

**UNIVERSIDADE FEDERAL DE MINAS GERAIS
INSTITUTO DE CIÊNCIAS EXATAS
DEPARTAMENTO DE QUÍMICA**

GLEISTON GONÇALVES DIAS

**RUTHENIUM(II) AND RHODIUM(III)-CATALYZED C–H ACTIVATION:
DIVERSIFYING BIOACTIVE AND FLUORESCENT COMPOUNDS *VIA*
ALKENYLATION, OXYGENATION AND ANNULATION PROTOCOLS**

BELO HORIZONTE

2021

UFMG/ICEX/DQ. 1.447

T. 658

GLEISTON GONÇALVES DIAS

**RUTHENIUM(II) AND RHODIUM(III)-CATALYZED C–H ACTIVATION:
DIVERSIFYING BIOACTIVE AND FLUORESCENT COMPOUNDS *VIA*
ALKENYLATION, OXYGENATION AND ANNULATION PROTOCOLS**

Thesis presented to the Department of
Chemistry of the Institute of Exact Sciences
of the Federal University of Minas Gerais as
a partial fulfillment for the Doctor of Science
degree - Chemistry

Advisor:

Professor Dr. Eufrânio Nunes da Silva Júnior

BELO HORIZONTE

2021

Ficha Catalográfica

D541r Dias, Gleiston Gonçalves
2021 Ruthenium(II) and rhodium(III)-catalyzed C-H
T activation [manuscrito] : diversifying bioactive and
fluorescent compounds via alkenylation, oxygenation
and annulation protocols / Gleiston Gonçalves Dias.
2021.
[xix, 239] f. : il.

Orientador: Eufrânio Nunes da Silva Júnior.

Tese (doutorado) - Universidade Federal de Minas
Gerais - Departamento de Química.

Inclui bibliografia.

1. Química orgânica - Teses. 2. Quinona - Teses. 3.
Rutênio - Teses. 4. Ródio - Teses. 5. Imidazóis -
Teses. 6. Catalisadores - Teses. 7. Ligação de
hidrogênio - Teses. 8. Compostos bioativos - Teses. 9.
Ressonância magnética nuclear - Teses. 10.
Cristalografia de raio X - Teses. I. Silva Júnior,
Eufrânio Nunes da, Orientador. II. Título.

CDU 043



UNIVERSIDADE FEDERAL DE MINAS GERAIS



"Ruthenium(ii) And Rhodium(iii)-catalyzed C-H Activation: Diversifying Bioactive And Fluorescent Compounds Via Alkenylation, Oxygenation And Annulation Protocols"

Gleiston Gonçalves Dias

Tese aprovada pela banca examinadora constituída pelos Professores:

Prof. Eufrânio Nunes da Silva Júnior - Orientador
UFMG

Profa. Maria Helena de Araujo
UFMG

Prof. Cleiton Moreira da Silva
UFMG

Prof. Márcio Weber Paixao
UFSCAR

Prof. Jason Guy Taylor
UFOP

Belo Horizonte, 19 de maio de 2021.



Documento assinado eletronicamente por **Marcio Weber Paixao, Usuário Externo**, em 19/05/2021, às 19:09, conforme horário oficial de Brasília, com fundamento no art. 5º do [Decreto nº 10.543, de 13 de novembro de 2020](#).



Documento assinado eletronicamente por **Eufranio Nunes da Silva Junior, Professor do Magistério Superior**, em 19/05/2021, às 19:11, conforme horário oficial de Brasília, com fundamento no art. 5º do [Decreto nº 10.543, de 13 de novembro de 2020](#).



Documento assinado eletronicamente por **Cleiton Moreira da Silva, Professor do Magistério Superior**, em 19/05/2021, às 19:12, conforme horário oficial de Brasília, com fundamento no art. 5º do [Decreto nº 10.543, de 13 de novembro de 2020](#).



Documento assinado eletronicamente por **Jason Guy Taylor, Usuário Externo**, em 19/05/2021, às 19:14, conforme horário oficial de Brasília, com fundamento no art. 5º do [Decreto nº 10.543, de 13 de novembro de 2020](#).



Documento assinado eletronicamente por **Maria Helena de Araujo, Membro**, em 19/05/2021, às 19:25, conforme horário oficial de Brasília, com fundamento no art. 5º do [Decreto nº 10.543, de 13 de novembro de 2020](#).



A autenticidade deste documento pode ser conferida no site https://sei.ufmg.br/sei/controlador_externo.php?acao=documento_conferir&id_orgao_acesso_externo=0, informando o código verificador **0721996** e o código CRC **13BE5582**.

I dedicate this thesis to my family, for all support.

To Vinicius Henrique Silveira, for being so understanding and present.

ACKNOWLEDGMENTS

To Professor Eufrânio Nunes da Silva Júnior, for the guidance and opportunity of developing science to the maximum of our ability.

To Prof. Lutz Ackermman and Prof. Claus Jacob, for receiving me in Germany and providing me a great opportunity of work.

To co-workers of the Ackermman and Jacob Research Groups, for providing me an environment of personal and professional growth.

To all the friends and co-workers of the Laboratory of Synthetic and Heterocyclic Chemistry over the last ten years. Many names to mention and even more great moments to record in memory.

To Renata Gomes Almeida, for sharing the challenges and overcoming of the post-graduation and for memorable moments in conferences.

To Esther Regina, for all the support in the final part of my research and for the opportunity of mutual teaching and learning.

To Wagner Valença and Eduardo H. G. Da Cruz for a great time in the lab and for learning with those who come first.

To Larissa Alves Corrêa, for the friendship, and many thoughtful conversations followed by an intense laughs. For sharing this long and intense road.

To my friends (“Topo”) from High/Technical School for the amazing moments over the last fifteen years.

To colleagues from the Department of Chemistry, for all the help in the reactions, sometimes providing chemicals and solvents and all support.

To Professors Solange de Castro and Rubem F. S. Menna-Barreto from Fiocruz, for joining forces with us in biological studies.

To Professor Carlos Simone, for the priceless contributions in X-ray crystallographic analysis.

To Professor Jarbas Magalhães Resende and LAREMAR team for NMR experiments and support.

To all the Professors in Department of Chemistry, for contributing to my academic and professional education. Special thanks to Professor Rosemeire Brondi Alves.

To Professor Luiz Alberto Cury, for the great and inspiring work on fluorescence studies.

To all Professors' members of the committee of evaluation of this work. I thank you for giving me the opportunity of learning even more.

To CNPQ for financial support and CAPES to the opportunity of developing part of my research in Germany *via* Programa Brasil-Alemanha (Probral). Also to FAPEMIG and PRPq-UFMG for the fundings.

**O correr da vida embrulha tudo.
A vida é assim: esquenta e esfria,
aperta e daí afrouxa,
sossega e depois desinquieta.
O que ela quer da gente é coragem”**
Guimarães Rosa, *Grande Sertão: Veredas*

“The strongest of all warriors are these two - Time and Patience.”
Liev Nikoláievich Tolstói, *War and Peace*

RESUMO

Esta tese descreve desenvolvimento de metodologias sintéticas, baseadas em ativação da ligação C–H, para promover alquenação e oxigenação de 1,4-naftoquinona e anelação de aril-lapimidazol. 1,4-naftoquinonas exibem baixa reatividade no anel benzenoide, *via* reações convencionais de areno, resultando em um escopo limitado de moléculas para serem aplicadas em Química Medicinal. Para superar essa limitação sintética, na primeira parte desta tese, alguns esforços no desenvolvimento da ativação de C–H *via* catálise com rutênio são descritos. Inicialmente, várias reações de otimização foram estudadas para encontrar a condição experimental adequada para realizar a funcionalização da ligação C–H do anel benzenoide de 1,4-naftoquinonas, com foco nas reações de alquenação e oxigenação. Após completar a otimização da reação, vários compostos 1,4-naftoquinoidais, contendo grupos doadores e retiradores de elétrons, foram preparados e submetidos aos protocolos de alquenação e oxigenação desenvolvidos. Os compostos obtidos foram avaliados contra o *Trypanosoma cruzi* e vários deles apresentaram promissora atividade biológica, principalmente os produtos contendo halogênios. Na segunda parte desta tese, são descritas as reações de anelação C–H /N–H em lapimidazol usando difenilacetileno. A maioria dos trabalhos na literatura relata reações semelhantes usando imidazóis simétricos, como estratégia para evitar isômeros. Assim, com o objetivo de superar essa limitação, foram realizados estudos de otimização utilizando lapimidazol não-simétrico. Vários derivados de lapimidazol, contendo diferentes grupos, foram sintetizados e submetidos à metodologia de anelação C–H/N–H. Em todos os casos, as anelações no lado do benzeno do lapimidazol foram observadas com maior rendimento, enquanto as anelações próximas ao lado alifático dos lapimidazóis foram observadas em menor rendimento. Os estudos de RMN e cristalografia de raios-X permitiram a correta distinção dos produtos e investigações mecanísticas foram realizadas justificando a maioria de um isômero. Além disso, estudos fotofísicos foram realizados com os produtos contendo os substituintes metoxila e nitro, bem como o produto sem substituinte. Em geral, os produtos exibiram emissão de fluorescência azul ou verde-amarelo enquanto que os produtos contendo o grupo nitro exibiram fluorescência de missão laranja/vermelho. Em conclusão, alquenação, oxigenação e anelação de ligações C–H desenvolvidas neste trabalho permitiram a obtenção de diversos compostos com propriedades biológicas ou fluorescentes.

Palavras-chave: ativação C–H, alquenação, oxigenação, anelação, quinona, imidazol

ABSTRACT

This thesis describes the development of synthetic methodologies, based on C–H bond activation, to perform alkenylation and oxygenation of 1,4-naphthoquinone and annulation of lapimidazole. 1,4-naphthoquinones exhibit low reactivity on the benzenoid ring by conventional arene reactions, resulting in a limited scope of molecules to be applied in Medicinal Chemistry. To overcome this synthetic restriction, in the first part of this thesis, some efforts in the development of C–H activation based on ruthenium catalysis are described. First, several optimization reactions were studied to find the suitable experimental condition to perform the functionalization of the C–H bond of the benzenoid ring of 1,4-naphthoquinones, focused on alkenylation and oxygenation reactions. After completing the optimization of the reaction, several 1,4-naphthoquinoidal compounds bearing electron-donating and withdrawing groups were prepared and subjected to C–H alkenylation and oxygenation protocols developed. The compounds obtained were subjected to biological assays against *Trypanosoma cruzi* and several of them presented promising biological activity, particularly products bearing halogens. In the second part of this thesis, C–H/N–H annulation reactions on imidazole using diphenyl acetylene are described. Most works in the literature report similar reactions using symmetrical imidazoles, as a strategy to avoid isomers. Thus, aiming to overcome this limitation, optimization studies were conducted using the non-symmetrical lapimidazole. Several lapimidazole derivatives, bearing different groups, were synthesized and subjected to C–H/N–H annulation methodology. In all cases, annulations in the benzene side of lapimidazole were observed in higher yield while the annulations close to the aliphatic side were observed in lower yield. NMR and X-ray crystallography studies enabled the correct distinction of both product and mechanistic investigations were carried out justifying the majority of one isomer. Also, photophysical studies were accomplished with the products bearing a methoxyl and nitro product as well as the product without substituent. In general, the products exhibited blue or green-yellow fluorescence emission while compounds bearing nitro group displayed orange-red fluorescence emission. In conclusion, C–H alkenylation, oxygenation and annulation developed in this work allowed to obtain diverse products with biological and fluorescent properties.

Keywords: C–H activation, alkenylation, oxygenation, annulation, quinone, imidazole.

LIST OF SCHEMES

Scheme 1. C–H activation as a methodology to direct functionalization.	1
Scheme 2. Comparison between Suzuki-Miyaura and C–H activation methodology by indazolidine arylation (Scheme adapted from ref. 6).	2
Scheme 3. One of the first examples of a metal-promoted ortho-directed C–H activation.	2
Scheme 4. Steric hindrance guides the selective arylation of indole (8).	3
Scheme 5. a) Directing group (DG) assistance in orientation and activation. b) Examples of directing groups.	4
Scheme 6. Ketone and ester as directing group in C–H alkylation catalyzed by Ru(II)-catalyzed.	5
Scheme 7. Frontier orbital interactions for electrophilic and nucleophilic mechanisms (adapted from ref. 25).	6
Scheme 8. Most common proposed mechanism pathways.	7
Scheme 9. Base-assisted C–H activation proposed mechanism.	8
Scheme 10. Selected examples of C–H alkenylation using acrylates.	11
Scheme 11. C–H oxygenation catalyzed by ruthenium reported by Ackermann and co-workers.	12
Scheme 12. Examples of oxygenation performed by Cu(II), Pd(II) and Ru(II).	13
Scheme 13. Chagas disease life cycle.	19
Scheme 14. Chemical approaches to achieve modified benzenoid ring of 1,4-naphthoquinone.	23
Scheme 15. Examples of juglone (74) synthesis.	24
Scheme 16. C–H oxygenation reported by Hong and co-workers. ¹²⁰	25
Scheme 17. C–H alkenylation of 1,4-naphthoquinone.	26
Scheme 18. Schematic representation of C–H metalation of 1,4-naphthoquinone followed by alkenylation and oxygenation described in the first part of this thesis.	27
Scheme 19. Proposed mechanism for C–H alkenylation of 1,4-naphthoquinone.	33
Scheme 20. C–H oxygenation reaction with anthraquinone (63).	35
Scheme 21. Mechanistic proposal of C–H oxygenation reactions.	37
Scheme 22. Schematic representation of 1,4-naphthoquinones derivatives substitution pattern.	37

Scheme 23. Synthesis of 2-(butylamino)naphthalene-1,4-dione (129), 2-methoxynaphthalene-1,4-dione (112) and -isopropoxynaphthalene-1,4-dione (131).....	39
Scheme 24. Synthesis of 2-chloronaphthalene-1,4-dione (132) and 2-bromonaphthalene-1,4-dione (133).....	39
Scheme 25. Synthesis of 2-chloro-3-methoxynaphthalene-1,4-dione (134) and 2,3-dimethoxynaphthalene-1,4-dione (135).....	40
Scheme 26. Synthesis of 2-methoxy-3-methylnaphthalene-1,4-dione (138).....	41
Scheme 27. Synthesis of α -lapachona (68).	41
Scheme 28. Synthesis of 5-nitronaphthalene-1,4-dione (102) and 5-aminonaphthalene-1,4-dione (103).....	42
Scheme 29. Synthesis of 6,7-dimethylnaphthalene-1,4-dione (141).	42
Scheme 30. Synthesis of anthracene-9,10-dione 122 , 144 and 145	43
Scheme 31. Synthesis of compounds 120 , 121 , 146 and 147	43
Scheme 32. a) Synthesis of compounds 149-151 and b) effect of the electron-donating groups in the reaction selectivity.....	44
Scheme 33. a) Unsuccessful synthesis of 152 and b) synthesis of 153-155 bearing methoxy group.....	45
Scheme 34. Synthesis of compounds 157	45
Scheme 35. Unsuccessful C–H alkenylation using substrates a) 132 , b) 126 and 127	46
Scheme 36. Synthesis of compounds 160-163	47
Scheme 37. Synthesis of compounds 164-167	47
Scheme 38. Synthesis of compounds 168-171	48
Scheme 39. Unsuccessful C–H alkenylation using substrates 102 and 103 modified in benzenoid ring with nitro and amine groups.	48
Scheme 40. a) Unsuccessful C–H oxygenation using substrates 124 , b) Synthesis of 114 and 175 c) regioselectivity possible explanation.....	49
Scheme 41. Synthesis of 178	50
Scheme 42. Attempt of C–H oxygenation using 2-isopropoxynaphthalene-1,4-dione (131)...	50
Scheme 43. a) Synthesis of 2-chloro-5-hydroxynaphthalene-1,4-dione (179) and 2-bromo-5-hydroxynaphthalene-1,4-dione (180). b) Orientation on C–H oxygenation. c) Traditional approach to synthesize 179 and 180	51
Scheme 44. Synthesis of 5-hydroxy-2-methylnaphthalene-1,4-dione (plumbagin, 186).	52
Scheme 45. Synthesis of plumbagin (186) carried out by Sun and co-workers. ¹⁴³	52

Scheme 46. Synthesis of 5-hydroxy-2-methoxy-3-methylnaphthalene-1,4-dione (191).....	53
Scheme 47. a) Synthesis 3-chloro-5-hydroxy-2-methoxynaphthalene-1,4-dione (192) and b) 5-hydroxy-2,3-dimethoxynaphthalene-1,4-dione (193).....	54
Scheme 48. a) Synthesis of 5-hydroxy-6,7-dimethylnaphthalene-1,4-dione (194) and attempts of C–H oxygenation using b) 5-nitronaphthalene-1,4-dione (102) and c) 5-aminonaphthalene-1,4-dione (103).	55
Scheme 49. Synthesis of oxygenated anthracene-9,10-dione 197 , 198 and 199	55
Scheme 50. Biological activity of selected product from C–H alkenylation. Values of IC ₅₀ in μM.	57
Scheme 51. Biological activity of selected product from C–H oxygenation. Values of IC ₅₀ in μM.	58
Scheme 52. 2,4,5-Triphenylimidazole (207) and 9,10-phenanthroimidazole (208).....	92
Scheme 53. Examples of fluorescent sensors 9,10-phenanthroimidazole-based to the detection of bisulfite, cysteine, homocysteine and Fe ³⁺ cation.	93
Scheme 54. C–H/N–H annulation reaction of 2-aryl-phenanthro[9,10- <i>d</i>]imidazoles with alkyne <i>via</i> rhodium(III) reported by Zheng and Hua.	95
Scheme 55. Examples of C–H/N–H oxidative annulation of 2-phenylbenzimidazole.	96
Scheme 56. C–H/N–H annulation of 10-phenyl-9H-pyreno[4,5- <i>d</i>]imidazole reported by Gandhi and co-workers.....	97
Scheme 57. Representation of symmetrical and non-symmetrical imidazole.	97
Scheme 58. Examples of non-symmetrical 2-phenyl-benzimidazole leading to isomeric products <i>via</i> C–H/N–H annulation reported by Dutta and Sen.	98
Scheme 59. Examples of lapimidazole 230 and its equivalents 231 and 232	99
Scheme 60. N–H equilibrium of imidazoles isomers.....	100
Scheme 61. Gram scale synthesis for preparing 235 and 236	103
Scheme 62. Scope of lapimidazole designed for C–H/N–H annulation.	104
Scheme 63. Mechanistic proposal of the synthesis of lapimidazoles.	105
Scheme 64. Substrate scope for C–H/N–H alkyne annulation of non-symmetric imidazole.	107
Scheme 65. Compounds 271 , 272 , 257 and 260 and their respective ortep-3 projection confirming the regioselectivity.	109
Scheme 66. a) Possible isomeric products pairs 279/283 and 282/284. b) X-ray crystallography studies of 279 and 280 confirming the regioselectivity.....	111

Scheme 67. Computed Gibbs free energies at $T = 373.15 \text{ K}$ ($\Delta G_{373.15}$) in kcal mol^{-1} for the annulation of **234**. Black curves are related to the pathway starting from the metalation of N^1 (benzenic side) while the pathway in red shows the annulation of **1a** following metalation at N^2 (aliphatic side). 113

Scheme 68. Catalytic cycle of the mechanism of C–H/N–H annulation proposed based on theoretical studies described..... 114

LIST OF FIGURES

Figure 1. Representation of different quinoidal structures	14
Figure 2. Selected examples of quinones with highlighted 1,4-quinone moiety.....	15
Figure 3. Selected examples of compounds with juglone moiety.	17
Figure 4. Benznidazole (88) Nifurtimox (89) and Crystal Violet (90).....	20
Figure 5. Examples of quinone with potent trypanocidal activity. ^a IC ₅₀ /24h values in μM for the activity on trypomastigotes.....	21
Figure 6. Naphthoquinones commercially obtained.....	38
Figure 7. Examples of imidazole compounds with biological properties.	91
Figure 8. Examples of products bearing a substituent in meta position.	108
Figure 9. ¹ H NMR (CDCl ₃ , 400 MHz) spectra of 271 and 272	110
Figure 10. Selected products 235/236 , 259/260 and 277/278 for photophysical studies.	115
Figure 11. Absorption and fluorescence spectra at room temperature for the 235/236 , 259/260 and 277/278 isomer pairs of solutions at 40 μM in ethyl acetate.....	116
Figure 12. ¹ H NMR spectrum (400 MHz, CDCl ₃) of compound 68	149
Figure 13. ¹³ C NMR spectrum (100 MHz, CDCl ₃) of compound 68	149
Figure 14. ¹ H NMR spectrum (400 MHz, CDCl ₃) of compound 102	150
Figure 15. ¹³ C NMR spectrum (100 MHz, CDCl ₃) of compound 102	150
Figure 16. ¹ H NMR spectrum (300 MHz, CDCl ₃) of compound 103	151
Figure 17. ¹³ C NMR spectrum (75 MHz, CDCl ₃) of compound 103	151
Figure 18. ¹ H NMR spectrum (300 MHz, CDCl ₃) of compound 112	152
Figure 19. ¹³ C NMR spectrum (75 MHz, CDCl ₃) of compound 112	152
Figure 20. ¹ H NMR spectrum (300 MHz, CDCl ₃) of compound 122	153
Figure 21. ¹³ C NMR spectrum (75 MHz, CDCl ₃) of compound 122	153
Figure 22. ¹ H NMR spectrum (300 MHz, CDCl ₃) of compound 129	154
Figure 23. ¹³ C NMR spectrum (75 MHz, CDCl ₃) of compound 129	154
Figure 24. ¹ H NMR spectrum (300 MHz, CDCl ₃) of compound 131	155
Figure 25. ¹³ C NMR spectrum (75 MHz, CDCl ₃) of compound 131	155
Figure 26. ¹ H NMR spectrum (300 MHz, CDCl ₃) of compound 132	156
Figure 27. ¹³ C NMR spectrum (75 MHz, CDCl ₃) of compound 132	156
Figure 28. ¹ H NMR spectrum (300 MHz, CDCl ₃) of compound 133	157
Figure 29. ¹³ C NMR spectrum (75 MHz, CDCl ₃) of compound 133	157

Figure 30. ^1H NMR spectrum (300 MHz, CDCl_3) of compound 134	158
Figure 31. ^{13}C NMR spectrum (75 MHz, CDCl_3) of compound 134	158
Figure 32. ^1H NMR spectrum (300 MHz, CDCl_3) of compound 135	159
Figure 33. ^{13}C NMR spectrum (75 MHz, CDCl_3) of compound 135	159
Figure 34. ^1H NMR spectrum (300 MHz, CDCl_3) of compound 137	160
Figure 35. ^{13}C NMR spectrum (75 MHz, CDCl_3) of compound 137	160
Figure 36. ^1H NMR spectrum (300 MHz, CDCl_3) of compound 138	161
Figure 37. ^{13}C NMR spectrum (75 MHz, CDCl_3) of compound 138	161
Figure 38. ^1H NMR spectrum (300 MHz, CDCl_3) of compound 141	162
Figure 39. ^{13}C NMR spectrum (75 MHz, CDCl_3) of compound 141	162
Figure 40. ^1H NMR spectrum (300 MHz, CDCl_3) of compound 144	163
Figure 41. ^{13}C NMR spectrum (75 MHz, CDCl_3) of compound 144	163
Figure 42. ^1H NMR spectrum (300 MHz, CDCl_3) of compound 156	164
Figure 43. ^{13}C NMR spectrum (75 MHz, CDCl_3) of compound 156	164
Figure 44. ^1H NMR spectrum (400 MHz, CDCl_3) of compound 120	166
Figure 45. ^{13}C NMR spectrum (100 MHz, CDCl_3) of compound 120	166
Figure 46. ^1H NMR spectrum (300 MHz, CDCl_3) of compound 121	167
Figure 47. ^{13}C NMR spectrum (75 MHz, CDCl_3) of compound 121	167
Figure 48. ^1H NMR spectrum (300 MHz, CDCl_3) of compound 146	168
Figure 49. ^{13}C NMR spectrum (75 MHz, CDCl_3) of compound 146	168
Figure 50. ^1H NMR spectrum (300 MHz, CDCl_3) of compound 147	169
Figure 51. ^{13}C NMR spectrum (75 MHz, CDCl_3) of compound 147	169
Figure 52. ^1H NMR spectrum (300 MHz, CDCl_3) of compound 149	170
Figure 53. ^{13}C NMR spectrum (75 MHz, CDCl_3) of compound 149	170
Figure 54. ^1H NMR spectrum (300 MHz, CDCl_3) of compound 150	171
Figure 55. ^{13}C NMR spectrum (75 MHz, CDCl_3) of compound 150	171
Figure 56. ^1H NMR spectrum (300 MHz, CDCl_3) of compound 151	172
Figure 57. ^{13}C NMR spectrum (75 MHz, CDCl_3) of compound 151	172
Figure 58. ^1H NMR spectrum (300 MHz, CDCl_3) of compound 153	173
Figure 59. ^{13}C NMR spectrum (75 MHz, CDCl_3) of compound 153	173
Figure 60. ^1H NMR spectrum (300 MHz, CDCl_3) of compound 154	174
Figure 61. ^{13}C NMR spectrum (75 MHz, CDCl_3) of compound 154	174
Figure 62. ^1H NMR spectrum (300 MHz, CDCl_3) of compound 155	175

Figure 63. ^{13}C NMR spectrum (75 MHz, CDCl_3) of compound 155	175
Figure 64. ^1H NMR spectrum (300 MHz, CDCl_3) of compound 157	176
Figure 65. ^{13}C NMR spectrum (75 MHz, CDCl_3) of compound 157	176
Figure 66. ^1H NMR spectrum (300 MHz, CDCl_3) of compound 160	177
Figure 67. ^{13}C NMR spectrum (75 MHz, CDCl_3) of compound 160	177
Figure 68. ^1H NMR spectrum (400 MHz, CDCl_3) of compound 162	178
Figure 69. ^{13}C NMR spectrum (100 MHz, CDCl_3) of compound 162	178
Figure 70. ^1H NMR spectrum (400 MHz, CDCl_3) of compound 163	179
Figure 71. ^{13}C NMR spectrum (100 MHz, CDCl_3) of compound 163	179
Figure 72. ^1H NMR spectrum (500 MHz, CDCl_3) of compound 164	180
Figure 73. ^{13}C NMR spectrum (125 MHz, CDCl_3) of compound 164	180
Figure 74. ^1H NMR spectrum (500 MHz, CDCl_3) of compound 165	181
Figure 75. ^{13}C NMR spectrum (125 MHz, CDCl_3) of compound 165	181
Figure 76. ^1H NMR spectrum (300 MHz, CDCl_3) of compound 166	182
Figure 77. ^{13}C NMR spectrum (75 MHz, CDCl_3) of compound 166	182
Figure 78. ^1H NMR spectrum (300 MHz, CDCl_3) of compound 167	183
Figure 79. ^{13}C NMR spectrum (75 MHz, CDCl_3) of compound 167	183
Figure 80. ^1H NMR spectrum (400 MHz, CDCl_3) of compound 168	184
Figure 81. ^{13}C NMR spectrum (100 MHz, CDCl_3) of compound 168	184
Figure 82. ^1H NMR spectrum (300 MHz, CDCl_3) of compound 169	185
Figure 83. ^{13}C NMR spectrum (75 MHz, CDCl_3) of compound 169	185
Figure 84. ^1H NMR spectrum (400 MHz, CDCl_3) of compound 170	186
Figure 85. ^{13}C NMR spectrum (100 MHz, CDCl_3) of compound 170	186
Figure 86. ^1H NMR spectrum (300 MHz, CDCl_3) of compound 171	187
Figure 87. ^{13}C NMR spectrum (75 MHz, CDCl_3) of compound 171	187
Figure 88. ^1H NMR spectrum (300 MHz, CDCl_3) of compound 74	189
Figure 89. ^{13}C NMR spectrum (75 MHz, CDCl_3) of compound 74	189
Figure 90. ^1H NMR spectrum (300 MHz, CDCl_3) of compound 114	190
Figure 91. ^{13}C NMR spectrum (75 MHz, CDCl_3) of compound 114	190
Figure 92. ^1H NMR spectrum (300 MHz, CDCl_3) of compound 123	191
Figure 93. ^{13}C NMR spectrum (75 MHz, CDCl_3) of compound 123	191
Figure 94. ^1H NMR spectrum (300 MHz, CDCl_3) of compound 124	192
Figure 95. ^{13}C NMR spectrum (75 MHz, CDCl_3) of compound 124	192

Figure 96. ^1H NMR spectrum (300 MHz, CDCl_3) of compound 178	193
Figure 97. ^{13}C NMR spectrum (75 MHz, CDCl_3) of compound 178	193
Figure 98. ^1H NMR spectrum (300 MHz, CDCl_3) of compound 179	194
Figure 99. ^{13}C NMR spectrum (75 MHz, CDCl_3) of compound 179	194
Figure 100. ^1H NMR spectrum (300 MHz, CDCl_3) of compound 180	195
Figure 101. ^{13}C NMR spectrum (75 MHz, CDCl_3) of compound 180	195
Figure 102. ^1H NMR spectrum (300 MHz, CDCl_3) of compound 186	196
Figure 103. ^{13}C NMR spectrum (75 MHz, CDCl_3) of compound 186	196
Figure 104. ^1H NMR spectrum (300 MHz, CDCl_3) of compound 191	197
Figure 105. ^{13}C NMR spectrum (75 MHz, CDCl_3) of compound 191	197
Figure 106. ^1H NMR spectrum (300 MHz, CDCl_3) of compound 192	198
Figure 107. ^{13}C NMR spectrum (75 MHz, CDCl_3) of compound 192	198
Figure 108. ^1H NMR spectrum (300 MHz, CDCl_3) of compound 193	199
Figure 109. ^{13}C NMR spectrum (75 MHz, CDCl_3) of compound 193	199
Figure 110. ^1H NMR spectrum (300 MHz, CDCl_3) of compound 194	200
Figure 111. ^{13}C NMR spectrum (75 MHz, CDCl_3) of compound 194	200
Figure 112. ^1H NMR spectrum (300 MHz, CDCl_3) of compound 196	201
Figure 113. ^{13}C NMR spectrum (75 MHz, CDCl_3) of compound 196	201
Figure 114. ^1H NMR spectrum (300 MHz, CDCl_3) of compound 198	202
Figure 115. ^{13}C NMR spectrum (75 MHz, CDCl_3) of compound 198	202
Figure 116. ^1H NMR spectrum (300 MHz, CDCl_3) of compound 199	203
Figure 117. ^{13}C NMR spectrum (75 MHz, CDCl_3) of compound 199	203
Figure 118. ^1H NMR spectrum (400 MHz, $\text{DMSO-}d_6$) of compound 234	205
Figure 119. ^1H NMR spectrum (400 MHz, $\text{DMSO-}d_6$) of compound 237	205
Figure 120. ^1H NMR spectrum (400 MHz, $\text{DMSO-}d_6$) of compound 238	206
Figure 121. ^1H NMR spectrum (400 MHz, $\text{DMSO-}d_6$) of compound 239	206
Figure 122. ^1H NMR spectrum (400 MHz, $\text{DMSO-}d_6$) of compound 240	207
Figure 123. ^1H NMR spectrum (400 MHz, $\text{DMSO-}d_6$) of compound 241	207
Figure 124. ^1H NMR spectrum (400 MHz, $\text{DMSO-}d_6$) of compound 242	208
Figure 125. ^1H NMR spectrum (400 MHz, $\text{DMSO-}d_6$) of compound 243	208
Figure 126. ^1H NMR spectrum (400 MHz, $\text{DMSO-}d_6$) of compound 244	209
Figure 127. ^1H NMR spectrum (400 MHz, $\text{DMSO-}d_6$) of compound 245	209
Figure 128. ^1H NMR spectrum (400 MHz, $\text{DMSO-}d_6$) of compound 246	210

Figure 129. ^1H NMR spectrum (400 MHz, DMSO- d_6) of compound 247	210
Figure 130. ^1H NMR spectrum (400 MHz, DMSO- d_6) of compound 248	211
Figure 131. ^1H NMR spectrum (400 MHz, DMSO- d_6) of compound 249	211
Figure 132. ^1H NMR spectrum (400 MHz, DMSO- d_6) of compound 250	212
Figure 133. ^1H NMR spectrum (400 MHz, CDCl_3) of compound 235	214
Figure 134. ^{13}C NMR spectrum (100 MHz, CDCl_3) of compound 235	214
Figure 135. ^1H NMR spectrum (400 MHz, CDCl_3) of compound 236	215
Figure 136. ^{13}C NMR spectrum (100 MHz, CDCl_3) of compound 236	215
Figure 137. ^1H NMR spectrum (400 MHz, CDCl_3) of compound 257	216
Figure 138. ^{13}C NMR spectrum (100 MHz, CDCl_3) of compound 257	216
Figure 139. ^1H NMR spectrum (400 MHz, CDCl_3) of compound 258	217
Figure 140. ^{13}C NMR spectrum (100 MHz, CDCl_3) of compound 258	217
Figure 141. ^1H NMR spectrum (600 MHz, CDCl_3) of compound 259	218
Figure 142. ^{13}C NMR spectrum (150 MHz, CDCl_3) of compound 259	218
Figure 143. ^1H NMR spectrum (600 MHz, CDCl_3) of compound 260	219
Figure 144. ^{13}C NMR spectrum (150 MHz, CDCl_3) of compound 260	219
Figure 145. ^1H NMR spectrum (400 MHz, CDCl_3) of compound 261	220
Figure 146. ^{13}C NMR spectrum (100 MHz, CDCl_3) of compound 261	220
Figure 147. ^1H NMR spectrum (400 MHz, CDCl_3) of compound 262	221
Figure 148. ^{13}C NMR spectrum (100 MHz, CDCl_3) of compound 262	221
Figure 149. ^1H NMR spectrum (400 MHz, CDCl_3) of compound 263	222
Figure 150. ^{13}C NMR spectrum (100 MHz, CDCl_3) of compound 263	222
Figure 151. ^1H NMR spectrum (400 MHz, CDCl_3) of compound 264	223
Figure 152. ^{13}C NMR spectrum (100 MHz, CDCl_3) of compound 264	223
Figure 153. ^1H NMR spectrum (400 MHz, CDCl_3) of compound 265	224
Figure 154. ^{13}C NMR spectrum (100 MHz, CDCl_3) of compound 265	224
Figure 155. ^1H NMR spectrum (400 MHz, CDCl_3) of compound 266	225
Figure 156. ^{13}C NMR spectrum (100 MHz, CDCl_3) of compound 266	225
Figure 157. ^1H NMR spectrum (400 MHz, CDCl_3) of compound 267	226
Figure 158. ^{13}C NMR spectrum (100 MHz, CDCl_3) of compound 267	226
Figure 159. ^1H NMR spectrum (400 MHz, CDCl_3) of compound 268	227
Figure 160. ^{13}C NMR spectrum (100 MHz, CDCl_3) of compound 268	227
Figure 161. ^1H NMR spectrum (400 MHz, CDCl_3) of compound 269	228

Figure 162. ^{13}C NMR spectrum (100 MHz, CDCl_3) of compound 269	228
Figure 163. ^1H NMR spectrum (400 MHz, CDCl_3) of compound 271	229
Figure 164. ^{13}C NMR spectrum (100 MHz, CDCl_3) of compound 271	229
Figure 165. ^1H NMR spectrum (400 MHz, CDCl_3) of compound 272	230
Figure 166. ^{13}C NMR spectrum (100 MHz, CDCl_3) of compound 272	230
Figure 167. ^1H NMR spectrum (400 MHz, CDCl_3) of compound 273	231
Figure 168. ^{13}C NMR spectrum (100 MHz, CDCl_3) of compound 273	231
Figure 169. ^1H NMR spectrum (400 MHz, CDCl_3) of compound 274	232
Figure 170. ^{13}C NMR spectrum (100 MHz, CDCl_3) of compound 274	232
Figure 171. ^1H NMR spectrum (400 MHz, CDCl_3) of compound 275	233
Figure 172. ^{13}C NMR spectrum (100 MHz, CDCl_3) of compound 275	233
Figure 173. ^1H NMR spectrum (400 MHz, CDCl_3) of compound 276	234
Figure 174. ^{13}C NMR spectrum (100 MHz, CDCl_3) of compound 276	234
Figure 175. ^1H NMR spectrum (600 MHz, CDCl_3) of compound 277	235
Figure 176. ^{13}C NMR spectrum (150 MHz, CDCl_3) of compound 277	235
Figure 177. ^1H NMR spectrum (400 MHz, CDCl_3) of compound 278	236
Figure 178. ^{13}C NMR spectrum (100 MHz, CDCl_3) of compound 278	236
Figure 179. ^1H NMR spectrum (400 MHz, CDCl_3) of compound 279	237
Figure 180. ^{13}C NMR spectrum (100 MHz, CDCl_3) of compound 279	237
Figure 181. ^1H NMR spectrum (400 MHz, CDCl_3) of compound 280	238
Figure 182. ^{13}C NMR spectrum (100 MHz, CDCl_3) of compound 280	238
Figure 183. ^1H NMR spectrum (400 MHz, CDCl_3) of compound 281	239
Figure 184. ^{13}C NMR spectrum (100 MHz, CDCl_3) of compound 281	239

LIST OF TABLES

Table 1. Catalyst and solvent screening.....	30
Table 2. Silver source and oxidants screening.....	31
Table 3. Studies of the amount of silver source and acrylate.	32
Table 4. Optimization of C–H oxygenation reactions of 1,4-naphthoquinone (61).	34
Table 5. Optimizations of oxygenation reactions of 1,4-dibromoanthracene-9,10-dione (122)	36
Table 6. Selected optimization results.	103
Table 7. Parameters obtained from the analysis of the absorption (λ_{abs}) and fluorescence (λ_{em}) spectra respectively for the solutions and dropcast films fabricated as described in the experimental section, being $\Delta\lambda = (\lambda_{\text{em}} - \lambda_{\text{abs}})$	116

LIST OF ABBREVIATIONS

AIE	Aggregation-induced emission
AMLA	Ambiphilic metal ligand activation
ATR	Attenuated total reflection
bs	Broad signal
CAN	Cerium ammonium nitrate
CAS	Ammonium cerium(IV) sulfate
CCDC	Cambridge Crystallographic Data Centre
CMD	Concerted metalation-deprotonation
d	Doublet
DCE	1,2-Dichloroethane
dd	Double doublet
ddd	Doublet of doublet of doublets
DDQ	2,3-Dichloro-5,6-dicyano- <i>p</i> -benzoquinone
DFT	Density functional theory
DG	Directing group
DMA	Dimethylacetamide
DMF	Dimethyl formamide
DNA	Deoxyribonucleic acid
EDG	Electron-donating group
EI	Electronic ionization
EWG	Electron-withdrawing group
FCC	Flash column chromatography
FG	Functional group
FGI	Functional group interconversion
HRMS	High resolution mass spectrometry
IC ₅₀	Half maximal inhibitory concentration
ICT	Intramolecular charge transfer
I. R.	infrared spectroscopy
<i>J</i>	Coupling constant
M	Molar
m	Multiplet

MCPBA	<i>Meta</i> -chloroperoxybenzoic acid
MHz	Mega Hertz
m. p.	melting point
NBS	<i>N</i> -bromosuccinimide
NCS	<i>N</i> -chlorosuccinimide
NMR	Nuclear Magnetic Resonance
NR	No Reaction
PIDA	(Diacetoxyiodo)benzene
PIFA	Bis(trifluoroacetoxy)iodobenzene
q	Quartet
ROS	Reactive oxygen species
rt	Room temperature
s	Singlet
sd	Septet of doublet
t	Triplet
TBAB	Tetrabutylammonium bromide
TBHP	Tert-butyl hydroperoxide
<i>T. cruzi</i>	<i>Trypanosoma cruzi</i>
td	Triplet of doublets
TFA	Trifluoroacetic acid
TFAA	Trifluoroacetic anhydride
THF	tetrahydrofuran
TLC	thin-layer chromatography
δ	chemical shift
$\tilde{\nu}$	wave number
σ (C–H)	sigma carbon-hydrogen bond orbital
σ^* (C–H)	sigma anti-bond carbon-hydrogen orbital

CONTENTS

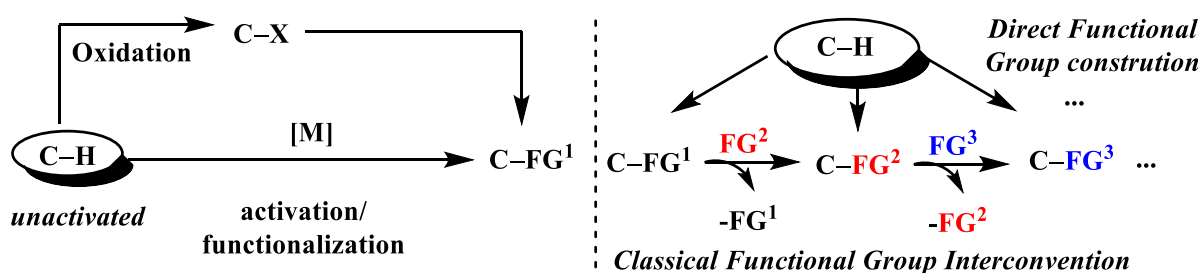
ACKNOWLEDGMENTS.....	II
RESUMO.....	V
ABSTRACT	VI
LIST OF SCHEMES.....	VII
LIST OF FIGURES.....	XI
LIST OF TABLES.....	XVII
LIST OF ABBREVIATIONS.....	XVIII
CONTENTS	XX
1. C–H ACTIVATION	1
1.1 Innate and Guided selectivity in C–H Bond activation.....	3
1.2 General aspects of mechanistic approach in C–H activation	5
PART I.....	9
1. INTRODUCTION	10
1.1 C–H alkenylation <i>via</i> acrylate.	10
1.2 C–H oxygenation.....	11
1.3 Quinone in Medicinal Chemistry.	13
1.4 Chagas disease.....	17
2. MOTIVATION	22
3. SYNTHETIC STRATEGY.....	25
4. RESEARCH PURPOSE	28
4.1. General purpose.....	28
4.1.1. Specific purpose.	28
5. RESULTS AND DISCUSSIONS.....	29
5.1 C–H alkenylation optimizations studies	29
5.2 Proposed C–H alkenylation mechanism.....	32
5.3 C–H oxygenations optimizations studies	33
5.4 Mechanism proposal.....	36
5.5 Synthesis of quinoidal substrates	37
5.6 Scope of the ruthenium(II) catalyzed C–H alkenylation	43
5.7 Scope of the ruthenium(II) catalyzed C–H oxygenation.....	48
5.8 Biological Assays against <i>Trypanosoma cruzi</i>	56
6. CONCLUSION	59
7. EXPERIMENTAL SECTION.....	60
7.1 Synthesis of Substrates.....	60
7.2 C–H alkenylation: general procedure A and characterization data of products.	68
7.3 C–H oxygenation: general procedure B and characterization data of products.....	81
7.4 C–H oxygenation of anthraquinone: general procedure C and characterization data of products.....	87
7.5 Trypanocidal Assays.....	89
PART II	90
1. INTRODUCTION	91

2. MOTIVATION	95
3. SYNTHETIC STRATEGY	99
4. RESEARCH PURPOSE	101
4.1. General Purpose	101
4.1.1 Specific Purpose	101
5. RESULTS AND DISCUSSIONS	102
5.1 C–H/N–H annulation optimizations	102
5.2 Gram scale synthesis for the preparation of 235 and 236	103
5.3 Synthesis of phenyl-lapimidazole derivatives	104
5.4 Scope of the rhodium(III)-catalyzed C–H/N–H annulation	105
5.5 Characterization	108
5.6 Mechanism proposal	111
5.7 Photophysical Studies	114
6. CONCLUSION	117
7. EXPERIMENTAL SECTION	118
7.1 Procedure for β-lapachone (228) synthesis	118
7.2 Synthesis of lapimidazole: general procedure D and characterization data of products.	118
7.3 C–H/N–H annulation: general procedure E and characterization data of products	126
7.4 Gram scale synthesis Procedure	144
7.5 Fluorescence studies	144
GENERAL CONCLUSION	146
APPENDICE	148

1. C–H ACTIVATION

Chemical modifications in organic molecules are focused on functional group interconversion (FGI) *via* bond cleavage, migration, and substitution. Those transformations are possible due to the relatively high energy level of the chemical bonds and favorable kinetic aspects. Bonds that undergo this kind of transformation are called activated bonds.¹ In contrast, deactivated bonds are thermodynamically and kinetically stable bonds and, consequently, unsusceptible to chemical transformation. Therefore, those bonds are rarely considered as a functional group. Nevertheless, they have been classified as an un-functional group.² C–H bonds in a hydrocarbon constitute a classic example of a deactivated bond, which makes the hydrocarbons the most common and ubiquitous organic functional group.

The direct chemical transformation of an inert C–H bond, intermediated by a transition metal (C–M as intermediate), without previous functionalization (oxidation), is called C–H activation (**Scheme 1**).³ This methodology is interesting because it allows building a functional group direct from an inert C–H bond reducing FGI and, consequently, it produce less waste.



Scheme 1. C–H activation as a methodology to direct functionalization.

Classical Suzuki cross-coupling reactions generally require an aryl or vinyl group (both pre-functionalized with a halogen or a pseudohalogen) and a boronic acid. However, in C–H activation processes at least one reagent does not need to be pre-functionalized. For example,

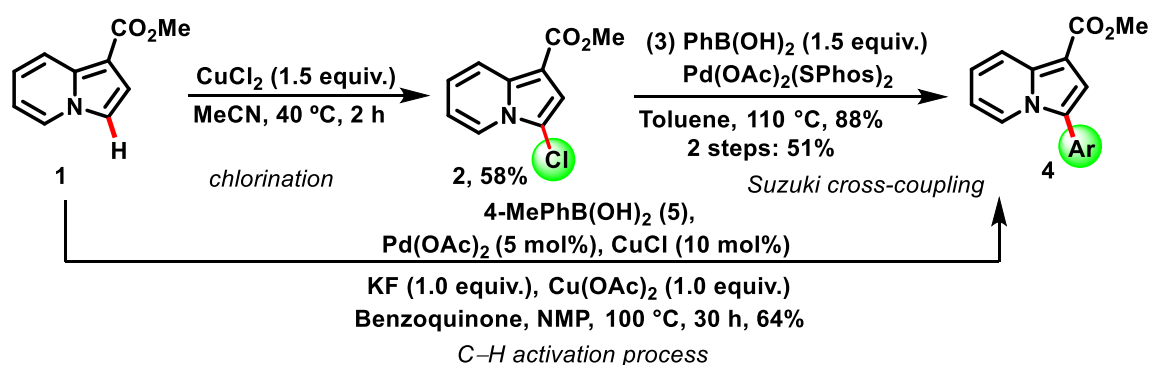
1. F. de Azambuja, C. R. D. Correia. O desafio da ativação das ligações C–H em síntese orgânica. *Quim. Nova*, **2011**, *34*, 1779-1790.

2. K. I. Goldberg; A. S. Goldman. *Activation and Functionalization of C–H Bonds*. ACS Symposium Series 885; *Am. Chem. Soc.* **2004**, Washington, DC, 1-43.

3. R. H. Crabtree. Alkane C–H activation and functionalization with homogeneous transition metal catalysts: a century of progress - a new millennium in prospect. *J. Chem. Soc., Dalton Trans.* **2001**, *0*, 2437-2450.

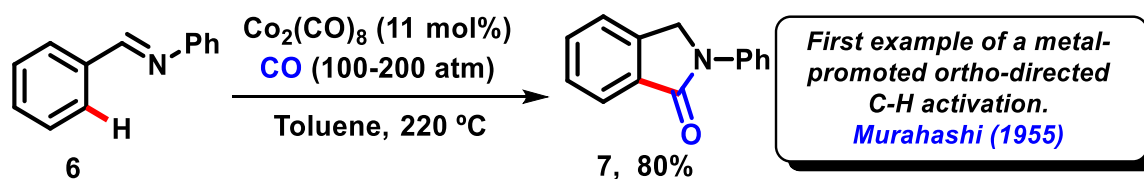
in 2010 You and co-workers⁴ reported a Pd/Cu as a catalyst system for direct arylation of heteroaromatic molecules without previous chlorine functionalization, as outlined in **Scheme 2**.⁵

Therefore, the direct arylation through C–H activation was performed and product **4** was obtained in 64% yield while in the previous methodology (chlorination and cross-coupling reaction), a similar product was obtained in 51% yield. Thus, the direct arylation was accomplished with less chemical, solvent, and time waste.



Scheme 2. Comparison between Suzuki-Miyaura and C–H activation methodology by indazole arylation (Scheme adapted from ref. 6).

Although there is no precise date for the first research about direct C–H activation was carried out, one of the oldest studies about a metal-promoted *ortho*-directed C–H activation can be attributed to Murahashi. The authors developed a methodology that produced amide **7** through a carbonyl addition and a ring-closure, catalyzed by $\text{Co}_2(\text{CO})_8$ in carbon monoxide atmosphere at high temperature (**Scheme 3**).⁷



Scheme 3. One of the first examples of a metal-promoted *ortho*-directed C–H activation.

4. B. Liu, X. Qin, K. Li, X. Li, Q. Guo, J. Lan, J. You. A palladium/copper bimetallic catalytic system: dramatic improvement for Suzuki-Miyaura-type direct C–H arylation of azoles with arylboronic acids. *Chem. Eur. J.* **2010**, *16*, 11836-11839.

5. J.-B. Xia, S.-L. You. Synthesis of 3-haloindolizines by copper(II) halide mediated direct functionalization of indolizines. *Org. Lett.* **2009**, *11*, 1187-1190.

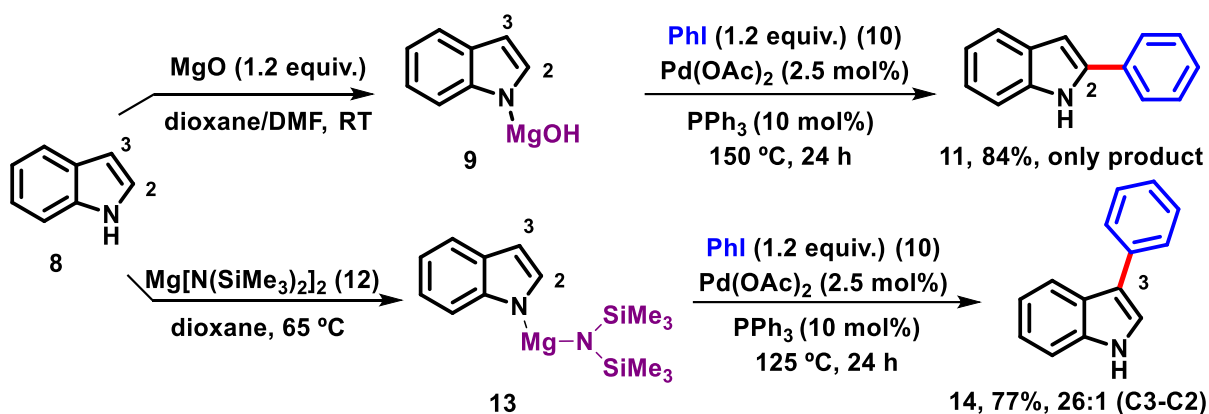
6. F. Azambuja, C. R. D. Correia. O desafio da ativação das ligações C–H em síntese orgânica. *Quim. Nova.* **2011**, *34*, 1779-1790.

7. S. Murahashi. Synthesis of phthalimidines from schiff bases and carbon monoxide. *J. Am. Chem. Soc.* **1955**, *77*, 6403-6404.

1.1 Innate and Guided selectivity in C–H Bond activation.

The reactional planning of organic transformations requires selective modification in molecules. Usually, *innate selectivity* in C–H activation can be achieved by electronic effects, such as electron-withdrawing (EWGs) or electron-donating groups (EDGs)⁸ or by steric effects, like bulky groups close to C–H bond prone to C–H bond activation.

For instance, C–H bonds at C-2 and C-3 positions in indole derivatives may undergo activation/functionalization based on acid and/or steric effects, because C–H bonds at C-2 position are more acid than at C-3 position. In 2005, Sames and co-workers reported⁹ that the C-2 position of indole (**8**) are more susceptible to Pd-catalyzed arylation when nitrogen atom bears less steric hindrance groups (-MgOH) as illustrated in **Scheme 4**. Nevertheless, bulkier groups (-MgN(SiMe₃)₂) can block C-2 position and allows only C-3 activation.



Scheme 4. Steric hindrance guides the selective arylation of indole (**8**).

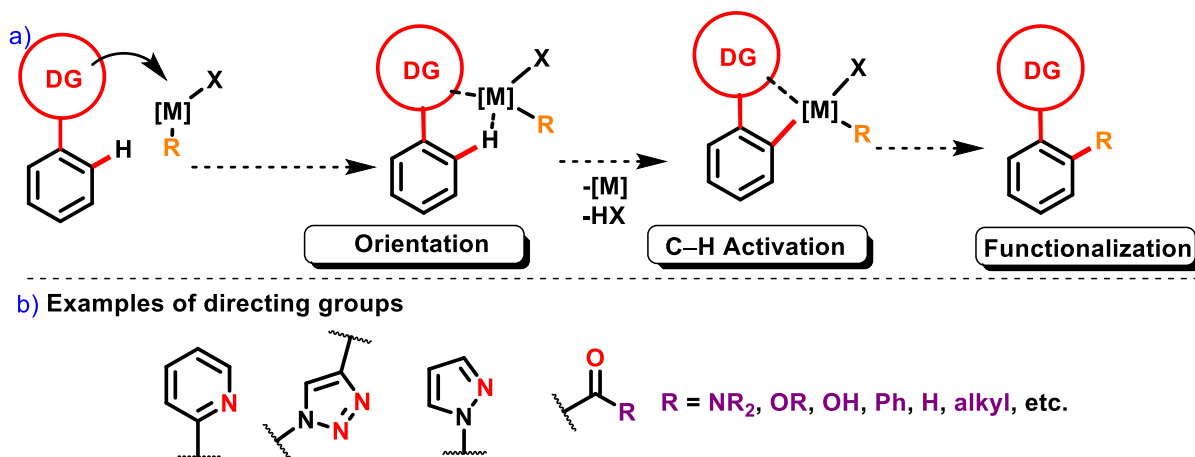
In *guided selectivity*, a directing group (DG), having free electron pairs, is necessary to coordinate to the transition metal leading to selectively *ortho*-cyclometallation and C–H activation.¹⁰ Then, a functional group, from another reagent, is transferred to metallacycle, followed by functionalization (**Scheme 5a**).

8. T. Newhouse, P. S. Baran. If C–H bonds could talk: selective C–H bond oxidation. *Angew. Chem. Int. Ed.* **2011**, *50*, 3362-3374.

9. B. S. Lane, M. A. Brown, D. Sames. Direct palladium-catalyzed C-2 and C-3 arylation of indoles: a mechanistic rationale for regioselectivity. *J. Am. Chem. Soc.* **2005**, *127*, 8050-8057.

10. T. Brückl, R. D. Baxter, Y. Ishihara, P. S. Baran. Innate and guided C–H functionalization logic. *Acc. Chem. Res.* **2012**, *45*, 826-839.

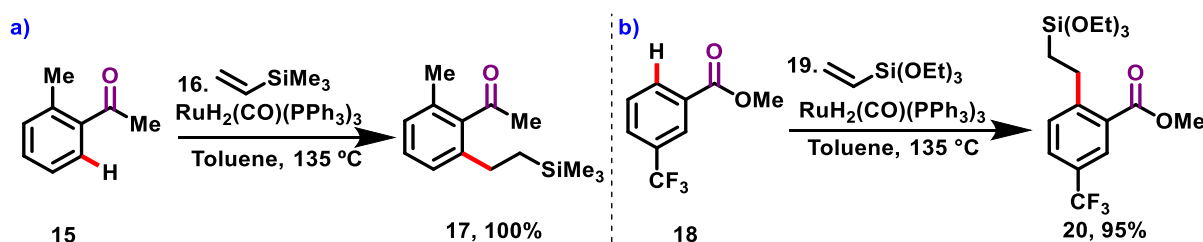
Different functional groups have been used as directing groups¹¹ such as pyridine, triazole,¹² pyrazole,¹³ amide,¹⁴ ester,¹⁵ carboxylic acid,¹⁶ ketone,¹⁷ and aldehyde¹⁸ (Scheme 5b). Currently, weak,¹⁹ modifiable²⁰ and removable²¹ DGs have been developed toward eco-friendly and economical organic synthesis.



Scheme 5. a) Directing group (DG) assistance in orientation and activation. b) Examples of directing groups.

11. Z. Chen, B. Wang, J. Zhang, W. Yu, Z. Liu, Y. Zhang. Transition metal-catalyzed C–H bond functionalizations by the use of diverse directing groups. *Org. Chem. Front.* **2015**, *2*, 1107-1295.
12. I. Guerrero, A. Correa. Metal-catalyzed C–H functionalization processes with “click”-triazole assistance. *Eur. J. Org. Chem.* **2018**, *44*, 6034-6049.
13. P. B. Arockiam, C. Fischmeister, C. Bruneau, P. H. Dixneuf. Ruthenium diacetate-catalysed oxidative alkenylation of C–H bonds in air: synthesis of alkenyl N-arylpyrazoles. *Green Chem.* **2011**, *13*, 3075-3078.
14. F. W. Patureau, F. Glorius. Rh catalyzed olefination and vinylation of unactivated acetanilides. *J. Am. Chem. Soc.* **2010**, *132*, 9982-9983.
15. B. Xiao, Y. Fu, J. Xu, T. Gong, J. Dai, J. Yi, L. Liu. Pd(II)-catalyzed C–H activation/aryl-aryl coupling of phenol esters. *J. Am. Chem. Soc.* **2010**, *132*, 468-469.
16. M. P. Drapeau, L. J. Gooben. Carboxylic acids as directing groups for C–H bond functionalization. *Chem. Eur. J.* **2016**, *22*, 18654-18677.
17. Z. Huang, H. N. Lim, F. Mo, M. C. Young, G. Dong. Transition metal-catalyzed ketone-directed or mediated C–H functionalization. *Chem. Soc. Rev.* **2015**, *44*, 7764-7786.
18. X. Liu, H. Park, J. Hu, Y. Hu, Q. Zhang, B. Wang, B. Sun, K. Yeung, F. Zhang, J.-Q. Yu. Diverse *ortho*-C(sp²)-H functionalization of benzaldehydes using transient directing groups. *J. Am. Chem. Soc.* **2017**, *139*, 888-896.
19. S. De Sarkar, W. Liu, S. I. Kozhushkov, L. Ackermann. Weakly coordinating directing groups for ruthenium (II)-catalyzed C–H activation. *Adv. Synth. Catal.* **2014**, *356*, 1461-1479.
20. F. Zhang, D. R. Spring. Arene C–H functionalization using a removable/ modifiable or a traceless directing group strategy. *Chem. Soc. Rev.* **2014**, *43*, 6906-6919.
21. G. Rousseau, B. Breit. Removable directing groups in organic synthesis and catalysis. *Angew. Chem. Int. Ed.* **2011**, *50*, 2450-2494.

Ru(II)-catalyzed *ortho*-C–H alkylation of aromatic ketones was reported by Murai and co-workers in 1993 in pioneering work.²² In that reaction, oxygen from ketone plays the role of a directing group leading to regioselectivity of *ortho*-C–H alkylation with vinyltrimethylsilane (**16**) (Scheme 6a). Later, in 1996, Murai and co-workers applied a similar methodology, using ester as DG to perform C–H alkylation of aromatic and heteroaromatic esters (Scheme 6b).²³



Scheme 6. Ketone and ester as directing group in C–H alkylation catalyzed by Ru(II)-catalyzed.

1.2 General aspects of mechanistic approach in C–H activation

The key step of the mechanism involved in C–H activation involves breaking the C–H bond and formation of C–M bond (metalation). Commonly, the metal coordinates to the directing group, when it is present, leading to cyclometalation.²⁴ Then, insertion of the functional group to the metallacycle intermediate leads to reductive elimination and subsequential formation of the product. The key step of the reaction is the metalation process, although several peculiarities concerning to the mechanism of C–H bond activation are involved such as the catalyst (metal, oxidation state, ligands, steric and electronic properties) and substrates.

The interaction of C–H with metal center (metalation) processes happens *via* a two-path charge transfer (CT) method: 1) from metal occupied $d\pi$ orbital to the σ^* orbital of C–H bond, named reverse CT process, and b) charge transfer from the filled σ orbital from C–H bond to an empty $d\sigma$ metal orbital, named forward CT process.²⁵ These two-paths charge transfer can contribute to weakening and breaking the C–H bond leading to its activation *via* metalation.²⁶

22. S. Murai, F. Kakiuchi, S. Sekine, Y. Tanaka, A. Kamatani, M. Sonoda, N. Chatani. Efficient catalytic addition of aromatic carbon-hydrogen bonds to olefins. *Nature*. **1993**, 366, 529-531.

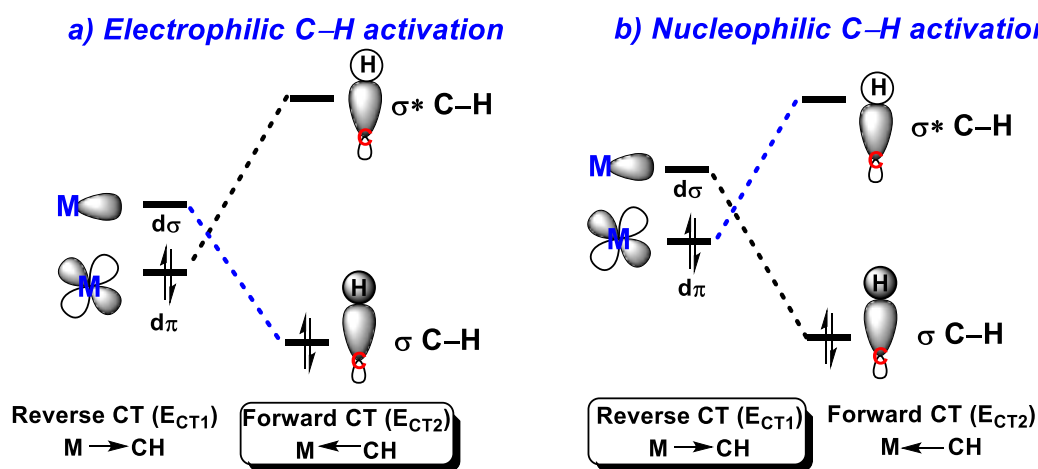
23. M. Sonoda, F. Kakiuchi, A. Kamatani, N. Chatani, S. Murai. Ruthenium-catalyzed addition of aromatic esters at the *ortho* C–H bonds to olefins. *Chem. Lett.* **1996**, 25, 109-110.

24. a) A. E. Shilov, G. B. Shul'pin. Activation of C–H bonds by metal complexes. *Chem. Rev.* **1997**, 97, 2879-2932. b) T. W. Lyons, M. S. Sanford. Palladium-catalyzed ligand-directed C–H functionalization reactions. *Chem. Rev.* **2010**, 110, 1147-1169.

25. F. Roudesly, J. Oble, G. Poli. Metal-catalyzed C–H activation/functionalization: The fundamentals. *J. Mol. Catal. A Chem.* **2017**, 426, 275-296.

26. D. H. Ess, W. A. Goddard III, R. A. Periana. Electrophilic, ambiphilic, and nucleophilic C–H bond activation: Understanding the electronic continuum of C–H bond activation through transition-state and reaction pathway interaction energy decompositions. *Organometallics*. **2010**, 29, 459–6472.

Electron-deficient metal species such as cationic and late transition metals Pd(II), Pt(II), Rh(III), Ir(III), and Ru(II) are known to possess low-energy $d\pi$ and $d\sigma$ electrons. Therefore, metallation processes occurs *via* a straightforward CT associated with coordination of strong σ -donation and weak π -back-donation leading to an *electrophilic C–H activation* (**Scheme 7a**). Then, a heterolytic cleavage occurs followed by the deprotonation usually assisted by an external anion. Moreover, electron-rich transition metal complex present high-energy $d\pi$ and $d\sigma$ electrons leading to reverse CT, which defines a *nucleophilic C–H activation* (**Scheme 7b**)



Scheme 7. Frontier orbital interactions for electrophilic and nucleophilic mechanisms (adapted from ref. 25).

There are some variations of the mechanism mentioned above. They involve intramolecular deprotonation by a heteroatom-based ligand *via* a cyclic concerted process. However, oxidative addition and electrophilic substitution approaches are the most used for explaining metallation. Some of these variants are described below:

a) Oxidative addition: electron-rich late transition metals (*i. e.* low oxidation states) coordinate *via* $d\pi$ -back-donation to the σ^* -C–H orbital and this strongly and synergistic interaction leads to the hemolytic bond cleavage and oxidation of the metal center in two units (**Scheme 8a**);

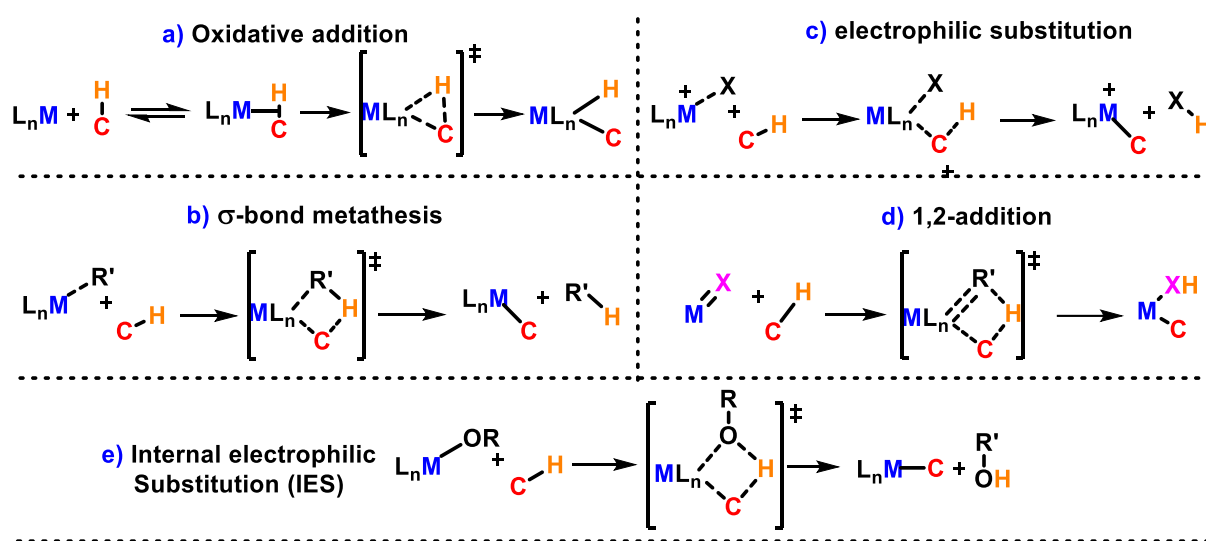
b) σ -bond metathesis: with early transition (poor electrons metals)²⁷ *via* a four-member metal-ligand cycle transition state without oxidation of metal (**Scheme 8b**);

27. Z. Lin. Current understanding of the σ -bond metathesis reactions of $L_nMR + R'-H \rightarrow L_nMR + R-H$. *Chem. Rev.* **2007**, *251*, 2280–2291.

c) Electrophilic activation: with electron-deficient late transition metals (**Scheme 8c**);²⁸

d) 1,2 addition: The M=X functionality (X= CR₂, CR, NR₂, NR, OR) adds to a C–H bond *via* formal [2σ + 2π] reaction (**Scheme 8d**);²⁹

e) IES (internal electrophilic substitution): mechanism happens *via* electrophilic attack of the metal and the deprotonation by an alkoxy ligand *via* a four-membered transition state. (**Scheme 8e**).³⁰



Scheme 8. Most common proposed mechanism pathways.

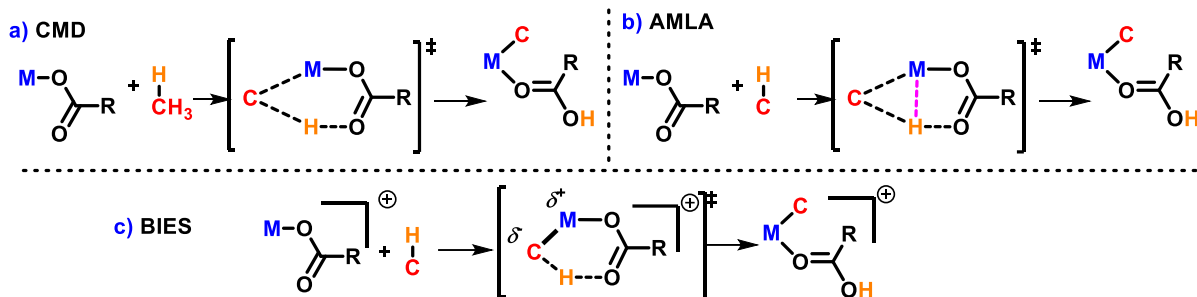
In the last years, experimental and computational reports have pointed out new insights about mechanisms *via* metal bearing a Lewis-basic ligand, usually oxygen bases or carboxylate additives. Fagnou has proposed an approach based on concerted metalation-deprotonation

28. a) D. Balcels, E. Clot, O. Eisenstein. C–H bond activation in transition metal species from a computational perspective. *Chem. Rev.* **2010**, *110*, 749-823. **b)** M. Lersch, M. Tilset. Mechanistic aspects of C–H activation by Pt complexes. *Chem. Rev.* **2005**, *105*, 2471-2526. **c)** V. Ritleng, C. Sirlin, M. Pfeffer. Ru-, Rh-, and Pd-Catalyzed C–C bond formation involving C–H activation and addition on unsaturated substrates: Reactions and mechanistic aspects. *Chem. Rev.* **2002**, *102*, 1731-1770.

29. a) T. R. Cundari, T. R. Klinckman, P. T. Wolczanski. Carbon–hydrogen bond activation by titanium imido complexes. Computational evidence for the role of alkane adducts in selective C–H activation. *J. Am. Chem. Soc.* **2002**, *124*, 1481-1487; **b)** J. L. Bennett, P. T. Wolczanski. Selectivities in hydrocarbon activation: kinetic and thermodynamic investigations of reversible 1,2-Rh-elimination from $(\text{silox})_2(\text{tBu}_3\text{SiNH})\text{TiR}$ ($\text{silox} = \text{tBu}_3\text{SiO}$). *J. Am. Chem. Soc.* **1997**, *119*, 10696-10719.

30. J. Oxgaard, W. J. Tenn, R. J. Nielsen, R. A. Periana, W. A. Goddard. Mechanistic analysis of iridium heteroatom C–H activation: evidence for an internal electrophilic substitution mechanism. *Organometallics.* **2007**, *26*, 1565-1567.

(CMD) (**Scheme 9a**)³¹ whereas MacGregor and Davies (**Scheme 9b**) have suggested CMD with the participation of hydrogen-based on ambiphilic metal ligand activation (AMLA).³² In the case of electron-rich arenes with acetate or carboxylate ligands, a base-assisted internal electrophilic substitution (BIES) has been proposed (**Scheme 9c**).³³



Scheme 9. Base-assisted C–H activation proposed mechanism.

This thesis will report the C–H activation development, focusing on alkenylation, oxygenation and annulation. In the first section, the development of a new synthetic approach about site-selective functionalize naphthoquinone with alkenyl and hydroxyl groups will be described to synthesize molecules with potential trypanocidal activity. In the second section, a new C–H/N–H annulation protocol, with emphasis on modifying fluorescent imidazoles prepared from quinoidal compounds, will be presented.

31. D. Lapointe, K. Fagnou. Overview of the mechanistic work on the concerted metalation–deprotonation pathway. *Chem. Lett.* **2010**, *39*, 1118-1126.

32. Y. Boutadla, D. L. Davies, S. A. Macgregor, A. I. Poblador-Bahamonde. Mechanisms of C–H bond activation: rich synergy between computation and experiment. *Dalton Trans.* **2009**, *30*, 5820-5831.

33. a) H. Wang, M. Moselage, M. J. González, L. Ackermann. Selective synthesis of indoles by cobalt(III)-catalyzed C–H/N–O functionalization with nitrones. *ACS Catal.* **2016**, *6*, 2705-2709; **b)** R. Mei, J. Loup, L. Ackermann. Oxazolinyll-assisted C–H amidation by cobalt(III) catalysis. *ACS Catal.* **2016**, *6*, 793-797; **c)** W. Ma, R. Mei, G. Tenti, L. Ackermann. Ruthenium(II)-catalyzed oxidative C–H alkenylations of sulfonic acids, sulfonyl chlorides and sulfonamides. *Chem. Eur. J.* **2014**, *20*, 15248-15251.

PART I

RUTHENIUM(II)-CATALYZED C–H ALKENYLATION AND OXYGENATION OF 1,4-NAPHTHOQUINONES: ACCESS TO POTENT TRYPANOCIDAL COMPOUNDS

New C–H activation protocols via ruthenium catalysis will be conducted in 1,4-naphthoquinones, focusing on alkenylation and oxygenation to achieve molecules with potent biological activity against Trypanossoma cruzi, the protozoan that causes Chagas disease.

1. INTRODUCTION

Several reactions based on C–H activation have been developed over the years to directly functionalize different substrates. Some examples of those reactions include arylation,³⁴ halogenation,³⁵ amination,³⁶ alkylation³⁷ among many others. In the first section of this work will particularly discuss efforts involving C–H alkenylation and C–H oxygenation as a synthetic platform to functionalize 1,4-naphthoquinones with potent trypanocidal activity.

1.1 C–H alkenylation *via* acrylate.

The transition metal-catalyzed reactions that convert inactive C–H bonds into substituted alkenes represents a powerful method for achieving value-added olefinic molecules. In this sense, several C–H alkenylation using acrylates have been widely studied.³⁸

In 2017, Wang and co-workers reported an alkenylation of phenyl-2-pyridylsulfonates³⁹ (**Scheme 10a**) and, in 2009, Wu and co-workers reported alkenylation reactions using quinoline-*N*-oxides under external-oxidant-free conditions (**Scheme 10b**).⁴⁰ In both studies, the authors employed palladium(II) acetate as catalyst.

On the other hand, under ruthenium catalyst, Miura and co-workers described the use of arylpyrazol (**83**) as a substrate (**Scheme 10c**)⁴¹ and Ackermann and co-workers disclosed the C–H alkenylation in anilide (**Scheme 10d**).⁴² Jeganmohan and co-workers have reported C–H

34. a) L. Ackermann, R. Vicente, A. R. Kapdi. Transition-metal-catalyzed direct arylation of (hetero)arenes by C–H bond cleavage. *Angew. Chem. Int. Ed.* **2009**, *48*, 9792-9826 b) I. Hussaina, T. Singh. Synthesis of biaryls through aromatic C–H bond activation: A review of recent developments. *Adv. Synth. Catal.* **2014**, *356*, 8, 1661-1696.

35. R. Das, M. Kapur. Transition-metal-catalyzed site-selective C–H halogenation reactions. *Asian J. Org. Chem.* **2018**, *7*, 1524-1541.

36. Y. Park, Y. Kim, S. Chang. Transition metal-catalyzed C–H amination: scope, mechanism, and applications. *Chem. Rev.* **2017**, *117*, 9247-9301.

37. Z. Dong, Z. Ren, S. J. Thompson, Y. Xu, G. Dong. Transition-metal-catalyzed C–H alkylation using alkenes. *Chem. Rev.* **2017**, *117*, 9333-9403.

38. W. Ma, P. Gandeepan, J. Li, L. Ackermann. Recent advances in positional-selective alkenylations: removable guidance for twofold C–H activation. *Org. Chem. Front.* **2017**, *4*, 1435-1467.

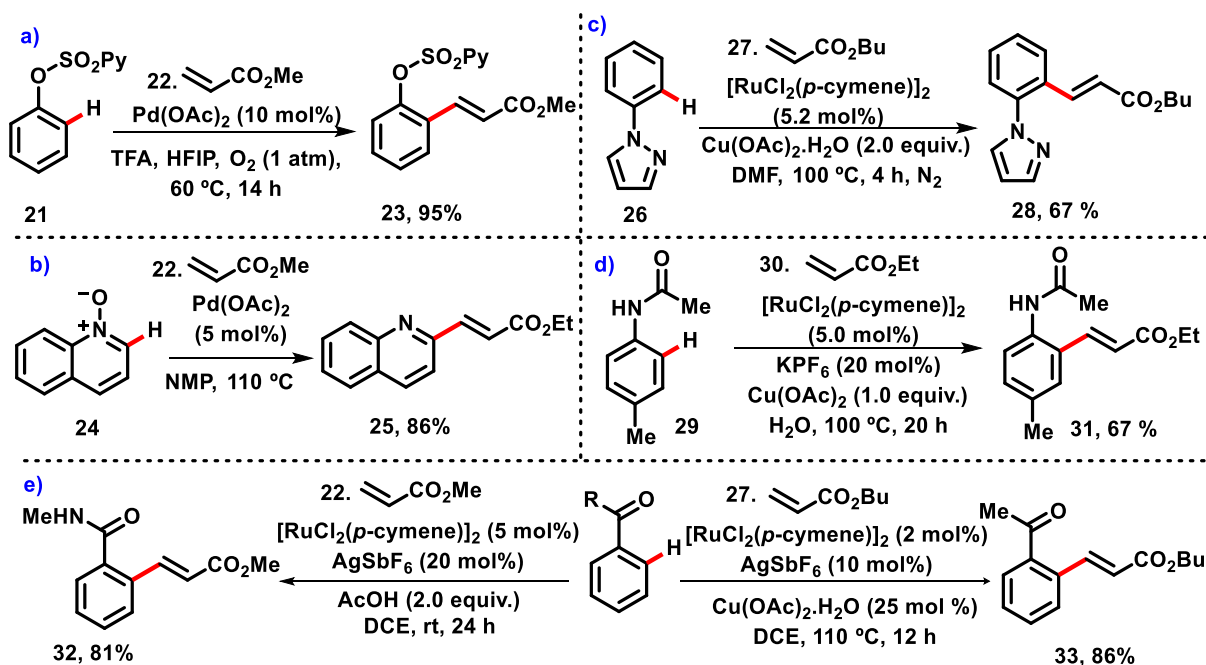
39. B. Li, D. Guo, S. Guo, G. Pan, Y. Gao, Y. Wang. Palladium-catalyzed C–H functionalization of phenyl-2-pyridylsulfonates. *Chem. Asian J.* **2017**, *12*, 130-144.

40. J. Wu, X. Cui, L. Chen, G. Jiang, Y. Wu. Palladium-catalyzed alkenylation of quinoline-*N*-oxides *via* C–H activation under external-oxidant-free conditions. *J. Am. Chem. Soc.* **2009**, *131*, 13888-13889.

41. Y. Hashimoto, T. Ueyama, T. Fukutani, K. Hirano, T. Satoh, M. Miura. Ruthenium-catalyzed oxidative alkenylation of arenes *via* regioselective C–H bond cleavage directed by a nitrogen-containing group. *Chem. Lett.* **2011**, *40*, 1165-1166.

42. L. Ackermann, L. Wang, R. Wolfram A. V. Lygin. Ruthenium-catalyzed oxidative C–H alkenylations of anilides and benzamides in water. *Org. Lett.* **2012**, *14*, 728-731.

alkenylation of aromatic ketone⁴³ and amide⁴⁴ via $[\text{RuCl}_2(p\text{-cymene})]_2$ catalyst in high yields (Scheme 10e). Several other similar reactions have been reported.⁴⁵



Scheme 10. Selected examples of C–H alkenylation using acrylates.

1.2 C–H oxygenation

Oxygenated aromatic molecules are strategic intermediates in organic synthesis. Despite the huge number of classical methods to achieve phenol derivatives already known, the demand for more sustainable and environmental approaches has directed synthetic efforts to developing C–H activation reactions.⁴⁶

In this sense, C–H oxygenation, catalyzed by metallic complexes, has been pointed as a new way to perform hydroxylation in an aromatic system to achieve phenols derivatives.⁴⁷ This

43. K. Padala, M. Jeganmohan. Ruthenium-catalyzed *ortho*-alkenylation of aromatic ketones with alkenes by C–H bond activation. *Org. Lett.* **2011**, *13*, 6144-6147.

44. R. Manikandan, P. Madasamy, M. Jeganmohan. Ruthenium-catalyzed *ortho* alkenylation of aromatics with alkenes at room temperature with hydrogen evolution. *ACS Catal.* **2016**, *6*, 230-234.

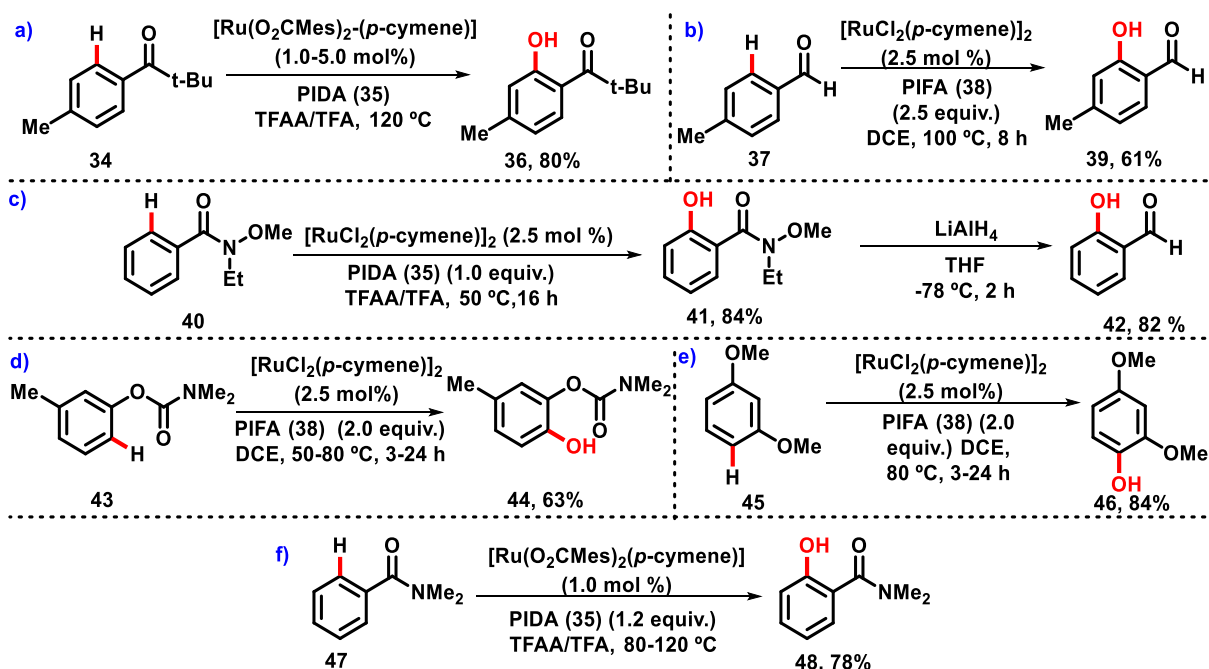
45. a) T. Gong, B. Xiao, Z. Liu, J. Wan, J. Xu, D. Luo, Y. Fu, L. Liu. Rhodium-catalyzed selective C–H activation/olefination of phenol carbamates. *Org. Lett.* **2011**, *13*, 3235-3237. b) T. Ueyama, S. Mochida, T. Fukutani, K. Hirano, T. Satoh, M. Miura. Ruthenium-catalyzed oxidative vinylation of heteroarene carboxylic acids with alkenes *via* regioselective C–H bond cleavage. *Org. Lett.* **2011**, *13*, 706-708.

46. S. Enthaler, A. Company. Palladium-catalysed hydroxylation and alkoxylation. *Chem. Soc. Rev.* **2011**, *40*, 4912-4924.

47. V. S. Thirunavukkarasu, S. I. Kozhushkov, L. Ackermann. C–H nitrogenation and oxygenation by ruthenium catalysis. *Chem. Commun.* **2014**, *50*, 29-39.

approach has advantages over classical reaction because of its general minimization of by-product formation (atom-economy), and its reaction steps (step economy).⁴⁸

Over the last years, Ackermann and co-workers have been exploring ruthenium catalysts as $[\text{RuCl}_2(p\text{-cymene})]_2$, biscarboxylate complex $[\text{Ru}(\text{O}_2\text{CMes})_2(p\text{-cymene})]$ or inexpensive $[\text{RuCl}_3 \cdot n\text{H}_2\text{O}]$ to performed C–H oxygenation. Usually these reactions were carried out using the oxidants (diacetoxyiodo)benzene (**35**, $\text{PhI}(\text{OAc})_2$, known as PIDA) or bis(trifluoroacetoxy)iodobenzene (**38**, $\text{PhI}(\text{F}_3\text{CCO}_2)_2$, known as PIFA). C–H oxygenation reaction were applied to different substrates (**Scheme 11**) such as aromatic ketone⁴⁹ and aldehyde,⁵⁰ aryl Weinreb amides,⁵¹ carbamate and anisoles,⁵² and benzamides.⁵³



Scheme 11. C–H oxygenation catalyzed by ruthenium reported by Ackermann and co-workers.

48. a) B. M. Trost. The atom economy—a search for synthetic efficiency. *Science*, **1991**, *254*, 1471-1477; b) B. M. Trost. On inventing reactions for atom economy. *Acc. Chem. Res.* **2002**, *35*, 695-705.

49. V. S. Thirunavukkarasu, L. Ackermann. Ruthenium-catalyzed C–H bond oxygenations with weakly coordinating ketones. *Org. Lett.* **2012**, *14*, 6206-6209.

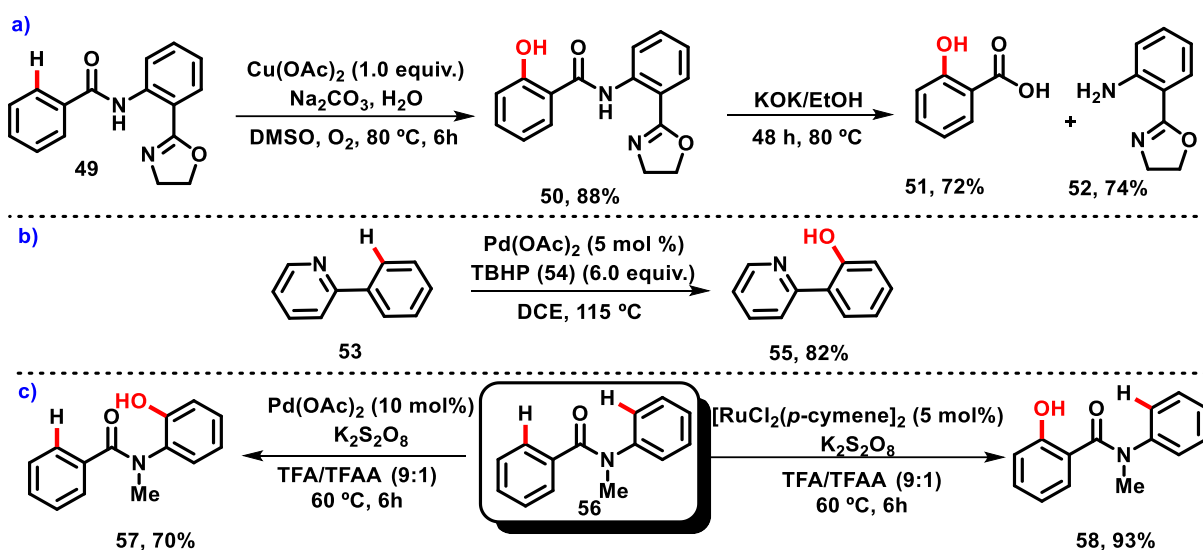
50. F. Yang, K. Rauch, K. Kettelhoit, L. Ackermann. Aldehyde-assisted ruthenium(II)-catalyzed C–H oxygenations. *Angew. Chem. Int. Ed.* **2014**, *126*, 11467-11470.

51. F. Yang, L. Ackermann. Ruthenium-catalyzed C–H oxygenation on aryl Weinreb amides. *Org. Lett.* **2013**, *15*, 718-720.

52. W. Liu, L. Ackermann. *Ortho*- and *para*-selective ruthenium-catalyzed $\text{C}(\text{sp}^2)\text{--H}$ oxygenations of phenol derivatives. *Org. Lett.* **2013**, *15*, 3484-3486.

53. V. S. Thirunavukkarasu, J. Hubrich, L. Ackermann. Ruthenium-catalyzed oxidative $\text{C}(\text{sp}^2)\text{--H}$ bond hydroxylation: site-selective C–O bond formation on benzamides. *Org. Lett.* **2012**, *14*, 4210-4213.

Beyond ruthenium catalysts, other metals have been used for oxygenation reactions. Yu and co-workers⁵⁴ applied $\text{Cu}(\text{OAc})_2/\text{Na}_2\text{CO}_3$ as a catalyst system in the oxygenation of benzamides, with oxazolamides as the removable directing groups (**Scheme 12a**). Sun and co-workers⁵⁵ developed a pyridyl-directed oxygenation catalyzed by $\text{Pd}(\text{OAc})_2$ /*tert*-butyl hydroperoxide (TBHP) (**Scheme 12b**). In a very interesting approach, Rao and co-workers⁵⁶ developed a methodology for the oxygenation of bioactive benzanilides with different regioselectivity using Ru(II) and Pd(II) catalysts (**Scheme 12c**).



Scheme 12. Examples of oxygenation performed by Cu(II), Pd(II) and Ru(II).

1.3 Quinone in Medicinal Chemistry.

According to IUPAC, quinones are compounds that exhibit a *fully conjugated cyclic dione structure*.⁵⁷ Those compounds can be classified into three categories related to their aromatic system: benzoquinones, naphthoquinones and anthraquinones. According to the position of carbonyl, quinones can be classified as 1,4-benzoquinone (**59**), 1,2-benzoquinone (**60**) 1,4-

54. S. Sun, M. Shang, H. Wang, H. Lin, H. Dai, J. Yu. Cu(II)-mediated $\text{C}(\text{sp}^2)\text{-H}$ hydroxylation. *J. Org. Chem.* **2015**, *80*, 8843-8848.

55. J. Dong, P. Liu, P. Sun. Palladium-catalyzed aryl $\text{C}(\text{sp}^2)\text{-H}$ bond hydroxylation of 2-arylpyridine using TBHP as oxidant. *J. Org. Chem.* **2015**, *80*, 2925-2929.

56. Y. Sun, T. Sun, Y. Wu, X. Zhang, Y. Rao. A diversity-oriented synthesis of bioactive benzanilides *via* a regioselective $\text{C}(\text{sp}^2)\text{-H}$ hydroxylation strategy. *Chem. Sci.* **2016**, *7*, 2229-2238.

57. IUPAC, Compendium of Chemical Terminology, 2nd ed. (the "Gold Book") (1997). <http://goldbook.iupac.org/html/Q/Q05015.html> accessed in 21.01.2018.

naphthoquinones (**61**), 1,2-naphthoquinones (**62**), 9,10-anthraquinone (**63**) (**Figure 1**) and other similar examples are possible as well.

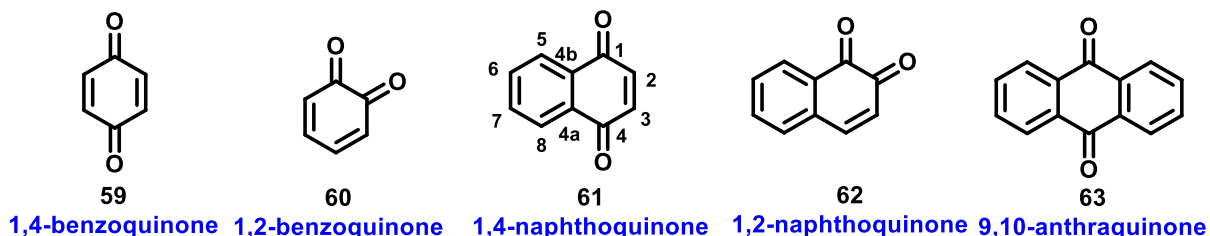


Figure 1. Representation of different quinoidal structures

Several quinones, some of them illustrated in **Figure 2**, have been isolated from different natural sources and/or have been synthesized by different methodologies. Some examples of 1,4-benzoquinone include blattellaquinone (**64**), a sex pheromone in cockroaches;⁵⁸ coenzyme Q₁₀ (**65**), also known as ubiquinone, important in aerobic cellular respiration;⁵⁹ and primin (**66**), which may cause dermatitis,⁶⁰ however, is commonly used treatment of basal cells carcinoma.⁶¹

Lapachol (**67**), is a natural product isolated from the heartwood of trees from the Bignoniaceae family (e. g. Brazilian Ipê tree).⁶² It has anti-inflammatory,⁶³ antimicrobial,⁶⁴ and antifungal⁶⁵ properties, and its α -lapachone derivative; menaquinone (K vitamin) (**69**),⁶⁶ it is important for blood coagulation.

58. S. Nojima, C. Schal, F. X. Webster, R. G. Santangelo, W. L. Roelofs. Identification of the sex pheromone of the German cockroach, *Blattella germanica*. *Science*. **2005**, 307, 1029-1031.

59. L. Ernster, G. Dallner. Biochemical, physiological and medical aspects of ubiquinone function. *Biochim. Biophys. Acta*. **1995**, 1271, 195-204.

60. C. Zachariae, K. Engkilde, J. D. Johansen, T. Menné. Primin in the European standard patch test series for 20 years. *Contact Derm*. **2007**, 56, 344-346.

61. L. W. Bieber, A. A. Chiappeta, M. A. M. Souza, M. Generino, P. R. Neto. Simple synthesis of primin and its analogues via lithiation of protected guaiacol. *J. Nat. Prod.* **1990**, 53, 706-709.

62. A. G. Ravelo, A. Estevez-Braun, E. Perez-Sacau. The chemistry and biology of lapachol and related natural products α and β -lapachones. *Stud. Nat. Prod. Chem.* **2003**, 29, 719-760.

63. E. R. Almeida, A. A. S. Filho, E. R. Santos, C. A. C. Lopes. Anti-inflammatory action of lapachol. *J. Ethnopharmacol.* **1990**, 29, 239-241.

64. K. O. Eyong, K. Krohn, H. Hussain, G. N. Folefoc, A. E. Nkengfack; B. Schulz, Q. Hu. Newbouldiaquinone and newbouldiamide: a new naphthoquinone–anthraquinone coupled pigment and a new ceramide from *Newbouldia laevis*. *Chem. Pharm. Bull.* **2005**, 53, 616-619.

65. K. O. Eyong, G. N. Folefoc, V. Kuete, V. P. Beng, K. Krohn, H. Hussain, A. E. Nkengfack, M. Saeftel, S. R. Sarite, A. Hoerauf. New bouldiaquinone A: a naphthoquinone–anthraquinone ether coupled pigment, as a potential antimicrobial and antimalarial agent from *Newbouldia laevis*. *Phytochem.* **2006**, 67, 605-609.

66. S. M. C. das Dôres, S. A. R. de Paiva, A. O. Campana. Vitamina K: Metabolismo e nutrição. *Rev. Nutr.* **2001**, 14, 207-218.

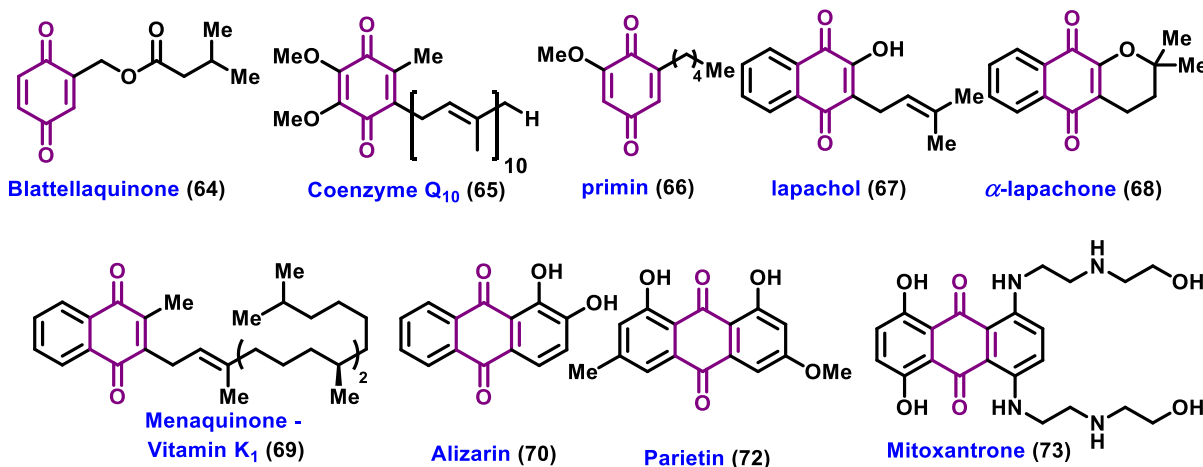


Figure 2. Selected examples of quinones with highlighted 1,4-quinone moiety.

Regarding 9,10-anthraquinone (63), we can highlight three examples: alizarin (70), a stain for calcium in bone; Parietin (72), a cortical pigment, which protects lichens (*Caloplaca*) against UV-B light;⁶⁷ and mitoxantrone (73), used for the treatment of acute myloid leukemia and improving the survival rate of children suffering from acute lymphoblastic leukemia.⁶⁸

A particular example of 1,4-naphthoquinone is 5-hydroxy-1,4-naphthoquinone (74), known as juglone (Figure 3).⁶⁹ It is a natural product found in plants from the *Juglandaceae* family, particularly the black walnut (*Juglans nigra*). It is traditionally used as a herbicide, a type of ink and as a natural orange dye for coloring fabric, mostly wool.⁷⁰

Juglone (74) has been studied for its anti-cancer properties, especially in decreasing the probability of intestinal tumors.⁷¹ This biological activity is associated with the formation of semiquinone, radical followed by superoxide anion radical production, in the mitochondria and cytosol,⁷² leading to cellular apoptosis.⁷³ A structural similar compound is 5,8-dihydroxy-1,4-

67. a) Y. Gauslaa, E. M. Estvedt. Is parietin a UV-B or a blue-light screening pigment in the lichen *Xanthoria parietina*? *Photochem. Photobiol. Sci.* **2003**, *2*, 424-432. b) A. S. Knut. UV-induction of sun-screening pigments in lichens. *New Phytologist.* **2003**, *158*, 91-100.

68. C. Parker, R. Waters, C. Leighton, J. Hancock, R. Sutton, A. V. Moorman, P. Ancliff, M. Morgan, A. Masurkar, N. Goulden, N. Green, T. Révész, P. Darbyshire, S. Love, V. Saha. Effect of mitoxantrone on outcome of children with first relapse of acute lymphoblastic leukaemia (ALL R3): an open-label randomised trial. *Lancet.* **2010**, *376*, 2009-2017.

69. M. P. Strugstad, S. Despotovski. A summary of extraction, synthesis, properties, and potential uses of juglone: A literature review. *J. Ecosyst. Manage.* **2012**, *13*, 1-16.

70. S. Topal, I. Kocaçaliskan, O. Arslan, A. Z. Tel. Herbicidal effects of juglone as an allelochemical. *Phyton.* **2007**, *46*, 259-269.

71. S. Sugie, K. Okamoto, K. M. W. Rahman, T. Tanaka, K. Kawai, J. Yamahara, H. Mori. Inhibitory effects of plumbagin and juglone on azoxymethane-induced intestinal carcinogenesis in rats. *Cancer Lett.* **1998**, *127*, 177-183.

72. J. J. Inbaraj, C. F. Chignell. Cytotoxic Action of juglone and plumbagin: A mechanistic study using HaCaT Keratinocytes. *Chem. Res. Toxicol.* **2004**, *17*, 55-62.

73. Y. Ji, Z. Qu, X. Zou. Juglone-induced apoptosis in human gastric cancer SGC-7901 cells *via* the mitochondrial pathway. *Exp. Toxicol. Pathol.* **2011**, *63*, 69-78.

naphthoquinone, also known as naphthazarin (**75**). It can be isolated from the wood bark of *Lomatia oblique* and from the walnut husks of *Juglans mandschurica maxim var.*⁷⁴

Examples of molecules with juglone moiety (**Figure 3**) include (-)-nocardione A (**76**), Cdc25B tyrosine phosphatase inhibitor, and (+)-nocardione A (**77**) with antifungal and cytotoxic activity.⁷⁵ Crassiflorone (**78**), isolated from tree *Diospyros crassiflora*, exhibits anti-mycobacterial and anti-gonorrhoeal properties.⁷⁶ Furthermore, juglomycin A (**79**),⁷⁷ (R)-8-hydroxy- α -dunnione (**80**)⁷⁸ and kidamycinone (**81**)⁷⁹ exhibit a different range of bioactivity. Marinone (**82**) and debromomarinone (**83**) present high activity against several bacteria lines.⁸⁰ Doxorubicin (**84**)⁸¹ and daunorubicin (**85**),⁸² both are used as potent drugs to treat different cancer cell lines. Besides, shikonin (**86**) and alkannin (**87**)⁸³ are also natural products that exhibit anti-microbial activity.⁸⁴

Quinone have received special attention in Medicinal Chemistry studies due to their important biological activities such as antibacterial,⁸⁵ antitumor,⁸⁶ antifungal,⁸⁷ and others. A particular case of quinone biological activity is focused on therapy against Chagas disease.⁸⁸

74 M. Moir, R. H. Thomson. Naphthaquinones in *Lomatia* species *Phytochemistry* **1973**, *12*, 1351-1353.

75. T. Otani, Y. Sugimoto, Y. Aoyagi, Y. Igarashi, T. Furumai, N. Saito, Y. Yamada, T. Asao, T. Oki. New Cdc25B Tyrosine phosphatase inhibitors, Nocardiones A and B, produced by *Nocardia sp.* TP-A0248. *J. Antibiot.* **2000**, *53*, 337-344.

76. J. Padwal, W. Lewis, C. J. Moody. Synthesis of the reported structure of crassiflorone, a naturally occurring quinone isolated from the African ebony *Diospyros crassiflora*, and regioisomeric entacyclic furocoumarin naphthoquinones. *Org. Biomol. Chem.* **2011**, *9*, 3484-3493.

77. H. Maeda, G. A. Kraus. A direct asymmetric synthesis of juglomycin A. *J. Org. Chem.* **1996**, *61*, 2986-2987.

78. X. H. Cai, X. D. Luo, J. Zhou, X. J. Hao. Quinones from *Chirita eburnea*. *J. Nat. Prod.* **2005**, *68*, 797-799.

79. T. Mabit, A. Siard, M. Pantin, D. Zon, L. Foulgoc, D. Sissouma, A. Guingant, M. Mathe-Allainmat, J. Lebreton, F. Carreaux, G. Dujardin, S. Collet. Total synthesis of #-indomycinone and kidamycinone by means of two regioselective Diels-Alder reactions *J. Org. Chem.* **2017**, *82*, 5710-5719.

80. C. Pathirana, P. R. Jensen, W. Fenical. Marinone and debromomarinone: Antibiotic sesquiterpenoid naphthoquinones of a new structure class from a marine bacterium. *Tetrahedron Lett.* **1992**, *33*, 7663-7666.

81. O. Tacar, P. Sriamornsak, C. R. Dassa. Doxorubicin: an update on anticancer molecular action, toxicity and novel drug delivery systems. *J. Pharm. Pharmacol.* **2013**, *65*, 157-170.

82. B. R. J. Abdella, J. Fisher. A chemical perspective on the anthracycline antitumor antibiotics. *Environ. Health Perspect.* **1985**, *64*, 3-18.

83. V. P. Papageorgiou, A. N. Assimopoulou, E. A. Couladouros, D. Hepworth, K. C. Nicolaou. The chemistry and biology of Alkannin, Shikonin, and related naphthazarin natural products. *Angew. Chem., Int. Ed.* **1999**, *38*, 270-300.

84. D. S. Bhakuni, M. L. Dhar, M. M. Dhar, B. N. Dhawan, B. N. Mehrotra. Screening of indian plants for biological activity. II. *Indian J. Exp. Biol.* **1969**, *7*, 250-262.

85. V. K. Tandon, H. K. Maurya, N. N. Mishra, P. K. Shukla. Design, synthesis and biological evaluation of novel nitrogen and sulfur-containing hetero-1,4-naphthoquinones as potent antifungal and antibacterial agents. *Eur. J. Med. Chem.* **2009**, *44*, 3130-3137.

86. N. Pradidphol, N. Kongkathip, P. Sittikul, N. Boonyalai, B. Kongkathip. First synthesis and anticancer activity of novel naphthoquinone amides. *Eur. J. Med. Chem.* **2012**, *49*, 253-270.

87. V. K. Tandon, R. B. Chhor, R. V. Singh, S. Rai, D. B. Yadav. Design, synthesis and evaluation of novel 1,4-naphthoquinone derivatives as antifungal and anticancer agents. *Bioorg. Med. Chem. Lett.* **2004**, *14*, 1079-1083.

88. S. L. de Castro, D. G. J. Batista, M. M. Batista, W. Batista, A. Daliry, E. M. de Souza, R. F. S. Menna-Barreto, G. M. Oliveira, K. Salomão, C. F. Silva, P. B. Silva, M. d. N. C. Soeiro. Experimental Chemotherapy for Chagas

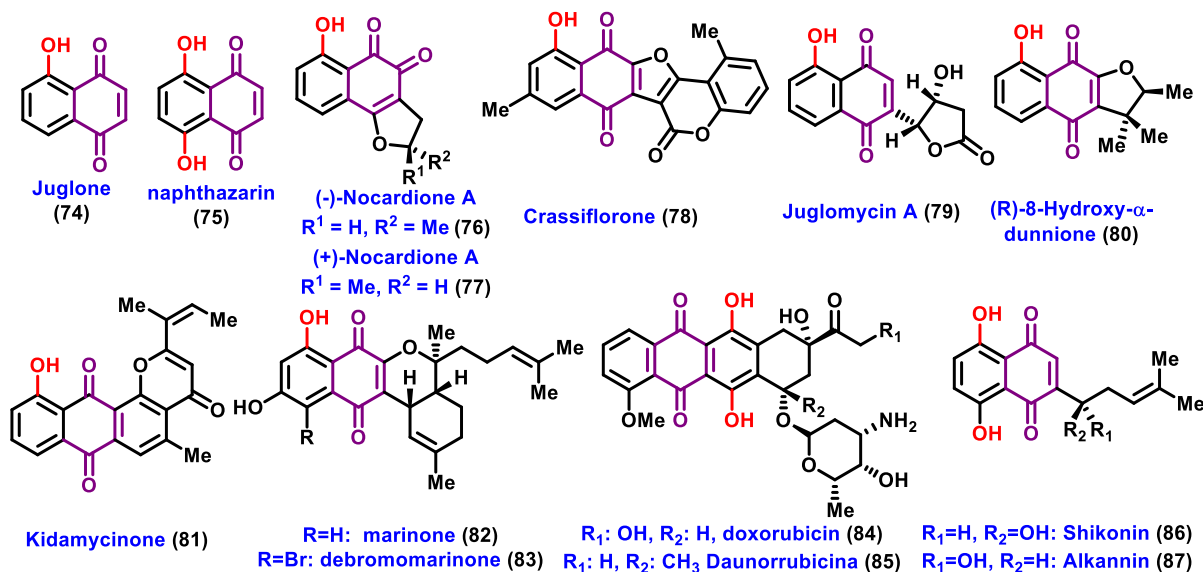


Figure 3. Selected examples of compounds with juglone moiety.

1.4 Chagas disease

In 1909, Dr. Carlos Ribeiro Justiniano das Chagas, one of the most important and recognized Brazilian scientists,⁸⁹ reported for the first time, a disease caused by the *Trypanosoma cruzi* (*T. cruzi*) parasite,⁹⁰ later named Chagas disease (CD). According to World Health Organization, CD is a neglected tropical disease⁹¹ that affects about 7 million people worldwide, mostly in Latin America.⁹²

The main transmission route of Chagas disease is *via* feces of sucking insects from the *Triatominae* subfamily, which can carry the *T. cruzi*. In Brazil, the most commonly infected insect is known as the barber bug and it is generally found in rural areas. Other routes of contaminations are possible, such as oral transmission, blood transfusion, mother-to-child (congenital) transmission, organ transplantation and even laboratory accidents.

disease: A morphological, biochemical, and proteomic overview of potential *Trypanosoma cruzi* targets of amines derivatives and naphthoquinones. *Mo. Bio. Internat.* **2011**, 2011,1-13.

89. a) L. A. B. A. Vasconcelos, L. C. P. K. Oliveira, F. L. Kaiber, J. M. R. Neto. Carlos Chagas, sua vida e sua arte. *Ver. Bras. Clin. Med.* **2011**, 9, 171-172 **b)** C. B. M. F. Gurgel, C. V. Magdalena, L. F. Prioli. Carlos Chagas e o enigma do prêmio Nobel. *Cad. Saúde Colet.* **2009**, 17, 799-809.

90. C. Chagas. Nova tripanozomíase humana: estudos sobre a morfologia e o ciclo evolutivo do *Schizotrypanum cruzi* n. gen., n. sp., agente etiológico de nova entidade morbida do homem. *Mem. Inst. Oswaldo Cruz* **1909**, 1, 159-218.

91. P. J. Hotez, S. Aksoy, P. J. Brindley, S. Kamhawi. What constitutes a neglected tropical disease? *PLoS Negl. Trop. Dis.* **2020**, 14, e0008001.

92. [https://www.who.int/en/news-room/fact-sheets/detail/chagas-disease-\(american-trypanosomiasis\)](https://www.who.int/en/news-room/fact-sheets/detail/chagas-disease-(american-trypanosomiasis)). Access in 08.04.2021.

In 2006, Brazil received the international certification of the interruption of vector transmission by *Triatoma infestans* that caused most of the transmissions in the past. However, the epidemiological surveillance remains, once the risk of Chagas disease transmission *via* contaminated food persists.⁹³ Currently, at least one million Brazilians are infected by *T. cruzi*, according to the Brazilian Ministry of Health.⁹⁴

The acute phase of Chagas disease last about two months after infection and it is characterized by a high number of *T. cruzi* present in the bloodstream.⁹⁵ In this initial phase, symptoms are absent or unspecific. They can be fever, swollen lymph nodes, headaches, or swelling at the bite site. Less than 50% of infected people develop skin lesions or a purplish swelling on the lids of one eye.⁹⁶

In the absence of appropriated treatment during the acute phase, the infection advances to the chronic phase, which 70% of infected people go through without any symptoms and 30% develop symptoms after 10-30 years of the infection. The most common symptoms are nerve damage, heart disease (45%), which can lead to heart failure, and digestive problems, like enlarged esophagus or enlarged colon.⁹⁷

T. cruzi parasite enters the human body over the bite of a contaminated insect. The bug defecates and releases *T. cruzi* in its feces, in trypomastigotes form, near the site bite. Trypomastigotes get into the host organism through the wound or intact mucosal membranes (1) (**Scheme 13**). Then, trypomastigotes invade cells near the site of inoculation and then differentiate into intracellular amastigotes (step 2), which undergoes several rounds of multiplication by binary fission (3). The replicated amastigotes form modifies back to trypomastigotes, that disrupt the host cell and get released into the bloodstream (4) spreading throughout the body and, so, leading to new infection sites over the years. The “kissing bug” gets infected by feeding on human or animal blood that contains trypomastigotes (5) that change to epimastigotes in the midgut of the vector (6). In the midgut, epimastigotes multiply and differentiate (7). Then, in the hindgut, they differentiate into infective metacyclic trypomastigotes (8).

93. M. T. Filigheddua, M. Górgolas, J. M. Ramos. Orally-transmitted Chagas disease. *Med. Clin.* **2017**, *148*, 125-131.

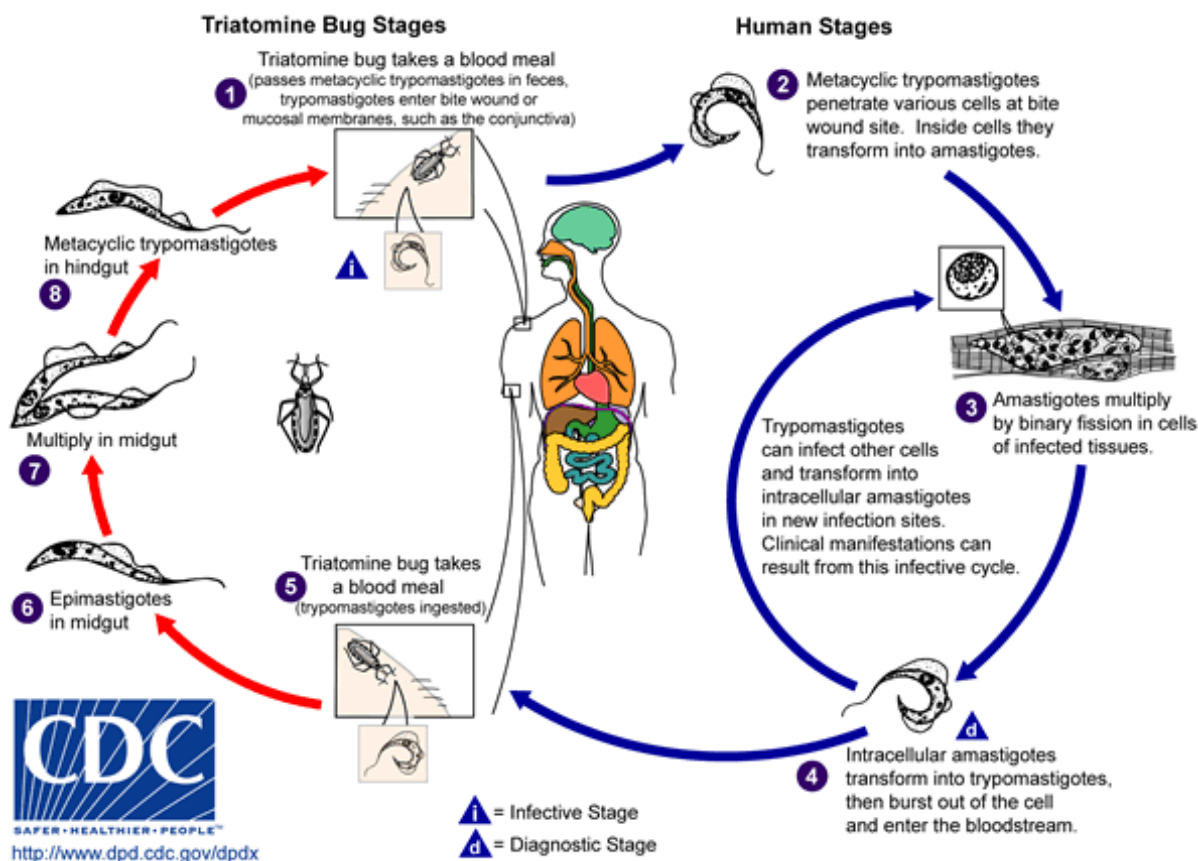
94. <https://saude.gov.br/saude-de-a-z/doenca-de-chagas>. Access in 08.04.2021.

95. R. C. Bezerra, V. A. Neto. *Trypanosoma cruzi*, hemocultura: uma abordagem prática. *Rev. Bras. Clín. Méd.* **2010**, *8*, 205-207.

96. R. L. Guerrant, D. H. Walker, P. F. Weller. American trypanosomiasis (Chagas' disease). *Tropical Infectious Diseases Principles, Pathogens, & Practice*. Philadelphia: Churchill Livingstone Elsevier, **2006**.

97. M. C. P. Nunes, A. Beaton, H. Acquatella, C. Bern, A. F. Bolger, L. E. Echeverría, W. O. Dutra, J. Gascon, C. A. Morillo, J. Oliveira-Filho, A. L. P. Ribeiro, J. A. Marin-Neto. Chagas cardiomyopathy: an update of current clinical knowledge and management: a scientific statement from the American Heart Association. *Circulation*. **2018**, *138*, 169–209.

The diagnosis of Chagas disease in the acute phase occurs when the *T. cruzi* is noted in the blood by microscopy. In the chronic phase, the diagnosis is made by finding antibodies to *T. cruzi* in the blood. The treatment for Chagas disease is based on an antiparasitic approach, for killing the parasite, and on a symptomatic treatment, to reduce the symptoms and signs of infection.



Scheme 13. Chagas disease life cycle.⁹⁸

The commonly recommend drugs for treating Chagas disease are benznidazole (**88**) and nifurtimox (**89**), although the first one is the only drug available in most Latin American countries (**Figure 4**). The treatment in acute phase is more effective, because it allows the elimination of the *T. cruzi* from the body of 50–80% of the patients, in contrast to the chronic phase, when 20–60% of the patients can eliminate it.⁹⁹ However, the parasite elimination does not cure the cardiac and gastrointestinal damage acquired in the chronic phase. Crystal violet (**90**) is used in the blood bank in endemic locaties, to ensure the decontamination of the blood stocks and avoiding contamination by blood transfusion.¹⁰⁰

98. www.cdc.gov/parasites/chagas/biology.html

99. J. Guarner. Chagas disease as example of a reemerging parasite. *Semin. Diagn. Pathol.* **2019**, *36*, 164-9.

100. G. C. Vilaseca, J. A. Cerisola, J. A. Olarte, A. Zothner. The use of Crystal violet in the prevention of the

Benznidazole (**88**) is considered the first-line treatment because it has milder adverse effects. However, its results are lower in people who have a long-term infection.¹⁰¹ The drug **88** presents several side effects, such as rash, numbness, fever, muscle pain, loss of appetite, and trouble for sleeping.¹⁰² Nifurtimox (**89**) is a second-line drug option used to treat Chagas disease and is effective for 97.5% of the individuals taking the drug. However, this compound presents some side effects as well, like abdominal pain, headache, nausea, weight loss, mood changes, insomnia, paresthesia, and peripheral neuropathy.¹⁰³ Considering the serious side effects of **88** and **89**, the development of more efficient drugs against *T. cruzi* remains necessary.

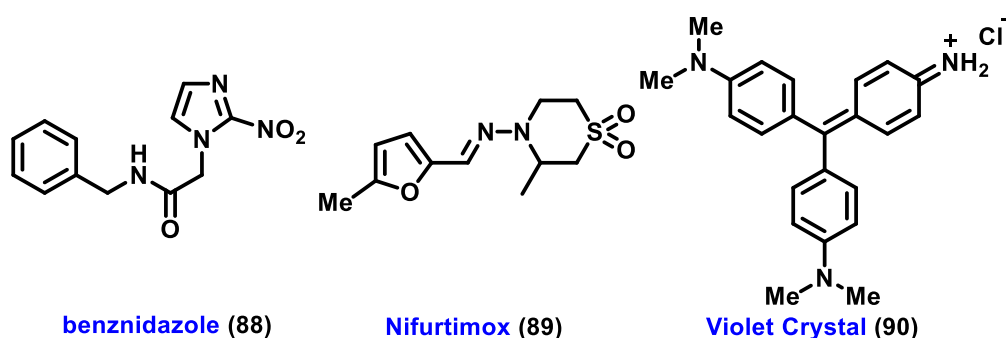


Figure 4. Benznidazole (**88**) Nifurtimox (**89**) and Crystal Violet (**90**).

As outlined, quinones exhibit several biological applications. Therefore, this class of compounds has been widely studied due to their potential application in Chagas disease chemotherapy.¹⁰⁴ Some examples of quinones with potent trypanocidal activity are displayed in **Figure 5**.¹⁰⁵

transfusional transmission of Chagas-Mazza disease. *Vox Snag.* **1966**, *11*, 711-716.

101. J. M. Kratz, F. G. Bournissen, C. J. Forsyth, S. Sosa-Estani. Clinical and pharmacological profile of benznidazole for treatment of Chagas disease. *Expert Rev. Clin. Pharmacol.* **2018**, *11*, 943-957.

102. J. A. Castro, M. M. Mecca, L. C. Bartel. Toxic side effects of drugs used to treat Chagas' disease (American trypanosomiasis). *Hum. Exp. Toxicol.* **2006**, *25*, 471-479.

103. P. A. Sales Junior, I. Molina, S. M. F. Murta, A. Sánchez-Montalvá, F. Salvador, R. Correa-Oliveira, C. M. Carneiro. Experimental and Clinical Treatment of Chagas Disease: A Review. *Am. J. Trop. Med. Hyg.* **2017**, *97*, 1289-1303.

104. a) J. R. Coura, S. L. De Castro. A critical review on Chagas Disease chemotherapy. *Mem. Inst Oswaldo Cruz.* **2002**, *97*, 3-24. **b)** E. N. da Silva Júnior, G. A. M. Jardim, R. F. S. Menna-Barreto, S. L. de Castro. Anti-*Trypanosoma cruzi* compounds: Our contribution for the evaluation and insights on the mode of action of naphthoquinones and derivatives. *J. Braz. Chem. Soc.* **2014**, *25*, 1780-1798.

105. E. N. da Silva Júnior, G. A.M. Jardim, C. Jacob, U. Dhawa, L. Ackermann, S. L. de Castro. Synthesis of quinones with highlighted biological applications: A critical update on the strategies towards bioactive compounds with emphasis on lapachones. *Eur. J. Med. Chem.* **2019**, *179*, 863-915.

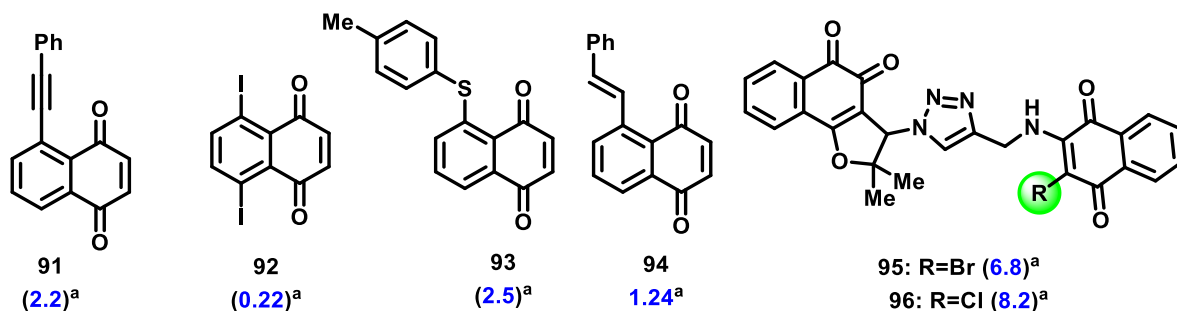


Figure 5. Examples of quinone with potent trypanocidal activity. ^aIC₅₀/24h values in μM for the activity on trypomastigotes.

The biological properties of quinoidal compounds are related to their ability to undergo biooxidation-reduction processes, focused on carbonyl moieties, leading to oxidative stress followed by cellular apoptosis. In healthy biological cells, there is a balance of Reactive Oxygen Species (ROS) such as HO•, O₂•⁻, e H₂O₂, usually produced in an anaerobic environment. The increase of these species, a phenomenon known as oxidative stress, leads the cell to apoptosis.¹⁰⁶ Biological *in vitro* tests have indicated that ROS generation processes may be related to the trypanocidal activity of quinones.¹⁰⁷ Another possible biological mechanism of those substances is the inhibition of the topoisomerase complex, which triggers cellular apoptosis.¹⁰⁸ Those biological processes can result in the death cell. For this reason, quinone compounds have been studied for their potential application against Chagas disease.

106. B. Halliwell. Biochemistry of oxidative stress. *Biochem. Soc. Trans.* **2007**, 35, 1147-1150.

107. M. P. M. Portela, S. H. F. Villamil, L. J. Perissinotti, A. O. M. Stoppani. Redox cycling of *o*-naphthoquinones in trypanosomatids - Superoxide and hydrogen peroxide production. *Biochemical Pharmacology* **1996**, 52, 1875-1882.

108. a) T. Andoh, R. Ishida. Catalytic inhibitors of DNA topoisomerase II. *Biochem. Biophys. Acta.* **1998**, 1400, 155-171. **b)** E. A. Hillard, F. C. de Abreu, D. C. M. Ferreira, G. Jaouen, M. O. F. Goulart, C. Amatore. Electrochemical parameters and techniques in drug development, with an emphasis on quinones and related compounds. *Chem. Commun.* **2008**, 0, 2612-2628.

2. MOTIVATION

The broad spectrum of biological activity of quinones inspired the development of synthetic methodologies for obtaining different compounds. However, in the case of 1,4-naphthoquinone (**61**), synthetic approaches are focused on quinone moiety modification and there is a lack of methodology to access benzenoid ring. As a consequence, biological studies with A-ring functionalized quinone are more limited, which represents a challenge in quinone chemistry.

The low reactivity of the benzenoid ring is associated to electronic deficiencies, caused by carbonyl as electronic deactivating groups. Precisely because of this, carbon C2 and C3 are more prone to nucleophilic substitution¹⁰⁹ and cycloadditions¹¹⁰

A few strategies for obtaining benzenoid-modified-naphthoquinones are showed in **Scheme 14**. For example, Diels-Alder's reaction between 1,4-benzoquinone (**59**) and isoprene (**97**) followed by dehydrogenation is an strategy to access A-ring naphthoquinone alkyl-substitutive (**99**) via annulation¹¹¹ (**Scheme 14a**). In 2015, Zeng and co-workers reported the oxidation of α -tetralone (**100**) by oxone[®] to achieve 6,7-dimethoxynaphthalene-1,4-dione (**101**) (**Scheme 14b**).¹¹² A classical functionalization of the benzenoid ring is nitration of **61** to achieve 5-nitronaphthalene-1,4-dione (**102**) followed by reduction to provide 5-aminonaphthalene-1,4-dione (**103**) (**Scheme 14c**).¹¹³ Oxidation of 1-phenylnaphthalene (**104**) to produce 5-phenylnaphthalene-1,4-dione (**105**) was reported by Mital and co-workers using chromium trioxide (**Scheme 14d**).¹¹⁴ Ishii and co-workers¹¹⁵ have reported oxidation of naphthols using Fremy's salt (**Scheme 14e**).

Those approaches have some disadvantages, for example: low yield; limited scope, the mixture of regioisomers and the use of a source of chromium - a toxic metal - as an oxidant.

109. A. D. Bukhtoyarova, T. V. Rybalova, L. V. Ektova. Amination of 5-hydroxy-1,4-naphthoquinone in the presence of copper acetate *Russ. J. Org. Chem.*, **2010**, *46*, 855-859.

110. J. Zhang, N. Redman, A. P. Litke, J. Zeng, J. Zhan, K. Y. Chan, C. -W. T. Chang. Synthesis and antibacterial activity study of a novel class of cationic anthraquinone analogs. *Bioorg. Med. Chem.*, **2011**, *19*, 498-503.

111. a) E. Torres, C. A. Panetta, N. E. Heimer, B. J. Clark, C. L. Hussey. Synthesis and properties of 6-(hydroxymethyl)-9,9,10,10-tetracyanonaphthoquinodimethane. *J. Org. Chem.* **1991**, *56*, 3737-3739 **b)** G. Huang, H. Zhao, W. Zhou, J. Dong, Q. Zhang, Q. Meng, B. Zhu, S. Li. 6-Substituted 1,4-naphthoquinone oxime derivatives (I): synthesis and evaluation of their cytotoxic activity. *Monatsh Chem.* **2017**, *148*, 1011-1023 **c)** J. Cai, Y. Li, J. Chen, P. Wang, M. Ji. Novel and convenient synthesis of 5-benzoyl-1,4-naphthoquinone and its derivatives. *Res. Chem. Intermed.* **2015**, *41*, 1-9.

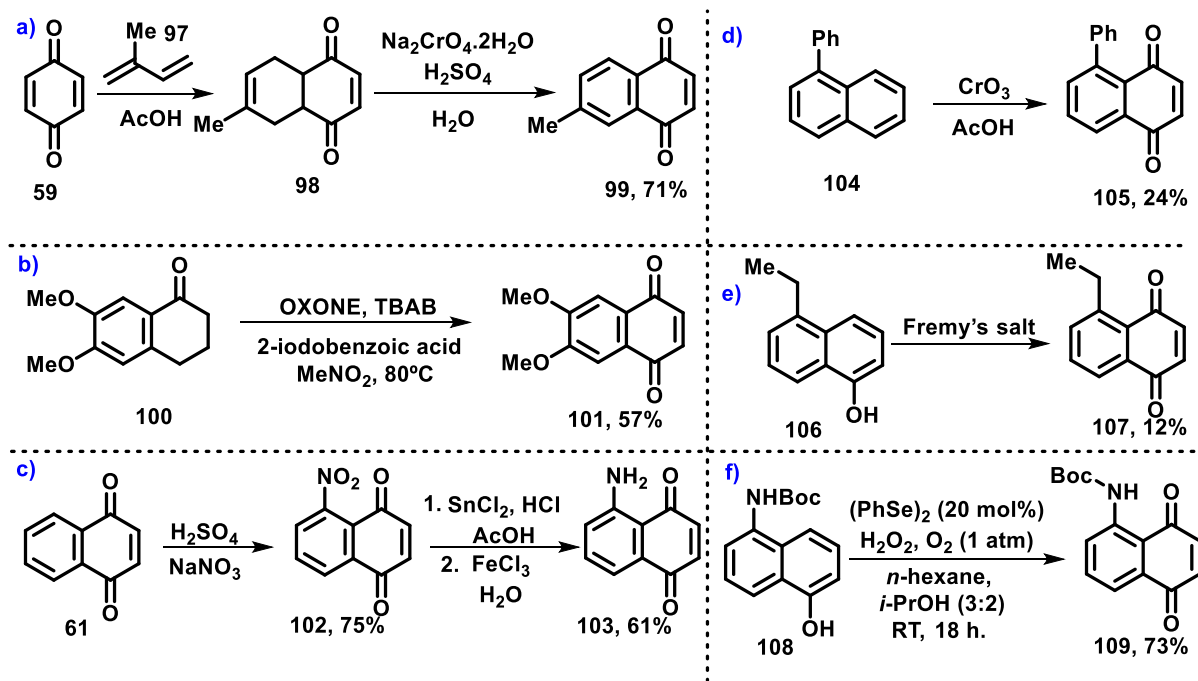
112. J. Ren, L. Lu, J. Xu, T. Yu, B. Zeng. Selective oxidation of 1-tetralones to 1,2-naphthoquinones with IBX and to 1,4-Naphthoquinones with oxone[®] and 2-Iodobenzoic acid. *Synthesis.* **2015**, *47*, 2270-2280.

113 H. Li, R. Liu, Y. Ji, Y. Wang. New method for the synthesis of juglone. *J. Chem. Pharm. Res.* **2014**, *6*, 72-76.

114. A. Mitala, V. S. Negia, U. Ramachandran. Synthesis and biological evaluation of naphthalene-1,4-dione derivatives as potent antimycobacterial agents. *Med. Chem.* **2008**, *4*, 492-497.

115. H. Ishii, T. Hanaoka, T. Asaka, Y. Harada, N. Ikeda. Oxidation with Fremy's salt-VIII. peri-effect of a group located at the C₅-position of 1-naphthol and related compounds. *Tetrahedron.* **1976**, *32*, 2693-2698.

Regarding oxidation of naphthols, in 2018, da Silva Júnior and co-workers developed a better strategy using a combination of aryl diselenides and hydrogen peroxide as a more efficient oxidant system. (**Scheme 14f**).¹¹⁶



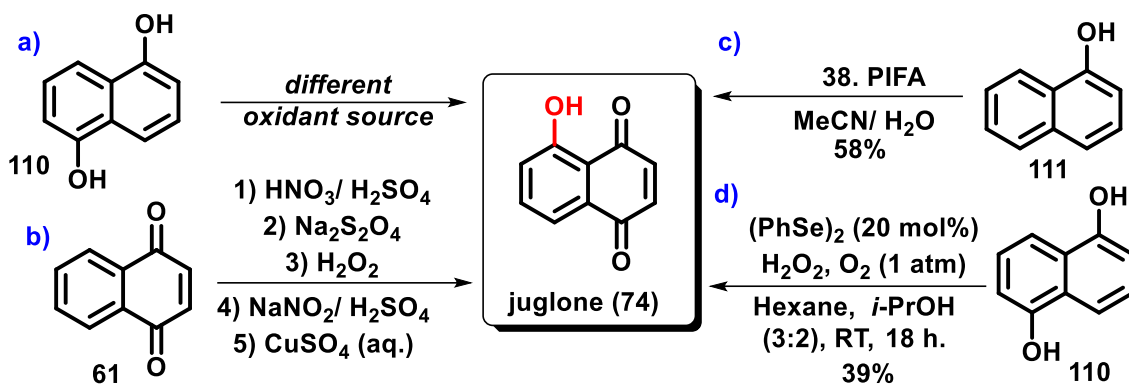
Scheme 14. Chemical approaches to achieve modified benzenoid ring of 1,4-naphthoquinone.

The specific case of hydroxyl-functionalized benzenoid ring of 1,4-naphthoquinone to obtain juglone (**74**), commonly involve oxidation of 1,5-dihydroxynaphthalene (**110**), by using different oxidants systems (**Scheme 15a**);¹¹⁷ or nitration of 1,4-naphthoquinone (**61**), followed by reduction and diazotization reaction (**Scheme 15b**). Other possibilities include oxidation of α -naphthol (**111**) using bis(trifluoroacetoxy)iodobenzene (PIFA, **38**) (**Scheme 15c**)¹¹⁸ or the using of diphenylselenide as oxidant (**Scheme 15d**).¹¹⁶

116. R. L. de Carvalho, G. A. M. Jardim, A. C. C. Santos, M. H. Araujo, W. X. C. Oliveira, A. C. S. Bombaça, R. F. S. Menna-Barreto, E. Gopi, E. Gravel, E. Doris, E. N. da Silva Júnior. Combination of aryl diselenides/hydrogen peroxide and carbon nanotube/Rhodium nano hybrids for naphthol oxidation: An efficient route towards trypanocidal quinones. *Chem. Eur. J.* **2018**, *24*, 15227-15235.

117. a) D. J. Crouse, M. M. Wheeler, M. Goemann, P. S. Tobin, S. K. Basu, D. M. S. Wheeler. Oxidation of 1,5-naphthalenediol and its methyl ether: preparation of juglone methyl ether monoacetal. *J. Org. Chem.* **1981**, *46*, 1815-1817. **b)** R. Barret, M. Daudon. An efficient synthesis of juglone. *Synth. commun.* **1990**, *20*, 2907-2912. **c)** R. T. Taylor, L. A. Flood. Polystyrene-bound phenylselenic acid: Catalytic oxidations of olefins, ketones, and aromatic systems. *J. Org. Chem.* **1983**, *48*, 5160-5164.

118. R. Barret, M. Daudon. Oxidation of phenols to quinones by bis(trifluoroacetoxy)iodobenzene. *Tetrahedron lett.* **1990**, *31*, 4871-4872.



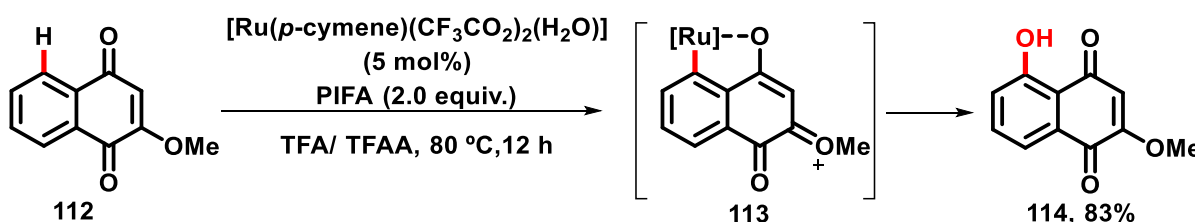
Scheme 15. Examples of juglone (74) synthesis.

In summary, 1,4-naphthoquinone derivatives have been described as target molecules in Medicinal Chemistry due to their potential biological activity against various diseases. Despite the large possibility of quinoidal modification, there are only a few limited strategies to access benzenoid-modified-1,4-naphthoquinones.

3. SYNTHETIC STRATEGY

To overcome the limitation of achieving 1,4-naphthoquinones modified at their benzenoid ring moiety, some recent approaches using C–H activation have been proposed in the literature. Those approaches are based on the carbonyl as a directing group to functionalize the benzenoid moiety *via* cyclometalation. Yet, the carbonyl groups of quinones are considered weak directing groups, which represents an additional challenge in this synthetic strategy.¹¹⁹

In 2015 Hong and co-workers¹²⁰ reported the oxygenation of flavones and chromones catalyzed by $[\text{Ru}(p\text{-cymene})(\text{CF}_3\text{CO}_2)_2(\text{H}_2\text{O})]$. Still, *only one single example of quinone* (2-methoxynaphthalene-1,4-dione, **112**) was described in order to obtain the oxygenated product **114** in 83% yield (**Scheme 16**). The methoxy group activated the reactivity of carbonyl leading to metalation and activation. Nevertheless, in the absence of this group, no C–H activation was observed.



Scheme 16. C–H oxygenation reported by Hong and co-workers.¹²⁰

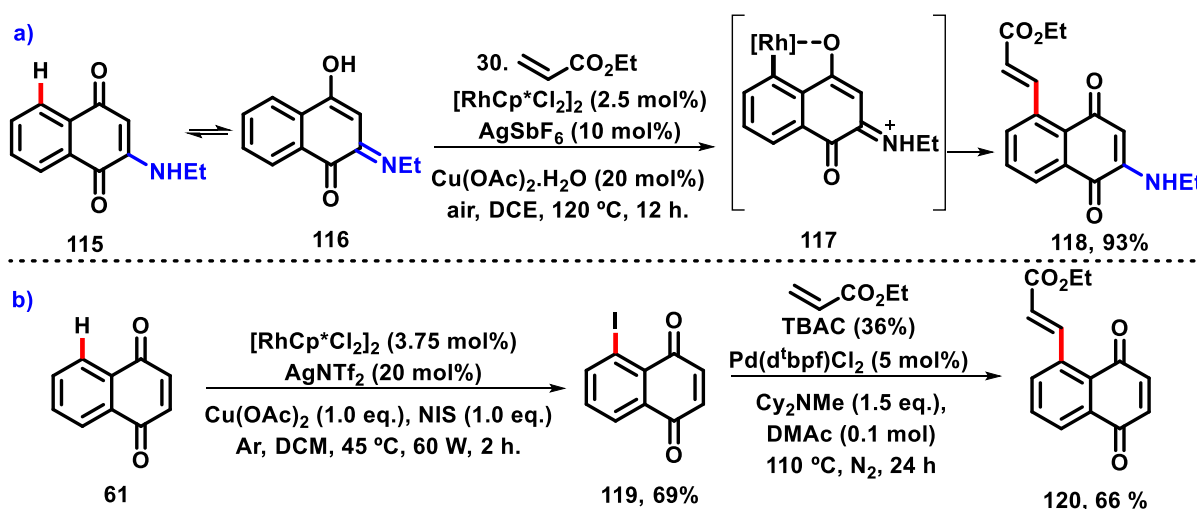
In 2014 Zhang and co-workers¹²¹ designed 2-(propylamino)naphthalene-1,4-dione (**115**) as substrate (**Scheme 17a**) for C–H alkenylation based on $[\text{RhCp}^*\text{Cl}_2]_2/\text{AgSbF}_6$, using ethyl acrylate (**30**) to achieve compound **118**. Similar to Hong and co-workers,¹²⁰ the authors discussed that electron-donating groups at C-2 or C-3 increase the coordinative ability of quinone carbonyl (intermediate **117**) and, in the absence of electron-donating groups, the reaction was not observed.

119. E. N. da Silva Júnior, G. A. M. Jardim, R. S. Gomes, Y.-F. Liang, L. Ackermann. Weakly-coordinating N-oxide and carbonyl groups for metal-catalyzed C–H activation: the case of A-ring functionalization. *Chem. Commun.* **2018**, 54, 7398-7411.

120. K. Kim, H. Choe, Y. Jeong, J. H. Lee, S. Hong. Ru(II)-catalyzed site-selective hydroxylation of flavone and chromone derivatives: The importance of the 5-hydroxyl Mmotif for the inhibition of Aurora Kinases. *Org. Lett.* **2015**, 17, 2550-2553.

121. C. Zhang, M. Wang, Z. Fan, L. P. Sun, A. Zhang. Substituent-enabled oxidative dehydrogenative cross-coupling of 1,4-naphthoquinones with alkenes. *J. Org. Chem.* **2014**, 79, 7626-7632.

Da Silva Júnior, Bower and co-workers¹²² have developed a methodology to obtain **117** regardless of the presence of electron-donating, an overcome of the limitation to modify the C-5 position of 1,4-naphthoquinone. The strategy involved selective C–H iodination of 1,4-naphthoquinone (**61**), to provide 5-iodonaphthalene-1,4-dione (**119**) followed by a Heck reaction to achieve the naphthoquinone **120** (**Scheme 17b**). The rhodium catalyst was needed, followed by a cross-coupling reaction with palladium. Despite the efficiency, this approach is quite expensive in both steps of the synthetic route and the desired product is obtained in moderate yield.

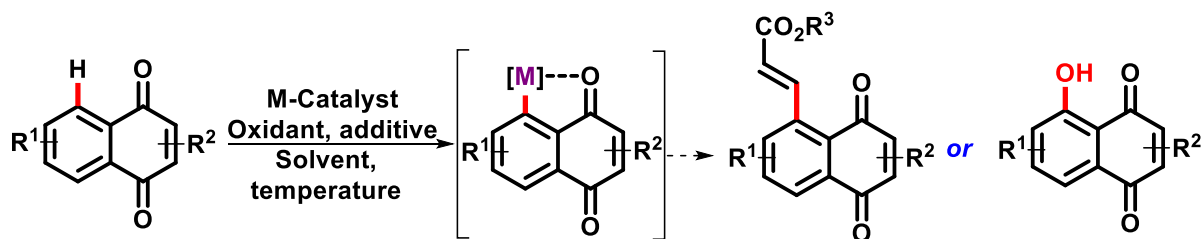


Scheme 17. C–H alkenylation of 1,4-naphthoquinone.

In summary, the development of methodologies, such as C–H oxygenation or C–H alkenylation have been raised as a promising field for obtaining 1,4-naphthoquinone with the modified-benzenoid ring. However, many challenges remain unexplored, for instance a small scope, the diversity of reaction, a less expensive catalyst and reactional the system.

*Aiming to overcome the limitation of accessing the benzenoid ring of 1,4-naphthoquinones, in the first part of this work, new efforts involving ruthenium catalyst to perform selective C–H oxygenation and alkenylation of 1,4-naphthoquinones will be described later (**Scheme 18**). In contrast with the researches previously described, in this work, different examples of quinoidal structures were applied to illustrate the functionality of the new approaches, regardless of the electron-donating group aspects.*

122. G. A. M. Jardim, E. N. da Silva Júnior, J. F. Bower. Overcoming naphthoquinone deactivation: rhodium-catalyzed C-5 selective C–H iodination as a gateway to functionalized derivatives. *Chem. Sci.* **2016**, *7*, 3780-3784.



Scheme 18. Schematic representation of C–H metalation of 1,4-naphthoquinone followed by alkenylation and oxygenation described in the first part of this thesis.

4. RESEARCH PURPOSE

4.1. General purpose

This work aimed to the development a new methodology to functionalize the C-5 position at the benzenoid ring of 1,4-naphthoquinone derivatives with acrylates and hydroxyl groups via C–H activation reaction. New products obtained were evaluated as their potential trypanocidal activity.

4.1.1. Specific purpose.

- To carry out methodological studies using different experimental conditions, such as different solvents, oxidants, additives, temperature, time of reaction and substrates;
- The synthesis of 1,4-naphthoquinone derivatives, followed by the C–H activation methodology to achieve new molecules;
- The evaluation of the biological properties of the new molecules against the *Trypanosoma cruzi* - the etiological agent of Chagas disease.

5. RESULTS AND DISCUSSIONS

5.1 C–H alkenylation optimizations studies

The methodological studies of C–H alkenylation were carried out using ethyl acrylate (**30**) and 1,4-naphthoquinone (**61**) as substrate, without substituents to avoid the influence of electron-donating or electron-withdrawing groups in the the reaction. The first attempts were based on previously published methodologies already described in this work. Our initial attempt involved the reaction of 1,4-naphthoquinone (**61**) with a $[\text{RuCl}_2(p\text{-cymene})]_2/\text{AgSbF}_6$ catalyst, ethyl acrylate as the alkenylating reagent, $\text{Cu}(\text{OAc})_2$ as the oxidant and DCE as solvent. Under that condition (**Table 1**, entry 1), the C-5 alkenylated product (**120**) was achieved in 33% yield.

In order to investigate the role of the catalyst in that reaction, C–H alkenylation studies were conduct under $[\text{RuClCp}^*(\text{COD})]$ (2 mol%) and Shvo's catalyst (2 mol%) catalysts in the same reactional condition of entry 1 (**Table 1**, entry 2 and 3). Yet, no product was observed. $\text{RuCl}_2(\text{PPh}_3)_3$, $\text{Ru}(\text{OAc})_2(\text{PPh}_3)_2$, $\text{Ru}(\text{OPiv})_2(\text{PPh}_3)_2$, $\text{Ru}(\text{O}_2\text{CAd})_2(\text{PPh}_3)_2$ (5 mol%) catalysts were also used, however without AgSbF_6 , and no product was achieved (**Table 1**, entries 4, 5, 6 and 7 respectively). Reestablishing the use of AgSbF_6 , $\text{Ru}(\text{O}_2\text{CMes})_2(p\text{-cymene})$ (5 mol%) and $\text{RuClCp}(\text{PPh}_3)_2$ (2 mol%) were used (**Table 1**, entry 8 and 9) and the product were obtained in 18% yield, in the first case, and 8% yield, respectively.

The role of solvent in a chemical reaction is crucial and is associated to different aspects, for instance: intermediate stabilization, chemicals solubility, and so on. Although in the first moment it is not simple to establish a connection between effects of the solvent in C–H alkenylation studies, different solvents were evaluated in this reaction. Even though a similar reaction had been already well described using DCE, the solvent was replaced for dioxane (15% yield), chlorobenzene (NR), dimethylacetamide (DMA) (13% yield), tetrahydrofuran (THF) (11% yield), chlorobenzene (NR), methanol (NR), *o*-xylol (NR) and water (NR) (**Table 1**, entries 10-17, respectively). However, in all cases, the solvent replacement was not satisfactory.

The initial reaction conditions were attempted again but replacing $\text{Cu}(\text{OAc})_2$ for $\text{Cu}(\text{OAc})_2 \cdot \text{H}_2\text{O}$. The product was obtained in 32% yield (**Table 1**, entry 18), a result similar to the first reaction. Then, the following reactions were evaluated using $\text{Cu}(\text{OAc})_2 \cdot \text{H}_2\text{O}$.

Table 1. Catalyst and solvent screening.

Entry	[Ru]-source (mol%)	Solvent	Yield 120/ 121 (%)	Entry	[Ru]-source (mol%)	Solvent	Yield 120/ 121 (%)
1	[RuCl ₂ (<i>p</i> -cymene)] ₂ (5 mol%)	DCE	33/0	10	[RuCl ₂ (<i>p</i> -cymene)] ₂ (5 mol%)	Dioxane	15/0
2	[RuClCp*(COD)] (2 mol%)	DCE	NR	11	[RuCl ₂ (<i>p</i> -cymene)] ₂ (5 mol%)	PhMe	NR
3	Shvo's catalyst (2 mol%)	DCE	NR	12	[RuCl ₂ (<i>p</i> -cymene)] ₂ (5 mol%)	DMA	13/0
4	RuCl ₂ (PPh ₃) ₃ (5 mol%)	DCE	NR	13	[RuCl ₂ (<i>p</i> -cymene)] ₂ (5 mol%)	THF	11/0
5	Ru(OAc) ₂ (PPh ₃) ₂ (5 mol%)	DCE	NR	14	[RuCl ₂ (<i>p</i> -cymene)] ₂ (5 mol%)	PhCl	NR
6	Ru(OPiv) ₂ (PPh ₃) ₂ (5 mol%)	DCE	NR	15	[RuCl ₂ (<i>p</i> -cymene)] ₂ (5 mol%)	Methanol	NR
7	Ru(O ₂ CAd) ₂ (PPh ₃) ₂ (5 mol%)	DCE	NR	16	[RuCl ₂ (<i>p</i> -cymene)] ₂ (5 mol%)	<i>o</i> -xilol	NR
8	Ru(O ₂ CMe) ₂ (<i>p</i> -cymene) (5 mol%)	DCE	18/0	17	[RuCl ₂ (<i>p</i> -cymene)] ₂ (5 mol%)	H ₂ O	NR
9	RuClCp(PPh ₃) ₂ (2 mol%)	DCE	8/0	18*	[RuCl ₂ (<i>p</i> -cymene)] ₂ (5 mol%)	DCE	32/0

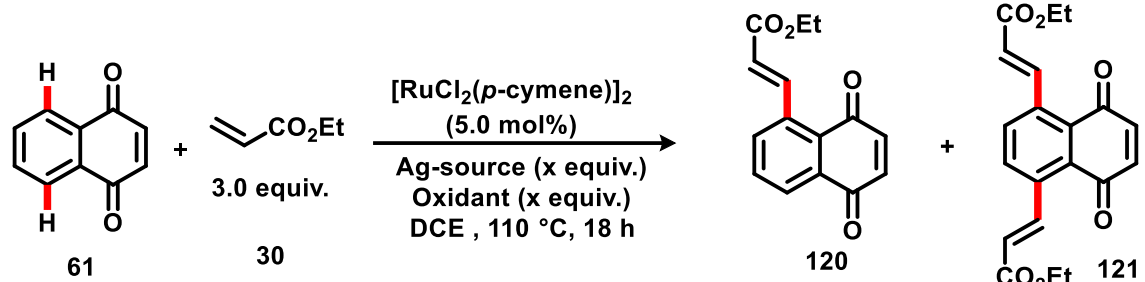
Reaction conditions: **1a** (0.40 mmol), ethylacrylate (1.2 equiv.), catalysts (2.0 or 5.0 mol %), AgSbF₆ (0.16 equiv.), Cu(OAc)₂ (2.0 equiv.), solvent (2.0 mL), 110 °C, 18 h. *Cu(OAc)₂·H₂O (2.0 equiv.). DCE: dichloroethane. NR (No reaction) = For all cases starting material was recovered. Yields of isolated products.

Copper acetate, Cu(OAc)₂, has been used as an oxidant for similar C–H alkenylation proving its importance in the reaction. Still, this compound was replaced by others oxidants in cases with unsatisfactory results. In that context, Cu(OTf)₂, CuSO₄, Zn(OAc)₂, OXONE[®], NaOAc, K₂S₂O₈, Cu(CF₃CO₂)₂, PIFA, and 2,3-dichloro-5,6-dicyano-*p*-benzoquinone (DDQ) (2.0) were used (**Table 2**, entries 1-9) and no product was obtained in any case. Those results describe other sources of copper, acetate or oxidants are not as effective as Cu(OAc)₂, thus, indicating that this compound plays an important role in the reaction.

In addition to a copper source, silver salts have been applied in a similar reactions as an additive. Aiming to achieve the more suitable source of silver, Cu(OAc)₂ was maintained and different silver additives were evaluated for this reaction such as Ag₂SO₄, Ag₂CO₃, AgBF₄, AgPF₆, AgNO₃, Ag₂O, AgOAc, AgNTf₂ (**Table 2**, entries 10-17). In general, in those cases no product was achieved, except when using AgNTf₂ and AgBF₄ (**Table 2**, entries 12 and 17) that resulted in product in 11 and 29% yield, respectively.

Furthermore, AgSbF₆ was replaced by KSbF₆ and no product was obtained (**Table 2**, entry 18). Therefore, those results lead us to the conclusion that silver and antimoniate, in different associations, are not as effective as AgSbF₆.

Table 2. Silver source and oxidants screening.



Entry	Silver source/ equiv.	Oxidant/ equiv.	Yield 120/ 121 (%)	Entry	Silver source/ equiv.	Oxidant/ equiv.	Yield 120/ 121 (%)
1	AgSbF ₆ (0.16)	Cu(OTf) ₂ (2.0)	NR	10	Ag ₂ SO ₄ (16%)	Cu(OAc) ₂ .H ₂ O (2.0)	NR
2	AgSbF ₆ (0.16)	CuSO ₄ (2.0)	NR	11	Ag ₂ CO ₃ (16%)	Cu(OAc) ₂ .H ₂ O (2.0)	NR
3	AgSbF ₆ (0.16)	Zn(OAc) ₂ (2.0)	NR	12	AgBF ₄ (16%)	Cu(OAc) ₂ .H ₂ O (2.0)	10/0
4	AgSbF ₆ (0.16)	OXONE (2.0)	NR	13	AgPF ₆ (16%)	Cu(OAc) ₂ .H ₂ O (2.0)	NR
5	AgSbF ₆ (0.16)	NaOAc (2.0)	NR	14	AgNO ₃ (100%)	Cu(OAc) ₂ .H ₂ O (2.0)	NR
6	AgSbF ₆ (0.16)	K ₂ S ₂ O ₈ (2.0)	NR	15	Ag ₂ O (50%)	Cu(OAc) ₂ .H ₂ O (2.0)	NR
7	AgSbF ₆ (0.16)	Cu(CF ₃ CO ₂) ₂ (2.0)	NR	16	AgOAc (0.16)	Cu(OAc) ₂ .H ₂ O (2.0)	NR
8	AgSbF ₆ (0.16)	PIFA (1.5)	NR	17	AgNTf ₂ (40%)	Cu(OAc) ₂ .H ₂ O (2.0)	29/0
9	AgSbF ₆ (0.16)	DDQ (2.0)	NR	18	KSbF ₆ (40%)	Cu(OAc) ₂ .H ₂ O (2.0)	NR

Reaction conditions: **61** (0.40 mmol), ethylacrylate (**30**) (1.2 or 3.0 equiv), [RuCl₂(*p*-cymene)]₂ (5 mol%), Ag source (X equiv.), oxidant source (X equiv.), solvent (2.0 mL), 110 °C, 18 h. DCE: dichloroethane. NR (No reaction) = For all cases starting material was recovered. Yields of isolated products.

At that point, it was clear that Cu(OAc)₂.H₂O and AgSbF₆ were important for the success of the reaction. Therefore, the amount of those chemicals and of acrylate were studied, as shown in **Table 3**.

The reaction was carried out in the absence of copper and no product was observed (**Table 3**, entry 1). Using Cu(OAc)₂.H₂O in 0.05; 0.5 and 1.0 equiv., instead of 2.0 equiv., the product was achieved in 6%, 17% and 20% yield, respectively (**Table 3**, entries 2, 3 and 4). The amount of AgSbF₆ was increased to 0.1, 0.6 and 1.0 equiv. (maintaining 2.0 equiv. of Cu(OAc)₂.H₂O) and the product was achieved in 36, 38 and 48% yield (**Table 3**, entries 5, 6 and 7). Using 1.0 equiv. of AgSbF₆ and 3.0 equiv. of ethyl acrylate, the product **120** and **121** were isolated in 50% and 40% yield (**Table 3**, entry 8). In that case, despite the low selectivity, the conversion was satisfactory.

Because of those interesting results, the amount of ethyl acrylate was maintained and the amount of AgSbF₆ was increased to 1.2, 1.4, 1.6 and 2.0 equiv. and **120/121** were achieved in 45/27, 48/35 and 48/38% yields, respectively. Then, increasing AgSbF₆ above 1.0 equiv. did

not make any difference in the yield and the best condition was assumed as the condition referred to entry 8. Although there is a lack of selectivity, the condition described in entry 8 leads to a 90% conversion of 1,4-naphthoquinone (**61**). Furthermore, these experimental conditions lead to a greater diversity of compounds due to the formation of two products, which allows more examples to be investigated regarding their biological activities. The optimized condition was performed in the absence of catalyst and no product was observed.

Table 3. Studies of the amount of silver source and acrylate.

Entry	Cu(OAc) ₂ ·H ₂ O (X equiv)	AgSbF ₆ (Y equiv)	Comp. 30 (X equiv)	Yield 120/121 (%)
1	-	0.16	1.2	NR
2	Cu(OAc) ₂ ·H ₂ O (0.05)	0.16	3.0	6/0
3	Cu(OAc) ₂ ·H ₂ O (0.5)	0.16	1.2	17/0
4	Cu(OAc) ₂ ·H ₂ O (1.0)	0.16	1.2	20/0
5	Cu(OAc) ₂ ·H ₂ O (2.0)	0.40	1.2	36/0
6	Cu(OAc) ₂ ·H ₂ O (2.0)	0.60	1.2	38/0
7	Cu(OAc) ₂ ·H ₂ O (2.0)	1.00	1.2	42/0
8	Cu(OAc)₂·H₂O (2.0)	1.00	3.0	50/40
9	Cu(OAc) ₂ ·H ₂ O (2.0)	1.20	3.0	30/18
10	Cu(OAc) ₂ ·H ₂ O (2.0)	1.40	3.0	45/27
11	Cu(OAc) ₂ ·H ₂ O (2.0)	1.60	3.0	48/35
12	Cu(OAc) ₂ ·H ₂ O (2.0)	2.00	3.0	48/38
13	Cu(OAc) ₂ ·H ₂ O (2.0)	-	3.0	NR

Reaction conditions: **61** (0.40 mmol), ethylacrylate (1.2 or 3.0 equiv), [RuCl₂(*p*-cymene)]₂ (5.0 mol %), AgSbF₆ (0.10-2.00 equiv), Cu(OAc)₂·H₂O (0.05-2.0 equiv), solvent (2.0 mL), 110 °C, 18 h. DCE:dichloroethane. NR = For all cases starting material was recovered. Yields of isolated products.

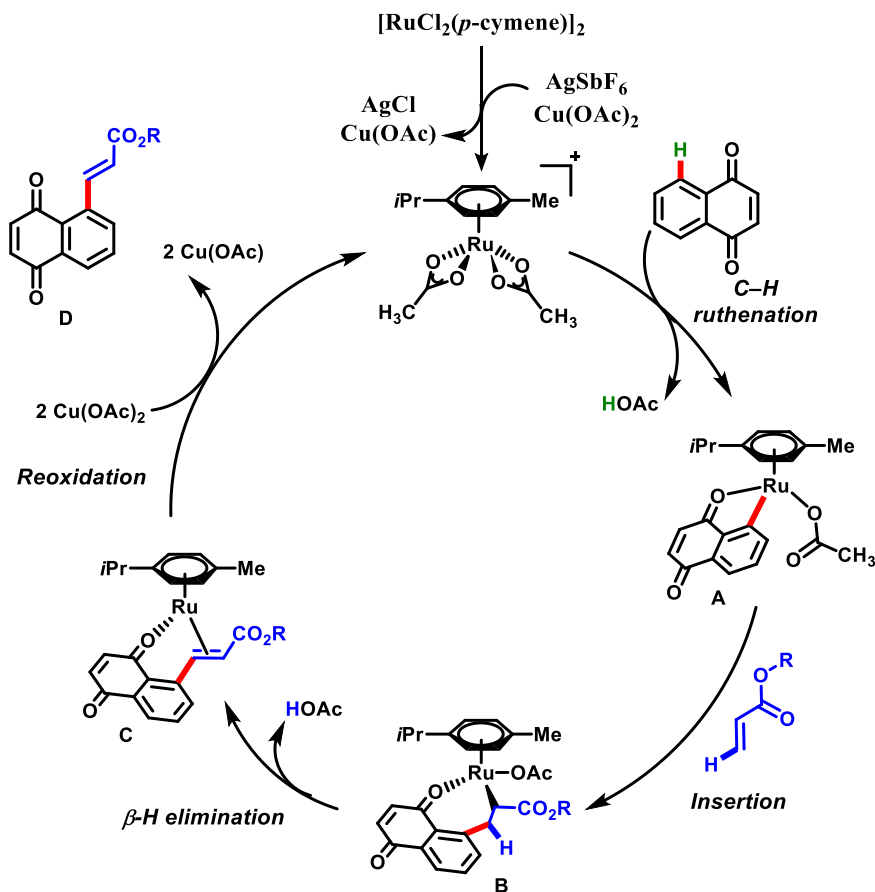
5.2 Proposed C–H alkenylation mechanism

The catalytic cycle proposed here (**Scheme 19**) is based on the previous report.¹²³ Initially, the pre-catalyst [RuCl₂(*p*-cymene)]₂ reacts with AgSbF₆/Cu(OAc)₂ to provide the active catalyst species [Ru(*p*-cymene)(OAc)₂] followed by carboxylate-assisted C–H ruthenation,¹²⁴

123. J. A. Leitch, P. B. Wilson, C. L. McMullin, M. F. Mahon, Y. Bhonoah, I. H. Williams, C. G. Frost. Ruthenium(II)-catalyzed C–H functionalization using the oxazolidinone heterocycle as a weakly coordinating directing group: Experimental and computational insights. *ACS Catal.* **2016**, *6*, 5520-5529.

124. A. Bechtoldt, C. Tirlor, K. Raghuvanshi, S. Warratz, C. Kornhaaß, L. Ackermann. Ruthenium oxidase catalysis for site-selective C–H alkenylations with ambient O₂ as the sole oxidant. *Angew. Chem., Int. Ed.* **2016**, *55*, 264-267.

via coordination with 1,4-naphthoquinone (**61**), affording the ruthena(II)cycle (**A**). Then, a migratory insertion of the acrylate leads to intermediate **B**, followed by a β -hydride elimination, leading to intermediate **C**. Finally, the reoxidation of the Ru(0) species by Cu(OAc)₂ regenerates the active catalyst leading to the desired product.



Scheme 19. Proposed mechanism for C–H alkenylation of 1,4-naphthoquinone.

5.3 C–H oxygenations optimizations studies

The methodological studies for C–H oxygenation reactions were carried out using 1,4-naphthoquinone (**61**) as substrate, using the catalyst $[\text{RuCl}_2(p\text{-cymene})]_2$ in 5 mol% and the oxidant [bis(trifluoroacetoxy)iodo]benzene (PIFA, **38**) in 2.0 equivalent for the reactional system. The reaction was conducted in a mixture of trifluoroacetic anhydride and trifluoroacetic acid (1.00:0.02) at 110 °C for 18 h, under air, in a sealed tube (**Table 4**, entry 1). The product juglone (**74**) was achieved in 53% yield and the double oxygenated product, naphtarazin (**75**), was achieved in 42%.

The previous result, poor selectivity and high conversion of 95%, indicates that harsh reaction conditions. Then, to use a milder conditions, the catalyst amount was decreased to 2

mol% and PIFA (**38**) to 1.2 equivalent, and the reaction was carried out at 80 °C for 18 hours (entry 2). In this case, juglone (**74**) was obtained in a higher yield of 87%, naphthazarin (**75**) in 5% yield.

Despite the interesting results, PIFA is not very stable and must be kept under an inert atmosphere and refrigeration. Then, PIFA was replaced by (diacetoxyiodo)benzene (PIDA) (entry 3), a more stable reactant, and by ammonium persulphate, (NH₄)₂S₂O₈ (entry 4). In the first case, juglone (**74**) was obtained in a lower yield of 71% and no naphthazarin (**75**) was observed. In the second case (entry 4), no product was observed.

The [RuCl₂(*p*-cymene)]₂ catalyst was replaced by RuCl₃.H₂O (5 mol%) (entry 5), [RhCp*Cl₂]₂ (5 mol %) (entry 6) and CoCp*(CO)I₂ (5 mol%) (entry 7) and no product was observed in those cases. Using Pd(OAc)₂ (5 mol%) any product was obtained and no 1,4-naphthoquinone (**61**) was recovered (entry 8).

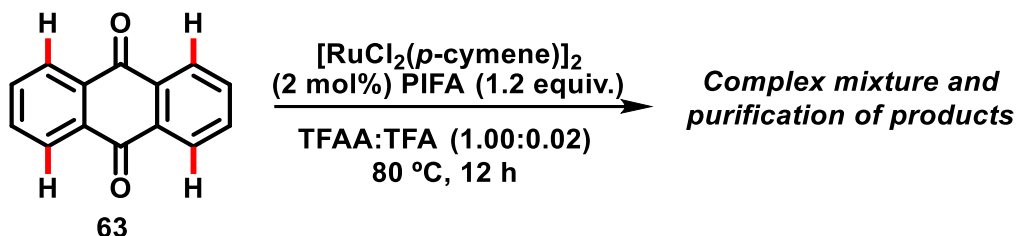
In the absence of a catalyst (entry 9), no product was obtained. Until that point, the best condition (entry 2) was carried out in less time, 12 h (entry 10), and surprisingly, juglone (**74**) was obtained in 92% yield and naphthazarin (**75**), in 3 % yield and. Consequently, the optimized condition was achieved.

Table 4. Optimization of C–H oxygenation reactions of 1,4-naphthoquinone (**61**).

Entry	[M]-source (mol %)	Oxidant	Y	Temp (°C)	74 (%)	75 (%)
1	[RuCl ₂ (<i>p</i> -cymene)] ₂ (5)	PIFA	2.0	110	53	42
2	[RuCl ₂ (<i>p</i> -cymene)] ₂ (2)	PIFA	1.2	80	87	5
3	[RuCl ₂ (<i>p</i> -cymene)] ₂ (2)	PIDA	1.2	80	71	Traces
4	[RuCl ₂ (<i>p</i> -cymene)] ₂ (2)	NH ₄ S ₂ O ₈	1.2	80	NR	NR
5	RuCl ₃ .H ₂ O (5)	PIFA	1.2	80	NR	NR
6	[RhCp*Cl ₂] ₂ (5)	PIFA	1.2	80	NR	NR
7	CoCp*(CO)I ₂ (5)	PIFA	1.2	80	NR	NR
8	Pd(OAc) ₂ (5)	PIFA	1.2	80	NR	NR
9	-	PIFA	1.2	80	NR	NR
10	[RuCl₂(<i>p</i>-cymene)]₂ (2)	PIFA	1.2	80	92	3

General reaction conditions: (**61**) (0.4 mmol), PIFA (0.5 mmol), [RuCl₂(*p*-cymene)]₂ (5.0 or 2.0 mol %); (TFAA) (1 mL) and TFA (0.02 mL); Entries 1-8, 18 h; Entries 9 and 10, 12 h. PIFA = PhI(CF₃CO₂)₂. PIDA = PhI(CH₃CO₂)₂. NR = No reaction.

To extend that methodology, anthraquinone (**63**) was used instead of 1,4-naphthoquinone (**61**). A complex mixture of products was achieved and the purification was unsuccessful (**Scheme 20**). The result was not that much surprising since multiple activation patterns are possible.

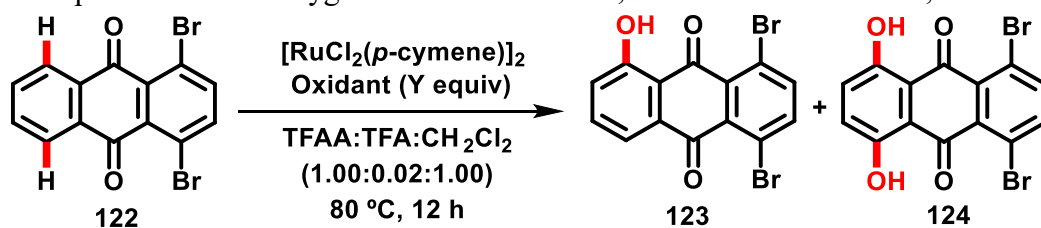


Scheme 20. C–H oxygenation reaction with anthraquinone (**63**).

Then, anthraquinone (**63**) was replaced by 1,4-dibromoanthracene-9,10-dione (**122**), with expectation of attaining better selectivity, considering that two possible positions were blocked by bromine. Applying the developed methodology to 1,4-naphthoquinone (**61**), the product 1,4-dibromo-5-hydroxyl-anthraquinone (**123**) was obtained in only 17% yield (**Table 5**, entry 1). In that case, the amount of catalyst was increased to 5 mol%, so the product was obtained in 15% and the 1,4-dibromo-5,8-dihydroxyl-anthraquinone (**124**), in 8% yield (entry 2).

The amount of PIFA (**38**) was increased to 2.0 equiv. for 5.0 mol% of the catalyst to provide 1,4-dibromo-5-hydroxyanthracene-9,10-dione (**123**) in 52% yield (entry 3). The replacement of PIFA 2.0 equiv. by PIDA (**35**, 2.3 equiv.) led to the product 1,4-dibromo-8-hydroxyl-anthraquinone in 70% yield and 1,4-dibromo-5,8-dihydroxyanthracene-9,10-dione (**124**), in 10% yield, so only 6% of starting material was recovered (entry 4), resulting in an optimized condition.

Table 5. Optimizations of oxygenation reactions of 1,4-dibromoanthracene-9,10-dione (**122**)



Entry	[Ru]-source (mol%)	Oxidant	Y	123	124	SM
1	[RuCl ₂ (<i>p</i> -cymene)] ₂ (2)	PIFA	1.2	17	-	65
2	[RuCl ₂ (<i>p</i> -cymene)] ₂ (5)	PIFA	1.2	15	8	51
3	[RuCl ₂ (<i>p</i> -cymene)] ₂ (5)	PIFA	2.0	52	10	35
4	[RuCl₂(<i>p</i>-cymene)]₂ (5)	PIDA	2.3	70	10	6

General reaction conditions: anthraquinone (0.3 mmol), PIDA (0.7 mmol), [RuCl₂(*p*-cymene)]₂ (5.0 mol %); (TFAA) (1 mL), TFA (0.02 mL) and CH₂Cl₂ (1 mL). Yields of isolated products. SM= starting material

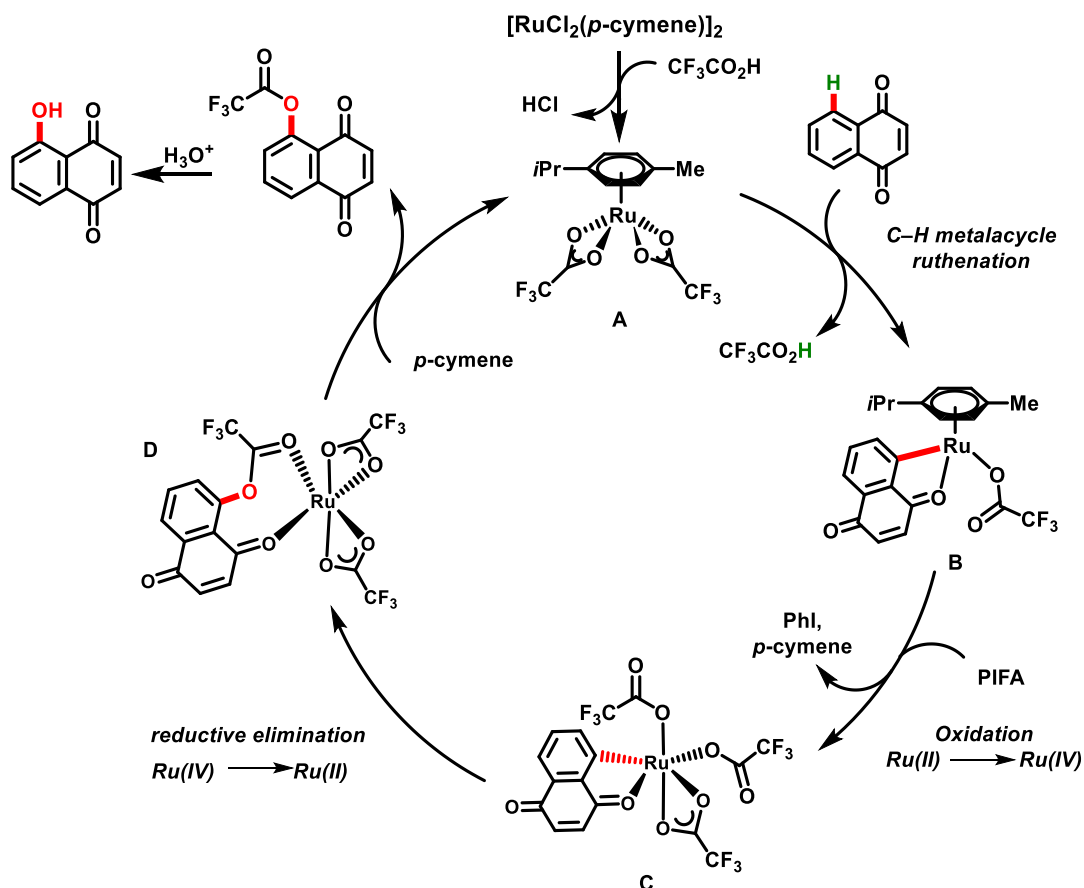
5.4 Mechanism proposal

The mechanistic proposal presented here (**Scheme 21**) is based on previous work propositions and, until now, there are no detailed studies regarding the mechanism of these reactions.

Initially, chloride from pre-catalyst [RuCl₂(*p*-cymene)]₂ is replaced by trifluoroacetate to provide the catalyst **A**. The correspondent 1,4-naphthoquinone coordinates to the metal, with the elimination of trifluoroacetate, followed by cycloruthenation processes to provide the intermediate **B**. The hypervalent iodine compound, PIFA, oxidizes the intermediate **B** to afford the intermediate **C**, by oxidation of Ru(II) to Ru(IV).¹²⁵

In the next step, reductive elimination takes place, by reduction of Ru(IV) to Ru(II), to provide the oxygenated intermediate **D** and then *p*-cymene coordinates to metal for the reestablishment of catalyst species **A** and release of the respective acetylated juglone. At this moment, the acid work-up of crude solution affords the oxygenated product.

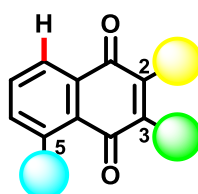
125. L. Ackermann, R. Vicente, H. K. Potukuchi, V. Pirovano. Mechanistic insight into direct arylations with ruthenium(II) carboxylate catalysts *Org. Lett.* **2010**, *12*, 5032-5035.



Scheme 21. Mechanistic proposal of C–H oxygenation reactions.

5.5 Synthesis of quinoidal substrates

Once the reaction optimization studies were concluded and the synthetic conditions were established, it was necessary to evaluate the applicability of the new methodology to similar substrates containing different groups in different positions. Accordingly, 1,4-naphthoquinones were designed to bear different substituents in positions 2, 3, and 5 (**Scheme 22**).



Scheme 22. Schematic representation of 1,4-naphthoquinones derivatives substitution pattern.

Compounds **61**, **124-127** (**Figure 6**) were commercially obtained and used without prior treatment. Unsubstituted 1,4-naphthoquinone (**61**) was used for optimization studies whereas

the 2-hydroxynaphthalene-1,4-dione (**124**) was selected to evaluate the effect of the hydroxyl group, as electron donor group, on the reactivity and selectivity of the moiety. Menadione (**125**), on the other hand, was thought of as a substrate bearing a methyl group, a less efficient donor than hydroxyl, which is not expected directly to interfere in the reaction. However it is a proper comparison with 1,4-naphthoquinone (**61**). 2,3-dichloronaphthalene-1,4-dione (**126**) and 2,3-dibromonaphthalene-1,4-dione (**127**) were selected due to the electron withdrawal effect of halogen, that enable the establishment of a relationship with donation groups. Furthermore, substrates **125-127** were used to access diversives 1,4-naphthoquinones.

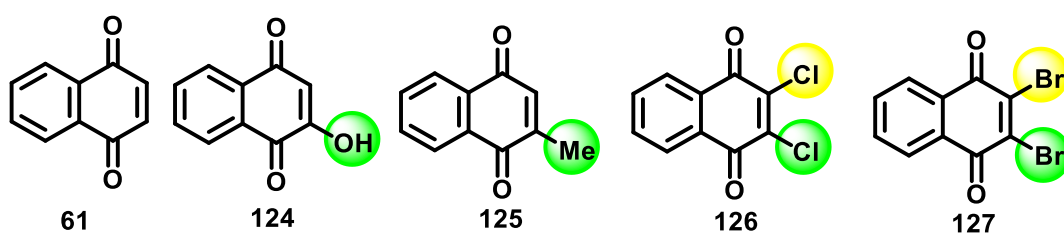


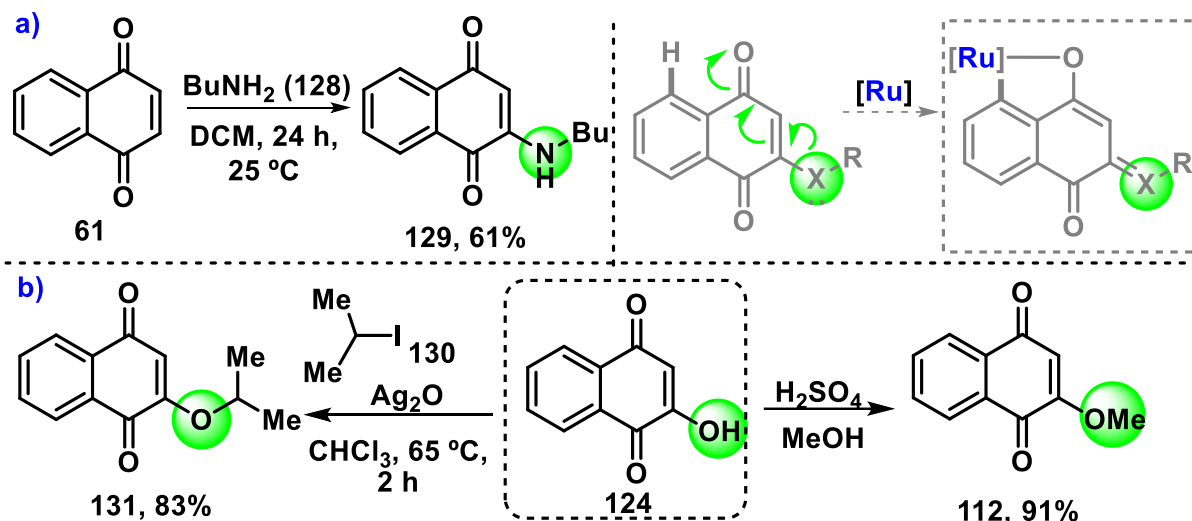
Figure 6. Naphthoquinones commercially obtained.

2-(butylamino)naphthalene-1,4-dione (**129**) was obtained in 61% yield *via* conjugated addition of buthylamine (**128**) to 1,4-naphthoquinone (**61**).¹²⁶ The amine moiety was incorporated to increase the electronic density at carbonyl to facilitate the metalation process during the C–H activation that is represented in the box in **Scheme 23a**. Two other similar examples of electron donor groups were considered based on alkylation hydroxy-group of **124** (**Scheme 23b**): 2-methoxynaphthalene-1,4-dione (**112**) was obtained *via* the addition of sulfuric acid to a methanolic solution of **124**¹²⁷ whereas 2-isopropoxynaphthalene-1,4-dione (**131**) was synthesized *via* reflux of mixture among **124**, 2-iodopropane (**130**) and Ag₂O in chloroform.¹²⁸

126. R. Patil, S. Bhand, V. B. Konkimalla, P. Banerjee, B. Ugale, D. Chadar, S. K. Saha, P. Pr. Praharaj, C. M. Nagaraja, D. Chakrovarty, S. Salunke-Gawali. Molecular association of 2-(*n*-alkylamino)-1,4-naphthoquinone derivatives: Electrochemical, DFT studies and antiproliferative activity against leukemia cell lines. *J. Mol. Struct.* **2016**, *1125*, 272-281

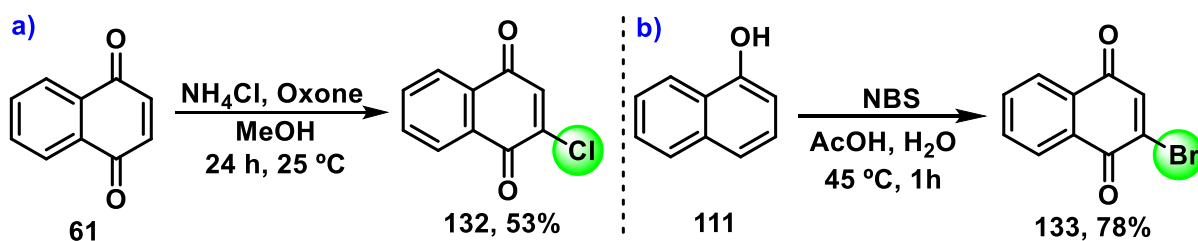
127. F. Brommel, P. Zou, H. Finkelmann, A. Hoffmann. Influence of the mesogenic shape on the molecular dynamics and phase-biaxiality of liquid crystal main-chain polymers. *Soft Matter*. **2013**, *9*, 1674-1677.

128. J.-C. Lien, L.-J. Huang, C.-M. Teng, J.-P. Wang, S.-C. Kuo. Synthesis of 2-alkoxy 1,4-naphthoquinone derivatives as antiplatelet, antiinflammatory, and antiallergic agents. *Chem. Pharm. Bull.* **2002**, *50*, 672-674.



Scheme 23. Synthesis of 2-(butylamino)naphthalene-1,4-dione (**129**), 2-methoxynaphthalene-1,4-dione (**112**) and -isopropoxynaphthalene-1,4-dione (**131**).

2-chloronaphthalene-1,4-dione (**132**), obtained in 53% yield from chlorination of **61**, was designed based on the electron-withdrawing effect of chlorine, which could interfere in the reactivity and selectivity of C–H activation reaction (**Scheme 24a**).¹²⁹ 2-bromonaphthalene-1,4-dione (**133**) was obtained *via* the reaction between naphthol (**111**) and N-bromosuccinimide (NBS) resulting in **133** in 78% yield (**Scheme 24b**).¹³⁰

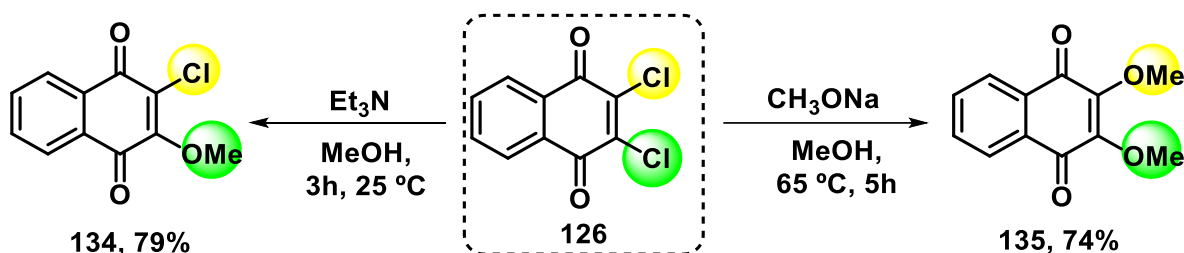


Scheme 24. Synthesis of 2-chloronaphthalene-1,4-dione (**132**) and 2-bromonaphthalene-1,4-dione (**133**).

129. a) S. Neufeind, N. Hülken, J.-M. Neudörfl, N. Schlörer and H.-G. Schmalz. Total synthesis of cyclo-mumbaistatin analogues through anionic homo-Fries rearrangement. *Chem. Eur. J.* **2011**, *17*, 2633-2641. **b)** P. Swamy, M. A. Kumar, M. M. Reddy, M. Naresh, K. Srujana, N. Narender. The vicinal functionalization of olefins: a facile route to the direct synthesis of β -chlorohydrins and β -chloroethers. *RSC Adv.* **2014**, *4*, 26288-26294.

130. P. Bachu, J. Sperry, M. A. Brimble. Chemoenzymatic synthesis of deoxy analogues of the DNA topoisomerase II inhibitor eleutherin and the 3C-protease inhibitor thysanone. *Tetrahedron*, **2008**, *64*, 4827-4834.

2,3-dichloronaphthalene-1,4-dione (**126**) enabled the obtaining two substrate: 2-chloro-3-methoxynaphthalene-1,4-dione (**134**) in 79% yield, *via* replacement of one chlorine,¹³¹ and 2,3-dimethoxynaphthalene-1,4-dione (**135**), as result of two chlorine substitution (**Scheme 25**).¹³² Compound **134** was thought as a substrate bearing one electron-withdrawing group, the chlorine; and an electron donating group, the methoxy, representing an interesting substrate to evaluate the competitive effect of those groups. Still, two methoxy groups in **135** could strongly increase the reactivity of 1,4-naphthoquinone (**61**) as a result of the double effect in the carbonyls.



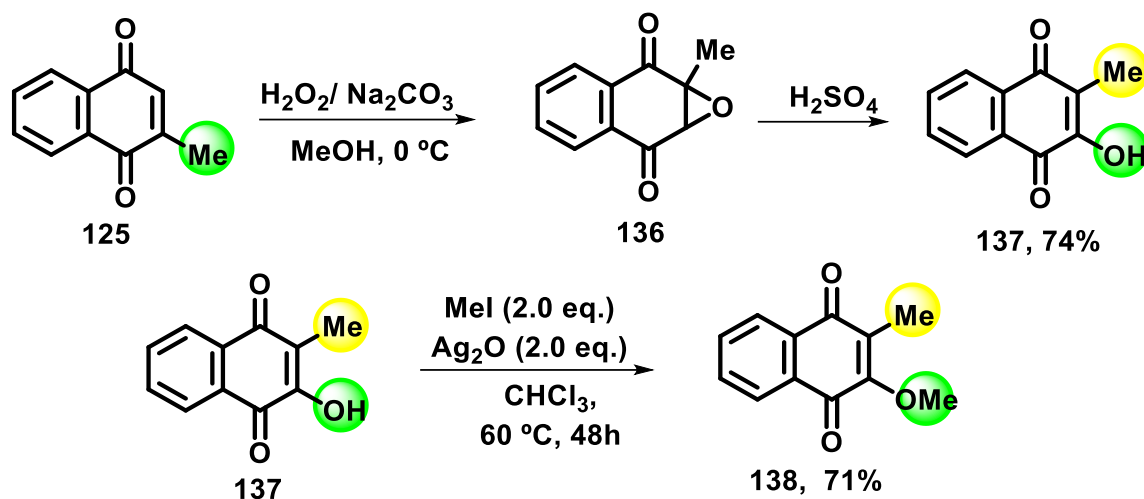
Scheme 25. Synthesis of 2-chloro-3-methoxynaphthalene-1,4-dione (**134**) and 2,3-dimethoxynaphthalene-1,4-dione (**135**).

2-methoxy-3-methylnaphthalene-1,4-dione (**138**), is another example of a compound bearing two electron-donating groups, although the electron donation of methoxy is clearly more effective than the inductive effect of methyl (**Scheme 26**). Menadione (**125**) epoxidation followed by the opening of the epoxy ring induced by sulfuric acid provided **137** in 74% yield. Posteriorly, the hydroxyl from **137** was methylated to provide 2-methoxy-3-methylnaphthalene-1,4-dione (**138**).¹³³

131. M. Delarmelina, R. D. Daltoé, M. F. Cerri, K. P. Madeira, L. B. A. Rangel, V. L. Júnior, W. Romão, A. G. Taranto, S. J. Greco. Synthesis, antitumor activity and docking of 2,3-(substituted)-1,4-naphthoquinone derivatives containing nitrogen, oxygen and sulfur. *J. Braz. Chem. Soc.* **2015**, *26*, 1804-1816.

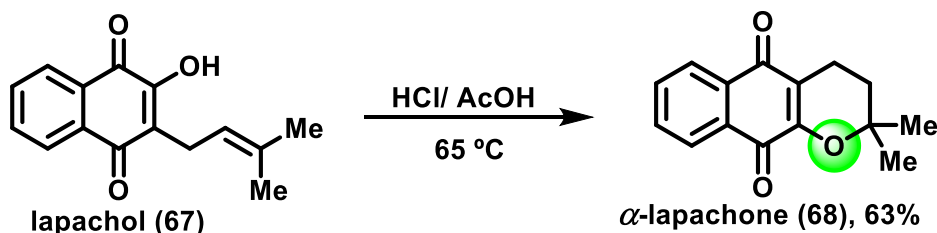
132. G. H. Jones, M. C. Venuti, J. M. Young, D. V. K. Murthy, B. E. Loe, R. A. Simpson, A. H. Berks, D. A. Spires, P. J. Maloney, M. Kruseman, S. Rouhafza, K. C. Kappas, C. C. Beard, S. H. Unger and P. S. Cheung. Topical nonsteroidal antipsoriatic agents. 1. 1,2,3,4-tetraoxygenated naphthalene derivatives. *J. Med. Chem.* **1986**, *29*, 1504-1511.

133. G. A. M. Jardim, E. H. G. da Cruz, W. O. Valença, D. J. B. Lima, B. C. Cavalcanti, C. Pessoa, J. Rafique, A. L. Braga, C. Jacob, E. N. da Silva Júnior. Synthesis of selenium-quinone hybrid compounds with potential antitumor activity via Rh-catalyzed C–H bond activation and Click Reactions. *Molecules.* **2018**, *23*, 83,1-16.



Scheme 26. Synthesis of 2-methoxy-3-methylnaphthalene-1,4-dione (**138**).

Lapachol (**67**), a natural and commercially available chemical, was cyclized in acid conditions to provide α -lapachone (**68**) in 63% yield (**Scheme 27**),¹³⁴ designed as a similar compound to 2-methoxynaphthalene-1,4-dione (**112**) and 2-isopropoxynaphthalene-1,4-dione (**131**).

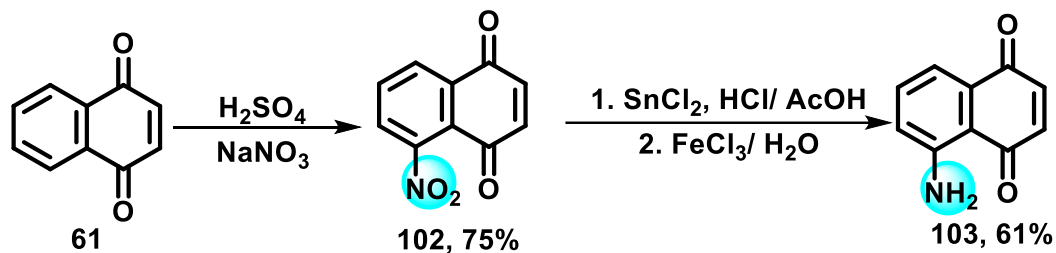


Scheme 27. Synthesis of α -lapachone (**68**).

Although examples of 1,4-naphthoquinones with benzenoid ring modified are not very common, two cases here were designed bearing a nitro group, an electron-withdrawing group, and an amine, an electron donor. Then, as described in **Scheme 28**, the nitration of **61** led to the formation of 5-nitronaphthalene-1,4-dione (**102**) in 75% yield followed by reduction of the nitro group by tin(II) chloride to achieve 5-aminonaphthalene-1,4-dione (**103**) in 61% yield.¹³⁵

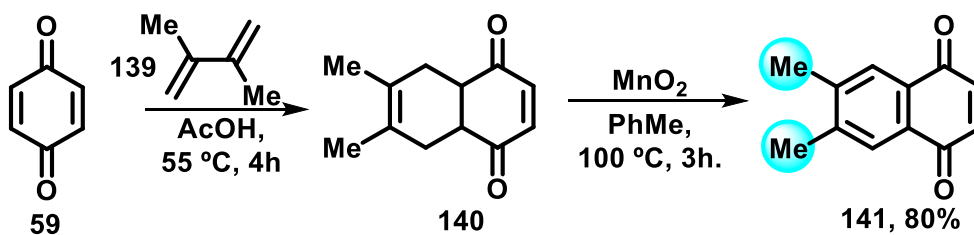
134. F. A. Calil, J. S. David, E. R. C. Chiappetta, F. Fumagalli, R. B. Mello, F. H. A. Leite, M. S. Castilho, F. S. Emery, M. C. Nonato. Ligand-based design, synthesis and biochemical evaluation of potent and selective inhibitors of *Schistosoma mansoni* dihydroorotate dehydrogenase. *Eur. J. Med. Chem.* **2019**, *167*, 357-366.

135. M. S. Shvartsberg, E. A. Kolodina, N. I. Lebedeva, L. G. Fedenok. Vicinal acetylenic derivatives of 2-amino-1,4-naphthoquinone as key precursors of heterocyclic quinones. *Russ. Chem. Bull., Int. Ed.* **2012**, *61*, 582-588.



Scheme 28. Synthesis of 5-nitronaphthalene-1,4-dione (**102**) and 5-aminonaphthalene-1,4-dione (**103**).

Another example of modified benzenoid-1,4-naphthoquinone includes the 6,7-dimethylnaphthalene-1,4-dione (**141**), obtained in 80% yield *via* Diels-Alder reaction between benzoquinone (**59**) and 2,3-dimethyl-1,3-butadiene (**139**), followed by the dehydrogenation of the intermediate **140** (Scheme 29).¹³⁶

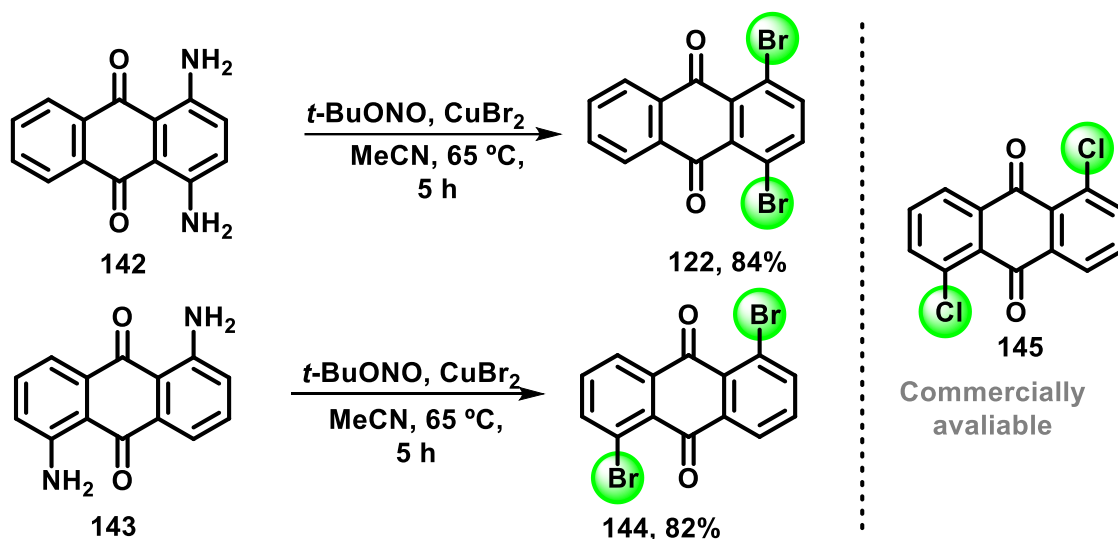


Scheme 29. Synthesis of 6,7-dimethylnaphthalene-1,4-dione (**141**).

Compounds 1,4-diaminoanthracene-9,10-dione (**142**) and 1,5-diaminoanthracene-9,10-dione (**143**) provided the correspondent 1,4-dibromoanthracene-9,10-dione (**122**) and 1,5-dibromoanthracene-9,10-dione (**144**) in 84 and 82% yield, respectively, *via* diazotization reaction¹³⁷ (Scheme 30). 1,5-dichloroanthracene-9,10-dione (**145**) was commercially obtained.

¹³⁶. D. J. Sullivan, R. Clérac, M. Jennings, A. J. Lough, K. E. Preuss. Trinuclear Mn(II) complex with paramagnetic bridging 1,2,3-dithiazolyl ligand *Chem. Commun.* **2012**, *48*, 10963-10965.

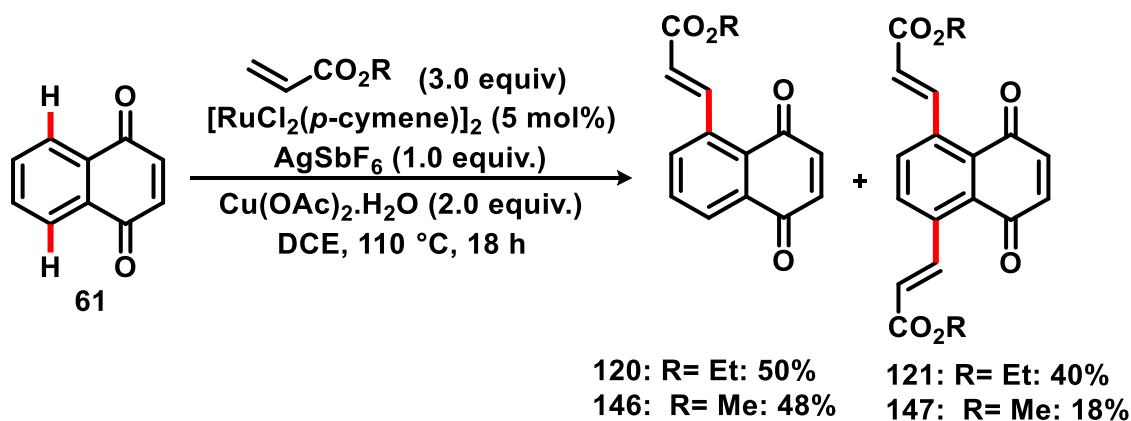
¹³⁷. B. VanVeller, D. Robinson, T. M. Swager. Triptycene Diols: A strategy for synthesizing planar p-systems through catalytic conversion of a poly(*p*-phenylene ethynylene) into a poly(*p*-phenylene vinylene). *Angew. Chem., Int. Ed.* **2012**, *51*, 1182-1186.



Scheme 30. Synthesis of anthracene-9,10-dione **122**, **144** and **145**.

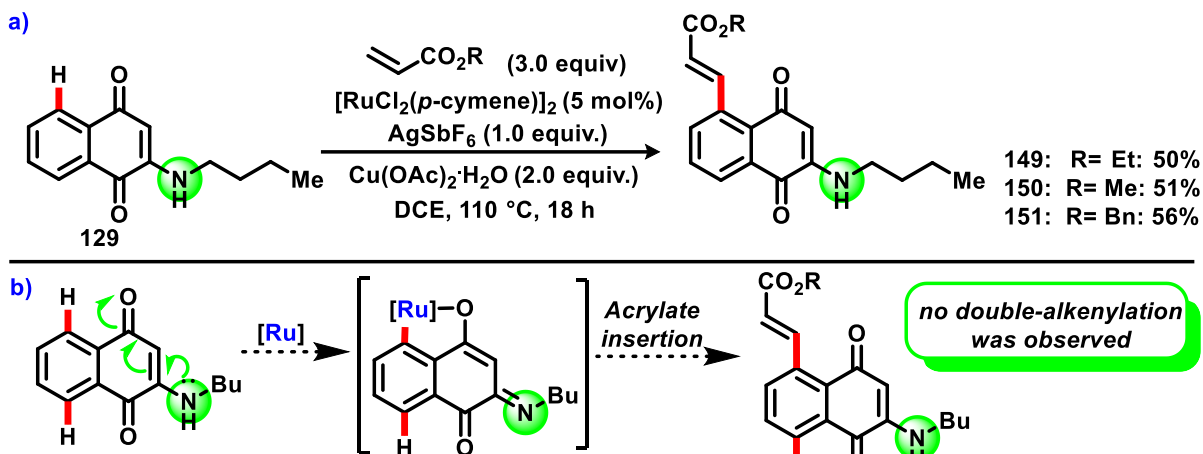
5.6 Scope of the ruthenium(II) catalyzed C–H alkenylation

With designed substrates fully synthesized and characterized, the viability of the C–H alkenylation protocol developed was evaluated using conditions previously studied. Firstly, methyl acrylate (**22**) was used, instead of ethyl acrylate (**30**) to provide **146** in 48% yield and **147** in 18% yield (Scheme 31). Interestingly, the replacement by methyl acrylate (**22**) reduced the yield of both products in comparison to **120** and **121**.



Scheme 31. Synthesis of compounds **120**, **121**, **146** and **147**.

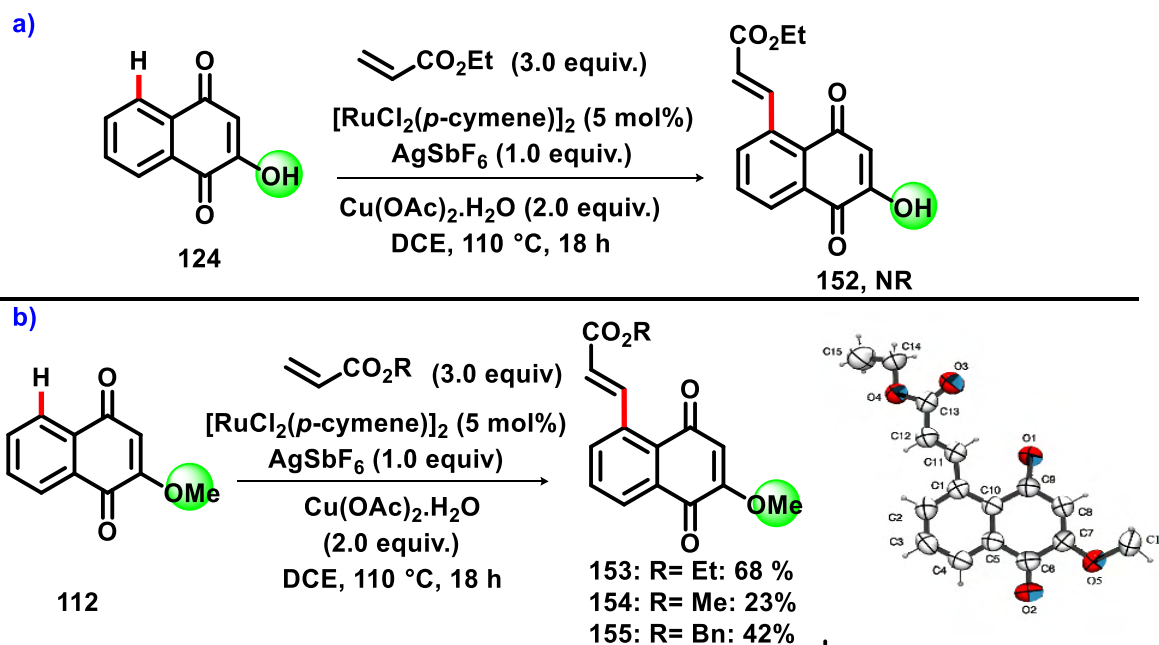
Compound **129** was subjected to C–H alkenylation using methyl acrylate (**22**), ethyl acrylate (**30**) and benzyl acrylate (**148**) to provide **149**, **150** and **151** in 50, 51 and 56% yield, respectively (Scheme 32a). In all cases, no double activation was observed, so it suggests the effectiveness of the electron-donating groups in the reaction selectivity (Scheme 32b).



Scheme 32. a) Synthesis of compounds **149-151** and b) effect of the electron-donating groups in the reaction selectivity.

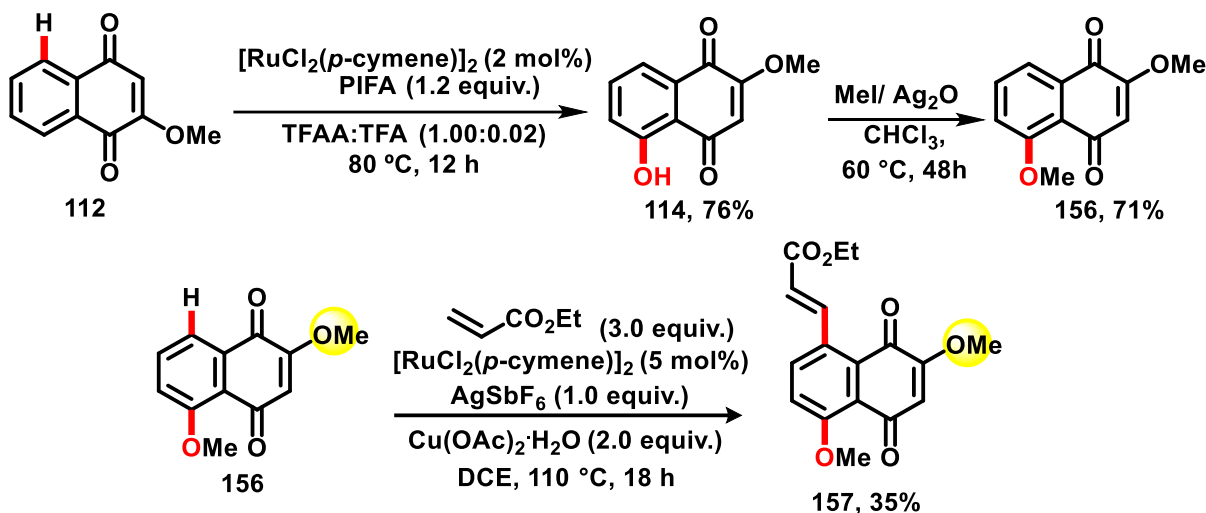
Surprisingly, no reaction was observed when 2-hydroxynaphthalene-1,4-dione (**124**) was submitted to C–H alkenylation reaction and **124** was almost totally recovered (**Scheme 33a**). Still, substrate bearing a methoxy group **112** led to **153** in 68% yield, when ethyl acrylate (**30**) was used. The reaction yield dropped sharply when ethyl acrylate (**30**) was replaced by methyl acrylate (**22**), leading to product **154**, which was obtained in 23% yield (**Scheme 33b**). This result is in agreement with previous ones indicating that methyl acrylate (**22**) is not suitable for those reactions. In the case of using benzyl acrylate (**148**), **155** was obtained in 42% yield.

In all reactions, no double activation was observed, so it corroborates, once again, the efficacy of the electron-donating groups in the reaction selectivity. Moreover, the recrystallization of **153** resulted in suitable crystals for X-ray crystallography studies, and in the ortep-3 projection of **153** is indicated in **Scheme 33**. It is possible to notice the regioselectivity of this reaction, as a result of increasing the electronic density in the orientation of the carbonyl in the alkenylation reaction



Scheme 33. a) Unsuccessful synthesis of **152** and b) synthesis of **153-155** bearing methoxy group.

C–H oxygenation reaction using 2-methoxynaphthalene-1,4-dione (**112**) provided **114** in 76% yield, which will be described later. Compound **114** was submitted to a methylation reaction¹³⁸ for obtaining **156** in 71% yield. Then, the C–H alkenylation was performed with **156**, using ethyl acrylate (**30**) to provide **157** in 35% yield (Scheme 34).

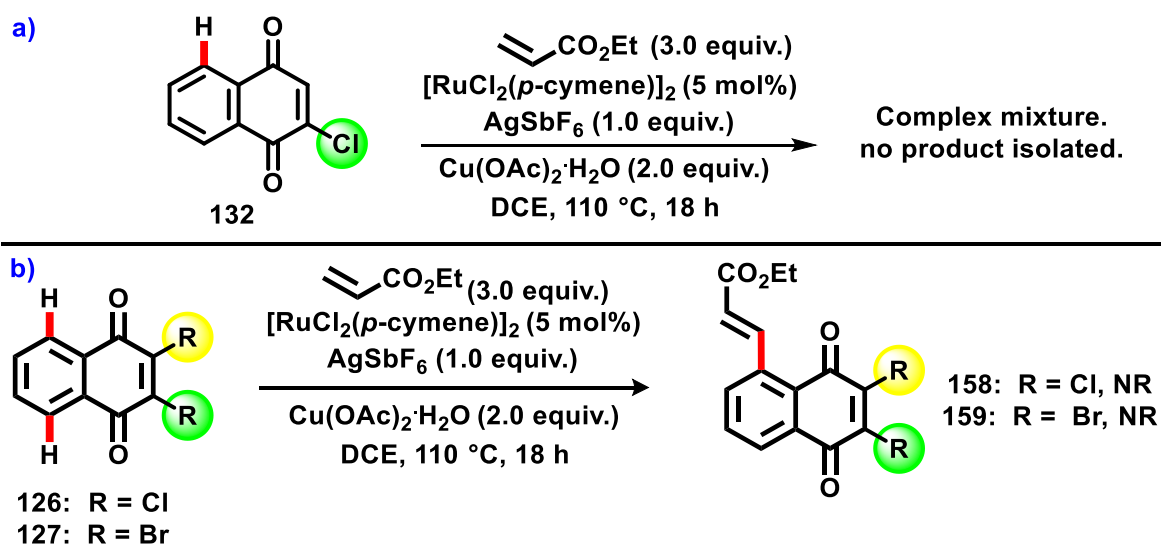


Scheme 34. Synthesis of compounds **157**.

¹³⁸ . M. Manickam, P. R. Boggu, J. Cho, Y. J. Nam, S. J. Lee, S.-H. Jung. Investigation of chemical reactivity of 2-alkoxy-1,4-naphthoquinones and their anticancer activity. *Bioorg. Med. Chem. Lett.* **2018**, *28*, 2023-2028.

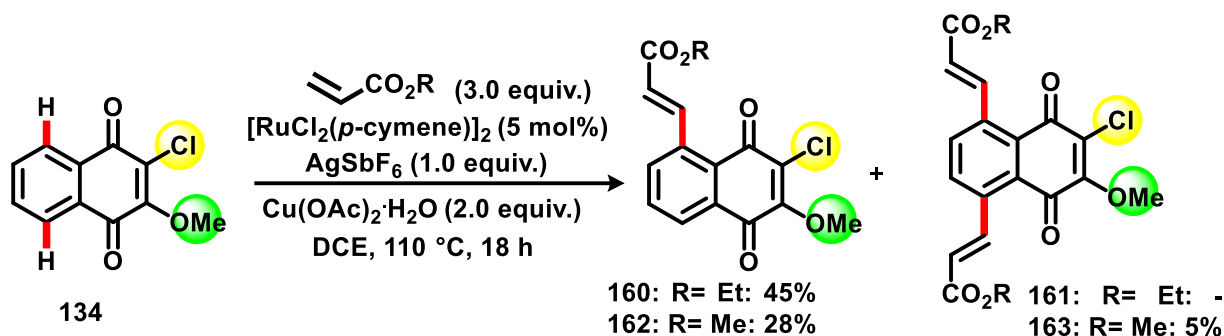
Those preliminaries result led to the conclusion that the presence of electron-donating groups do not significantly increased the reaction yield (optimized in 50%). Therefore, those groups do not significantly interfere in the reaction yield. Yet, as demonstrated in the following examples, those groups increase the selective of reaction.

C–H alkenylation with 2-chloronaphthalene-1,4-dione (**132**) using ethyl acrylate (**30**) led to a complex mixture and no compound was successfully isolated for further characterization (Scheme 35a). In case of 2,3-dichloronaphthalene-1,4-dione (**126**) and 2,3-dibromonaphthalene-1,4-dione (**127**) no product was obtained and both halogenated substrates were almost completely recovered (Scheme 35b). The lack of reactivity of bis-halogenated substrates is probably associated with the deactivation of α -carbonyl caused by the electron-withdrawing effect of the halogens. This deactivation reduces the ability of the carbonyl group to bond to metal for performing the catalytic reaction.



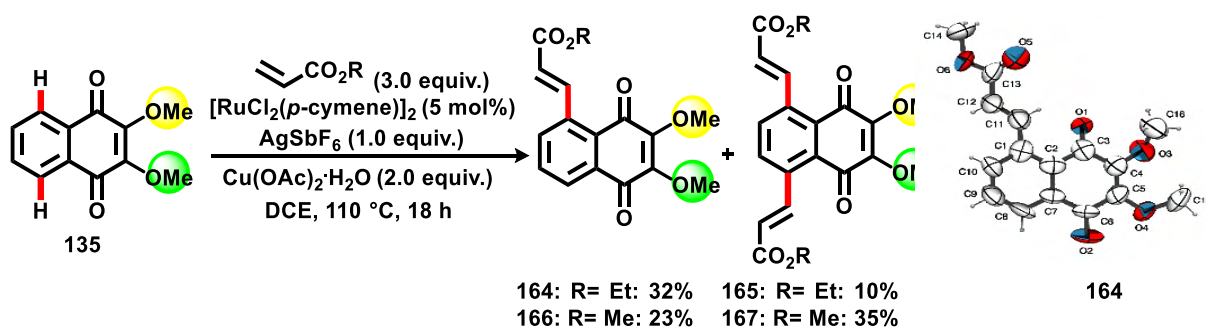
Scheme 35. Unsuccessful C–H alkenylation using substrates a) **132**, b) **126** and **127**.

Then, to evaluate a halogenated substrate associated to an electron donating group, compounds **134** was subjected to C–H alkenylation using ethyl acrylate (**30**) and so the product **160** was achieved in 45% yield and **161** was not obtained. It is important to highlight that product **160** was obtained in satisfactory yield and the regioselectivity indicated that the methoxy group was more efficient in increase the reactivity of the carbonyl than the electron-withdrawing effect of the halogen. When methyl acrylate (**22**) was used, compound **162** was obtained in 28% yield, whilst the double C–H activated product (**163**) was isolated in only 5% yield (Scheme 36).



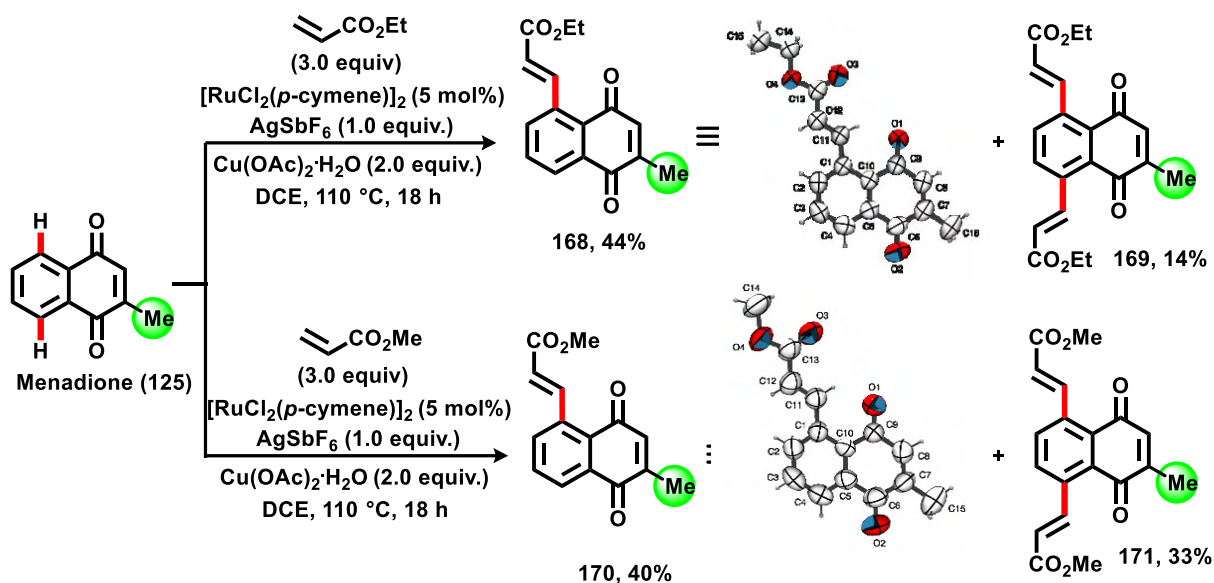
Scheme 36. Synthesis of compounds 160-163.

Compound 2,3-dimethoxynaphthalene-1,4-dione (**135**) was submitted to C–H alkenylation using ethyl acrylate (**30**), resulting in **164** in 32% yield and the double activated product (**165**), in 10% yield (Scheme 37). Similarly, using methyl acrylate (**22**), product **166** was obtained in 23% yield and the double activated product (**167**), in 35% yield.



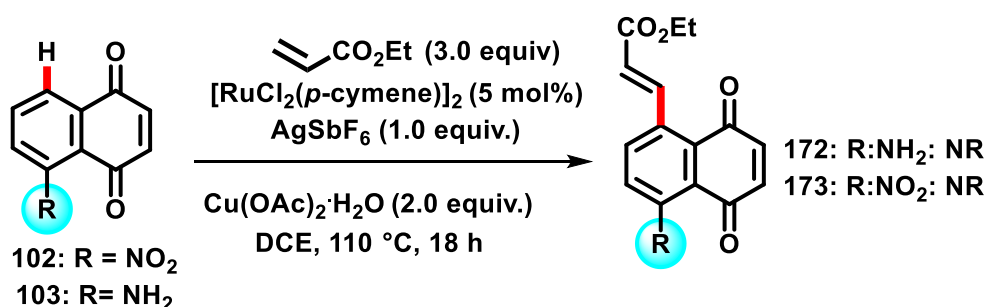
Scheme 37. Synthesis of compounds 164-167.

2-methyl-1,4-naphthoquinone (**125**) was submitted to C–H alkenylation using ethyl acrylate (**30**) to provide product **168** in 44% yield and **169** in 14% yield. A similar reaction using methyl acrylate (**22**) led to product **170** in 40% yield and **171** in 33% yield (Scheme 38). Recrystallization of **168** and **170** followed by X-ray crystallography studies revealed that inductive effects were enough to induce the regioselectivity of those reaction, despite the absence of an electron donating group from methyl groups.



Scheme 38. Synthesis of compounds 168-171.

Compounds **102** and **103** bearing on the benzenoid ring a nitro group and an amine group, respectively, were evaluated for C–H alkenylation reaction. However, in both cases, no product was achieved (**Scheme 39**). Probably, the nitro group reduces sharply the reactivity of the benzenoid ring due to the electron-withdrawing effect. Furthermore, the low reactivity of **103** may be associated to the interaction between amino moiety and copper present in the reaction, causing the prevention of the reaction course.



Scheme 39. Unsuccessful C–H alkenylation using substrates **102** and **103** modified in benzenoid ring with nitro and amine groups.

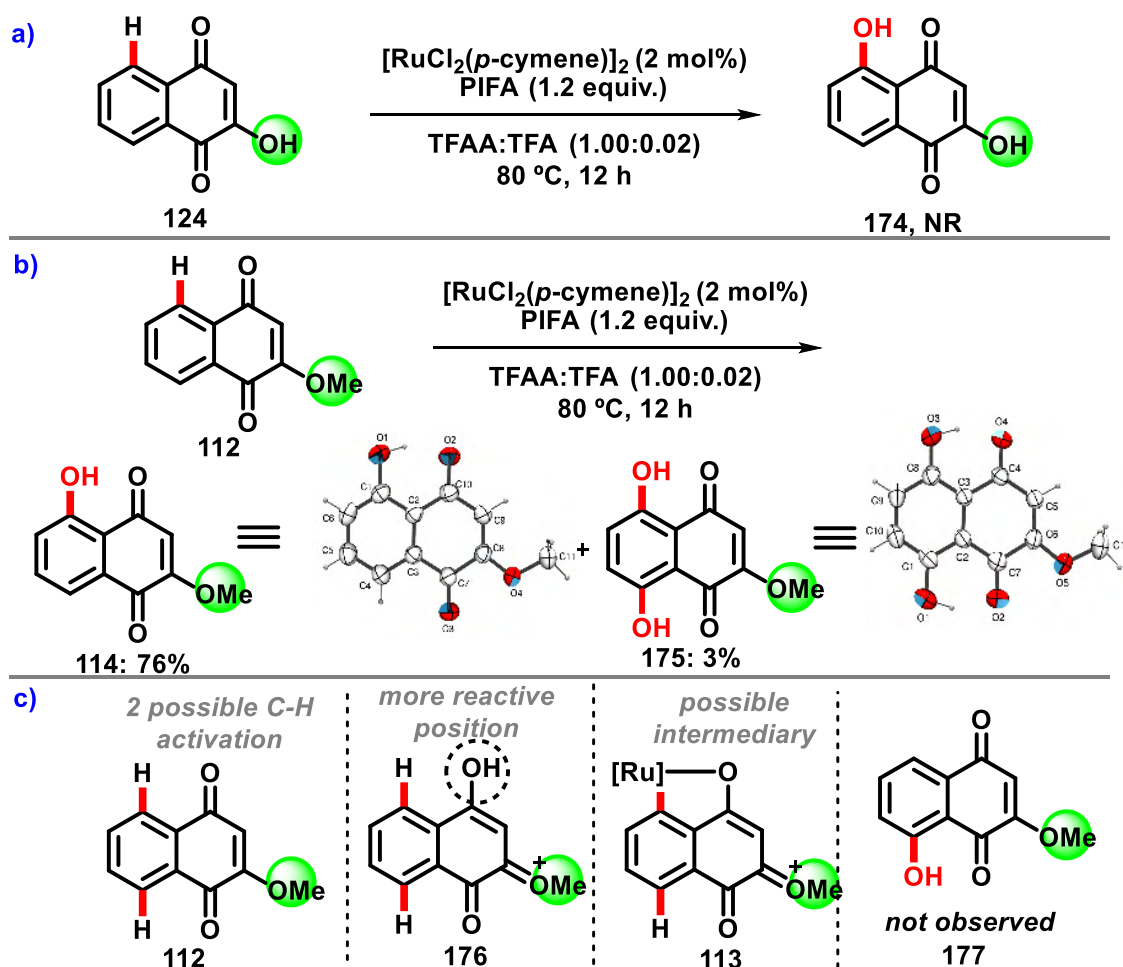
5.7 Scope of the ruthenium(II) catalyzed C–H oxygenation

The prepared quinoidal substrates were submitted to the optimized C–H oxygenation reaction protocol to evaluate the applicability of this reaction. Compound **124** was firstly used however no product was obtained (**Scheme 40a**). A similar result for C–H alkenylation of **124**

had been already observed (**Scheme 33a**) which indicates that 2-hydroxynaphthalene-1,4-dione (**124**) is not a substrate suitable for C–H activation in those reactional conditions.

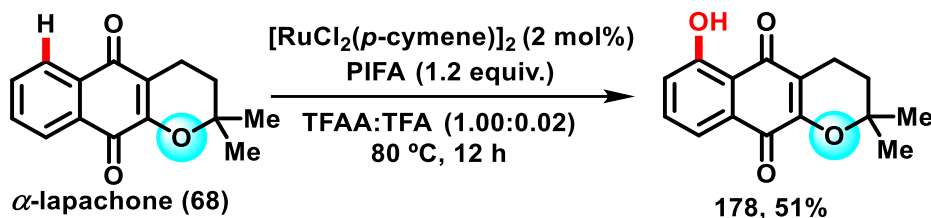
On the other hand, C–H oxygenation using 2-methoxynaphthalene-1,4-dione (**112**) led to the formation of 5-hydroxy-2-methoxynaphthalene-1,4-dione (**114**) in 76% yield and 5,8-dihydroxy-2-methoxynaphthalene-1,4-dione (**175**) in 3% yield (**Scheme 40b**).

Both products **114** and **175** were recrystallized and the projection ortep-3 from X-ray crystallography studies confirmed undoubtedly the position of hydroxyl in **114**. Those results suggest that the regioselectivity of this reaction is associated with the ability of the methoxy group to increase the electronic density of carbonyl fomenting the coordination with the metal followed by C–H activation (**Scheme 40c**). A similar observation was reported C–H alkenylation previously describe. Furthermore, no 8-hydroxy-2-methoxynaphthalene-1,4-dione (**177**, **Scheme 40c**) was observed which may indicate that 5,8-dihydroxy-2-methoxynaphthalene-1,4-dione (**175**), isolated in 3% came from **114**.



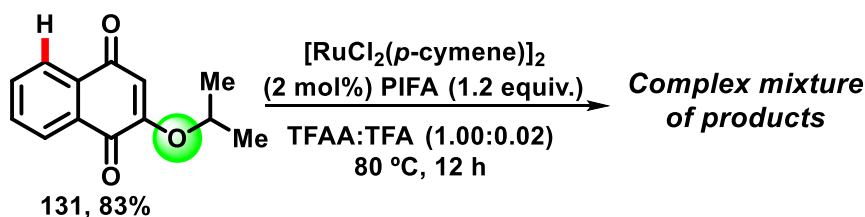
Scheme 40. a) Unsuccessful C–H oxygenation using substrates **124**, b) Synthesis of **114** and **175** c) regioselectivity possible explanation.

Compound α -lapachone (**68**) displays similar reactivity to 2-methoxynaphthalene-1,4-dione (**112**) and, indeed, C–H oxygenation resulted in a similar product **178** in 51% yield and no other product was isolated (**Scheme 41**).¹³⁹



Scheme 41. Synthesis of **178**.

Similarly, 2-isopropoxynaphthalene-1,4-dione (**131**) was submitted to the C–H oxygenation conditions, however, surprisingly, the reaction afforded a complex mixture and no product was isolated (**Scheme 42**). Probably, the reaction conditions employed led to side reactions involving the isopropoxy group.



Scheme 42. Attempt of C–H oxygenation using 2-isopropoxynaphthalene-1,4-dione (**131**).

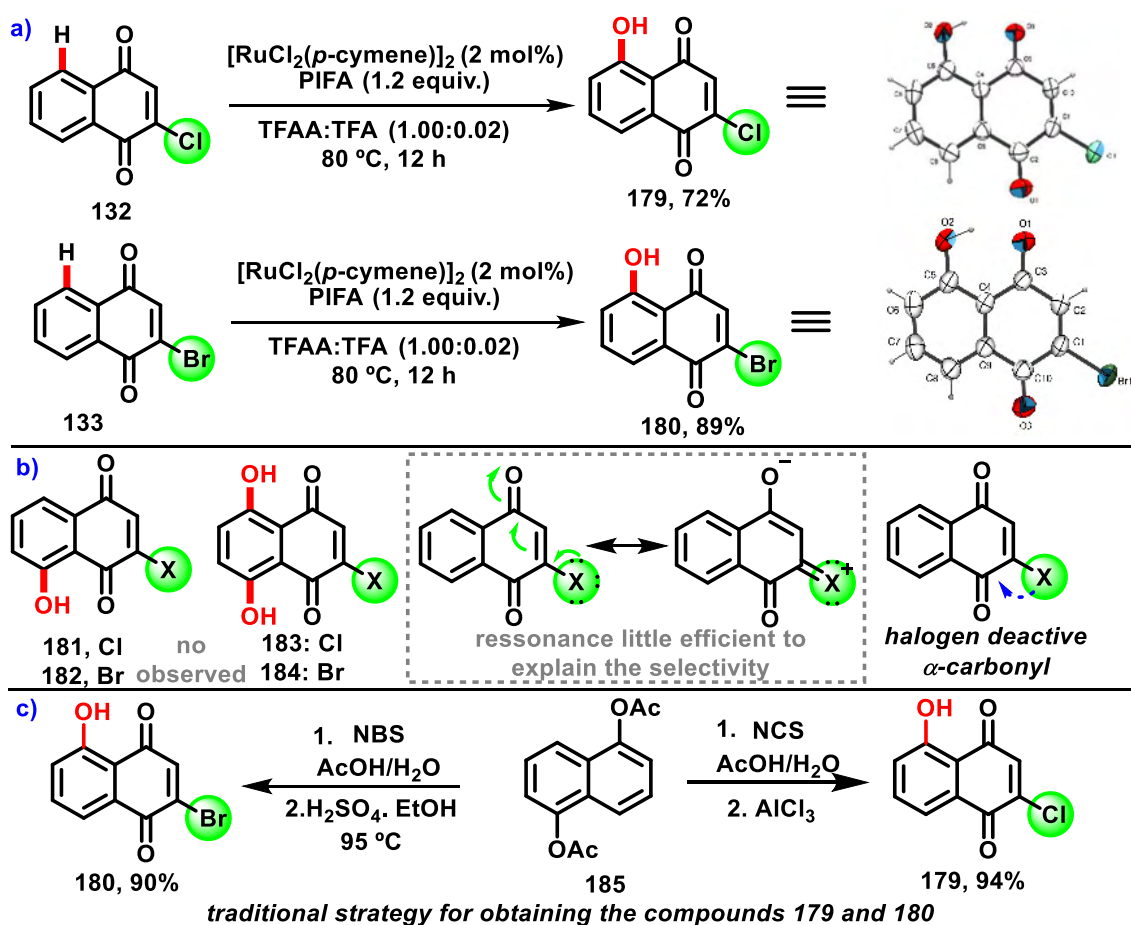
The halogenated quinoidal substrates 2-chloronaphthalene-1,4-dione (**132**) and 2-bromonaphthalene-1,4-dione (**133**) afforded the respective oxygenated products 2-chloro-5-hydroxynaphthalene-1,4-dione (**179**) in 72% yield and 2-bromo-5-hydroxynaphthalene-1,4-dione (**180**) in 89% yield (**Scheme 43a**). The X-ray diffraction studies of single crystals of **179** and **180** confirmed the regioselectivity of the C–H activation similar to the previously product.

Interestingly, no 2-halo-8-hydroxynaphthalene-1,4-dione (**181** and **182**) neither double oxygenated products (**183** or **184**) were observed (**Scheme 43b**). Although chlorine and bromine can donate electrons by resonance activating carbonyl, in a similar way to the one discussed above, this phenomenon is not efficient enough to justify the observed regioselectivity.

139. Y. Brandy, N. Brandy, E. Akinboye, M. Lewis, C. Mouamba, S. Mack, R. J. Butcher, A. J. Anderson, O. Bakare. Synthesis and characterization of novel unsymmetrical and symmetrical 3-halo- or 3-methoxy-substituted 2-dibenzoylamino-1,4-naphthoquinone derivatives. *Molecules*. **2013**, *18*, 1973-1984.

Probably, the inductive electron-withdrawing effect of the halogens deactivates the alpha-carbonyl to such an extent that prevented coordination with the metal.

Traditionally, compounds 2-chloro-5-hydroxynaphthalene-1,4-dione (**179**)¹⁴⁰ and 2-bromo-5-hydroxynaphthalene-1,4-dione (**180**)¹⁴¹ are obtained using radical oxidation of acetylated 1,5-dihydroxynaphthalene (**185**) with N-chlorosuccinimide (NCS) and N-bromosuccinimide (NBS), respectively, in acid conditions (Scheme 43c). Furthermore, **179** and **180** are strategical compounds to obtain other juglones derivatives with important biological activity.¹⁴² The C–H oxygenation developed provided an alternative of both compounds with good yields.



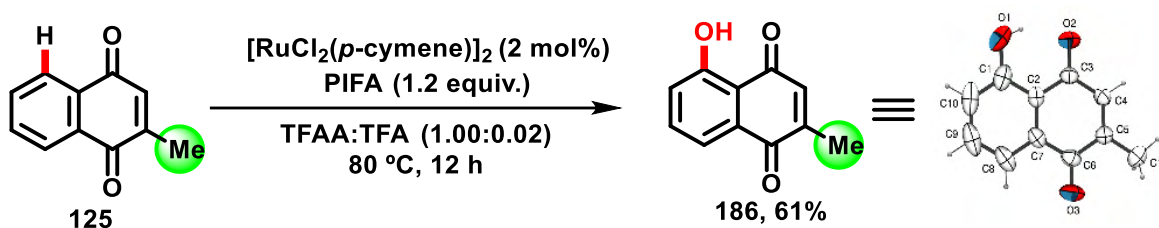
Scheme 43. a) Synthesis of 2-chloro-5-hydroxynaphthalene-1,4-dione (**179**) and 2-bromo-5-hydroxynaphthalene-1,4-dione (**180**). b) Orientation on C–H oxygenation. c) Traditional approach to synthesize **179** and **180**.

140. G. Wurm, U. Geres. Untersuchungen an 1,4-Naphthochinonen, 20. Mitt. 1): Droseron, Ether und Isomere aus Juglon. *Arch. Pharm.* **1990**, *323*, 319-322.

141. Y. Zhang, Q. Ye, X. Wang, Q. She, J. S. Thorson. A divergent enantioselective strategy for the synthesis of griseusins. *Angew. Chem. Int. Ed.* **2015**, *54*, 11219-11222.

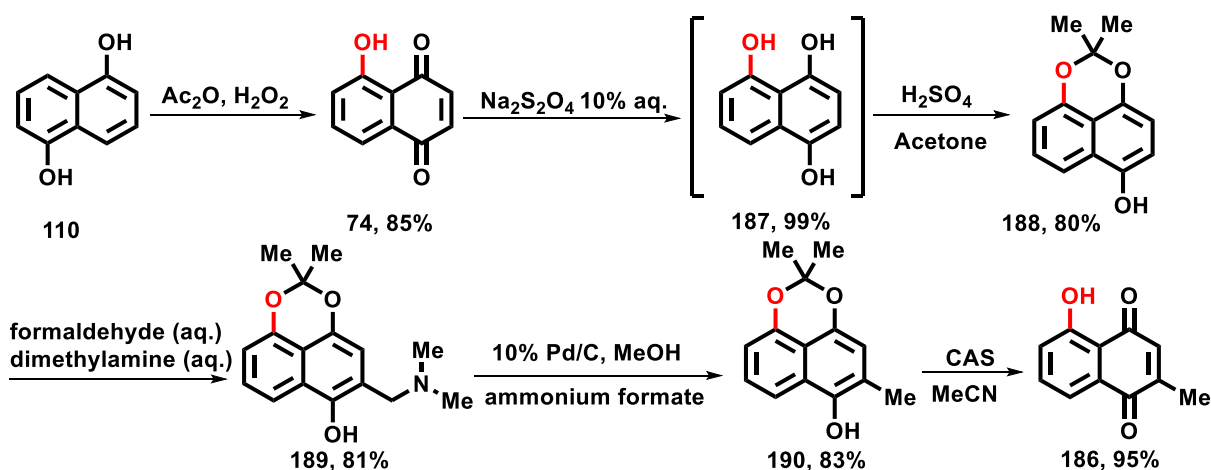
142. E. Brötz, J. Herrmann, J. Wiese, H. Zinecker, A. Maier, G. Kelter, J. F. Imhoff, R. Müller, T. Paululat. Synthesis and cytotoxic activity of a small naphthoquinone library: First synthesis of juglonbutin. *Eur. J. Org. Chem.* **2014**, *24*, 5318-5330.

C–H oxygenation conditions were employed to the commercially available 2-methylnaphthalene-1,4-dione (also known as menadione, **125**) and the product 5-hydroxy-2-methylnaphthalene-1,4-dione (**186**), commonly called plumbagin, was achieved in 61% yield (**Scheme 44**). The regioselectivity of the C–H oxygenation was confirmed by X-ray diffraction of a single crystal of the product and, despite the absence of electron donor effect by resonance, same regioselectivity pattern was observed, an intriguing question that requires more careful investigation. Furthermore, no other product was obtained.



Scheme 44. Synthesis of 5-hydroxy-2-methylnaphthalene-1,4-dione (plumbagin, **186**).

In 2018, Sun and co-workers synthesized **186**, as shown in **Scheme 45**, in 6 steps in 45% global yield.¹⁴³ Here, the synthesis of **186** is reported in one single step with 61% yield. Given the relevance of this expensive¹⁴⁴ compound with a broad spectrum of biological applicability, this new synthetic methodology represents a new advance in the synthesis of plumbagin (**186**).

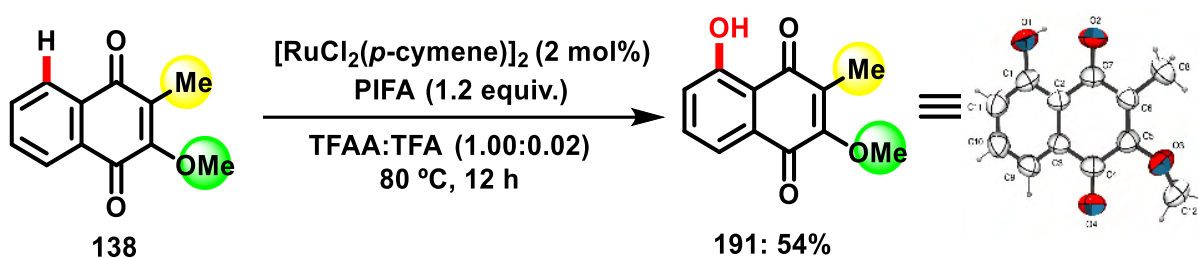


Scheme 45. Synthesis of plumbagin (**186**) carried out by Sun and co-workers.¹⁴³

143. N. Bao, J. Ou, W. Shi, N. Li, L. Chen, J. Sun. Highly efficient synthesis and structure–activity relationships of a small library of Substituted 1,4-naphthoquinones. *Eur. J. Org. Chem.* **2018**, *19*, 2254-2258.

144. For example: 100 mg = R\$ 408.00. site: [Plumbagin | 481-42-5 | Sigma-Aldrich](#) (accessed 24.02.2021).

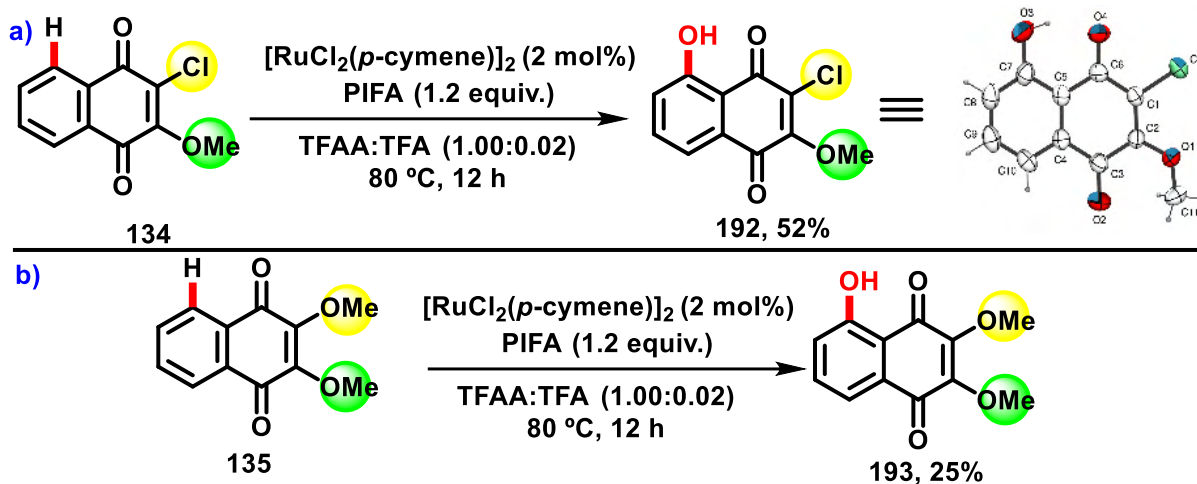
2-methoxy-3-methylnaphthalene-1,4-dione (**138**) was used as a substrate for C–H oxygenation resulting in the compound 5-hydroxy-2-methoxy-3-methylnaphthalene-1,4-dione (**191**) in 54% yield and no other product was isolated (**Scheme 46**). The corrected assignment of the hydroxyl group was accomplished *via* the ortep-3 projection obtained *via* X-ray diffraction of a single crystal of **191**. Once again, the effect of the methoxy group in activating a carbonyl followed by induction of C–H activation was observed.



Scheme 46. Synthesis of 5-hydroxy-2-methoxy-3-methylnaphthalene-1,4-dione (**191**).

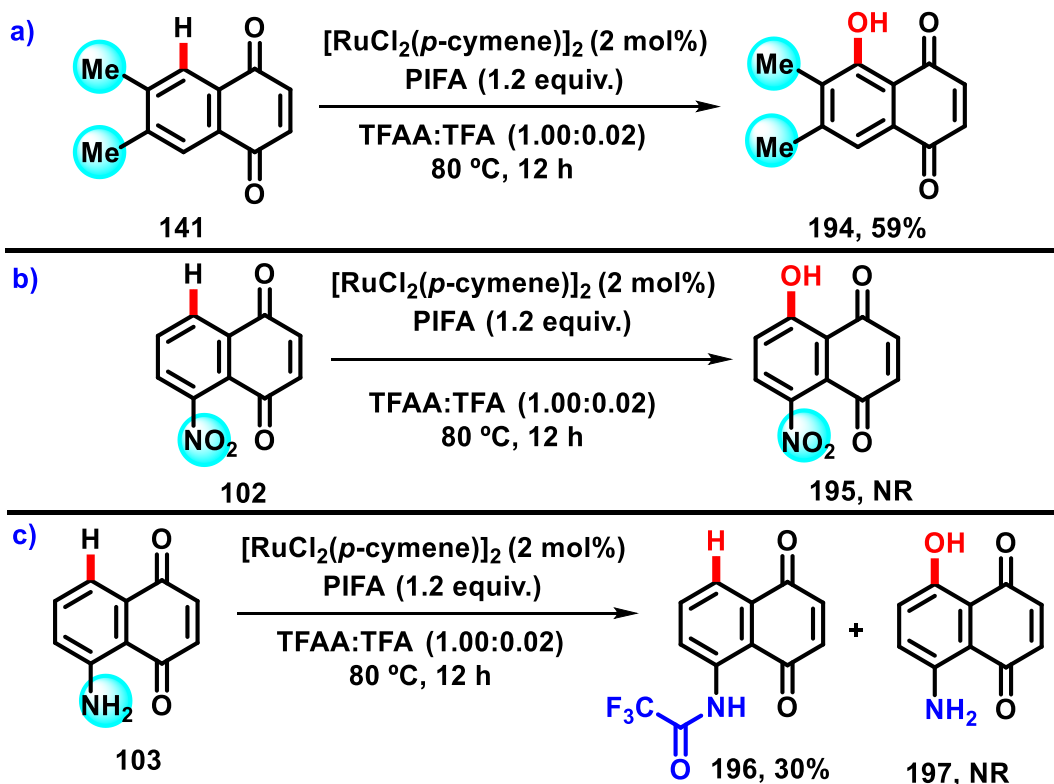
Still aiming to evaluate the effect of donor groups and counter with the effect of withdrawal group, compound 2-chloro-3-methoxynaphthalene-1,4-dione (**134**) was submitted to C–H oxygenation conditions resulting in compound 3-chloro-5-hydroxy-2-methoxy-naphthalene-1,4-dione (**192**) in 52% yield and no other product was observed (**Scheme 47a**). In accordance with previous results, ortep-3 projection of **192** indicated the position of hydroxy group.

In the case of the substrate bearing two methoxy groups, 2,3-dimethoxynaphthalene-1,4-dione (**135**), product 5-hydroxy-2,3-dimethoxynaphthalene-1,4-dione (**193**) was isolated unfortunately in only 25% yield and no other product neither started material was isolated (**Scheme 47b**). Then, tune modification in optimized conditions was performed to increase the yield of reaction. Those modifications included performing the reaction in absence of TFA; additions of 1 mL of DCM to increase the solubility of **135** in TFAA; decrease the temperature of reaction to 60 °C and in none of those modifications the yield of reaction change significantly.



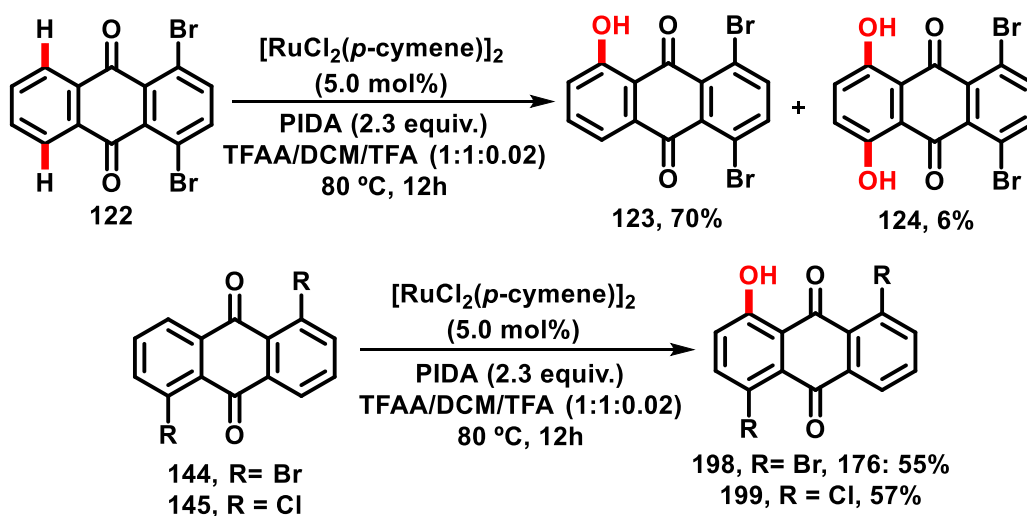
Scheme 47. a) Synthesis 3-chloro-5-hydroxy-2-methoxynaphthalene-1,4-dione (**192**) and b) 5-hydroxy-2,3-dimethoxynaphthalene-1,4-dione (**193**).

Three examples of 1,4-naphthoquinone with modified benzenoid rings were used in C–H oxygenation reactions. Compound 6,7-dimethylnaphthalene-1,4-dione (**141**) led to the formation of product 5-hydroxy-6,7-dimethylnaphthalene-1,4-dione (**194**) in 59% yield (**Scheme 48a**) whereas for 5-nitronaphthalene-1,4-dione (**102**) no product was achieved and **102** was recovered (**Scheme 48b**). 5-aminonaphthalene-1,4-dione (**103**) submitted to C–H alkenylation also resulted in no desired product, however, the acetylated substrate (**196**) was isolated in 30% yield (**Scheme 48c**).



Scheme 48. a) Synthesis of 5-hydroxy-6,7-dimethylnaphthalene-1,4-dione (**194**) and attempts of C–H oxygenation using b) 5-nitronaphthalene-1,4-dione (**102**) and c) 5-aminonaphthalene-1,4-dione (**103**).

The applicability of C–H oxygenation methodology for anthracene-9,10-dione derivatives was studied in three examples (**Scheme 49**). Compounds **122**, **144** and **145** were submitted to C–H oxygenation reactions, as previously optimized for anthracene-9,10-dione substrates, to provide **197** in 70% yield, **198** in 55% yield and **199** in 57% yield.



Scheme 49. Synthesis of oxygenated anthracene-9,10-dione **197**, **198** and **199**.

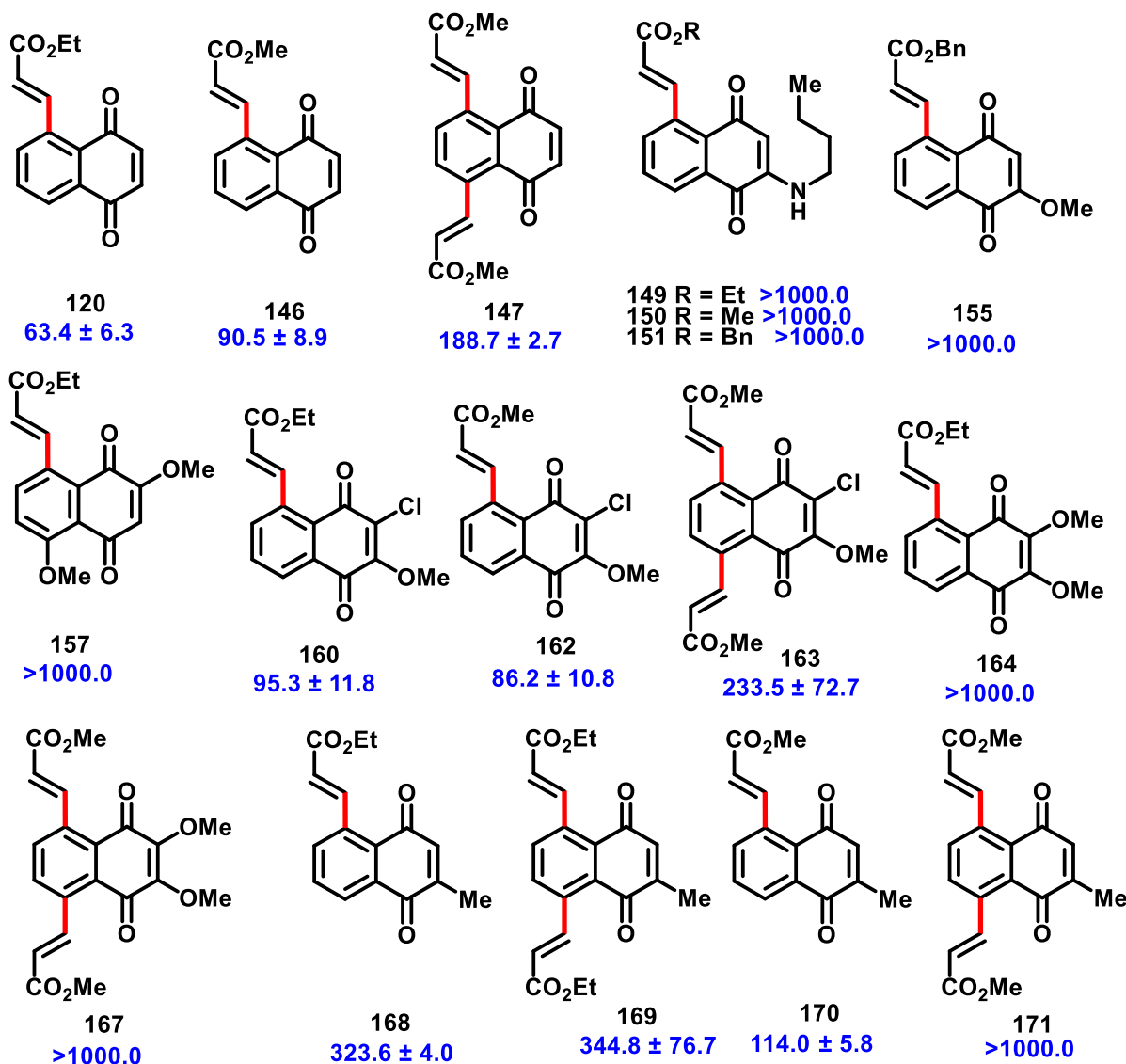
5.8 Biological Assays against *Trypanosoma cruzi*

Biological assays against *T. cruzi* with selected naphthoquinones obtained through C–H oxygenation and alkenylation were carried out by the group of Dr. R. Menna-Barreto and the results are demonstrated in **Scheme 50** and **Scheme 51**.

Compounds **120** ($IC_{50} = 63.4 \pm 6.3$) and **146** ($IC_{50} = 90.5 \pm 8.9$) were more active than benznidazole ($IC_{50} = 103.6 \pm 0.6$).¹⁴⁵ **147** ($IC_{50} = 188.7 \pm 2.7$), besides also active, was less active than **146**. Electron-donating groups in quinone such as amine (**149-151**), methoxy (**155-157**) and 2,3-dimethoxy (**164** and **167**) led to inactive substances against the parasite. However, compounds bearing an electron donating groups associated with chlorine were active, as **160** ($IC_{50} = 95.3 \pm 11.8 \mu\text{M}$), **162** ($IC_{50} = 86.2 \pm 10.8 \mu\text{M}$) and **163** ($IC_{50} = 233.5 \pm 72.7 \mu\text{M}$). Menadione derivatives **168** ($IC_{50} = 323.6 \pm 4.0 \mu\text{M}$), **169** ($IC_{50} = 344.8 \pm 76.7 \mu\text{M}$) presented good activity and **170** ($IC_{50} = 114.0 \pm 5.8$) was almost as active as the benznidazole ($IC_{50} = 103.6 \pm 0.6$). However, **171** was not active and, in general way, bis-acrylated substances were not active or less active than the respective mono-acrylated product.

Those biological assays against *T. cruzi* indicate that new 1,4-naphthoquinones prototypes could be planned based on mono-alkenylation with chlorine and/or methyl at position C-2/C-3 or without substituents in those positions.

145. a) M. N. Soeiro, S. L. de Castro. *Trypanosoma cruzi* targets for new chemotherapeutic approaches. *Expert Opin. Ther. Targets*. **2009**, *13*, 105-121; **b)** J. A. Urbina. Specific chemotherapy of Chagas disease: Relevance, current limitations and new approaches. *Acta Trop.* **2010**, *115*, 55-68.



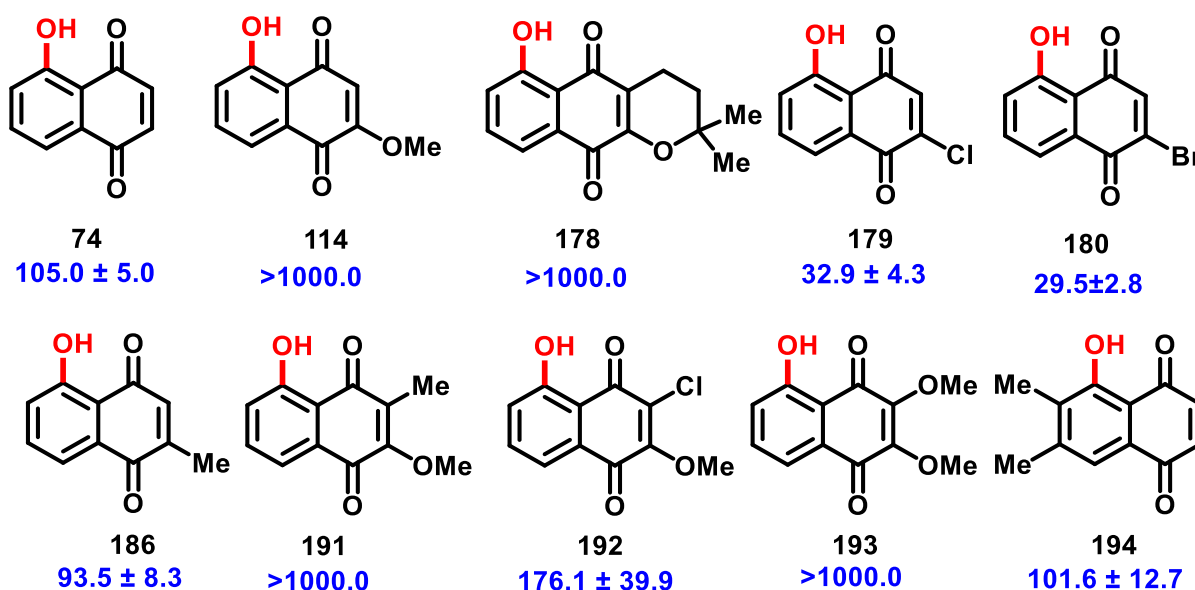
Scheme 50. Biological activity of selected product from C–H alkenylation. Values of IC₅₀ in μM.

As previously described, compounds bearing a juglone moiety exhibit different biological activity, in this sense, the molecules here obtained *via* C–H oxygenation methodology were subject to biological assays to evaluate its potential activity against *T. cruzi* as well.

Biological assays results have indicated that juglone (**74**) exhibit activity against *T. cruzi* with IC₅₀ = 105.0 ± 5.0 μM, however, the insertion of the methoxy group in compound **114** leads to inactivity of this class of compounds (**Scheme 51**).

On the other hand, halogen at compounds **179** and **180** increases the activity of the juglone to IC₅₀ = 32.9 ± 4.3 μM and 29.5 ± 2.8 μM. Compound **114**, considered inactive, became active with the insertion of chlorine and the substance **160** present moderate activity with IC₅₀ = 176.1 ± 39.9.

It is noteworthy to mention that compound **179** and **180** present IC_{50} much lower than benznidazole ($IC_{50} = 103.6 \pm 0.6$), the standard drugs for the treatment of Chagas disease. Those results showed that the presence of halogen leads to the increase of biological activity of juglones derivatives against *T. cruzi*. The compound **180**, plumbagin, recognized for potent activity antimicrobial,¹⁴⁶ antimalarial,¹⁴⁷ anti-inflammatory,¹⁴⁸ anticarcinogenic,¹⁴⁹ and others exhibited high activity with $IC_{50} = 93.5 \pm 8.3$. Unfortunately, compounds **191**, **193**, and **178** were not active.



Scheme 51. Biological activity of selected product from C–H oxygenation. Values of IC_{50} in μM .

146. S. R. de Paiva, M. R. Figueiredo, T. V. Aragão, M. A. C. Kaplan. Antimicrobial activity *in vitro* of plumbagin isolated from *Plumbago* species. *Mem. Inst. Oswaldo Cruz.* **2003**, *98*, 959-961.

147. K. Likhitwitayawuid, R. Kaewamatawong, N. Ruangrunsi, J. Krungkrai. Antimalarial naphthoquinones from *Nepenthes thorelii*. *Planta Med.* **1998**, *64*, 237-241.

148. R. Checker, D. Sharma, S. K. Sandur, G. Subrahmanyam, S. Krishnan, T. B. Poduval, K. B. Sainis. Plumbagin inhibits proliferative and inflammatory responses of T cells independent of ROS generation but by modulating intracellular thiols. *J. Cell. Biochem.* **2010**, *110*, 1082-1093.

149. B. R. Subramaniya, G. Srinivasan, S. S. Sadullah, N. Davis, L. B. Subhadara, D. Halagowder, N. D. Sivasi-tambaram. Apoptosis inducing effect of plumbagin on colonic cancer cells depends on expression of COX-2. *PLoS ONE.* **2011**, *6*, 18695.

6. CONCLUSION

Several reaction conditions based on C–H alkenylation and oxygenation were accomplished to develop new protocols to modify the benzenoid ring of 1,4-naphthoquinones. Those studies allow us to establish a new C–H alkenylation protocol, which, although offered a modest yield, resulted in different products *via* efficient and practical procedures. New C–H oxygenation protocol allowed us to obtain juglones derivatives in satisfactory yields *via* efficient as well.

The present work contributed to development of more efficient synthetic strategies to modify the benzenoid moiety of 1,4-naphthoquinones and increase the scope of this class of molecule in new 20 examples (alkenylated molecules). Although juglone derivatives have already been published, here a new synthetic alternative has been presented to obtain such compounds. The relevance of this new alternative is rooted in their potent biological activity.

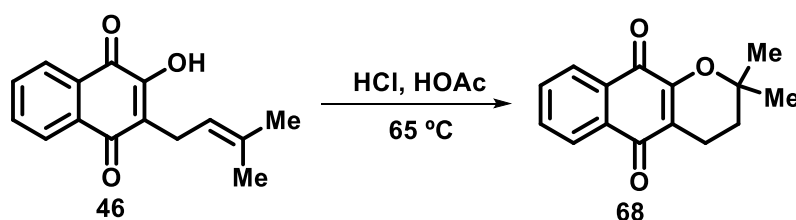
Compounds obtained here (21 alkenylated products and 10 juglones derivatives) were evaluated against the *Trypanosoma cruzi* and several of them displayed potent activity. For example, compounds **120**, **160** and **162** exhibited IC₅₀ less than benznidazole, the standard drug for the treatment of Chagas disease. Compounds **179** and **180** were three times more potent against the *Trypanosoma cruzi* compared to benznidazole.

7. EXPERIMENTAL SECTION

General Remarks

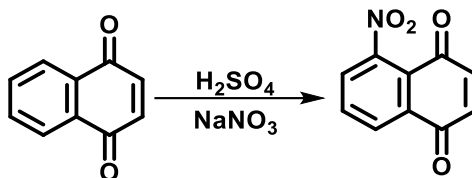
All catalytic reactions were carried out under air using pre-dried 25 mL Schlenk- or pressure tubes. 1,4-Naphthoquinone (**61**) was purified *via* reduced pressure sublimation using a cold finger sublimation apparatus (50 °C, 0.9 mbar) and stored in a glovebox to prevent contact with moisture. Other chemicals were obtained from commercial sources and used without further purification. Yields refer to isolated compounds, estimated to be > 95% pure as determined by ¹H NMR and GC. TLC: Merck, TLC Silica gel 60 F₂₅₄, detection at 254 nm. Chromatographic separations were carried out on Merck Geduran SI-60 (0.040–0.063 mm). IR spectra were recorded on a Bruker ATR FT-IR Alpha device. MS: EI-MS: Jeol AccuTOF at 70 eV; ESI-MS: Bruker maXis and MicrOTOF. High-resolution mass spectrometry (HRMS): Bruker maXis, Bruker MicrOTOF and Jeol AccuTOF. Melting points (M.p.): Büchi 540 capillary melting point apparatus, values are uncorrected. NMR spectra were recorded on Varian Mercury VX 300, Inova-500, Inova-600 and Bruker Avance 300, Avance III 300, Avance III HD 400, Avance III 400, Avance III HD 500 instruments, chemical shifts (δ) are provided in ppm. ChemDraw Professional 16.0 was used to generate the IUPAC names of the compounds.

7.1 Synthesis of Substrates

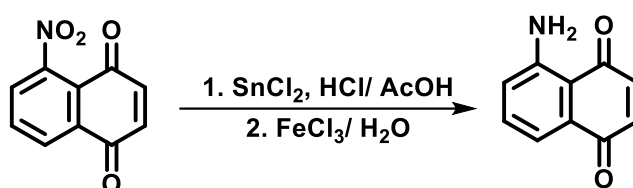


α -lapachone (68): Lapachol (**67**) (0.97 g, 4.00 mmol) was dissolved in HCl (40 mL) and HOAc (15 mL) at 25 °C. Then, the mixture was heated to 65 °C for 1 h. After cooling to 25 °C, cold H₂O (250 mL) was added and the solid was filtered off. Recrystallization from EtOH provided α -lapachone (**68**) (0.61 g, 63%) as a yellow solid. ¹H NMR (400 MHz, CDCl₃) δ : 8.02 (t, J = 8.0, 2H), 7.66-7.59 (m, 2H), 2.57 (t, J = 6.4 Hz, 2H), 1.77 (t, J = 6.4 Hz, 2H), 1.39 (s, 6H). ¹³C NMR (100 MHz, CDCl₃) δ : 184.3, 179.9, 154.6, 133.8, 132.9, 131.1, 126.2, 125.9, 120.1, 78.1,

31.4, 26.4, 16.7. **m. p.** (°C) = 113-115. Data are consistent with those reported in the literature (ref. 134, p. 41).

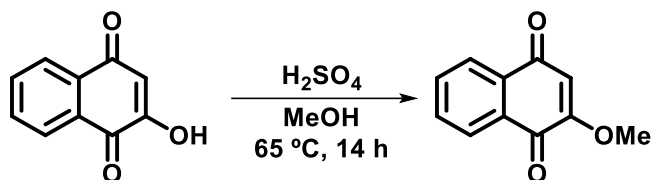


5-nitronaphthalene-1,4-dione (102): 1,4-naphthoquinone (**61**) (6.3 mmol, 1.00 g) was added slowly, over 10 minutes, to vigorously stirred concentrated sulfuric acid (15 ml) at 0 °C. A solution of NaNO₃ (41 mmol, 3.5 g) in concentrated sulfuric acid (5 mL) was then added over 3 minutes. The ice bath was removed and the mixture was stirred at 25 °C for 1h. The reaction mixture was then heated at 40 °C for 15 minutes, cooled to 25 °C, and the resulting orange solution was poured onto ice (100 g). The yellow precipitate was filtered, washed with water and dried under vacuum. After dried, the crude product was purified by column chromatography in silica gel (*n*-hexane/EtOAc 25:1) to afford 5-nitronaphthalene-1,4-dione (**102**, 934 mg, 73%). ¹H NMR (400 MHz, CDCl₃) δ: 8.25 (dd, *J* = 7.6 and 1.2 Hz, 1H), 7.87 (t, *J* = 8.0 Hz, 1H), 7.71 (dd, *J* = 8.0 and 0.8 Hz, 1H), 7.03 (d, *J* = 10.4 Hz, 1H), 6.99 (d, *J* = 10.4 Hz, 1H). ¹³C NMR (100 MHz, CDCl₃) δ: 182.5; 181.2, 139.0, 138.1, 134.7, 132.6, 128.9, 127.5 122.8. **m. p.** (°C) = 167-168. Data are consistent with those reported in the literature (ref. 135, p. 41).

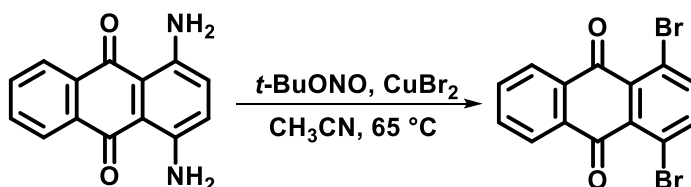


5-aminonaphthalene-1,4-dione (103): 5-nitronaphthalene-1,4-dione (2.5 mmol, 0.5 g) was dissolved in AcOH (20 mL) and heated at 50 °C in a 100 mL round bottom flask. Then, a solution of SnCl₂·2H₂O (13.3 mmol, 3.00 g) in concentrated HCl (5 mL) was added. The mixture was heated at 70 °C for 40 minutes and cooled at 25 °C. A solution of FeCl₃·6H₂O (16.1 mmol, 4.35 g) in cold H₂O (5 mL) was added and stirring was continued for 30 minutes. The mixture was poured into ice (50 g) and kept under the refrigerator for 12 h. The resulting solid was filtered, washed with water and dried under reduced pressure to 5-aminonaphthalene-1,4-dione (**103**) (260 mg, 60% yield) as a purple solid; ¹H NMR (400 MHz, CDCl₃) δ: 7.40-7.39

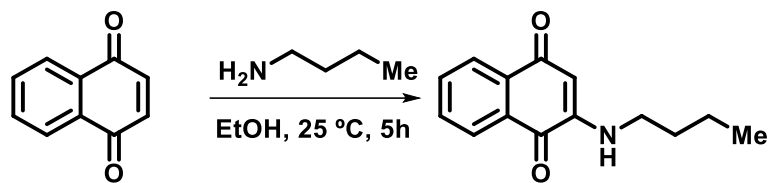
(m, 2H), 6.94-6.90 (m, 1H), 6.85 (d, $J = 8.0$ Hz, 1H), 6.81 (d, $J = 8.0$ Hz, 1H), 6.64 (bs, 2H). ^{13}C NMR (100 MHz, CDCl_3) δ : 187.1, 185.4, 150.1, 140.6, 137.3, 134.6, 132.9, 123.2, 117.0, 112.3. **m. p.** ($^\circ\text{C}$) = 188-189. Data are consistent with those reported in the literature (ref. 135, p. 41).



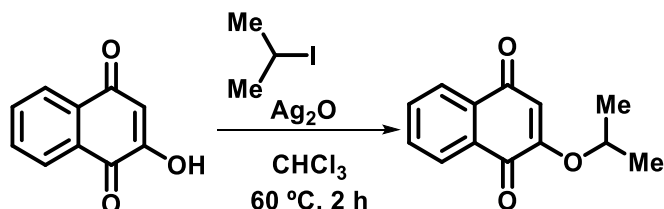
2-methoxynaphthalene-1,4-dione (112): 2-hydroxynaphthalene-1,4-dione (**124**) (1.04 g, 6.00 mmol) and concentrated sulfuric acid (0.4 mL) were added to MeOH (150 mL). The mixture was heated to $65\text{ }^\circ\text{C}$ for 14 h and cooled to $25\text{ }^\circ\text{C}$, then the solid was filtered and washed with MeOH (50 mL) and H_2O (100 mL) to provide 2-methoxynaphthalene-1,4-dione (**112**) (1.03 g, 91%). ^1H NMR (300 MHz, CDCl_3) δ : 8.09-8.06 (m, 1H), 8.04-8.02 (m, 1H), 7.73-7.63 (m, 2H), 6.13 (s, 1H), 3.87 (s, 3H); ^{13}C NMR (75 MHz, CDCl_3) δ : 184.6, 179.9, 160.3, 134.2, 133.2, 131.9, 130.9, 126.6, 126.1, 109.8, 56.4; **m. p.** ($^\circ\text{C}$) = 186-188. Data are consistent with those reported in the literature (ref. 127, p. 38).



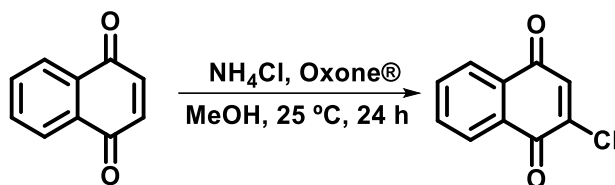
1,4-dibromoanthracene-9,10-dione (122): 1,4-diaminoanthracene-9,10-dione (**142**) (2.00 g, 8.39 mmol), CuBr_2 (4.23 g, 18.9 mmol) and tert-butyl nitrite, $t\text{-BuONO}$ (1.95 g, 18.9 mmol) were added to MeCN (15 mL). The mixture was heated to $65\text{ }^\circ\text{C}$ for 5 h and then cooled to $25\text{ }^\circ\text{C}$. An aqueous solution of HCl (1M, 100 mL) was added and the solution was extracted with CH_2Cl_2 (4 x 20 mL). Subsequently, the organic extracts were dried over Na_2SO_4 and the solvent was evaporated under reduced pressure. Then, the product was purified by column chromatography (PhMe) to yield 1,4-dibromoanthracene-9,10-dione (**122**) (2.58 g, 84%) as a yellow solid. ^1H NMR (300 MHz, CDCl_3) δ : 8.14 (dd, $J = 6.0$ and 0.3 Hz, 2H), 7.76 (s, 2H), 7.75-7.73 (m, 2H); ^{13}C NMR (75 MHz, CDCl_3) δ : 181.4, 140.5, 134.1, 133.4, 133.3, 126.8, 122.0; **m. p.** ($^\circ\text{C}$) = 220-221. Data are consistent with those reported in the literature (ref. 137, p. 42).



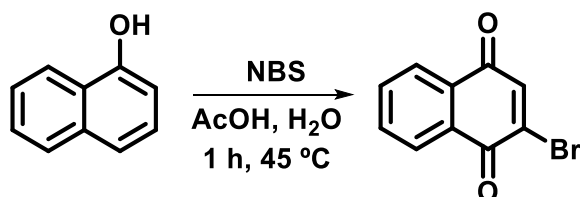
2-(butylamino)naphthalene-1,4-dione (129): 1,4-Naphthoquinone (**61**) (950 mg, 6.00 mmol) in dichloromethane (5 mL) was added slowly to a solution of *n*-butylamine (1.8 mL, 18 mmol) in ethanol (10 mL) under magnetic stirring at 25 °C. After 5 h the solvent was evaporated and the product was purified by using silica gel column chromatography (*n*-hexane/EtOAc 20:1) to provide the product 2-(butylamino)naphthalene-1,4-dione (**129**) as an orange solid (839 mg, 61%). ¹H NMR (300 MHz, CDCl₃) δ: 8.06 (dd, *J* = 7.5 and 1.2 Hz, 1H), 8.00 (dd, *J* = 7.5 and 1.2 Hz, 1H), 7.68 (td, *J* = 7.5 and 1.5 Hz, 1H), 7.57 (td, *J* = 7.5 and 1.5 Hz, 1H), 5.86 (s, 1H), 5.70 (s, 1H), 3.18-3.12 (m, 2H), 1.70-1.60 (m, 2H), 1.44-1.37 (m, 2H), 0.94 (t, *J* = 7.5 Hz, 3H). ¹³C NMR (75 MHz, CDCl₃): 182.7, 181.8, 147.8, 134.6, 133.6, 131.8, 130.4, 126.1, 126.0, 100.7, 42.3, 30.3, 20.3, 13.8. **m. p.** (°C) = 122-124. Data are consistent with those reported in the literature (ref. 126, p. **Erro! Indicador não definido.**).



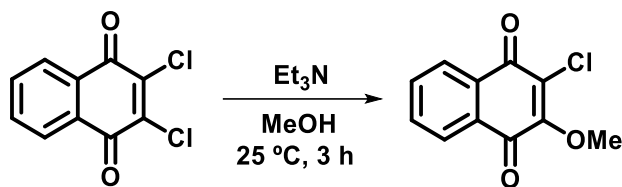
2-isopropoxynaphthalene-1,4-dione (131): 2-hydroxynaphthalene-1,4-dione (**90**) (376 mg, 2.00 mmol), Ag₂O (0.7 g, 3.0 mmol) and 2-iodo-propane (0.40 mL, 4.00 mmol) were dissolved in CHCl₃ (50 mL) and heated to 60 °C for 48 h. After cooling to 25 °C, the solids were removed through filtration through a Celite pad. The solvent was evaporated under reduced pressure. After purification by column chromatography on silica gel (*n*-hexane/EtOAc 5:1) the 2-isopropoxynaphthalene-1,4-dione (**131**) (287 mg, 71%) was obtained as a yellow solid in 83% yield. ¹H NMR (300 MHz, CDCl₃) δ: 8.07 (ddd, *J* = 7.5, 0.9 and 0.6 Hz, 1H); 7.84 (dd, *J* = 7.5 and 0.9 Hz, 1H); 7.64 (td, *J* = 7.5 and 1.5 Hz, 1H); 7.54 (td, *J* = 7.5 and 1.5 Hz, 1H); 5.91 (d, *J* = 0.3 Hz, 1H); 4.70 (sd, *J* = 6.0 and 0.6 Hz, 1H); 1.45 (d, *J* = 6.0 Hz, 6H). ¹³C NMR (75 MHz, CDCl₃) δ: 179.5, 179.3, 166.6, 134.7, 132.4, 131.3, 130.5, 128.8, 124.8, 103.8, 73.0, 21.6; **m. p.** (°C) = 121-122. Data are consistent with those reported in the literature (ref. 128, p. 38).



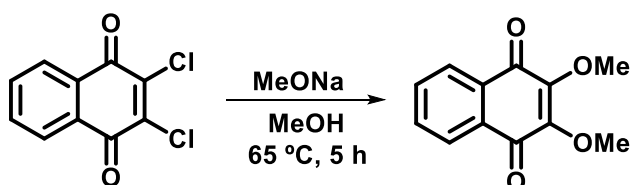
2-chloronaphthalene-1,4-dione (132): 1,4-naphthoquinone (61) (158 mg, 1.00 mmol) and NH_4Cl (60 mg, 1.1 mmol) were added to MeOH (5 mL) under vigorous stirring. Oxone® (338 mg, 1.1 mmol) was slowly added and the solution was allowed to stir at 25 °C for 24 hours. H_2O was added (5 mL), the organic phase was extracted with EtOAc (10 mL) and dried over Na_2SO_4 . Purification by column chromatography on silica gel (*n*-hexane/EtOAc 25:1) yielded 2-chloronaphthalene-1,4-dione (132) (102 mg, 53%) as a yellow solid. $^1\text{H NMR}$ (400 MHz, CDCl_3) δ : 8.05-8.03 (m, 1H), 7.97-7.94 (m, 1H), 7.67-7.63 (m, 2H), 7.09 (s, 1H); $^{13}\text{C NMR}$ (100 MHz, CDCl_3) δ : 182.9, 178.2, 146.6, 136.1, 134.7, 134.4, 132.0, 131.5, 127.7, 127.0; **m. p.** (°C) = 72-75. Data are consistent with those reported in the literature (ref. 129, p. 39).



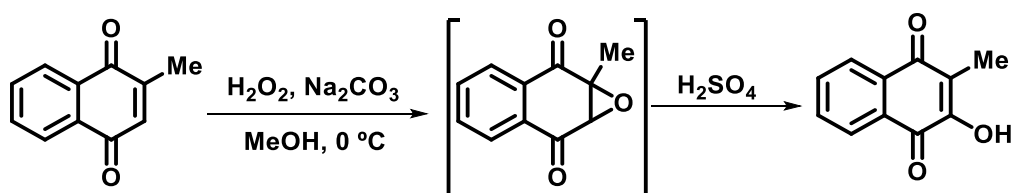
2-bromonaphthalene-1,4-dione (133): 1-Naphthol (111) (1.0 g, 7.0 mmol) was dissolved in HOAc (70 mL) and added dropwise to a solution of *N*-bromosuccinimide (4.5 g, 26 mmol in 70 mL HOAc/70 mL H_2O) at 45 °C. After 1 h the mixture was cooled to 25 °C and H_2O (70 mL) was added. The mixture was extracted with CH_2Cl_2 and the organic layer was washed with sat. aq. NaHCO_3 and dried over Na_2SO_4 . The solvent was removed and the crude product purified by column chromatography on silica gel (*n*-hexane/EtOAc 20:1) to yield 2-bromonaphthalene-1,4-dione (133) (78%). $^1\text{H NMR}$ (400 MHz, CDCl_3) δ : 8.15-8.12 (m, 1H), 8.06-8.04 (m, 1H), 7.77-7.71 (m, 2H), 7.48 (s, 1H); $^{13}\text{C NMR}$ (100 MHz, CDCl_3) δ : 182.4, 177.8, 140.3, 140.1, 134.4, 134.1, 131.7, 130.9, 127.8, 126.8; **m. p.** (°C) = 130-132. Data are consistent with those reported in the literature (ref. 130, p. 39).



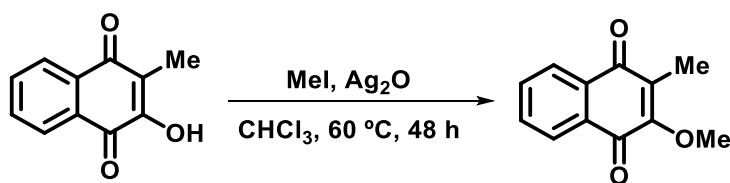
2-chloro-3-methoxynaphthalene-1,4-dione (134): 2,3-Dichloronaphthalene-1,4-dione (**126**) (0.91 g, 4.00 mmol) and Et₃N (0.61 mL, 4.40 mmol) were dissolved in MeOH (35 mL) at 25 °C. After 3 h, the solid was filtered off and washed with cold H₂O (50 mL) to afford 2-chloro-3-methoxynaphthalene-1,4-dione (**134**) (705 mg, 79%) as a green solid. ¹H NMR (300 MHz, CDCl₃) δ: 8.12-8.09 (m, 1H), 8.06-8.03 (m, 1H), 7.73-7.70 (m, 2H), 4.28 (s, 3H); ¹³C NMR (75 MHz, CDCl₃) δ: 179.5, 178.4, 156.6, 134.2, 133.8, 131.0, 128.2, 127.7, 126.9, 126.8, 61.8; **m. p.** (°C) = 143-145. Data are consistent with those reported in the literature (ref. 131, p. 40).



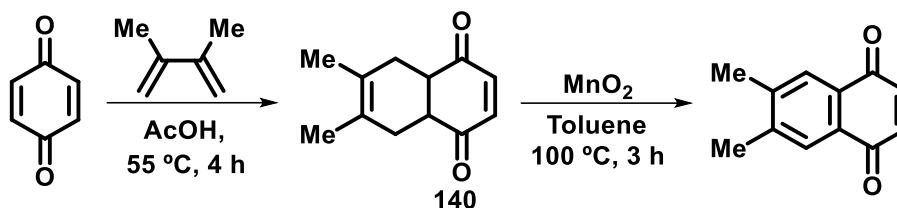
2,3-dimethoxynaphthalene-1,4-dione (135): 2,3-Dichloronaphthalene-1,4-dione (**126**) (1.09 g, 5.00 mmol) and NaOMe (0.81 g, 15.0 mmol) were dissolved in MeOH (25 mL) and heated to 65 °C for 5 h. Then, a second portion of MeONa (0.81 g, 15.0 mmol) was added and the mixture was heated to 65 °C for 1 h. The solvent was evaporated and H₂O (20 mL) was added. The solid was filtered off and washed with H₂O (100 mL) to provide 2,3-dimethoxynaphthalene-1,4-dione (**135**) (810 mg, 74%) as a yellow solid. ¹H NMR (300 MHz, CDCl₃) δ: 7.97 (d, *J* = 5.7 Hz, 1H), 7.96 (d, *J* = 5.7 Hz, 1H), 7.62 (d, *J* = 5.7 Hz, 1H), 7.61 (d, *J* = 5.7 Hz, 1H), 4.04 (s, 6H); ¹³C NMR (75 MHz, CDCl₃) δ: 181.6, 147.3, 133.5, 130.6, 126.0, 61.3; **m. p.** (°C) = 112-114. Data are consistent with those reported in the literature (ref. 132, p. 40).



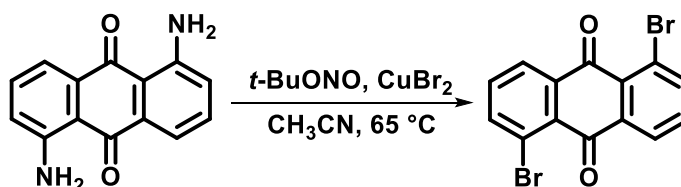
2-hydroxy-3-methylnaphthalene-1,4-dione (137): 2-Methyl-1,4-naphthoquinone (**125**), (1.0 g, 5.8 mmol) was dissolved in methanol (10 mL) at 0 °C. Then, a solution of Na₂CO₃ (0.2 g in 1 mL of water) and H₂O₂ (1 mL of H₂O₂ 30 % in 5 mL of water) were added slowly. Water (100 mL) was added and 2-methyl-1,4-naphthoquinone oxide precipitated as a white solid, which was filtered off. Concentrated H₂SO₄ (5 mL) was added and the mixture was kept in rest for 10 min. Addition of water (20 mL) provided a yellow solid, which was filtered and purified by column chromatography on silica gel (*n*-hexane/EtOAc 4:1) to provide 2-hydroxy-3-methylnaphthalene-1,4-dione (**137**) (808 mg, 74%) as a yellow solid. ¹H NMR (300 MHz, CDCl₃) δ: 8.08 (dd, *J* = 7.5 and 1.5 Hz, 1H), 8.03 (dd, *J* = 7.5 and 1.5 Hz, 1H), 7.71 (td, *J* = 7.5 and 1.5 Hz, 1H), 7.64 (td, *J* = 7.5 and 1.5 Hz, 1H), 7.30 (s, 1H), 2.08 (s, 3H); ¹³C NMR (75 MHz, CDCl₃) δ: 185.0, 181.1, 153.1, 134.8, 132.8, 132.9, 129.4, 126.7, 126.1, 120.5, 8.7; **m. p.** (°C) = 173-174. Data are consistent with those reported in the literature (ref. 133, p. 40).



2-methoxy-3-methylnaphthalene-1,4-dione (138): 2-hydroxy-3-methylnaphthalene-1,4-dione (**137**) (376 mg, 2.00 mmol), Ag₂O (0.7 g, 3.0 mmol) and MeI (250 μL, 4.00 mmol) were dissolved in CHCl₃ (50 mL) and heated to 60 °C for 48 h. After cooling to 25 °C, the solids were removed through filtration through a Celite pad. The solvent was evaporated under reduced pressure. After purification by column chromatography on silica gel (*n*-hexane/EtOAc 5:1) the 2-methoxy-3-methylnaphthalene-1,4-dione (**138**) (287 mg, 71%) was obtained as a yellow solid. ¹H NMR (300 MHz, CDCl₃) δ: 8.04-8.00 (m, 2H), 7.67-7.64 (m, 2H), 4.09 (s, 3H), 2.07 (s, 3H); ¹³C NMR (75 MHz, CDCl₃) δ: 185.6, 181.1, 157.7, 133.6, 133.1, 131.9, 131.7, 131.4, 126.1, 126.0, 61.0, 9.4; **m. p.** (°C) = 101-102. Data are consistent with those reported in the literature (ref. 133, p. 40).

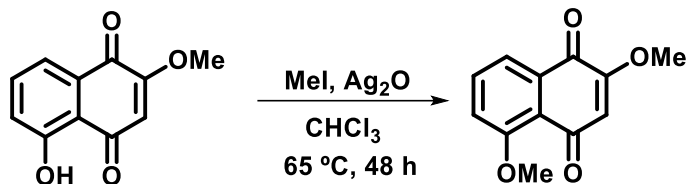


6,7-dimethylnaphthalene-1,4-dione (141): 2,3-Dimethyl-1,3-butadiene (1.2 mL, 10.2 mmol) and *p*-benzoquinone (**59**) (1.03 g, 9.50 mmol,) were dissolved in HOAc (10 mL) and the solution was heated to 55 °C for 4 h. After cooling to 25 °C, HOAc was evaporated under reduced pressure and EtOH (20 mL) was added. The solid was filtered off and washed with H₂O (100 mL), EtOH (50 mL) and Et₂O (50 mL) to provide a white solid **140**. Without further purification, compound **140** was dissolved in PhMe (100 mL) and heated to 100 °C. MnO₂ (13.0 g, 87.0 mmol) was added slowly over a period of 10 min and the solution was heated to 100 °C for 3 h. The solution was filtered through a pad of Celite and the filtrate was evaporated under reduced pressure. The crude product was recrystallized from EtOH to afford 6,7-dimethylnaphthalene-1,4-dione (**141**) (2.0 g, 80%) as a yellow solid. ¹H NMR (300 MHz, CDCl₃) δ: 7.77 (s, 2H), 6.86 (s, 2H), 2.36 (s, 6H); ¹³C NMR (75 MHz, CDCl₃) δ: 185.1, 143.6, 138.4, 129.8, 127.3, 20.2; **m. p.** (°C) = 115-117. Data are consistent with those reported in the literature (ref. 136, p. 42).



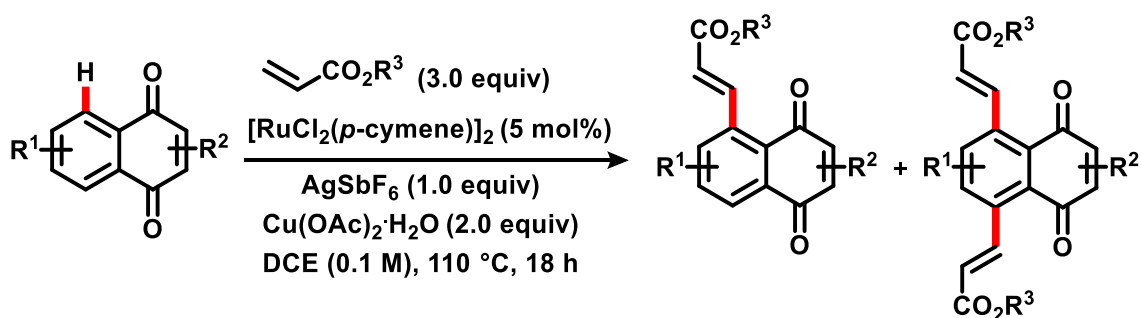
1,5-dibromoanthracene-9,10-dione (144): 1,5-Diaminoanthracene-9,10-dione (**143**) (2.00 g, 8.39 mmol), CuBr₂ (4.23 g, 18.9 mmol) and tert-butyl nitrite, *t*-BuONO, (1.95 g, 18.9 mmol) were added to MeCN (15 mL). The mixture was heated to 65 °C for 5 h and then cooled to 25 °C. An aqueous solution of HCl (1M, 100 mL) was added and the solution was extracted with CH₂Cl₂ (4 x 20 mL). Subsequently, the organic extract was dried over Na₂SO₄ and solvent was evaporated under reduced pressure. Then, the product was purified by column chromatography (PhMe) to yield 1,5-dibromoanthracene-9,10-dione (**144**) (2.58 g, 84%) as a yellow solid. ¹H NMR (300 MHz, CDCl₃) δ: 8.29 (dd, *J* = 7.8 and 1.2 Hz, 1H), 7.99 (dd, *J* = 7.8 and 1.2 Hz, 1H), 7.57 (t, *J* = 7.8 Hz, 1H). ¹³C NMR (75 MHz, CDCl₃) δ: 181.0, 140.8, 137.1, 134.1, 130.2,

127.7, 122.0; **m. p.** (°C) = 294-296. Data are consistent with those reported in the literature (ref. 137, p. 42).

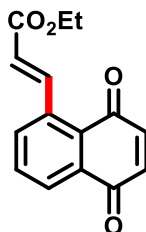


2,5-dimethoxynaphthalene-1,4-dione (156): 5-Hydroxy-2-methoxy-1,4-naphthoquinone (**114**) (228 mg, 1.00 mmol), Ag₂O (468 mg, 2.00 mmol) and iodomethane (125 μ L, 2.00 mmol) were dissolved in CHCl₃ (25 mL). The mixture was heated to reflux for 48 h and then cooled to 25 °C. The solid was removed by filtration through a pad of celite and the solvent was evaporated under reduced pressure. The residue was purified by column chromatography in silica gel (*n*-hexane/EtOAc 10:3) to afford 2,5-dimethoxynaphthalene-1,4-dione (**156**) (535 mg, 71%). ¹H NMR (300 MHz, CDCl₃) δ : 7.80 (d, *J* = 6.0 Hz, 1H), 7.67-7.63 (m, 1H), 7.32 (d, *J* = 6.0 Hz, 1H), 6.09 (s, 1H), 4.01 (s, 3H), 3.87 (s, 3H). ¹³C NMR (75 MHz, CDCl₃) δ : 184.6, 180.4, 159.4, 158.4, 134.3, 133.4, 119.6, 118.6, 112.1, 56.5, 56.2. **m. p.** (°C) = 199-200. Data are consistent with those reported in the literature (ref. 138, p. **Erro! Indicador não definido.**).

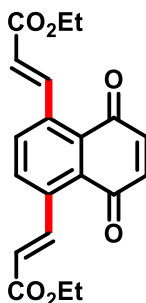
7.2 C–H alkenylation: general procedure A and characterization data of products.



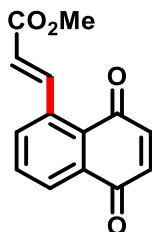
General Procedure A: To an oven-dried re-sealable tube, naphthoquinoidal substrates (0.40 mmol), [RuCl₂(*p*-cymene)]₂ (12.0 mg, 0.02 mmol, 5 mol%), AgSbF₆ (137 mg, 0.40 mmol, 1.0 equiv), Cu(OAc)₂·H₂O (160 mg, 0.80 mmol, 2.00 equiv.) were added. Acrylates (3.0 equiv.) and DCE (2 mL) were added *via* syringe, and the tube was sealed and submitted to heating (110 °C) and stirring for 18 hours. Then the reaction mixture was filtered through a pad of celite, and the crude product was purified *via* column chromatography under the conditions noted.



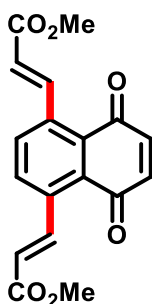
ethyl (*E*)-3-(5,8-dioxo-5,8-dihydronaphthalen-1-yl)acrylate (120): The general procedure A was followed using 1,4-naphthoquinone (**61**) as starting material (63.6 mg, 0.40 mmol) and ethyl acrylate (**30**) (130 μ L, 1.20 mmol). Purification by column chromatography (*n*-hexane/EtOAc 20:1) led to product **120** (51.3 mg, 0.20 mmol, 50% yield), obtained as a yellow solid. $^1\text{H NMR}$ (400 MHz, CDCl_3) δ : 8.57 (d, $J = 16.0$ Hz, 1H), 8.14 (dd, $J = 7.2$ and 2.0 Hz, 1H), 7.77-7.71 (m, 2H), 6.94 (s, 2H), 6.25 (d, $J = 16.0$ Hz, 1H), 4.27 (q, $J = 7.2$ Hz, 2H), 1.33 (t, $J = 7.2$ Hz, 3H). $^{13}\text{C NMR}$ (100 MHz, CDCl_3) δ : 186.2 (C), 184.7 (C), 166.2 (C), 144.0 (CH), 140.0 (CH), 137.3 (CH), 137.2 (C), 134.1 (CH), 133.6 (CH), 133.1 (C), 129.1 (C), 128.1 (CH), 122.8 (CH), 60.8 (CH_2), 14.3 (CH_3). **IR** (ATR): $\tilde{\nu} = 2910, 1720, 1654, 1195 \text{ cm}^{-1}$; **m. p.** ($^\circ\text{C}$) = 135-136. **HRMS** (ESI $^+$): 279.0629 $[\text{M}+\text{Na}]^+$. Calcd. for $[\text{C}_{15}\text{H}_{12}\text{NaO}_4]^+$: 279.0628.



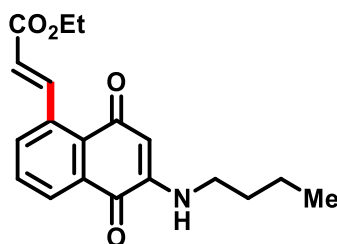
diethyl 3,3'-(5,8-dioxo-5,8-dihydronaphthalene-1,4-diyl)(2*E*,2'*E*)-diacrylate (121): **121** was obtained as a yellow solid (56.7 mg, 0.16 mmol, 40% yield). $^1\text{H NMR}$ (300 MHz, CDCl_3) δ : 8.45 (d, $J = 16.0$ Hz, 2H), 7.72 (s, 2H), 6.93 (s, 2H), 6.24 (d, $J = 16.0$ Hz, 2H), 4.28 (q, $J = 5.4$ Hz, 4H), 1.33 (t, $J = 5.4$ Hz, 6H). $^{13}\text{C NMR}$ (75 MHz, CDCl_3) δ : 158.9 (C), 166.0 (C), 143.9 (CH), 138.4 (C), 138.3 (CH), 133.9 (C), 130.5 (CH), 122.7 (CH), 60.8 (CH_2), 14.4 (CH_3). **IR** (ATR): $\tilde{\nu} = 2961, 1720, 1660, 1278, 850 \text{ cm}^{-1}$; **m. p.** ($^\circ\text{C}$) = 156-157. **HRMS** (ESI $^+$): 355.1176 $[\text{M}+\text{H}]^+$. Calcd. for $[\text{C}_{20}\text{H}_{19}\text{O}_6]^+$: 355.1181



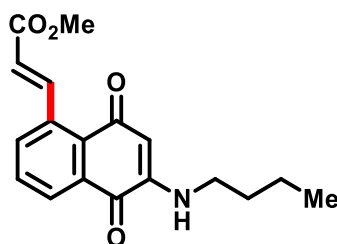
methyl (*E*)-3-(5,8-dioxo-5,8-dihydronaphthalen-1-yl)acrylate (146): The general procedure A was followed using 1,4-naphthoquinone (**61**) as starting material (63.6 mg, 0.40 mmol) and methyl acrylate (**22**) (110 μ L, 1.20 mmol). Purification by column chromatography (*n*-hexane/EtOAc 25:1) led to product **146** (46.5 mg, 0.19 mmol, 48% yield), obtained as a yellow solid. $^1\text{H NMR}$ (300 MHz, CDCl_3) δ : 8.55 (d, $J = 15.9$ Hz, 1H), 8.15 (dd, $J = 6.6$ and 2.4 Hz, 1H), 7.74-7.71 (m, 2H), 6.93 (s, 2H), 6.24 (d, $J = 15.9$ Hz, 1H), 3.80 (s, 3H). $^{13}\text{C NMR}$ (75 MHz, CDCl_3) δ : 186.0 (C), 184.4 (C), 166.4 (CH), 144.1 (CH), 139.8 (CH), 137.2 (C), 137.0 (CH), 134.0 (C), 133.5 (C), 133.0 (CH), 129.0 (C), 128.0 (CH), 122.2 (CH), 51.9 (CH_3). **IR** (ATR): $\tilde{\nu} = 2955, 1708, 1655, 1282, 784$ cm^{-1} ; **m. p.** ($^{\circ}\text{C}$) = 147-149; **HRMS** (ESI^+): 243.0650 $[\text{M}+\text{H}]^+$. Calcd. for $[\text{C}_{14}\text{H}_{11}\text{O}_4]^+$: 243.0652.



dimethyl 3,3'-(5,8-dioxo-5,8-dihydronaphthalene-1,4-diyl)(2*E*,2'*E*)-diacrylate (147): **147** was obtained as a yellow solid (23.5 mg, 0.07 mmol, 18% yield). $^1\text{H NMR}$ (300 MHz, CDCl_3) δ : 8.45 (d, $J = 15.8$ Hz, 2H), 7.71 (s, 2H), 6.93 (s, 2H), 6.24 (d, $J = 15.8$ Hz, 2H), 3.82 (s, 6H). $^{13}\text{C NMR}$ (75 MHz, CDCl_3) δ : 185.9 (C), 166.4 (C), 144.2 (CH), 138.3 (C), 133.9 (C), 130.5 (CH), 122.2 (CH), 52.0 (CH_3). **IR** (ATR): $\tilde{\nu} = 2956, 1717, 1655, 1277, 840$ cm^{-1} . **m. p.** ($^{\circ}\text{C}$) = 157-159; **HRMS** (ESI^+): 349.0689 $[\text{M}+\text{Na}]^+$. Calcd. for $[\text{C}_{18}\text{H}_{14}\text{NaO}_6]^+$: 349.0683.

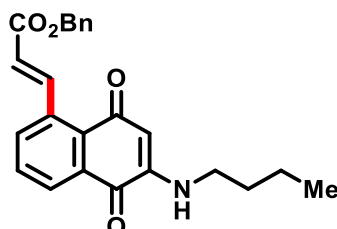


ethyl (*E*)-3-(6-(butylamino)-5,8-dioxo-5,8-dihydronaphthalen-1-yl)acrylate (149): The general procedure A was followed using 2-(butylamino)naphthalene-1,4-dione (**129**) as starting material (91.7 mg, 0.40 mmol) and ethyl acrylate (**30**) (130 μ L, 1.20 mmol). Purification by column chromatography (*n*-hexane/EtOAc 20:3) led to product **149** (65.5 mg, 0.20 mmol, 50% yield), obtained as a red solid. $^1\text{H NMR}$ (300 MHz, CDCl_3) δ : 8.72 (d, $J = 15.9$ Hz, 1H), 8.10 (dd, $J = 7.6$ and 1.5 Hz, 1H), 7.68 (ddd, $J = 7.8$, 1.5 and 0.6 Hz, 1H), 7.57 (td, $J = 7.2$ and 0.6 Hz, 1H), 6.14 (d, $J = 15.9$ Hz, 1H), 5.73 (t, $J = 6.8$ Hz, 1H), 5.68 (s, 1H), 4.26 (q, $J = 7.1$ Hz, 2H), 3.17-3.11 (m, 2H), 1.67-1.62 (m, 2H), 1.45-1.37 (m, 2H), 1.32 (t, $J = 7.1$ Hz, 3H), 0.94 (t, $J = 7.3$ Hz, 3H). $^{13}\text{C NMR}$ (75 MHz, CDCl_3) δ : 184.3 (C), 181.6 (C), 166.4 (C), 146.8 (C), 145.5 (CH), 136.8 (CH) 135.1 (C), 131.7 (C), 131.5 (CH), 130.5 (CH), 127.8 (C), 121.2 (CH), 102.3 (CH), 60.6 (CH_2), 42.3 (CH_2), 30.4 (CH_2), 20.2 (CH_2), 14.4 (CH_3), 13.8 (CH_3). **IR** (ATR): $\tilde{\nu} = 3351, 2947, 1702, 1608, 1222 \text{ cm}^{-1}$; **m. p.** ($^\circ\text{C}$) = 99-100; **HRMS** (ESI^+): 328.1543 $[\text{M}+\text{H}]^+$. Calcd. for $[\text{C}_{19}\text{H}_{22}\text{NO}_4]^+$: 328.1549.

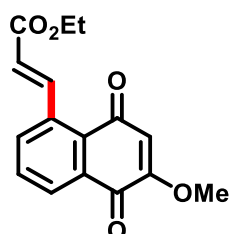


methyl (*E*)-3-(6-(butylamino)-5,8-dioxo-5,8-dihydronaphthalen-1-yl)acrylate (150): The general procedure A was followed using and 2-(butylamino)naphthalene-1,4-dione (**129**) as starting material (91.7 mg, 0.40 mmol) and methyl acrylate (**22**) (110 μ L, 1.20 mmol). Purification by column chromatography (*n*-hexane/EtOAc 5:1) led to product **150** (63.9 mg, 0.20 mmol, 51% yield), obtained as a red solid. $^1\text{H NMR}$ (300 MHz, CDCl_3) δ : 8.76 (d, $J = 16.0$ Hz, 1H), 8.11 (ddd, $J = 7.8$, 1.4 and 0.3 Hz, 1H), 7.71 (ddd, $J = 7.8$, 1.4 and 0.3 Hz, 1H), 7.60 (td, $J = 7.7$ and 0.6 Hz, 1H), 6.15 (d, $J = 16.0$ Hz, 1H), 5.73 (bs, 1H), 5.68 (s, 1H), 3.80 (s, 3H), 3.18-3.11 (m, 2H), 1.67-1.62 (m, 2H), 1.46-1.37 (m, 2H), 0.94 (t, $J = 7.3$ Hz, 3H). $^{13}\text{C NMR}$

(75 MHz, CDCl₃) δ : 184.2 (C), 181.6 (C), 166.8 (CH), 146.7 (CH), 145.8 (C), 136.7 (C), 135.1 (CH), 131.6 (C), 131.5 (CH), 130.5 (C), 127.9 (CH), 120.6 (C), 102.2 (CH), 51.8 (CH₂), 42.2 (CH₂), 30.3 (CH₃), 20.2 (CH₂), 13.7 (CH₃). **IR** (ATR): $\tilde{\nu}$ = 3351, 2951, 1707, 1604. cm⁻¹; **m. p.** (°C) = 111-113; **HRMS** (ESI⁺): 314.1387 [M+H]⁺. Cald. for [C₁₈H₂₀NO₄]⁺: 314.1392.

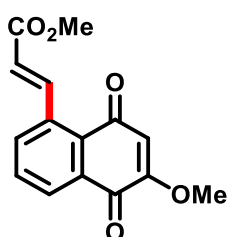


benzyl (E)-3-(6-(butylamino)-5,8-dioxo-5,8-dihydronaphthalen-1-yl)acrylate (151): The general procedure A was followed using 2-(butylamino)naphthalene-1,4-dione (**129**) as starting material (91.7 mg, 0.40 mmol) and benzyl acrylate (**148**) (200 μ L, 1.20 mmol). Purification by column chromatography (*n*-hexane/EtOAc 25:3) led to product **151** (87.2 mg, 0.22 mmol, 56% yield), obtained as a red solid. **¹H NMR** (300 MHz, CDCl₃) δ : 8.82 (d, *J* = 15.5 Hz, 1H), 8.11 (dd, *J* = 7.6 and 1.7 Hz, 1H), 7.69 (ddd, *J* = 7.8, 1.4 Hz and 0.6, 1H), 7.58 (td, *J* = 7.7 and 0.5 Hz, 1H), 7.45-7.33 (m, 5H), 6.22 (d, *J* = 15.5 Hz, 1H), 5.77 (t, *J* = 5.4, 1H), 5.71 (s, 1H), 5.28 (s, 2H), 3.18-3.12 (m, 2H), 1.71-1.61 (m, 2H), 1.50-1.36 (m, 2H), 0.97 (t, *J* = 7.3 Hz, 3H). **¹³C NMR** (75 MHz, CDCl₃) δ : 184.2 (C), 181.6 (C), 166.1 (C), 146.7 (C), 146.2 (C), 136.6 (CH), 136.0 (CH), 135.1 (C), 131.6 (CH), 131.5 (CH), 130.5 (CH), 128.4 (CH), 128.1 (CH), 128.0 (CH), 127.9 (CH), 120.2 (C), 102.2 (C), 66.3 (CH₂), 42.3 (CH₂), 30.3 (CH₂), 20.2 (CH₂), 13.8 (CH₃). **IR** (ATR): $\tilde{\nu}$ = 3362, 2953, 1712, 1608, 1167 cm⁻¹. **m. p.** (°C) = 102-103. **HRMS** (ESI⁺): 390.1694 [M+H]⁺. Cald. for [C₂₄H₂₄NO₄]⁺: 390.1705

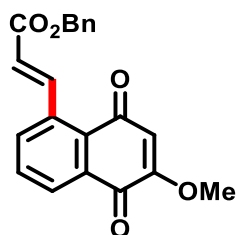


ethyl (E)-3-(6-methoxy-5,8-dioxo-5,8-dihydronaphthalen-1-yl)acrylate (153): The general procedure A was followed using 2-methoxynaphthalene-1,4-dione (**112**) as starting material (72.3 mg, 0.40 mmol) and ethyl acrylate (**30**) (130 μ L, 1.20 mmol). Purification by column chromatography (*n*-hexane/EtOAc 4:1) led to product **153** (77.9 mg, 0.26 mmol, 68% yield),

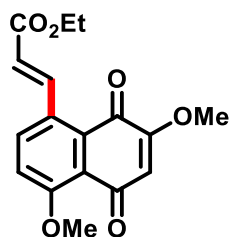
obtained as a yellow solid. $^1\text{H NMR}$ (300 MHz, CDCl_3) δ : 8.63 (d, $J = 15.9$ Hz, 1H), 8.21 (dd, $J = 7.4$ and 1.5 Hz, 1H), 7.76 (ddd, $J = 5.7$, 1.5 and 0.6, 1H), 7.73-7.68 (m, 1H), 6.24 (d, $J = 15.9$ Hz, 1H), 6.17 (s, 1H), 4.30 (q, $J = 7.1$ Hz, 2H), 3.90 (s, 3H), 1.35 (t, $J = 7.1$ Hz, 3H). $^{13}\text{C NMR}$ (75 MHz, CDCl_3) δ : 186.1 (C), 179.9 (C), 166.3 (C), 159.4 (C), 144.6 (CH) 137.1 (CH), 134.8 (CH), 133.0 (CH), 132.4 (C), 129.2 (C), 128.4 (C), 122.5 (CH), 111.4 (CH), 60.9 (CH_3), 56.6 (CH_2), 14.6 (CH_3). **IR** (ATR): $\tilde{\nu} = 2991, 1705, 1680, 1619, 1233 \text{ cm}^{-1}$. **m. p.** ($^\circ\text{C}$) = 183-184. **HRMS** (ESI^+): 287.0909 $[\text{M}+\text{H}]^+$. Cald. for $[\text{C}_{16}\text{H}_{15}\text{O}_5]^+$: 287.0914; *The structure of the product was also confirmed by X-ray diffraction (CCDC number = 1877203).*



methyl (*E*)-3-(6-methoxy-5,8-dioxo-5,8-dihydronaphthalen-1-yl)acrylate (154): The general procedure A was followed using 2-methoxynaphthalene-1,4-dione (**112** as starting material) (72.3 mg, 0.40 mmol) and methyl acrylate (**22**) (110 μL , 1.20 mmol). Purification by column chromatography (hexane/EtOAc 4:1) led to product **154** (25.0 mg, 0.09 mmol, 23% yield), obtained as an yellow solid. $^1\text{H NMR}$ (300 MHz, CDCl_3) δ : 8.65 (d, $J = 15.9$ Hz, 1H), 8.22 (dd, $J = 7.2$ and 1.8 Hz, 1H), 7.76-7.71 (m, 2H), 6.25 (d, $J = 15.9$ Hz, 1H), 6.17 (s, 1H), 3.92 (s, 3H), 3.85 (s, 3H). $^{13}\text{C NMR}$ (75 MHz, CDCl_3) δ : 185.9 (C), 179.7 (CH), 166.6 (C), 159.2 (CH), 144.7 (CH), 136.8 (CH), 134.6 (C), 132.9 (C), 132.2 (CH), 129.0 (C), 128.3 (C), 121.8 (CH), 111.2 (C), 56.5 (CH_3), 51.9 (CH_3). **IR** (ATR): $\tilde{\nu} = 3058, 1711, 1677, 1617, 1244 \text{ cm}^{-1}$. **m. p.** ($^\circ\text{C}$) = 215-217; **HRMS** (ESI^+): 273.0761 $[\text{M}+\text{H}]^+$. Cald. for $[\text{C}_{15}\text{H}_{13}\text{O}_5]^+$: 273.0757;

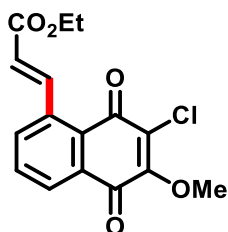


benzyl (*E*)-3-(6-methoxy-5,8-dioxo-5,8-dihydronaphthalen-1-yl)acrylate (155): The general procedure A was followed using 2-methoxynaphthalene-1,4-dione (**112**) as starting material (72.3 mg, 0.40 mmol) and benzyl acrylate (**148**) (200 μ L, 1.20 mmol). Purification by column chromatography (hexane/EtOAc 10:1) led to product **155** (58.5 mg, 0.17mmol, 42% yield), obtained as a yellow solid. $^1\text{H NMR}$ (300 MHz, CDCl_3) δ : 8.66 (d, $J = 15.9$ Hz, 1H), 8.18 (dd, $J = 5.7$ and 1.8 Hz, 1H), 7.73-7.765 (m, 2H), 7.43-7.32 (m, 5H), 6.26 (d, $J = 15.9$ Hz, 1H), 6.13 (s, 1H), 5.26 (s, 2H), 3.86 (s, 3H). $^{13}\text{C NMR}$ (75 MHz, CDCl_3) δ : 185.8 (C), 179.6 (C), 165.9 (C), 159.2 (C), 145.0 (CH), 136.7 (CH), 135.9 (CH), 134.5 (C), 132.8 (C), 132.1 (CH), 129.0 (CH), 128.5 (CH), 128.3 (CH), 128.2(CH), 128.1 (CH), 121.8 (CH), 111.2 (C), 66.4 (CH_3), 56.4 (CH_2). **IR** (ATR): $\tilde{\nu} = 2993, 1709, 1636, 1621, 1235 \text{ cm}^{-1}$. **m. p.** ($^\circ\text{C}$) = 171-173. **MS** (ESI $^+$): 371.0 $[\text{M}+\text{Na}]^+$. Calcd. for $[\text{C}_{21}\text{H}_{16}\text{NaO}_5]^+$: 371.0;



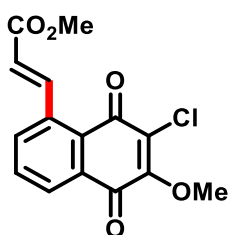
ethyl (*E*)-3-(4,7-dimethoxy-5,8-dioxo-5,8-dihydronaphthalen-1-yl)acrylate (157): The general procedure A was followed using 2,5-dimethoxynaphthalene-1,4-dione (**156**) as starting material (87.3 mg, 0.40 mmol) and ethyl acrylate (**30**) (130 μ L, 1.20 mmol). Purification by column chromatography (*n*-hexane/EtOAc 2:1) led to product **157** (44.3 mg, 0.14 mmol, 35% yield), obtained as a yellow solid. $^1\text{H NMR}$ (300 MHz, CDCl_3) δ : 8.39 (d, $J = 15.8$ Hz, 1H), 7.68 (dd, $J = 5.4$ and 0.3 Hz, 1H), 7.33 (d, $J = 5.1$ Hz, 1H), 6.18 (d, $J = 15.8$ Hz, 1H), 6.09 (s, 1H), 4.28 (q, $J = 4.2$ Hz, 2H), 4.03 (s, 3H), 3.87 (s, 3H), 1.35 (t, $J = 4.2$ Hz, 3H). $^{13}\text{C NMR}$ (75 MHz, CDCl_3) δ : 184.3 (C), 181.7 (C), 166.4 (C), 160.3 (C), 158.7 (C), 144.5 (CH), 135.0 (CH), 130.7 (C), 130.0 (C), 121.2 (CH), 120.2 (C), 118.6 (CH), 110.9 (CH), 60.6 (CH_2), 56.7 (CH_3),

56.3 (CH₃), 14.3 (CH₃). **IR** (ATR): $\tilde{\nu}$ = 2972, 1702, 1621, 1273, 1032 cm⁻¹. **m. p.** (°C) = 156-158; **HRMS** (ESI⁺): 316.0947 [M+H]⁺. Calcd. for [C₁₇H₁₆O₆]⁺: 316.0947.



ethyl (E)-3-(7-chloro-6-methoxy-5,8-dioxo-5,8-dihydronaphthalen-1-yl)acrylate (160):

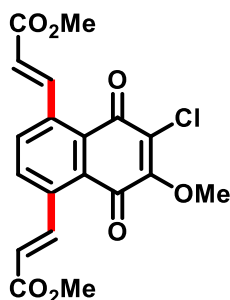
The general procedure A was followed using 2-chloro-3-methoxynaphthalene-1,4-dione (**134**) as starting material (89.0 mg, 0.40 mmol) and ethyl acrylate (**30**) (130 μ L, 1.20 mmol). Purification by column chromatography (*n*-hexane/EtOAc 5:1) led to product **160** (57.7 mg, 0.18 mmol, 45% yield), obtained as a yellow solid. **¹H NMR** (300 MHz, CDCl₃) δ : 8.57 (d, *J* = 15.9 Hz, 1H), 8.16 (dd, *J* = 6.4 and 2.8 Hz, 1H), 7.75-7.73 (m, 2H), 6.23 (d, *J* = 15.9 Hz, 1H), 4.31-4.29 (m, 5H), 1.35 (t, *J* = 7.1 Hz, 3H). **¹³C NMR** (75 MHz, CDCl₃) δ : 179.3 (C), 179.2 (C), 165.9 (CH), 155.7 (C), 143.8 (CH), 137.6 (CH), 134.8 (C), 133.4 (C), 132.0 (C), 128.8 (C), 128.3 (CH), 127.9 (C), 123.0 (CH), 61.8 (CH₃), 60.8 (CH₃), 14.4 (CH₂). **IR** (ATR): $\tilde{\nu}$ = 2956, 1705, 1673, 1607, 1242 cm⁻¹; **m. p.** (°C) = 97-99; **HRMS** (ESI⁺): 343.0345 [M+Na]⁺. Calcd. for [C₁₆H₁₃ClNaO₅]⁺: 343.0344.



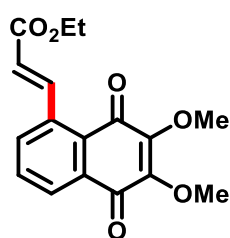
methyl (E)-3-(7-chloro-6-methoxy-5,8-dioxo-5,8-dihydronaphthalen-1-yl)acrylate (162):

The general procedure A was followed using 2-chloro-3-methoxynaphthalene-1,4-dione (**134**) as starting material (89.0 mg, 0.40 mmol) and methyl acrylate (**22**) (110 μ L, 1.20 mmol). Purification by column chromatography (*n*-hexane/EtOAc 5:1) led to product **162** (34.4 mg, 0.11 mmol, 28% yield), obtained as a yellow solid. **¹H NMR** (400 MHz, CDCl₃) δ : 8.56 (d, *J* = 16.0 Hz, 1H), 8.14 (dd, *J* = 4.8 and 1.8 Hz, 1H), 7.73-7.70 (m, 2H), 6.21 (d, *J* = 16.0 Hz, 1H), 4.28 (s, 3H), 3.80 (s, 3H). **¹³C NMR** (100 MHz, CDCl₃) δ : 179.5 (C), 179.3 (C), 166.5 (C),

155.9 (C), 144.2 (CH), 137.6 (CH), 134.7 (C), 133.5 (C), 132.0 (C), 128.9 (C), 128.4 (CH), 128.0 (CH), 122.6 (CH), 61.8 (CH₃), 51.9 (CH₃). **IR** (ATR): $\tilde{\nu}$ = 2955, 1724, 1670, 1435, 1242 cm⁻¹. **m. p.** (°C) = 170-172; **HRMS** (ESI⁺): 329.0183 [M+Na]⁺. Cald. for [C₁₅H₁₁ClNaO₅]⁺: 329.0187.

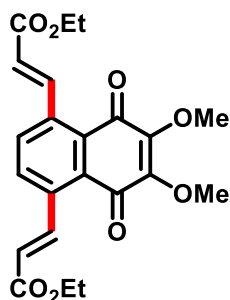


dimethyl 3,3'-(6-chloro-7-methoxy-5,8-dioxo-5,8-dihydronaphthalene-1,4-diyl)(2E,2'E)-diacrylate (163): **163** was obtained as yellow solid (9.7 mg, 0.02 mmol, 5% yield). **¹H NMR** (400 MHz, CDCl₃) δ : 8.46 (d, 1H, J = 15.6 Hz), 8.36 (d, J = 16.0 Hz, 1H), 7.72-7.67 (m, 2H), 6.27 (d, J = 15.6 Hz, 1H), 6.21 (d, J = 15.6 Hz, 1H), 4.27 (s, 3H), 3.82 (s, 3H), 3.81 (s, 3H). **¹³C NMR** (100 MHz, CDCl₃) δ : 180.5 (C), 179.4 (C), 166.5 (C), 166.4 (C), 156.5 (C), 144.3 (CH), 143.8 (CH), 134.4 (C), 133.9 (C), 122.6 (CH), 122.5 (CH), 61.8 (CH₃), 52.0 (CH₃), 51.9 (CH₃). **IR** (ATR): $\tilde{\nu}$ = 2957, 1720, 1660, 1430, 1247 cm⁻¹. **m. p.** (°C) = 90-91; **HRMS** (ESI⁺): 413.0401 [M+Na]⁺. Cald. for [C₁₉H₁₅ClNaO₇]⁺: 413.0404.

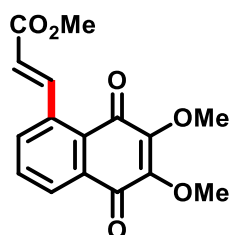


ethyl (E)-3-(6,7-dimethoxy-5,8-dioxo-5,8-dihydronaphthalen-1-yl)acrylate (164): The general procedure A was followed using 2,3-dimethoxynaphthalene-1,4-dione (**135**) as starting material (87.3 mg, 0.40 mmol) and ethyl acrylate (**30**) (130 μ L, 1.20 mmol). Purification by column chromatography (*n*-hexane/EtOAc 4:1) led to product **164** (40.5 mg, 0.13 mmol, 32% yield), obtained as a yellow solid. **¹H NMR** (300 MHz, CDCl₃) δ : 8.58 (d, J = 15.9 Hz, 1H), 8.15 (dd, J = 7.2 and 1.5 Hz, 1H), 7.73-7.64 (m, 2H), 6.25 (d, J = 15.9 Hz, 1H), 4.29 (q, J = 7.1 Hz, 2H), 4.11 (s, 3H), 4.10 (s, 3H), 1.36 (t, J = 7.1 Hz, 3H). **¹³C NMR** (75 MHz, CDCl₃) δ :

182.9 (C), 181.6 (C), 166.2 (C), 147.8 (C), 146.4 (C), 144.2 9 (CH), 137.0 (C), 134.0 (CH), 133.3 (CH), 132.0 (C), 127.9 (C), 127.8 (CH), 122.6 (CH), 61.5 (CH₃), 61.3 (CH₃), 60.7 (CH₂), 14.3 (CH₃). **IR** (ATR): $\tilde{\nu}$ = 2948, 1716, 1618, 1280, 1187 cm⁻¹; **m. p.** (°C) = 83-84; **MS** (ESI⁺): 339.1 [M+Na]⁺. Cald. for [C₁₇H₁₆NaO₆]⁺: 339.1.

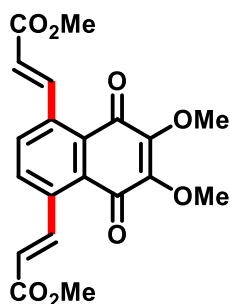


diethyl 3,3'-(6,7-dimethoxy-5,8-dioxo-5,8-dihydronaphthalene-1,4-diyl)(2E,2'E)-diacrylate (165): **165** was obtained as yellow solid (16.6 mg, 0.04 mmol, 10% yield). **¹H NMR** (500 MHz, CDCl₃) δ : 8.45 (d, J = 15.8 Hz, 2H), 7.67 (s, 1H), 6.23 (d, J = 15.8 Hz, 2H), 4.28 (q, J = 7.1 Hz, 4H), 4.09 (s, 6H), 1.35 (t, J = 7.1 Hz, 6H). **¹³C NMR** (125 MHz, CDCl₃) δ : 182.7 (C), 166.1 (C), 146.6 (C), 144.2 (CH), 138.2 (C), 133.7 (CH), 129.4 (C), 122.5 (CH), 61.4 (CH₃), 60.8 (CH₂), 14.3 (CH₃). **IR** (ATR): $\tilde{\nu}$ = 2960, 1708, 1624, 1260, 1164 cm⁻¹; **m. p.** (°C) = 83-85; **HRMS** (ESI⁺): 415.1384 [M+H]⁺. Cald. for [C₂₂H₂₃O₈]⁺: 415.1393.

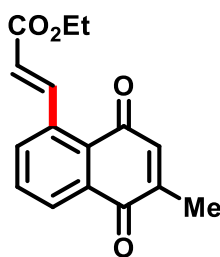


methyl (E)-3-(6,7-dimethoxy-5,8-dioxo-5,8-dihydronaphthalen-1-yl)acrylate (166): The general procedure A was followed using 2,3-dimethoxynaphthalene-1,4-dione (**135**) as starting material (87.3 mg, 0.40 mmol) and methyl acrylate (**22**) (110 μ L, 1.20 mmol). Purification by column chromatography (*n*-hexane/EtOAc 4:1) led to product **166** (27.8 mg, 0.05 mmol, 23% yield), obtained as a yellow solid. **¹H NMR** (300 MHz, CDCl₃) δ : 8.57 (d, J = 15.9 Hz, 1H), 8.15 (dd, J = 6.9 and 2.4 Hz, 1H), 7.77-7.67 (m, 2H), 6.25 (d, J = 15.9 Hz, 1H), 4.10 (s, 3H), 4.09 (s, 3H), 3.83 (s, 3H). **¹³C NMR** (75 MHz, CDCl₃) δ : 182.8 (C), 181.3 (C), 166.5 (C), 147.7 (CH), 146.4 (CH), 144.4 (C), 136.8 (C), 133.9 (CH), 133.2 (CH), 132.0 (C), 127.9 (C), 127.8

(CH), 122.0 (C), 61.5 (CH₃), 61.3 (CH₃), 51.9 (CH₃). **IR** (ATR): $\tilde{\nu}$ = 2957, 1720, 1614, 1430, 1161 cm⁻¹. **m. p.** (°C) = 138-140; **HRMS** (ESI⁺): 325.0680 [M+Na]⁺. Cald. for [C₁₆H₁₄NaO₆]⁺: 325.0683. The structure of the product was also confirmed by X-ray diffraction (CCDC number = 1877197).

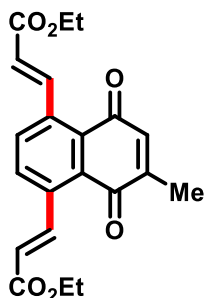


dimethyl 3,3'-(6,7-dimethoxy-5,8-dioxo-5,8-dihydronaphthalene-1,4-diyl)(2E,2'E)-diacrylate (167): **167** was obtained as yellow solid (54.1 mg, 0.14 mmol, 35% yield). **¹H NMR** (300 MHz, CDCl₃) δ : 8.47 (d, *J* = 15.8 Hz, 2H), 7.67 (s, 2H), 6.24 (d, *J* = 15.8 Hz, 2H), 4.10 (s, 6H), 3.84 (s, 6H). **¹³C NMR** (75 MHz, CDCl₃) δ : 182.6 (C), 166.4 (CH), 146.6 (CH), 144.4 (C), 138.0 (C), 133.6 (CH), 129.4 (C), 122.0 (C), 61.4 (CH₃), 51.9 (CH₃). **IR** (ATR): $\tilde{\nu}$ = 2954, 1711, 1619, 1434, 1166 cm⁻¹; **m. p.** (°C) = 179-181; **HRMS** (ESI⁺): 387.1089 [M+H]⁺. Cald. for [C₂₀H₁₉O₈]⁺: 387.1074.

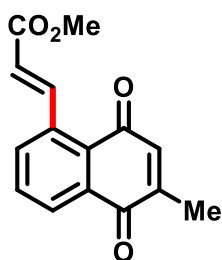


ethyl (E)-3-(6-methyl-5,8-dioxo-5,8-dihydronaphthalen-1-yl)acrylate (168): The general procedure A was followed using 2-methylnaphthalene-1,4-dione (**125**) as starting material (68.9 mg, 0.40 mmol) and ethyl acrylate (**30**) (130 μ L, 1.20 mmol). Purification by column chromatography (*n*-hexane/EtOAc 1:20) led to product **168** (47.6 mg, 0.13 mmol, 44% yield), obtained as a yellow solid. **¹H NMR** (400 MHz, CDCl₃) δ : 8.55 (d, *J* = 16.0 Hz, 1H), 8.10 (d, *J* = 6.4 Hz, 1H), 7.70-7.63 (m, 2H), 6.75 (s, 1H), 6.20 (d, *J* = 16.0 Hz, 1H), 4.24 (q, *J* = 7.2 Hz, 2H), 2.11 (s, 3H), 1.30 (t, *J* = 7.2 Hz, 3H). **¹³C NMR** (100 MHz, CDCl₃) δ : 186.3 (C), 185.3 (C), 166.4 (C), 146.9 (C), 144.3 (CH), 137.1 (C), 134.6 (C), 133.9 (CH), 133.4 (CH), 129.4 (C),

128.4 (CH), 127.9 (CH), 122.7 (CH), 60.8 (CH₂), 16.1(CH₃), 14.3 (CH₃). **IR** (ATR): $\tilde{\nu}$ = 2956, 1728, 1655, 1431, 1158 cm⁻¹. **m. p.** (°C) = 96-98. **HRMS** (EI⁺): 293.0797 [M+Na]⁺. Cald. for [C₁₆H₁₄NaO₄]: 293.0790; *The structure of the product was also confirmed by X-ray diffraction* (CCDC number = 1877202).

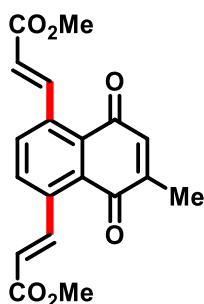


diethyl 3,3'-(6-methyl-5,8-dioxo-5,8-dihydronaphthalene-1,4-diyl)(2E,2'E)-diacrylate (169): **169** was obtained as yellow solid (20.6 mg, 0.06 mmol, 14% yield). **¹H NMR** (300 MHz, CDCl₃) δ : 8.45 (t, J = 16.2 Hz, 2H), 7.67 (d, J = 1.5 Hz, 2H), 6.79 (q, J = 1.5 Hz, 1H), 6.22 (d, J = 15.9 Hz, 1H), 6.21 (d, J = 15.9 Hz, 1H), 4.28 (q, J = 7.2, 2H), 4.27 (q, J = 7.2, 2H), 2.15 (d, J = 1.5 Hz, 3H), 1.33 (t, J = 6.9 Hz, 3H), 1.32 (td, J = 6.9 Hz, 3H). **¹³C NMR** (75 MHz, CDCl₃) δ : 186.7 (C), 186.0 (C), 166.2 (C), 148.0 (C), 144.7 (CH), 144.3 (CH), 138.7 (C), 138.3 (C), 135.7 (C), 133.8 (C), 131.1 (CH), 130.9 (CH), 122.7 (CH), 122.5 (CH), 61.1 (CH₂), 16.6 (CH₃), 14.6 (CH₃). **IR** (ATR): $\tilde{\nu}$ = 2981, 1699, 1632, 1273, 1170 cm⁻¹. **m. p.** (°C) = 128-130. **HRMS** (ESI⁺): 391.1146 [M+Na]⁺. Cald. for [C₂₁H₂₀NaO₆]⁺: 391.1158.



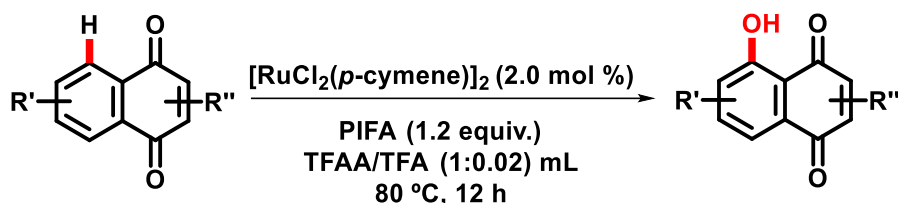
methyl (E)-3-(6-methyl-5,8-dioxo-5,8-dihydronaphthalen-1-yl)acrylate (170): The general procedure A was followed using 2-methylnaphthalene-1,4-dione (**125**) as starting material (68.9 mg, 0.40 mmol) and methyl acrylate (**22**) (110 μ L, 1.20 mmol). Purification by column chromatography (*n*-hexane/EtOAc 5:1) led to product **170** (41.0 mg, 0.16 mmol, 40% yield), obtained as a yellow solid. **¹H NMR** (400 MHz, CDCl₃) δ : 8.57 (d, J = 15.6 Hz, 1H), 8.13 (d,

$J = 6.4$ Hz, 1H), 7.71-7.65 (m, 2H), 6.77 (s, 1H), 6.22 (d, $J = 15.6$ Hz, 1H), 3.79 (s, 3H), 2.13 (s, 3H). ^{13}C NMR (100 MHz, CDCl_3) δ : 186.1 (C), 185.1 (C), 166.7 (C), 146.8 (C), 144.4 (CH), 136.9 (CH), 136.7 (C), 133.7 (CH), 133.3 (CH), 133.2 (C), 129.3 (C), 128.2 (CH), 122.0 (CH), 51.8 (CH_3), 15.9 (CH_3). **m.p.** ($^\circ\text{C}$) = 135-137; **IR** (ATR): $\tilde{\nu} = 2956, 1728, 1655, 1431, 1158$ cm^{-1} ; **HRMS** (ESI^+): 279.0625 $[\text{M}+\text{Na}]^+$. Cald. for $[\text{C}_{15}\text{H}_{12}\text{NaO}_4]$: 279.0633; *The structure of the product was also confirmed by X-ray diffraction (CCDC number = 1877196).*

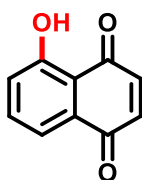


dimethyl 3,3'-(6-methyl-5,8-dioxo-5,8-dihydronaphthalene-1,4-diyl)(2E,2'E)-diacrylate (171): 171 was obtained as yellow solid (44.2 mg, 0.13 mmol, 33% yield). ^1H NMR (300 MHz, CDCl_3) δ : 8.50-8.40 (m, 2H), 7.68 (d, $J = 1.2$ Hz, 2H), 6.79 (q, $J = 1.5$ Hz, 1H), 6.82 (q, $J = 1.5$ Hz, 1H), 6.22 (d, $J = 15.6$ Hz, 1H), 6.21 (d, $J = 15.6$ Hz, 1H), 3.81 (s, 3H), 3.81 (s, 3H), 2.14 (d, $J = 1.4$ Hz, 3H). ^{13}C NMR (75 MHz, CDCl_3) δ : 186.5 (C), 185.8 (C), 166.5 (C), 166.4 (C), 147.8 (C), 144.8 (CH), 144.4 (CH), 138.4 (C), 138.0 (C), 135.5 (C), 133.6 (C), 130.9 (CH), 130.7 (CH), 122.0 (CH), 121.8 (CH), 52.0 (CH_3), 16.4 (CH_3). **IR** (ATR): $\tilde{\nu} = 2954, 1703, 1652, 1254, 1166$ cm^{-1} . **m. p.** ($^\circ\text{C}$) = 173-174. **HRMS** (ESI^+): 363.0835 $[\text{M}+\text{Na}]^+$. Cald. for $[\text{C}_{19}\text{H}_{16}\text{NaO}_6]^+$: 363.0839.

7.3 C–H oxygenation: general procedure B and characterization data of products.

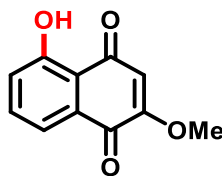


General Procedure B: The corresponding naphthoquinone (0.4 mmol), [bis(trifluoroacetoxy)iodo]benzene (PIFA) (215 mg, 0.50 mmol) and $[\text{RuCl}_2(p\text{-cymene})]_2$ (5 mg, 2.0 mol %) were added to a pressure tube. Trifluoroacetic anhydride (TFAA) (1 mL) and trifluoroacetic acid (0.02 mL) was subsequently added. The tube was sealed and the mixture was stirred at 80 °C for 12 h and then cooled to 25 °C. The mixture was transferred to a 25 mL flask and, under vigorous magnetic stirring, CH_2Cl_2 (1 mL), H_2O (1 mL) and a solution of HCl (1M, 0.2 mL) were added dropwise. After 5 min, the solution was extracted with CH_2Cl_2 (3 x 10 mL) and dried over Na_2SO_4 . The solvent was evaporated under reduced pressure and the crude product was purified by column chromatography on silica gel (*n*-hexane/EtOAc).



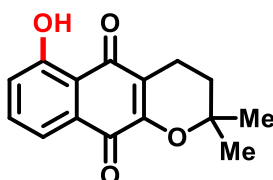
5-hydroxynaphthalene-1,4-dione (74): The general procedure B was followed using 1,4-naphthoquinone (**61**) as starting material (64 mg, 0.4 mmol). Purification by column chromatography on silica gel (*n*-hexane/EtOAc 50:1) yielded **74** (64 mg, 92%) as an orange solid. $^1\text{H NMR}$ (300 MHz, CDCl_3) δ : 11.85 (s, 1H), 7.60-7.57 (m, 2H), 7.23 (dd, $J = 7.3$ and 1.8 Hz, 1H), 6.90 (s, 2H); $^{13}\text{C NMR}$ (75 MHz, CDCl_3) δ : 190.0 (C), 184.0 (C), 161.3 (CH), 139.4 (CH), 138.5 (C), 136.4 (C), 131.6 (C), 124.4 (CH), 119.0 (CH), 114.9 (CH); **IR** (ATR): $\tilde{\nu} = 1678, 1625, 1597, 1444, 1219, 1075, 769 \text{ cm}^{-1}$; **m. p.** ($^\circ\text{C}$) = 160-162; **HRMS** (EI): Calcd for $\text{C}_{10}\text{H}_6\text{O}_3$ $[\text{M}]^+$ 174.0317, found 174.0309. 5,8-Dihydroxy-1,4-naphthoquinone (**75**) was also isolated in 3% yield. The data are consistent with those reported in the literature.¹⁵⁰

150. O. Suchard, R. Kane, B. J. Roe, E. Zimmermann, C. Jung, P. A. Waske, J. Mattay, M. Oelgemöller. Photooxygenations of 1-naphthols: an environmentally friendly access to 1,4-naphthoquinones. *Tetrahedron*, **2006**, *62*, 1467-1473.



5-hydroxy-2-methoxynaphthalene-1,4-dione (114): The general procedure B was followed using 2-methoxynaphthalene-1,4-dione (112) as starting material (75 mg, 0.4 mmol). Purification by column chromatography on silica gel (*n*-hexane/EtOAc 10:1) yielded **148** (62 mg, 76%) as a yellow solid. $^1\text{H NMR}$ (300 MHz, CDCl_3) δ : 12.13 (s, 1H), 7.58 (dd, $J = 7.5$ and 1.2 Hz, 1H), 7.79 (m, 1H), 7.19 (dd, $J = 7.5$ and 1.2 Hz, 1H), 6.03 (s, 1H), 3.85 (s, 3H); $^{13}\text{C NMR}$ (75 MHz, CDCl_3) δ : 190.5 (C), 179.1 (C), 160.9 (C), 160.9 (C), 135.3 (CH), 130.9 (C), 125.1 (CH), 119.4 (CH), 114.1 (C), 109.4 (CH), 56.6 (CH_3); **IR** (ATR): $\tilde{\nu} = 1678, 1625, 1597, 1444, 1219, 1075, 769 \text{ cm}^{-1}$; **m. p.** ($^\circ\text{C}$) = 162-163; **HRMS** (EI): Calcd for $\text{C}_{11}\text{H}_8\text{O}_4$ $[\text{M}]^+$ 204.0423, found 204.0415. The structure of the product was also confirmed by *X-ray diffraction* (CCDC number = 1859289).

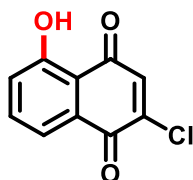
5,8-Dihydroxy-2-methoxy-1,4-naphthoquinone (**175**) was also isolated in 3% yield and the structure was solved by *X-ray diffraction* (CCDC number = 1859290). **HRMS** (EI): Calcd for $\text{C}_{11}\text{H}_9\text{O}_5$ $[\text{M}+\text{H}]^+$ 221.0450, found 221.0448. The data are consistent with those reported in the literature.¹⁵¹



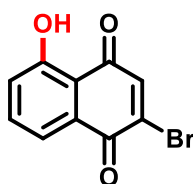
6-hydroxy-2,2-dimethyl-3,4-dihydro-2H-benzo[g]chromene-5,10-dione (178): The general procedure B was followed using α -lapachone (**68**) as starting material (97 mg, 0.4 mmol). Purification by column chromatography on silica gel (*n*-hexane/EtOAc 20:1) yielded **166** (53 mg, 51%) as a yellow solid; $^1\text{H NMR}$ (300 MHz, CDCl_3) δ : 12.32 (s, 1H), 7.58 (dd, $J = 7.3$ and 1.5 Hz, 1H), 7.49-7.44 (m, 1H), 7.16 (dd, $J = 8.4$ and 1.2 Hz, 1H), 2.55 (t, $J = 6.6$ Hz, 2H), 1.79 (t, $J = 6.6$ Hz, 2H), 1.40 (s, 6H); $^{13}\text{C NMR}$ (75 MHz, CDCl_3) δ : 189.8 (C), 179.0 (C), 160.7 (C),

¹⁵¹. Y. Zhou, B. Yang, Y. Jiang, Z. Liu, Y. Liu, X. Wang and H. Kuang. Studies on cytotoxic activity against HepG-2 cells of naphthoquinones from green walnut husks of *Juglans mandshurica* Maxim. *Molecules*. **2015**, *20*, 15572-15588.

155.2 (C), 134.9 (CH), 131.0 (C), 124.6 (CH), 119.4 (C), 119.0 (CH), 114.0 (C), 78.6 (C), 31.3 (CH₃), 26.6 (CH₃), 16.2 (CH₂); **IR** (ATR): $\tilde{\nu}$ = 1680, 1628, 1601, 1258, 1158, 831, 769 cm⁻¹; **m. p.** (°C) = 176-177; **HRMS** (ESI): Calcd for C₁₅H₁₄NaO₄ [M+Na]⁺ 281.0790, found 281.0784. The data are consistent with those reported in the literature.¹⁵²



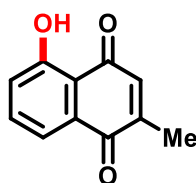
2-chloro-5-hydroxynaphthalene-1,4-dione (179): The general procedure B was followed using 2-chloronaphthalene-1,4-dione (**132**) as starting material (77 mg, 0.4 mmol). Purification by column chromatography on silica gel (*n*-hexane/EtOAc 100:3) yielded **179** (60 mg, 72%) as a yellow solid. **¹H NMR** (300 MHz, CDCl₃) δ : 11.76 (s, 1H), 7.69 (dd, *J* = 8.1 and 1.2 Hz, 1H), 7.64-7.59 (m, 1H), 7.28 (dd, *J* = 8.4 and 1.2 Hz, 1H), 7.16 (s, 1H); **¹³C NMR** (75 MHz, CDCl₃) δ : 187.7 (C), 177.1 (C), 161.5 (C), 147.0 (C), 136.4 (CH), 135.7 (CH), 131.0 (C), 125.2 (CH), 120.6 (CH), 114.5 (C); **IR** (ATR): $\tilde{\nu}$ = 1674, 1637, 1589, 1240, 891, 746 cm⁻¹; **m. p.** (°C) = 107-108; **HRMS** (EI): Calcd for C₁₀H₅³⁵ClO₃ [M, ³⁵Cl]⁺ 207.9927, found 207.9927; calcd for C₁₀H₅³⁷ClO₃ [M, ³⁷Cl]⁺ 209.9898, found 209.9910. The data are consistent with those reported in the literature (ref. 140 p. 51). *The structure of the product was also confirmed by X-ray diffraction* (CCDC number = 1859455).



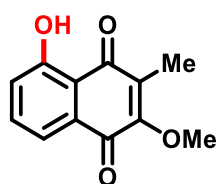
2-bromo-5-hydroxynaphthalene-1,4-dione (180): The general procedure B was followed using 2-bromonaphthalene-1,4-dione (**133**) as starting material (95 mg, 0.4 mmol). Purification by column chromatography on silica gel (*n*-hexane/EtOAc 100:3) yielded **180** (90 mg, 89%) as a yellow solid. **¹H NMR** (300 MHz, CDCl₃) δ : 11.73 (s, 1H), 7.70 (dd, *J* = 7.5 and 1.2 Hz, 1H), 7.64-7.58 (m, 1H), 7.46 (s, 1H), 7.28 (dd, *J* = 8.4 and 1.2 Hz, 1H); **¹³C NMR** (75 MHz, CDCl₃)

152. C. Ríos-Luci, E. L. Bonifazi, L. G. León, J. C. Montero, G. Burton, A. Pandiella, R. I. Misico, J. M. Padrón. β -Lapachone analogs with enhanced antiproliferative activity. *Eur. J. Med. Chem.* **2012**, *53*, 264-274.

δ : 187.3 (C), 177.0 (C), 161.6 (C), 140.8 (C), 140.2 (CH), 136.3 (CH), 130.6 (C), 125.0 (CH), 120.9 (CH), 114.6 (C). **IR** (ATR): $\tilde{\nu}$ = 1675, 1633, 1586, 1451, 1196, 893, 745 cm^{-1} ; **m. p.** ($^{\circ}\text{C}$) = 138-139; **HRMS** (EI): Calcd for $\text{C}_{10}\text{H}_5^{79}\text{BrO}_3$ [$\text{M}, ^{79}\text{Br}$] $^+$ 251.9422, found 251.9427. Calcd for $\text{C}_{10}\text{H}_5^{81}\text{BrO}_3$ [$\text{M}, ^{81}\text{Br}$] $^+$ 253.9402, found 253.9390. *The structure of the product was also confirmed by X-ray diffraction* (CCDC number = 1859287). The data are consistent with those reported in the literature (ref. 141, p. 51).

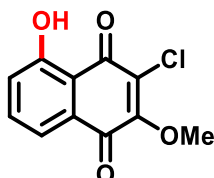


5-hydroxy-2-methylnaphthalene-1,4-dione (186): The general procedure B was followed using 2-methyl-1,4-naphthoquinone (**125**) as starting material (69 mg, 0.4 mmol). Purification by column chromatography on silica gel (*n*-hexane/EtOAc 50:1) yielded **186** (46 mg, 61%) as a yellow solid. **^1H NMR** (300 MHz, CDCl_3) δ : 11.92 (s, 1H), 7.58-7.55 (m, 2H), 7.21 (dd, J = 7.5 and 2.1, 1H), 6.76 (q, J = 1.5 Hz, 1H), 2.15 (d, J = 1.5 Hz, 3H); **^{13}C NMR** (75 MHz, CDCl_3) δ : 190.0 (C), 184.6 (C), 161.0 (C), 149.5 (C), 136.0 (CH), 135.3 (CH), 132.0 (C), 124.1 (CH), 119.2 (CH), 115.1 (C), 16.6 (CH₃); **IR** (ATR): $\tilde{\nu}$ = 1661, 1641, 1603, 1451, 1228, 833, 745 cm^{-1} ; **m.p.** ($^{\circ}\text{C}$) = 77-78; **HRMS** (EI): Calcd for $\text{C}_{11}\text{H}_8\text{O}_3$ [M] $^+$ 188.0473, found 188.0478. *The structure of the product was also confirmed by X-ray diffraction* (CCDC number = 1859288). The data are consistent with those reported in the literature (ref. 143, p. 52).

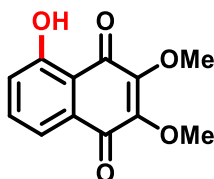


5-hydroxy-2-methoxy-3-methylnaphthalene-1,4-dione (191): The general procedure B was followed using 2-methoxy-3-methylnaphthalene-1,4-dione (**138**) as starting material (81 mg, 0.4 mmol). Purification by column chromatography on silica gel (*n*-hexane/EtOAc 50:1) yielded **191** (47 mg, 54%) as a yellow solid. **^1H NMR** (300 MHz, CDCl_3) δ : 12.21 (s, 1H), 7.52-7.49 (m, 2H), 7.17 (dd, J = 7.0 and 2.7 Hz, 1H), 4.11 (s, 3H), 2.03 (s, 3H); **^{13}C NMR** (75 MHz, CDCl_3) δ : 191.0 (C), 180.4 (C), 160.7 (C), 158.2 (C), 135.2 (CH), 131.4 (C), 130.7 (C),

124.4 (CH), 118.8 (CH), 114.3 (C), 61.1 (CH₃), 8.7 (CH₃); **IR** (ATR): $\tilde{\nu}$ = 1666, 1608, 1454, 1258, 1158, 763, 686 cm⁻¹; **m. p.** (°C) = 130-131; **HRMS** (ESI): Calcd for C₁₂H₁₁O₄ [M+H]⁺ 219.0652, found 219.0644; C₁₂H₁₀NaO₄ [M+Na]⁺ 241.0471, found 241.0468. *The structure of the product was also confirmed by X-ray diffraction* (CCDC number = 1859454). The data are consistent with those reported in the literature.¹⁵³



3-chloro-5-hydroxy-2-methoxynaphthalene-1,4-dione (192): The general B procedure was followed using 2-chloro-3-methoxynaphthalene-1,4-dione (**134**) as starting material (90 mg, 0.4 mmol). Purification by column chromatography on silica gel (*n*-hexane/EtOAc 20:1) yielded **192** (50 mg, 52%) as a yellow solid. **¹H NMR** (300 MHz, CDCl₃) δ : 11.83 (s, 1H), 7.56-7.54 (m, 2H), 7.22 (dd, *J* = 6.6 and 3.0 Hz, 1H), 4.30 (s, 3H); **¹³C NMR** (75 MHz, CDCl₃) δ : 183.6 (C), 178.7 (C), 161.1 (C), 157.1 (C), 135.8 (CH), 130.7 (C), 126.8 (CH), 125.1 (C), 119.9 (CH), 113.3 (C), 62.0 (CH₃); **IR** (ATR): $\tilde{\nu}$ = 3440, 1630, 1671, 1245, 747 cm⁻¹; **m. p.** (°C) = 140-142; **HRMS** (ESI): calcd for C₁₁H₇³⁵ClNaO₄ [M+Na, ³⁵Cl]⁺ 260.9931, found 260.9925 and calcd for C₁₁H₇³⁷ClNaO₄ [M+Na³⁷Cl]⁺ 262.9901, found 262.9896. *The structure of the product was also confirmed by X-ray diffraction* (CCDC number = 1859453). The data are consistent with those reported in the literature.¹⁵⁴

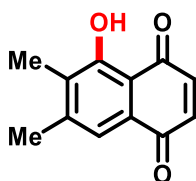


5-hydroxy-2,3-dimethoxynaphthalene-1,4-dione (193): The general procedure B was followed using 2,3-dimethoxynaphthalene-1,4-dione (**135**) as starting material (87 mg, 0.4

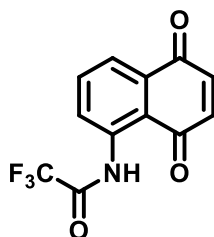
153. R. G. F. Giles, G. H. P. Roos. Syntheses of substituted 1,4-naphthoquinones by Diels–Alder addition of methoxycyclohexadienes to substituted 1,4-benzoquinones. *J. Chem. Soc., Perkin Trans 1*, **1976**, 19, 2057-2060.

154. G. Wurm, H.-J. Gurka, U. Geres. Untersuchungen an 1,4-Naphthochionen, 15. Mitt. Reaktion von 2- und 3-Chlor/Bromjuglonderivaten mit methanolischer Lauge (Teil 1: Monomere Produkte) *Arch. Pharm.* **1986**, 319, 1106-1113.

mmol). Purification by column chromatography on silica gel (*n*-hexane/EtOAc 10:1) yielded **193** (23 mg, 25%) as a yellow solid. $^1\text{H NMR}$ (300 MHz, CDCl_3) δ : 11.87 (s, 1H), 7.55 (dd, J = 4.5 and 0.6 Hz, 1H), 7.54-7.50 (m, 1H), 7.18 (dd, J = 5.1 and 0.6 Hz, 1H), 4.09 (s, 3H), 4.06 (s, 3H); $^{13}\text{C NMR}$ (75 MHz, CDCl_3) δ : 187.2 (C), 181.2 (C), 161.2 (C), 148.1 (C), 146.6 (C), 136.0 (CH), 130.8 (C), 124.5 (CH), 119.1 (CH), 113.3 (C), 61.7 (CH_3), 61.4 (CH_3); **IR** (ATR): $\tilde{\nu}$ = 1670, 1640, 1441, 1303, 1069, 758 cm^{-1} ; **m. p.** ($^\circ\text{C}$) = 88-89; **HRMS** (ESI): Calcd for $\text{C}_{12}\text{H}_{11}\text{O}_5$ $[\text{M}+\text{H}]^+$ 235.0606, found 235.0597. The data are consistent with those reported in the literature.¹⁵⁵



5-hydroxy-6,7-dimethylnaphthalene-1,4-dione (194): The general procedure B was followed using 6,7-dimethylnaphthalene-1,4-dione (**141**) as starting material (75 mg, 0.4 mmol). Purification by column chromatography on silica gel (*n*-hexane/EtOAc 100:3) yielded **194** (48 mg, 59%) as a yellow solid. $^1\text{H NMR}$ (300 MHz, CDCl_3) δ : 12.27 (s, 1H), 7.39 (s, 1H), 6.85 (s, 1H), 6.84 (s, 1H), 2.35 (s, 3H), 2.23 (s, 3H); $^{13}\text{C NMR}$ (75 MHz, CDCl_3) δ : 189.9 (C), 184.4 (C), 159.8 (C), 146.1 (C), 139.2 (CH), 138.5 (CH), 133.0 (C), 128.5 (C), 120.8 (CH), 112.4 (C), 20.9 (CH_3), 11.8 (CH_3); **IR** (ATR): $\tilde{\nu}$ = 2924, 1668, 1598, 1392, 1308, 1143, 1057 cm^{-1} ; **m. p.** ($^\circ\text{C}$) = 132-134; **HRMS** (ED): Calcd. for $\text{C}_{12}\text{H}_{10}\text{O}_3$ $[\text{M}]^+$ 202.0630, found 202.0633.

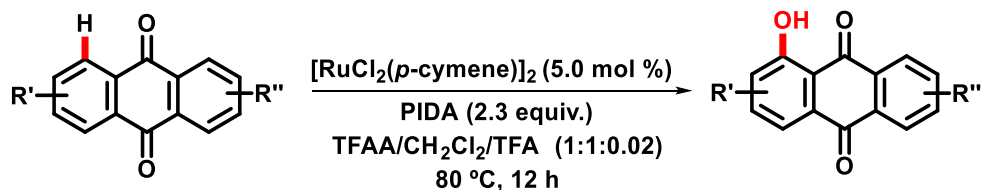


N-(5,8-dioxo-5,8-dihydronaphthalen-1-yl)-2,2,2-trifluoroacetamide (196): This product was isolated from reaction using general procedure B. $^1\text{H NMR}$ (300 MHz, CDCl_3) δ : 12.89 (s, 1H), 8.97 (dd, J = 6.0 and 1.2 Hz, 1H), 7.95 (dd, J = 6.3 and 1.5 Hz, 1H), 7.84-7.78 (m, 1H), 6.98 (s, 1H), 6.97 (s, 1H); $^{13}\text{C NMR}$ (75 MHz, CDCl_3) δ : 189.1, 183.6, 156.0 (q, J = 22.5 Hz),

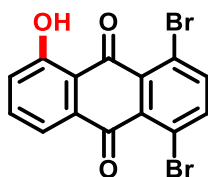
155. V. Ph. Anufriev, V. L. Novikov. Fluoride salts-alcohols-alumina as reagents for nucleophilic substitution of chlorine atoms for alkoxy groups in 2,3-dichlorosubstituted jugiones, naphthazarines, and quinizarines. *Tetrahedron Lett.* **1995**, 36, 2515-2518.

139.4, 138.4, 138.3, 136.0, 126.0 123.7, 117.4, 116.6, 114.3. **m. p.** (°C) = 135-137. **HRMS** (EI): Calcd. For C₁₂H₆F₃NNaO₃ [M+Na]⁺ 292.0197, found 292.0200.

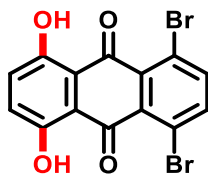
7.4 C–H oxygenation of anthraquinone: general procedure C and characterization data of products.



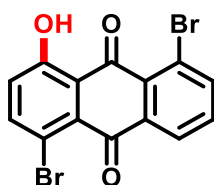
General Procedure C: The corresponding 9,10-anthraquinone (0.3 mmol), (diacetoxy-iodo)benzene (PIDA) (0.7 mmol) and [RuCl₂(*p*-cymene)]₂ (9 mg, 5.0 mol%) was added to a pressure and trifluoroacetic anhydride (TFAA) (1 mL), trifluoroacetic acid (0.02 mL) and CH₂Cl₂ (1 mL) were added. The mixture was stirred at 80 °C for 12 h. Then, the mixture was cooled to 25 °C and transferred to a 25 mL flask. CH₂Cl₂ (1 mL), H₂O (1 mL) and a solution of HCl (1M, 0.1 mL) were added dropwise. After 5 min, the solution was extracted with CH₂Cl₂ (3 x 10 mL) and dried over Na₂SO₄. The solvent was evaporated under reduced pressure and the crude product was purified by column chromatography on silica gel (PhMe).



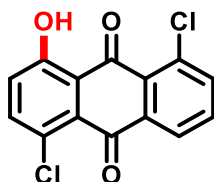
1,4-dibromo-5-hydroxyanthracene-9,10-dione (123): The general procedure C was followed using 1,4-dibromoanthracene-9,10-dione (**122**) as starting material (110 mg, 0.30 mmol). Purification by column chromatography on silica gel (PhMe) yielded **123** (80 mg, 70%) as a yellow solid. ¹H NMR (300 MHz, CDCl₃) δ: 12.09 (s, 1H), 7.80 (bs, 2H), 7.72 (dd, *J* = 7.5 and 1.5 Hz, 1H), 7.68-7.65 (m, 1H), 7.28 (dd, *J* = 8.4 and 1.5 Hz, 1H); ¹³C NMR (75 MHz, CDCl₃) δ: 185.9 (C), 180.7 (C), 161.8 (C), 141.1 (CH), 141.0 (CH) 136.9 (CH), 133.7 (C), 133.4 (C), 132.6 (C), 124.1 (C), 124.0 (C), 122.5 (CH), 119.3 (C), 116.0 (CH); IR (KBr): $\tilde{\nu}$ = 2923, 1711, 1671, 1454, 1301, 1235, 717 cm⁻¹; **m. p.** (°C) = 129-131; **HRMS** (EI): Calcd for C₁₄H₆O₃⁷⁹Br₂ [M, ⁷⁹Br]⁺ 379.8684, found 379.8690;



1,4-Dibromo-5,8-dihydroxy-9,10-anthraquinone (124): Compound **124** was isolated in 6% yield. $^1\text{H NMR}$ (300 MHz, CDCl_3) δ : 12.57 (s, 2H), 7.83 (s, 2H), 7.30 (s, 2H); $^{13}\text{C NMR}$ (75 MHz, CDCl_3) δ : 184.3 (C), 157.3 (C), 141.4 (C), 132.9 (CH), 129.3 (C), 122.8 (C), 112.6 (CH). **IR** (KBr): $\tilde{\nu}$ = 2924, 1668, 1635, 1538, 1454, 1302, 1236, 769 cm^{-1} ; **m. p.** ($^\circ\text{C}$) = 155-157; **HRMS** (EI): Calcd. for $\text{C}_{14}\text{H}_6\text{O}_4^{79}\text{Br}_2$ [M , ^{79}Br] $^+$ 395.8633, found 395.8634.



1,5-dibromo-4-hydroxyanthracene-9,10-dione (198): The general procedure C was followed using 1,5-dibromo-9,10-anthraquinone (**144**) as starting material (73 mg, 0.2 mmol). Purification by column chromatography on silica gel (PhMe) yielded **198** (42 mg, 55%) as a yellow solid. $^1\text{H NMR}$ (300 MHz, CDCl_3) δ : 12.97 (s, 1H), 8.30 (dd, J = 7.8 and 1.2 Hz, 1H), 8.02 (dd, J = 7.8 and 1.2 Hz, 1H), 7.84 (dd, J = 8.7 and 0.3 Hz, 1H), 7.61-7.58 (m, 1H), 7.14 (d, J = 8.7 Hz, 1H); $^{13}\text{C NMR}$ (75 MHz, CDCl_3) δ : 186.5 (C), 180.3 (C), 162.6 (C), 143.4 (CH), 141.3 (CH), 136.8 (C), 134.5 (CH), 129.6 (CH), 129.4 (CH), 127.8 (C), 125.4 (C), 122.3 (C), 118.2 (C), 112.6 (C); **IR** (ATR): $\tilde{\nu}$ = 1634, 1411, 1328, 1266, 1219, 1158, 1123, 789, 745, 441 cm^{-1} ; **m. p.** ($^\circ\text{C}$) = 218-219; **HRMS** (EI): Calcd for $\text{C}_{14}\text{H}_6\text{O}_3^{79}\text{Br}_2$ [M , ^{79}Br] $^+$ 379.8684, found 379.8675.



1,5-dichloro-4-hydroxyanthracene-9,10-dione (199): The general procedure C was followed using 1,5-dichloro-9,10-anthraquinone (**145**) as starting material (68 mg, 0.3 mmol). Purification by column chromatography on silica gel (PhMe) yielded **199** (49 mg, 57%) as a yellow solid. $^1\text{H NMR}$ (300 MHz, CDCl_3) δ : 13.01 (s, 1H), 8.26 (dd, J = 7.6 and 1.5 Hz, 1H), 7.79

(dd, $J = 7.9$ and 1.4 Hz, 1H), 7.71 (d, $J = 7.9$ Hz, 1H), 7.64 (d, $J = 9.2$ Hz, 1H), 7.25 (d, $J = 5.1$ Hz, 1H); ^{13}C NMR (75 MHz, CDCl_3) δ : 186.8 (C), 180.3 (C), 162.0 (C), 140.1 (CH), 137.6 (CH), 136.8 (C), 135.1 (C), 134.5 (CH), 128.2 (C), 128.1 (C), 127.1 (CH), 125.9 (C), 125.5 (CH), 117.8 (C); IR (ATR): $\tilde{\nu} = 1627, 1574, 1443, 1413, 1332, 1261, 1216, 1126, 769, 751$ cm^{-1} ; **m. p.** ($^{\circ}\text{C}$) = 250-251; **HRMS** (EI): Calcd for $\text{C}_{14}\text{H}_6\text{O}_3^{35}\text{Cl}_2$ [$\text{M}, ^{35}\text{Cl}$] $^{+}$ 291.9694, found 291.9698.

7.5 Trypanocidal Assays

Stock solutions of the compounds were prepared in dimethylsulfoxide (DMSO), with the final concentration of the latter in the experiments never exceeding 0.1%. Preliminary experiments showed that concentrations up to 0.5%, DMSO have no deleterious effect on the parasites. Bloodstream trypomastigotes of the Y strain were obtained at the peak of parasitaemia from infected albino mice, isolated by differential centrifugation and resuspended in Dulbecco's modified Eagle medium (DME) to a parasite concentration of 107 cells/mL in the presence of 10% of mouse blood. This suspension (100 μL) was added in the same volume of each compound previously prepared at twice the desired final concentrations. Cell counts were performed in Neubauer chamber and the trypanocidal activity was expressed as IC_{50} , corresponding to the concentration that leads to lysis of 50% of the parasites.

PART II

RHODIUM(III)-CATALYZED ANNULATION REACTIONS: DIVERSIFYING FLUORESCENT COMPOUNDS

In the second section of this thesis, it is present a new C–H activation/annulation protocols on lapimidazole, via rhodium catalyst, which was studied to obtain fluorescent compounds.

1. INTRODUCTION

Azoles are 5-membered aromatic heterocycles with a nitrogen atom and at least one more heteroatom. A representative example of this class is imidazole (200, Figure 7), which bears an additional N–H group, therefore called 1,3-diazole. This heterocycle can present a different pattern of substitution at 2, 4 and 5 positions and modifications on N–H group.

Several examples of imidazole derivatives have been described in literature and widely applied, particularly as bioactive compounds. For example, natural products, such as amino acid L-histidine (201) and hormone histamine (202), exhibit imidazole in their structure.¹⁵⁶ Other examples are antifungal miconazole (203)¹⁵⁷ and benznidazole (88), used in the treatment of Chagas disease;¹⁵⁸ antitumoral albendazole (204)¹⁵⁹ and, antibiotic metronidazole (205),¹⁶⁰ used for the treatment of many parasitic worm infestations; the sedative midazolam (206),¹⁶¹ and other examples.¹⁶²

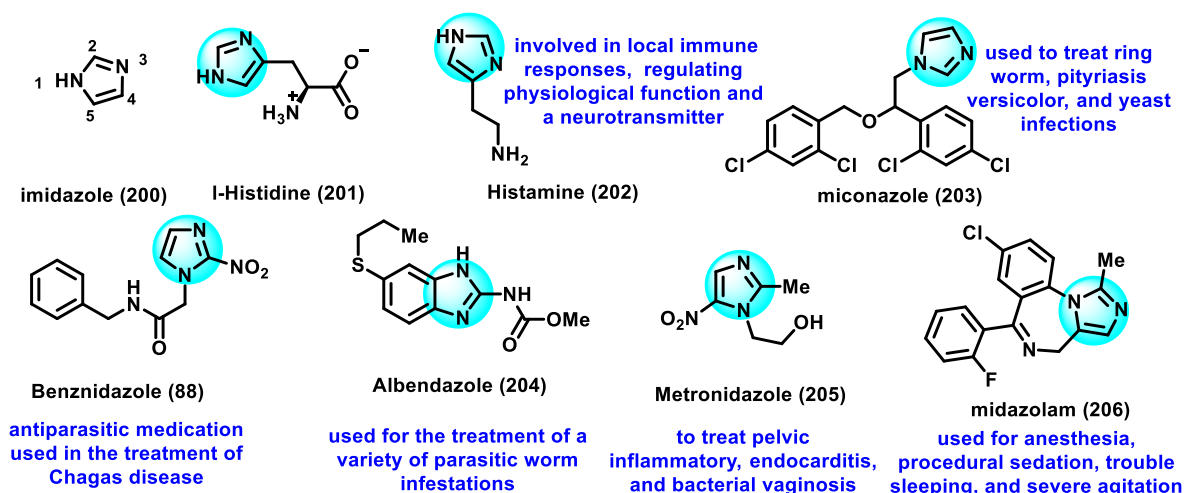


Figure 7. Examples of imidazole compounds with biological properties.

156. G. Nieto-Alamilla, R. Márquez-Gómez, A. M. García-Gálvez, G. E. Morales-Figueroa, J. A. Arias-Montaño. The Histamine H₃ Receptor: Structure, Pharmacology, and Function. *Mol. Pharmacol.* **2016**, *90*, 649-673.

157. A. Sadique, S. H. Khalid, S. Asghar, M. Irfan, I. U. Khan, A. Rasul, M. I. Qadir, K. Abbas. Miconazole nitrate microemulsion: preparation, characterization and evaluation for enhancement of antifungal activity. *Lat. Am. J. Pharm.* **2018**, *37*, 1578-86.

158. C. A. Morillo, J. A. Marin-Neto, A. Avezum, S. Sosa-Estani, A. Rassi, Jr., F. Rosas, E. Villena, R. Quiroz, R. Bonilla, C. Britto, F. Guhl, E. Velazquez, L. Bonilla, B. Meeks, P. Rao-Melacini, J. Pogue, A. Mattos, J. Lazdins, A. Rassi, S. J. Connolly, S. Yusuf. Randomized trial of benznidazole for chronic Chagas' Cardiomyopathy. *N. Engl. J. Med.* **2015**, *373*, 1295-1306.

159. L. S. E. P. W. Castro, M. R. Kvicinski, F. Ourique, E. B. Parisotto, V. M. A. S. Grinevicius, J. F. G. Correia, D. W. Filho, R. C. Pedrosa. Albendazole as a promising molecule for tumor control. *Redox Biol.* **2016**, *10*, 90-99.

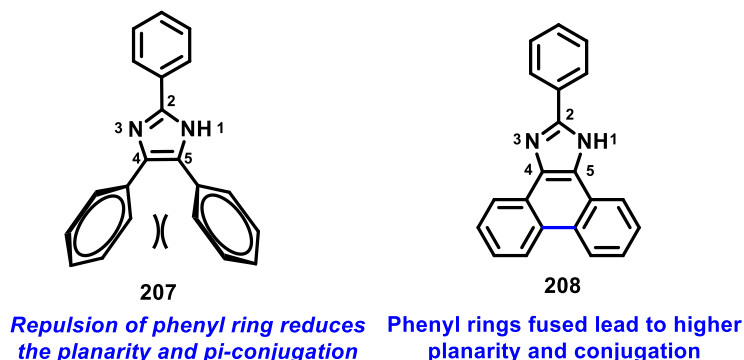
160. T. E. Rams, J. E. Degener, A. J. van Winkelhoff. Antibiotic resistance in human peri-implantitis microbiota. *Clin. Oral Impl. Res.* **2014**, *25*, 82-90

161. A. Conway, J. Rolley, J. R. Sutherland. Midazolam for sedation before procedures. *Cochrane Database of Syst. Rev.* **2016**, *5*, 1-89.

162. X. Zheng, Z. Ma, D. Zhang. Synthesis of imidazole-based medicinal molecules utilizing the Van Leusen imidazole synthesis. *Pharmaceuticals.* **2020**, *13*, 1-19.

Highly π -conjugated and planar compounds, such as imidazole 2,4,5-triphenyl-1*H*-imidazole (**207**) and 2-phenyl-1*H*-phenanthro[9,10-*d*]imidazole (**208**), illustrated in **Scheme 52**, may exhibit fluorescence properties. Hence, both compounds were investigated by Guo and co-workers.¹⁶³ The authors have concluded from density functional theory, that phenyl rings at 4 and 5 positions in **207** are out of the plane of imidazole, which results in steric effects (**Scheme 52**), reducing the planarity and the conjugation of π -system. Yet, both phenyl rings are fused to the imidazole ring in compound **208**, which results in the enhancement of the planarity and the rigidity.

As a consequence of this expansion of π -system conjugation, a decrease of the energy gap between HOMO and LUMO orbitals was observed, related to 2,4,5-triphenylimidazole (**207**), resulting in increasing the fluorescence quantum yield and the bathochromic effects in absorption end emission. Therefore, phenanthro[9,10-*d*]imidazole compounds are usually more fluorescents than 2,4,5-triphenyl-1*H*-imidazole. Indeed, those compounds may exhibit biological applications and optical uses.



Scheme 52. 2,4,5-Triphenylimidazole (**207**) and 9,10-phenanthroimidazole (**208**).

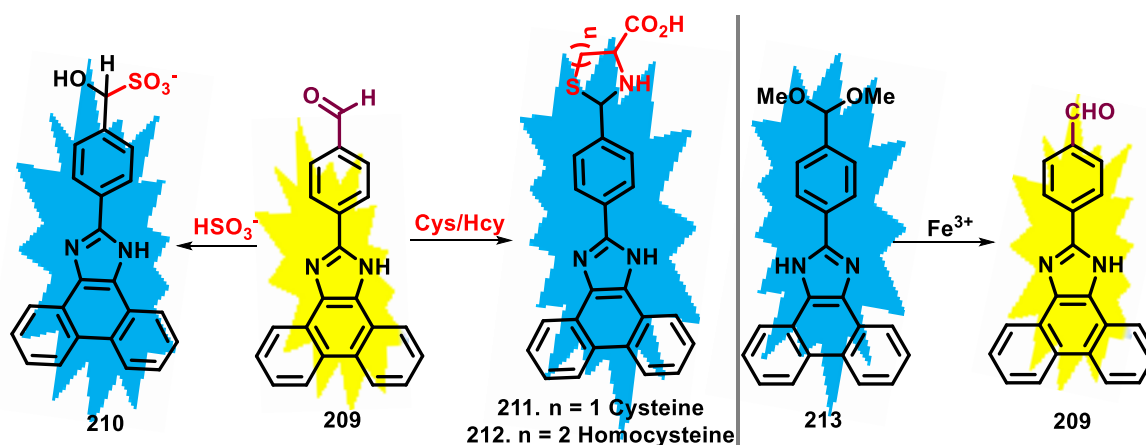
Fluorescents properties of phenanthro[9,10-*d*]imidazole have been widely investigated, addressed mainly to their potential application as a sensor probes for recognition and quantification of ionic and molecular species. For instance, phenanthro[9,10-*d*]imidazole **209** displayed yellowish-green fluorescence emission, associated with intramolecular charge transfer (ICT). Notwithstanding, hydrogen sulfite anions react with the formyl moiety resulting in aldehyde–hydrogen sulfite adduct, which displays blue fluorescence (**Scheme 53a**).¹⁶⁴ This change in

163. M. Tian, C. Wang, L. Wang, K. Luo, A. Zhao, C. Guo. Study on the synthesis and structure-effect relationship of multi-aryl imidazoles with their fluorescence properties. *Luminescence*. **2014**, 29, 540-548.

164. X. Cheng, H. Jia, J. Feng, J. Qin, Z. Li. “Reactive” probe for hydrogen sulfite: Good ratiometric response and bioimaging application. *Sens. Actuators B. Chem.* **2013**, 184, 274-280.

fluorescence emission, which does not occur for other anions, may lead **209** to be applied as an optical sensor for hydrogen sulfite anions. A similar approach using the same compound was described for the detection of cysteine and homocysteine.¹⁶⁵

In an appositional molecular designer, Long and co-workers have described the blue fluorescent phenanthro[9,10-*d*]imidazole **213**, that could undergo deacetylation induced by Fe³⁺ cation, leading to the formation of **209**, recovering the green-yellowish fluorescence of **209** (Scheme 53b).¹⁶⁶ In this sense, **213** could be used to detect Fe³⁺ cation, once no other cation provides the same reaction. Also, fluorescence modulation of phenanthro[9,10-*d*]imidazoles through selective reaction and/or interaction with analyte have been designed to fluorescent sensor toward hydrazine,¹⁶⁷ Cu²⁺,¹⁶⁸ ClO⁻,¹⁶⁹ F⁻,¹⁷⁰ Hg²⁺,¹⁷¹ Ag⁺,¹⁷² NO₂⁻,¹⁷³ Cr³⁺,¹⁷⁴ and others.



Scheme 53. Examples of fluorescent sensors 9,10-phenanthroimidazole-based to the detection of bisulfite, cysteine, homocysteine and Fe³⁺ cation.

- 165.** W. Lin, L. Long, L. Yuan, Z. Cao, B. Chen, W. Tan. A ratiometric fluorescent probe for cysteine and homocysteine displaying a large emission shift. *Org. Lett.* **2008**, *10*, 5577-5580.
- 166.** L. Long, L. Zhou, L. Wang, S. Meng, A. Gong, C. Zhang. A ratiometric fluorescent probe for iron(III) and its application for detection of iron(III) in human blood serum. *Anal. Chim. Acta.* **2014**, *812*, 145-151.
- 167.** H. Xu, B. Gu, Y. Li, Z. Huang, W. Su, X. Duan, P. Yin, H. La, S. Yao. A highly selective, colorimetric and ratiometric fluorescent probe for NH₂NH₂ and its bioimaging. *Talanta.* **2018**, *180*, 199-205.
- 168.** W. Lin, L. Yuan, W. Tan, J. Feng, L. Long. Construction of fluorescent probes via protection/deprotection of functional groups: A ratiometric fluorescent probe for Cu²⁺. *Chem. Eur. J.* **2009**, *15*, 1030-1035.
- 169.** W. Lin, L. Long, B. Chen, W. Tan. A ratiometric fluorescent probe for hypochlorite based on a deoxygenation reaction. *Chem. Eur. J.* **2009**, *15*, 2305-2309.
- 170.** R. Ali, S. S. Razi, M. Shahid, P. Srivastava, A. Misra. Off-On-Off fluorescence behavior of an intramolecular charge transfer probe toward anions and CO₂. *Spectrochim. Acta A.* **2016**, *168*, 21-28.
- 171.** Y. Guo, Y. Yan, X. Zhi, C. Yang, H. Xu. Phenanthroimidazole-based thiobenzamide as an effective sensor for highly selective detection of mercury(II). *Bioorg. Med. Chem. Lett.* **2013**, *23*, 3382-3384.
- 172.** G. Asaithambi, V. Periasamy. Phenanthrene-imidazole-based fluorescent sensor for selective detection of Ag⁺ and F⁻ ions: real sample application and live cell imaging. *Res. Chem. Intermediat.* **2019**, *45*, 1295-1308.
- 173.** B. Gu, L. Huang, J. Hu, J. Liu, W. Su, X. Duan, H. Li, S. Yao. Highly selective and sensitive fluorescent probe for the detection of nitrite. *Talanta.* **2016**, *152*, 155-161.
- 174.** C. Fan, X. Huang, C. A. Black, X. Shen, J. Qi, Y. Yi, Z. Lu, Y. Nie, G. Sun. A fast-response, fluorescent 'turn-on' chemosensor for selective detection of Cr³⁺. *RSC Adv.* **2015**, *5*, 70302-70308.

Beyond optical applications, phenanthro[9,10-*d*]imidazoles have been investigated for their biological properties. For instance, Patel and co-workers have described aryl-phenanthro[9,10-*d*]imidazole with potent activity against human colon cancer cell line HCT116,¹⁷⁵ whereas a similar structure with polyglycol side chains have demonstrated activity against different tumor cell lines, such as HL-60 (immature granulocyte leukemia), Bel-7402 (liver carcinoma), BGC-823 (gastrocarcinoma) and KB (nasopharyngeal carcinoma).¹⁷⁶ An outstanding biological application of phenanthro[9,10-*d*]imidazole against 60 tumoral human cell lines was investigated by Paul and co-workers.¹⁷⁷

175. A. Patel, S. Y. Sharp, K. Hall, W. Lewis, M. F. G. Stevens, P. Workman, C. J. Moody. Fused imidazoles as potential chemical scaffolds for inhibition of heat shock protein 70 and induction of apoptosis. Synthesis and biological evaluation of phenanthro[9,10-*d*]imidazoles and imidazo[4,5-*f*][1,10]phenanthrolines *Org. Biomol. Chem.* **2016**, *14*, 3889-3905.

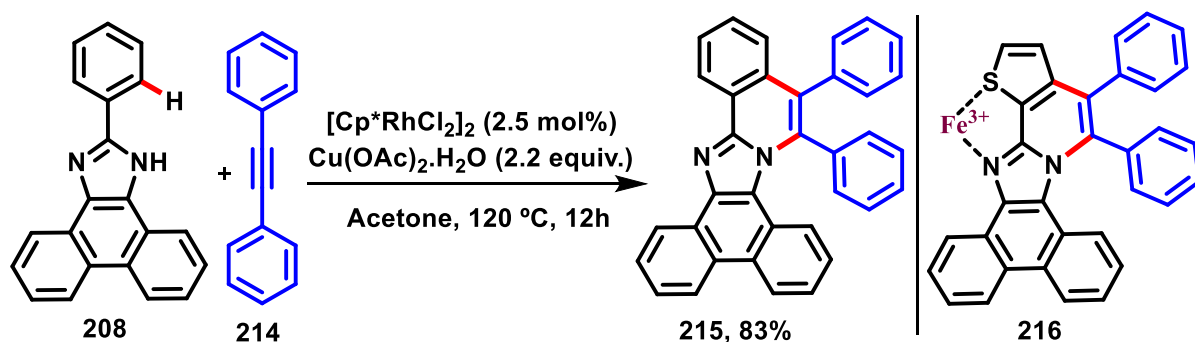
176. S. Wang, H. Li, C. Chen, J. Zhang, S. Li, X. Qin, X. Li, K. Wang. Cytotoxicity and DNA binding property of phenanthrene imidazole with polyglycol side chains. *Bioorg. Med. Chem. Lett.* **2012**, *22*, 6347-6351.

177. a) I. Singh, R. Rani, V. Luxami, K. Paul. Synthesis of 5-(4-(1*H*-phenanthro[9,10-*d*]imidazol-2-yl)benzylidene)thiazolidine-2,4-dione as promising DNA and serum albumin-binding agents and evaluation of antitumor activity. *Eur. J. Med. Chem.* **2019**, *166*, 267-280. **b)** I. Singh, V. Luxami, K. Paul. Synthesis of naphthalimide-phenanthro[9,10-*d*]imidazole derivatives: In vitro evaluation, binding interaction with DNA and topoisomerase inhibition *Bioorg. Chem.* **2020**, *96*, 103631.

2. MOTIVATION

The biological and fluorescent application of phenanthro[9,10-*d*]imidazoles has inspired scientists to develop synthetic strategies to obtain and modify of this heterocycle. The modification on those structures may modulate mainly fluorescent properties *via* the extension of π -conjugation. One of those emergent synthetic studies involves C–H/N–H annulation with an alkyne, a particular case of C–H activation.

For instance, in 2014, Zheng and Hua reported C–H/N–H annulation of 2-aryl-phenanthro[9,10-*d*]imidazoles with alkyne *via* rhodium catalyst (**Scheme 54**).¹⁷⁸ This synthetic approach led to a higher π -conjugated system. The authors applied the methodology to design a similar product **216** having a thiophene moiety. Fluorescent studies have indicated that Fe³⁺ cation can coordinate with **216**, leading to the increase of fluorescence emission, whereas no significant modification was observed for other cations.



Scheme 54. C–H/N–H annulation reaction of 2-aryl-phenanthro[9,10-*d*]imidazoles with alkyne *via* rhodium(III) reported by Zheng and Hua.

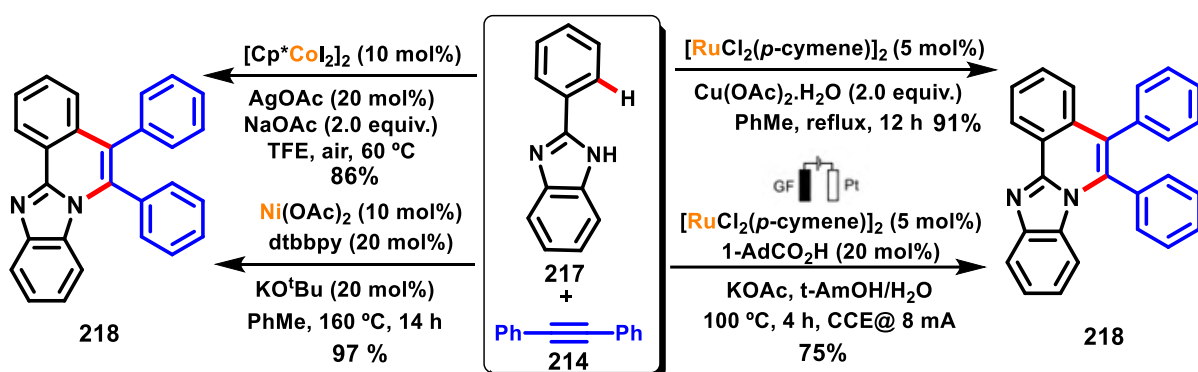
Similar reactions using phenyl-benzimidazole have been developed using ruthenium(II), cobalt(III), nickel(0) and nickel(II) as catalysts. Chandrasekhar and co-workers have described the oxidative annulation of **217** in reflux of toluene, using [RuCl₂(*p*-cymene)]₂ as a catalyst and Cu(OAc)₂·H₂O as oxidant (**Scheme 55**).¹⁷⁹ The replacement of toluene by PEG-400 (polyethylene glycol 400) led to the formation of **218** in similar yields, at room temperature

¹⁷⁸ L. Zheng, R. Hua. Modular assembly of ring-fused and π -extended phenanthroimidazoles *via* C–H activation and alkyne annulation. *J. Org. Chem.* **2014**, *79*, 3930-3936.

¹⁷⁹ N. Kavitha, G. Sukumar, V. P. Kumar, P. S. Mainkar, S. Chandrasekhar. Ruthenium-catalyzed benzimidazoisoquinoline synthesis *via* oxidative coupling of 2-arylbenzimidazoles with alkynes. *Tetrahedron Lett.* **2013**, *54*, 4198-4201

with the possibility of catalyst and PEG-400 recyclability for a few times without any significant loss of activity.

In 2018, Dutta and Sen reported the same reaction using a less expensive catalyst $[\text{Cp}^*\text{CoI}_2]_2$ (Scheme 55).¹⁸⁰ Chatani and co-workers have established a chemical protocol to achieve **218** via nickel catalysts.¹⁸¹ Recently, Ackermann and co-workers have envisaged the use of electrocatalysis, a more sustainable approach without metal oxidant, to provide dehydrogenative C–H/N–H annulation reaction of imidazoles using $[\text{RuCl}_2(p\text{-cymene})]_2$ as a catalyst (Scheme 55).¹⁸²



Scheme 55. Examples of C–H/N–H oxidative annulation of 2-phenylbenzimidazole.

Those examples described 2-aryl-phenanthro[9,10-*d*]imidazoles and 2-aryl-1*H*-benzo[*d*]imidazole as platforms to C–H/N–H annulation with an alkyne. However, the wide application of pyrene (**219**, Scheme 56), a polyaromatic hydrocarbon (PAH), as fluorescent probes¹⁸³ and organic semiconductors,¹⁸⁴ have inspired Gandhi and co-workers to perform similar reactions using 10-phenyl-9*H*-pyreno[4,5-*d*]imidazole (**220**, Scheme 56).¹⁸⁵ This strategy was applied as an attempt to introduce bulky aryl substituents into the π -extended conjugated

180. P. K. Dutta, S. Sen. (Benz)imidazole-directed cobalt(III)-catalyzed C–H activation of arenes: A facile strategy to access polyheteroarenes by oxidative annulation. *Eur. J. Org. Chem.* **2018**, 5512-5519.

181. A. Obata, A. Sasagawa, K. Yamazaki, Y. Ano, N. Chatani. Nickel-catalyzed oxidative C–H/N–H annulation of *N*-heteroaromatic compounds with alkynes. *Chem. Sci.* **2019**, *10*, 3242-3248.

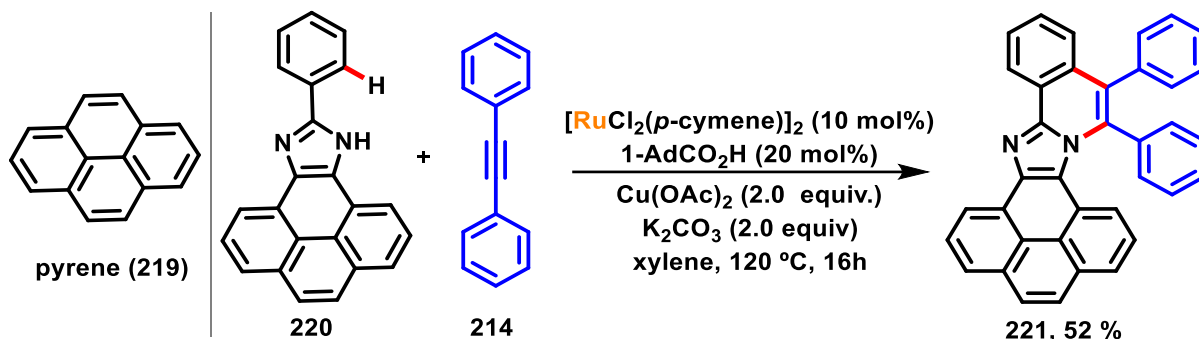
182. L. Yang, R. Steinbock, A. Scheremetjew, R. Kuniyil, L. H. Finger, A. M. Messinis, L. Ackermann. Azaruthena(II)-bicyclo-[3.2.0]-heptadiene: Key intermediate for ruthenaelectro(II/III/I)-catalyzed alkyne annulations. *Angew. Chem. Int. Ed.* **2020**, *59*, 11130-11135.

183. S. Karuppannan, J.-C. Chambron. Supramolecular chemical sensors based on pyrene monomer–excimer dual luminescence. *Chem. - Asian J.* **2011**, *6*, 964-984.

184. T. M. Figueira-Duarte, K. Müllen. Pyrene-based materials for organic electronics. *Chem. Rev.* **2011**, *111*, 7260-7314.

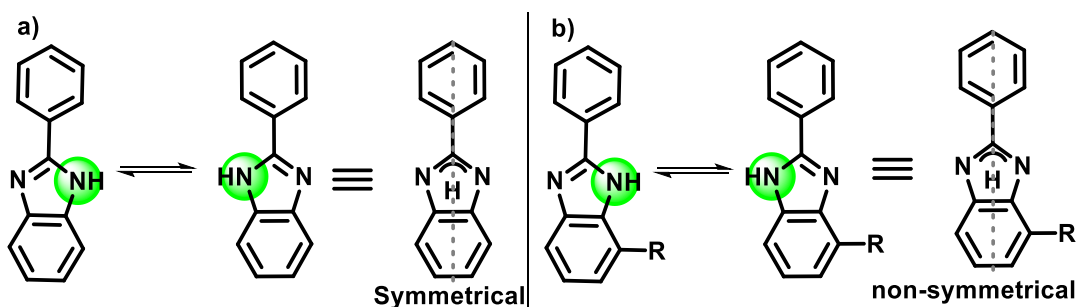
185. S. Karthik, J. Ajantha, C. M. Nagaraja, S. Easwaramoorthi, T. Gandhi. Synthesis and photophysics of extended π -conjugated systems of substituted 10-aryl-pyrenoimidazoles. *Org. Biomol. Chem.* **2016**, *14*, 10255-10266.

system (**221**) to avoid the π - π stacking or to provide aggregation-induced emission (AIE), resulting in a fluorescence enhancement.



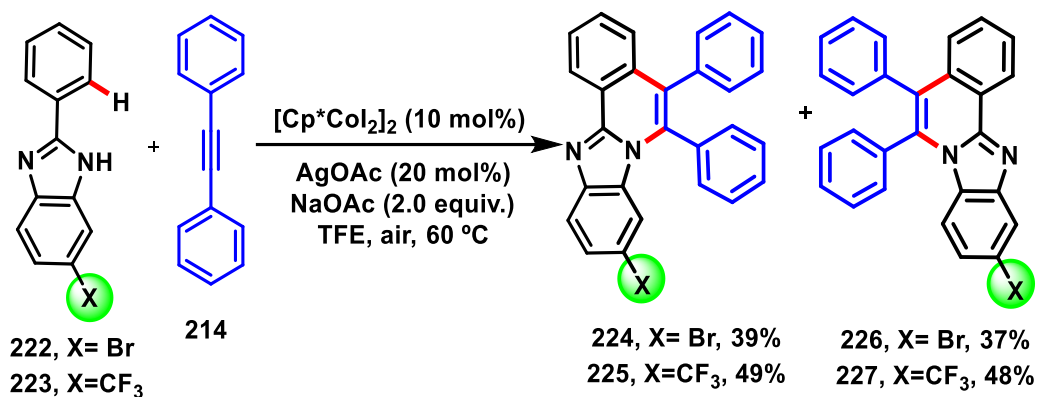
Scheme 56. C–H/N–H annulation of 10-phenyl-9*H*-pyreno[4,5-*d*]imidazole reported by Gandhi and co-workers.

Imidazole can be described in two tautomeric forms, since the hydrogen from N–H may be bound to one or other nitrogen (**Scheme 57a**). In absence of an element of asymmetry, imidazole can be considered a symmetrical molecule. Still, a substituent in the phenyl group and/or in the benzimidazole core could result in a non-symmetrical compound (**Scheme 57b**).



Scheme 57. Representation of symmetrical and non-symmetrical imidazole.

A careful observation of the previous C–H/N–H annulation reactions indicates the particular use of symmetrical imidazole instead of non-symmetrical imidazole. Probably, the choice of the symmetrical structure aims to avoid the formation of possible isomers. For instance, Dutta and Sen have reported two cases of non-symmetrical benzimidazole bearing a bromide (**222**) and trifluoromethyl (**223**) groups, which have resulted in the almost equimolar formation of two regioisomers in each case (**Scheme 58**).¹⁸⁰ Similar results were achieved by Chandrasekhar as well.¹⁷⁹

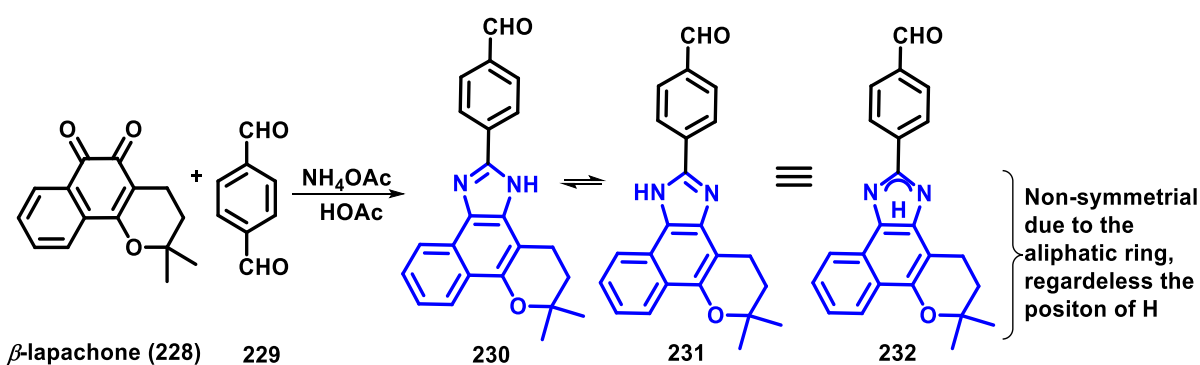


Scheme 58. Examples of non-symmetrical 2-phenyl-benzimidazole leading to isomeric products *via* C–H/N–H annulation reported by Dutta and Sen.

The lack of procedures involving C–H/N–H annulation in non-symmetric imidazole using alkyne illustrated by several examples, inspired us to pursue a new protocol to achieve a regioisomeric excess of one π -extend product. This possible regioselectivity was designed considering imidazole with a molecular group capable of inducing some selectivity.

3. SYNTHETIC STRATEGY

Imidazole obtained from β -lapachone (**228**), through a multicomponent reaction using an aldehyde and ammonium acetate, is an example of non-symmetrical imidazole due to the aliphatic ring. This class of imidazole, similar to phenanthro[9,10-*d*]imidazole and here generally called aryl-lapimidazole, is illustrated in **Scheme 59** for compound **230**. On the contrary of benzimidazole tautomeric forms described in **Scheme 57a**, tautomeric forms of lapimidazole (**230-231**) are different structures due to their lack of symmetry, which indicates that both structures can be found distinctly in equilibrium with a possible predominance of one of them, as it will be described below.



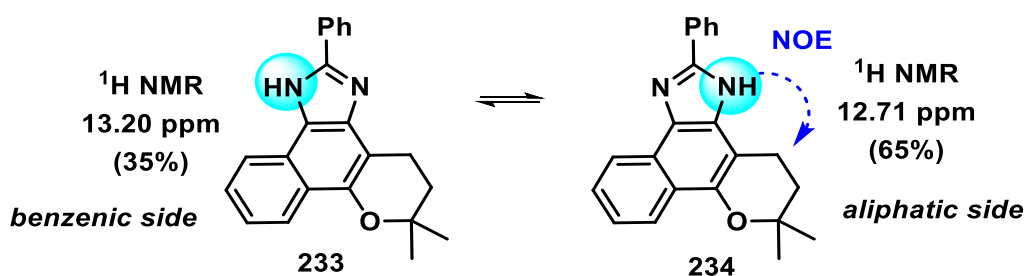
Scheme 59. Examples of lapimidazole **230** and its equivalents **231** and **232**.

For that reason, Carvalho and co-workers have reported a study about this equilibrium of phenyl-lapimidazole (**233**) as a prototype.¹⁸⁶ NMR spectra of **233** exhibited two signals associated with N–H, at 12.71 ppm (65%) and 13.20 ppm (35%). When ^1H NMR experiments are conducted in CDCl_3 or $\text{DMSO-}d_6$ with water, no signal is observed for N–H. The authors have associated this result to the quick exchange with hydrogen chloride (CDCl_3) and water (DMSO), present in these solvents. The origin for two ^1H NMR signals was attributed to two interconvertible isomers **233** and **234** (**Scheme 60**). Irradiation of ^1H NMR at signal 12.71 ppm, led to an increase in signal at 3.1 ppm (CH_2 from C ring), *via* Nuclear Overhauser Enhancement (NOE). Therefore, the signal in 13.20 was attributed to isomer **233** and the signal in 12.71 ppm to isomer **234**. In a concentrated solution of the compound in anhydrous $\text{DMSO-}d_6$ (50 mg/0.5

186. C. E. M. Carvalho, M. A. A. Silva, I. M. Brin, M. C. R. Pinto, A.V. Pinto, J. Schripsema, R. L. Longo. Tautomerization in the ground and first excited singlet states of phenyl-lapimidazole. *J. Lumin.* **2004**, *109*, 207-214.

mL), the coalescence of the signals was observed at 323 K, suggesting an intermolecular proton transfer process.

The approximate 1:2 ratio of N–H signals (35% for 13.20 and 65% for 12.71 ppm and ppm) indicates that, under these conditions, isomer **234** is more stable than isomer **233**, which was supported by theoretical calculation and photophysical experiments. Furthermore, the first X-ray crystallographic studies of that class of compounds confirms unequivocally the position of N–H on lapimidazole, at least in the solid-state.¹⁸⁷



Scheme 60. N–H equilibrium of imidazoles isomers.

Lapimidazole has been widely investigated since 1990, mainly as its potential application as trypanocidal agents.¹⁸⁸ More recently, fluorescent properties of this non-symmetrical azole have been applied to investigate intracellular compartments as well. For instance, lapimidazole **230**, described in **Scheme 59**, was designed to display intense blue/green fluorescence and evaluated as a bioprobe for mitochondria in MCF-7 cells (human breast adenocarcinoma cells).¹⁸⁹

*Based on the interaction between N–H group from non-symmetrical lapimidazole and the aliphatic ring, in addition to the equilibrium between **233** and **234**, described in **Scheme 60**, we found the hypothesis that regioselective C–H/N–H annulation via alkyne insertion could be envisaged for lapimidazole. Therefore, a similar synthetic methodology described in literature and previously discussed here, could be studied to modify non-symmetrical imidazole.*

187. K. C. G. Moura, P. F. Carneiro, M. C. F. R. Pinto, J. A. da Silva, V. R. S. Malta, C. A. de Simone, G. G. Dias, G. A. M. Jardim, J. Cantos, T. S. Coelho, P. E. A. da Silva, E. N. da Silva Junior. 1,3-Azoles from *ortho*-naphthoquinones: Synthesis of aryl substituted imidazoles and oxazoles and their potent activity against *Mycobacterium tuberculosis*. *Bioorg. Med. Chem.* **2012**, *20*, 6482-6488.

188. K. C. G. de Moura, F. S. Emery, C. N. Pinto, M. C. F. R. Pinto, A. P. Dantas, K. Salomão, S. L. de Castro, A. V. Pinto. Trypanocidal activity of isolated naphthoquinones from *Tabebuia* and some heterocyclic derivatives: A review from an interdisciplinary study. *J. Braz. Chem. Soc.* **2001**, *12*, 325-338.

189. F. S. dos Santos, G. G. Dias, R. P. de Freitas, L. S. Santos, G. F. de Lima, H. A. Duarte, C. A. de Simone, L. M. S. L. Rezende, M. J. X. Vianna, J. R. Corrêa, B. A. D. Neto, E. N. da Silva Junior. Redox center modification of lapachones towards the synthesis of nitrogen heterocycles as selective fluorescent mitochondrial imaging probes. *Eur. J. Org. Chem.* **2017**, *2017*, 3763-3773.

4. RESEARCH PURPOSE

4.1. General Purpose

This work aimed to develop a synthetic protocol involving C–H/N–H annulation reaction of phenyl-lapimidazole derivatives with an alkyne to achieve compounds with potential fluorescent and medicinal application.

4.1.1 Specific Purpose

- Methodological studies were conducted using different experimental conditions, such as different solvents, oxidants, additives, temperatures, reaction time;
- Synthesis of different aryl-lapimidazole followed by C–H/N–H annulation reaction to achieve new molecules;
- Photophysical studies with the fluorescent compounds were accomplished.

5. RESULTS AND DISCUSSIONS

5.1 C–H/N–H annulation optimizations

The first optimization studies of C–H/N–H annulation were based on studies previously described in the introduction using phenyl-lapimidazole (**234**) and diphenylacetylene (**214**) under different catalyst systems. The initial reactions were performed through $\text{RuCl}_3 \cdot \text{H}_2\text{O}/\text{AgOAc}$ and $\text{RuO}_3/\text{AgOAc}$ catalytic systems at 100 °C. Yet, after 24 h of reaction, no product was achieved and the starting materials were recovered (**Table 6**, entries 1 and 2). $[\text{Ru}(p\text{-cymene})\text{Cl}_2]_2/\text{AgOAc}$ catalyst system was also evaluated, resulting in the formation of annulated products **235** and **236** in 16%/10% (**Table 6**, entry 3). However, increasing the amount of silver source decreased the yield of **235** to 12% with a concomitant increase of **236** to 38% yield (**Table 6**, entry 4).

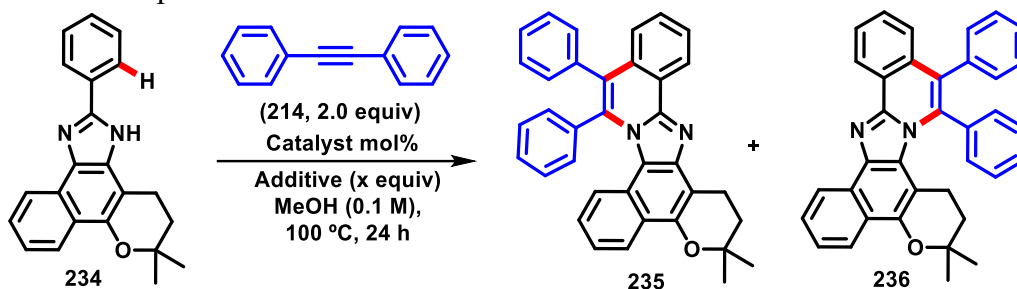
Other metal catalysts, like $\text{CoCp}^*(\text{CO})\text{I}_2$ and $\text{Pd}(\text{OAc})_2$, were evaluated as well, but the same unsuccessful results were obtained. $\text{Ir}(1,5\text{-cod})\text{Cl}]_2/\text{AgOAc}$ under similar conditions resulted in the desired products in 26%/5% yield (**Table 6**, entry 8), although they are unpromising results.

Finally, the product **235** was obtained in 48% yield and **236** in 9% yield when the reaction was carried out *via* $[\text{RhCp}^*\text{Cl}_2]_2/\text{AgOAc}$ (**Table 6**, entry 9). This promising result pointed to the possibility of yield improvement by increasing the amount of catalyst from 2 mol% to 5 mol%, from which the product **235** was obtained in 59% yield (**Table 6**, entry 10) and its respective isomer in only 19% yield. Same reaction conditions were carried out under an inert atmosphere with no significant improvement (**Table 6**, entry 11).

Prominent results under rhodium catalysis highlighted the possibility of using a similar catalyst to result in a good yield too. However, products **235** and **236** were not obtained when $[\text{Rh}(\text{OAc})_2]_2$, $[\text{Rh}(\text{nbd})\text{Cl}_2]_2$, $[\text{Rh}(\text{cod})\text{Cl}_2]_2$, $[\text{Rh}(\text{coe})_2\text{Cl}_2]_2$ were used in similar conditions.

The methodological studies have indicated that entry 10 was the best result. It had the majority asymmetric product isolated in moderate 59% yield, despite the by-side product in 19% yield. Moreover, this result showed an interesting observation: *although a pair of isomers was obtained, one of them was obtained with a considerable high yield, unlike the similar reaction to phenylbenzoimidazol, reported by Dutta and Sen (Scheme 58, p. 98).¹⁸⁰ The present result already indicated an overcoming in terms of regioselectivity in the methodologies previously discussed.*

Table 6. Selected optimization results.

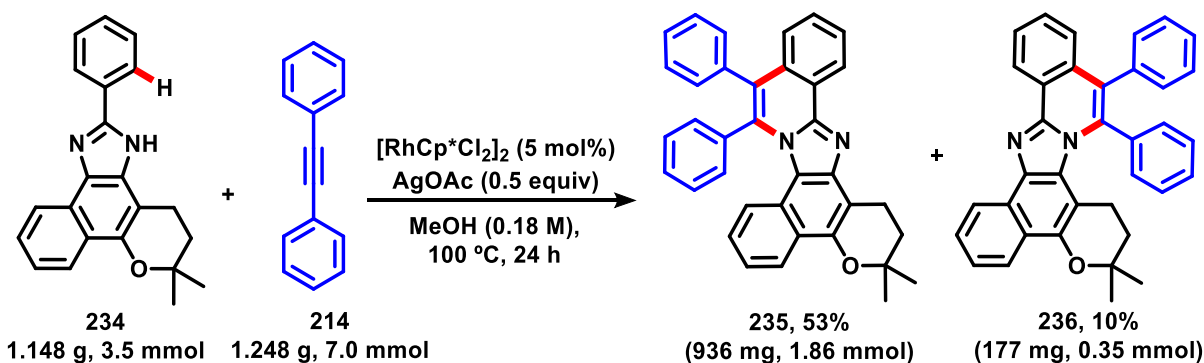


Entry	Catalyst (mol %)	Additive (equiv)	235/236 (%)	Entry	Catalyst (mol %)	Additive (equiv)	235/236 (%)
1	RuCl ₃ ·H ₂ O (5)	AgOAc (1.0)	NR/NR	11 ^b	[RhCp*Cl ₂] ₂ (5)	AgOAc (0.5)	60/17
2	RuO ₃ (10)	AgOAc (1.0)	NR/NR	12	[Rh(OAc) ₂] ₂ (2)	AgOAc (1.0)	NR/NR
3	[Ru(<i>p</i> -cymene)Cl ₂] ₂ (5)	AgOAc (0.5)	16/10	13	[Rh(nbd)Cl ₂] ₂ (5)	AgOAc (0.5)	trace
4	[Ru(<i>p</i> -cymene)Cl ₂] ₂ (5)	AgOAc (1.0)	12/38	14	[Rh(cod)Cl ₂] ₂ (5)	AgOAc (0.5)	trace
5	CoCp*(CO) ₂ (5)	AgOAc (1.0)	NR/NR	15	[Rh(coe) ₂ Cl ₂] ₂ (5)	AgOAc (0.5)	trace
6 ^a	CoCp*(CO) ₂ (10)	AgOAc (0.2)/NaOAc (2.0)	NR/NR	16	[RhCp*Cl ₂] ₂ (5)	AgOAc (2.0)	45/5
7	Pd(OAc) ₂ (5)	AgOAc (0.5)	NR/NR	17	[RhCp*Cl ₂] ₂ (5)	Cu(OAc) ₂ ·H ₂ O (2.0)	35/5
8	[Ir(1,5-cod)Cl] ₂ (5)	AgOAc (0.5)	26/5	18 ^a	[RhCp*Cl ₂] ₂ (5)	AgOAc (0.5)	46/7
9	[RhCp*Cl ₂] ₂ (2)	AgOAc (1.0)	48/9	19 ^c	[RhCp*Cl ₂] ₂ (5)	AgOAc (0.5)	41/8
10	[RhCp*Cl ₂] ₂ (5)	AgOAc (0.5)	59/19	20	-	AgOAc (0.5)	NR/NR

Reaction conditions: **234** (0.1 mmol), **214** (0.2 mmol), catalyst (5.0, 2.0 or 10 mol %), MeOH (1 mL), air. ^aReaction performed with TFE (1 mL) as solvent. ^bReaction performed at N₂ atmosphere. NR = No reaction. ^cReaction performed with *t*-AmOH (1 mL) as solvent. Yields of isolated products.

5.2 Gram scale synthesis for the preparation of **235** and **236**

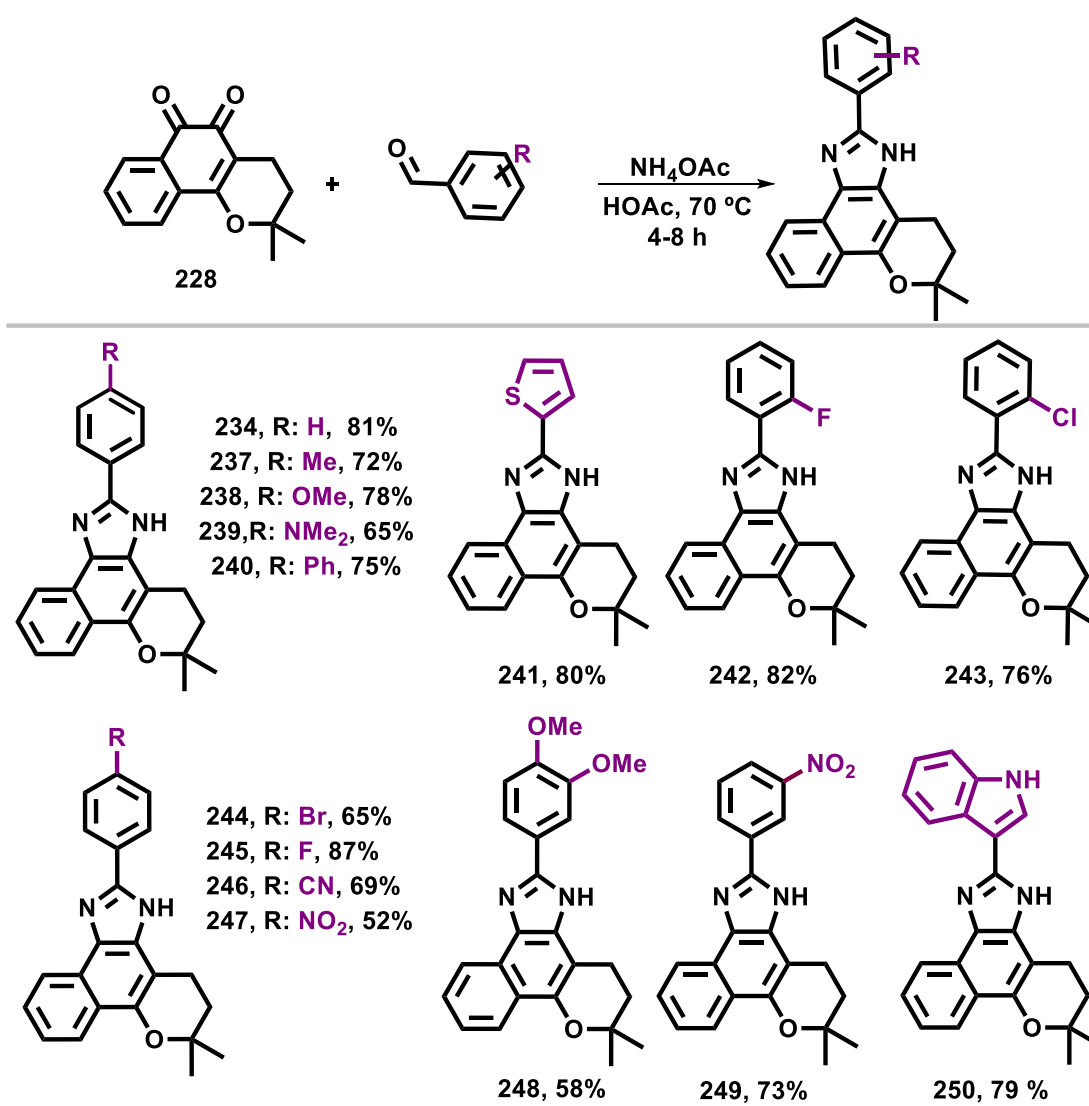
The practicality of the C–H/N–H annulation of phenyl-lapimidazole (**234**) has also been demonstrated by performing the reaction up to gram scale (**Scheme 61**). The product **235** was obtained in 53% yield and **236** was isolated in 10% yield, which demonstrates that the synthetic methodology applied is operational on a large scale.



Scheme 61. Gram scale synthesis for preparing **235** and **236**.

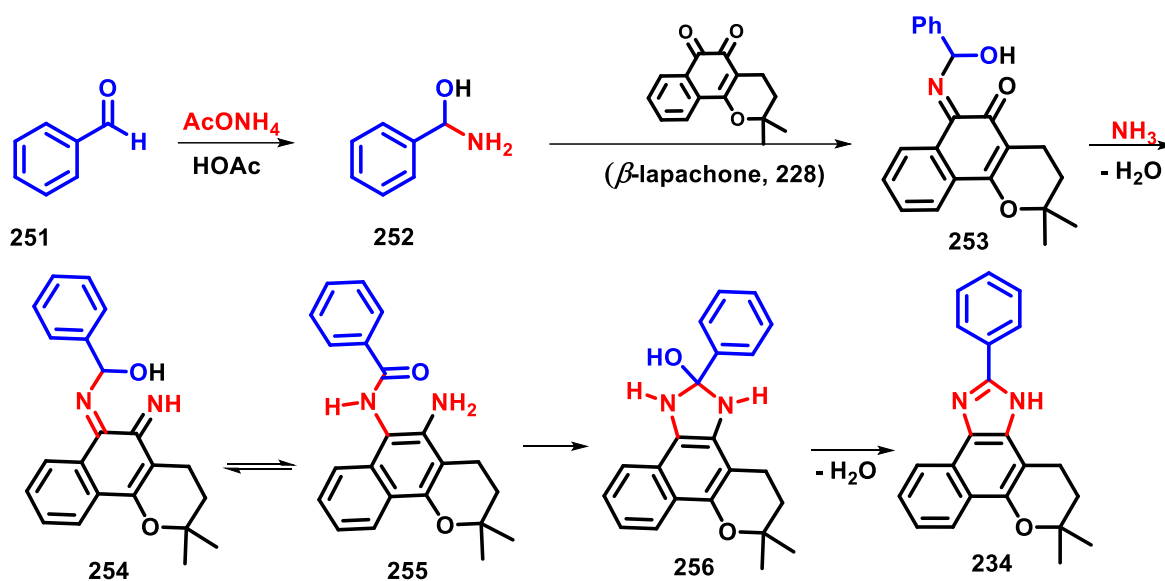
5.3 Synthesis of phenyl-lapimidazole derivatives

To investigate the applicability of the new developed C–H/N–H annulation, several aryl-lapimidazole were synthesized based on well-established protocols reported in the literature (mentioned in the experimental section) and products **240** and **248** are described here for the first time. Lapimidazoles were designed to bear different withdrawing and donating groups as well as one example of heterocycle group and one additional phenyl moiety (**Scheme 62**). Products were obtained in good yield (52–88% yield).



Scheme 62. Scope of lapimidazole designed for C–H/N–H annulation.

The lapimidazole synthesis mechanism is proposed in **Scheme 63**. The reaction between benzaldehyde (**251**) and ammonium acetate, in acetic acid, provides the aminoalcohol **252**, which reacts with β -lapachone (**228**), leading to the intermediate **253**. Posteriorly, **253** reacts with ammonia, from ammonium acetate, to achieve **254**, followed by the equilibrium to form amide **255**. Amine group of **255** attacks carbonyl moieties leading to an intramolecular heterocyclization, and then, to dehydration for providing phenyl-lapimidazole (**234**).



Scheme 63. Mechanistic proposal of the synthesis of lapimidazoles.

5.4 Scope of the rhodium(III)-catalyzed C–H/N–H annulation

The developed C–H/N–H annulation methodology was applied to aryl-lapimidazole previously described (**Scheme 62**), using optimized conditions in order to evaluate the applicability of this new synthetic approach. Results displayed in **Scheme 64** (p. 107) disclose that products of type **235** were obtained in a substantially higher yield than the product of type **236** in all the cases. This set of results reiterates the reaction regioselectivity using non-symmetrical imidazole, as previously described. Beyond that, in general, the main product was obtained in moderate yield (51-75% yield) whereas the second product was achieved in low yield (trace-22%).

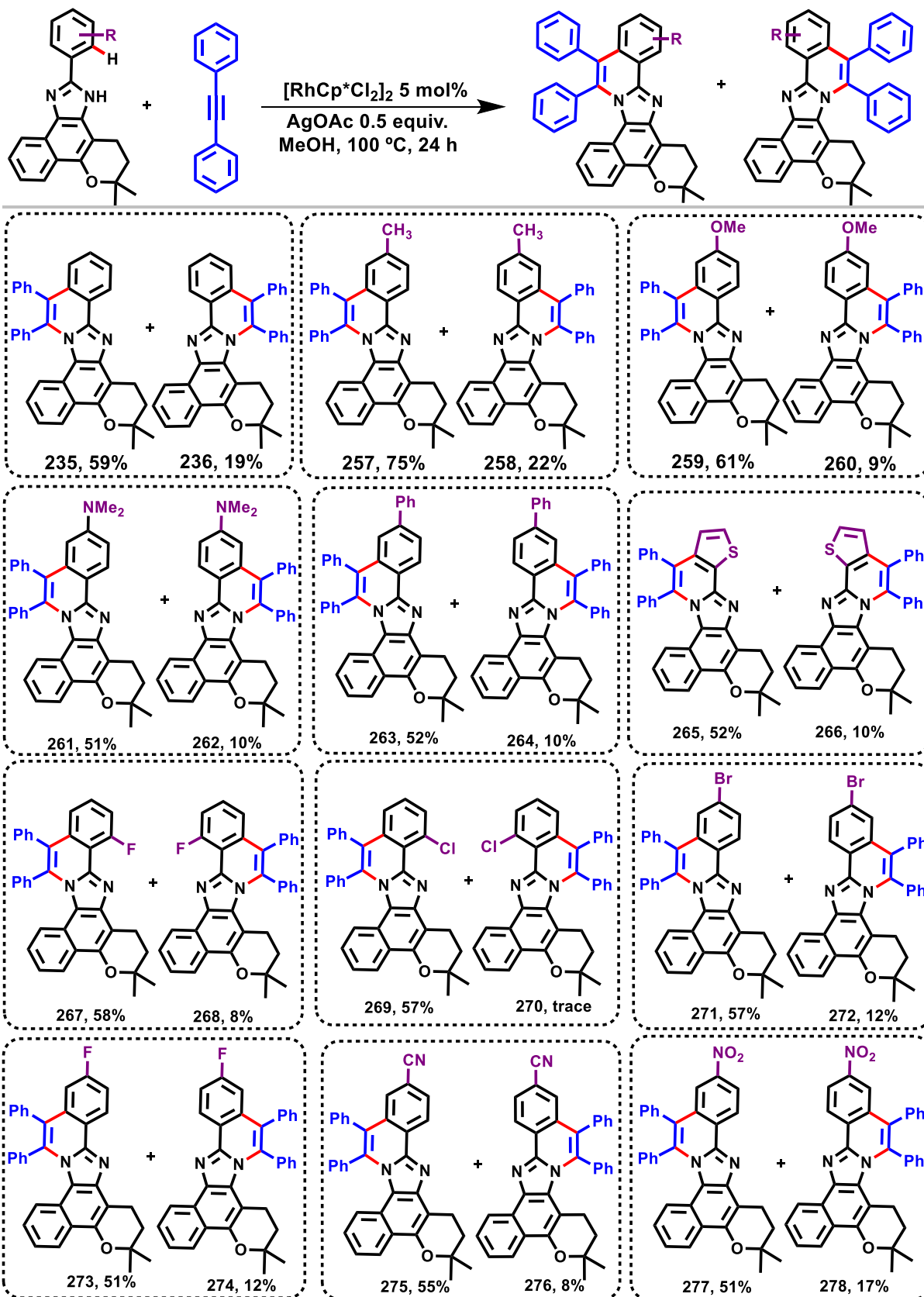
Phenyl-lapimidazole bearing a methyl group (**237**) led to the formation of annulated product **257** in 75% yield and its isomer in **258** in only 22% yield. Both products were obtained in higher yield than the isomers **235/236**. Similarly, phenyl-lapimidazole bearing a methoxy

group (**238**) resulted in the formation of products **259** and **260** in 61 % and 9% yield, respectively. With these first two examples, a hypothesis was built: electron donating groups could increase the reaction yield. Nevertheless, when imidazole containing an amino group **239** was used, a reduction to 51% and 10% yield of **261** and **262**, respectively, was observed. The presence of an additional phenyl group and the heterocyclic ring thiophene led to the products **263/264** and **265/266** in similar results of 52%/10% yield, respectively.

Examples bearing electron-withdrawing groups (EWG) were evaluated and resulted products in moderate yield. For example, phenyl-lapimidazol with *ortho*-fluor resulted in products **267** and **268** in 58%/8% yield, with a similar results to the *ortho*-chlorine substrate in 57% yield of **269**, although only trace of **270** was observed. *Para*-electron-withdrawing (EWG) group in lapimidazole such as bromine (**244**), fluor (**245**), nitrile (**246**) and nitro (**247**) led to the formation of isomeric pairs **271/272**, **273/274**, **275/276** and **277/278** in similar results of 57%/12%, 51%/12%, 55%/8% and 51%/17% yield, respectively.

These results indicate that the strength of electron-withdrawing groups, as well as its position at phenyl ring, do not cause significant modification in the yield. Also, those groups do not interfere in the reaction, which is resilient to electron-withdrawing groups. Although electron-donating groups methoxy and methyl have resulted in a higher yield, it was not the same standard for the amine group. These results disclose that a further investigation is necessary with similar groups to investigate a possible relationship between electron donating groups and reaction yields.

Two examples of phenyl-lapimidazole bearing a substituent at *meta* position, **248** and **249**, were evaluated for C–H/N–H annulation (**Figure 8**, p. 108). In those cases, product **279** was obtained in 49% yield whereas its isomer, **280**, was isolated in only 5% yield. The product bearing a nitro group, **281**, was isolated in 52% yield and its isomer was not obtained. When imidazole **250** was submitted to C–H/N–H annulation, no product was obtained.



Scheme 64. Substrate scope for C–H/N–H alkyne annulation of non-symmetric imidazole.

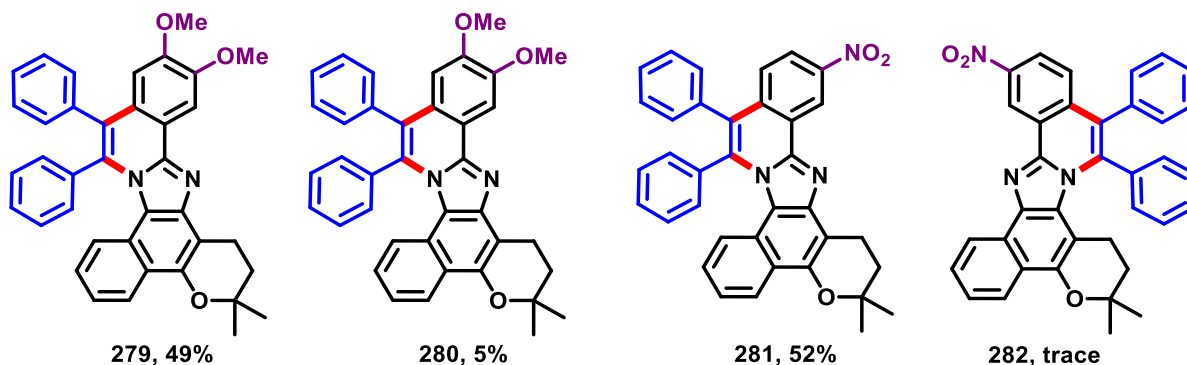
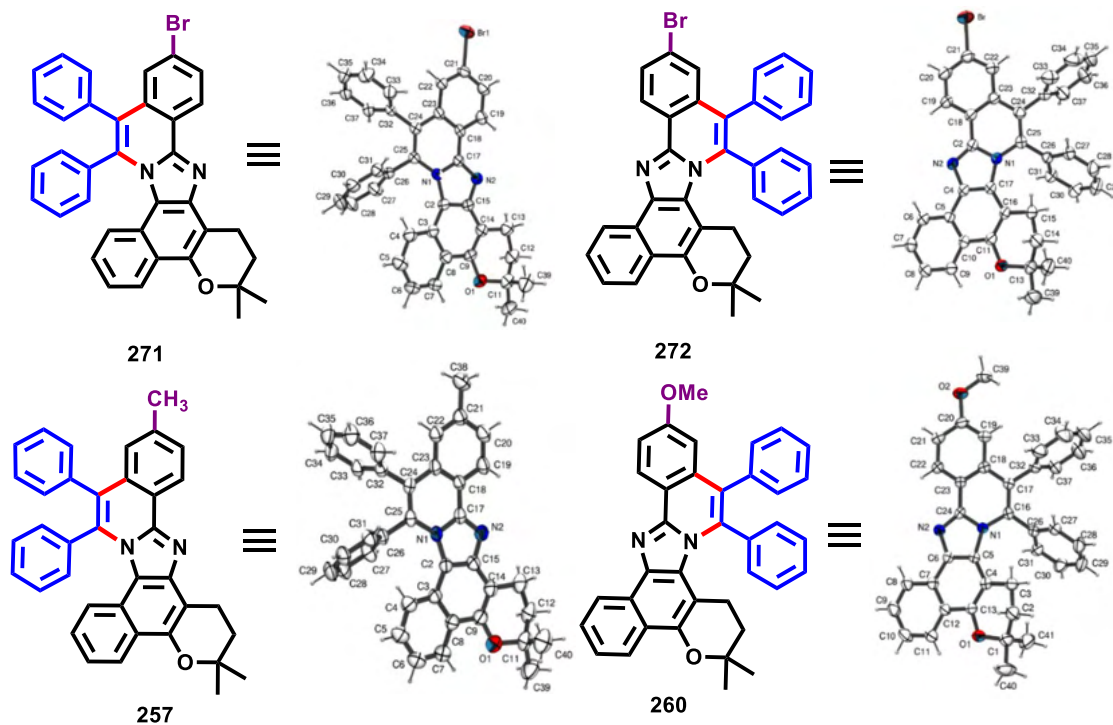


Figure 8. Examples of products bearing a substituent in *meta* position.

5.5 Characterization

As previously described in the optimization and scope studies, two isomeric products were isolated from C–H/N–H annulation. Aware of the proton equilibrium (**Scheme 60**, p. 100) and the general non-symmetry of lapimidazole (**Scheme 59**, p. 99), we have envisaged the possibility of C–H/N–H annulation in both sides of lapimidazole, here named aliphatic side and benzenic side, as illustrated in the **Scheme 64**. Indeed, High-Resolution Mass Spectrometry (HRMS) results have indicated that the two products from each reaction exhibited the same molecular mass, confirming the isomerism.

In order to undoubtedly determine the structure, compounds **271** and **272** were recrystallized by slow evaporation of a solvent mixture (ethyl acetate and hexane 1:20 mL) of 5 mg of the compounds. A pair of crystals of **271** and **272** suitable for X-ray diffraction studies were obtained and results confirmed the initial proposition of C–H/N–H annulation in both sides of lapimidazole (**Scheme 65**). Later, crystals of **257** and **260** were obtained as well, reinforcing the regioselectivity observed.



Scheme 65. Compounds **271**, **272**, **257** and **260** and their respective ortep-3 projection confirming the regioselectivity.

Furthermore, ^1H NMR experiments of isomeric pair **271** and **272** were conducted to compare both spectra and established differences between them (**Figure 9**). It is known that the ^1H NMR signals correspond methylene groups of β -lapachone derivatives appear approximately at 2.57 (t, $J = 6.7$ Hz) and 1.86 (t, $J = 6.7$ Hz) ppm.¹⁹⁰ For compound **271** the correspondent signals at methylene groups were observed at 3.37 (t, $J = 6.8$ Hz, 2H) and 2.05 (t, $J = 6.8$ Hz, 2H) ppm, less shielded concerning β -lapachone. Curiously, signals of those groups for isomer **272** were observed at 1.39-1.36 (m, 2H) and 1.31-1.28 (m, 2H), indicating that both methylene groups are highly shielded. Ortep-3 projection of **272** (**Scheme 65**) shows that phenyl is located near to methylene groups which could explain the shield of those groups.

In addition, compounds **257** and **260**, both confirmed by X-ray crystallography (**Scheme 65**), showed similar ^1H NMR behavior. Signals of methylene groups of **257** were observed at 3.41 (t, $J = 6.4$, 2H) and 2.05 (t, $J = 6.4$, 2H) ppm, as expected, whereas same groups were observed at 1.39 (t, $J = 6.6$ Hz, 2H) and 1.30 (t, $J = 6.6$ Hz, 2H) ppm for **260**. Those ^1H NMR enabled correct distinction of both isomers for all other compounds.

190. G. G. Dias, P. V. B. Pinho, H. A. Duarte, J. M. Resende, A. B. B. Rosa, J. R. Correa, B. A. D. Neto, E. N. da Silva Júnior. Fluorescent oxazoles from quinones for bioimaging applications. *RSC Adv.* **2016**, *6*, 76056-76063.

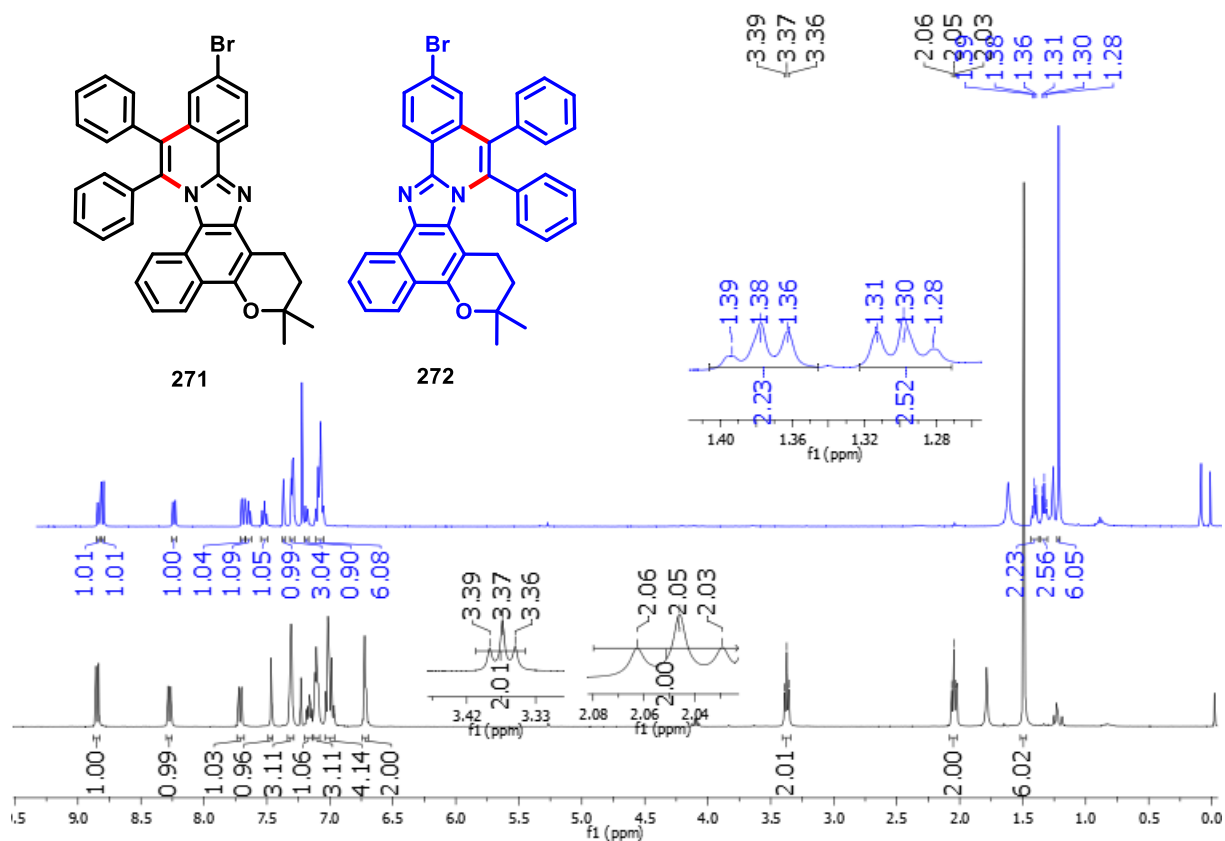
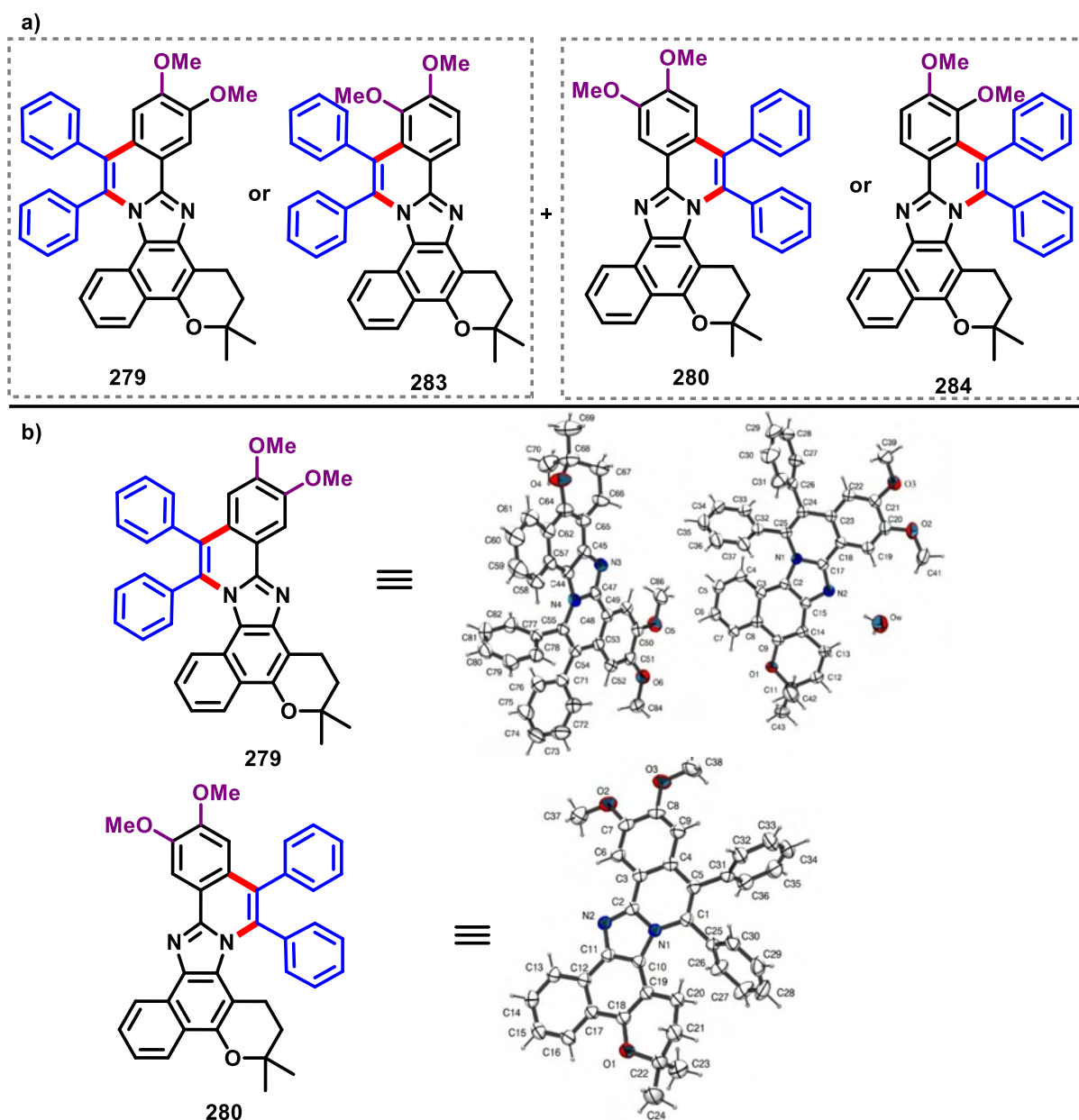


Figure 9. ^1H NMR (CDCl₃, 400 MHz) spectra of **271** and **272**.

In the case of lapimidazole bearing a *meta* substituent, four products are expected as results of the equilibrium of proton imidazole and the non-symmetry of the substrate, both scenarios were already described (**Scheme 57**, p. 97). For instance, possible products of lapimidazole **248** are shown in **Scheme 66a**, however, only products **279** and **280** were obtained (**Scheme 66b**). Crystallization of both products afforded suitable crystals for X-ray crystallography studies and the ortep-3 projection of those compounds unequivocally confirmed their structure.

An important highlight here is that, in the case of products **279** and **280**, the methoxy group is not close to the phenyl groups, as suggested for possible structures **283** and **284** (**Scheme 66**). This suggests that *meta* substituent may induce some stereoselectivity in this C–H/N–H annulation as result of repulsive interaction during the reaction. Although no suitable crystals for X-ray crystallography studies of **281** (**Figure 8**) were obtained, the structure of **281** is proposed here as a result of those observations. Also, further studies for confirm undoubtedly the structure will be carried out in due course.



Scheme 66. a) Possible isomeric products pairs **279/283** and **282/284**. b) X-ray crystallography studies of **279** and **280** confirming the regioselectivity.

5.6 Mechanism proposal

Once the synthetic methodology, scope and characterization, were well established we dedicated our efforts to understand the mechanism of this reaction. In contrast to C–H oxygenation and C–H alkenylation, described in the first section of this work, the mechanism of C–H/N–H annulation of imidazole is not well established yet. In this sense, detailed computational calculations were accomplished, *via* density functional theory (DFT), to clarify a mechanism

proposition. Theoretical studies were performed on both isomers **235** and **236** to elucidate preferential formation from **235** over **236**. The computed Gibbs free energies of all steps proposed for this reaction are illustrated in **Scheme 67** as well as the correspondent catalytic cycle of the mechanism in **Scheme 68**. The results described here first refers to the deprotonated N–H bond of the imidazole ring turned to the benzenic side to explain the formation of preferential product **235**.

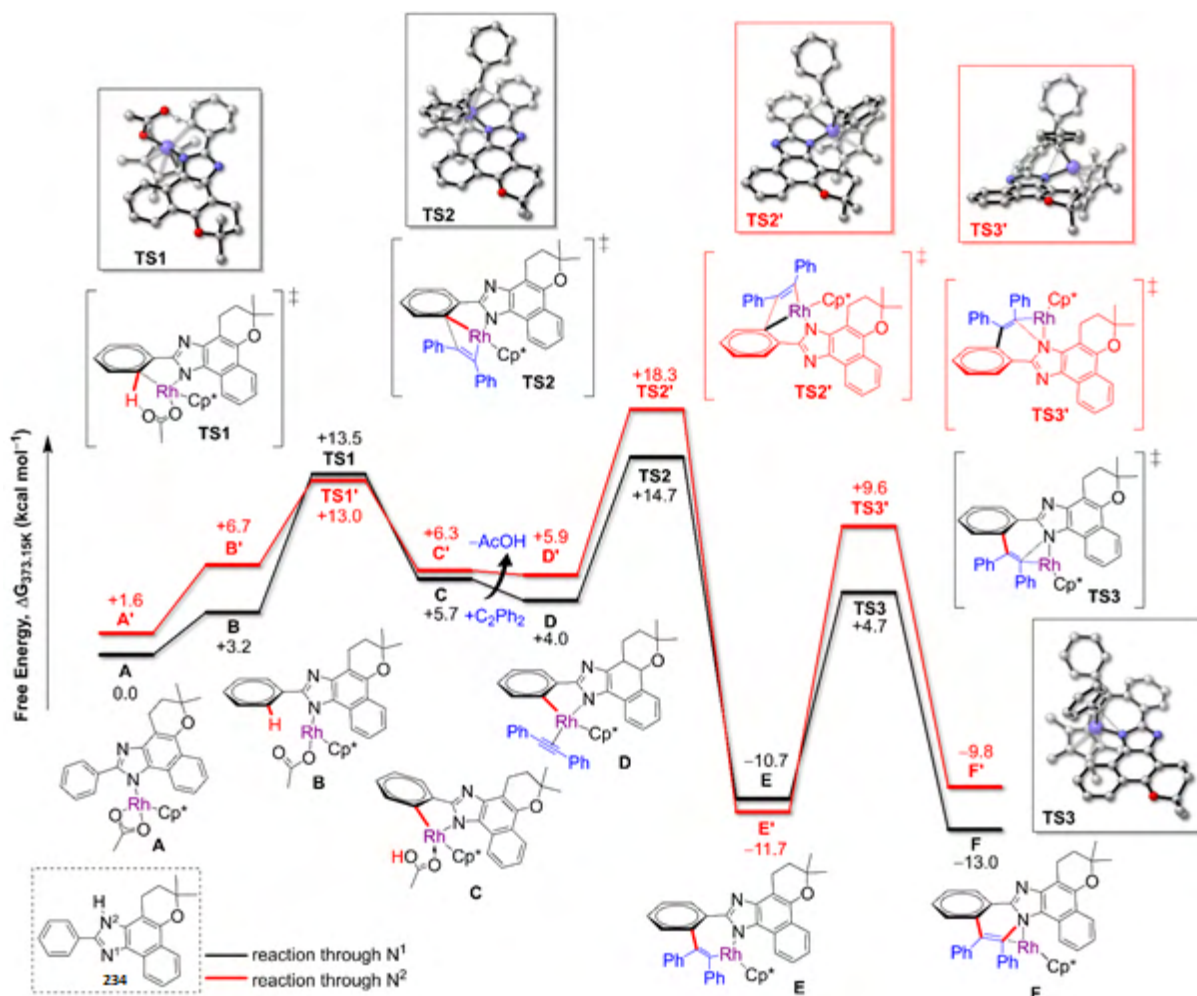
Initially, the deprotonation of N–H bond of lapimidazole and tautomerization to the benzenic side followed by metalation with [Cp*Rh(OAc)] resulted in the intermediate **A**. After that, one of the oxygen atoms of acetate was detached from Rh as a result of the metal interaction with the appropriate phenyl carbon atom, leading to intermediate **B**, *via* a slightly endergonic process ($\Delta G_{373.15} = 3.2 \text{ kcal mol}^{-1}$). The transition state **TS1**, with a free energy barrier of $+10.3 \text{ kcal mol}^{-1}$, was achieved, then, with the interaction between acetate and the carbon prone to C–H activation in an appropriated conformation. The proton abstraction by acetate with carbon-metal bond formation was established to form intermediate **C** and to release of AcOH and alkyne coordination (diphenylacetylene, **214**), resulting in the intermediate **D**.

The next step involves the alkyne insertion mediated by rhodium leading to **TS2** located $+14.7 \text{ kcal mol}^{-1}$ above **A**, followed by the formation of the seven-membered rhodacycle **E** slightly exoergic ($\Delta G_{373.15} = -3.2 \text{ kcal mol}^{-1}$). Then, **E** led to **TS3**, with the weakening of Rh-nitrogen bond and the concomitant interaction between carbon from alkyne and nitrogen from imidazole. **TS3** is achieved with the largest free energy barrier ($+15.4 \text{ kcal mol}^{-1}$) among the ones related to the formation of **235**. Then, Rh-mediated carbon-nitrogen coupling resulted in intermediate **F** *via* **TS3**, and, finally, the demetallation processes lead to the desired annulated product.

Similar studies were conducted using N–H bond of the imidazole ring, turned the aliphatic as a model to provide the minor product **236**. The results indicated that except for the seven-membered rhodacycles **E/E'**, the relative free energies of the structures after the alkyne coordination are systematically more positive than those from the other tautomer.

The transition states **TS2'** and **TS3'** are located $+18.3$ and $+9.6 \text{ kcal mol}^{-1}$ above **A**, respectively 3.6 and $4.9 \text{ kcal mol}^{-1}$ higher than **TS2** and **TS3**. Accordingly, **TS3'** has the largest free energy barrier ($+21.3 \text{ kcal mol}^{-1}$) among the ones obtained here, and the $\Delta G_{373.15}$ of the corresponding metallated product **F'** is $3.2 \text{ kcal mol}^{-1}$ higher than the $\Delta G_{373.15}$ of **F**. Those results can be attributed to the more sterically crowded aliphatic side of phenyl-lapimidazole than the benzenic side. Therefore, the coordination of alkyne and the subsequent migratory insertion

are less favorable in the tautomer where the N–H bond is turned to the aliphatic side, which might explain the observed preference for annulation at the benzenic side.



Scheme 67. Computed Gibbs free energies at $T = 373.15\text{ K}$ ($\Delta G_{373.15}$) in kcal mol^{-1} for the annulation of **234**. Black curves are related to the pathway starting from the metalation of N^1 (benzenic side) while the pathway in red shows the annulation of **1a** following metalation at N^2 (aliphatic side).

inversion of the quantum yields values, being larger for **278** than for **277** solutions, in the contrary of what was observed for the methoxy group of isomers.

Photophysical results of those selected compounds disclosed interesting findings, with respect to the effects of substituents in the absorption and emission of modified lapimidazole that was obtained. The results involving fluorescents properties make this new class of compounds suitable for technological applications, such as bioprobes. Further studies on Time-Correlated Single Photon Counting and application in cellular biology are being carried out.

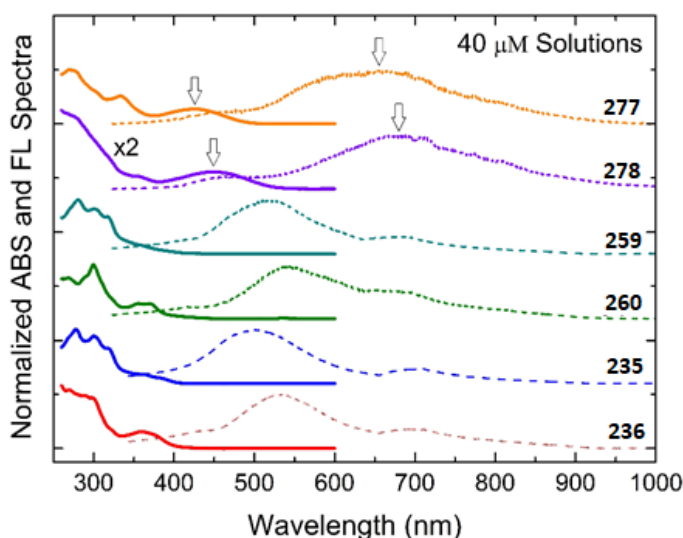


Figure 11. Absorption and fluorescence spectra at room temperature for the **235/236**, **259/260** and **277/278** isomer pairs of solutions at 40 μM in ethyl acetate.

Table 7. Parameters obtained from the analysis of the absorption (λ_{abs}) and fluorescence (λ_{em}) spectra respectively for the solutions and dropcast films fabricated as described in the experimental section, being $\Delta\lambda = (\lambda_{\text{em}} - \lambda_{\text{abs}})$.

	Compound	λ_{abs} (nm) \pm 10 nm	λ_{em} (nm) \pm 10 nm	$\Delta\lambda$ (nm) \pm 20 nm	$\phi \pm$ 15 %
Solution	235	409	629	220	0.256
	236	401	670	269	0.076
	259	412	663	251	0.232
	260	431	728	297	0.147
	277	490	874	384	0.114
	278	527	924	397	0.194
Film	235	425	606	181	-
	236	500	597	97	-
	259	436	605	169	-
	260	442	607	165	-
	277	552	802	250	-
	278	563	802	239	-

6. CONCLUSION

In this work, synthetic efforts were addressed to develop a synthetic methodology to perform the C–H/N–H annulation of lapimidazole. Despite the expensive rhodium catalyst, the reaction was carried out under air atmosphere, with no need of prior solvent treatment, and products were easily purified. A remarkable achievement of this synthetic approach is related to regioselectivity, once non-symmetrical imidazoles were used. Different lapimidazole substrates were used to demonstrate that reaction efficiency with a satisfactory yield over 51%. Curiously, substituents on lapimidazole did not affect systematically the yield of the reaction.

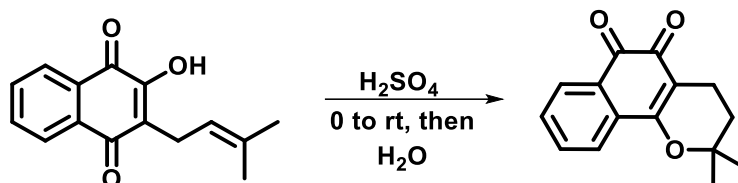
Furthermore, *via* theoretical calculation, it was possible to establish a mechanism proposition and a plausible explanation for the regioselectivity, as a result of the repulsive interaction between diphenylacetylene and the aliphatic moiety of lapimidazole. Crystallography of X-ray associated with NMR and HMRS enabled the characterization of the obtained products.

Photophysical studies were carried out with selected products, not only in ethyl acetate solution, but in solid-state as well. The results have demonstrated that those compounds exhibited intense fluorescence emission under condition studies. The major product displays blueshift emission in respect to the minor product, probably as a result of a minor efficiency in the pi-conjugation system of the major product.

Due to the easy-to-obtain process, stability and fluorescent properties, the obtained products could be a promising new class of compounds, with potent application in different fields of optical interest. Therefore, further studies involving the use of those compounds as bioprobes to investigate the cellular environment will be carried out.

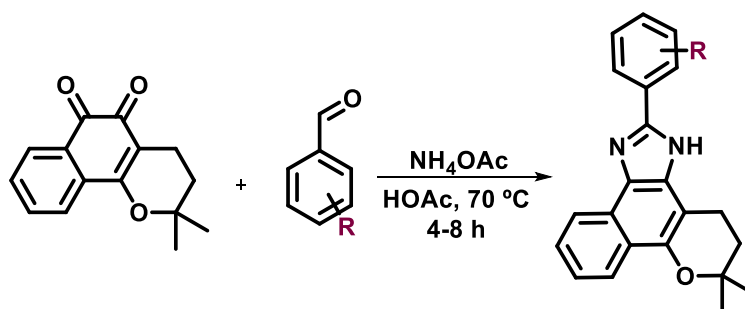
7. EXPERIMENTAL SECTION

7.1 Procedure for β -lapachone (**228**) synthesis



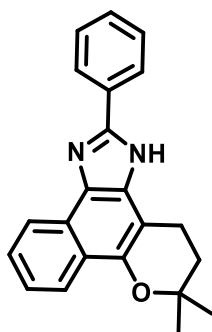
Sulfuric acid was slowly added to lapachol (**67**) (1 mmol, 242 mg) until complete dissolution of the quinone. Then, ice and water were added resulting in a precipitate which was filtered out and washed with water. Purification by column chromatography on silica gel (*n*-hexane/EtOAc 10:1) yielded β -lapachone (**228**) (240 mg, 90% yield) as an orange solid. $^1\text{H NMR}$ (400 MHz, CDCl_3 , 303 K) δ : 8.06 (dd, $J = 7.6$ and 1.4 Hz, 1H), 7.81 (dd, $J = 7.8$ and 1.1 Hz, 1H), 7.65 (ddd, $J = 7.8$, 7.6 and 1.4 Hz, 1H), 7.51 (m, 1H), 2.57 (t, 2H, $J = 6.7$ Hz), 1.86 (t, $J = 6.7$ Hz, 2H), 1.47 (s, 6H). $^{13}\text{C NMR}$ (100 MHz, CDCl_3 , 303 K) δ : 179.8, 178.5, 162.0, 134.7, 132.6, 130.6, 130.1, 128.5, 124.0, 112.7, 79.3, 31.6, 26.8, 16.2. **m. p.** ($^\circ\text{C}$): 153-155. Data are consistent with those reported in the literature (ref. 190. p. **Erro! Indicador não definido.**).

7.2 Synthesis of lapimidazole: general procedure D and characterization data of products.

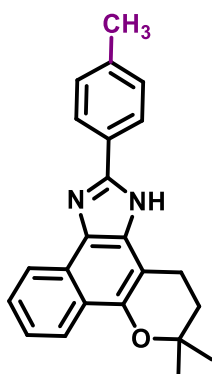


General Procedure D: β -lapachone (**228**, 242 mg, 1.0 mmol) was added to acetic acid (6 mL) at 70 $^\circ\text{C}$ under stirring followed by the correspondent aldehyde (1.2 mmol). Ammonium acetate (1.54 g, 16.5 mmol), was slowly added, and reflux was maintained for 4-6h. All the reactions were monitored by thin-layer chromatography. At the end of the reaction, ice and water were added to the mixture and the precipitate was filtered and washed with cold water (50 mL). Solid

was purified by column chromatography using as eluent a mixture of hexane/ethyl acetate, with a gradient of increasing polarity.¹⁹¹



6,6-dimethyl-2-phenyl-3,4,5,6-tetrahydrobenzo[7,8]chromeno[5,6-d]imidazole (234): The general procedure D was followed using β -lapachone (**228**) (242 mg, 1.0 mmol) and benzaldehyde (112.0 μ L, 1.1 mmol). Product was recrystallized in *n*-hexane/EtOAc 50:1 and yielded **234** (266 mg, 81%, 0.81 mmol) as a white solid. ¹H NMR (400 MHz, DMSO-*d*₆) δ : 13.23 and 12.74 (s, 1H), 8.41 (d, *J* = 8.0 Hz, 1H), 8.25 (d, *J* = 7.6 Hz, 2H), 8.14 (d, *J* = 6.3 Hz, 1H), 7.58-7.53 (m, 3H), 7.46-7.41 (m, 2H), 3.06 (bs, 2H), 1.97 (bs, 2H), 1.42 (s, 6H). **m. p.** (°C) = 273-275. Data are consistent with those reported in the literature.¹⁹²

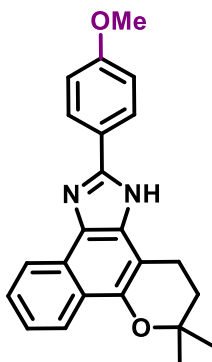


6,6-dimethyl-2-(*p*-tolyl)-3,4,5,6-tetrahydrobenzo[7,8]chromeno[5,6-d]imidazole (237): The general procedure D was followed using β -lapachone (**228**) (242 mg, 1.00 mmol) and 4-methylbenzaldehyde (130 μ L, 1.10 mmol). Product was recrystallized in (*n*-hexane/EtOAc 50:1) yielded **237** (247 mg, 72%, 0.72 mmol) as a white solid. ¹H NMR (400 MHz, DMSO-*d*₆) δ : 13.13 and 12.64 (s, 1H), 8.42-8.37 (m, 1H), 8.14 (bs, 3H), 7.57-7.53 (m, 1H), 7.43-7.40 (m,

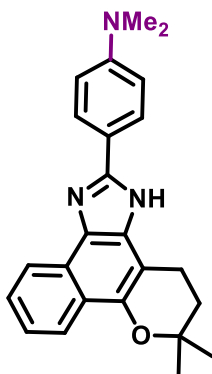
191. K. C. G. Moura, K. Salomão, R. F. S. Menna-Barreto, F. S. Emery, M. C. F. R. Pinto, A. V. Pinto, S. L. de Castro. Studies on the trypanocidal activity of semi-synthetic pyran[*b*-4,3]naphtho[1,2-*d*]imidazoles from β -lapachone. *Eur. J. Med. Chem.* **2004**, *39*, 639-645.

192. R. F. S. Menna-Barreto, A. Henriques-Pons, A. V. Pinto, J. A. Morgado-Diaz, M. J. Soares, S. L. De Castro. Effect of a β -lapachone-derived naphthoimidazole on *Trypanosoma cruzi*: identification of target organelles. *J. Antimicrob. Chemother.* **2005**, *56*, 1034-1041.

1H), 7.36-7.34 (m, 2H), 3.10-3.04 (m, 2H), 2.38 (s, 3H), 1.98-1.94 (m, 2H), 1.42 (s, 6H). **m. p.** (°C) = 230-232. Data are consistent with those reported in the literature.¹⁹¹



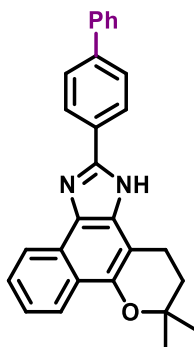
2-(4-methoxyphenyl)-6,6-dimethyl-3,4,5,6-tetrahydrobenzo[7,8]chromeno[5,6-*d*]imidazole (238): The general procedure D was followed using β -lapachone (**228**) (242 mg, 1.00 mmol) and 4-methoxybenzaldehyde (134 μ L, 1.10 mmol). Product was recrystallized in (*n*-hexane/EtOAc 50:1) yielded **238** (280 mg, 78%, 0.78 mmol) as a white solid. ¹H NMR (400 MHz, DMSO-*d*₆) δ : 13.04 and 12.57 (s, 1H), 8.38 (d, *J* = 6.8 Hz, 1H), 8.18 (d, *J* = 8.4 Hz, 2H), 8.13 (d, *J* = 8.4 Hz, 1H), 7.54 (t, *J* = 7.2 Hz, 1H), 7.40 (t, *J* = 7.2 Hz, 1H), 7.12 (d, *J* = 8.8 Hz, 2H), 3.84 (s, 3H), 3.06 (bs, 2H), 2.01-1.96 (m, 2H), 1.41 (s, 6H). **m. p.** (°C) = 110-120. Data are consistent with those reported in the literature.¹⁹³



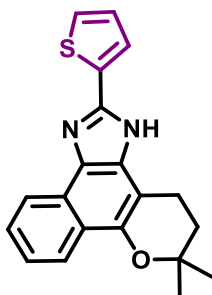
4-(6,6-dimethyl-3,4,5,6-tetrahydrobenzo[7,8]chromeno[5,6-*d*]imidazol-2-yl)-N,N-dimethylaniline (239): The general procedure D was followed using β -lapachone (**228**) (242 mg, 1.00 mmol) and 4-(dimethylamino)benzaldehyde (164 mg, 1.10 mmol). Purification by column chromatography on silica gel (*n*-hexane/EtOAc 5:1) yielded **239** (242 mg, 65%, 0.65 mmol) as

193. C. N. Pinto, A. P. Dantas, K. C. G. De Moura, F. S. Emery, P. F. Polequevitch, M. C. F. R. Pinto, S. L. de Castro, A. V. Pinto. Chemical reactivity studies with naphthoquinones from *Tabebuia* with anti-trypanosomal efficacy. *Arzneim.-Forsch./Drug Res.* **2000**, *12*, 1120-1128.

a white solid. $^1\text{H NMR}$ (400 MHz, DMSO- d_6) δ : 12.37 (bs, 1H), 8.30 (d, $J = 8.0$ Hz, 1H), 8.06 (d, $J = 8.0$ Hz, 1H), 8.01 (d, $J = 8.0$ Hz, 2H), 7.46 (t, $J = 8.0$ Hz, 1H), 7.31 (t, $J = 8.0$ Hz, 1H), 6.78 (d, $J = 8.0$ Hz, 2H), 2.99 (t, $J = 6.4$ Hz, 2H), 2.92 (s, 6H), 1.89 (t, $J = 6.4$ Hz, 2H), 1.34 (s, 6H). **m. p.** ($^\circ\text{C}$) = 217-219. Data are consistent with those reported in the literature (ref. 191, p. **Erro! Indicador não definido.**).

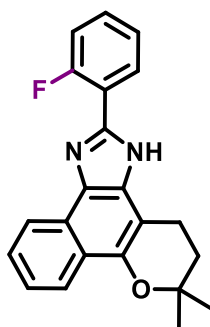


2-([1,1'-biphenyl]-4-yl)-6,6-dimethyl-3,4,5,6-tetrahydrobenzo[7,8]chromeno[5,6-*d*]imidazole (240): The general procedure D was followed using β -lapachone (**228**) (242 mg, 1.00 mmol) and biphenyl-4-carboxaldehyde (207 mg, 1.10 mmol). Purification by column chromatography on silica gel (*n*-hexane/EtOAc 5:1) yielded **240** (202 mg, 75%, 0.75 mmol) as a white solid. $^1\text{H NMR}$ (400 MHz, DMSO- d_6) δ : 13.27 and 12.79 (s, 1H), 8.43 (bs, 1H), 8.35 (d, $J = 8.0$ Hz, 2H), 8.16 (d, $J = 8.0$ Hz, 1H), 7.87 (d, $J = 8.0$ Hz, 2H), 7.78 (d, $J = 8.0$ Hz, 2H), 7.58 (t, $J = 7.6$ Hz, 1H), 7.50 (t, $J = 7.6$, 2H), 7.46-7.38 (m, 2H), 3.08 (bs, 2H), 1.98 (bs, 2H), 1.43 (s, 6H). **m. p.** ($^\circ\text{C}$) = 219-221.

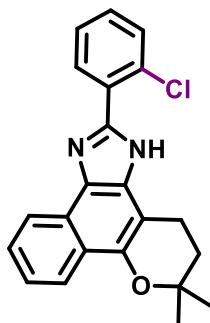


6,6-dimethyl-2-(thiophen-2-yl)-3,4,5,6-tetrahydrobenzo[7,8]chromeno[5,6-*d*]imidazole (241): The general procedure D was followed using β -lapachone (**228**) (242 mg, 1.00 mmol) and 2-thiophenecarboxaldehyde (103 μL , 1.10 mmol). Product was recrystallized in (*n*-hexane/EtOAc 50:1) yielded **241** (268 mg, 80%, 0.80 mmol) as a white solid. $^1\text{H NMR}$ (400 MHz, DMSO- d_6) δ : 13.30 and 12.85 (s, 1H), 8.32 (dd, $J = 22.8$ and 8.4 Hz, 1H), 8.11 (t, $J = 8.4$ Hz, 1H), 7.86-7.84 (m, 1H), 7.65 (dd, $J = 13.0$ and 4.8 Hz, 1H), 7.59-7.52 (m, 1H), 7.45-7.40 (m,

1H), 7.25-7.20 (m, 1H), 3.07-2.99 (m, 2H), 2.00-1.91 (m, 2H), 1.42 (s, 6H). **m. p.** (°C) = 183-185. Data are consistent with those reported in the literature.¹⁹⁴



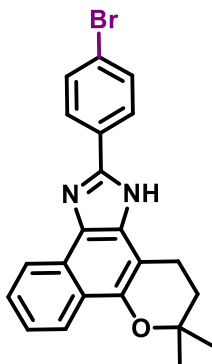
2-(2-fluorophenyl)-6,6-dimethyl-3,4,5,6-tetrahydrobenzo[7,8]chromeno[5,6-*d*]imidazole (242): The general procedure D was followed using β -lapachone (**228**) (242 mg, 1.00 mmol) and 2-fluorobenzaldehyde (116 μ L, 1.10 mmol). Product was recrystallized in (*n*-hexane/EtOAc 50:1) yielded **242** (284 mg, 82%, 0.82 mmol) as a white solid. ¹H NMR (400 MHz, DMSO-*d*₆) δ : 12.84 (bs, 1H), 8.44 (d, *J* = 8.0 Hz, 1H), 8.13 (d, *J* = 8.0 Hz, 2H), 8.07 (td, *J* = 7.6 and 1.6 Hz, 1H), 7.57-7.48 (m, 2H), 7.45-7.35 (m, 3H), 3.02 (t, *J* = 6.0 Hz, 2H), 1.91 (t, *J* = 6.0 Hz, 2H), 1.37 (s, 6H). **m. p.** (°C) = 200-201. Data are consistent with those reported in the literature (ref. 191, p. **Erro! Indicador não definido.**).



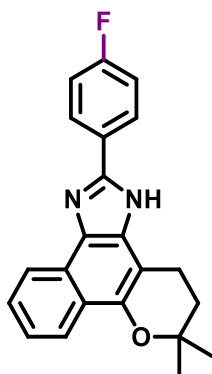
2-(2-chlorophenyl)-6,6-dimethyl-3,4,5,6-tetrahydrobenzo[7,8]chromeno[5,6-*d*]imidazole (243): The general procedure D was followed using β -lapachone (**228**) (242 mg, 1.00 mmol) and 2-chlorobenzaldehyde (124 μ L, 1.10 mmol). Product was recrystallized in (*n*-hexane/EtOAc 50:1) yielded **243** (305 mg, 76%, 0.76 mmol) as a white solid. ¹H NMR (400 MHz, DMSO-*d*₆) δ : 13.28 and 12.82 (s, 1H), 8.37 (bs, 1H), 8.16 (d, *J* = 8.0 Hz, 1H), 7.85-7.82 (m, 1H), 7.68-7.66 (m, 1H), 7.58-7.52 (m, 3H), 7.44 (t, *J* = 7.4, 1H), 2.99 (bs, 2H) 1.96 (bs, 2H),

194. A. M. Silva, L. Araújo-Silva, A. C. S. Bombaça, R. F. S. Menna-Barreto, C. E. R. Santos, A. B. B. Ferreira, S. L. de Castro. Synthesis and biological evaluation of N-alkyl naphthoimidazoles derived from β -lapachone against *Trypanosoma cruzi* bloodstream trypomastigotes. *Med. Chem. Commun.* **2017**, *8*, 952-959.

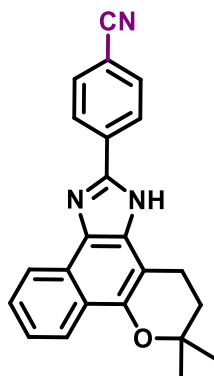
1.42 (s, 6H). **m. p.** (°C) = 132-133. Data are consistent with those reported in the literature (ref. 191, p. **Erro! Indicador não definido.**).



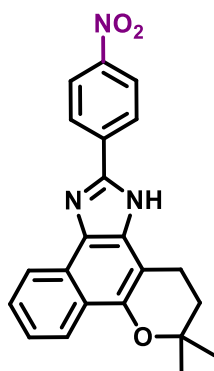
2-(4-bromophenyl)-6,6-dimethyl-3,4,5,6-tetrahydrobenzo[7,8]chromeno[5,6-*d*]imidazole (244): The general procedure D was followed using β -lapachone (**228**) (242 mg, 1.00 mmol) and 4-bromobenzaldehyde (204 mg, 1.10 mmol). Purification by column chromatography on silica gel (*n*-hexane/EtOAc 5:1) yielded **244** (265 mg, 65%, 0.65 mmol) as a white solid. ^1H NMR (400 MHz, DMSO-*d*₆) δ : 13.29 and 12.80 (s, 1H), 8.42-8.35 (m, 1H), 8.21-8.13 (m, 3H), 7.76-7.42 (m, 2H), 7.58-7.54 (m, 1H), 7.58-7.54 (m, 1H), 7.45-7.41 (m, 1H), 3.09-3.02 (m, 2H), 1.98-1.94 (m, 2H), 1.42 (s, 6H). **m. p.** (°C) = 255-257. Data are consistent with those reported in the literature (ref. 187, p. 100).



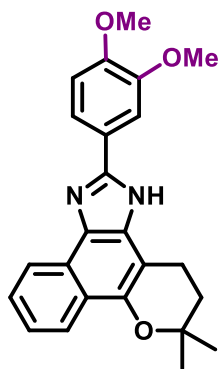
2-(4-fluorophenyl)-6,6-dimethyl-3,4,5,6-tetrahydrobenzo[7,8]chromeno[5,6-*d*]imidazole (245): The general procedure D was followed using β -lapachone (**228**) (242 mg, 1.00 mmol) and *p*-fluorobenzaldehyde (118 μL , 1.10 mmol). Product was recrystallized in (*n*-hexane/EtOAc 50:1) yielded **245** (300 mg, 87%, 0.87 mmol) as a white solid. ^1H NMR (400 MHz, DMSO-*d*₆) δ : 13.23 and 12.74 (s, 1H), 8.38 (dd, J = 22.8 and 8.0 Hz, 1H), 8.32-8.25 (m, 2H), 8.14 (t, J = 8.4 Hz, 1H), 7.56 (dd, J = 8.4 and 8.0 Hz, 1H), 7.45-7.37 (m, 3H), 3.11-3.01 (m, 2H), 2.00-1.92 (m, 2H), 1.40 (m, 6H). **m. p.** (°C) = 297-299. Data are consistent with those reported in the literature (ref. 191, p. **Erro! Indicador não definido.**).



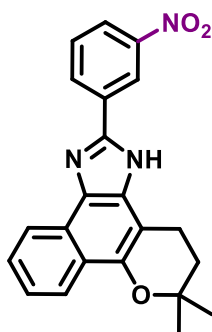
4-(6,6-dimethyl-3,4,5,6-tetrahydrobenzo[7,8]chromeno[5,6-*d*]imidazol-2-yl)benzonitrile (246): The general procedure D was followed using β -lapachone (**228**) (242 mg, 1.0 mmol) and 4-formylbenzonitrile (144 mg, 1.10 mmol). Purification by column chromatography on silica gel (*n*-hexane/EtOAc 5:2) yielded **246** (244mg, 69%, 0.69 mmol) as a white solid. $^1\text{H NMR}$ (400 MHz, DMSO-*d*₆) δ : 13.48 and 12.97 (s, 1H), 8.45-8.36 (m, 3H), 8.15 (t, $J = 8.4$ Hz, 1H), 8.01-7.97 (m, 2H), 7.59 (dd, $J = 7.2$ and 7.2 Hz, 1H), 7.45 (dd, $J = 7.2$ and 7.2 Hz, 1H), 3.02 (t, $J = 6.4$ Hz, 2H), 1.98 (t, $J = 6.4$ Hz, 2H). 1.42 (s, 6H). **m. p.** ($^{\circ}\text{C}$) = 160-162. Data are consistent with those reported in the literature (ref. 191, p. **Erro! Indicador não definido.**).



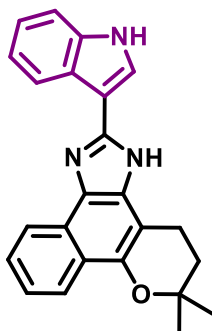
6,6-dimethyl-2-(4-nitrophenyl)-3,4,5,6-tetrahydrobenzo[7,8]chromeno[5,6-*d*]imidazole (247): The general procedure D was followed using β -lapachone (**228**) (242 mg, 1.00 mmol) and 4-nitrobenzaldehyde (166 μL , 1.10 mmol). Purification by column chromatography on silica gel (*n*-hexane/EtOAc 5:2) yielded **247** (194 mg, 52%, 0.52 mmol) as a red solid. $^1\text{H NMR}$ (400 MHz, DMSO-*d*₆) δ : 13.57 and 13.06 (s, 1H), 8.43-8.37 (m, 5H), 8.14 (d, $J = 7.2$ Hz, 1H), 7.59-7.46 (m, 2H), 3.02 (bs, 2H), 1.96 (bs, 2H), 1.41 (s, 6H). **m. p.** ($^{\circ}\text{C}$) = 193-195. Data are consistent with those reported in the literature (ref. 193, p. 120).



2-(3,4-dimethoxyphenyl)-6,6-dimethyl-3,4,5,6-tetrahydrobenzo[7,8]chromeno[5,6-*d*]imidazole (248): The general procedure D was followed using β -lapachone (**228**) (242 mg, 1.00 mmol) and 3,4-dimethoxybenzaldehyde (183 mg, 1.10 mmol). Purification by column chromatography on silica gel (*n*-hexane/EtOAc 5:2) yielded **248** (225 mg, 58%, 0.58 mmol) as a yellow solid. $^1\text{H NMR}$ (400 MHz, DMSO-*d*₆) δ : 12.99 and 12.57 (s, 1H), 8.39 (d, $J = 7.2$ Hz, 1H), 8.14 (d, $J = 8.4$ Hz, 1H), 7.83-7.82 (m, 2H), 7.55 (t, $J = 7.6$ Hz, 1H), 7.41 (t, $J = 7.6$ Hz, 1H), 7.13 (d, $J = 8.4$ Hz, 1H), 3.92 (s, 3H), 3.84 (s, 3H), 3.07 (bs, 2H), 1.98-1.97 (m, 2H), 1.42 (s, 6H). **m. p.** ($^{\circ}\text{C}$) = 193-195.



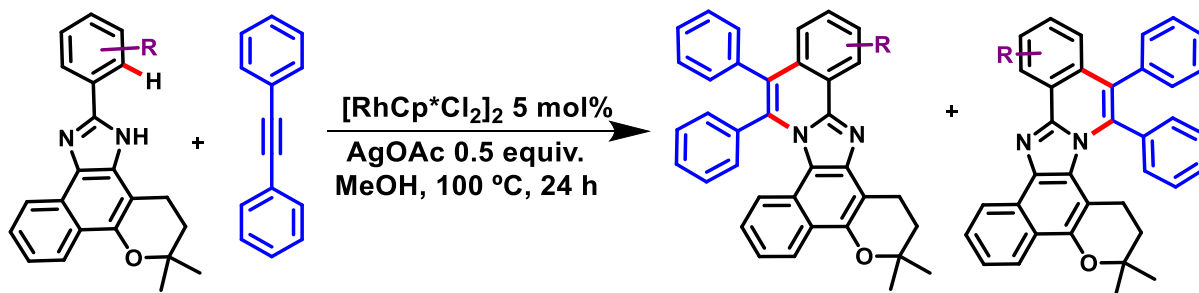
6,6-dimethyl-2-(3-nitrophenyl)-3,4,5,6-tetrahydrobenzo[7,8]chromeno[5,6-*d*]imidazole (249): The general procedure D was followed using β -lapachone (**228**) (242 mg, 1.00 mmol) and 3-nitrobenzaldehyde (166 mg, 1.10 mmol). Product was recrystallized in (*n*-hexane/EtOAc 50:1) and yielded **249** (273 mg, 73%, 0.73 mmol) as a yellow solid. $^1\text{H NMR}$ (400 MHz, DMSO-*d*₆) δ : 13.07 and 11.99 (s, 1H), 9.07 (s, 1H), 8.66 (d, $J = 7.2$ Hz, 1H), 8.42 (bs, 1H), 8.25 (dd, $J = 7.6$ and 1.6 Hz, 1H), 8.14 (d, $J = 8.0$ Hz, 1H), 7.81 (t, $J = 8.0$ Hz, 1H), 7.59 (t, $J = 7.2$ Hz, 1H), 7.45 (t, $J = 8.0$ Hz, 1H), 3.05 (bs, 2H), 1.97 (t, $J = 6.0$ Hz, 2H), 1.42 (s, 6H). **m. p.** ($^{\circ}\text{C}$) = 256-257. Data are consistent with those reported in the literature (ref. 187, p. 100).



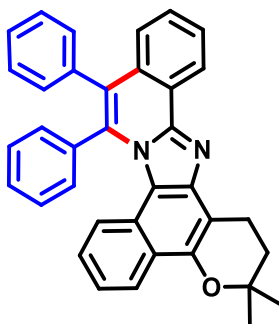
2-(1*H*-indol-3-yl)-6,6-dimethyl-3,4,5,6-tetrahydrobenzo[7,8]chromeno[5,6-*d*]imidazole

(**250**): The general procedure D was followed using β -lapachone (**228**) (242 mg, 1.00 mmol) and indole-3-carbaldehyde (160 mg, 1.10 mmol). Product was recrystallized in (*n*-hexane/EtOAc 50:1) and yielded **250** (290 mg, 79%, 0.79 mmol) as a yellow solid. $^1\text{H NMR}$ (400 MHz, DMSO-*d*₆) δ : 12.59 (bs, 1H), 11.46 (s, 1H), 8.54-8.52 (m, 1H), 8.32 (d, $J = 7.6$ Hz, 1H), 8.11-8.10 (m, 1H), 8.05 (d, $J = 8.0$ Hz, 1H), 7.47-7.44 (m, 1H), 7.46 (t, $J = 7.2$ Hz, 1H), 7.41-7.40 (m, 1H), 7.30 (t, $J = 7.2$ Hz, 1H) 7.15-7.10 (m, 2H), 3.00 (t, $J = 5.6$ Hz, 2H), 1.89 (t, $J = 5.6$ Hz, 2H), 1.33 (s, 6H). **m. p.** ($^{\circ}\text{C}$) = 272-274. Data are consistent with those reported in the literature (ref. 191, p. **Erro! Indicador não definido.**).

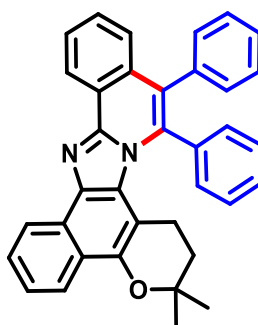
7.3 C–H/N–H annulation: general procedure E and characterization data of products



General Procedure E: To an oven-dried re-sealable tube, lapimidazole substrates (0.20 mmol), diphenylacetylene (71.2 mg, 0.40 mmol), $[\text{RhCp}^*\text{Cl}_2]_2$ (6.0 mg, 0.01 mmol, 5 mol%), AgOAc (16.6 mg, 0.10 mmol, 0.5 equiv) were added followed of methanol (2 mL). The tube was sealed and submitted to heating (100 $^{\circ}\text{C}$) and stirring for 24 hours. Then the reaction mixture was filtered through a pad of celite, and the crude product was purified *via* column chromatography under the conditions noted using silica gel and mixture of ethyl acetate and *n*-hexane.

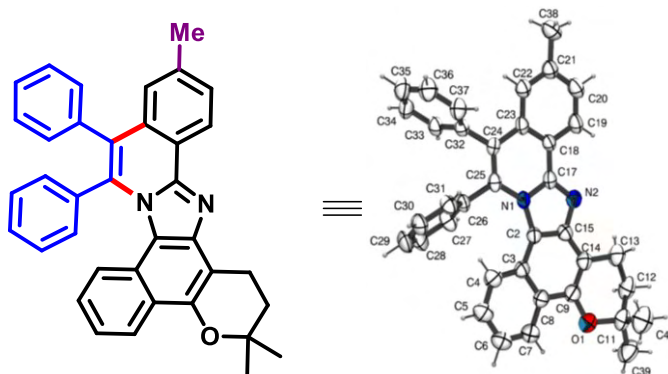


3,3-dimethyl-10,11-diphenyl-2,3-dihydro-1H-benzo[7',8']chromeno[5',6':4,5]imidazo[2,1-a]isoquinoline (235): The general procedure E was followed by using **234** as starting material (66 mg, 0.2 mmol). Purification by column chromatography on silica gel (*n*-hexane/EtOAc 20:1) yielded **235** (59.5 mg, 59%, 0.12 mmol) as a white solid. $^1\text{H NMR}$ (400 MHz, CDCl_3) δ : 9.00 (d, $J = 8.0$ Hz, 1H), 8.28 (d, $J = 8.0$ Hz, 1H), 7.66-7.62 (m, 1H), 7.50-7.46 (m, 1H), 7.35 (d, $J = 8.0$ Hz, 1H), 7.32-7.29 (m, 3H), 7.18-7.14 (m, 3H), 7.10-7.06 (m, 3H), 7.01-6.98 (m, 2H), 6.79 (d, $J = 8.0$ Hz, 1H), 6.74-6.70 (m, 1H), 3.42 (t, $J = 6.8$ Hz, 2H), 2.06 (t, $J = 6.8$ Hz, 2H), 1.50 (s, 6H). $^{13}\text{C NMR}$ (100 MHz, CDCl_3) δ : 148.0 (C), 146.9 (C), 143.2 (C), 137.2 (C), 135.7 (C), 135.1 (C), 131.7 (CH), 131.5 (C), 130.1 (CH), 128.8 (CH), 128.2 (CH), 128.1 (CH), 128.0 (CH), 127.6 (CH), 127.1 (CH), 126.2 (CH), 125.1 (C), 124.5 (CH), 123.9 (CH), 123.6 (C), 123.3 (C), 122.8 (CH), 122.3 (CH), 122.1 (C), 121.9 (CH), 119.9 (C), 107.1 (C), 74.9 (C), 32.6 (CH_2), 26.9 (CH_3), 18.7 (CH_2). **IR** (KBr): $\tilde{\nu} = 3441, 3048, 3020, 2971, 2941, 1592, 1575, 1513, 1449, 1346, 1329, 1157, 754, 705$ cm^{-1} ; **m. p.** ($^\circ\text{C}$) = 254-256. **HRMS** (ESI+): Calcd. for $[\text{C}_{36}\text{H}_{29}\text{N}_2\text{O}]^+ [\text{M}+\text{H}]^+$ 505.2274, found 505.2281.

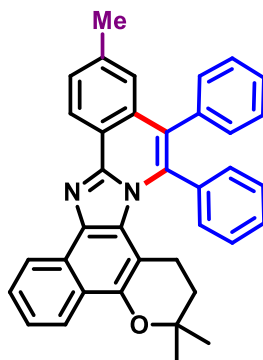


3,3-dimethyl-14,15-diphenyl-2,3-dihydro-1H-benzo[7',8']chromeno[6',5':4,5]imidazo[2,1-a]isoquinoline (236): The product **236** was obtained (*n*-hexane/EtOAc 20:1) as an orange solid (19.1 mg, 19%, 0.04 mmol). $^1\text{H NMR}$ (400 MHz, CDCl_3) δ : 8.99 (d, $J = 8.0$ Hz,

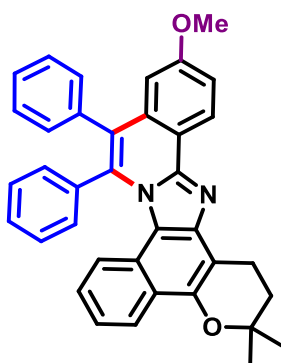
1H), 8.92 (d, $J = 8.0$ Hz, 1H), 8.28 (d, $J = 8.0$ Hz, 1H), 7.68 (t, $J = 8.0$ Hz, 1H), 7.63 (t, $J = 8.0$ Hz, 1H), 7.55 (t, $J = 8.0$ Hz, 1H), 7.45 (t, $J = 8.0$ Hz, 1H), 7.31-7.30 (m, 3H), 7.29-7.25 (m, 1H), 7.23-7.19 (m, 1H), 7.14-7.11 (m, 6H), 1.44-1.41 (m, 2H), 1.34-1.31 (m, 2H), 1.21 (s, 6H). ^{13}C NMR (100 MHz, CDCl_3) δ : 146.6 (C), 145.2 (C), 137.2 (C), 136.6 (C), 135.2 (C), 135.0 (C), 131.6 (CH), 131.5 (C), 130.3 (CH), 128.5 (CH), 128.2 (CH), 128.1 (CH), 128.0 (C), 127.8 (CH), 127.2 (CH), 126.3 (CH), 126.1 (C), 125.1 (CH), 124.9 (C), 124.6 (C), 124.2 (CH), 124.0 (C), 122.5 (CH), 122.3 (CH), 105.1 (C), 74.1 (C), 32.6 (CH_2), 26.4 (CH_3), 22.1 (CH_2). IR (KBr): $\tilde{\nu} = 3415, 3059, 2968, 2917, 1574, 1528, 1450, 1409, 1367, 1309, 1160, 1117, 768, 703$ cm^{-1} ; m. p. ($^\circ\text{C}$) = 250-251. HRMS (ESI+): Cald. for $[\text{C}_{36}\text{H}_{29}\text{N}_2\text{O}]^+$ $[\text{M}+\text{H}]^+$ 505.2274, found 505.2266.



3,3,13-trimethyl-10,11-diphenyl-2,3-dihydro-1H-benzo[7',8']chromeno[5',6':4,5]imidazo[2,1-a]isoquinoline (257): The general procedure E was followed by using **237** as starting material (68 mg, 0.2 mmol). The product **257** was obtained (*n*-hexane/EtOAc 20:1) as a white solid (77.8 mg, 75%, 0.15 mmol). ^1H NMR (400 MHz, CDCl_3) δ : 8.90 (d, $J = 8.0$ Hz, 1H), 8.27 (d, $J = 8.0$ Hz, 1H), 7.47 (d, $J = 8.0$ Hz, 1H), 7.31-7.30 (m, 3H), 7.16-7.11 (m, 4H), 7.09-7.04 (m, 3H), 7.00-6.97 (m, 2H), 6.77 (d, $J = 8.4$ Hz, 1H), 6.73-6.69 (m, 1H), 3.41 (t, $J = 6.4$, 2H), 2.39 (s, 3H), 2.05 (t, $J = 6.4$, 2H), 1.50 (s, 6H). ^{13}C NMR (100 MHz, CDCl_3) δ : 148.2 (C), 146.8 (C), 143.2 (C), 139.0 (C), 137.3 (C), 135.7 (C), 135.1 (C), 131.8 (CH), 131.6 (C), 130.1 (CH), 129.3 (CH), 128.1 (CH), 128.0 (CH), 127.9 (CH), 127.1 (CH), 125.9 (CH), 125.0 (C), 124.5 (CH), 123.8 (CH), 123.4 (C), 122.7 (CH), 122.2 (CH), 122.1 (C), 121.8 (CH), 121.1 (C), 119.7 (C), 107.1 (C), 74.8 (C), 32.6 (CH_2), 26.9 (CH_3), 22.0 (CH_3), 18.7 (CH_2). IR (KBr): $\tilde{\nu} = 3412, 3054, 2964, 2923, 1734, 1616, 1591, 1572, 1515, 1477, 1325, 1158, 1098, 758, 731, 698$ cm^{-1} ; m. p. ($^\circ\text{C}$) = 245-247. HRMS (ESI+): Cald. for $[\text{C}_{37}\text{H}_{31}\text{N}_2\text{O}]^+$ $[\text{M}+\text{H}]^+$ 519.2431, found 519.2430. The structure of the product was also confirmed by X-ray diffraction (CCDC number = 2025253).

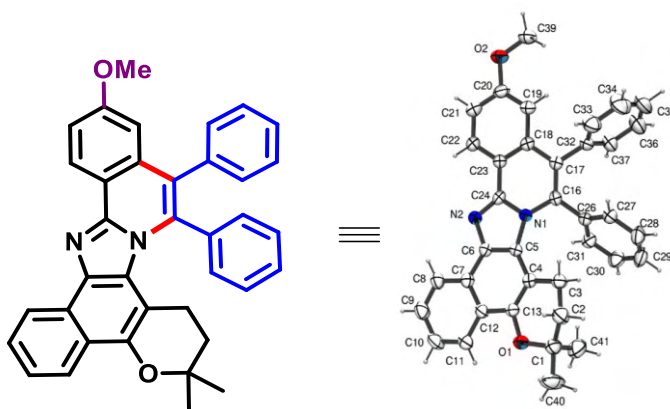


3,3,12-trimethyl-14,15-diphenyl-2,3-dihydro-1H-benzo[7',8']chromeno[6',5':4,5]imidazo[2,1-a]isoquinoline (258): Purification by column chromatography on silica gel (*n*-hexane/EtOAc 20:1) yielded **258** (22.9 mg, 22%, 0.04 mmol) as a yellow solid. $^1\text{H NMR}$ (400 MHz, CDCl_3) δ : 8.89-8.85 (m, 2H), 8.25 (d, $J = 8.0$ Hz, 1H), 7.67-7.63 (m, 1H), 7.54-7.49 (m, 1H), 7.44 (d, $J = 8.0$ Hz, 1H), 7.30-7.29 (m, 3H), 7.20-7.16 (m, 1H), 7.12-7.08 (m, 6H), 7.03 (s, 1H), 2.36 (s, 3H), 1.40 (t, $J = 6.4$, 2H), 1.30 (t, $J = 6.4$, 2H), 1.19 (s, 6H). $^{13}\text{C NMR}$ (100 MHz, CDCl_3) δ : 146.9 (C), 145.0 (C), 138.7 (C), 137.3 (C), 136.7 (C), 135.1 (C), 135.0 (C), 131.6 (CH), 131.5 (C), 130.4 (CH), 129.3 (CH), 128.1 (CH), 128.0 (CH), 127.7 (CH), 127.1 (CH), 126.2 (CH), 126.1 (CH), 126.0 (C), 125.0 (CH), 124.8 (C), 124.6 (C), 124.2 (CH), 122.5 (CH), 122.3 (CH), 121.7 (C), 105.1 (C), 74.0 (C), 32.6 (CH_2), 26.5 (CH_3), 22.1 (CH_2), 22.0 (CH_3). **IR** (KBr): $\tilde{\nu} = 3429, 3054, 2971, 2918, 1576, 1529, 1451, 1411, 1167, 1158, 1118, 764, 739, 698$ cm^{-1} ; **m. p.** ($^\circ\text{C}$) = 278-280. **HRMS** (ESI $^+$): Cald. for $[\text{C}_{37}\text{H}_{31}\text{N}_2\text{O}]^+$ $[\text{M}+\text{H}]^+$ 519.2431, found 519.2431.



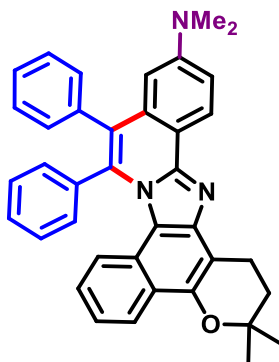
13-methoxy-3,3-dimethyl-10,11-diphenyl-2,3-dihydro-1H-benzo[7',8']chromeno[5',6':4,5]-imidazo[2,1-a]isoquinoline (259): The general procedure E was followed by using **238** as starting material (72 mg, 0.2 mmol). The product **259** was obtained (*n*-hexane/EtOAc 25:2) as a white solid (65.2 mg, 61%, 0.12 mmol). $^1\text{H NMR}$ (600 MHz, CDCl_3) δ : 8.93 (d, $J = 9.0$ Hz, 1H), 8.28 (d, $J = 8.4$ Hz, 1H), 7.31-7.30 (m, 3H), 7.27-7.24 (m, 1H), 7.16-7.14 (m, 3H),

7.11-7.07 (m, 3H), 7.02-6.99 (m, 2H), 6.77-6.71 (m, 3H), 3.72 (s, 3H), 3.42 (t, $J = 6.6$ Hz, 2H), 2.06 (t, $J = 6.6$ Hz, 2H), 1.51 (s, 6H). ^{13}C NMR (150 MHz, CDCl_3) δ : 160.1 (C), 148.2 (C), 146.8 (C), 143.2 (C), 137.3 (C), 135.7 (C), 135.6 (C), 133.3 (C), 131.6 (CH), 130.1 (CH), 128.2 (CH), 128.1 (CH), 127.9 (CH), 127.1 (CH), 126.4 (CH), 124.7 (C), 123.8 (CH), 123.3 (C), 122.6 (CH), 122.1 (C), 122.0 (CH), 121.8 (CH), 119.5 (C), 117.4 (C), 116.6 (CH), 108.2 (CH), 107.1 (C), 74.8 (C), 55.2 (CH_3), 32.6 (CH_2), 26.9 (CH_3), 18.7 (CH_2). IR (KBR): $\tilde{\nu} = 3435$, 3053, 2970, 2930, 1616, 1517, 1475, 1326, 1281, 1096, 1216 1034, 756, 735, 698 cm^{-1} ; **m. p.** ($^\circ\text{C}$) = 219-220; HRMS (ESI+): Cald. for $[\text{C}_{37}\text{H}_{31}\text{N}_2\text{O}_2]^+$ $[\text{M}+\text{H}]^+$ 535.2380, found 535.2389.

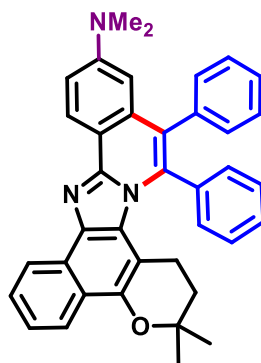


12-methoxy-3,3-dimethyl-14,15-diphenyl-2,3-dihydro-1H-benzo[7',8']-Schromeno-

Z[6',5':4,5]imidazo[2,1-a]isoquinoline (260): Purification by column chromatography on silica gel (*n*-hexane/EtOAc 25:2) yielded **260** (10.0 mg, 9%, 0.02 mmol) as a yellow solid. ^1H NMR (600 MHz, CDCl_3) δ : 8.89 (d, $J = 9.0$ Hz, 1H), 8.86 (d, $J = 7.0$ Hz, 1H), 8.24 (d, $J = 8.4$ Hz, 1H), 7.65-7.63 (m, 1H), 7.52-7.49 (m, 1H), 7.29-7.28 (m, 3H), 7.23 (s, 1H), 7.20-7.17 (m, 1H), 7.11-7.08 (m, 6H), 6.66 (d, $J = 3.0$ Hz, 1H), 3.71 (s, 3H), 1.39 (t, $J = 6.6$ Hz, 2H), 1.30 (t, $J = 6.6$ Hz, 2H), 1.18 (s, 6H). ^{13}C NMR (150 MHz, CDCl_3) δ : 160.0 (C), 146.9 (C), 144.8 (C), 137.2 (C), 136.6 (C), 135.6 (C), 135.1 (C), 133.3 (C), 131.5 (CH), 130.3 (CH), 128.2 (CH), 128.1 (CH), 127.9 (C), 127.8 (CH), 127.2 (CH), 126.2 (CH), 126.1 (CH), 125.9 (C), 125.0 (CH), 124.5 (C), 124.5 (C), 122.5 (CH), 122.3 (CH), 118.0 (C), 116.2 (CH), 108.9 (CH), 105.2 (C), 74.0 (C), 55.2 (CH_3), 32.6 (CH_2), 26.5 (CH_3), 22.1 (CH_2). IR (KBR): $\tilde{\nu} = 3430$, 3062, 3018, 2962, 2924, 1617, 1594, 1481, 1376, 1322, 1226, 1047, 1030, 760, 723, 700 cm^{-1} ; **m. p.** ($^\circ\text{C}$) = 301-303. HRMS (ESI+): Cald. for $[\text{C}_{37}\text{H}_{31}\text{N}_2\text{O}_2]^+$ $[\text{M}+\text{H}]^+$ 535.2380, found 535.2389. The structure of the product was also confirmed by X-ray diffraction (CCDC number = 2025259).

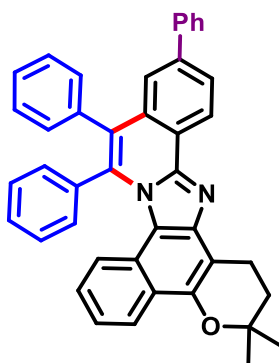


N,N,3,3-tetramethyl-10,11-diphenyl-2,3-dihydro-1H-benzo[7',8']chromeno[5',6':4,5]imidazo[2,1-a]isoquinolin-13-amine (261): The general procedure E was followed by using **239** as starting material (74 mg, 0.2 mmol). The product **261** was obtained (*n*-hexane/EtOAc 20:1) as a yellow solid (56.2 mg, 51%, 0.10 mmol). $^1\text{H NMR}$ (400 MHz, CDCl_3) δ : 8.82 (d, $J = 8.0$ Hz, 1H), 8.25 (d, $J = 8.0$ Hz, 1H), 7.30-7.26 (m, 3H) 7.15-7.10 (m, 4H), 7.08-7.06 (m, 3H), 7.00-6.96 (m, 2H), 6.76 (d, $J = 8.0$ Hz, 1H), 6.71-6.67 (m, 1H), 6.41 (d, $J = 2.4$ Hz, 1H), 3.40 (t, $J = 6.8$ Hz, 2H), 2.88 (s, 6H), 2.04 (t, $J = 6.8$ Hz, 2H), 1.48 (s, 6H). $^{13}\text{C NMR}$ (100 MHz, CDCl_3) δ : 150.7 (C), 149.0 (C), 146.5 (C), 143.2 (C), 137.8 (C), 136.0 (C), 135.2 (C), 133.3 (C), 131.7 (CH), 130.2 (CH), 128.0 (CH), 127.9 (CH), 126.9 (CH), 125.9 (CH), 125.0 (C), 123.7 (CH), 122.9 (C), 122.5 (CH), 122.1 (C), 121.8 (CH), 121.7 (CH), 119.4 (C), 114.3 (CH), 113.7 (C), 107.0 (C), 106.6 (CH), 74.7 (C), 40.1 (CH_3), 32.6 (CH_2), 26.9 (CH_3), 18.8 (CH_2). IR (KBr): $\tilde{\nu} = 3425, 3049, 2971, 2925, 1613, 1448, 1594, 1441, 1157, 119, 1094, 759, 722, 700$ cm^{-1} ; **m. p.** ($^\circ\text{C}$) = 264-265. **HRMS** (ESI $^+$): Cald. for $[\text{C}_{38}\text{H}_{34}\text{N}_3\text{O}]^+$ $[\text{M}+\text{H}]^+$ 548.2696, found 548.2722.

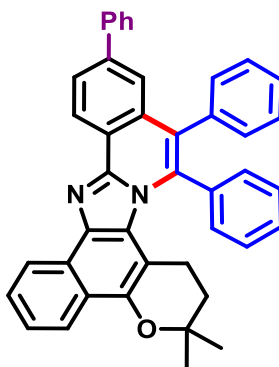


N,N,3,3-tetramethyl-14,15-diphenyl-2,3-dihydro-1H-benzo[7',8']chromeno[6',5':4,5]imidazo[2,1-a]isoquinolin-12-amine (262): Purification by column chromatography on silica gel (*n*-hexane/EtOAc 20:1) yielded **262** (10.9 mg, 10%, 0.02 mmol) as a yellow solid. $^1\text{H NMR}$ (400 MHz, CDCl_3) δ : 8.88 (d, $J = 8.0$ Hz, 1H), 8.82 (d, $J = 8.8$ Hz, 1H), 8.26 (d, $J = 8.0$ Hz,

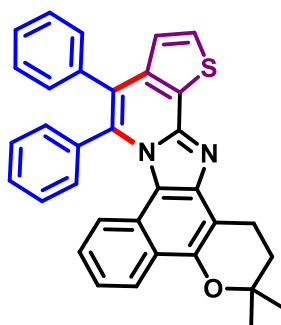
1H), 7.66-7.63 (m, 1H), 7.53-7.49 (m, 1H), 7.30-7.28 (m, 3H), 7.21-7.17 (m, 1H), 7.14-7.12 (m, 3H), 7.11-7.10 (m, 4H), 6.38 (d, $J = 2.4$ Hz, 1H), 2.89 (s, 6H), 1.41 (t, $J = 6.0$ Hz, 2H), 1.32 (t, $J = 6.0$ Hz, 2H), 1.20 (s, 6H). ^{13}C NMR (100 MHz, CDCl_3) δ : 150.6 (C), 147.7 (C), 144.4 (C), 137.4 (C), 136.9 (C), 135.1 (C), 135.0 (C), 133.2 (C), 131.6 (CH), 130.4 (CH), 128.0 (CH), 127.9 (CH), 127.7 (CH), 126.9 (CH), 125.9 (CH), 125.8 (C), 125.5 (CH), 124.9 (CH), 124.7 (C), 124.3 (C), 122.5 (CH), 122.2 (CH), 114.2 (CH), 114.1 (C), 107.1 (CH), 105.3 (C), 73.9 (C), 40.2 (CH_3), 32.6 (CH_2), 26.5 (CH_3), 22.1 (CH_2). IR (KBr): $\tilde{\nu} = 3424, 3057, 2973, 2918, 1615, 1378, 1158, 1119, 954, 765, 701, \text{cm}^{-1}$; **m. p.** ($^\circ\text{C}$) = 162-164. HRMS (ESI+): Calcd. for $[\text{C}_{38}\text{H}_{34}\text{N}_3\text{O}]^+ [\text{M}+\text{H}]^+ 548.2696$, found 548.2722.



3,3-dimethyl-10,11,13-triphenyl-2,3-dihydro-1H-benzo[7',8']chromeno[5',6':4,5]imidazo[2,1-a]isoquinoline (263): The general procedure E was followed by using **240** as starting material (81 mg, 0.2 mmol). Purification by column chromatography on silica gel (*n*-hexane/EtOAc 25:2) yielded **263** (60.1 mg, 52%, 0.10 mmol) as a yellow solid. ^1H NMR (400 MHz, CDCl_3) δ : 9.06 (d, $J = 8.0$ Hz, 1H), 8.29 (d, $J = 8.0$ Hz, 1H), 7.89 (d, $J = 8.0$ Hz, 1H), 7.57 (s, 1H), 7.53 (d, $J = 8.0$ Hz, 2H), 7.41-7.38 (m, 2H), 7.33-7.30 (m, 4H), 7.20-7.17 (m, 3H), 7.11-7.08 (m, 3H), 7.03-6.99 (m, 2H), 6.80 (d, $J = 8.0$ Hz, 1H), 6.75-6.72 (m, 1H), 3.43 (t, $J = 6.4$, 2H), 2.07 (t, $J = 6.4$, 2H), 1.51 (s, 6H). ^{13}C NMR (100 MHz, CDCl_3) δ : 147.8 (C), 146.9 (C), 143.4 (C), 141.4 (C), 140.7 (C), 137.1 (C), 135.7 (C), 135.5 (C), 131.8 (C), 131.7 (CH), 130.1 (CH), 128.8 (CH), 128.3 (CH), 128.1 (CH), 128.0 (CH), 127.6 (CH), 127.3 (CH), 127.2 (CH), 126.8 (CH), 125.3 (C), 125.1 (CH), 124.4 (CH), 123.9 (CH), 123.6 (C), 122.9 (CH), 122.4 (CH), 122.3 (C), 122.1 (C), 121.9 (CH), 119.9 (C), 107.1 (C), 74.9 (C), 32.6 (CH_2), 26.9 (CH_3), 18.8 (CH_2). IR (KBr): $\tilde{\nu} = 3424, 3059, 2968, 2927, 1589, 1573, 1467, 1415, 1324, 1157, 1118, 1099, 7564, 727, 700 \text{cm}^{-1}$; **m. p.** ($^\circ\text{C}$) = 296-298. HRMS (ESI+): Calcd. for $[\text{C}_{42}\text{H}_{33}\text{N}_2\text{O}]^+ [\text{M}+\text{H}]^+ 581.2587$, found 581.2608.

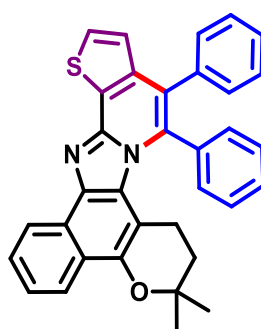


3,3-dimethyl-12,14,15-triphenyl-2,3-dihydro-1H-benzo[7',8']chromeno[6',5':4,5]imidazo[2,1-a]isoquinoline (264): The product **264** was obtained (*n*-hexane/EtOAc 25:2) as a yellow solid (12.1 mg, 10%, 0.02 mmol). $^1\text{H NMR}$ (400 MHz, CDCl_3) δ : 9.05 (d, $J = 8.0$ Hz, 1H), 8.93 (d, $J = 8.0$ Hz, 1H), 8.29 (d, $J = 8.0$ Hz, 1H), 7.89 (dd, $J = 6.8$ and 1.6 Hz, 1H), 7.69 (t, $J = 8.0$ Hz, 1H), 7.58-7.49 (m, 4H), 7.42-7.39 (m, 2H), 7.34-7.32 (m, 4H), 7.24-7.21 (m, 1H), 7.19-7.16 (m, 2H), 7.14-7.13 (m, 4H), 1.45-1.42 (m, 2H), 1.35-1.32 (m, 2H), 1.22 (s, 6H). $^{13}\text{C NMR}$ (100 MHz, CDCl_3) δ : 146.5 (C), 145.3 (C), 141.2 (C), 140.7 (C), 137.0 (C), 136.6 (C), 135.4 (C), 135.3 (C), 131.9 (C), 131.6 (CH), 130.4 (CH), 128.8 (CH), 128.3 (C), 128.2 (CH), 128.1 (CH), 127.8 (CH), 127.5 (CH), 127.3 (CH), 127.0 (CH), 126.3 (CH), 126.1 (C), 125.2 (CH), 125.0 (C), 124.8 (CH), 124.7 (C), 124.6 (CH), 123.0 (C), 122.5 (CH), 122.4 (CH), 105.1 (C), 74.1 (C), 32.6 (CH_2), 26.5 (CH_3), 22.1 (CH_2). **IR** (KBr): $\tilde{\nu} = 3433, 3059, 2967, 2922, 1572, 1529, 1487, 1440, 1408, 1332, 1247, 1160, 1117, 756, 699$ cm^{-1} ; **m. p.** ($^\circ\text{C}$) = 310-312. **HRMS** (ESI $^+$): Calcd. for $[\text{C}_{42}\text{H}_{33}\text{N}_2\text{O}]^+$ $[\text{M}+\text{H}]^+$ 581.2587, found 581.2607.

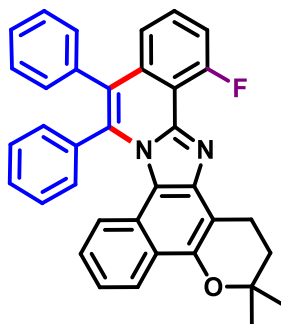


12,12-dimethyl-4,5-diphenyl-12,13,14,15b-tetrahydro-3aH-benzo[7',8']chromeno[5',6':4,5]-imidazo[1,2-a]thieno[3,2-c]pyridine (265): The general procedure E was followed by using **241** as starting material (67 mg, 0.2 mmol). The product **265** was obtained (*n*-hexane/EtOAc 25:2) as a white solid (53.1 mg, 52%, 0.10 mmol). $^1\text{H NMR}$

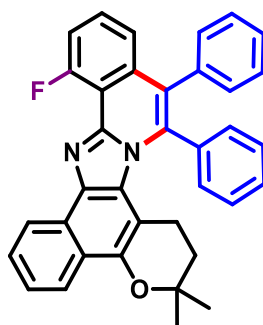
(400 MHz, CDCl₃) δ : 8.28 (d, J = 8.0 Hz, 1H), 7.47 (d, J = 8.0 Hz, 1H), 7.28-7.27 (m, 3H), 7.16-7.12 (m, 4H), 7.08-7.01 (m, 4H), 6.96 (d, J = 5.2, 1H), 6.75-6.69 (m, 2H), 3.37 (t, J = 6.8 Hz, 2H), 2.04 (t, J = 6.8 Hz, 2H), 1.49 (s, 6H). ¹³C NMR (100 MHz, CDCl₃) δ : 147.2 (C), 145.5 (C), 144.1 (C), 138.9 (C), 137.9 (C), 135.1 (C), 134.8 (C), 130.9 (CH), 130.2 (CH), 128.3 (CH), 128.2 (CH), 128.1 (CH), 127.8 (CH), 127.1 (CH), 126.3 (C), 125.2 (CH), 123.9 (CH), 123.4 (C), 123.1 (C), 122.7 (CH), 122.2 (CH), 122.1 (C), 121.9 (CH), 119.0 (C), 107.0 (C), 74.9 (C), 32.5 (CH₂), 26.9 (CH₃), 18.8 (CH₂). IR (KBr): $\tilde{\nu}$ = 3426, 3049, 3020, 2970, 2938, 1610, 1593, 1483, 1318, 1157, 1120, 1089, 754, 727, 693 cm⁻¹; m. p. (°C) = 258-260. HRMS (ESI+): Cald. for [C₃₄H₂₇N₂OS]⁺ [M+H]⁺ 511.1839, found 511.1849.



9,9-dimethyl-4,5-diphenyl-8,9-dihydro-7H-benzo[7',8']chromeno[6',5':4,5]imidazo[1,2-a]-thieno[2,3-c]pyridine (266): Purification by column chromatography on silica gel (*n*-hexane/EtOAc 25:2) yielded **266** (10.0 mg, 10%, 0.02 mmol) as a yellow solid. ¹H NMR (400 MHz, CDCl₃) δ : 8.88 (d, J = 8.0 Hz, 1H), 8.28 (d, J = 8.0 Hz, 1H), 7.67 (t, J = 8.0 Hz, 1H), 7.55 (t, J = 8.0 Hz, 1H), 7.45 (d, J = 5.2 Hz, 1H), 7.30-7.29 (m, 3H), 7.26 (s, 1H), 7.16-7.12 (m, 6H), 6.92 (d, J = 5.2 Hz, 1H), 1.44 (t, J = 6.4, 2H), 1.32 (t, J = 6.4, 2H), 1.22 (s, 6H). ¹³C NMR (100 MHz, CDCl₃) δ : 145.0 (C), 144.3 (C), 138.5 (C), 137.8 (C), 136.1 (C), 136.0 (C), 134.7 (C), 130.8 (CH), 130.4 (CH), 128.2 (CH), 128.1 (CH), 128.0 (CH), 127.4 (C), 127.2 (CH), 127.1 (CH), 126.2 (CH), 125.9 (C), 125.3 (CH), 125.2 (C), 124.9 (C), 122.8 (CH), 122.7 (C), 122.3 (CH), 105.2 (C), 74.1 (C), 32.7 (CH₂), 26.5 (CH₃), 22.2 (CH₂). IR (KBr): $\tilde{\nu}$ = 3420, 3052, 3021, 2961, 2923, 1610, 1598, 1573, 1485, 1409, 1367, 1165, 1135, 1120, 1087, 752, 714, 700 cm⁻¹; m. p. (°C) = 254-255. HRMS (ESI+): Cald. for [C₃₄H₂₇N₂OS]⁺ [M+H]⁺ 511.1839, found 511.1849.

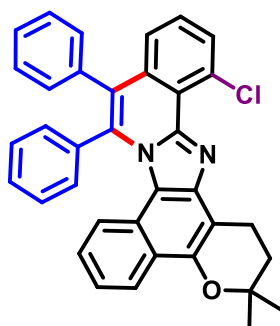


3,3-dimethyl-13-nitro-10,11-diphenyl-2,3-dihydro-1H-benzo[7',8']chromeno[5',6':4,5]imidazo[2,1-a]isoquinoline (267): The general procedure E was followed by using **242** as starting material (69 mg, 0.2 mmol). Purification by column chromatography on silica gel (*n*-hexane/EtOAc 25:2) yielded **267** (60.6 mg, 58%, 0.12 mmol) as a yellow solid. $^1\text{H NMR}$ (400 MHz, CDCl_3) δ : 8.30 (d, $J = 8.0$ Hz, 1H), 7.43-7.37 (m, 2H), 7.34-7.32 (m, 3H), 7.21-7.16 (m, 4H), 7.10 (d, $J = 8.0$ Hz, 1H), 7.06-7.04 (m, 2H), 7.02-6.98 (m, 2H), 6.88 (d, $J = 8.0$ Hz, 1H), 6.78-6.74 (m, 1H), 3.47 (d, $J = 6.4$ Hz, 1H), 2.07 (d, $J = 6.4$ Hz, 1H), 1.52 (s, 6H). $^{13}\text{C NMR}$ (100 MHz, CDCl_3) δ : 159.6 (C, d, $J^{13\text{C}-19\text{F}} = 260$ Hz), 147.0 (C), 144.5 (C), 144.4 (C), 143.6 (C, d, $J^{13\text{C}-19\text{F}} = 10$ Hz), 137.1 (C), 136.1 (C), 135.3 (C), 134.0 (C), 131.7 (CH), 130.0 (CH), 128.7 (CH, d, $J^{13\text{C}-19\text{F}} = 8.0$ Hz), 128.4 (CH), 128.2 (CH), 127.9 (CH), 127.3 (CH), 123.9 (CH), 123.8 (C), 123.0 (CH), 122.6 (CH), 122.2 (CH, d, $J^{13\text{C}-19\text{F}} = 4$ Hz), 122.1 (CH), 121.9 (CH), 121.8 (C), 119.0 (C), 114.1 (CH, d, $J^{213\text{C}-19\text{F}} = 21$ Hz), 112.7 (C, d, $J^{13\text{C}-19\text{F}} = 10$ Hz), 107.3 (C), 75.0 (C), 32.5 (CH_2), 26.9 (CH_3), 18.7 (CH_2). **IR** (KBR): $\tilde{\nu} = 3431, 3055, 3021, 2973, 2929, 1591, 1471, 1158, 1119, 754, 708, \text{cm}^{-1}$; **m. p.** ($^\circ\text{C}$) = 205-207. **HRMS** (ESI+): Calcd. for $[\text{C}_{36}\text{H}_{28}\text{FN}_2\text{O}]^+ [\text{M}+\text{H}]^+ 523.2180$, found 523.2186.



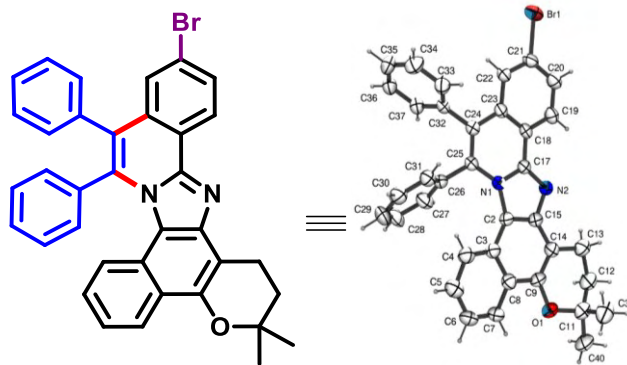
3,3-dimethyl-13-nitro-10,11-diphenyl-2,3-dihydro-1H-benzo[7',8']chromeno[5',6':4,5]imidazo[2,1-a]isoquinoline (268): The product **268** was obtained (*n*-hexane/EtOAc 25:2) as a yellow solid (8 mg, 8%, 0.02 mmol). $^1\text{H NMR}$ (400 MHz, CDCl_3) δ : 8.93 (d, $J = 8.0$ Hz, 1H), 8.25 (d, $J = 8.0$ Hz, 1H), 7.67 (t, $J = 8.0$ Hz, 1H), 7.53 (t, $J = 8.0$ Hz, 1H), 7.36-7.32 (m, 2H),

7.31-7.29 (m, 3H), 7.19-7.17 (m, 1H), 7.12-7.09 (m, 3H), 7.07-7.05 (m, 4H), 1.39 (t, $J = 6.4$ Hz, 2H), 1.30 (t, $J = 6.4$ Hz, 2H), 1.18 (s, 6H). ^{13}C NMR (100 MHz, CDCl_3) δ : 159.3 (C, d, $J^1_{13\text{C}-19\text{F}} = 258$ Hz), 158.0 (C), 145.7 (C), 143.0 (C), 142.9 (C, d, $J^3_{13\text{C}-19\text{F}} = 9$ Hz), 137.1 (C), 136.3 (C), 136.0 (C), 135.7 (C), 134.0 (C), 131.6 (CH), 130.2 (CH), 128.5 (CH, d, $J^3_{13\text{C}-19\text{F}} = 9$ Hz), 128.3 (CH), 128.4 (CH), 127.8 (CH), 127.4 (CH), 126.5 (CH), 126.2 (C), 125.3 (CH), 124.7 (C), 124.3 (C), 122.9 (CH), 122.3 (CH, d, $J^4_{13\text{C}-19\text{F}} = 3$ Hz), 114.4 (CH, d, $J^2_{13\text{C}-19\text{F}} = 20$ Hz), 113.3 (C, d, $J^2_{13\text{C}-19\text{F}} = 10$ Hz), 104.8 (C), 74.3 (C), 32.5 (CH_2), 26.5 (CH_3), 22.2 (CH_2). IR (KBR): $\tilde{\nu} = 3431, 3066, 3015, 2972, 2927, 1592, 1471, 1158, 1118, 754, 711$ cm^{-1} ; m. p. ($^\circ\text{C}$) = 205-207. HRMS (ESI+): Cald. for $[\text{C}_{36}\text{H}_{28}\text{FN}_2\text{O}]^+$ $[\text{M}+\text{H}]^+ 523.2180$, found 523.2188.



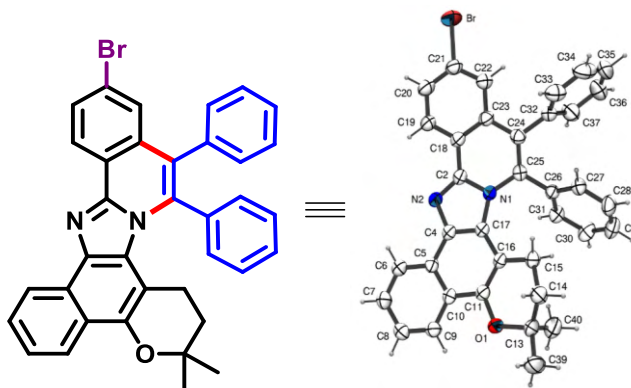
10-chloro-3,3-dimethyl-14,15-diphenyl-2,3-dihydro-1H-

benzo[7',8']chromeno[6',5':4,5]imidazo[2,1-a]isoquinoline (269): The general procedure E was followed by using **243** as starting material (73 mg, 0.2 mmol). The product **269** was obtained (*n*-hexane/EtOAc 50:1) as a white solid (61.0 mg, 57%, 0.11 mmol). ^1H NMR (400 MHz, CDCl_3) δ : 8.29 (d, $J = 8.0$ Hz, 1H), 7.34 (dd, $J = 7.2$ and 1.6 Hz, 1H), 7.35-7.32 (m, 5H), 7.21-7.19 (m, 1H), 7.17-7.15 (m, 2H), 7.10-7.07 (m, 1H), 7.04-6.96 (m, 4H), 6.92 (d, $J = 8.0$ Hz, 1H), 6.78-6.74 (m, 1H), 3.47 (t, $J = 6.6$ Hz, 2H), 2.08 (t, $J = 6.6$ Hz, 2H), 1.52 (s, 6H). ^{13}C NMR (100 MHz, CDCl_3) δ : 146.9 (C), 145.9 (C), 143.1 (C), 137.3 (C), 135.9 (C), 135.3 (C), 134.1 (C), 131.8 (CH), 131.6 (CH), 130.6 (C), 129.8 (CH), 128.3 (CH), 128.2 (CH), 127.9 (CH), 127.3 (C), 127.4 (CH), 125.4 (CH), 124.7 (C), 124.0 (CH), 123.8 (C), 123.0 (CH), 122.7 (CH), 121.9 (CH), 121.9 (C), 120.8 (C), 119.0 (C), 107.4 (C), 32.6 (CH_2), 27.0 (CH_3), 18.7 (CH_2). IR (KBR): $\tilde{\nu} 3429, 3060, 3017, 2972, 1592, 1471, 1160, 1114, 754, 710$ cm^{-1} m. p. ($^\circ\text{C}$) = 223-225. HRMS (ESI+): Cald. for $[\text{C}_{36}\text{H}_{28}\text{ClN}_2\text{O}]^+$ $[\text{M}+\text{H}]^+ 539.1885$, found 539.1895.



13-bromo-3,3-dimethyl-10,11-diphenyl-2,3-dihydro-1H-

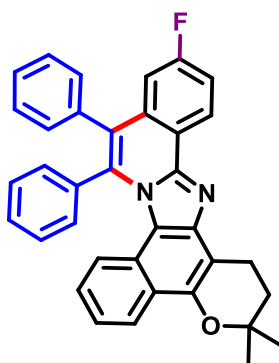
benzo[7',8']chromeno[5',6':4,5]imidazo[2,1-a]isoquinoline (271): The general procedure E was followed by using **244** as starting material (82 mg, 0.2 mmol). The product **271** was obtained (*n*-hexane/EtOAc 25:2) as a yellow solid (65.9 mg, 57%, 0.11 mmol). $^1\text{H NMR}$ (400 MHz, CDCl_3) δ : 8.85 (d, $J = 8.0$ Hz, 1H), 8.27 (d, $J = 8.0$ Hz, 1H), 7.71 (dd, $J = 8.0$ and 2.0 Hz, 1H), 7.46 (d, $J = 1.6$ Hz, 1H), 7.32-7.30 (m, 3H), 7.18-7.14 (m, 1H), 7.12-7.09 (m, 3H), 7.03-6.97 (m, 4H), 6.72-6.71 (m, 2H), 3.37 (t, $J = 6.8$ Hz, 2H), 2.05 (t, $J = 6.8$ Hz, 2H), 1.49 (s, 6H). $^{13}\text{C NMR}$ (100 MHz, CDCl_3) δ : 147.3 (C), 147.1 (C), 143.3 (C), 136.4 (C), 136.2 (C), 135.2 (C), 132.8 (C), 131.6 (CH), 130.7 (CH), 130.0 (CH), 128.6 (CH), 128.5 (CH), 128.3 (CH), 128.0 (CH), 127.4 (CH), 126.2 (CH), 124.1 (C), 124.2 (CH), 123.7 (C), 123.3 (C), 122.8 (CH), 122.5 (CH), 122.0 (C), 121.9 (CH), 121.8 (C), 119.8 (C), 106.9 (C), 74.9 (C), 32.5 (CH_2), 26.9 (CH_3), 18.7 (CH_2). IR (KBr): $\tilde{\nu} = 3431, 3058, 2967, 2923, 1596, 1514, 1417, 1319, 1158, 1119, 883, 758, 722, 704 \text{ cm}^{-1}$; **m. p.** ($^\circ\text{C}$) = 277-279. **HRMS** (ESI $^+$): Calcd. for $[\text{C}_{36}\text{H}_{28}\text{BrN}_2\text{O}]^+$ $[\text{M}+\text{H}]^+$ 583.1380, found 583.1378. The structure of the product was also confirmed by X-ray diffraction (CCDC number = 2025256).



12-bromo-3,3-dimethyl-14,15-diphenyl-2,3-dihydro-1H-

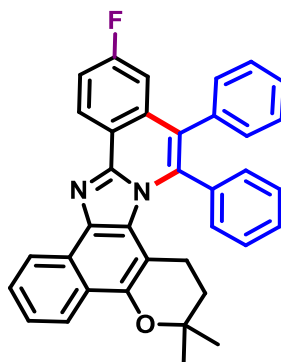
benzo[7',8']chromeno[6',5':4,5]imidazo[2,1-a]isoquinoline (272): Purification by column chromatography on silica gel (*n*-hexane/EtOAc 25:2) yielded **272** (13.8 mg, 12%, 0.02 mmol) as a yellow solid. $^1\text{H NMR}$ (400 MHz, CDCl_3) δ : 8.85 (d, $J = 8.0$ Hz, 1H), 8.82 (d, $J = 8.0$ Hz,

1H), 8.25 (d, $J = 8.0$ Hz, 1H), 7.67 (dd, $J = 6.4$ and 2.0 Hz, 1H), 7.68-7.64 (m, 1H), 7.55-7.51 (m, 1H), 7.37 (d, $J = 1.6$ Hz, 1H), 7.31-7.30 (m, 3H), 7.20-7.18 (m, 1H), 7.10-7.06 (m, 6H), 1.39-1.36 (m, 2H), 1.31-1.28 (m, 2H), 1.18 (s, 6H). ^{13}C NMR (100 MHz, CDCl_3) δ : 146.0 (C), 145.5 (C), 136.4 (C), 136.3 (C), 136.2 (C), 135.4 (C), 132.9 (C), 131.5 (CH), 130.9 (CH), 130.3 (CH), 128.7 (CH), 128.4 (CH), 128.3 (C), 127.8 (CH), 127.5 (CH), 126.4 (CH), 126.0 (C), 125.9 (CH), 125.3 (CH), 124.7 (C), 123.8 (C), 122.9 (C), 122.7 (C), 122.5 (CH), 122.4 (CH), 105.0 (C), 74.2 (C), 32.5 (CH_2), 26.4 (CH_3), 22.1 (CH_2). IR (KBr): $\tilde{\nu} = 3427, 3062, 2967, 2920, 1572, 1527, 1485, 1442, 1159, 1117, 767, 713, 703$ cm^{-1} ; m. p. ($^\circ\text{C}$) = 298-300. HRMS (ESI+): Cald. for $[\text{C}_{36}\text{H}_{28}\text{BrN}_2\text{O}]^+ [\text{M}+\text{H}]^+$ 583.1380, found 583.1369. The structure of the product was also confirmed by X-ray diffraction (CCDC number = 2025254).

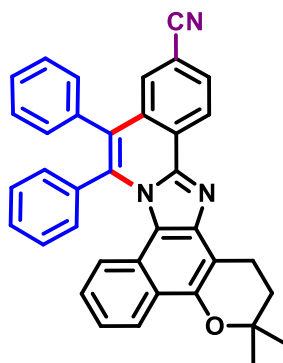


13-fluoro-3,3-dimethyl-10,11-diphenyl-2,3-dihydro-1H-

benzo[7',8']chromeno[5',6':4,5]imidazo[2,1-a]isoquinoline (273): The general procedure E was followed by using **245** as starting material (69 mg, 0.2 mmol). The product **273** was obtained (*n*-hexane/EtOAc 10:1) as a yellow solid (53 mg, 51%, 0.10 mmol). ^1H NMR (400 MHz, CDCl_3) δ : 9.05-9.01 (m, 1H), 8.31 (d, $J = 8.4$ Hz, 1H), 7.41-7.33 (m, 4H), 7.22-7.13 (m, 4H), 7.10-7.08 (m, 2H), 7.06-7.04 (m, 2H), 7.02-7.01 (m, 1H), 6.78-6.73 (m, 2H), 3.43 (t, $J = 6.8$ Hz, 2H), 2.09 (t, $J = 6.8$ Hz, 2H), 1.54 (s, 6H). ^{13}C NMR (100 MHz, CDCl_3) δ : 154.0 (C, d, $J^1_{13\text{C}-19\text{F}} = 250$ Hz), 147.5 (C), 147.0 (C), 143.2 (C), 136.7 (C), 136.3 (C), 135.4 (C), 133.4 (C, d, $J^3_{13\text{C}-19\text{F}} = 9.0$ Hz), 131.6 (CH), 130.1 (CH), 128.5 (CH), 128.3 (CH), 128.0 (CH), 127.3 (CH, d, $J^3_{13\text{C}-19\text{F}} = 9.0$ Hz), 127.2 (CH), 127.1 (CH), 124.4 (C), 124.3 (C), 124.0 (CH), 123.6 (C), 122.7 (CH), 122.4 (CH), 122.0 (CH), 121.9 (CH), 119.8 (C, d, $J^4_{13\text{C}-19\text{F}} = 2.0$ Hz), 119.7 (C), 116.3 (CH, $J^2_{13\text{C}-19\text{F}} = 24.0$ Hz), 111.4 (CH, $J^2_{13\text{C}-19\text{F}} = 24$ Hz), 107.0 (C), 74.9 (C), 32.5 (CH_2), 26.9 (CH_3), 18.7 (CH_2). IR (KBr): $\tilde{\nu} = 3428, 3053, 2931, 1615, 1594, 1572, 1517, 1433, 1316, 1195, 1160, 759, 735, 699$ cm^{-1} ; m. p. ($^\circ\text{C}$) = 296-298. HRMS (ESI+): Cald. for $[\text{C}_{36}\text{H}_{28}\text{FN}_2\text{O}]^+ [\text{M}+\text{H}]^+$ 523.2180, found 523.2195.

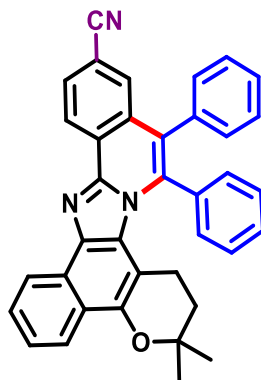


2-fluoro-3,3-dimethyl-14,15-diphenyl-2,3-dihydro-1H-benzo[7',8']chromeno[6',5':4,5]imidazo[2,1-a]isoquinoline (274): Purification by column chromatography on silica gel (*n*-hexane/EtOAc 10:1) yielded **274** (12.5 mg, 12%, 0.02 mmol) as a yellow solid. $^1\text{H NMR}$ (400 MHz, CDCl_3) δ : 8.98 (m, 1H), 8.88 (d, $J = 8.0$ Hz, 1H), 8.27 (d, $J = 8.0$ Hz, 1H), 7.70-7.66 (m, 1H), 7.57-7.53 (m, 1H), 7.35-7.31 (m, 4H), 7.24-7.21 (m, 1H), 7.13-7.10 (m, 6H), 6.92 (dd, $J = 8.0$ and 2.4 Hz, 1H), 1.41 (t, $J = 6.0$ Hz, 2H), 1.32 (t, $J = 6.0$ Hz, 2H), 1.21 (s, 6H). $^{13}\text{C NMR}$ (100 MHz, CDCl_3) δ : 162.3 (C, d, $J^{13\text{C}-19\text{F}} = 246.0$ Hz), 146.2 (C), 145.3 (C), 136.7 (C), 136.3 (C), 136.2 (C), 133.5 (C, $J^{13\text{C}-19\text{F}} = 9.0$ Hz), 131.5 (CH), 130.3 (CH), 128.4 (CH), 128.1 (C), 127.8 (CH), 127.4 (CH), 126.8 (CH, d, $J^{13\text{C}-19\text{F}} = 9.0$ Hz), 126.4 (CH), 126.0 (C), 125.2 (CH), 124.7 (C), 124.2 (C, d, $J^{13\text{C}-19\text{F}} = 3.0$ Hz), 122.4 (CH), 122.3 (CH), 120.6 (C), 120.5 (C), 116.3 (CH, d, $J^{13\text{C}-19\text{F}} = 24.0$ Hz), 111.6 (CH, d, $J^{13\text{C}-19\text{F}} = 23.0$ Hz), 105.0 (C), 74.1 (C), 32.6 (CH_2), 26.4 (CH_3), 22.1 (CH_2). **IR** (KBr): $\tilde{\nu} = 3444, 3058, 2967, 2915, 1674, 1531, 1450, 1409, 1167, 1196, 1157, 766, 744, 700$ cm^{-1} ; **m. p.** ($^\circ\text{C}$) = 293-295. **HRMS** (ESI $^+$): Calcd. for $[\text{C}_{36}\text{H}_{28}\text{FN}_2\text{O}]^+$ $[\text{M}+\text{H}]^+$ 523.2180, found 523.2180.

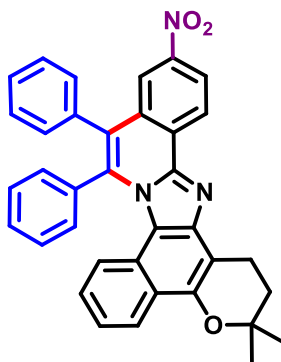


3,3-dimethyl-10,11-diphenyl-2,3-dihydro-1H-benzo[7',8']chromeno[5',6':4,5]imidazo[2,1-a]isoquinoline-13-carbonitrile (275): The general procedure E was followed by using **246** as starting material (71 mg, 0.2 mmol). The product **275** was obtained (*n*-hexane/EtOAc 25:2) as a yellow solid (58.0 mg, 55%, 0.11 mmol). $^1\text{H NMR}$ (400 MHz, CDCl_3) δ : 9.07 (d, J

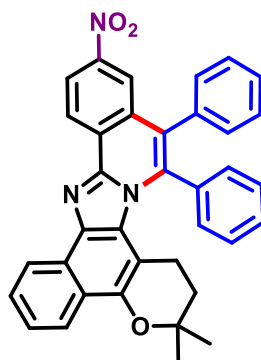
= 8.4 Hz, 1H), 8.31 (d, J = 8.0 Hz, 1H), 7.80 (dd, J = 6.8 and 1.2 Hz, 1H), 7.97 (d, J = 1.2 Hz, 1H), 7.36-7.35 (m, 3H), 7.24-7.19 (m, 1H), 7.17-7.10 (m, 3H), 7.04-7.02 (m, 4H), 6.78-6.72 (m, 2H), 3.39 (t, J = 6.4 Hz, 2H), 2.08 (t, J = 6.4 Hz, 2H), 1.52 (s, 6H). ^{13}C NMR (100 MHz, CDCl_3) δ : 147.4 (C), 146.2 (C), 143.7 (C), 136.8 (C), 135.8 (C), 134.9 (C), 131.5 (CH), 131.1 (CH), 131.0 (C), 129.9 (CH), 129.1 (CH), 128.8 (CH), 128.5 (CH), 128.1 (CH), 127.8 (CH), 125.5 (C), 125.4 (CH), 124.2 (CH), 123.9 (C), 123.1 (CH), 123.0 (CH), 122.0 (CH), 121.8 (C), 120.3 (C), 119.0 (C), 111.6 (C), 106.9 (C), 75.1 (C), 32.4 (CH_2), 26.9 (CH_3), 18.6 (CH_2). IR (KBr): $\tilde{\nu}$ = 3447, 2931, 2227, 1623, 1570, 1516, 1423, 1324, 1160, 1121, 1100, 763, 730, 703 cm^{-1} ; m. p. ($^\circ\text{C}$) = 308-310. HRMS (ESI+): Cald. for $[\text{C}_{37}\text{H}_{28}\text{N}_3\text{O}]^+$ $[\text{M}+\text{H}]^+$ 530.2227, found 530.2226.



3,3-dimethyl-14,15-diphenyl-2,3-dihydro-1H-benzo[7',8']chromeno[6',5':4,5]imidazo[2,1-a]-12-carbonitrile (276): Purification by column chromatography on silica gel (*n*-hexane/EtOAc 25:2) yielded **276** (8.4 mg, 8%, 0.02 mmol) as a yellow solid. ^1H NMR (400 MHz, CDCl_3) δ : 9.06 (d, J = 8.4 Hz, 1H), 8.90 (d, J = 8.0 Hz, 1H), 8.30 (d, J = 8.4 Hz, 1H), 7.82 (dd, J = 7.2 and 1.2 Hz, 1H), 7.74-7.70 (m, 1H), 7.61-7.58 (m, 2H), 7.38-7.36 (m, 3H), 7.18-7.12 (m, 7H), 1.42 (t, J = 6 Hz, 2H), 1.35 (t, J = 6 Hz, 2H), 1.23 (s, 6H). ^{13}C NMR (100 MHz, CDCl_3) δ : 146.3 (C), 144.9 (C), 136.8 (C), 135.8 (C), 135.9 (C), 135.8 (C), 131.4 (CH), 131.2 (C), 131.1 (CH), 130.2 (CH), 129.5 (CH), 128.7 (C), 128.6 (CH), 128.5 (CH), 127.9 (CH), 127.8 (CH), 126.7 (CH), 126.5 (C), 126.1 (C), 125.7 (CH), 125.0 (CH), 123.7 (C), 122.5 (CH), 122.4 (CH), 119.1 (C), 111.3 (C), 104.7 (C), 74.4 (C), 32.5 (CH_2), 26.4 (CH_3), 22.0 (CH_2). IR (KBr): $\tilde{\nu}$ = 3066, 2967, 2921, 2229, 1527, 1485, 1444, 1411, 1333, 1167, 1159, 1117, 832, 767, 700 cm^{-1} ; m. p. ($^\circ\text{C}$) = 299-300. HRMS (ESI+): Cald. for $[\text{C}_{37}\text{H}_{27}\text{N}_3\text{NaO}]^+$ $[\text{M}+\text{Na}]^+$ 552.2046, found 552.2062.

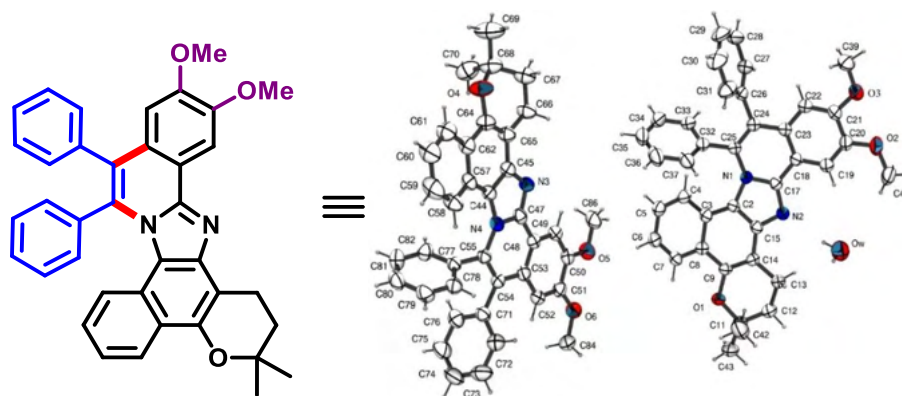


3,3-dimethyl-13-nitro-10,11-diphenyl-2,3-dihydro-1H-benzo[7',8']chromeno[5',6':4,5]imidazo[2,1-a]isoquinoline (277): The general procedure E was followed by using **247** as starting material (75 mg, 0.2 mmol). The product **277** was obtained (*n*-hexane/EtOAc 20:1) as a red solid (56.1 mg, 51%, 0.10 mmol). $^1\text{H NMR}$ (400 MHz, CDCl_3) δ : 9.10 (d, $J = 8.0$, 1H), 8.38 (dd, $J = 8.0$ and 2.0 Hz, 1H), 8.29 (d, $J = 8.0$ Hz, 1H), 8.23 (d, $J = 2.0$ Hz, 1H), 7.35-7.34 (m, 3H), 7.22-7.18 (m, 1H), 7.14-7.12 (m, 3H), 7.05-6.99 (m, 4H), 6.76-6.72 (m, 2H), 3.38 (t, $J = 6.8$ Hz, 2H), 2.06 (t, $J = 6.8$ Hz, 2H), 1.50 (s, 6H). $^{13}\text{C NMR}$ (100 MHz, CDCl_3) δ : 147.6 (C), 147.4 (C), 146.1 (C), 144.0 (C), 137.2 (C), 135.7 (C), 134.9 (C), 131.5 (CH), 131.2 (C), 130.0 (CH), 128.8 (CH), 128.5 (CH), 128.2 (CH), 127.9 (CH), 126.9 (C), 125.9 (CH), 124.7 (C), 124.4 (C), 124.3 (CH), 123.2 (CH), 122.1 (CH), 121.9 (C), 121.5 (CH), 120.5 (C), 106.9 (C), 75.2 (C), 32.4 (CH_2), 26.9 (CH_3), 18.6 (CH_2). **IR** (KBR): $\tilde{\nu} = 3486, 3058, 2925, 1520, 1340, 1150, 1099, 828, 763, 703, \text{cm}^{-1}$; **m. p.** ($^\circ\text{C}$) = 267-269. **HRMS** (ESI $^+$): Cald. for $[\text{C}_{36}\text{H}_{27}\text{N}_3\text{NaO}_3]^+ [\text{M}+\text{Na}]^+$ 572.1945, found 572.1963.



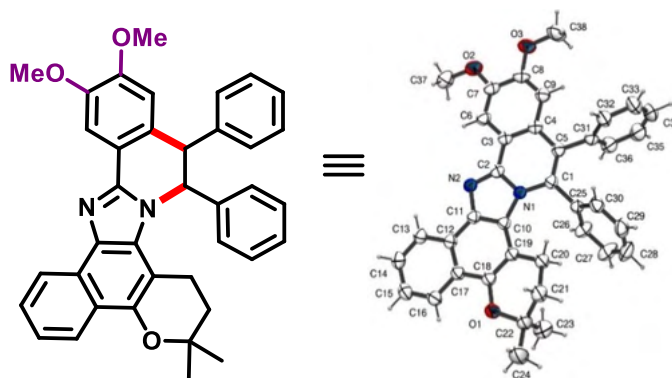
3,3-dimethyl-12-nitro-14,15-diphenyl-2,3-dihydro-1H-benzo[7',8']chromeno[6',5':4,5]imidazo[2,1-a]isoquinoline (278): Purification by column chromatography on silica gel (*n*-hexane/EtOAc 20:1) yielded **278** (18.7 mg, 17%, 0.03 mmol) as a red solid. $^1\text{H NMR}$ (400 MHz, CDCl_3) δ : 9.09 (d, $J = 8.8$, 1H), 8.90 (d, $J = 8.0$, 1H), 8.39 (dd, $J = 8.8$ and 2.0 Hz, 1H), 8.29 (d, $J = 8.0$ Hz, 1H), 8.16 (d, $J = 2.0$, 1H), 7.73-7.70 (m, 1H), 7.61-7.57 (m, 1H), 7.37-7.36 (m,

3H), 7.26-7.25 (m, 1H), 7.18-7.11 (m, 6H), 1.43 (t, $J = 6.0$ Hz, 2H), 1.34 (t, $J = 6.0$ Hz, 2H), 1.22 (s, 6H). ^{13}C NMR (100 MHz, CDCl_3) δ : 147.2 (C), 146.5 (C), 144.7 (C), 137.1 (C), 136.3 (C), 135.9 (C), 135.7 (C), 131.4 (CH), 131.3 (C), 130.2 (CH), 128.9 (C), 128.7 (CH), 128.6 (CH), 128.0 (CH), 127.9 (CH), 126.8 (CH), 126.1 (C), 125.8 (CH), 125.4 (C), 125.1 (C), 124.3 (C), 122.6 (CH), 122.5 (CH), 122.1 (CH), 121.8 (CH), 104.7 (C), 74.5 (C), 32.5 (CH_2), 26.4 (CH_3), 22.0 (CH_2). IR (KBR): $\tilde{\nu} = 3441, 3018, 2963, 2924, 1742, 1617, 1529, 1481, 1339, 1226, 1158, 1117, 891, 760, 741, 714$ cm^{-1} ; m. p. ($^\circ\text{C}$) = 246-248. HRMS (ESI+): Calcd. for $[\text{C}_{36}\text{H}_{27}\text{N}_3\text{NaO}_3]^+ [\text{M}+\text{Na}]^+$ 572.1945, found 572.1942.



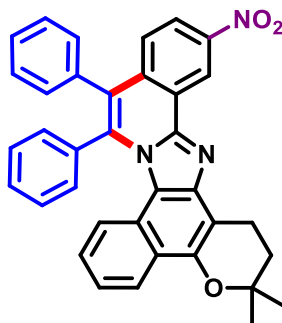
13,14-dimethoxy-3,3-dimethyl-10,11-diphenyl-2,3-dihydro-1H-

benzo[7',8']chromeno[5',6':4,5]imidazo[2,1-a]isoquinoline (279): The general procedure E was followed by using **248** as starting material (75 mg, 0.2 mmol). Purification by column chromatography on silica gel (*n*-hexane/EtOAc 5:1) yielded **279** (55.3 mg, 49%, 0.10 mmol) as a white solid. ^1H NMR (400 MHz, CDCl_3) δ : 8.42 (s, 1H), 8.29 (d, $J = 8.0$ Hz, 1H), 7.34-7.32 (m, 3H), 7.19-7.17 (m, 3H), 7.12-7.07 (m, 3H), 7.02 (d, $J = 8.0$ Hz, 2H), 6.80 (d, $J = 8.0$ Hz, 1H), 6.76-6.74 (m, 1H), 6.73 (s, 1H), 4.21 (s, 3H), 3.73 (s, 3H), 3.44 (t, $J = 6.4$ Hz, 2H), 2.08 (t, $J = 6.4$ Hz, 2H), 1.52 (s, 6H). ^{13}C NMR (100 MHz, CDCl_3) δ : 150.8 (C), 150.0 (C), 146.8 (C), 137.5 (C), 135.8 (C), 133.7 (C), 131.6 (CH), 130.1 (CH), 128.1 (CH), 128.0 (CH), 127.9 (CH), 127.2 (CH), 126.5 (C), 124.9 (C), 123.8 (CH), 123.3 (C), 122.6 (CH), 122.1 (CH), 121.8 (CH), 119.5 (C), 117.6 (C), 106.9 (CH), 104.9 (CH), 74.8 (C), 56.5 (OCH_3), 55.7 (OCH_3), 32.6 (CH_2), 26.9 (CH_3), 18.8 (CH_2). IR (KBr): $\tilde{\nu} = 3060, 3026, 2970, 2928, 1615, 1592, 1486, 1438, 1363, 1155, 1119, 1097, 861, 754, 727, 696, 587$ cm^{-1} . m. p. ($^\circ\text{C}$) = 191-192. HRMS (ESI+): Calcd for $[\text{C}_{38}\text{H}_{33}\text{N}_2\text{O}_3]^+ [\text{M}+\text{H}]^+$ 565.2486, found 565.2481. The structure of the product was also confirmed by X-ray diffraction (CCDC number = 2043364).



11,12-dimethoxy-3,3-dimethyl-14,15-diphenyl-2,3-dihydro-1H-

benzo[7',8']chromeno[6',5':4,5]imidazo[2,1-a]isoquinoline (280): Purification by column chromatography on silica gel (*n*-hexane/EtOAc 5:1) yielded **280** (5.6 mg, 5%, 0.01 mmol) as a white solid. $^1\text{H NMR}$ (400 MHz, CDCl_3) δ : 8.91 (d, $J = 8.0$ Hz, 1H), 8.41 (s, 1H), 8.28 (d, $J = 8.0$ Hz, 1H), 7.70-7.66 (m, 1H), 7.57-7.52 (m, 1H), 7.33-7.31 (m, 3H), 7.22-7.19 (m, 1H), 7.16-7.13 (m, 2H), 7.12-7.11 (m, 4H), 6.65 (s, 1H), 4.21 (s, 3H), 3.71 (s, 3H), 1.44 (t, $J = 6.4$ Hz, 2H), 1.33 (t, $J = 6.4$ Hz, 2H), 1.22 (s, 6H). $^{13}\text{C NMR}$ (100 MHz, CDCl_3) δ : 150.5 (C), 150.0 (C), 146.6 (C), 144.8 (C), 137.5 (C), 136.8 (C), 133.6 (C), 131.5 (CH), 130.3 (CH), 128.2 (CH), 127.9 (CH), 127.8 (CH), 127.2 (CH), 126.3 (C), 126.2 (CH), 126.0 (C), 125.1 (CH), 124.7 (C), 124.6 (C), 122.5 (CH), 122.4 (CH), 118.4 (C), 107.3 (CH), 105.3 (C), 104.9 (CH), 74.0 (C), 56.5 (OCH₃), 55.7 (OCH₃), 32.6 (CH₂), 26.5 (CH₃), 22.1 (CH₂). **IR** (KBr): $\tilde{\nu} = 3051, 2972, 2925, 1612, 1497, 1293, 1244, 1209, 1166, 1097, 1047, 950, 864, 696, 581$ cm^{-1} . **m. p.** ($^\circ\text{C}$) = 289-290. **HRMS** (ESI⁺): Calcd for $[\text{C}_{38}\text{H}_{33}\text{N}_2\text{O}_3]^+$ $[\text{M}+\text{H}]^+$ 565.2486, found 565.2459. *The structure of the product was also confirmed by X-ray diffraction* (CCDC number = 2043280).



3,3-dimethyl-14-nitro-10,11-diphenyl-2,3-dihydro-1H-benzo[7',8']chromeno[5',6':4,5]imidazo[2,1-a]isoquinoline (281): The general procedure E was followed by using **249** as starting

material (75 mg, 0.2 mmol) Purification by column chromatography on silica gel (*n*-hexane/EtOAc 20:1) yielded **281** (57.4 mg, 52%, 0.10 mmol) as a red solid. $^1\text{H NMR}$ (400 MHz, CDCl_3) δ : 9.85 (d, $J = 2.0$ Hz, 1H), 8.28 (d, $J = 8.0$ Hz, 1H), 8.21 (dd, $J = 9.2$ and 2.4 Hz, 1H), 7.46 (d, $J = 8.0$ Hz, 1H), 7.34-7.33 (m, 3H), 7.19-7.17 (m, 1H), 7.15-7.12 (m, 3H), 7.09-7.03 (m, 4H), 6.74-6.70 (m, 2H), 3.40 (t, $J = 6.4$ Hz, 2H), 2.07 (t, $J = 6.4$ Hz, 2H), 1.50 (s, 6H). $^{13}\text{C NMR}$ (100 MHz, CDCl_3) δ : 147.6 (C), 146.7 (C), 146.3 (C), 143.6 (C), 138.6 (C), 136.2 (C), 135.1 (C), 134.9 (C), 131.6 (CH), 130.0 (CH), 129.0 (CH), 128.5 (CH), 128.2 (CH), 127.7 (CH), 127.6 (CH), 124.3 (CH), 124.1 (C), 124.0 (C), 123.1 (C), 123.0 (CH), 122.3 (CH), 122.1 (CH), 121.9 (C), 120.7 (CH), 120.0 (C), 107.1 (C), 75.2 (C), 32.5 (CH_2), 26.9 (CH_2), 18.7 (CH_2). IR (KBr): $\tilde{\nu} = 3058, 2922, 2849, 1515, 1339, 1148, 1099, 829, 740, 695 \text{ cm}^{-1}$. m. p. ($^\circ\text{C}$) = 255-256. HRMS (ESI+): Calcd for $[\text{C}_{36}\text{H}_{28}\text{N}_3\text{O}_3]^+ [\text{M}+\text{H}]^+$ 550.2125, found 550.2098.

7.4 Gram scale synthesis Procedure.

To an oven-dried re-sealable tube, the phenyl-lapimidazole **234** (1.148 g, 3.5 mmol), diphenylacetylene (**214**) (1.248 g, 7.0 mmol), $[\text{RhCp}^*\text{Cl}_2]_2$ (108.0 mg, 0.175 mmol, 5 mol%), AgOAc (292.0 mg, 1.75 mmol, 0.5 equiv) were added followed of methanol (20 mL). The tube was sealed, submitted to heating (100 $^\circ\text{C}$) using an oil bath heating system and stirring for 24 hours. Then, the reaction mixture was filtered through a pad of celite, and the crude product was purified *via* column chromatography under the conditions noted using silica gel and a mixture of ethyl acetate and *n*-hexane as eluent.

7.5 Fluorescence studies

Dropcast films and solutions of **235/236**, **259/260** and **277/278** were investigated by steady-state fluorescence and absorption at room temperature. The optically studied solutions of the isomer pairs were prepared at 40 μM concentration in ethyl acetate. Dropcast films were fabricated from initial solutions at a higher concentration (400 μM) in ethyl acetate. The dropcast films **235** and **236** were fabricated following the procedure of the sequential cycles of spreading and natural drying of the respective isomeric solutions on glass substrates, under

atmospheric conditions. The dropcast **259/260** and **277/278** were fabricated by the same procedure but using only five sequential cycles of spreading and natural drying of the respective isomeric solutions on glass substrates.

The steady-state fluorescence measurements of all dropcast films were measured in air at room temperature. The laser beam on the film surfaces was not focused, enabling a maximum area of excitation. Quartz cuvettes of 10 mm pathway were used for the acquisition of fluorescence spectra of dilute solutions (40 μM). In this case, the laser beam was focused on the solution, corresponding to a minimum width of the exciting light trace crossing the cuvette. For all fluorescence measurements of dropcast films and solutions, the excitation of the samples was made by a CW laser emitting at 375 nm. The scattered fluorescence emissions of all samples were acquired into an ANDOR-Shamrock-303i spectrometer.

UV-Vis absorption measurements of dropcast films **235/236**, **259/260** and **277/278**, and their respective solutions at 40 μM of concentration were performed at room temperature in a spectrophotometer Shimadzu, model 3600.

The emission quantum yields (Φ) of the solutions were measured by the integrating sphere (Ocean Optics) method.¹⁹⁵ The respective solutions were injected inside a thin quartz tube, which in turn was placed at the entrance of the integrating sphere. It is worth noticing that the same volume (25 μL) for each solution was used, making the emission quantum yield measurements more uniform. For the excitation of the solutions, the incident laser beam was addressed vertically, without focusing, crossing the quartz tube from top to bottom.

195. a) L.-O. Pallsson, A. P. Monkman. Measurements of solid-state photoluminescence quantum yields of films using a fluorimeter. *Adv. Mater.* **2002**, *14*, 757-758. **b)** J. C. de Mello, H. F. Wittmann, R. H. Friend. An improved experimental determination of external photoluminescence quantum efficiency. *Adv. Mater.* **1997**, *9*, 230-232.

GENERAL CONCLUSION

Metal-promoted C–H activation has been extensively investigated due to the possibility of sustainable organic transformation associated with synthetic steps reduction. In the course of this doctoral thesis, developed methodologies involving C–H alkenylation and oxygenation on quinoidal compounds, as well as C–H/N–H annulation reactions on lapimidazole were described. The new established protocols have contributed to the development of new strategies to overcome the limitation of accessing benzenoid of 1,4-naphthoquinones. The obtained products from C–H alkenylation and oxygenation were evaluated against *T. cruzi* give rising to other potential drugs for the treatment of Chagas disease. New protocols for C–H/N–H annulation on lapimidazole allowed us to obtain regioselectively non-symmetrical products and computational studies clarified the mechanism and selectivity of this reaction. In addition, fluorescence studies were carried out with products obtained. In conclusion, the results concerning C–H activation protocols represent a significant contribution to the field of organic synthesis.

This work is a detailed collection manuscript of 4 already published reports:

1. G. G. Dias, T. Rogge, R. Kuniyil, C. Jacob, R. F. S. Menna-Barreto, E. N. da Silva Júnior, L. Ackermann. Ruthenium-catalyzed C–H oxygenation of quinones by weak *O*-coordination for potent trypanocidal agentes. *Chem. Commun.* **2018**, 54, 12840-12843.

2. G. G. Dias, T. A. do Nascimento, A. K. A. de Almeida, A. Cristina S. Bombaça, R. F. S. Menna-Barreto, C. Jacob, S. Warratz, E. N. da Silva Júnior, L. Ackermann. Ruthenium(II)-catalyzed C–H alkenylation of quinones: diversity-oriented strategy for trypanocidal compounds. *Eur. J. Org. Chem.* **2019**, 2344-2353.

3. G. G. Dias, E. R. S. Paz, J. Y. Kadooca, A. A. Sabino, L. A. Cury, K. Torikai, C. A. de Simone, F. Fantuzzi, E. N. da Silva Júnior. Rhodium(III)-Catalyzed C–H/N–H Alkyne Annulation of Nonsymmetric 2-Aryl (Benz)imidazole Derivatives: Photophysical and Mechanistic Insights. *J. Org. Chem.* **2021**, 86, 264-278.

4. R. L. Carvalho, G. G. Dias, C. L. M. Pereira, P. Ghosh, D. Maiti, E. N. da Silva Júnior. A Catalysis Guide Focusing on C–H Activation Processes. *J. Braz. Chem. Soc.* **2021**, 00, 1-36.

Others reports out of the scope of this thesis project:

5. G. G. Dias, Aaron King, F. de Moliner, M. Vendrell, Eufrânio N. da Silva Júnior. Quinone-based fluorophores for imaging biological processes. *Chem. Soc. Rev.* **2018**, 47, 12-27.

6. Z. Cheng, W. O. Valença, G. G. Dias, J. Scott, N. D. Barth, F. de Moliner, G. B. P. Souza, R. J. Mellanby, M. Vendrell, E. N. da Silva Júnior. Natural product-inspired profluorophores for imaging NQO1 activity in tumour tissues. *Bioorg. Med. Chem.* **2019**, 27, 3938-3946.

APPENDICE

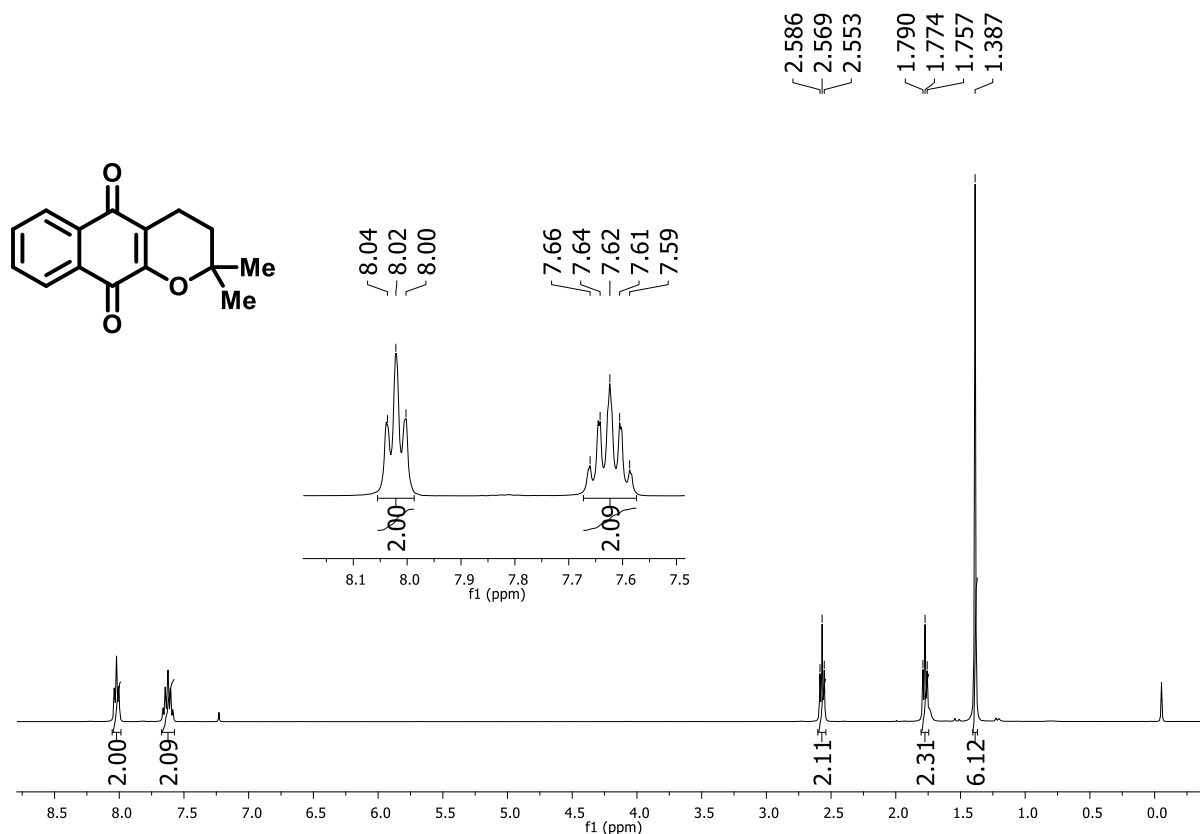


Figure 12. ^1H NMR spectrum (400 MHz, CDCl_3) of compound **68**.

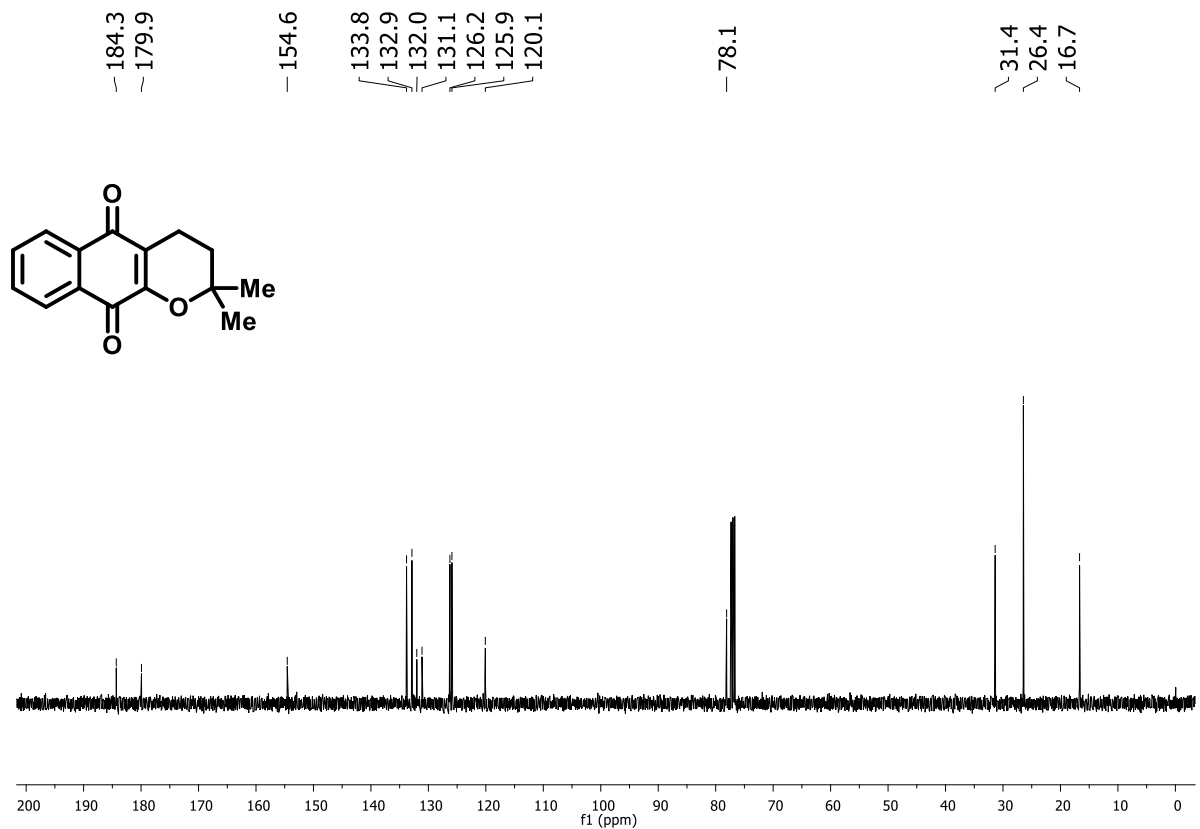


Figure 13. ^{13}C NMR spectrum (100 MHz, CDCl_3) of compound **68**.

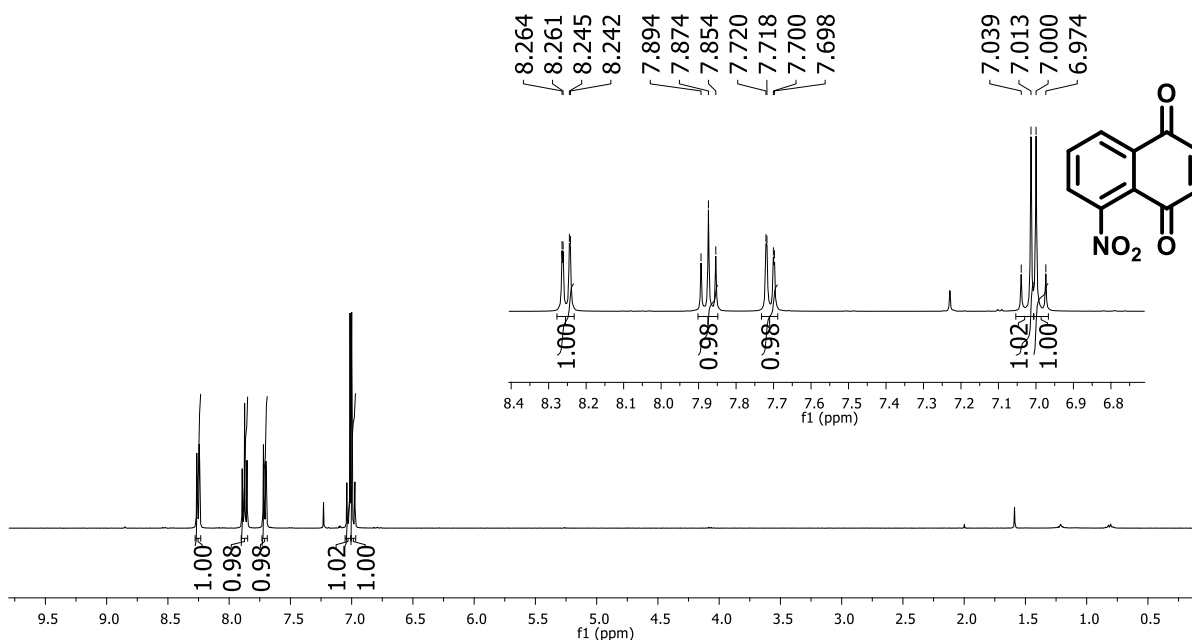


Figure 14. ¹H NMR spectrum (400 MHz, CDCl₃) of compound 102.

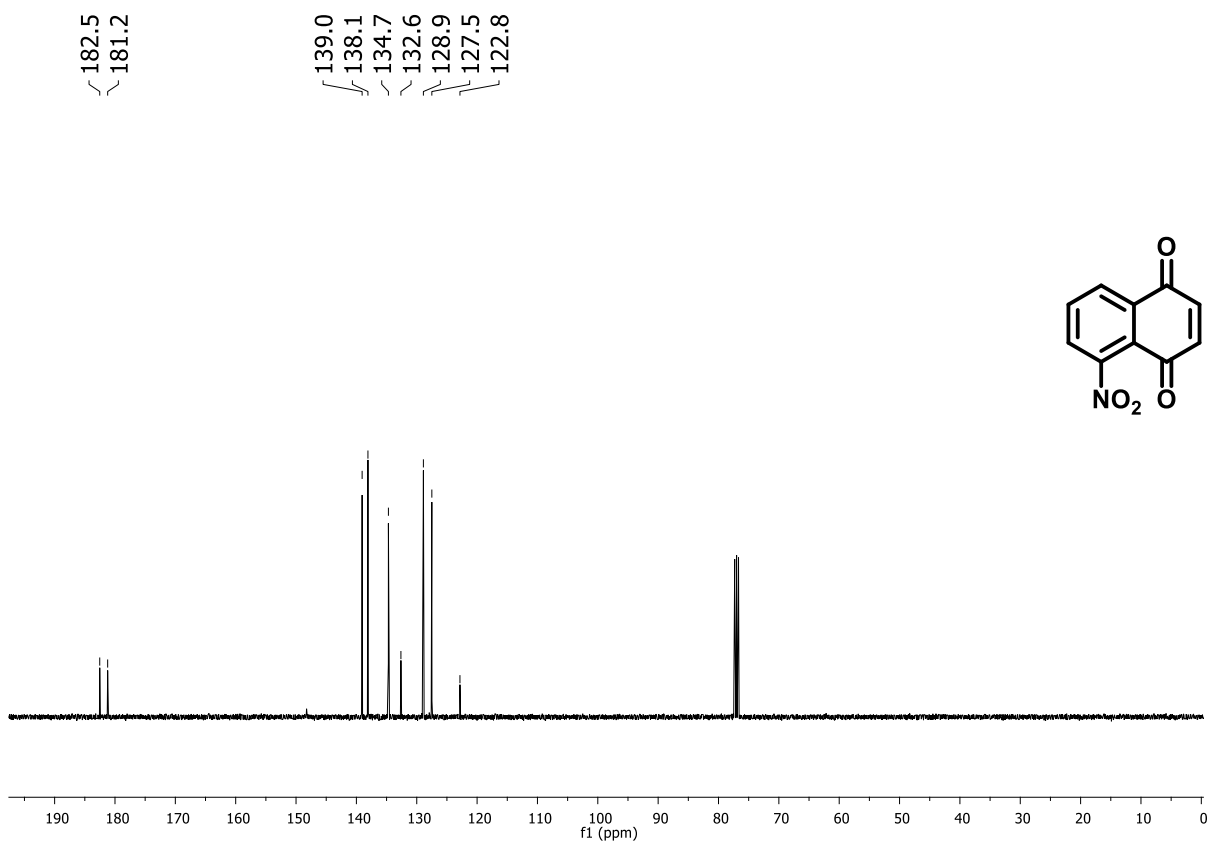


Figure 15. ¹³C NMR spectrum (100 MHz, CDCl₃) of compound 102.

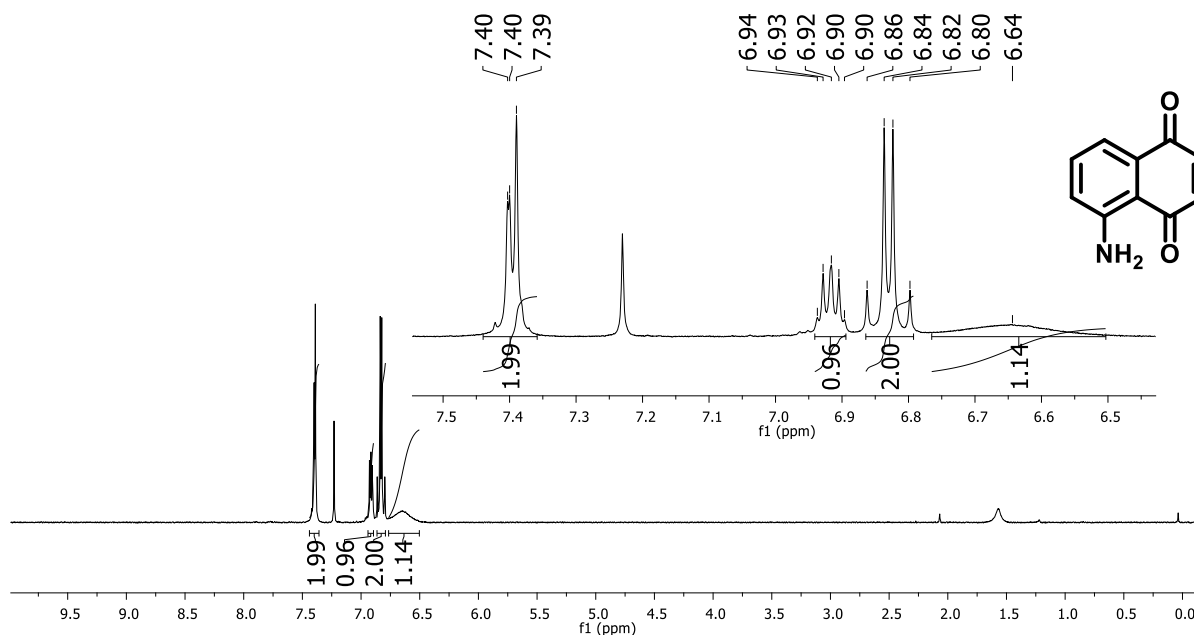


Figure 16. ^1H NMR spectrum (300 MHz, CDCl_3) of compound 103.

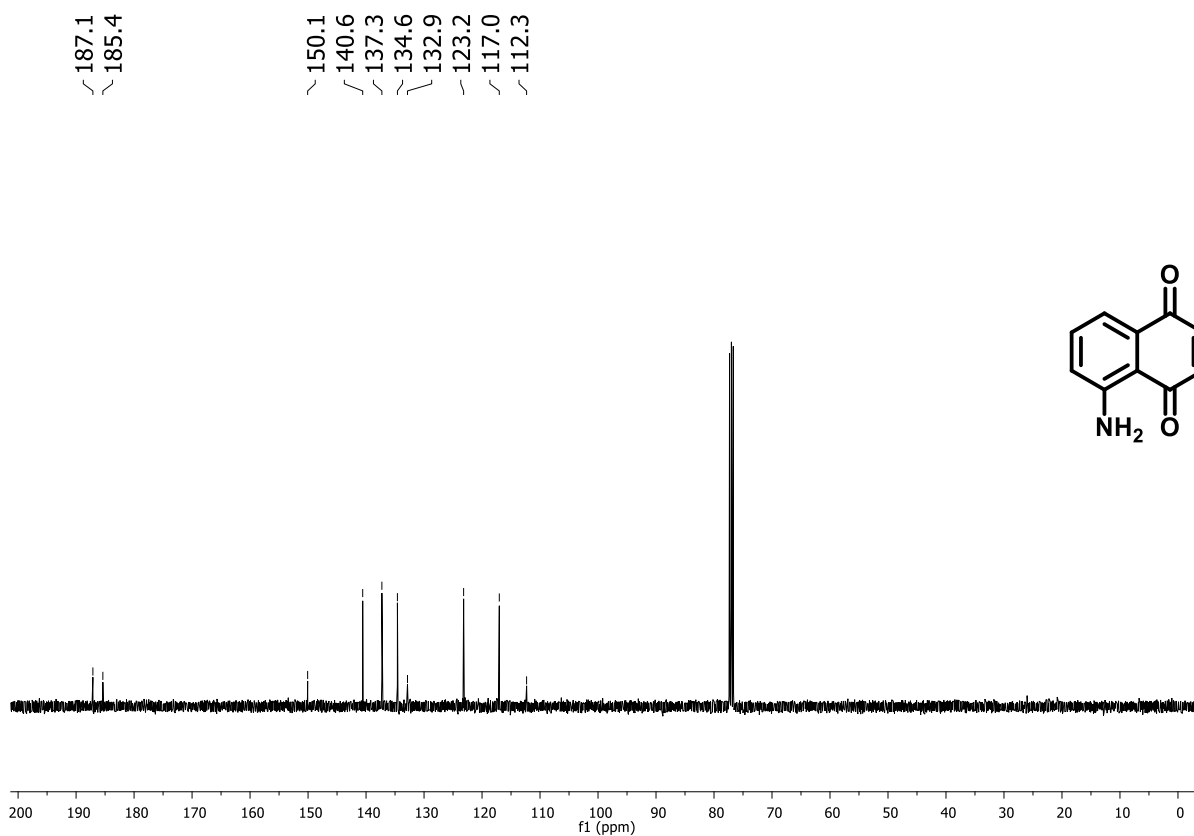


Figure 17. ^{13}C NMR spectrum (75 MHz, CDCl_3) of compound 103.

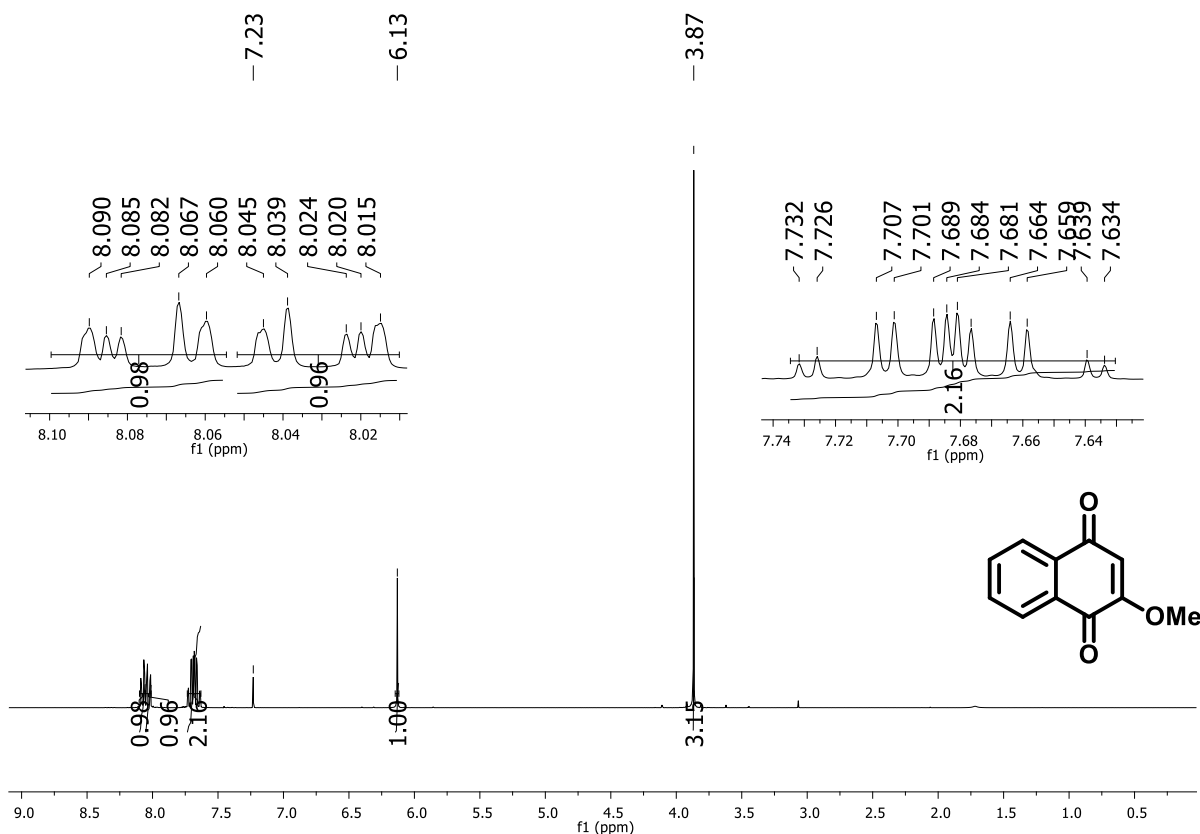


Figure 18. ¹H NMR spectrum (300 MHz, CDCl₃) of compound 112.

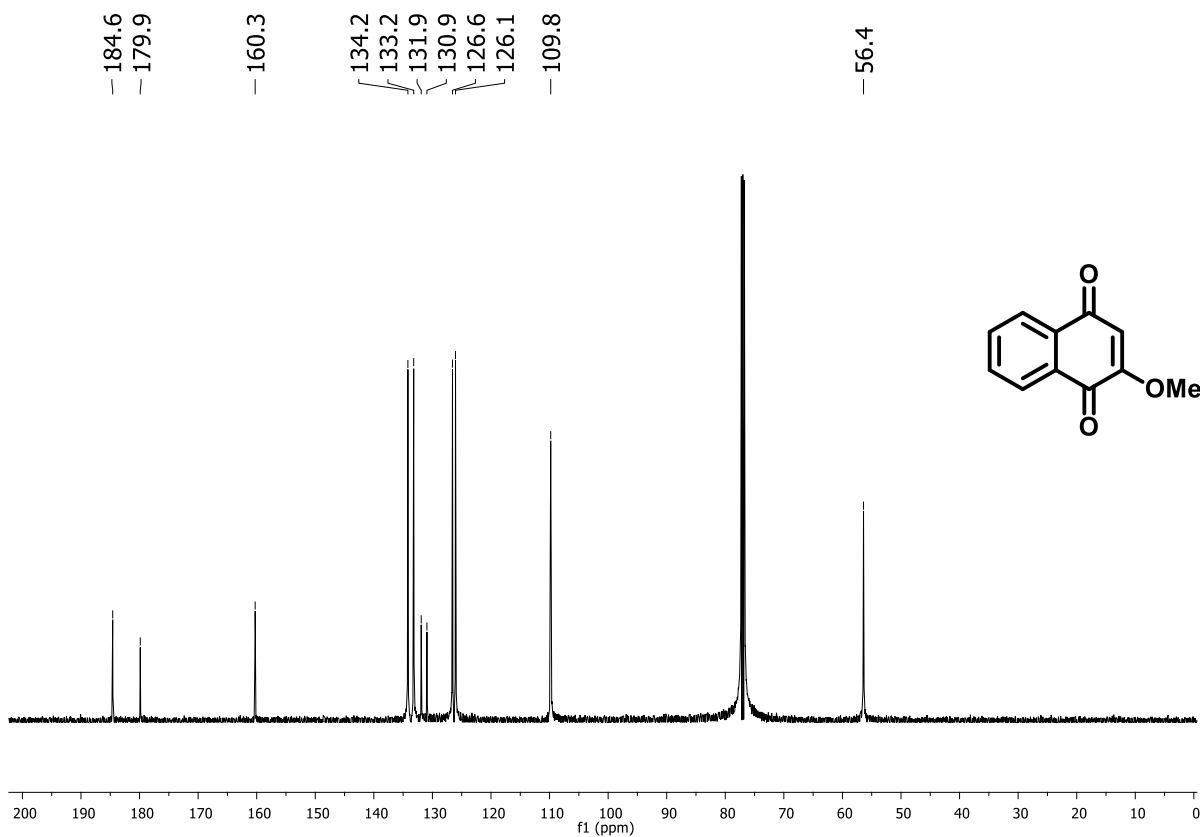


Figure 19. ¹³C NMR spectrum (75 MHz, CDCl₃) of compound 112.

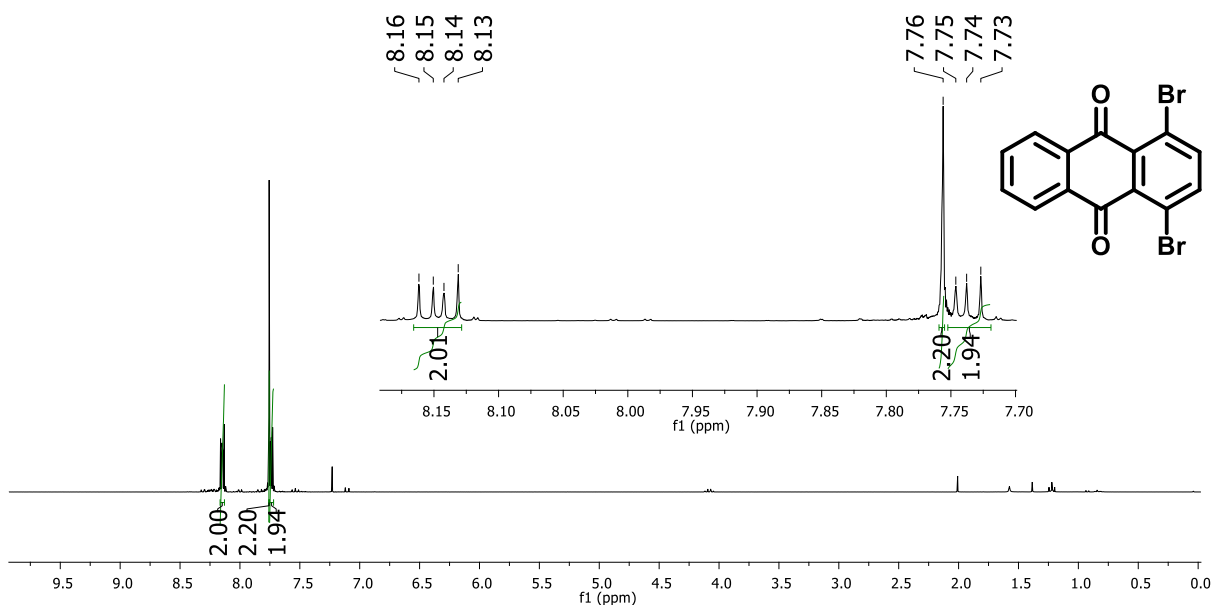


Figure 20. ^1H NMR spectrum (300 MHz, CDCl_3) of compound 122.

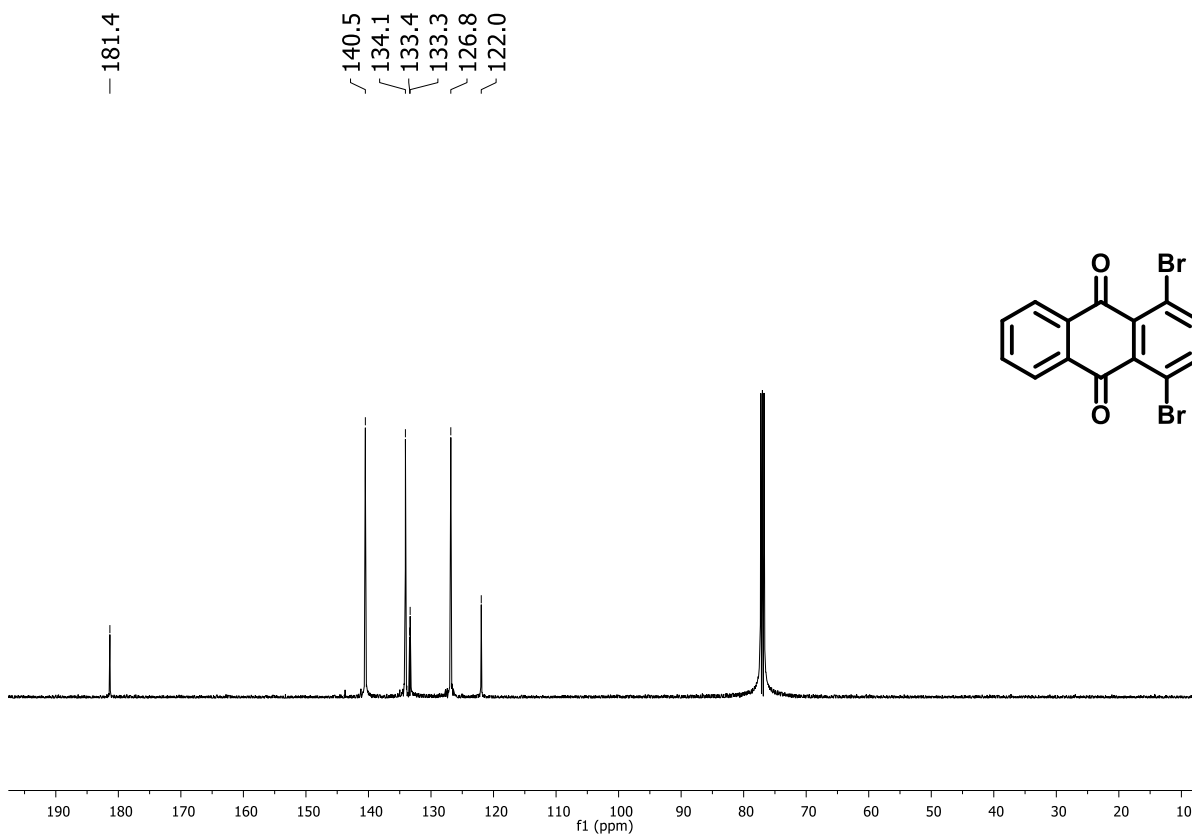


Figure 21. ^{13}C NMR spectrum (75 MHz, CDCl_3) of compound 122.

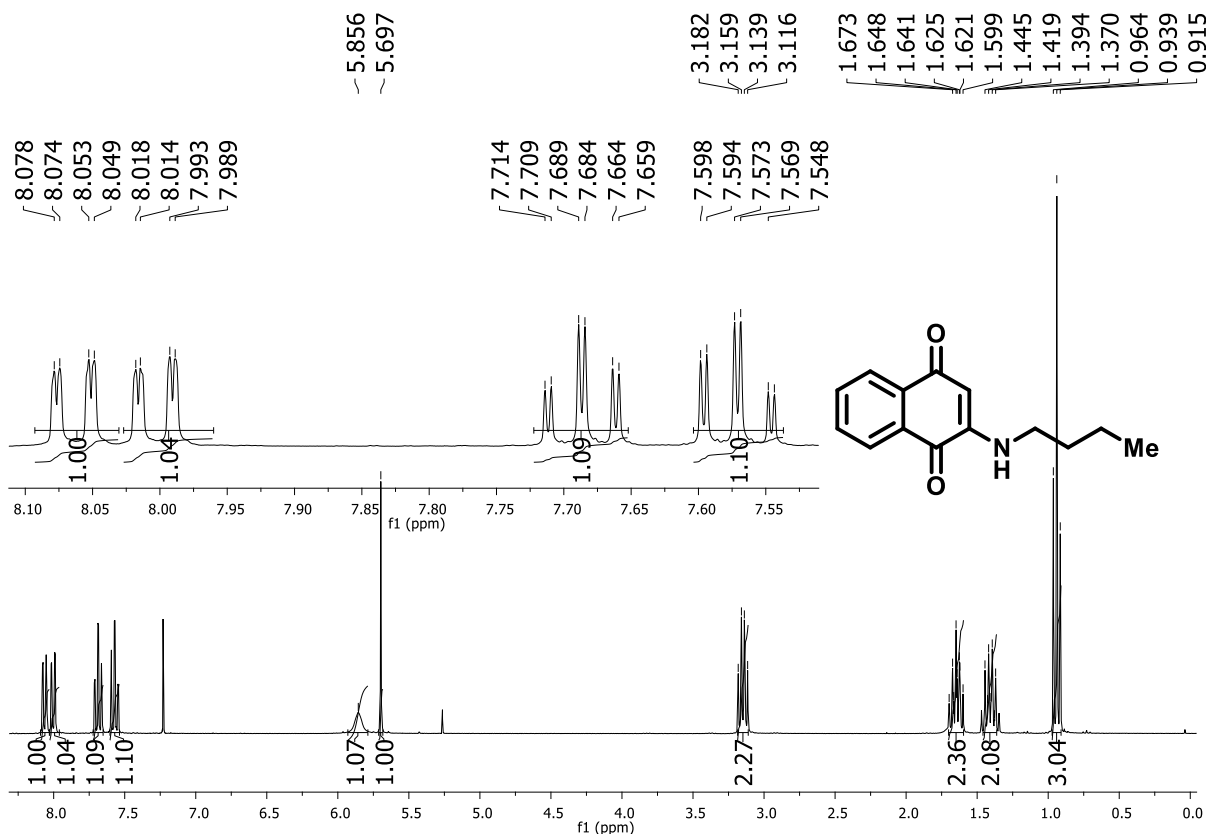


Figure 22. ¹H NMR spectrum (300 MHz, CDCl₃) of compound 129.

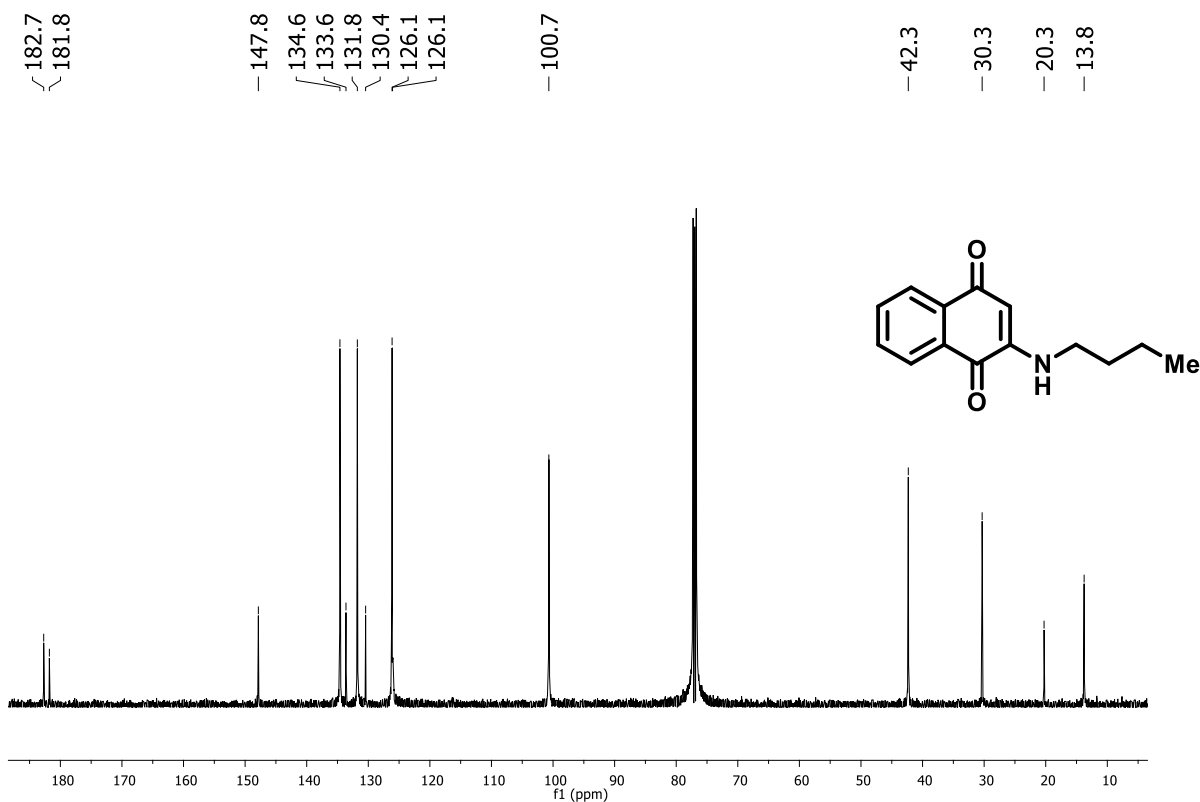


Figure 23. ¹³C NMR spectrum (75 MHz, CDCl₃) of compound 129.

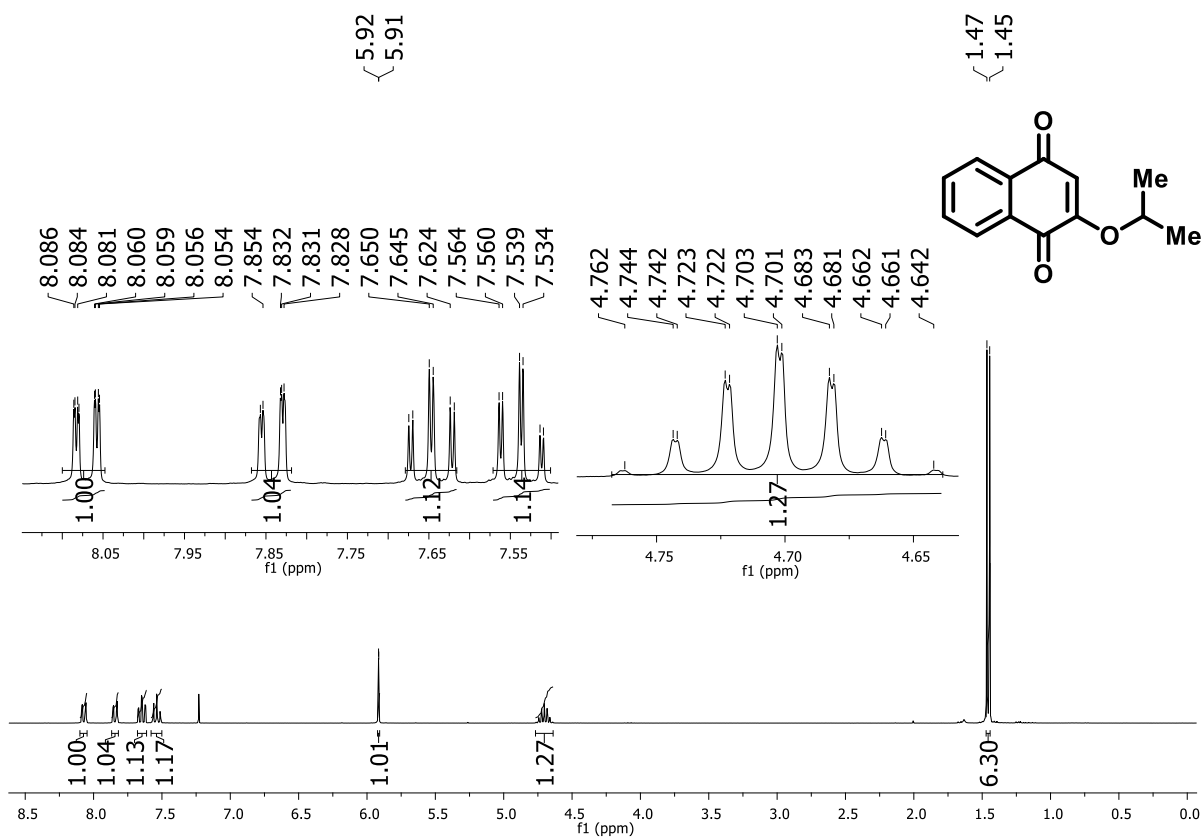


Figure 24. ^1H NMR spectrum (300 MHz, CDCl_3) of compound **131**.

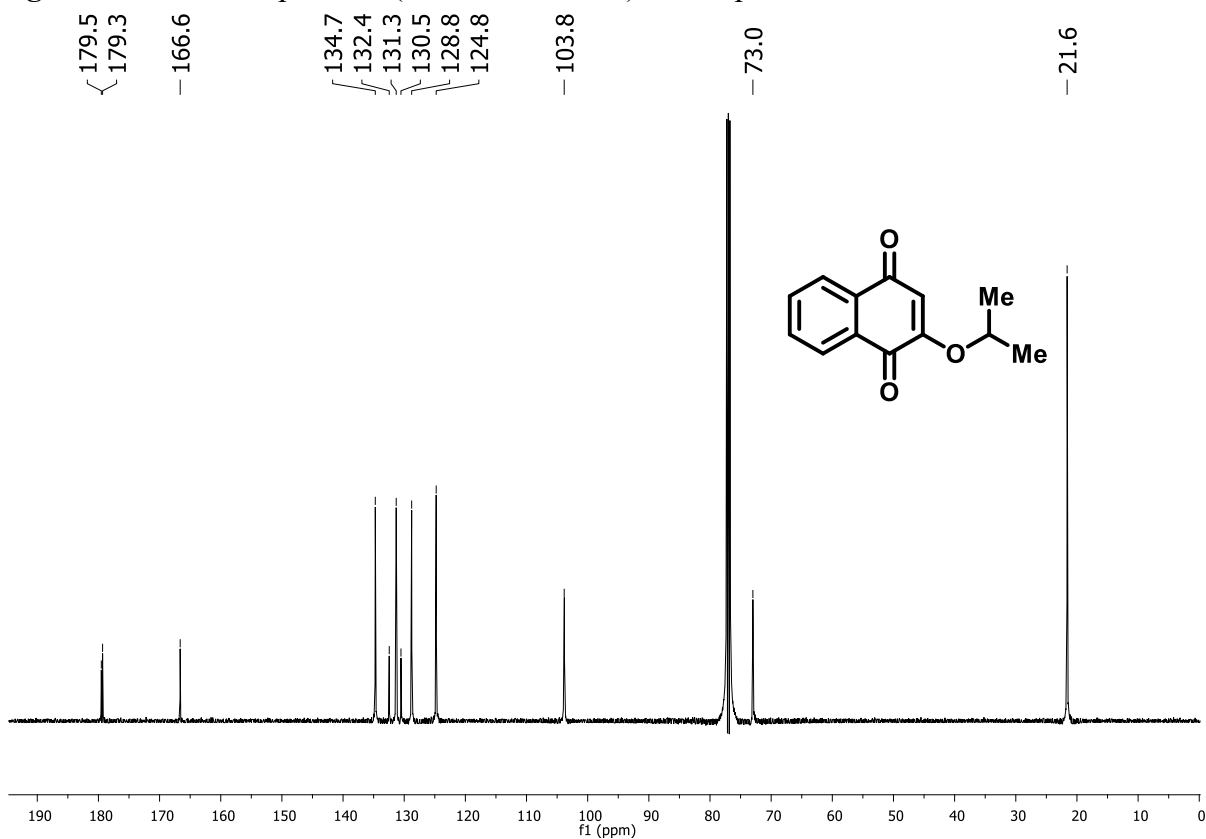


Figure 25. ^{13}C NMR spectrum (75 MHz, CDCl_3) of compound **131**.

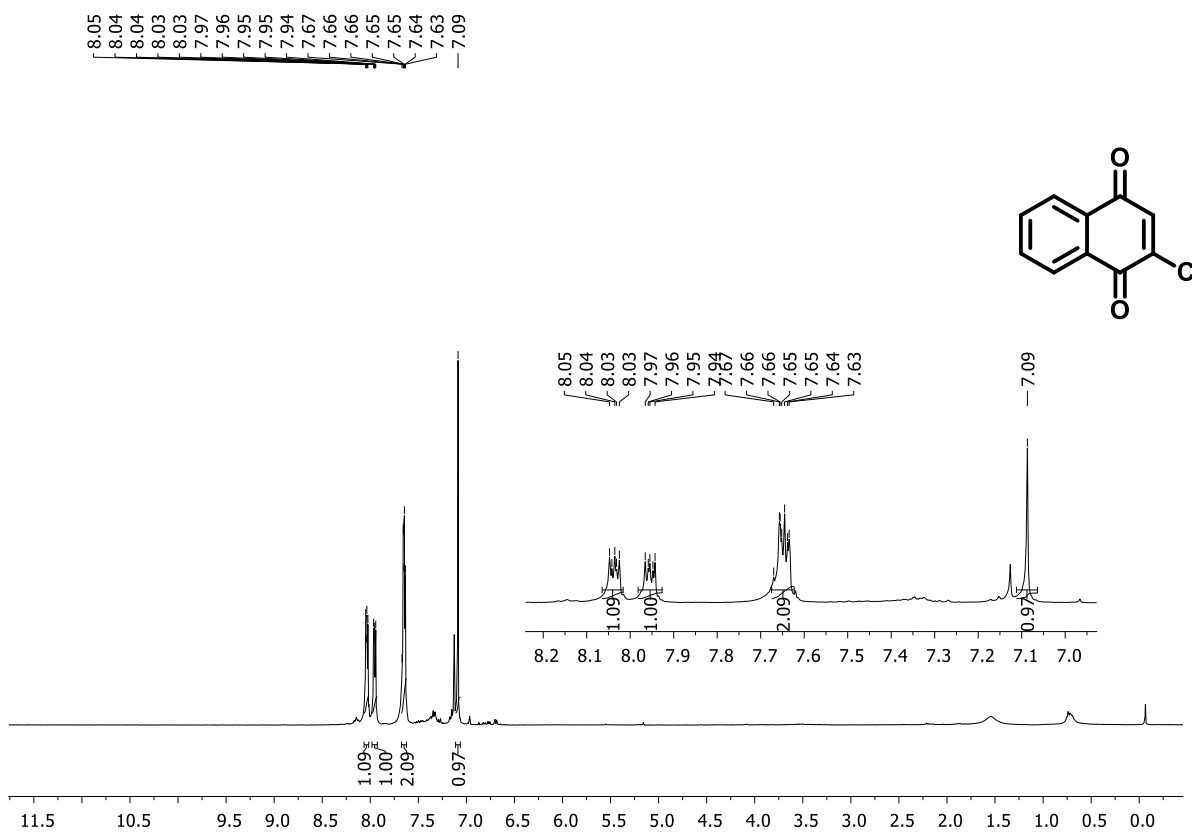


Figure 26. ¹H NMR spectrum (300 MHz, CDCl₃) of compound 132.

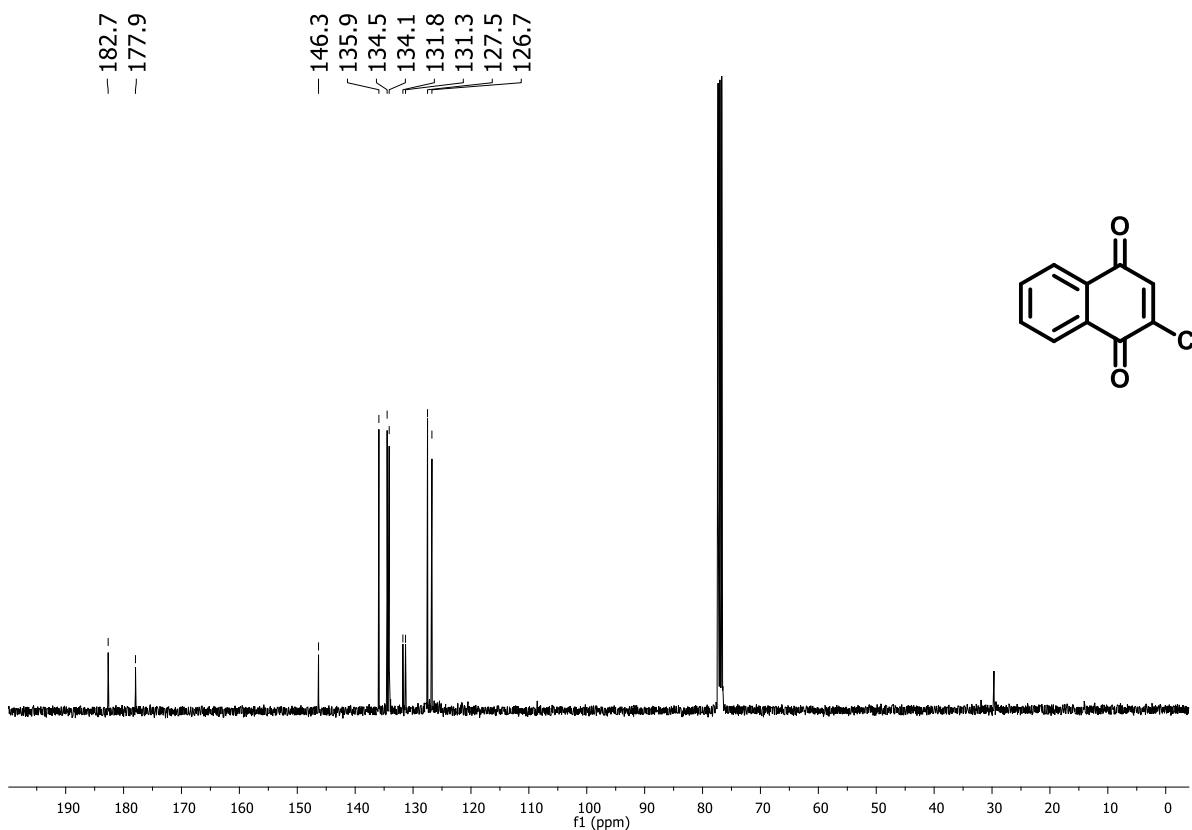


Figure 27. ¹³C NMR spectrum (75 MHz, CDCl₃) of compound 132.

– 7.48

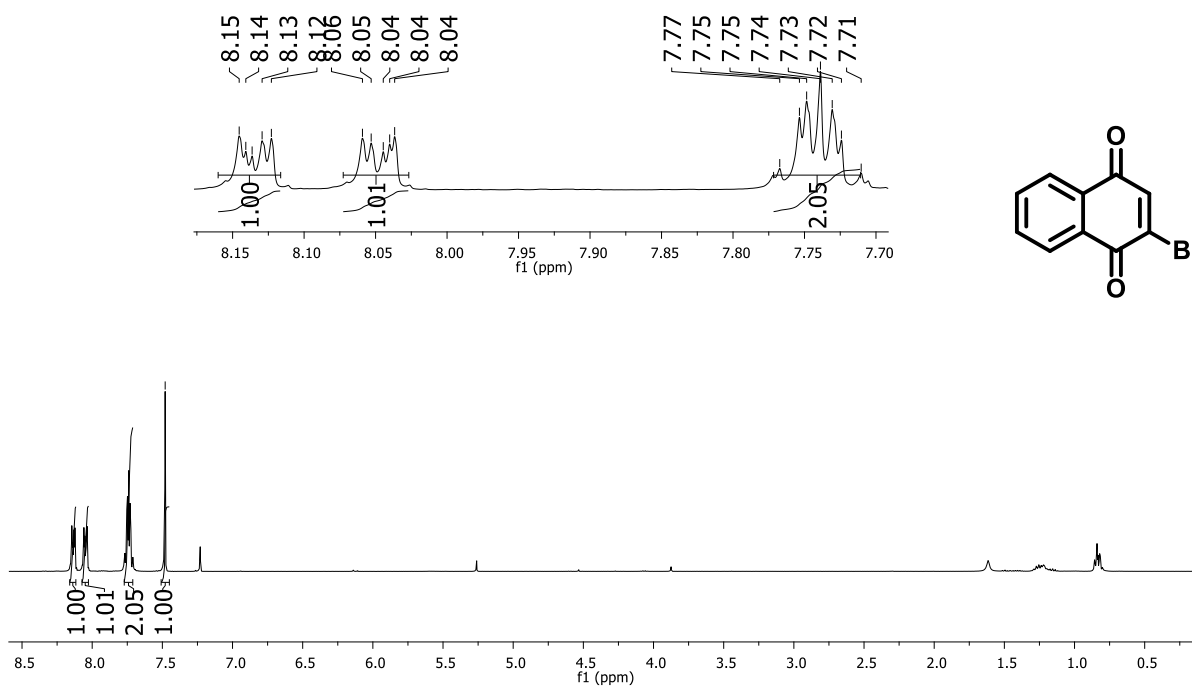


Figure 28. ¹H NMR spectrum (300 MHz, CDCl₃) of compound 133.

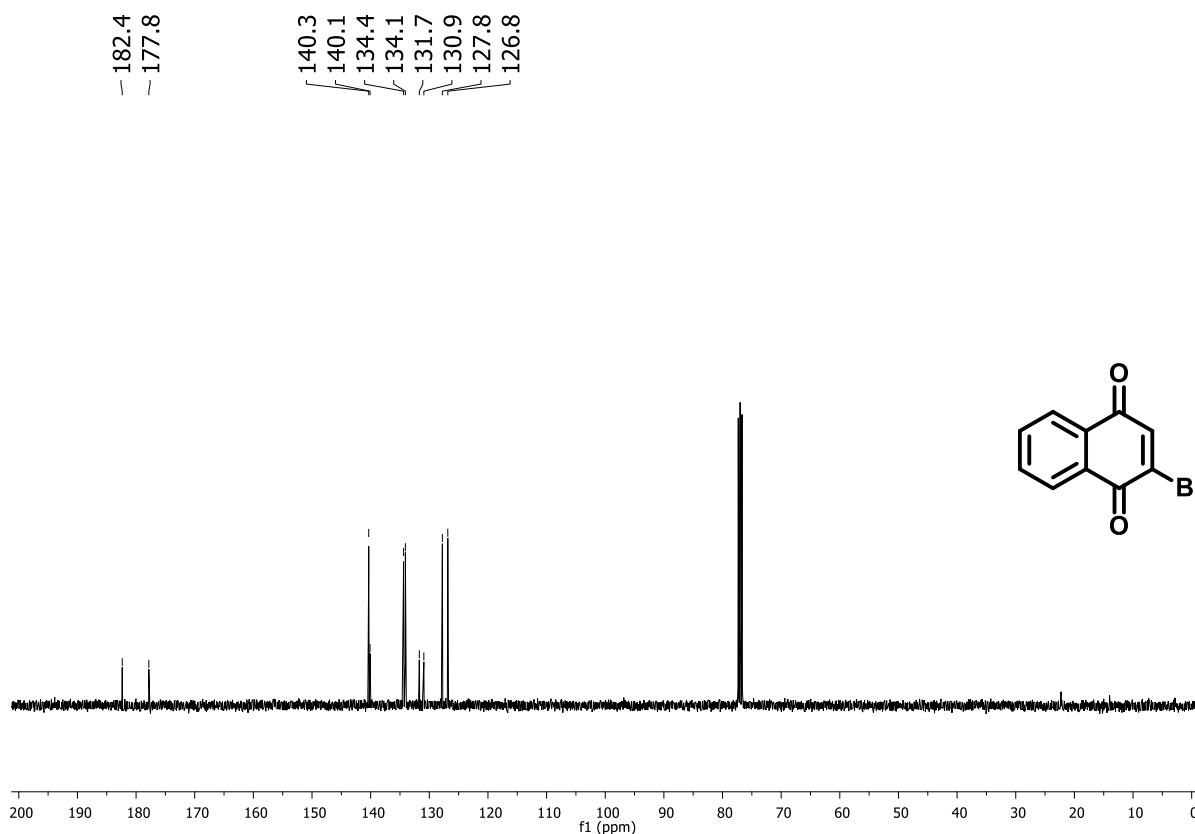


Figure 29. ¹³C NMR spectrum (75 MHz, CDCl₃) of compound 133.

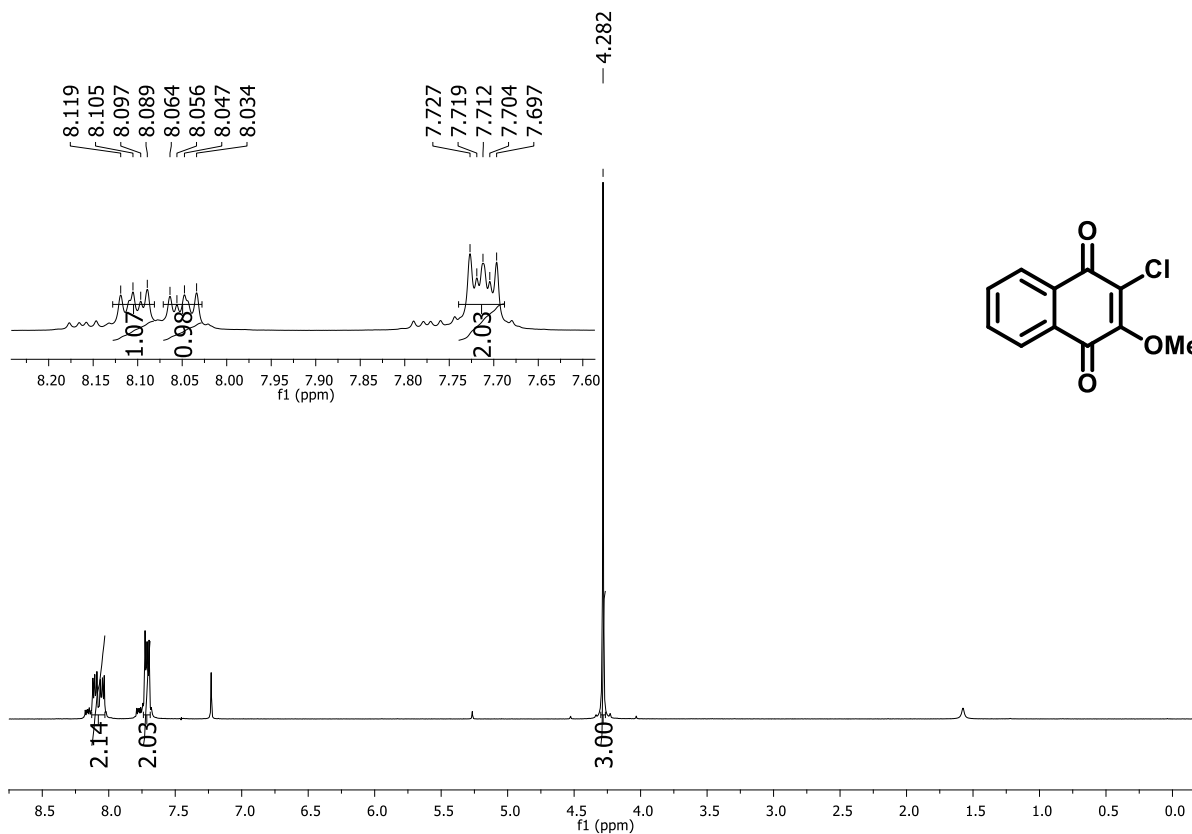


Figure 30. ^1H NMR spectrum (300 MHz, CDCl_3) of compound 134.

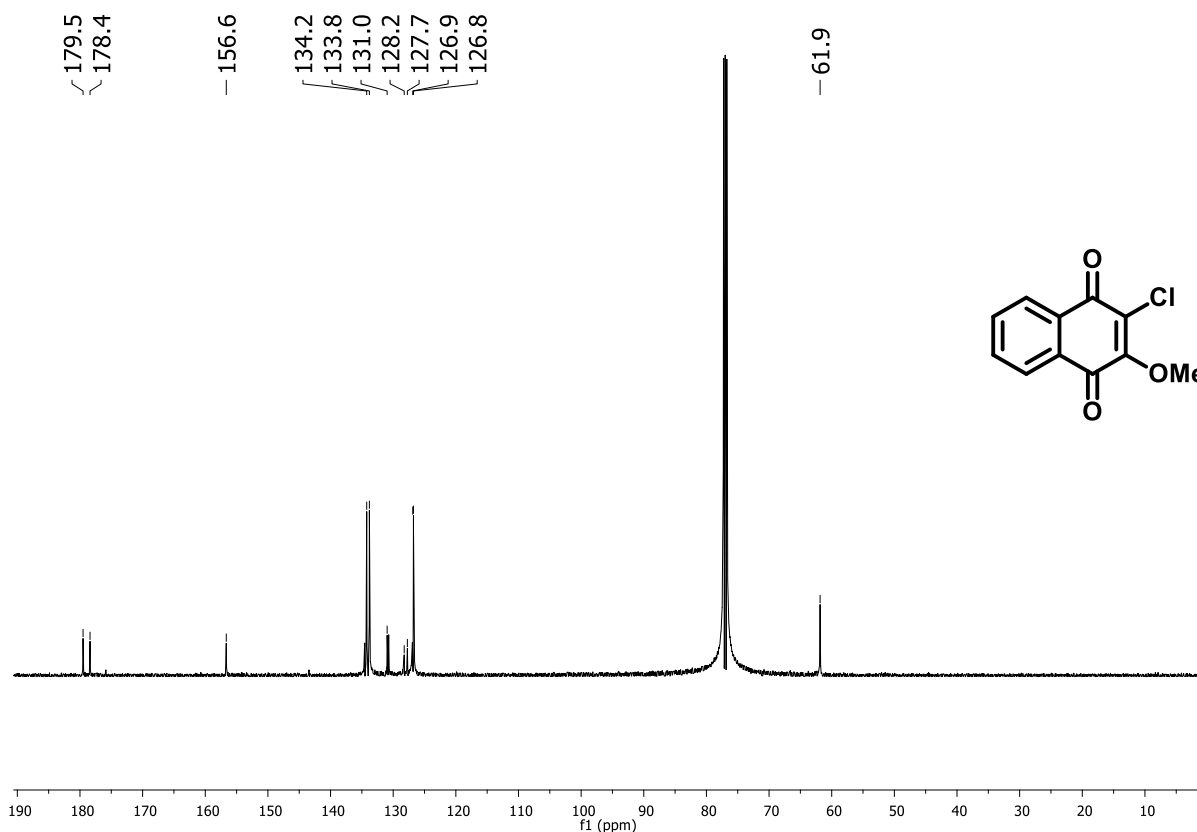


Figure 31. ^{13}C NMR spectrum (75 MHz, CDCl_3) of compound 134.

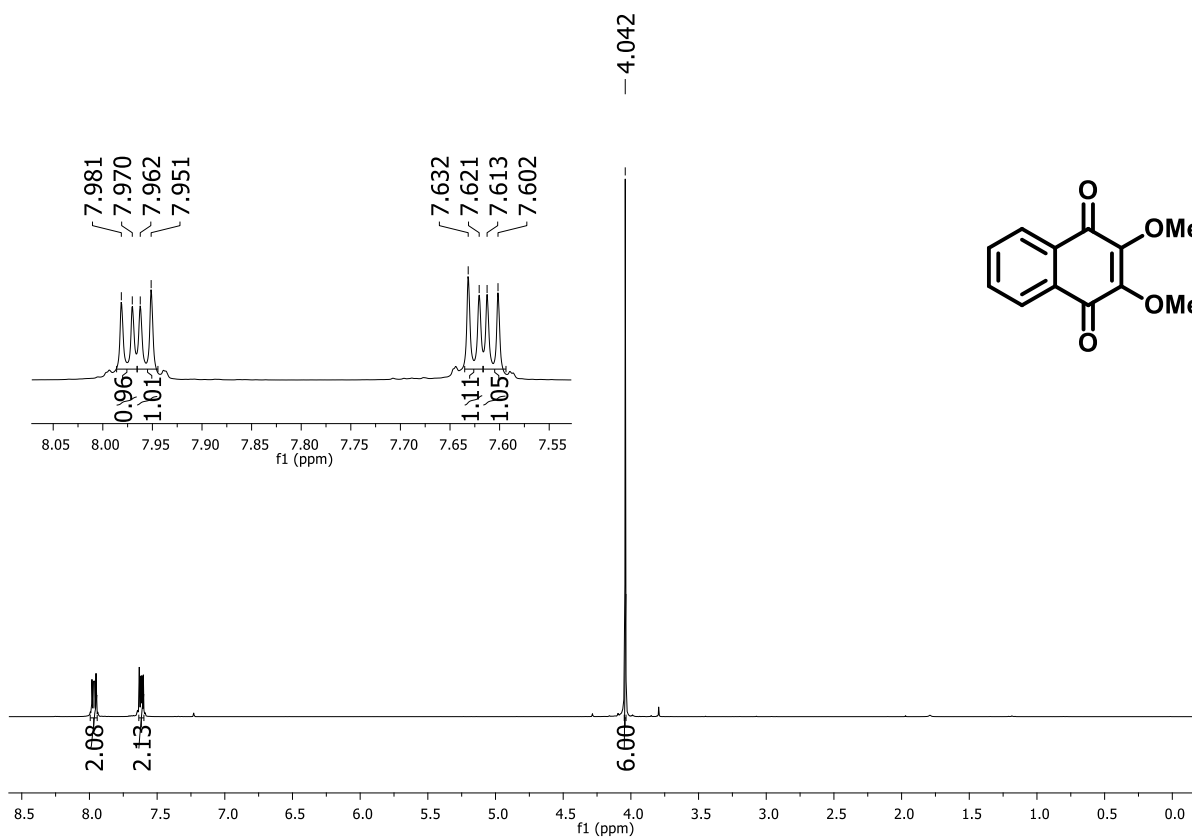


Figure 32. ¹H NMR spectrum (300 MHz, CDCl₃) of compound 135.

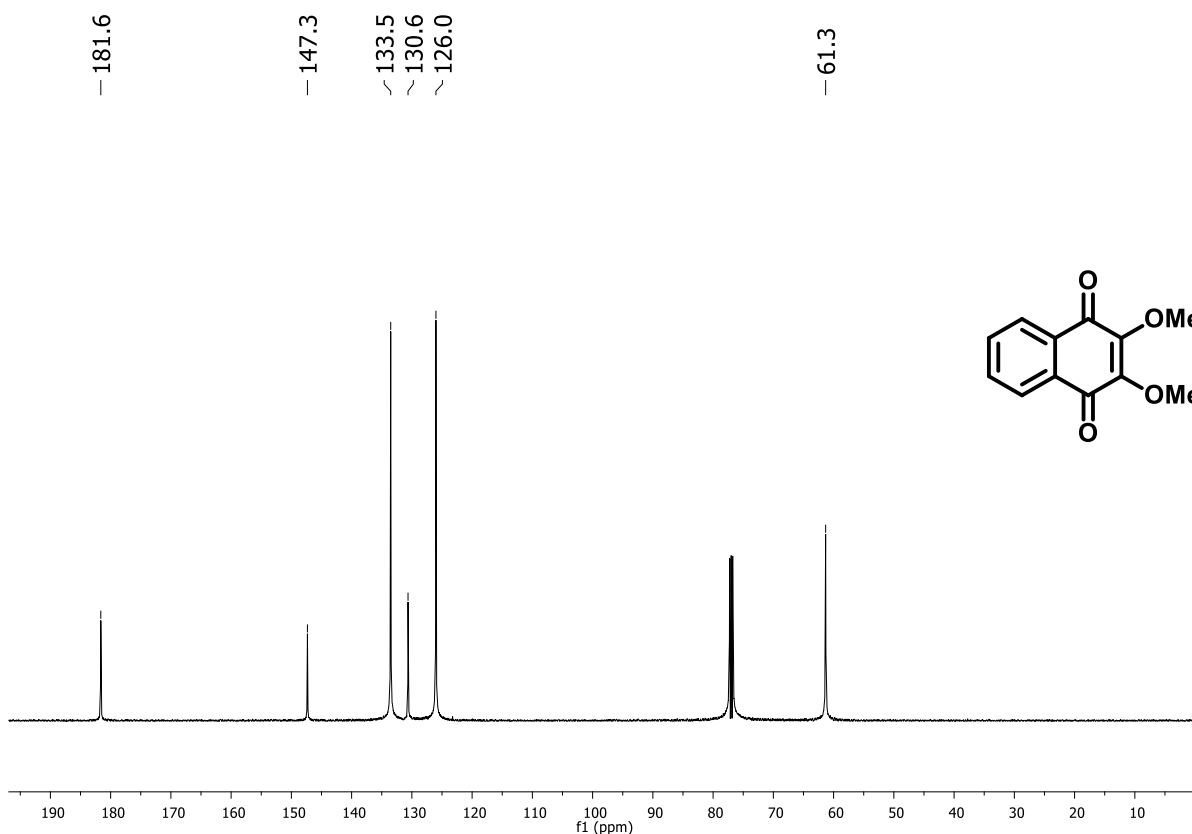


Figure 33. ¹³C NMR spectrum (75 MHz, CDCl₃) of compound 135.

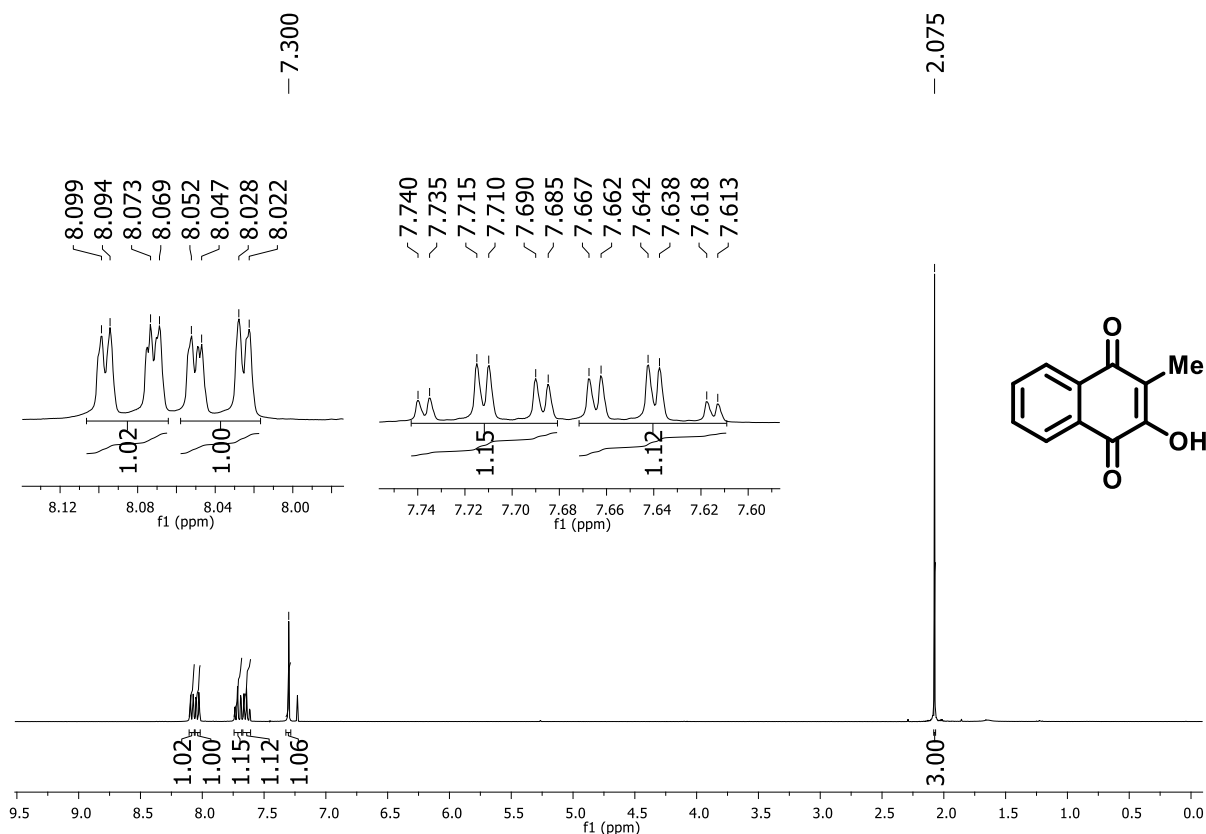


Figure 34. ¹H NMR spectrum (300 MHz, CDCl₃) of compound 137.

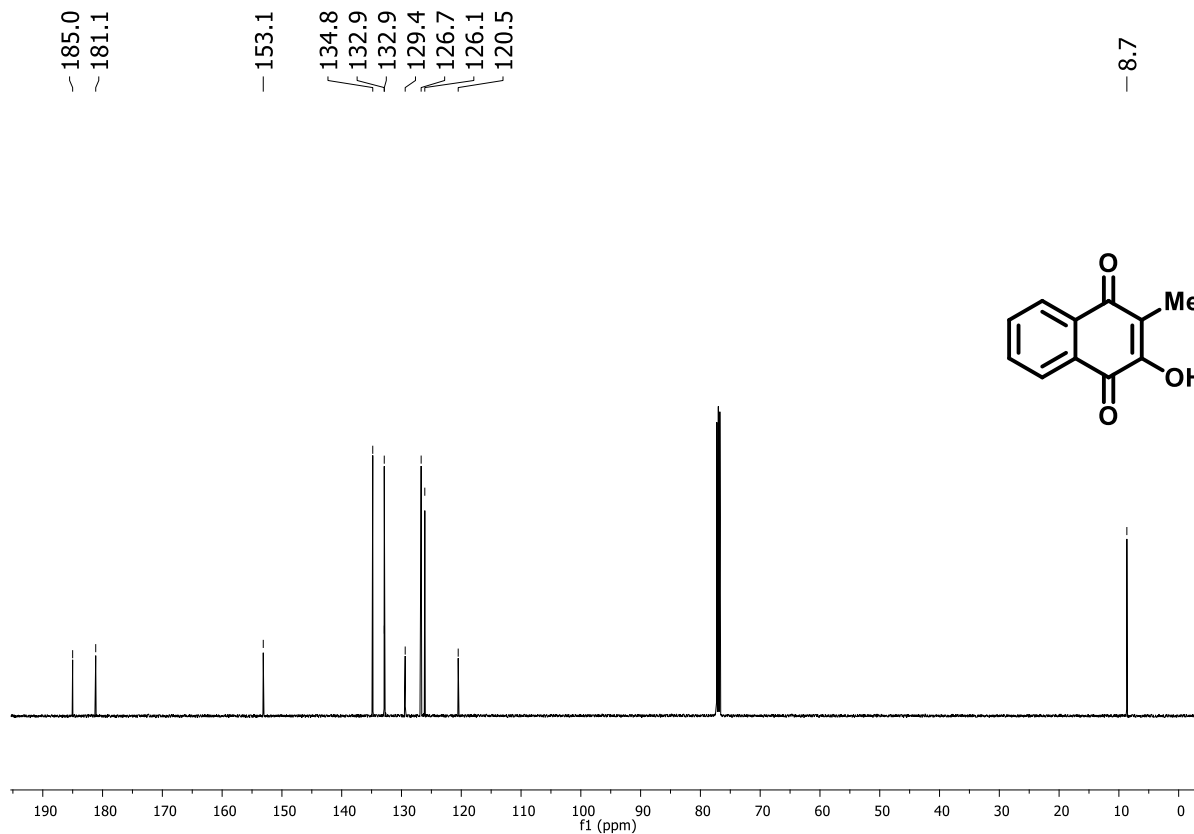


Figure 35. ¹³C NMR spectrum (75 MHz, CDCl₃) of compound 137.

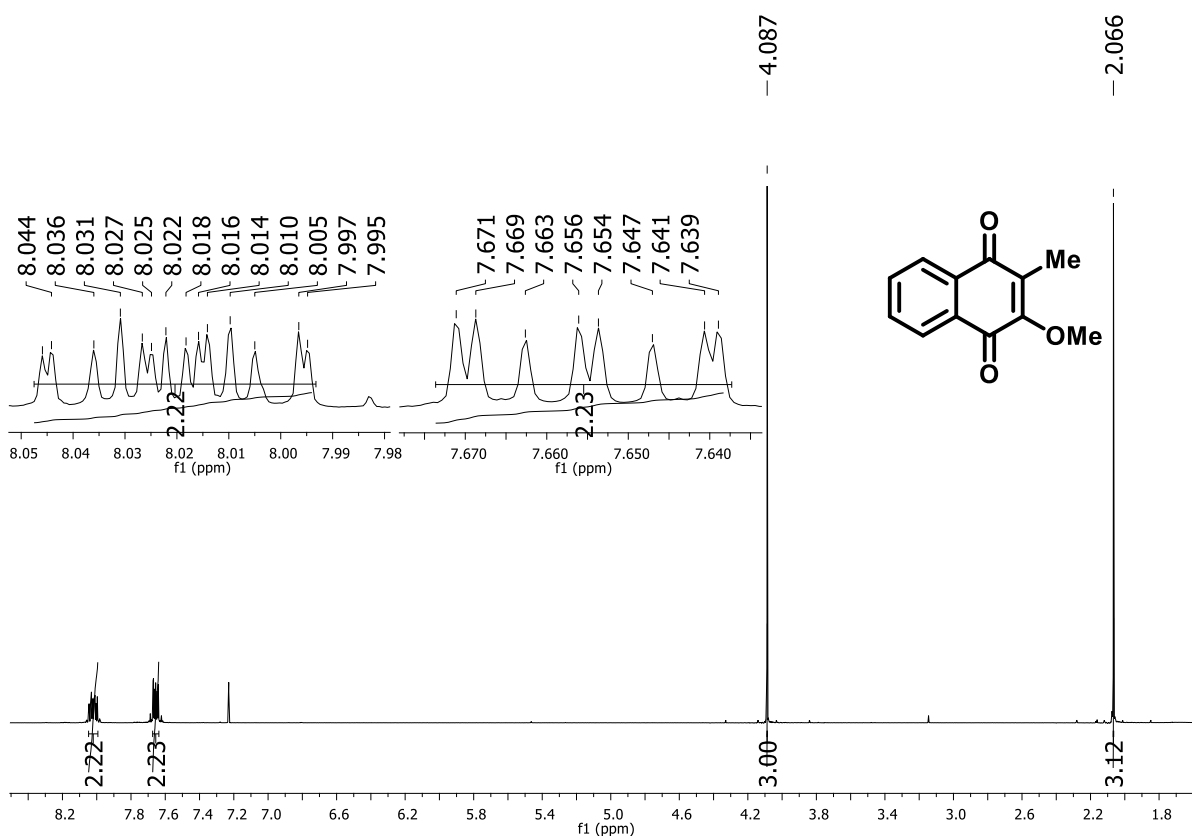


Figure 36. ^1H NMR spectrum (300 MHz, CDCl_3) of compound **138**.

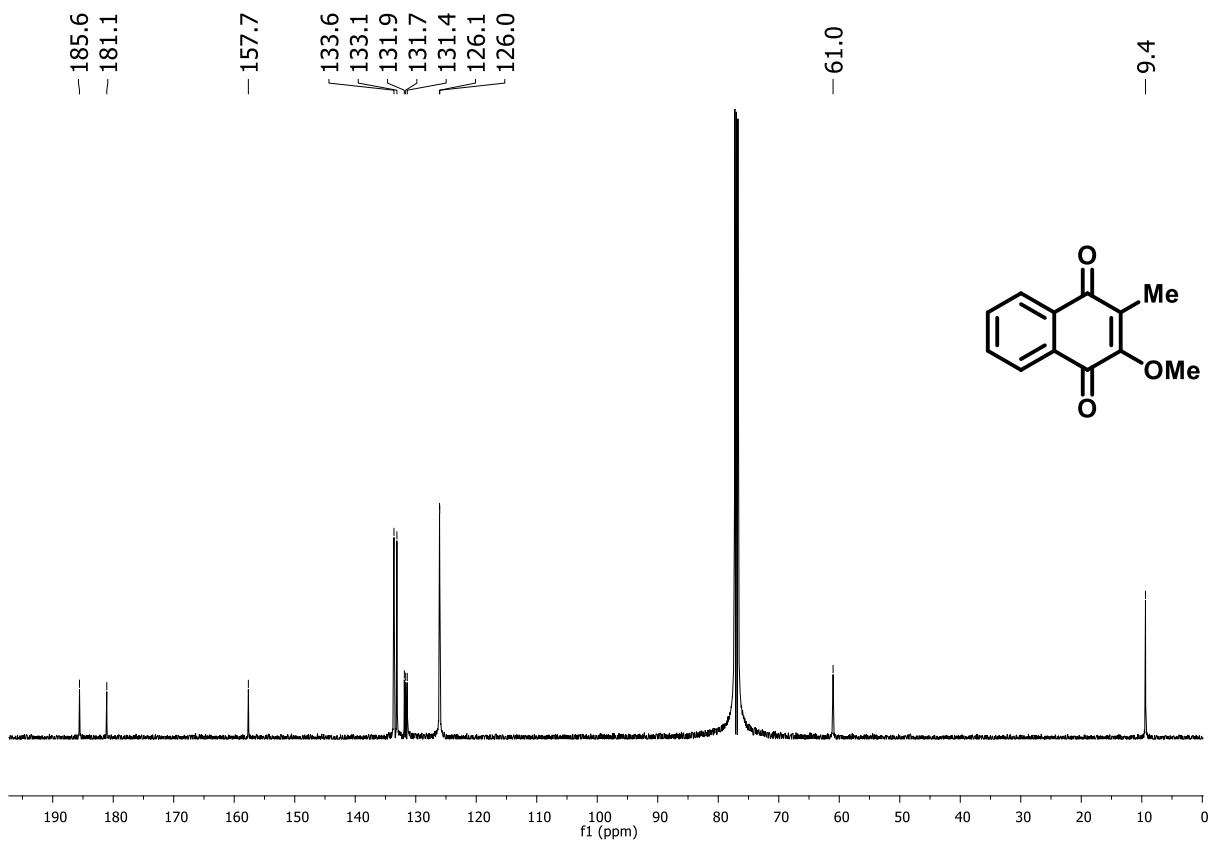


Figure 37. ^{13}C NMR spectrum (75 MHz, CDCl_3) of compound **138**.

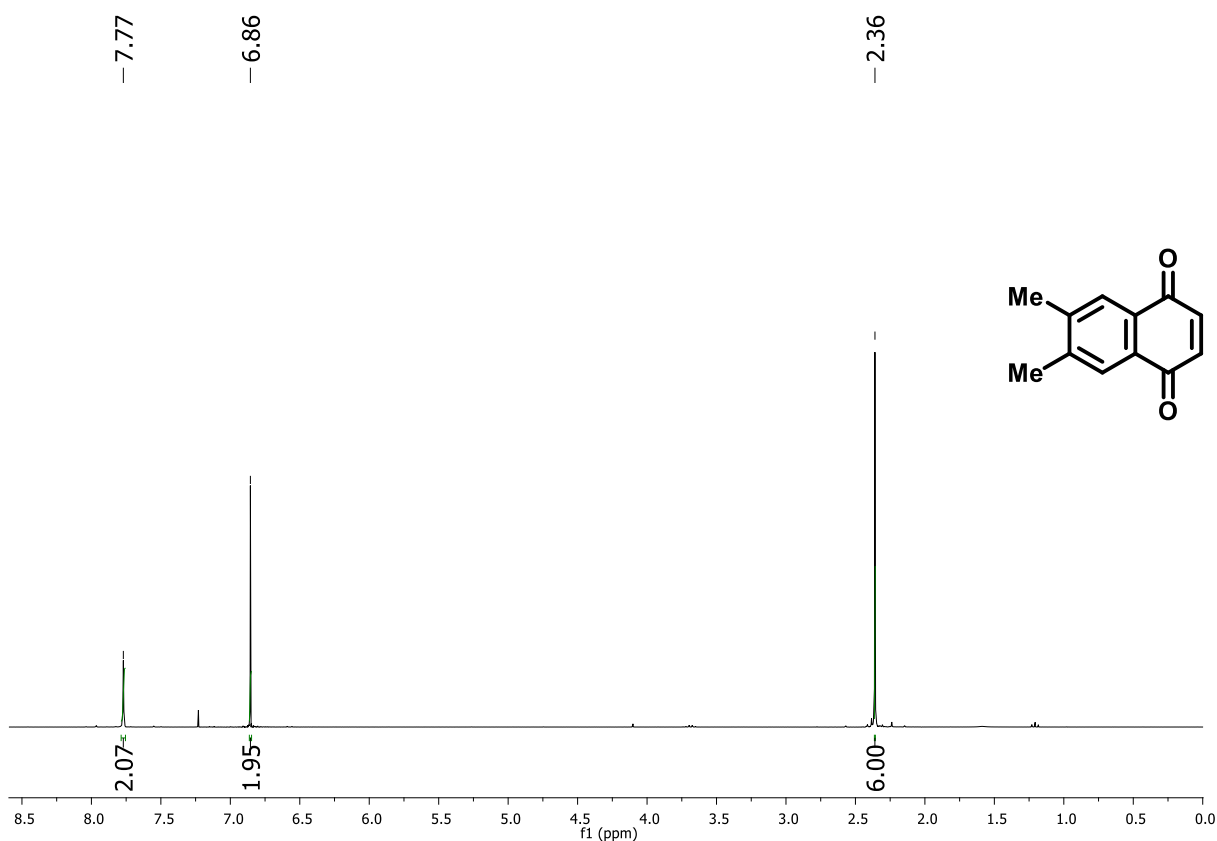


Figure 38. ¹H NMR spectrum (300 MHz, CDCl₃) of compound 141.

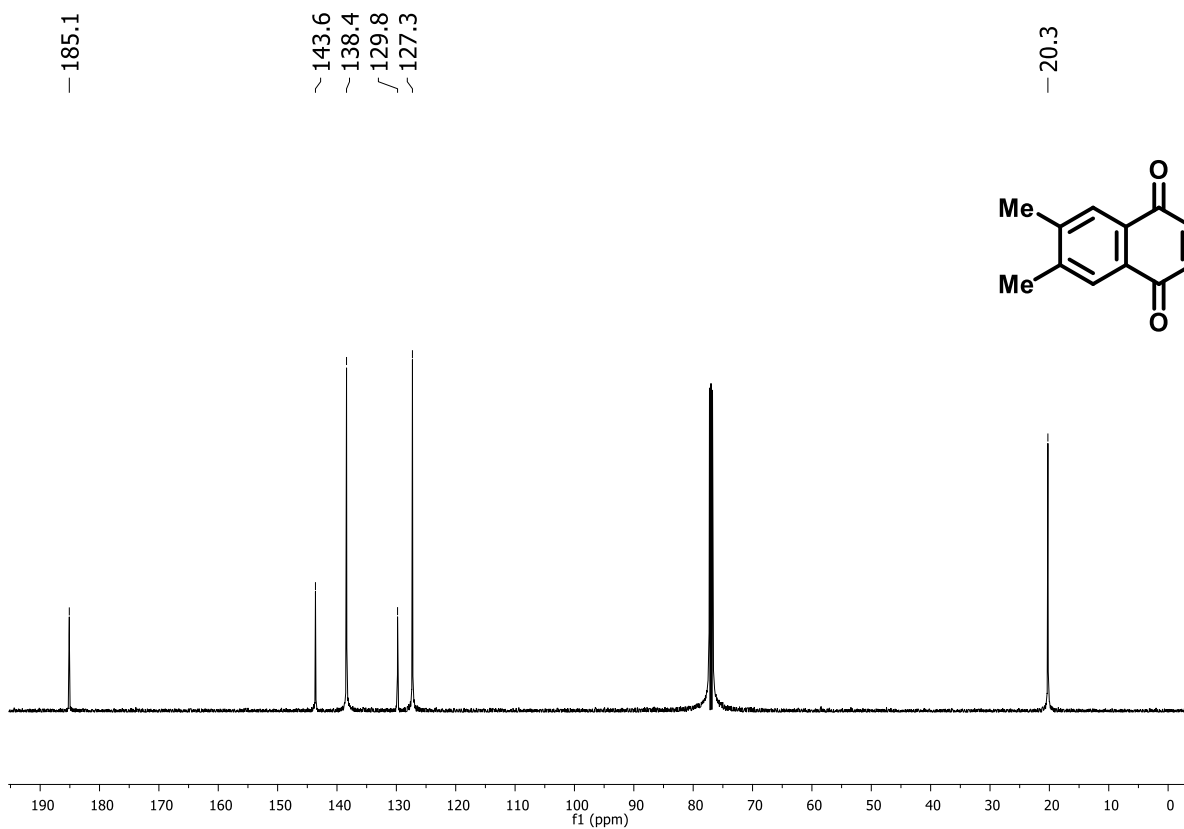


Figure 39. ¹³C NMR spectrum (75 MHz, CDCl₃) of compound 141.

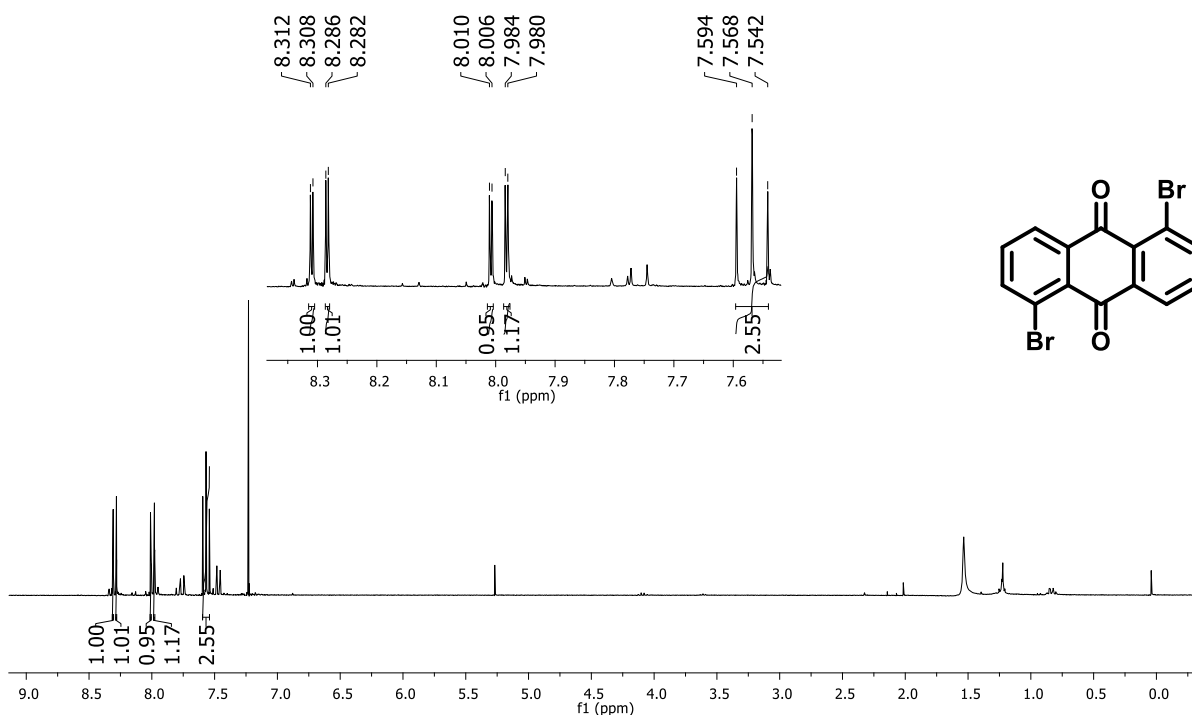


Figure 40. ¹H NMR spectrum (300 MHz, CDCl₃) of compound 144.

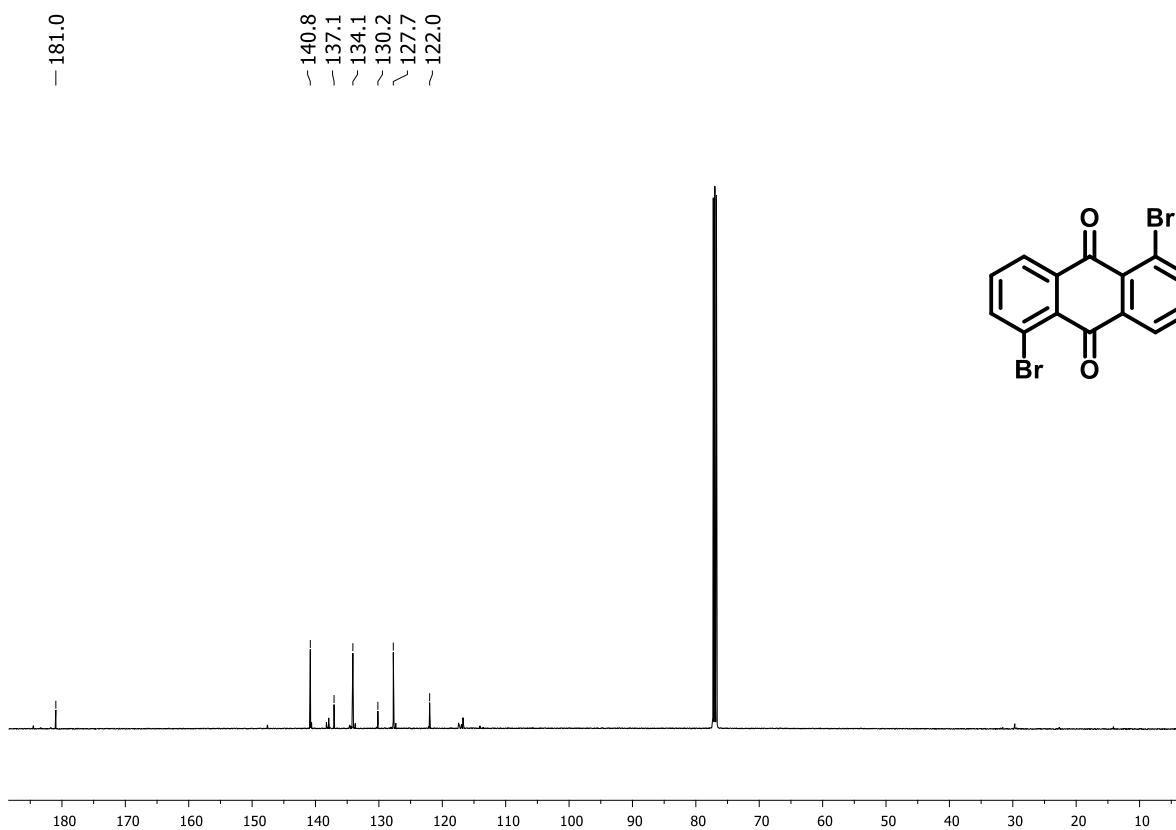


Figure 41. ¹³C NMR spectrum (75 MHz, CDCl₃) of compound 144.

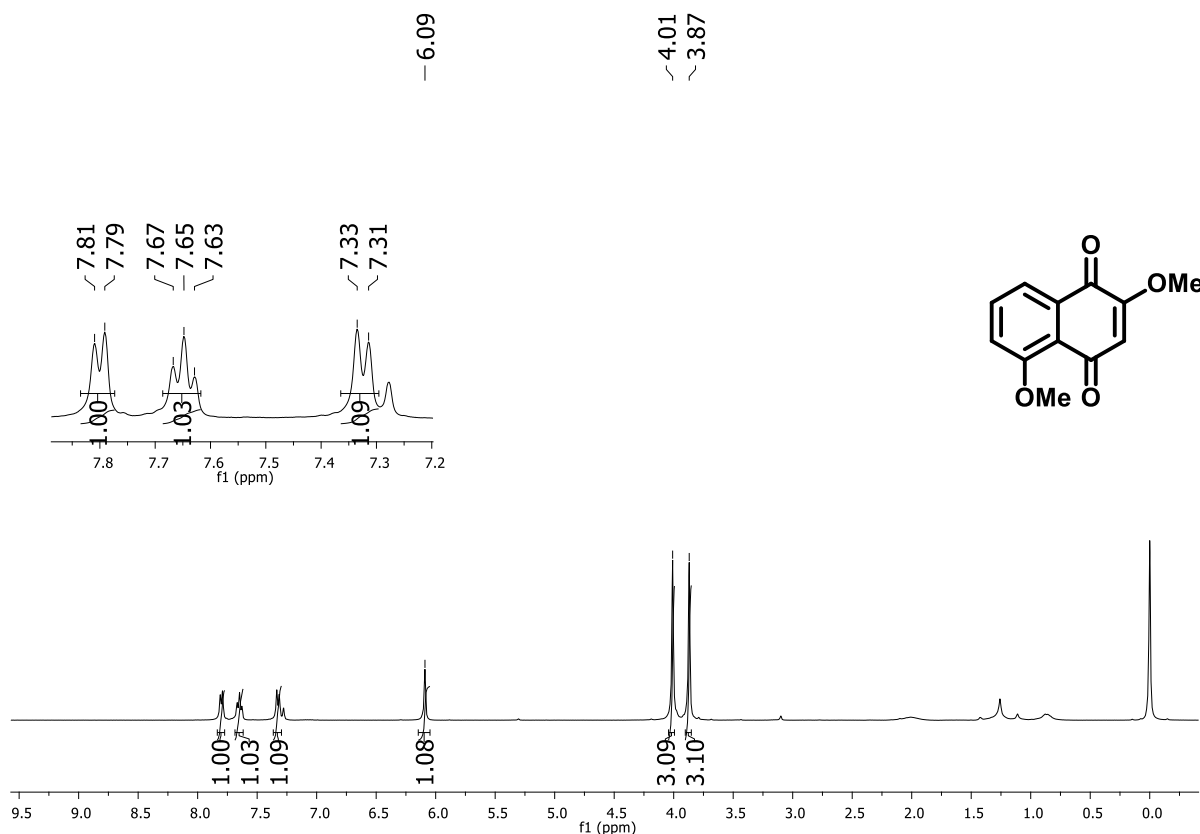


Figure 42. ^1H NMR spectrum (300 MHz, CDCl_3) of compound 156.

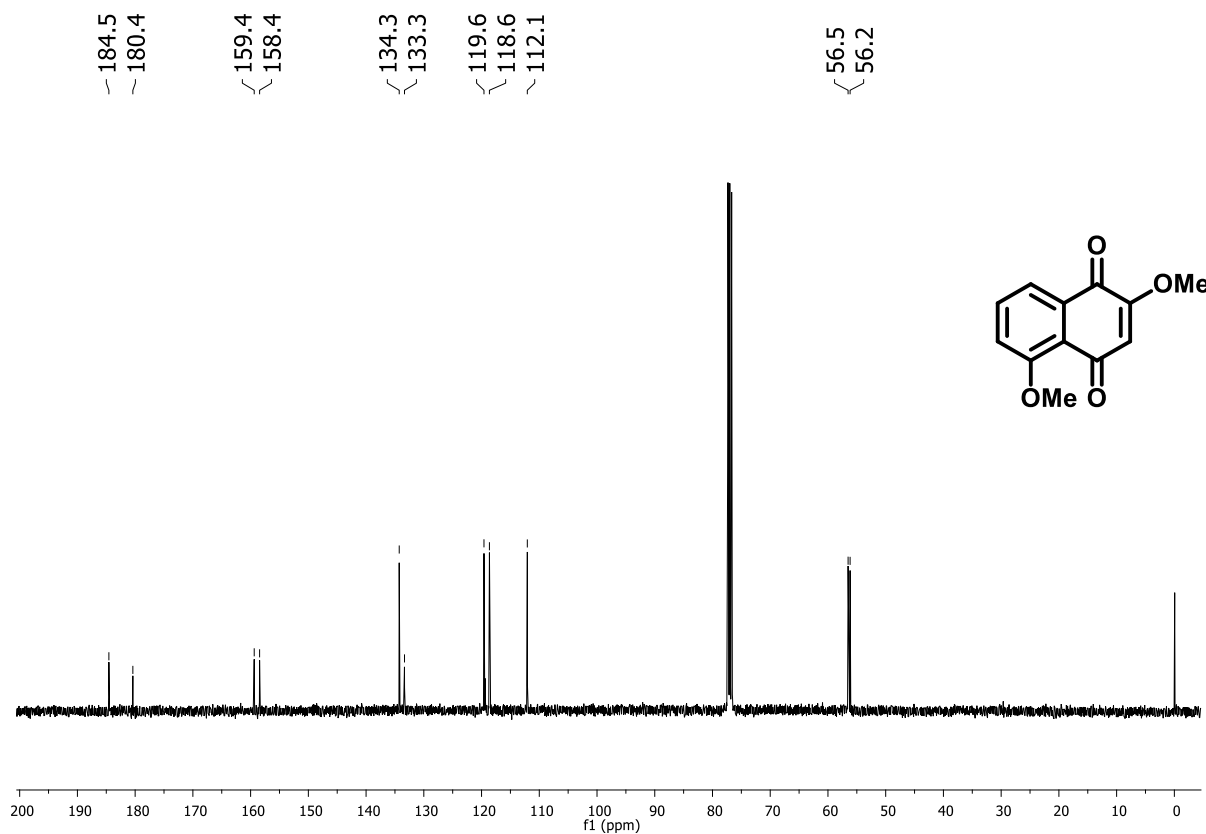


Figure 43. ^{13}C NMR spectrum (75 MHz, CDCl_3) of compound 156.

Spectra of alkenylated product

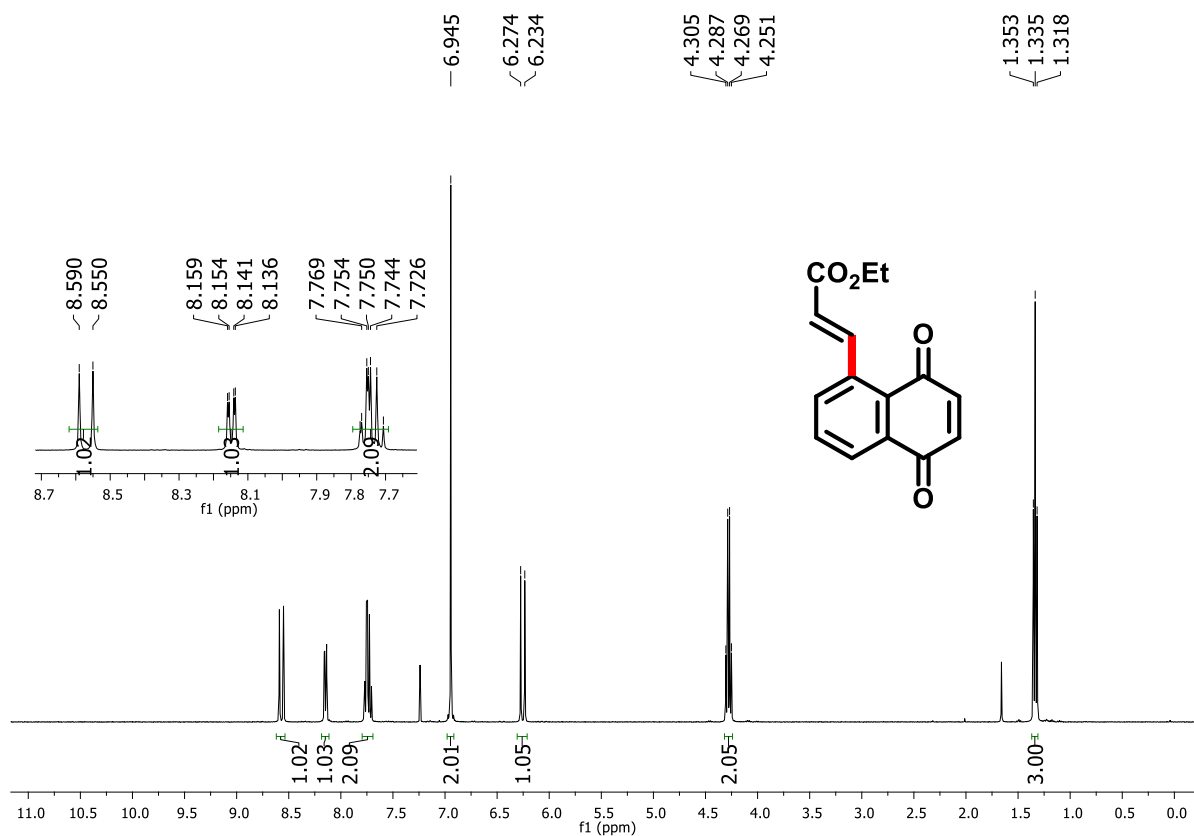


Figure 44. ^1H NMR spectrum (400 MHz, CDCl_3) of compound 120.

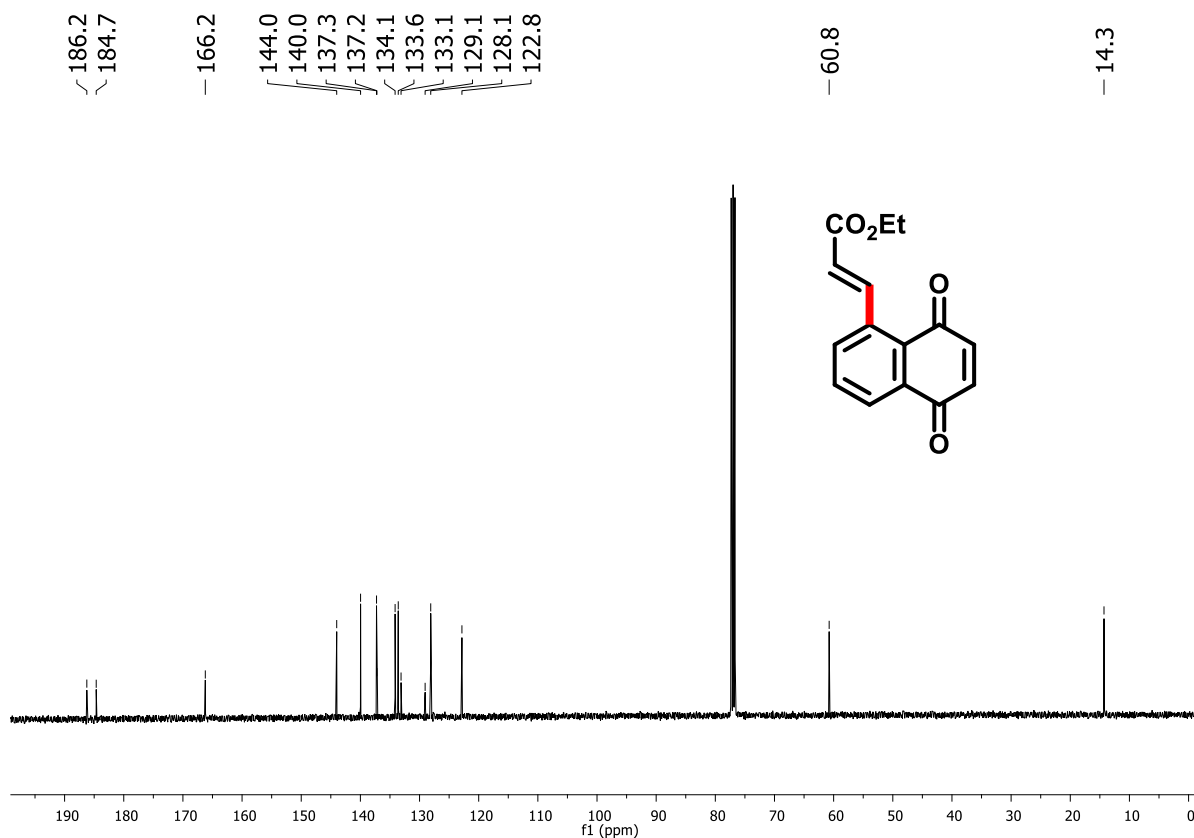


Figure 45. ^{13}C NMR spectrum (100 MHz, CDCl_3) of compound 120.

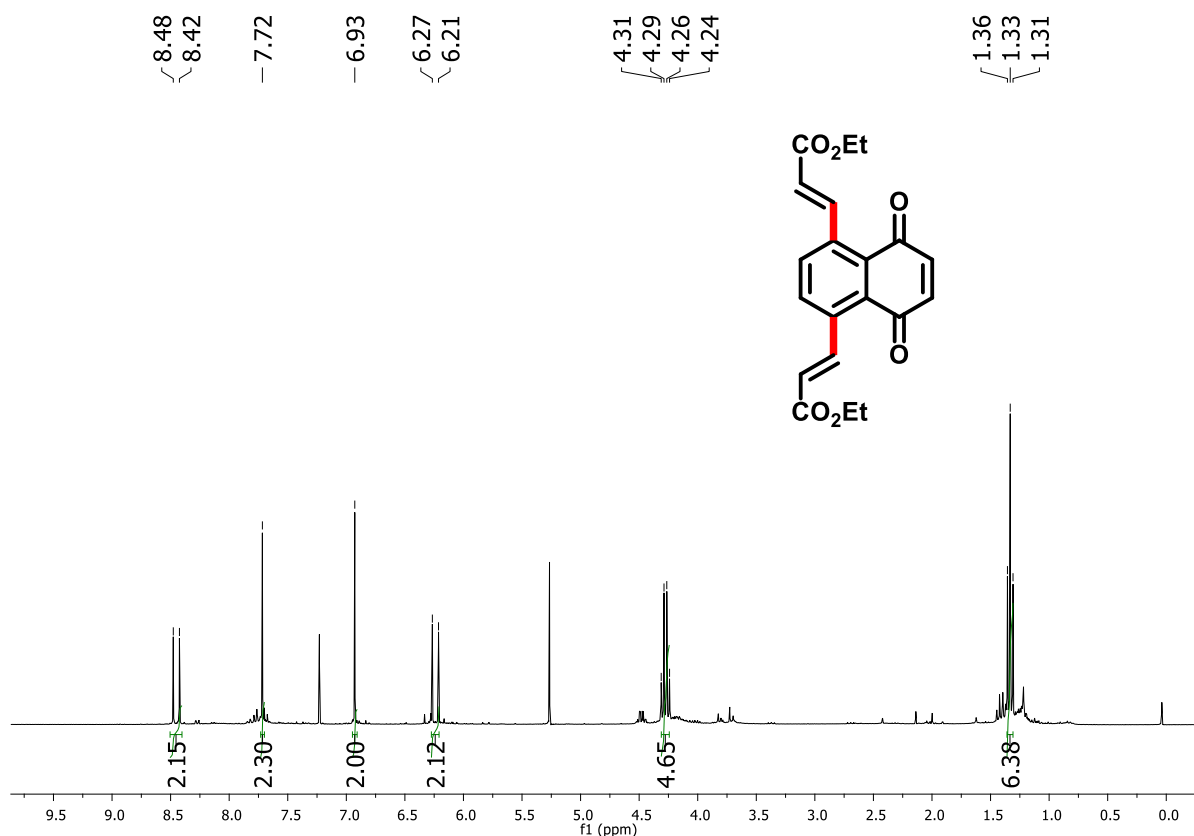


Figure 46. ^1H NMR spectrum (300 MHz, CDCl_3) of compound 121.

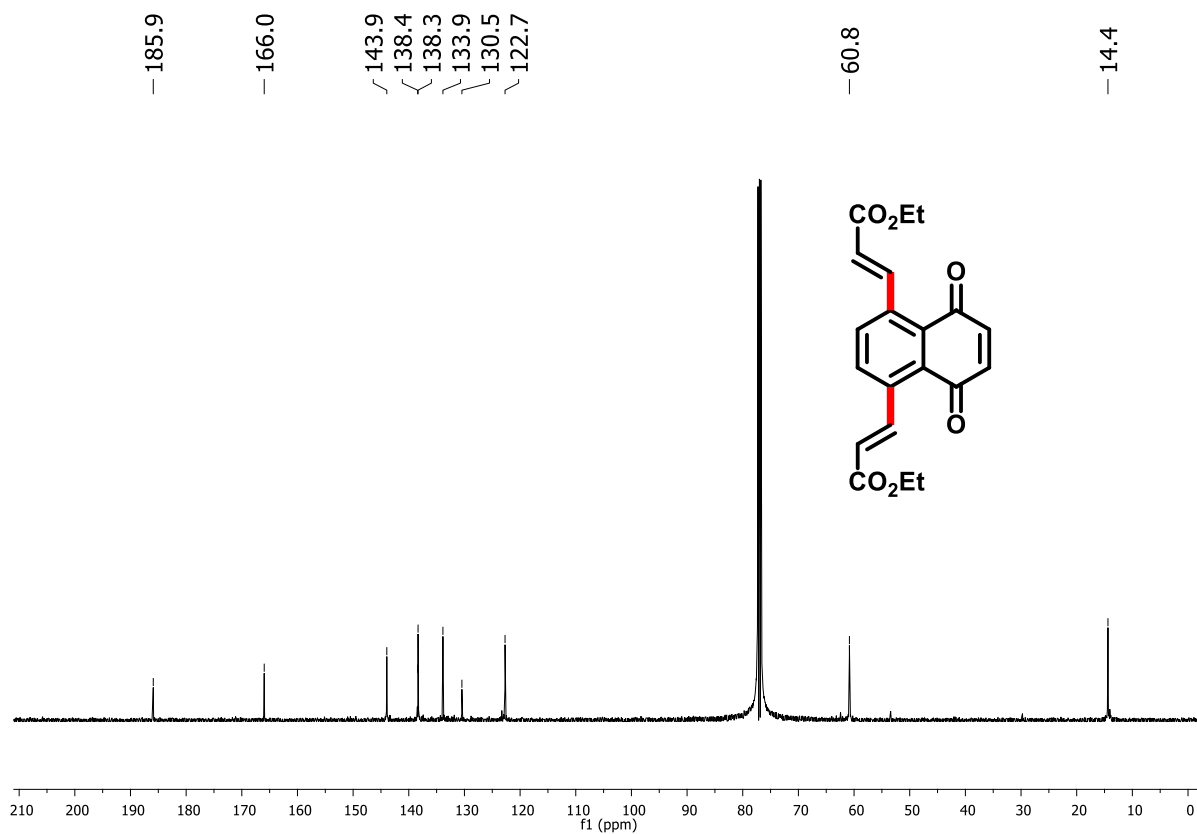


Figure 47. ^{13}C NMR spectrum (75 MHz, CDCl_3) of compound 121.

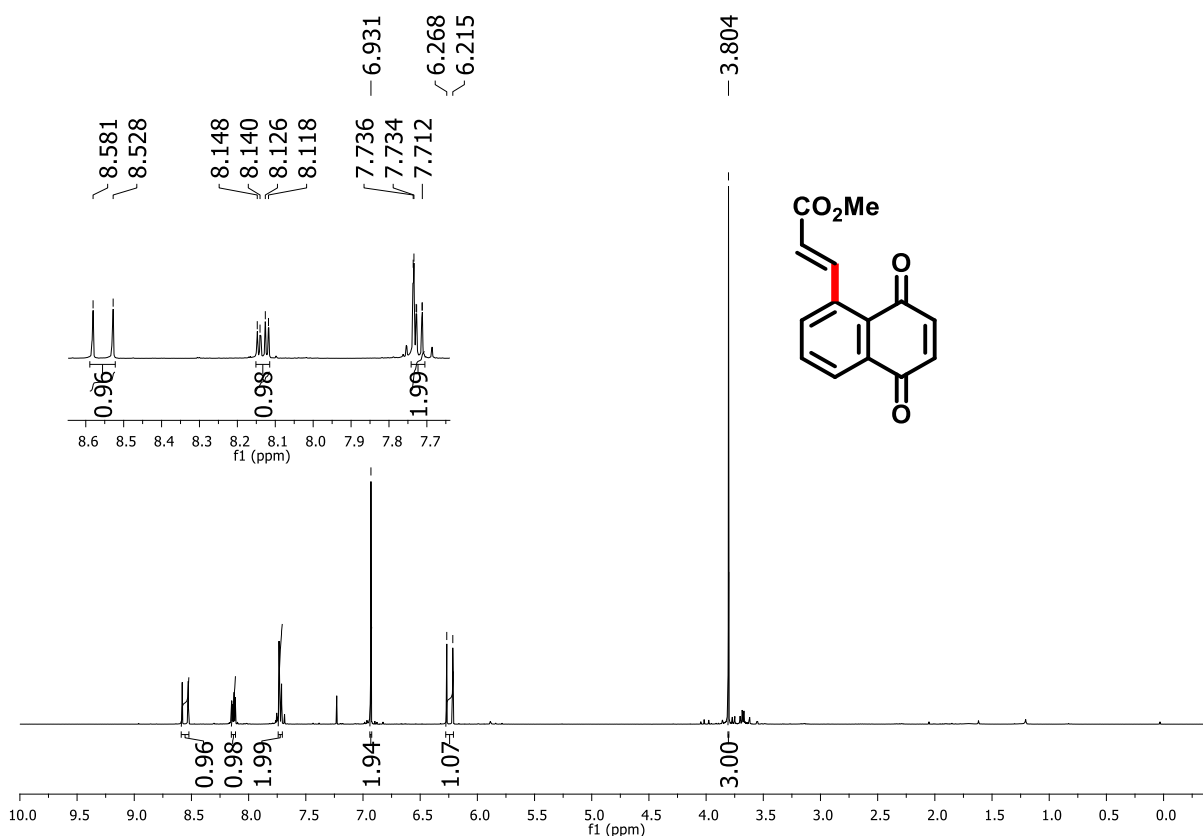


Figure 48. ^1H NMR spectrum (300 MHz, CDCl_3) of compound 146.

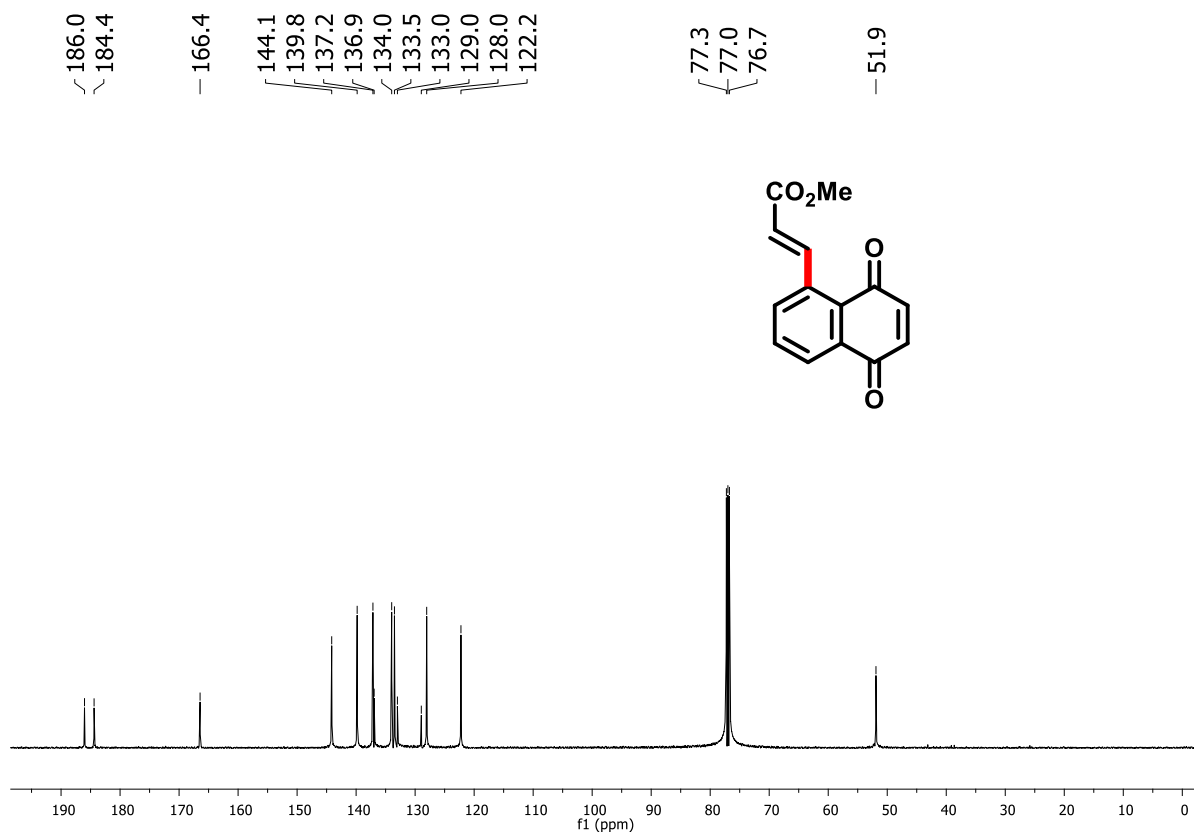


Figure 49. ^{13}C NMR spectrum (75 MHz, CDCl_3) of compound 146.

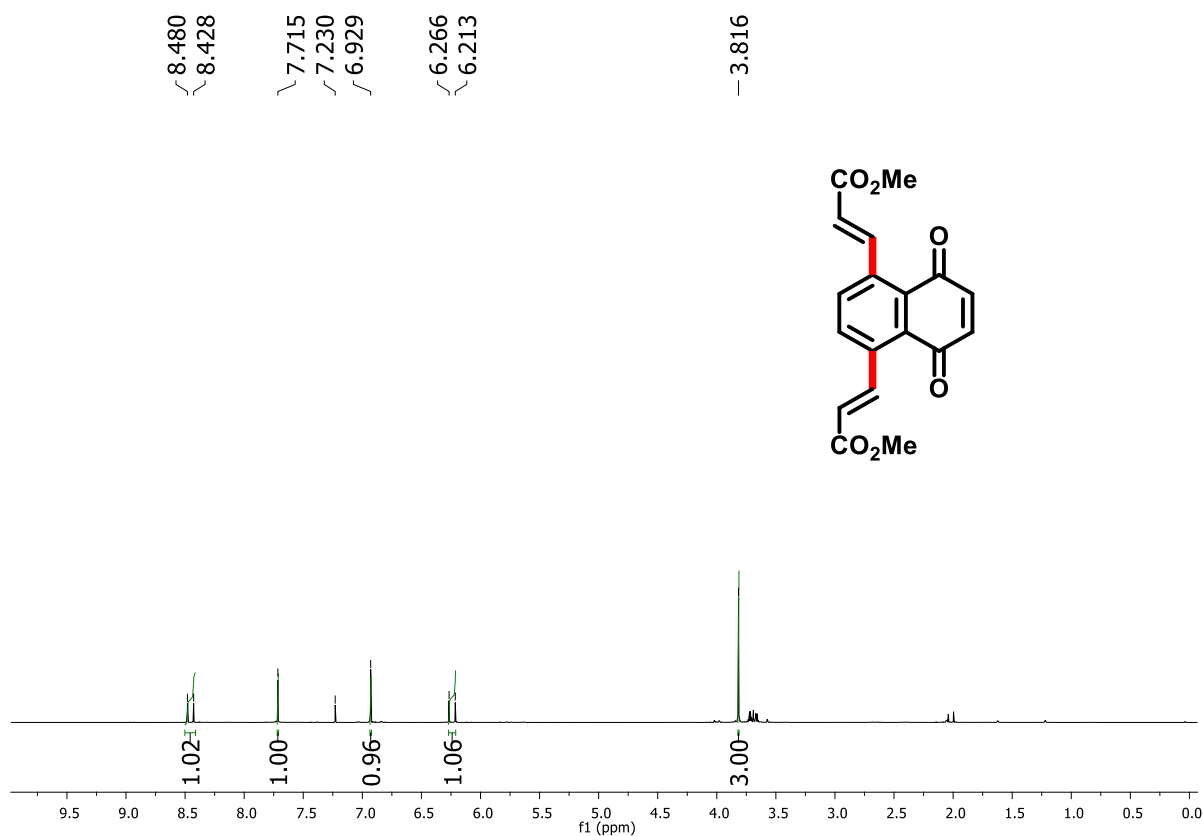


Figure 50. ¹H NMR spectrum (300 MHz, CDCl₃) of compound 147.

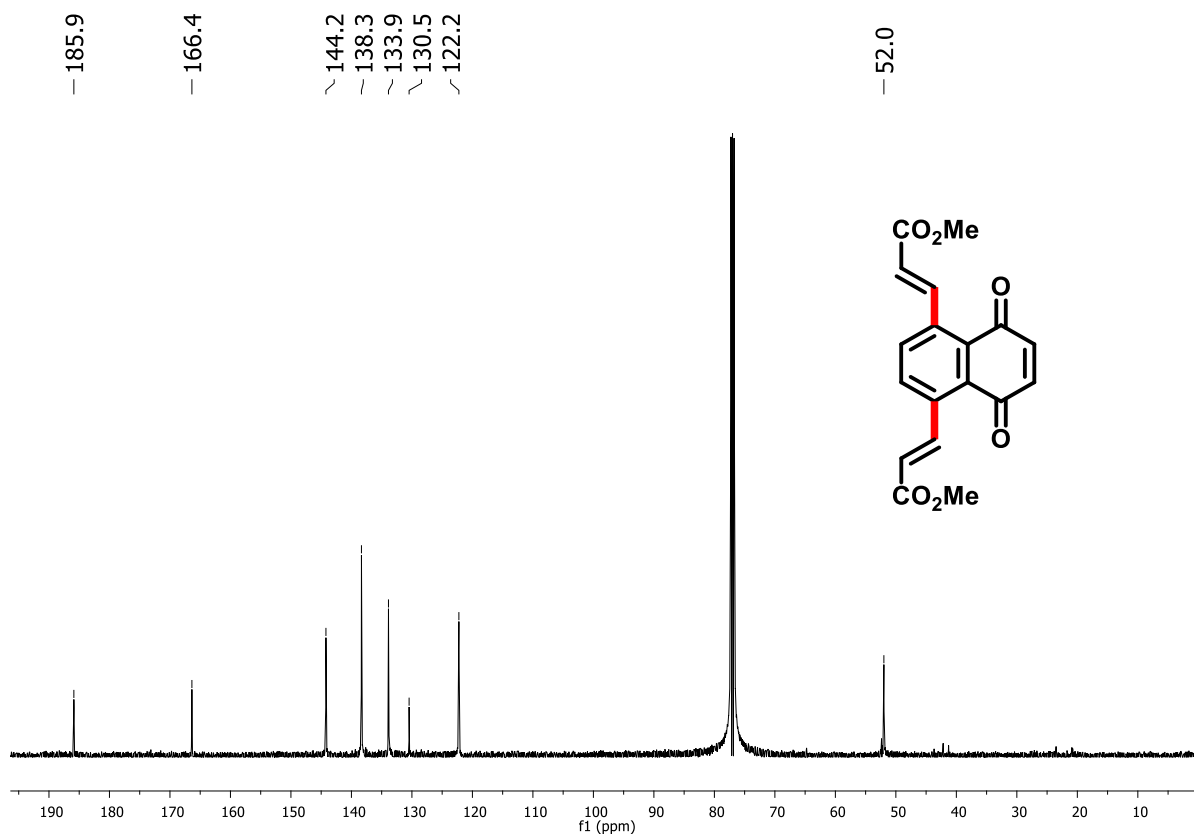


Figure 51. ¹³C NMR spectrum (75 MHz, CDCl₃) of compound 147.

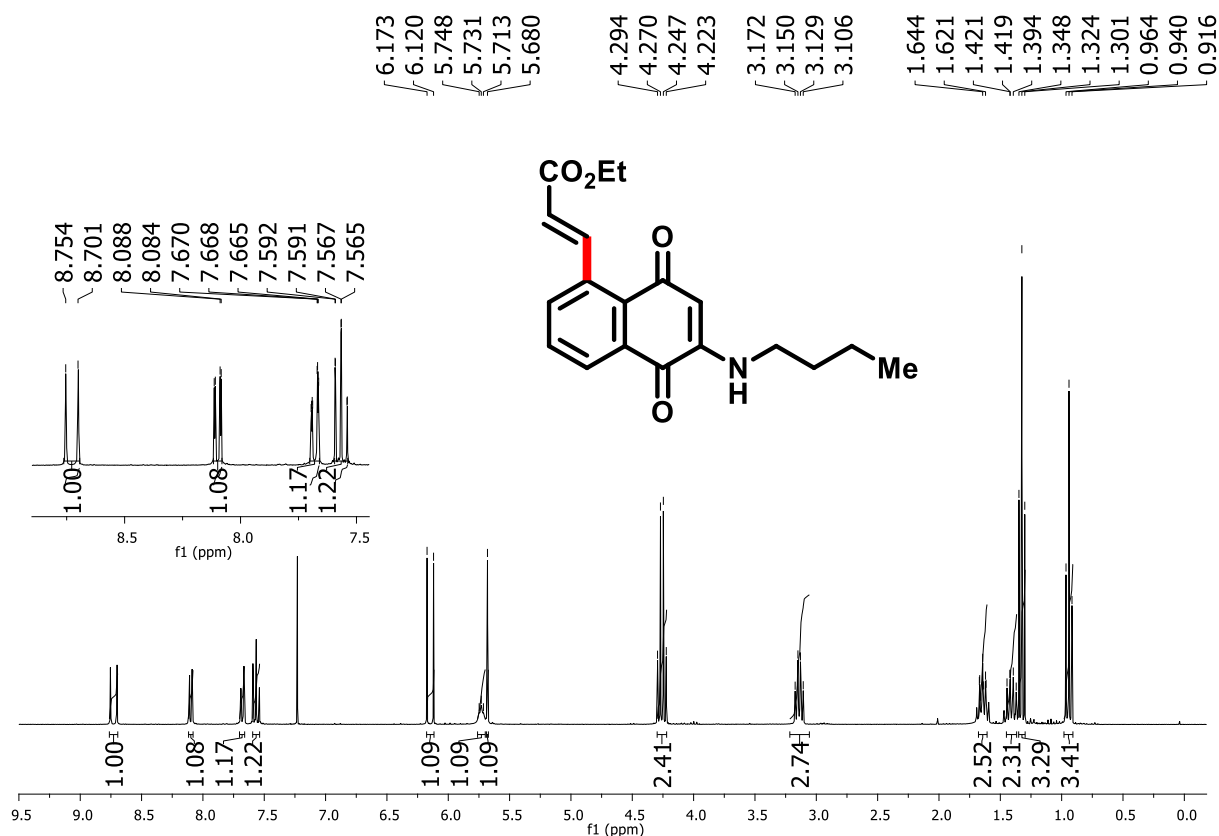


Figure 52. ¹H NMR spectrum (300 MHz, CDCl₃) of compound 149.

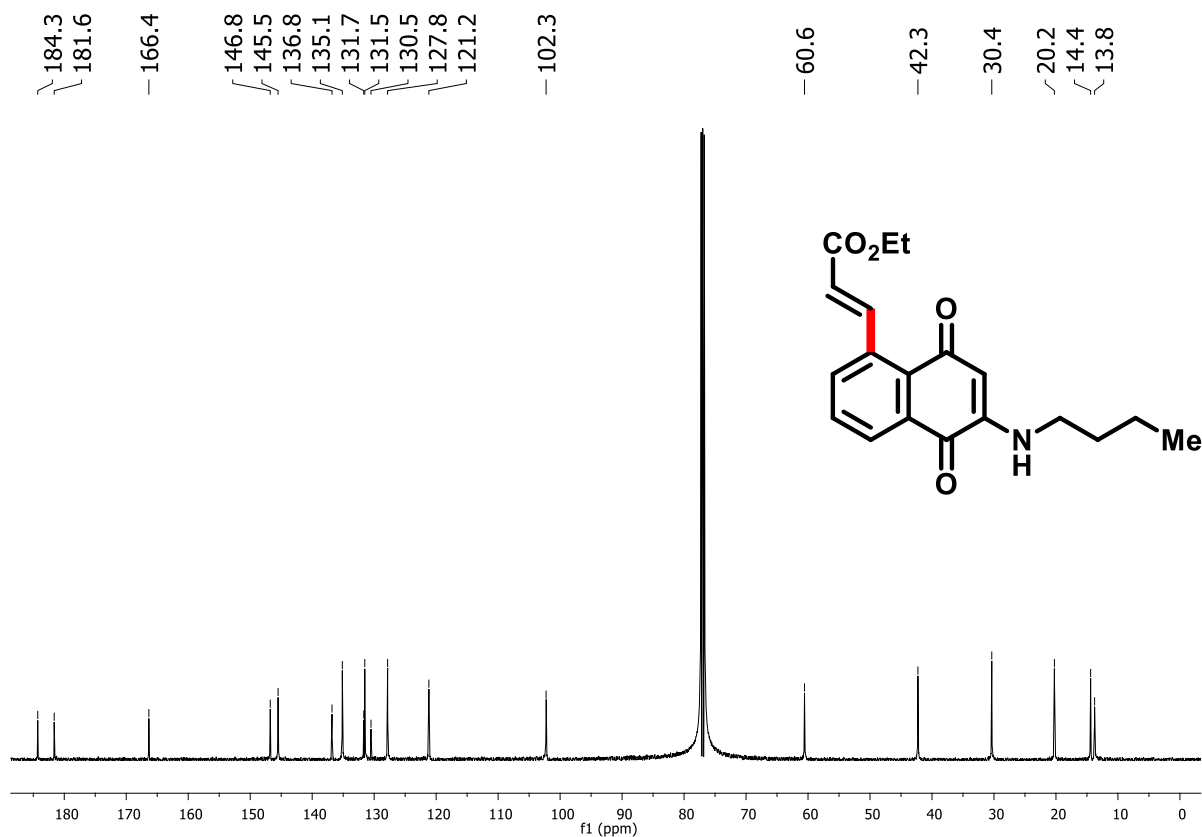


Figure 53. ¹³C NMR spectrum (75 MHz, CDCl₃) of compound 149.

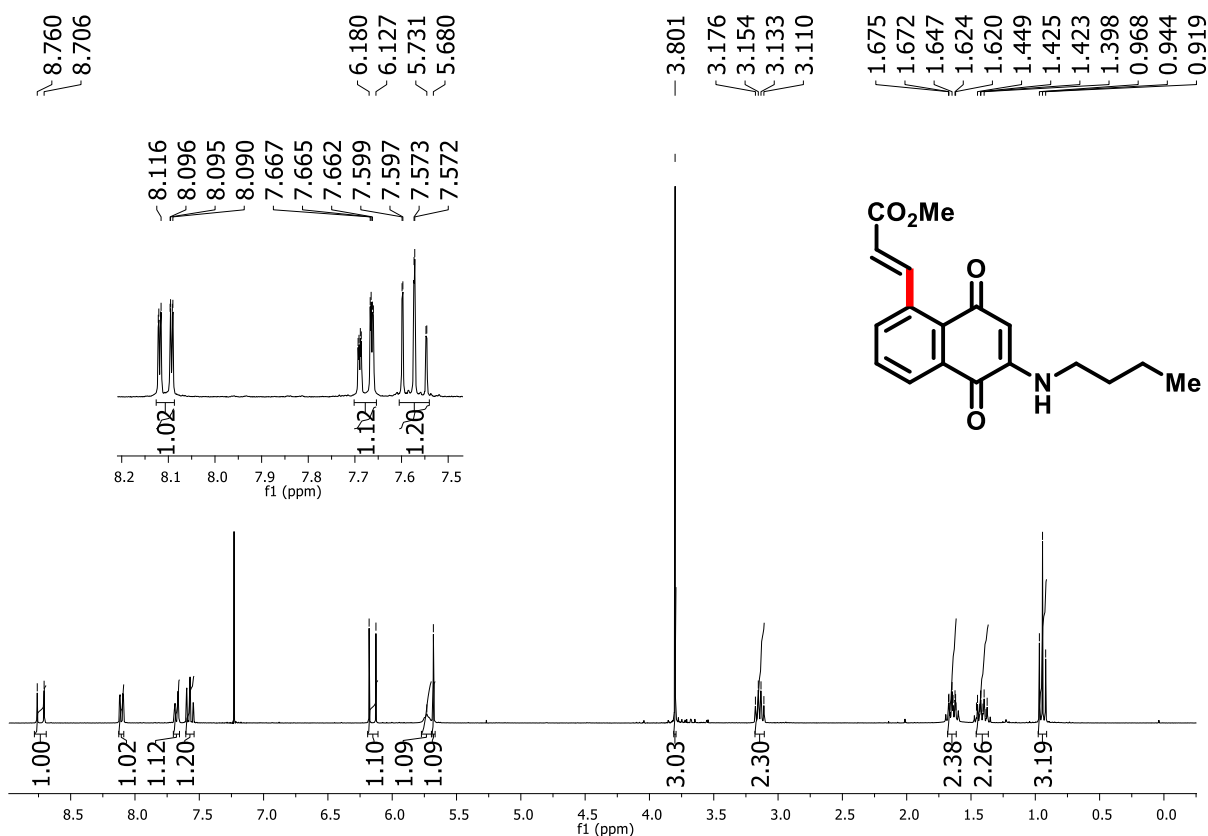


Figure 54. ¹H NMR spectrum (300 MHz, CDCl₃) of compound 150.

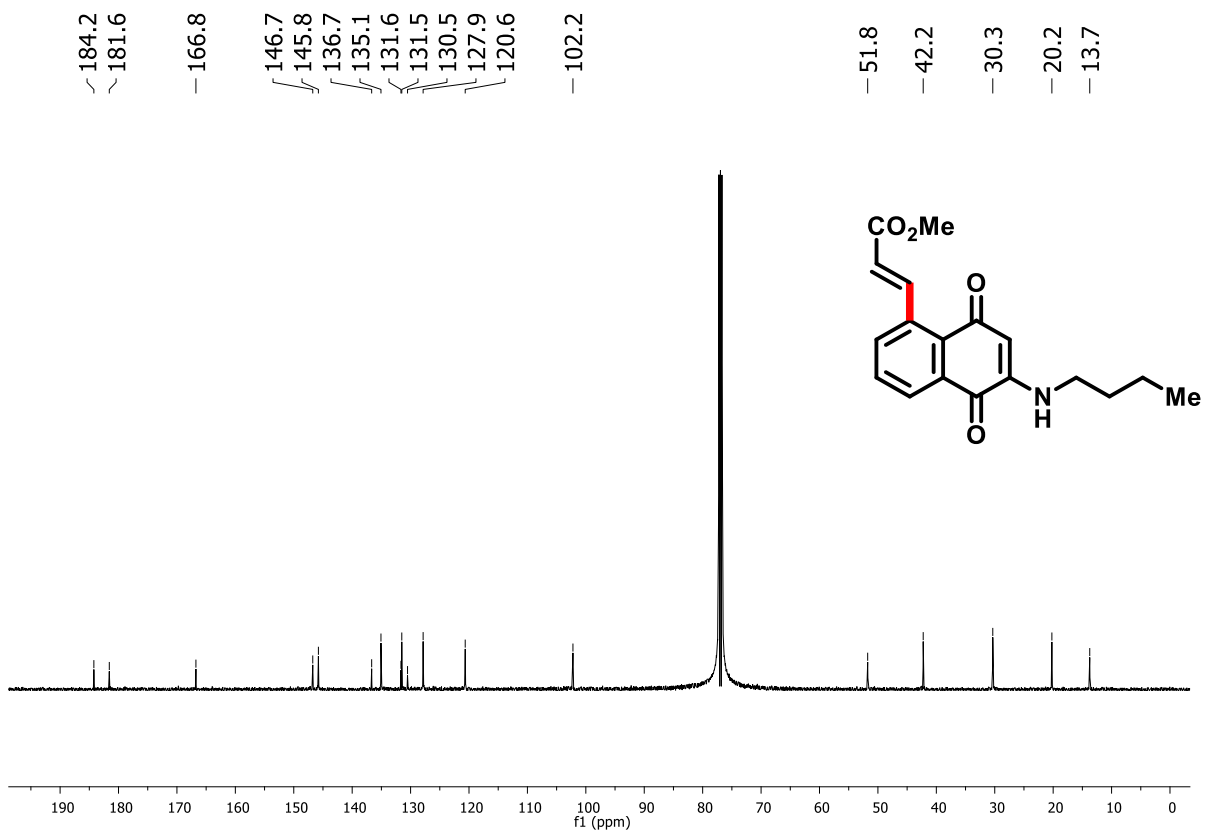


Figure 55. ¹³C NMR spectrum (75 MHz, CDCl₃) of compound 150.

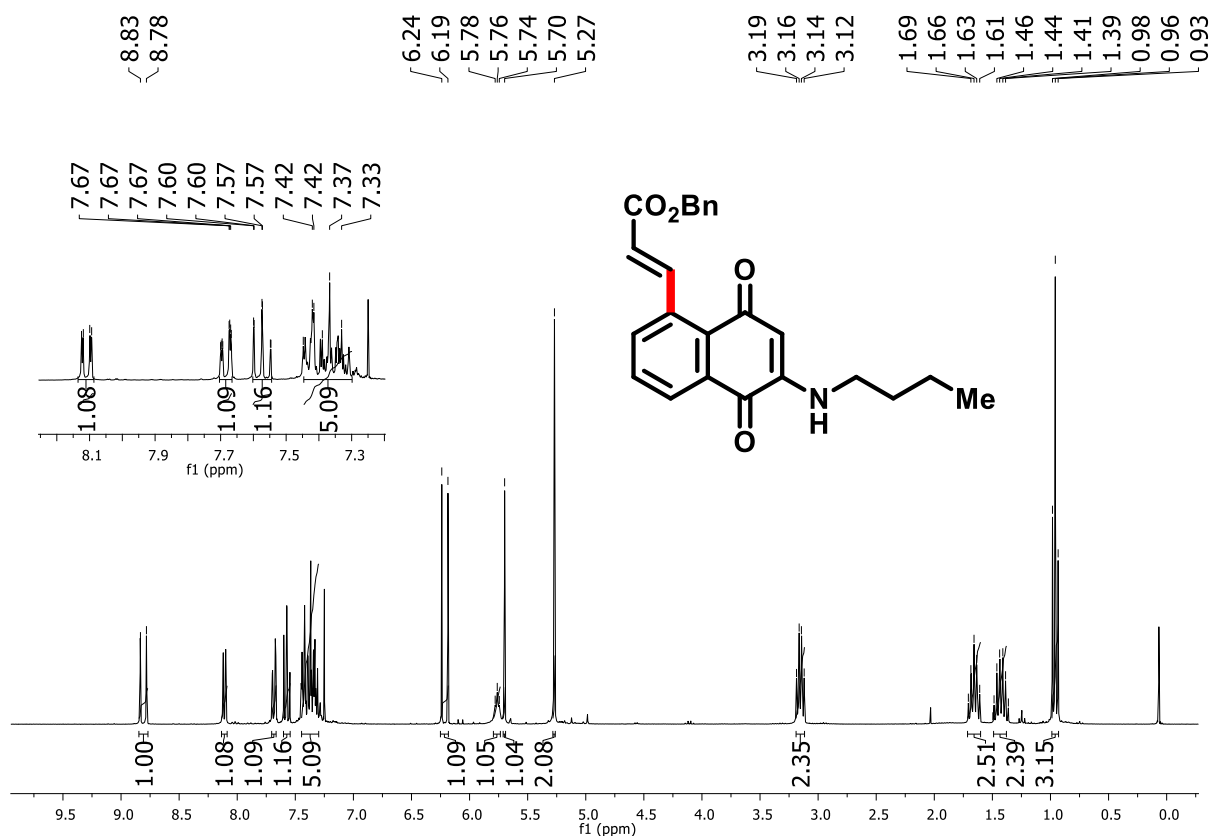


Figure 56. ¹H NMR spectrum (300 MHz, CDCl₃) of compound 151.

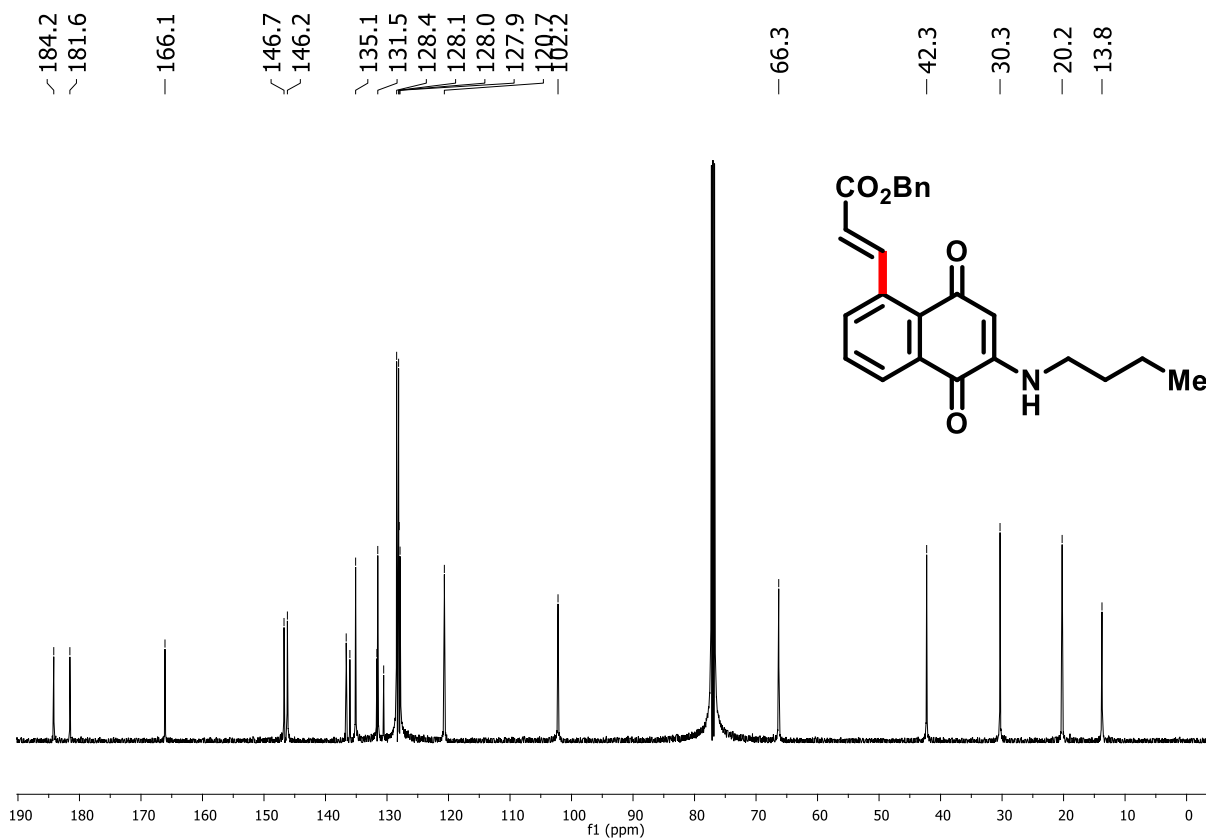


Figure 57. ¹³C NMR spectrum (75 MHz, CDCl₃) of compound 151.

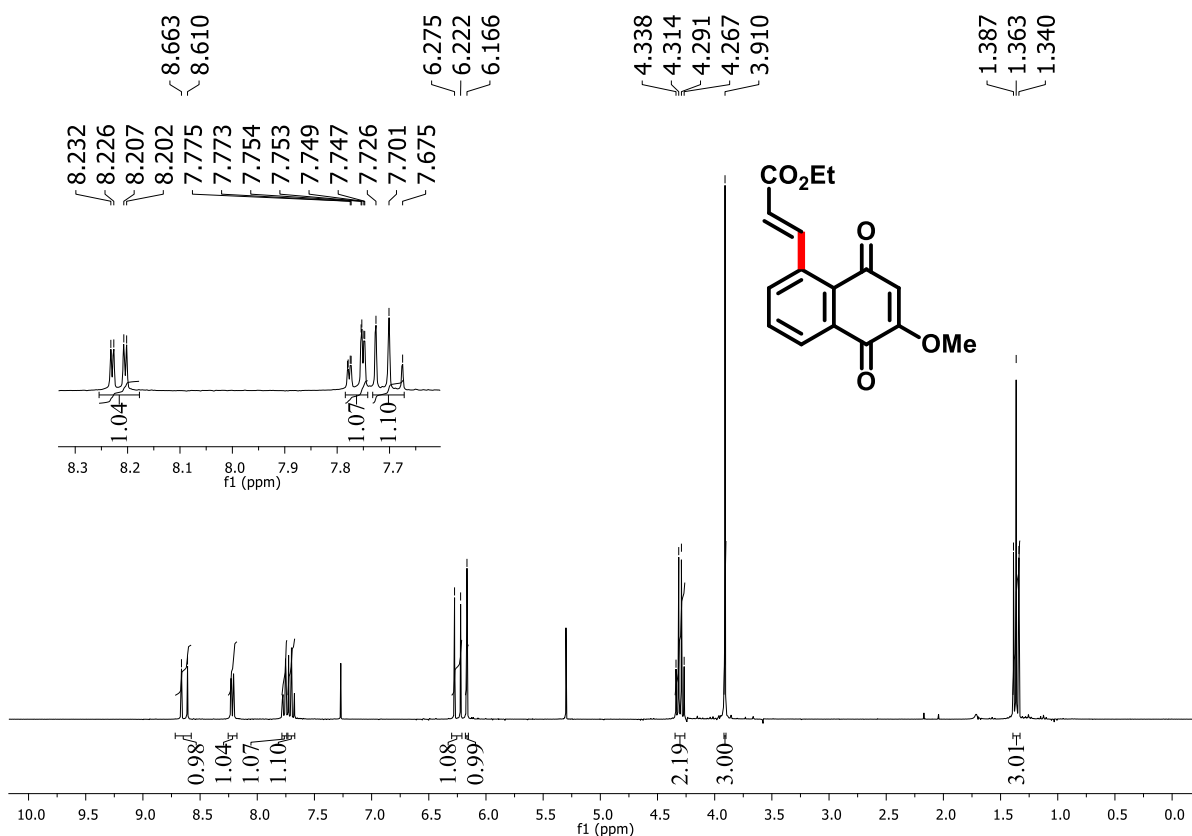


Figure 58. ¹H NMR spectrum (300 MHz, CDCl₃) of compound 153.

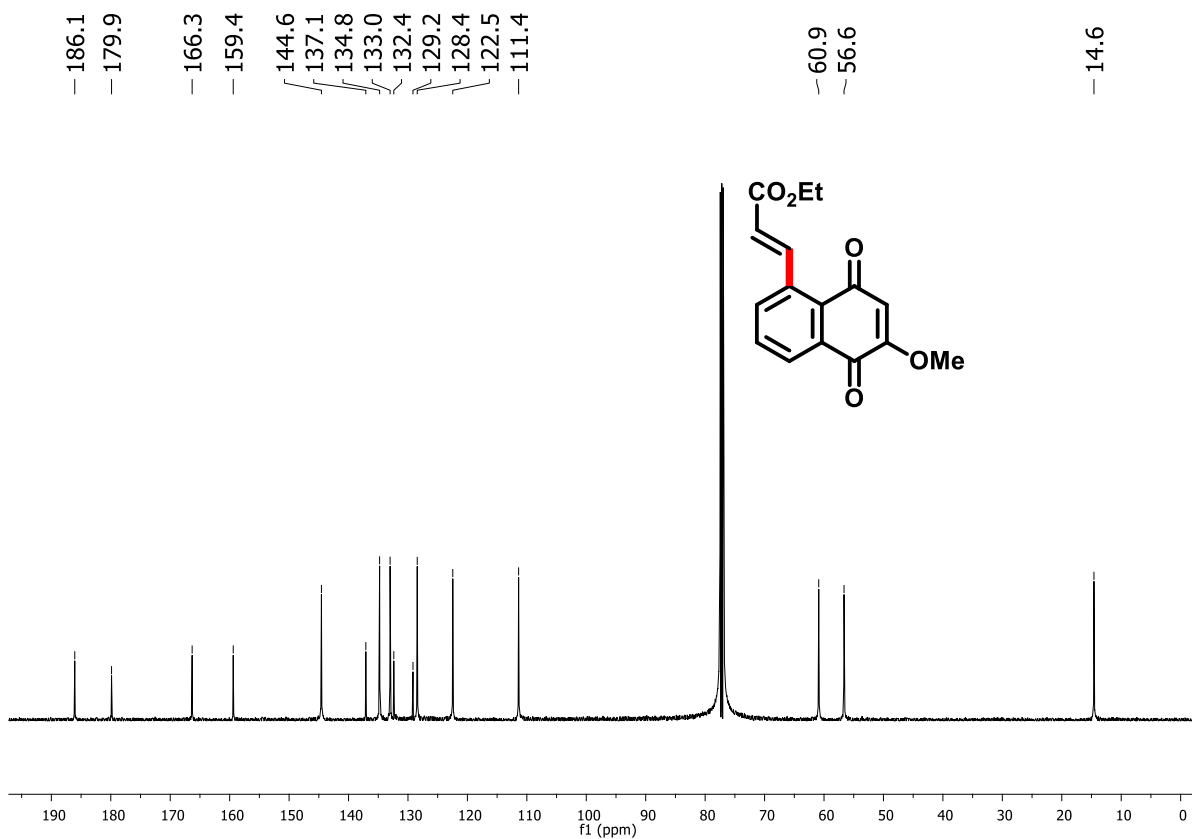


Figure 59. ¹³C NMR spectrum (75 MHz, CDCl₃) of compound 153.

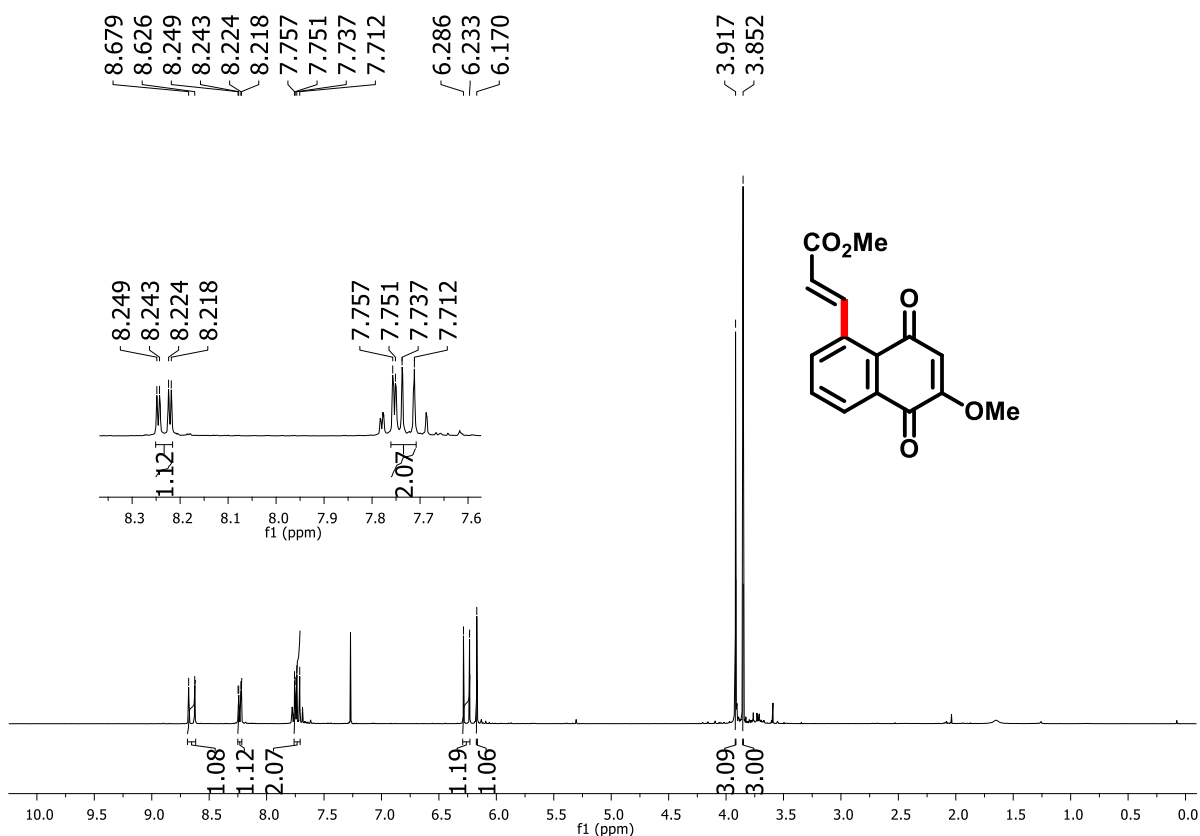


Figure 60. ^1H NMR spectrum (300 MHz, CDCl_3) of compound 154.

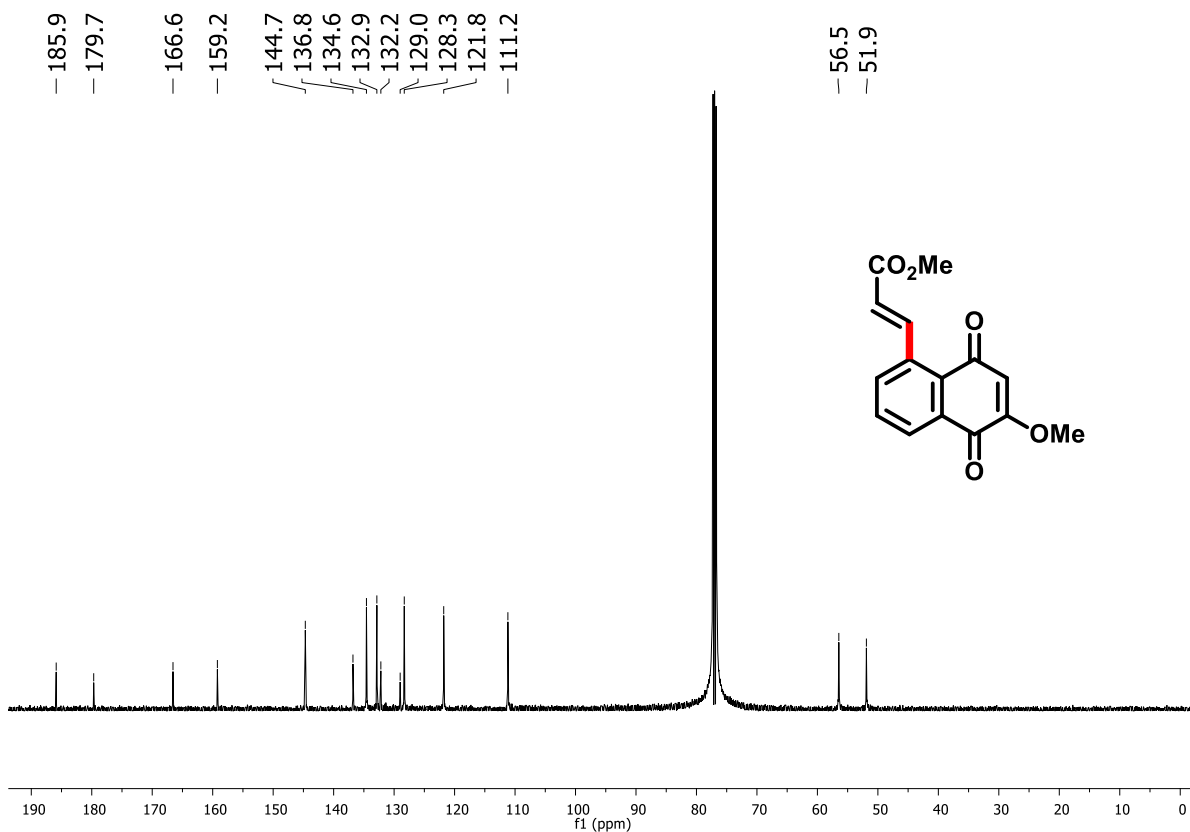


Figure 61. ^{13}C NMR spectrum (75 MHz, CDCl_3) of compound 154.

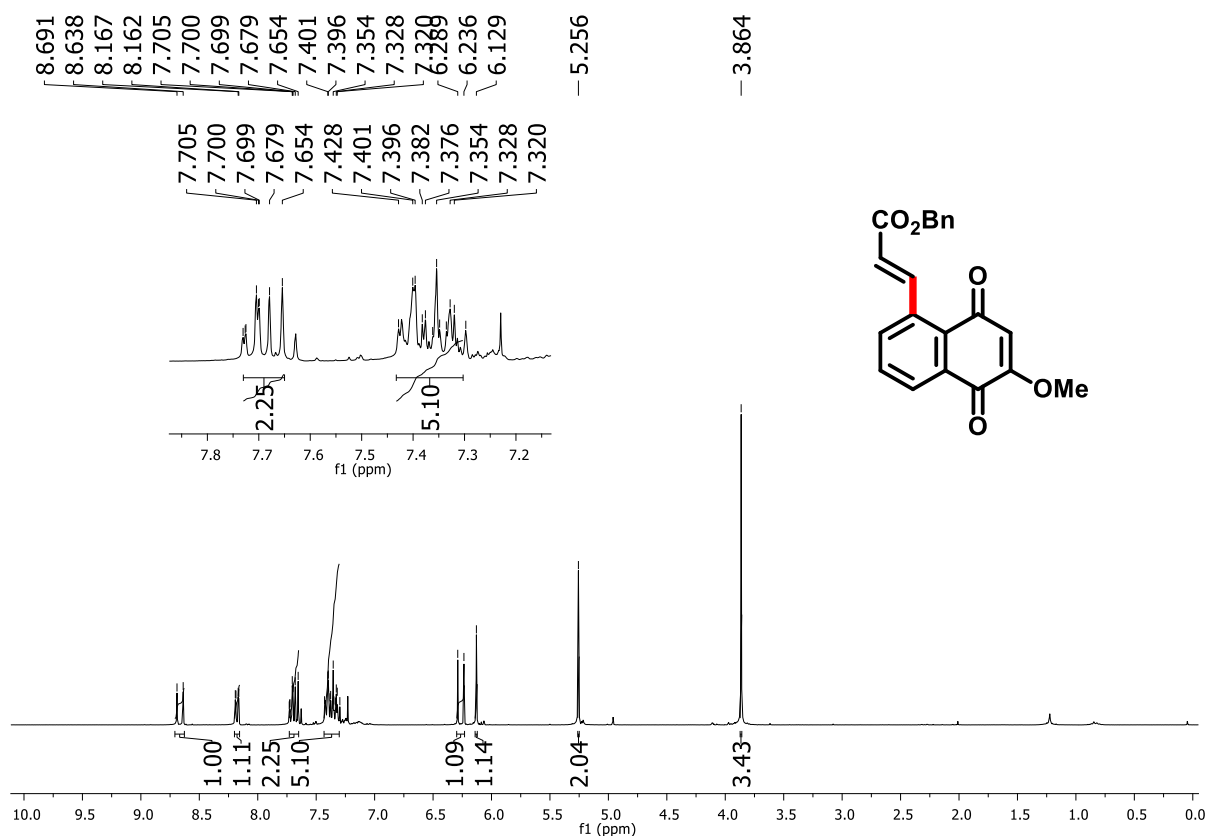


Figure 62. ¹H NMR spectrum (300 MHz, CDCl₃) of compound 155.

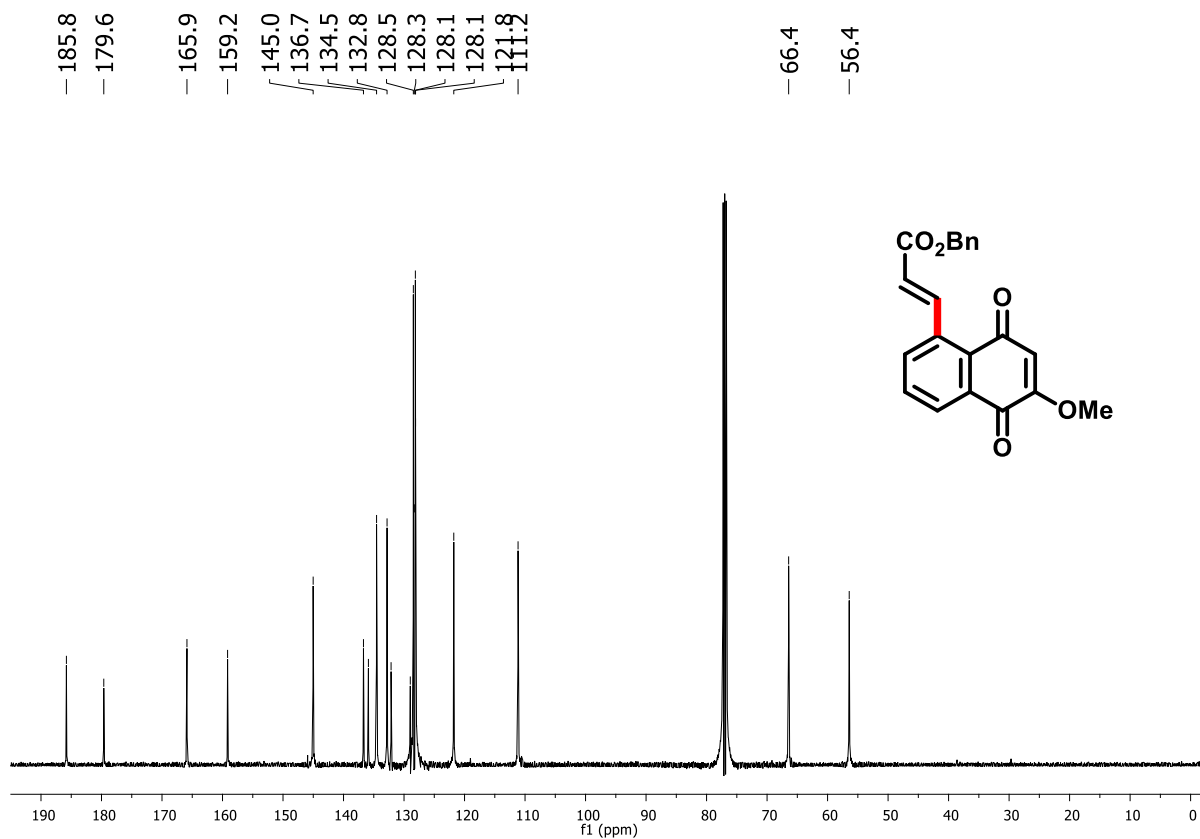


Figure 63. ¹³C NMR spectrum (75 MHz, CDCl₃) of compound 155.

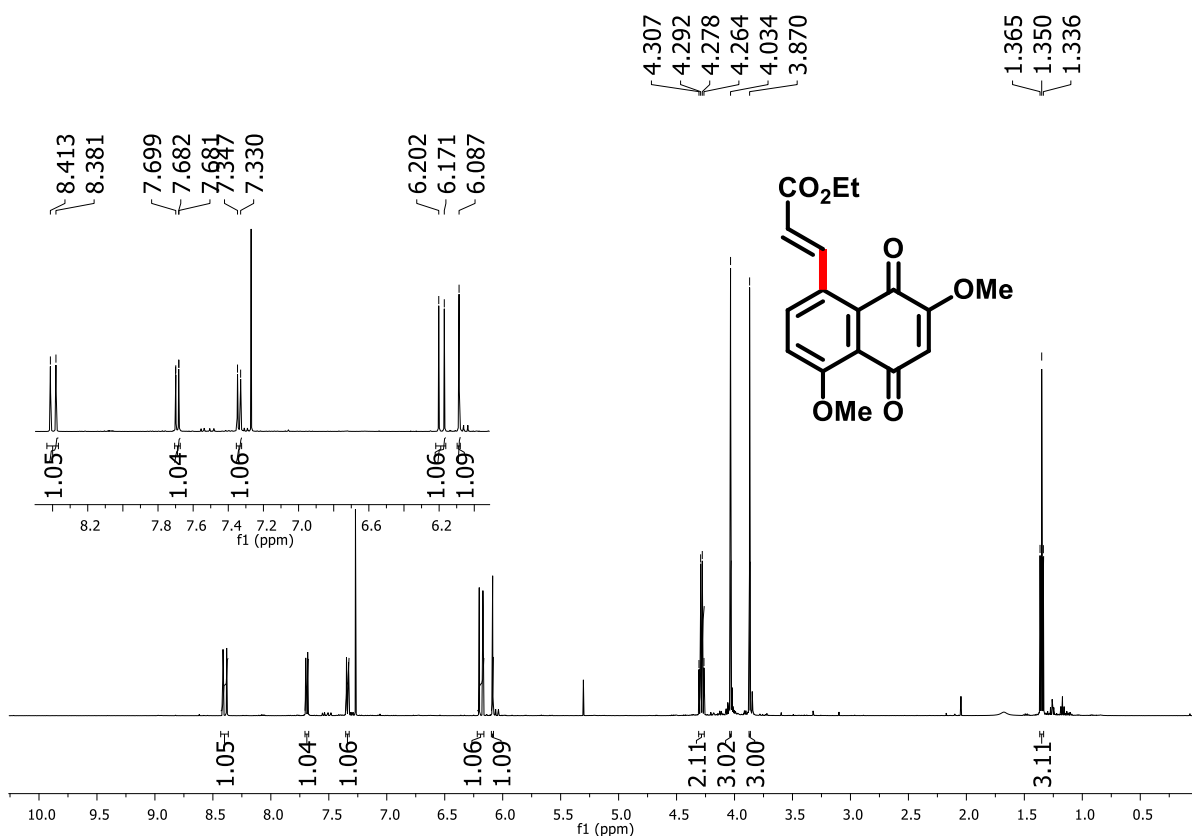


Figure 64. ¹H NMR spectrum (300 MHz, CDCl₃) of compound 157.

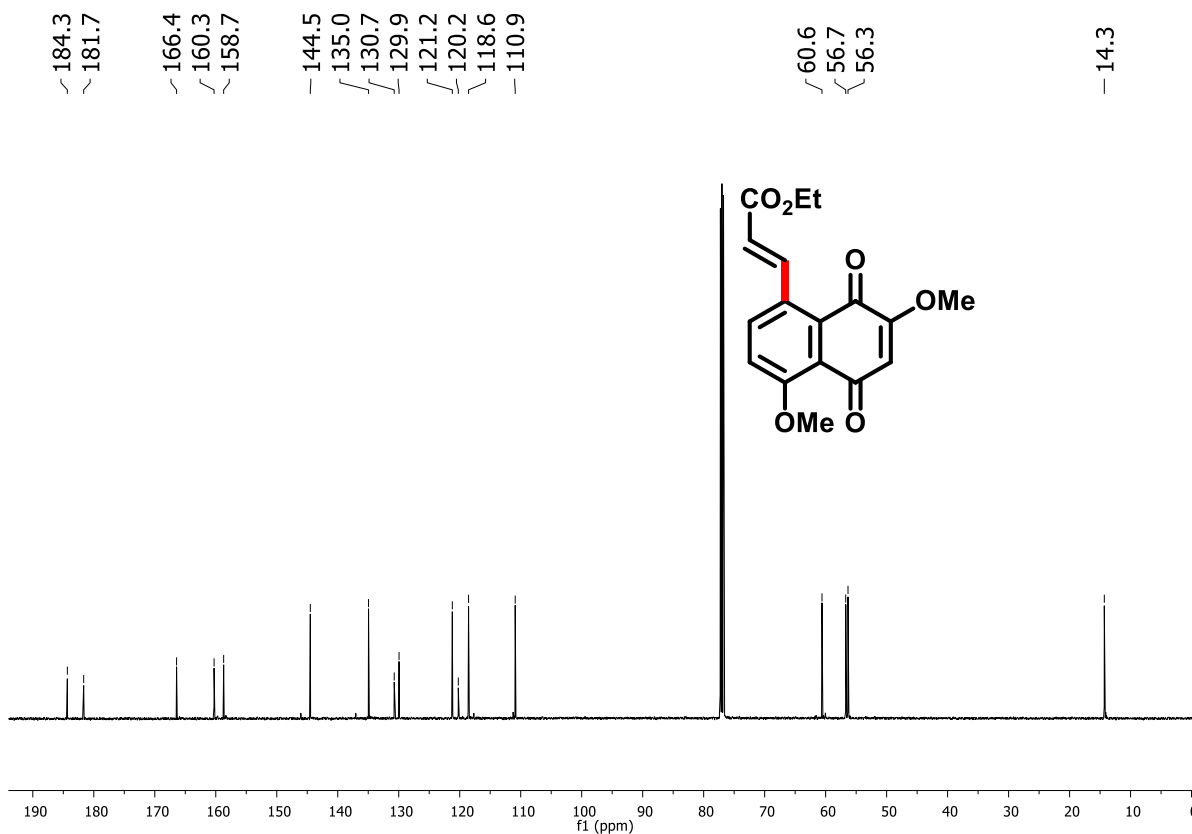
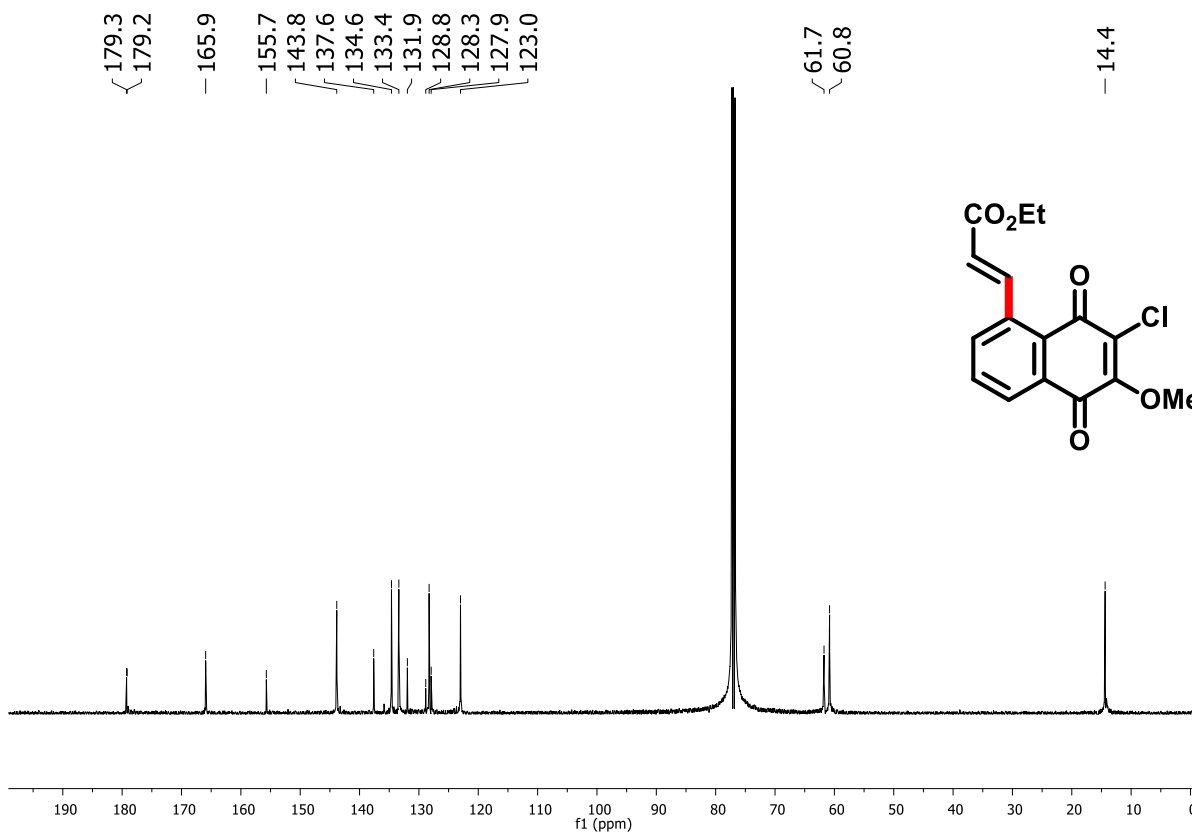
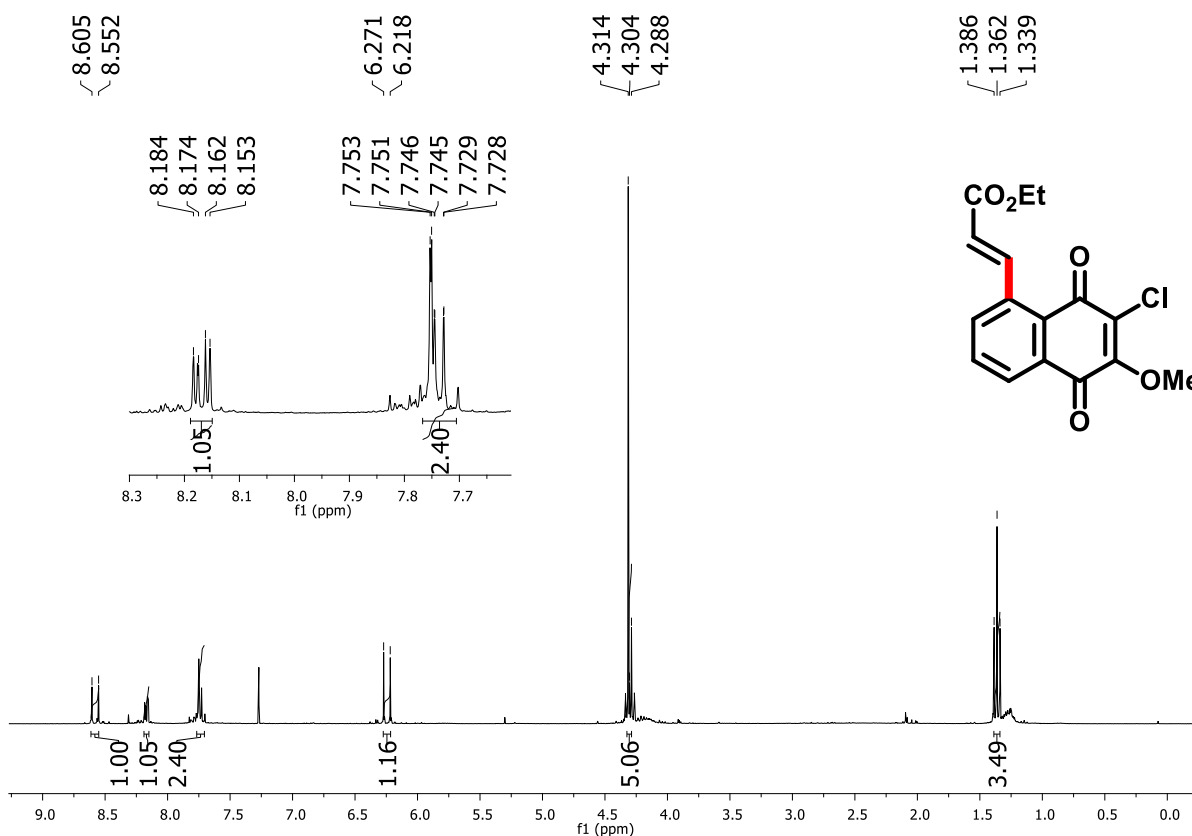


Figure 65. ¹³C NMR spectrum (75 MHz, CDCl₃) of compound 157.



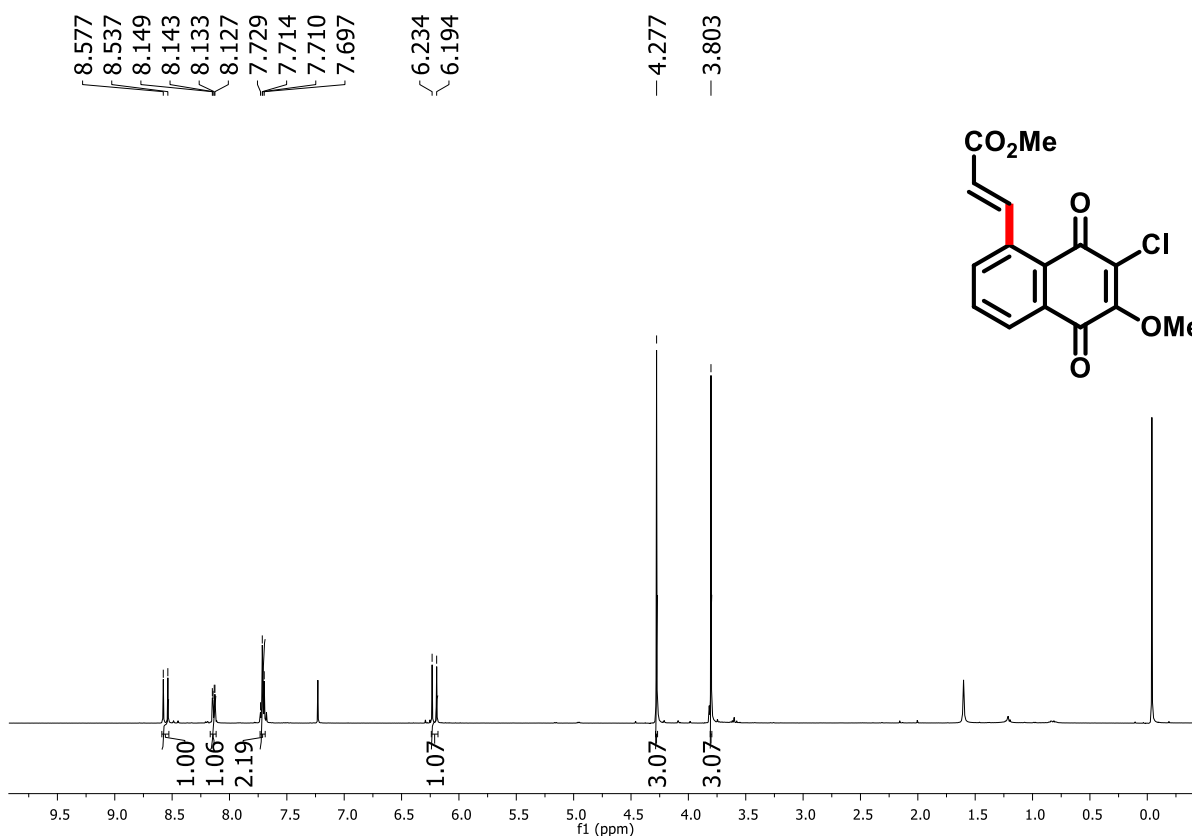


Figure 68. ^1H NMR spectrum (400 MHz, CDCl_3) of compound 162.

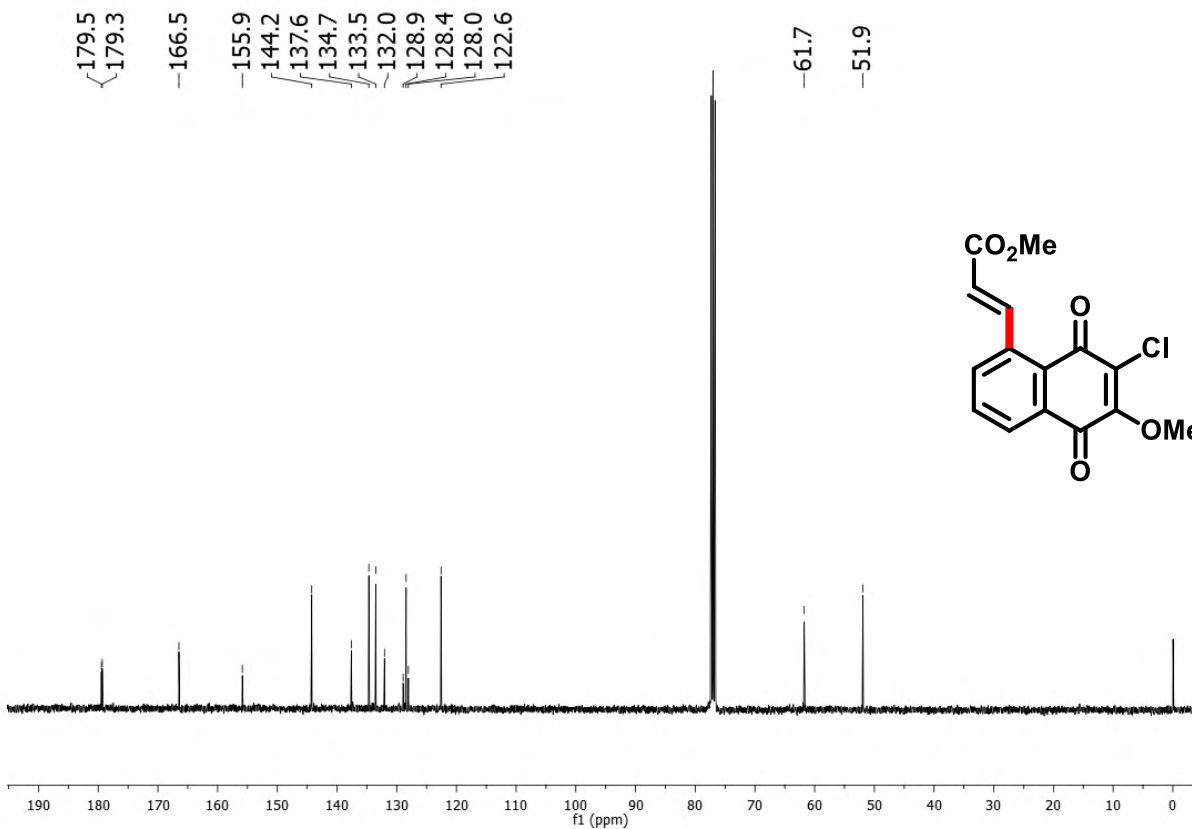


Figure 69. ^{13}C NMR spectrum (100 MHz, CDCl_3) of compound 162.

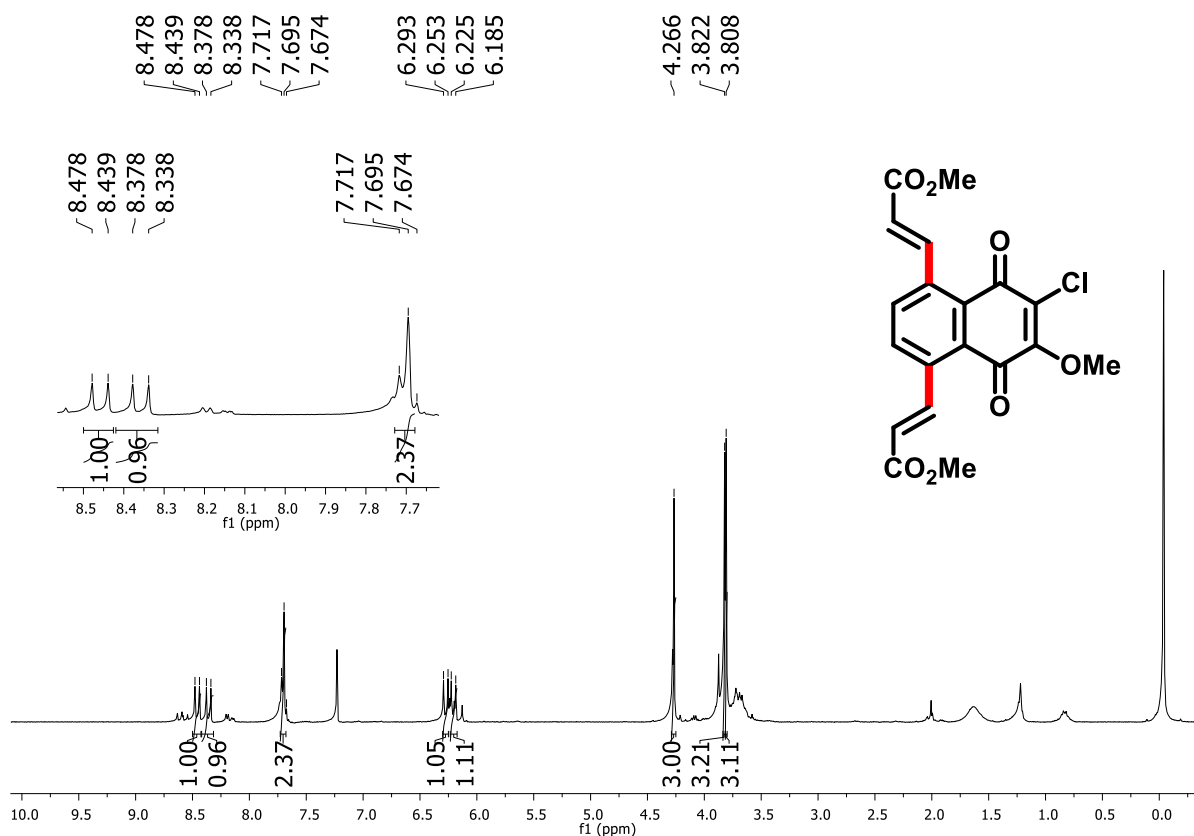


Figure 70. ¹H NMR spectrum (400 MHz, CDCl₃) of compound 163.

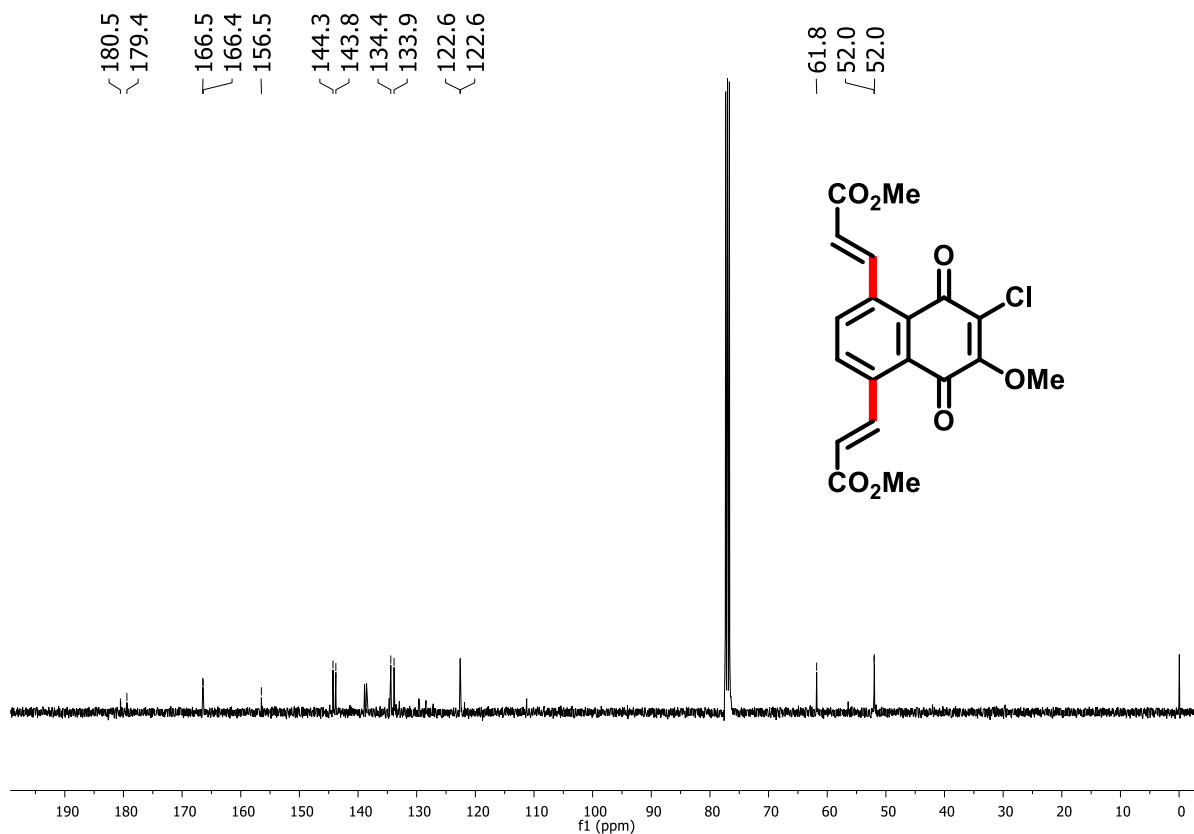


Figure 71. ¹³C NMR spectrum (100 MHz, CDCl₃) of compound 163.

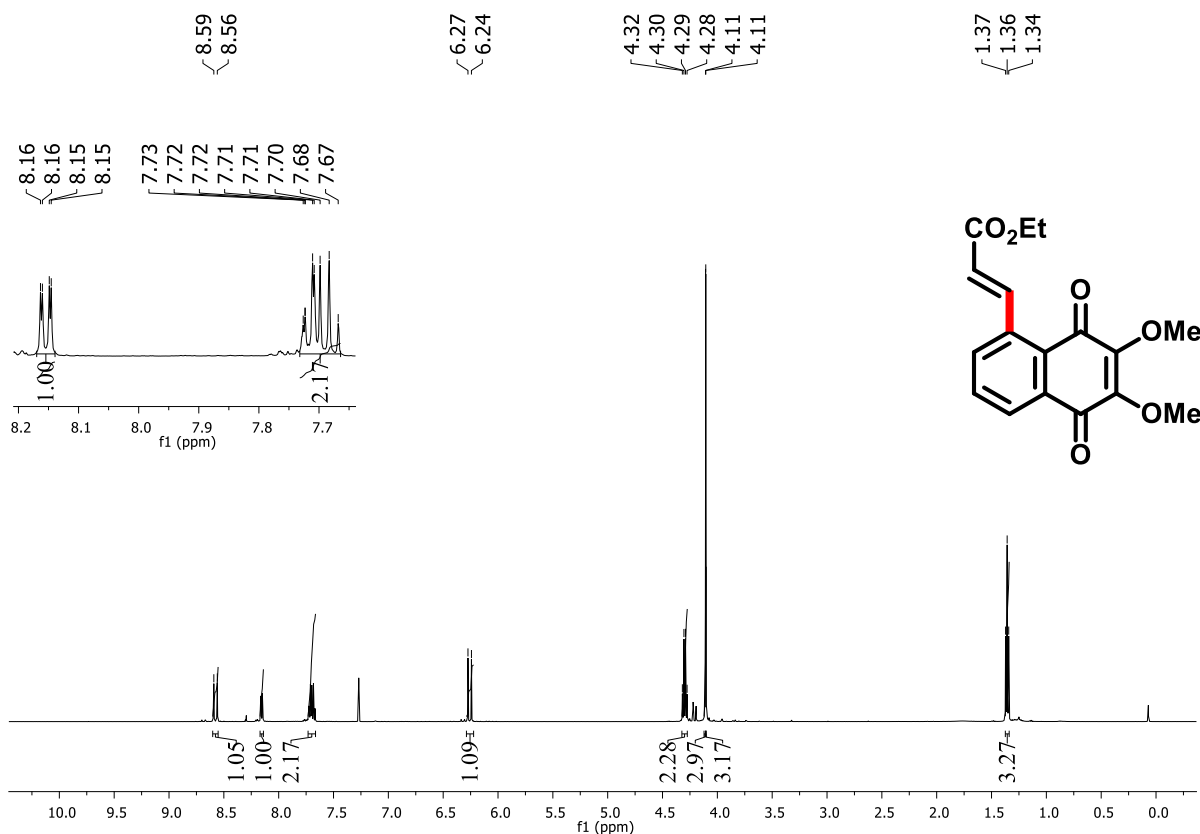


Figure 72. ^1H NMR spectrum (500 MHz, CDCl_3) of compound 164.

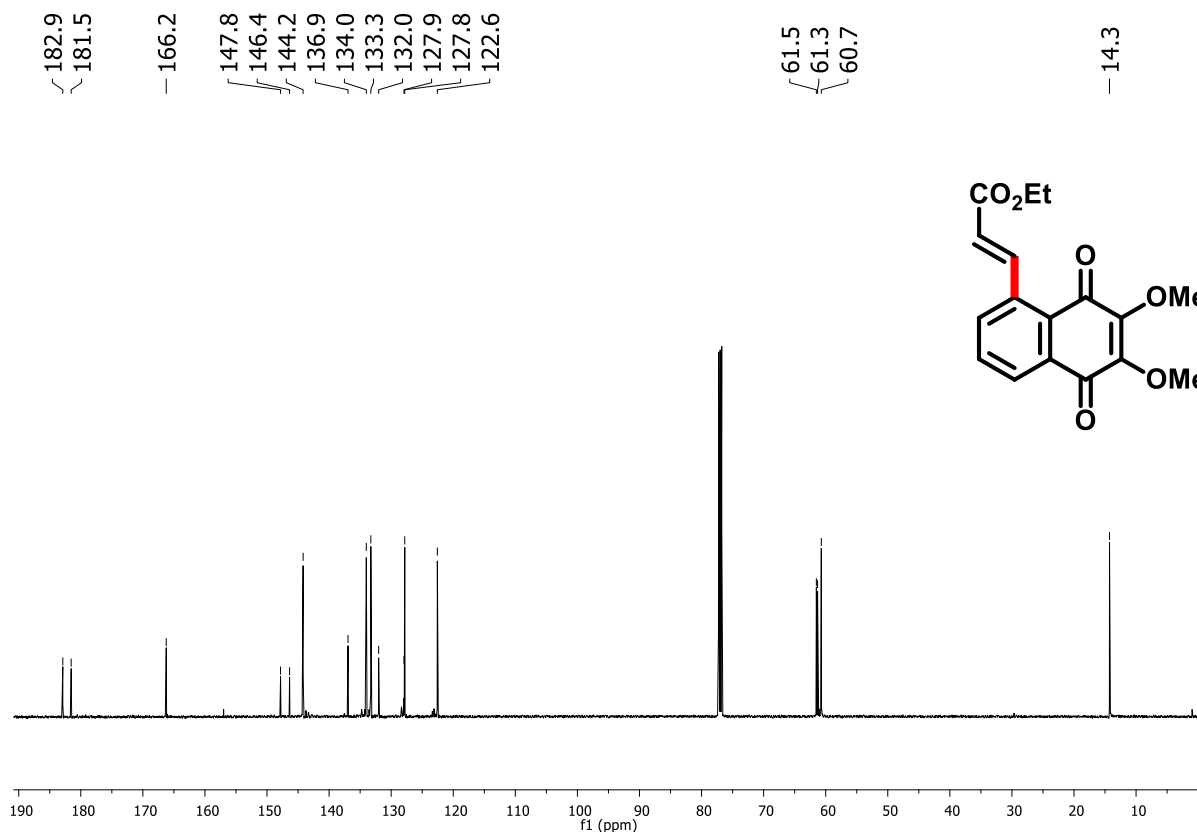


Figure 73. ^{13}C NMR spectrum (125 MHz, CDCl_3) of compound 164.

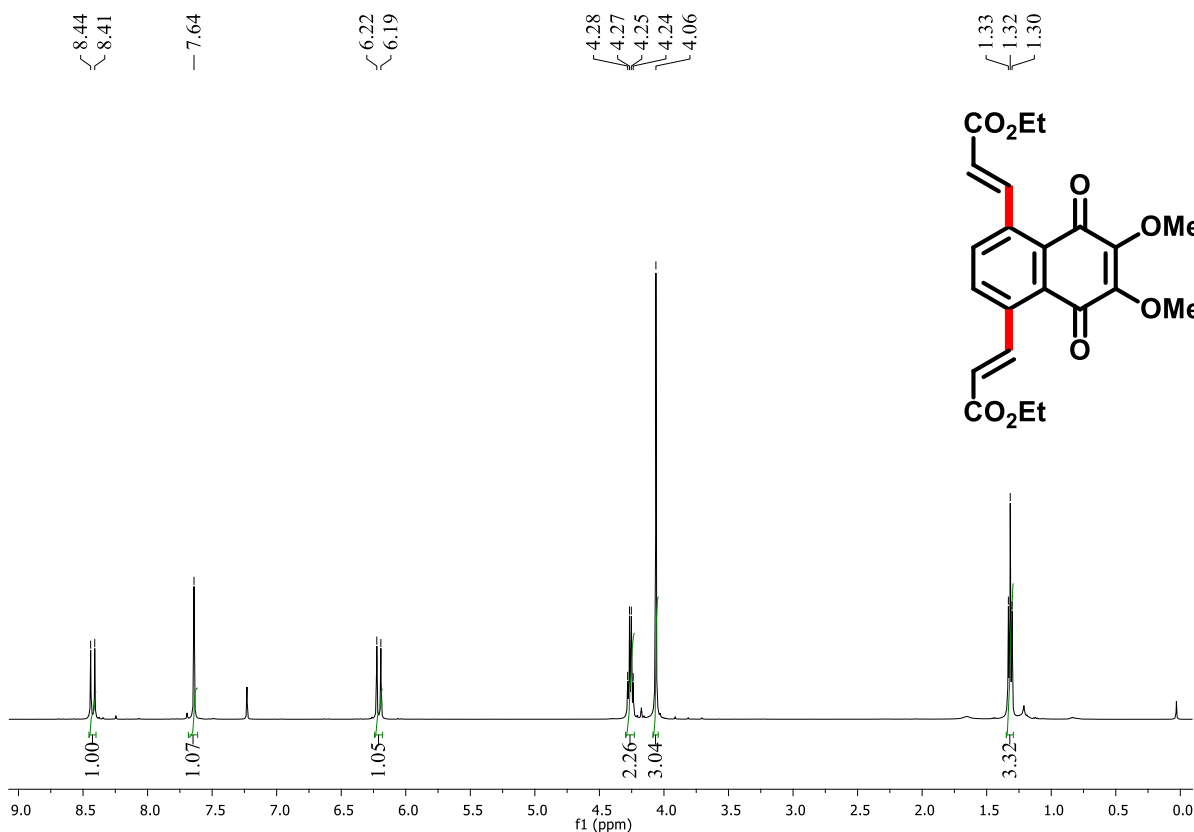


Figure 74. ^1H NMR spectrum (500 MHz, CDCl_3) of compound 165.

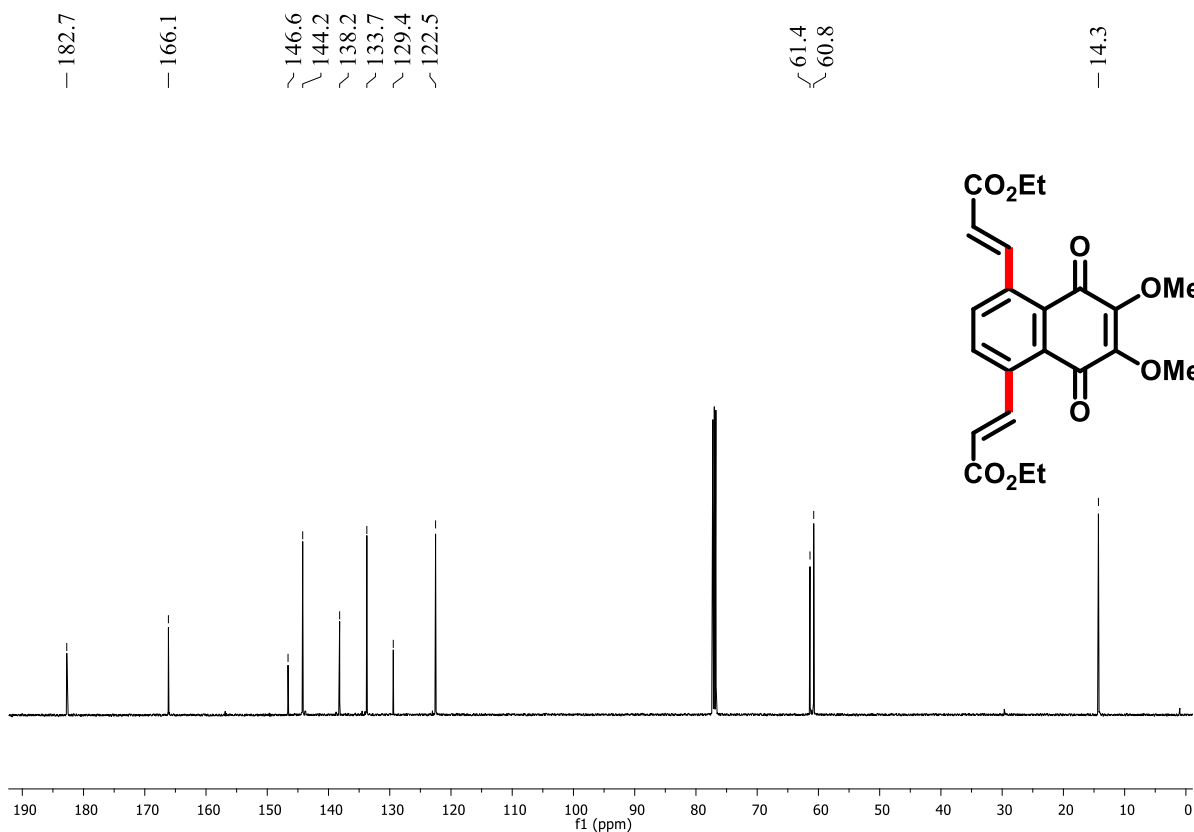


Figure 75. ^{13}C NMR spectrum (125 MHz, CDCl_3) of compound 165.

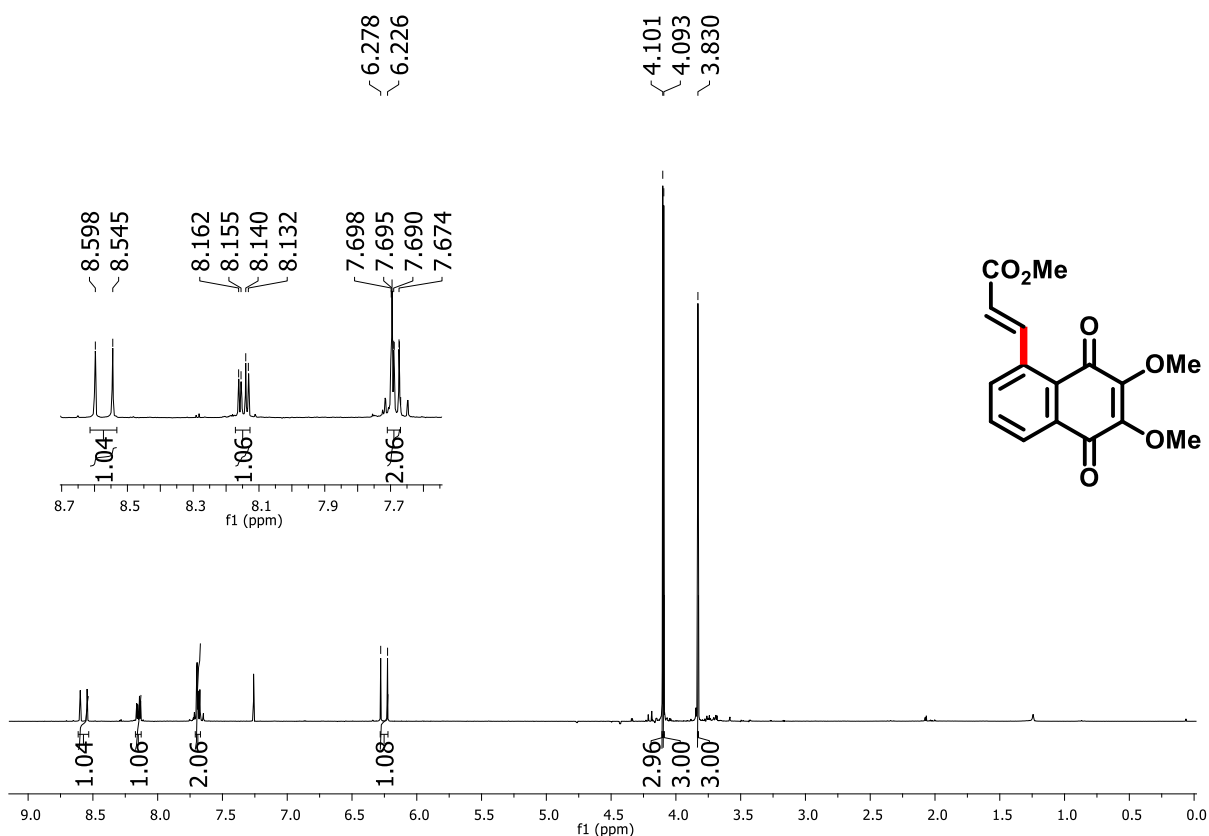


Figure 76. ^1H NMR spectrum (300 MHz, CDCl_3) of compound 166.

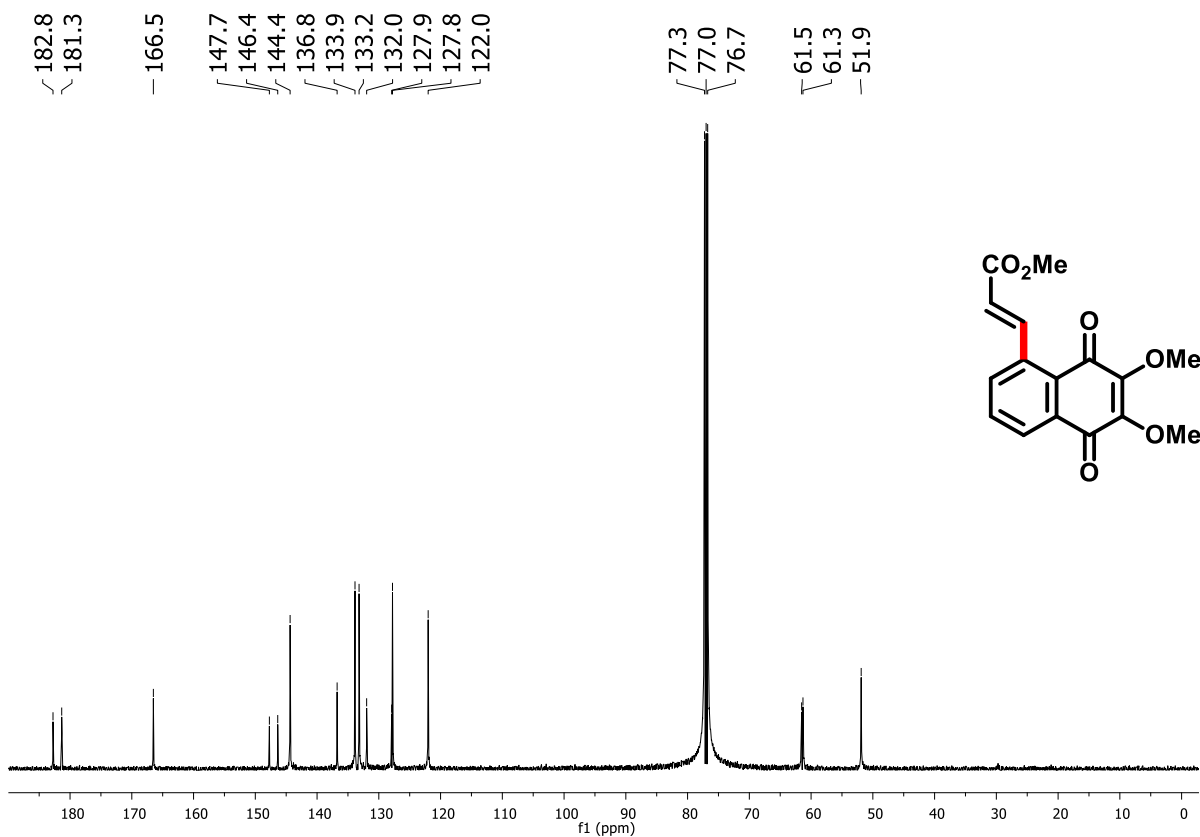


Figure 77. ^{13}C NMR spectrum (75 MHz, CDCl_3) of compound 166.

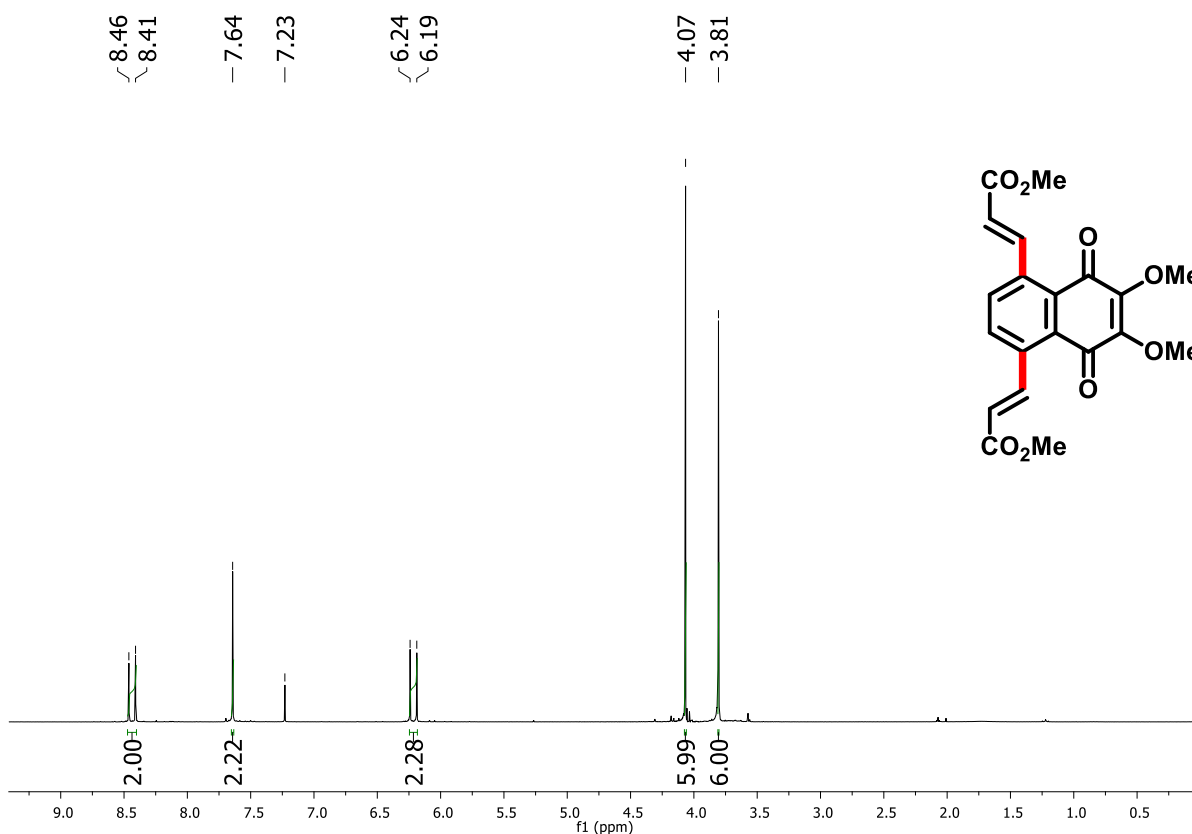


Figure 78. ^1H NMR spectrum (300 MHz, CDCl_3) of compound 167.

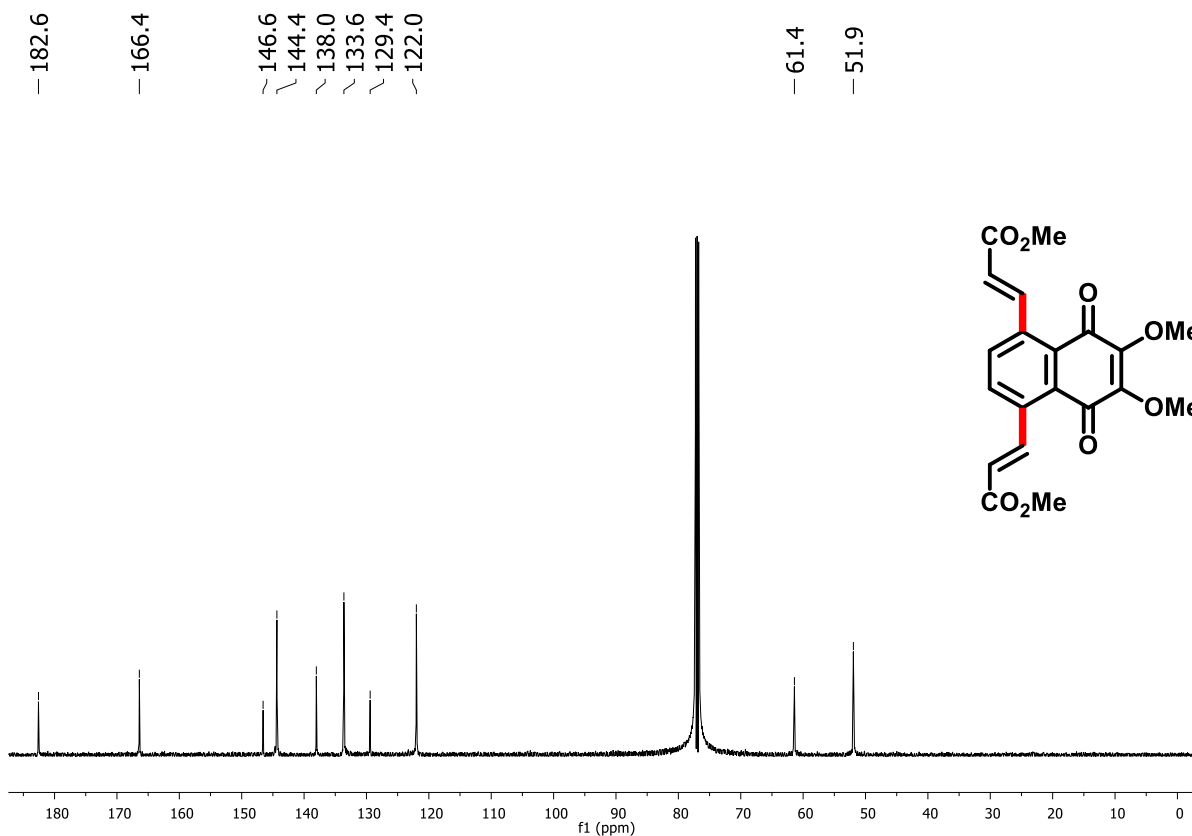


Figure 79. ^{13}C NMR spectrum (75 MHz, CDCl_3) of compound 167.

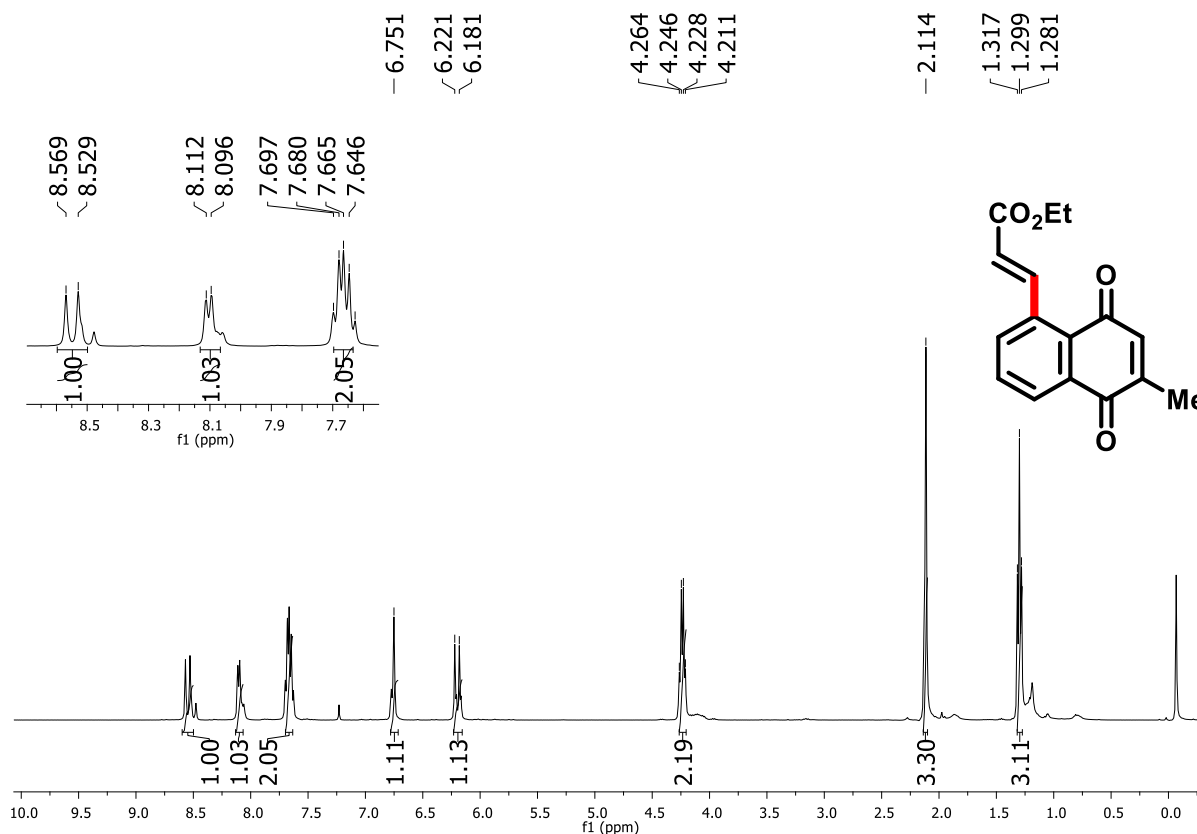


Figure 80. ¹H NMR spectrum (400 MHz, CDCl₃) of compound 168.

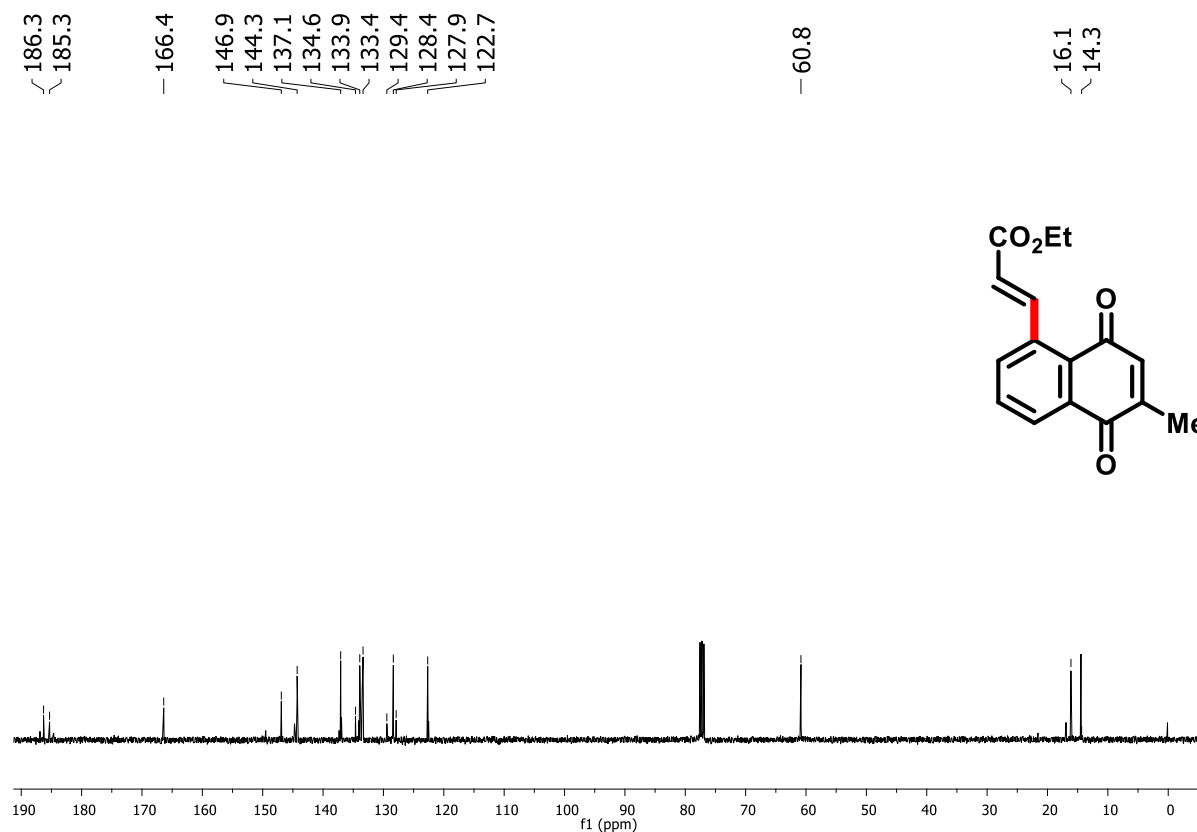


Figure 81. ¹³C NMR spectrum (100 MHz, CDCl₃) of compound 168.

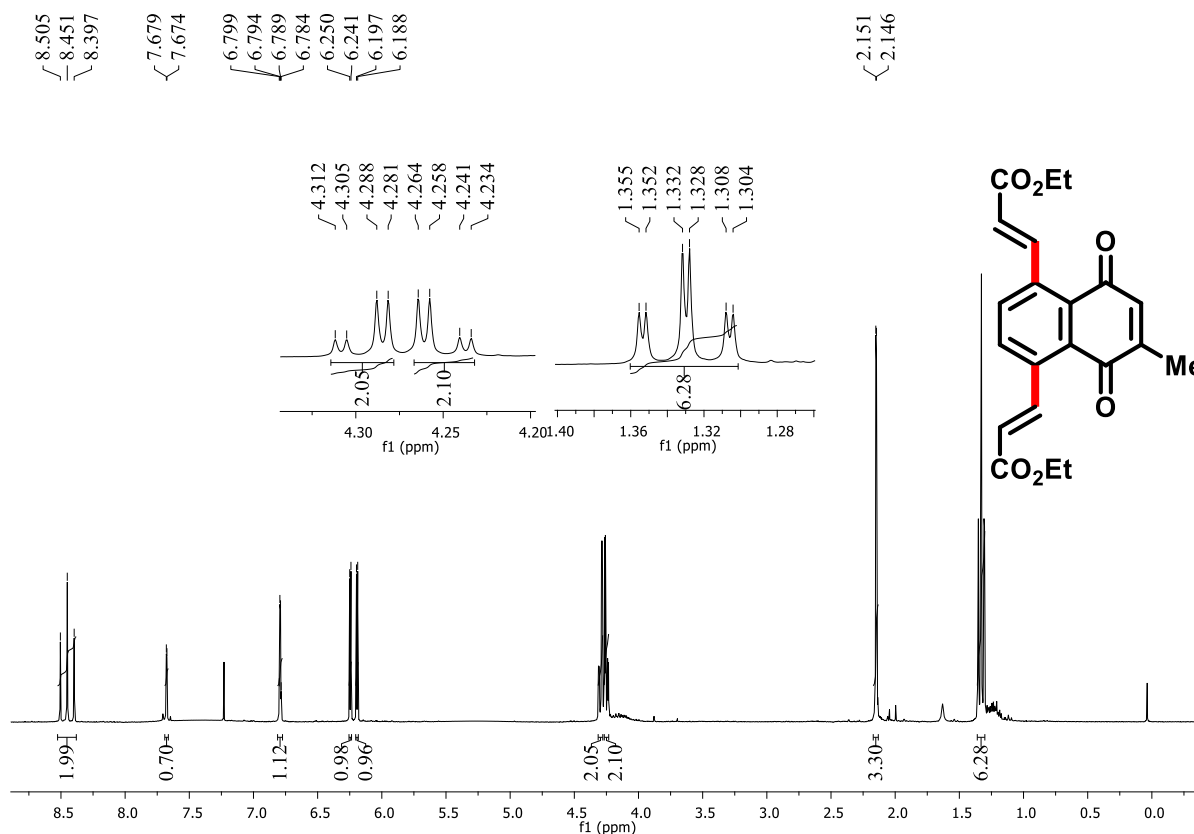


Figure 82. ¹H NMR spectrum (300 MHz, CDCl₃) of compound 169.

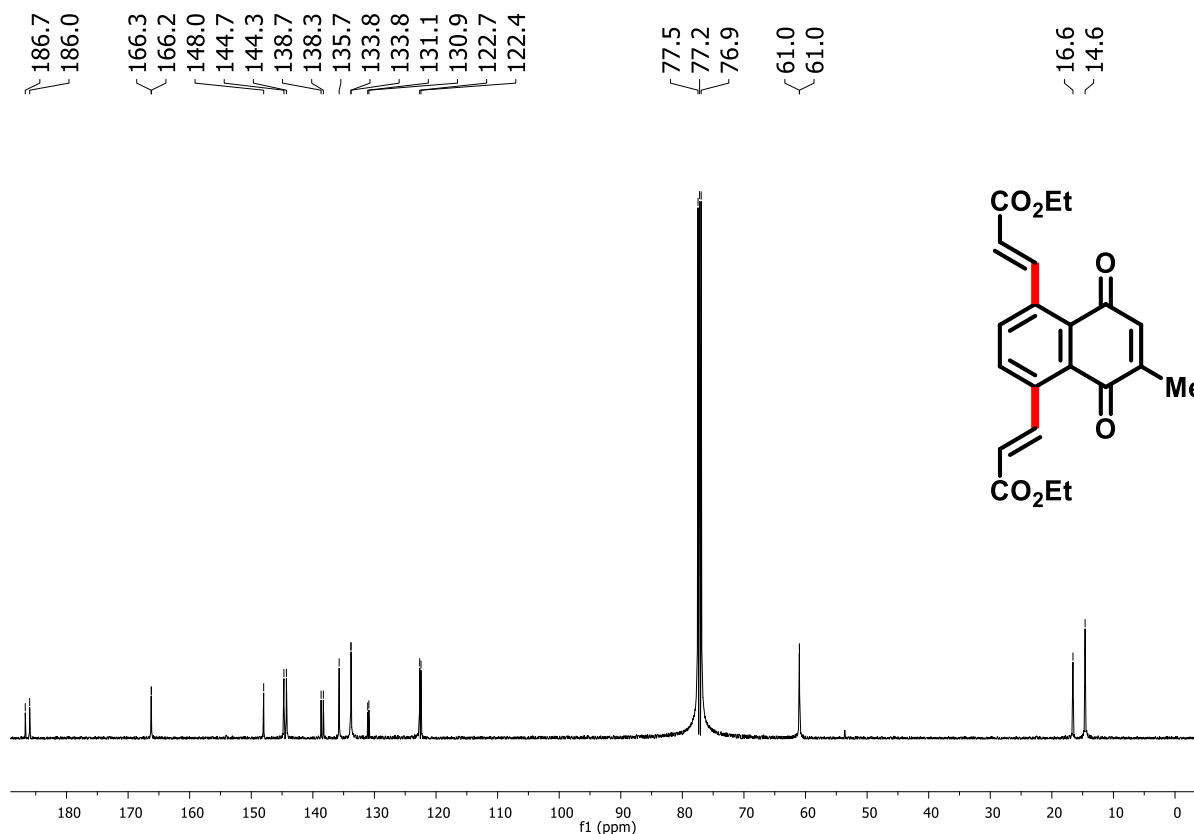


Figure 83. ¹³C NMR spectrum (75 MHz, CDCl₃) of compound 169.

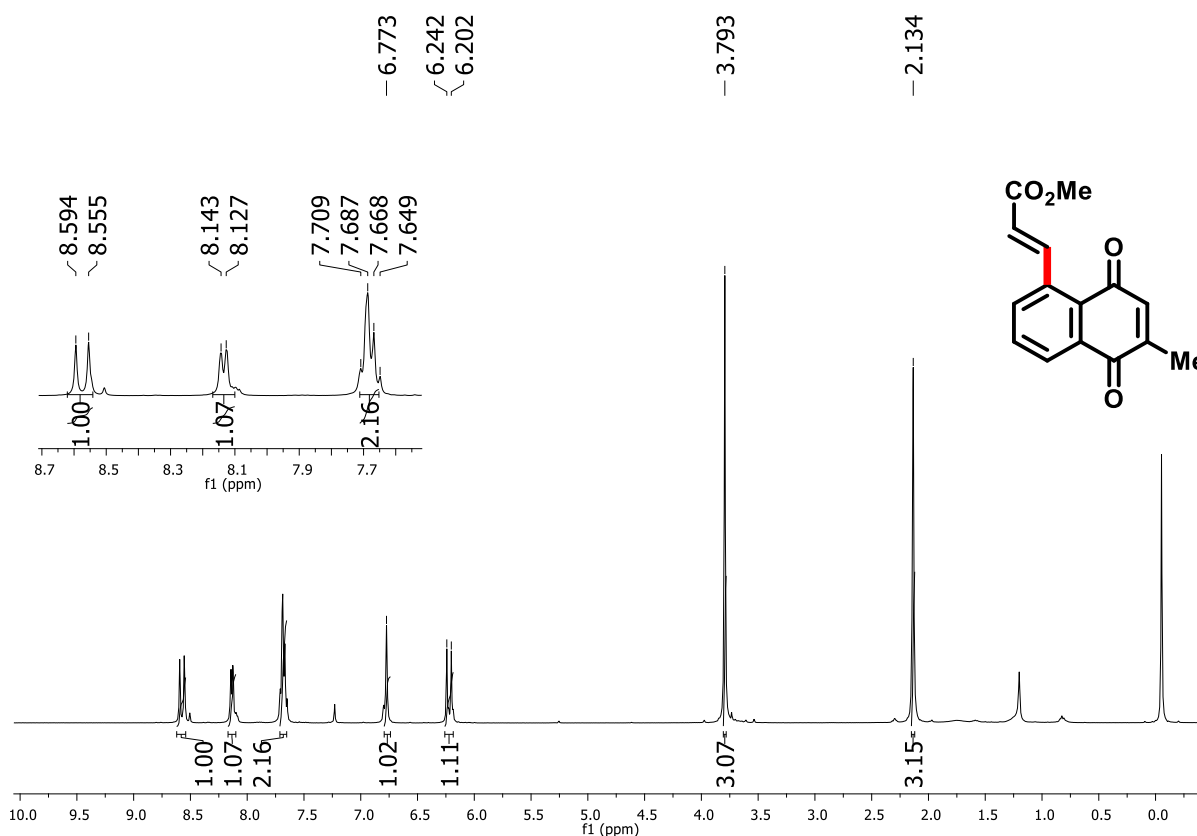


Figure 84. ^1H NMR spectrum (400 MHz, CDCl_3) of compound 170.

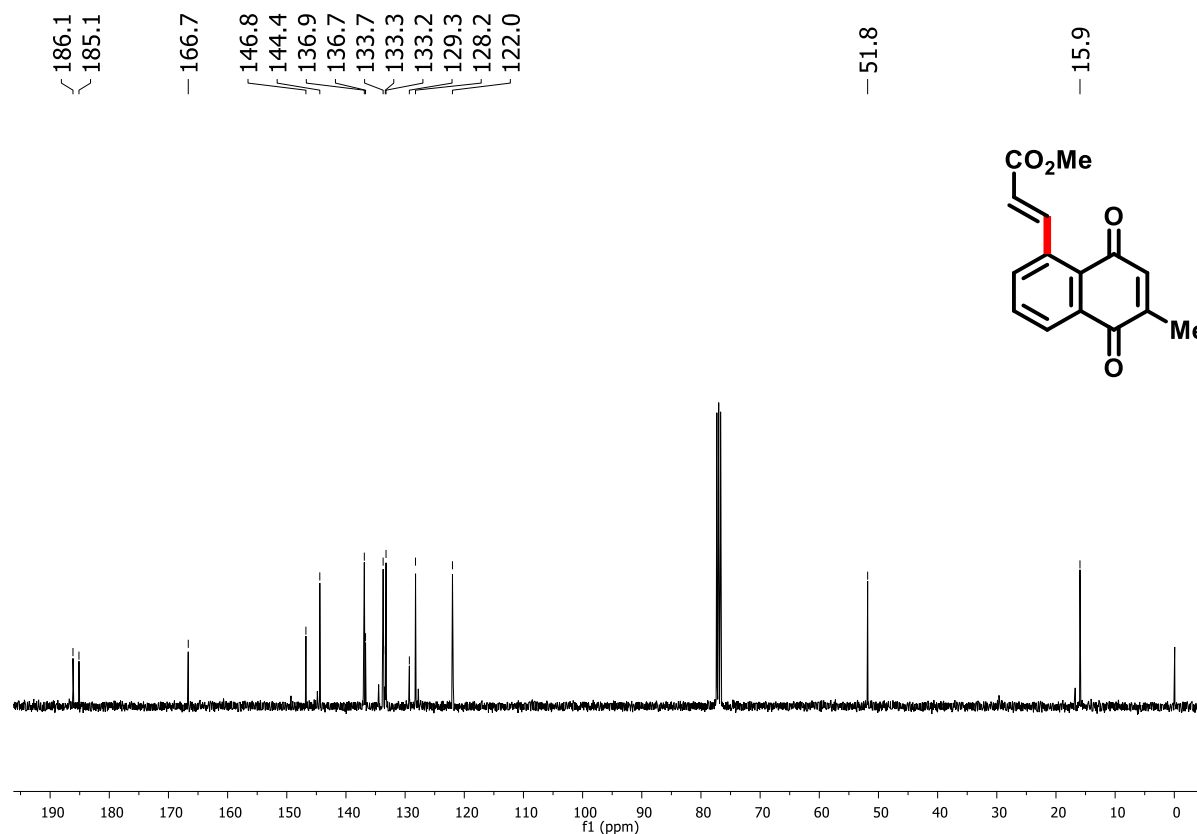
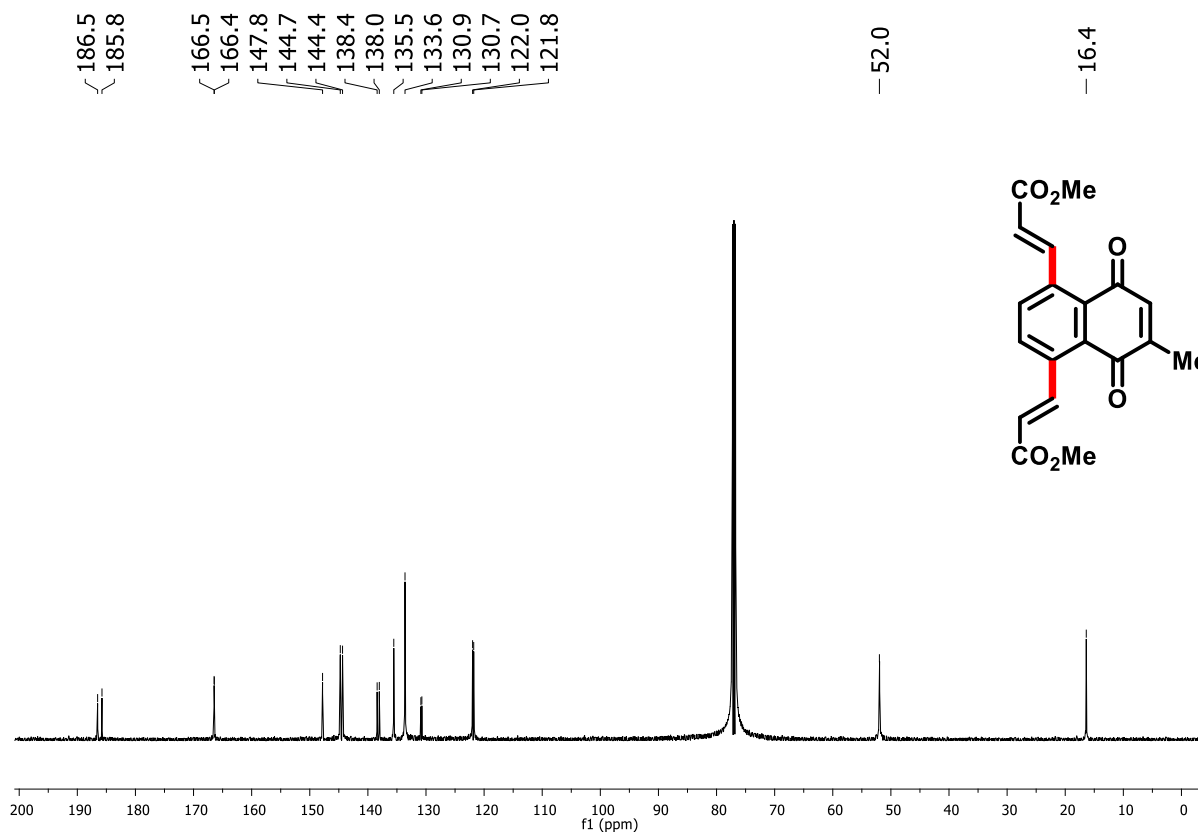
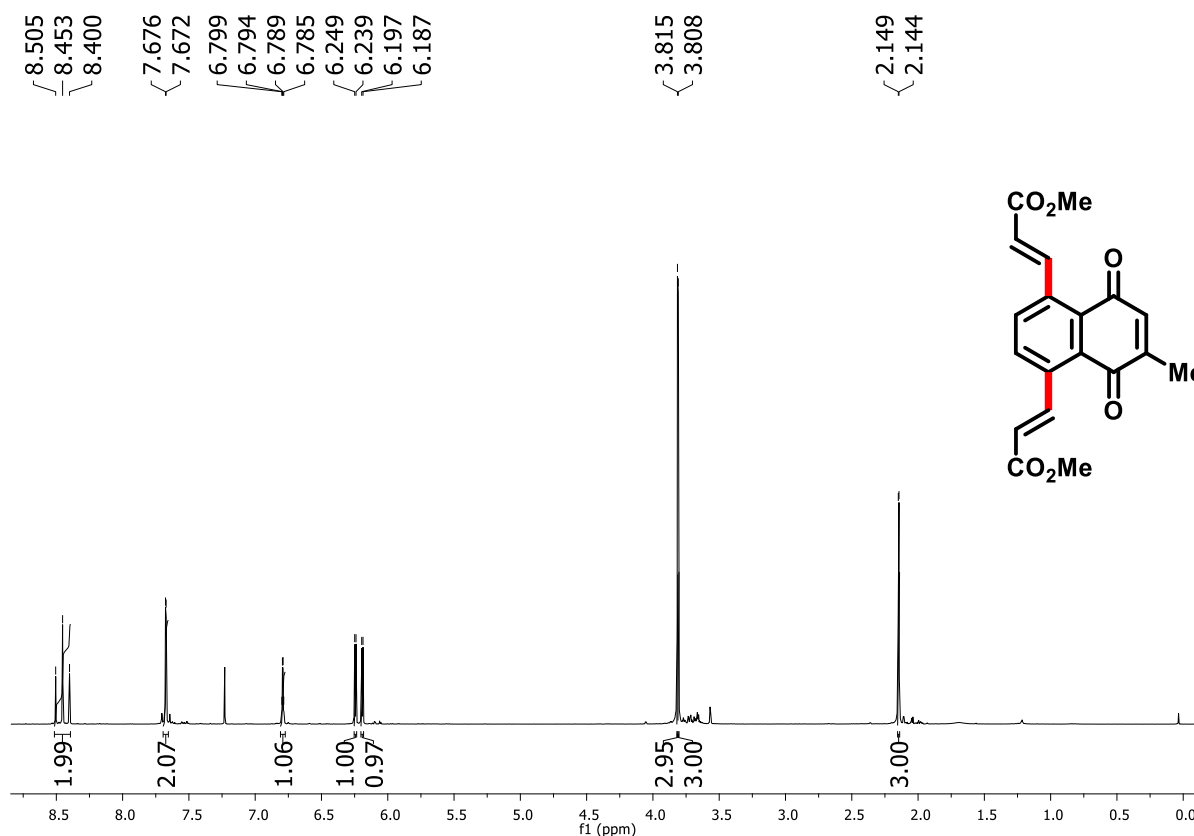


Figure 85. ^{13}C NMR spectrum (100 MHz, CDCl_3) of compound 170.



Spectra of oxygenated products

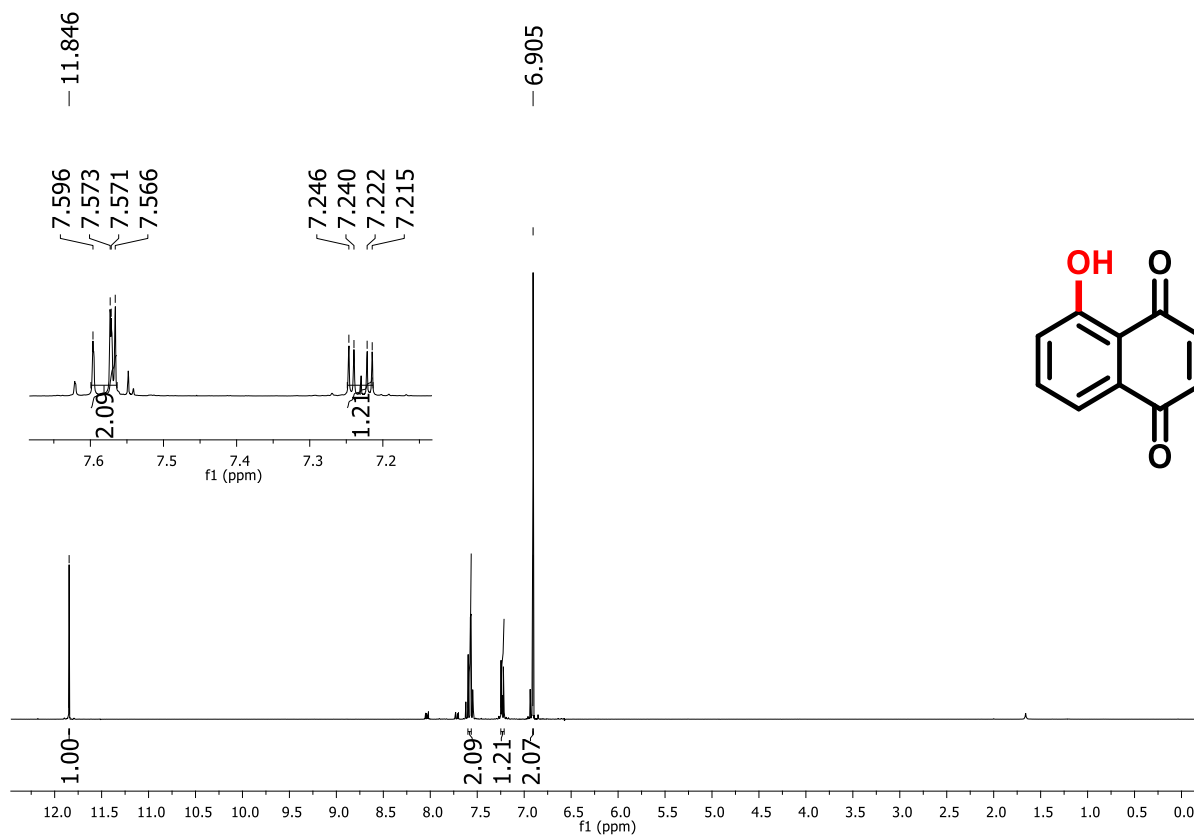


Figure 88. ¹H NMR spectrum (300 MHz, CDCl₃) of compound 74.

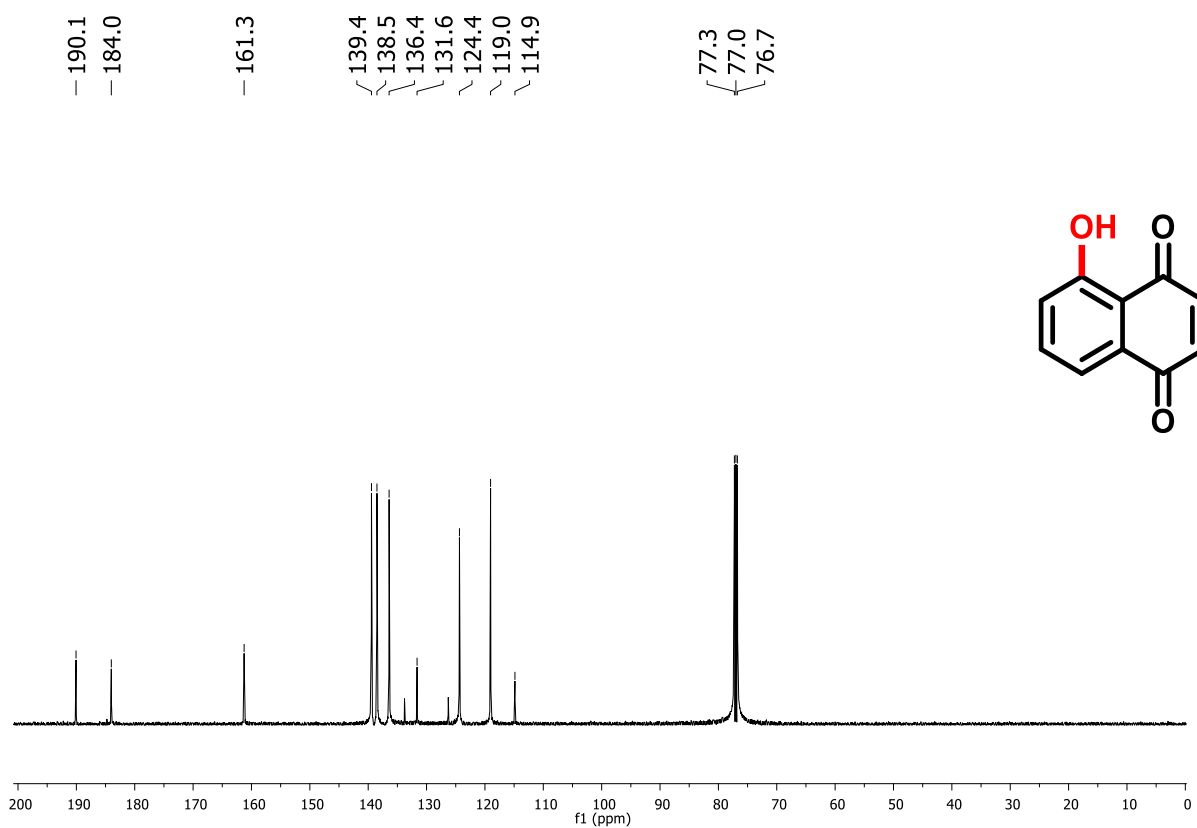


Figure 89. ¹³C NMR spectrum (75 MHz, CDCl₃) of compound 74.

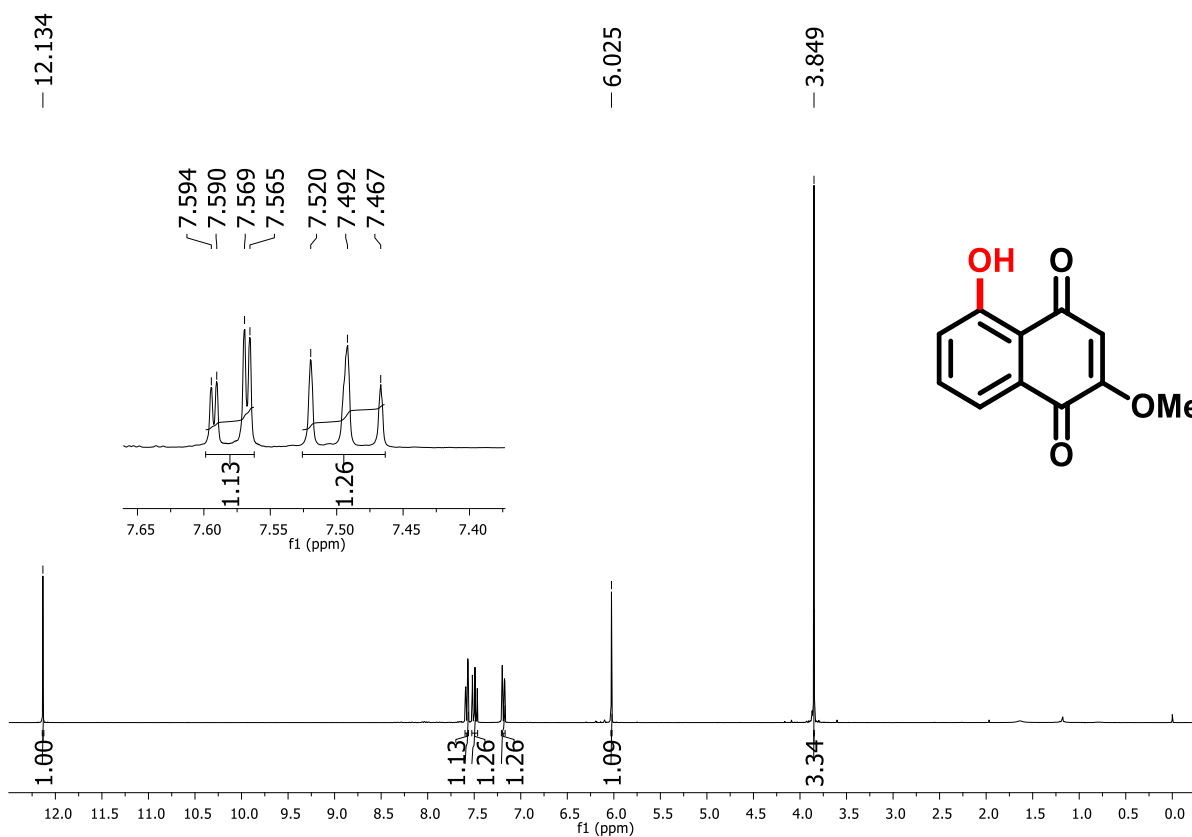


Figure 90. ^1H NMR spectrum (300 MHz, CDCl_3) of compound 114.

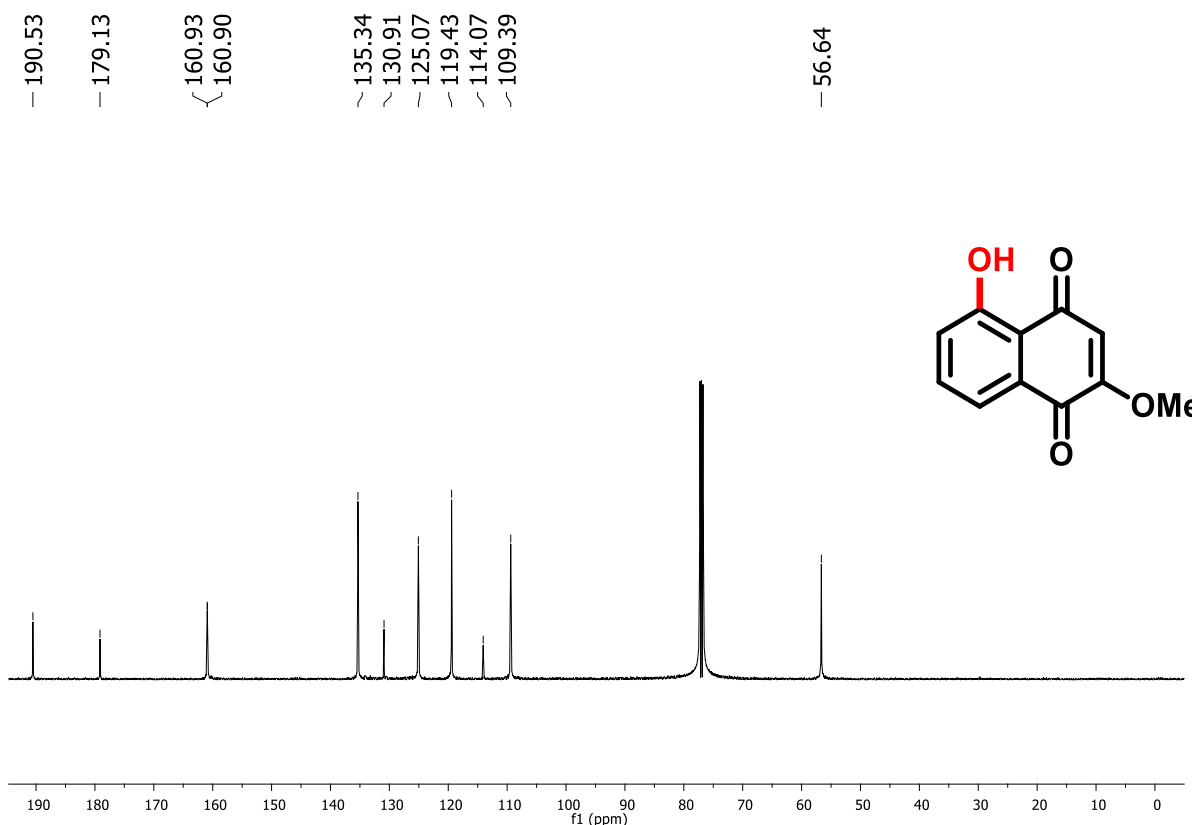


Figure 91. ^{13}C NMR spectrum (75 MHz, CDCl_3) of compound 114.

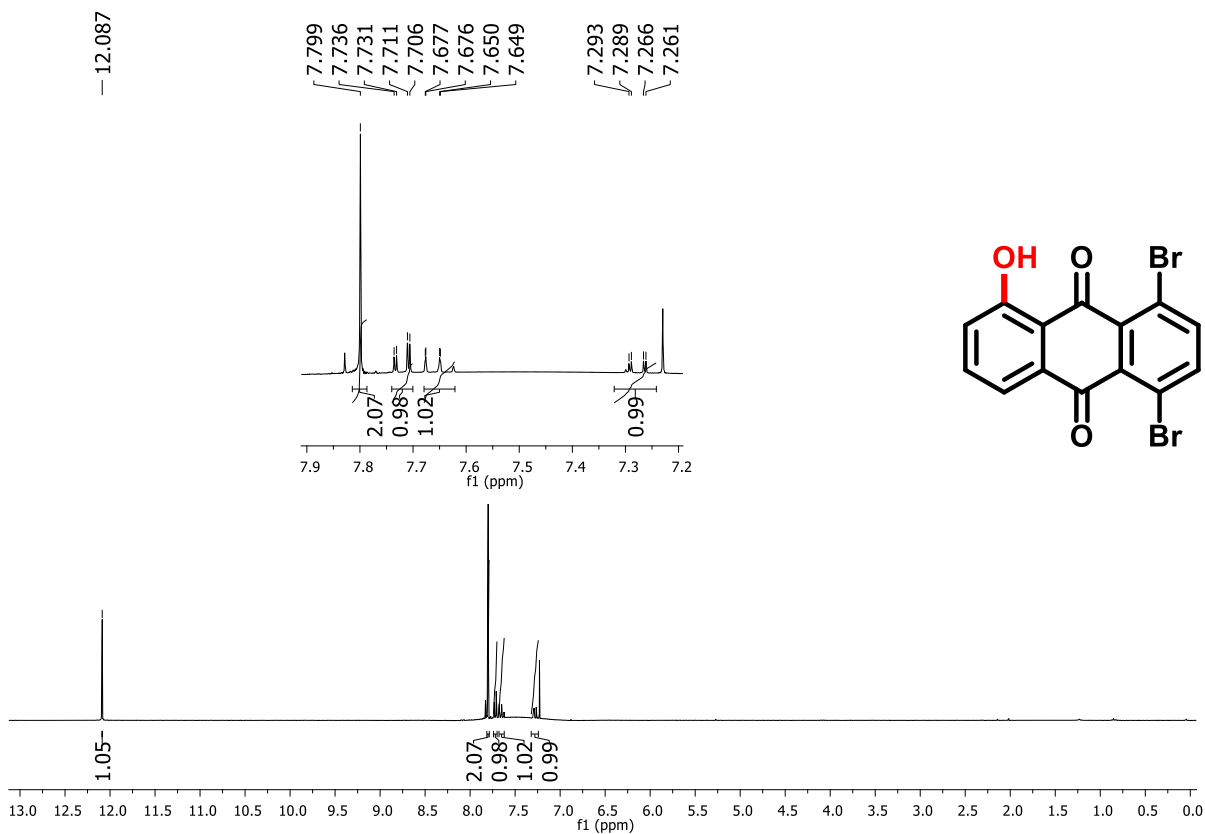


Figure 92. ^1H NMR spectrum (300 MHz, CDCl_3) of compound 123.

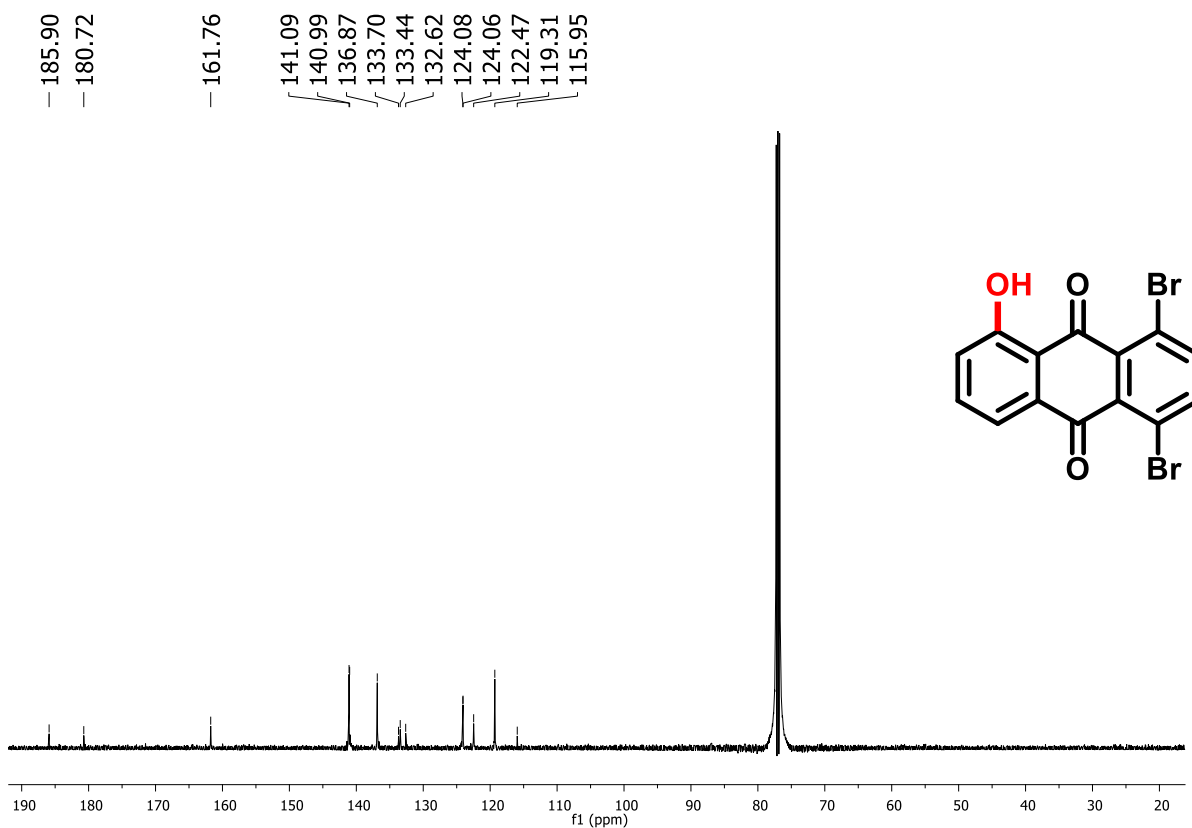


Figure 93. ^{13}C NMR spectrum (75 MHz, CDCl_3) of compound 123.

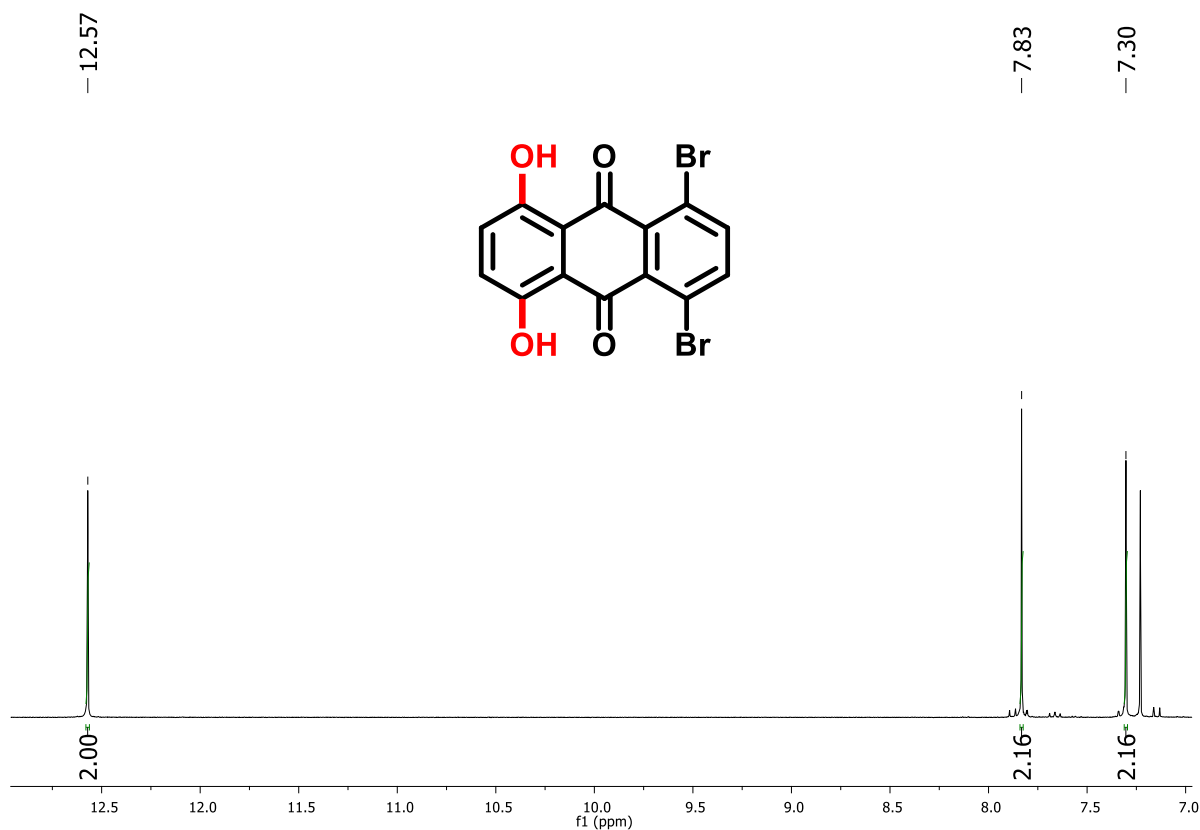


Figure 94. ¹H NMR spectrum (300 MHz, CDCl₃) of compound 124.

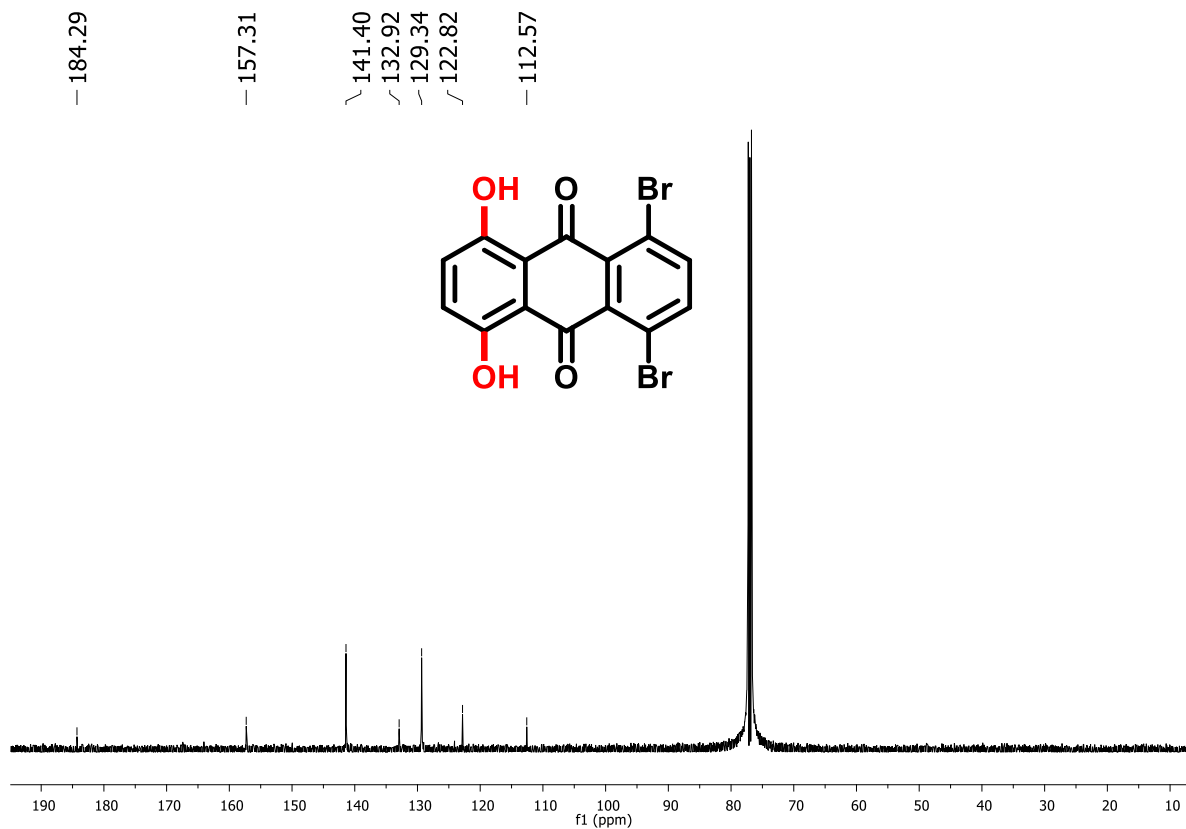


Figure 95. ¹³C NMR spectrum (75 MHz, CDCl₃) of compound 124.

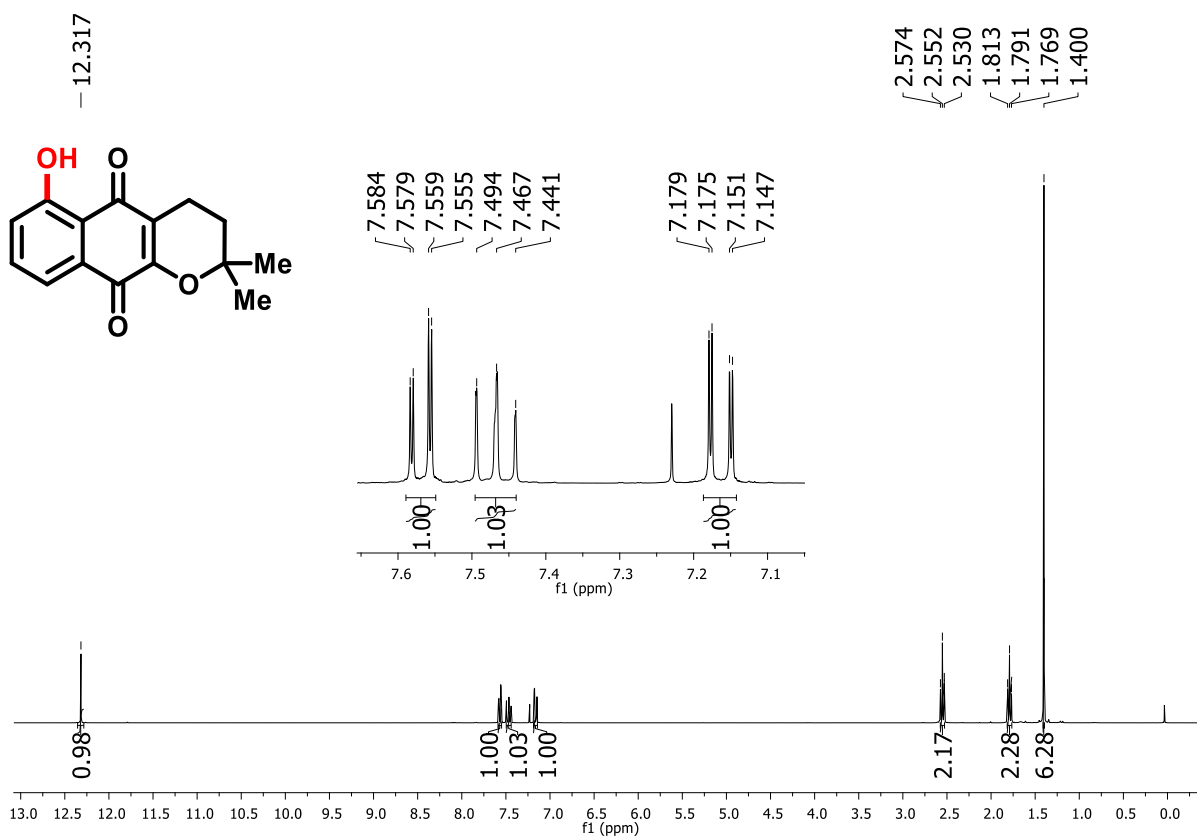


Figure 96. ¹H NMR spectrum (300 MHz, CDCl₃) of compound 178.

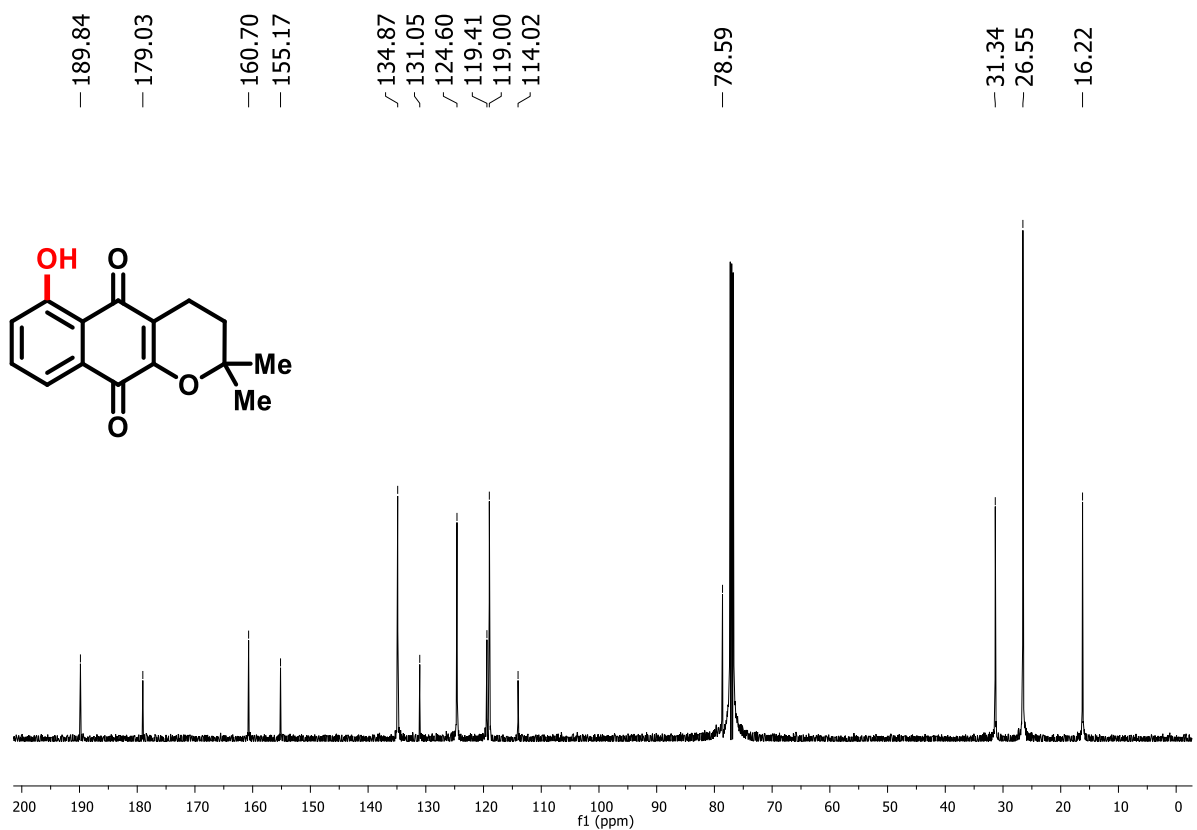


Figure 97. ¹³C NMR spectrum (75 MHz, CDCl₃) of compound 178.

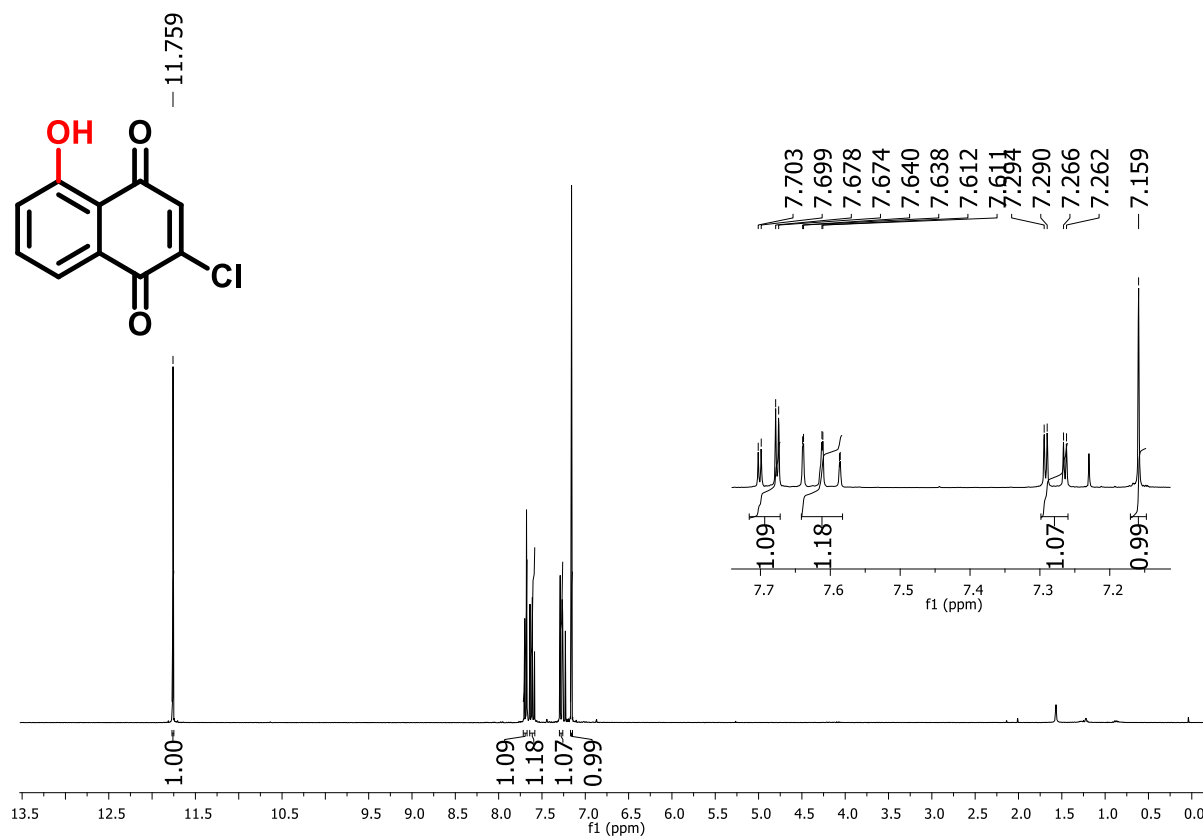


Figure 98. ¹H NMR spectrum (300 MHz, CDCl₃) of compound 179.

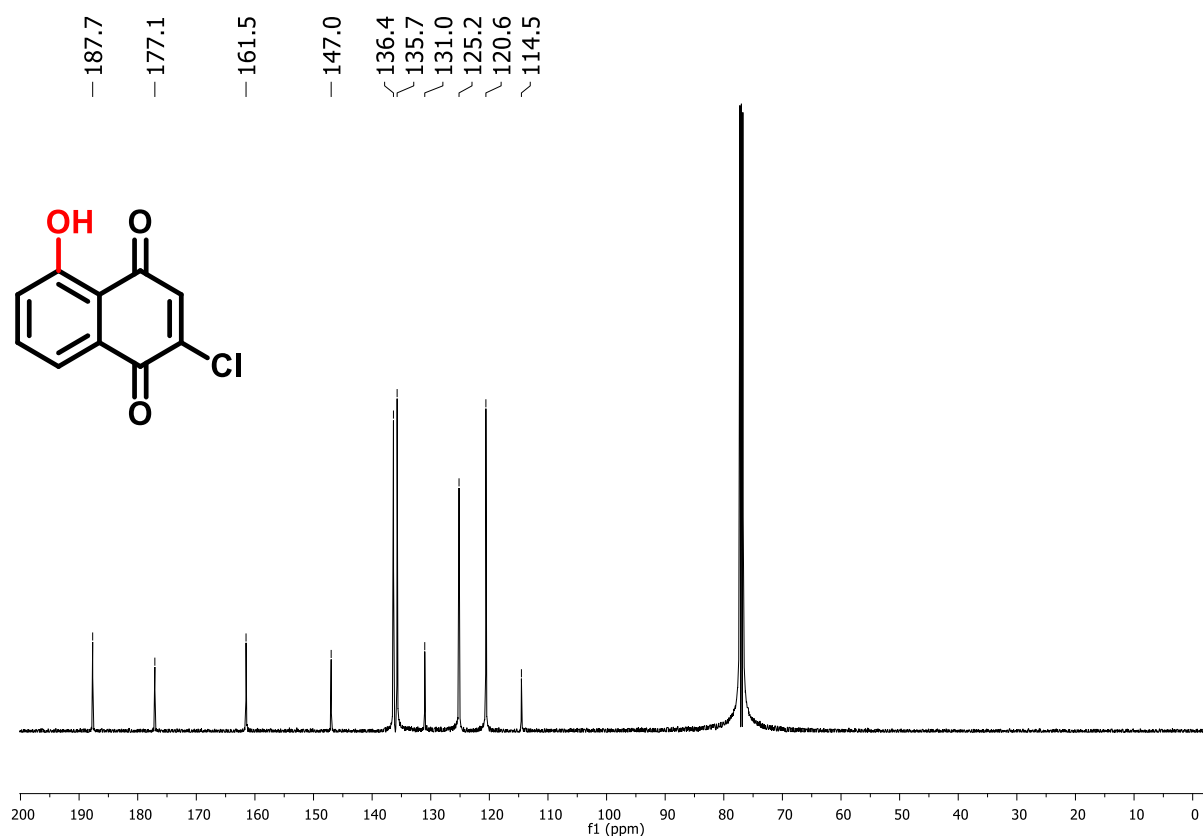


Figure 99. ¹³C NMR spectrum (75 MHz, CDCl₃) of compound 179.

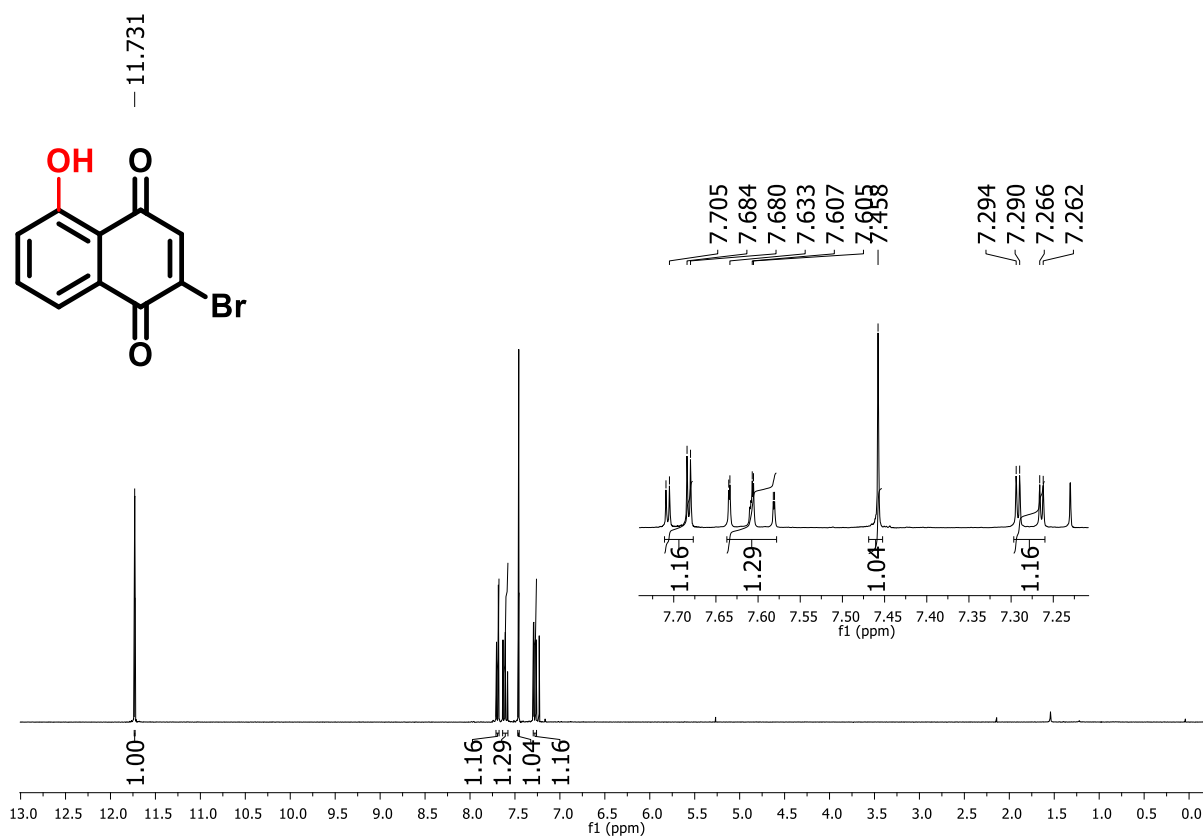


Figure 100. ¹H NMR spectrum (300 MHz, CDCl₃) of compound 180.

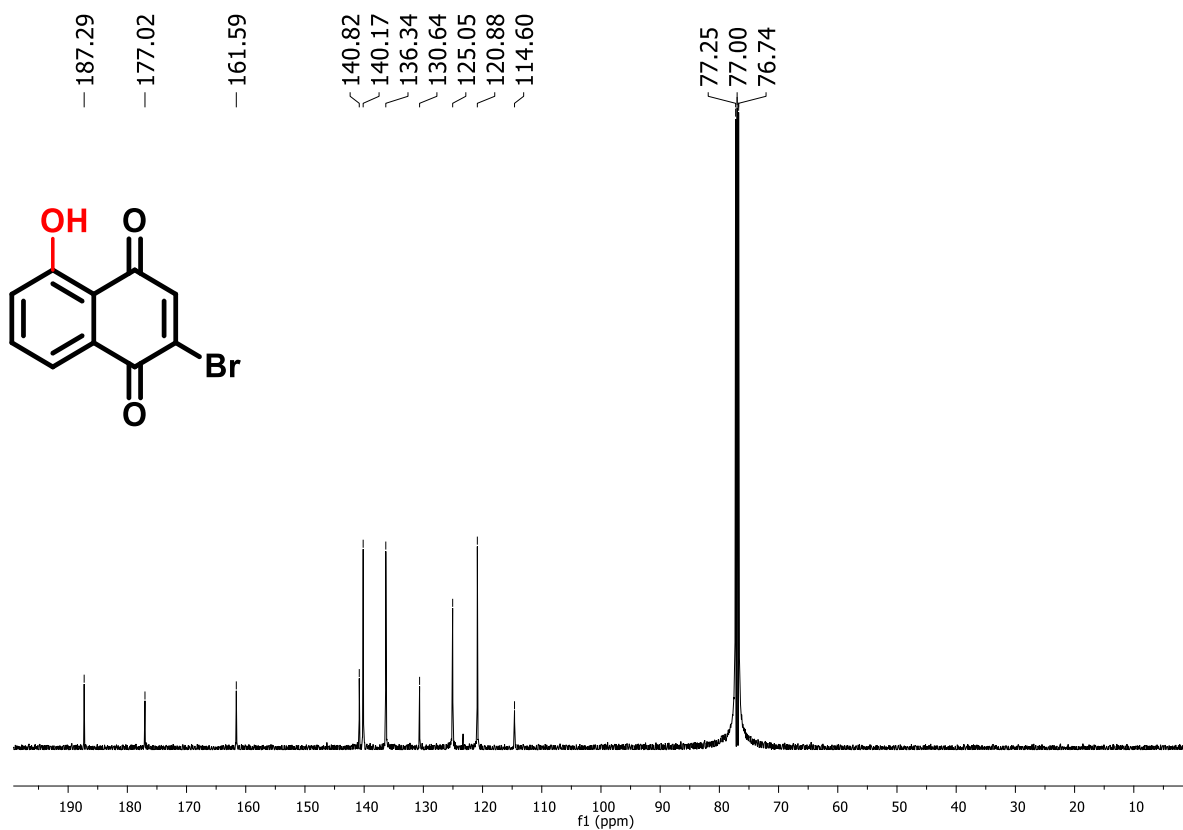


Figure 101. ¹³C NMR spectrum (75 MHz, CDCl₃) of compound 180.

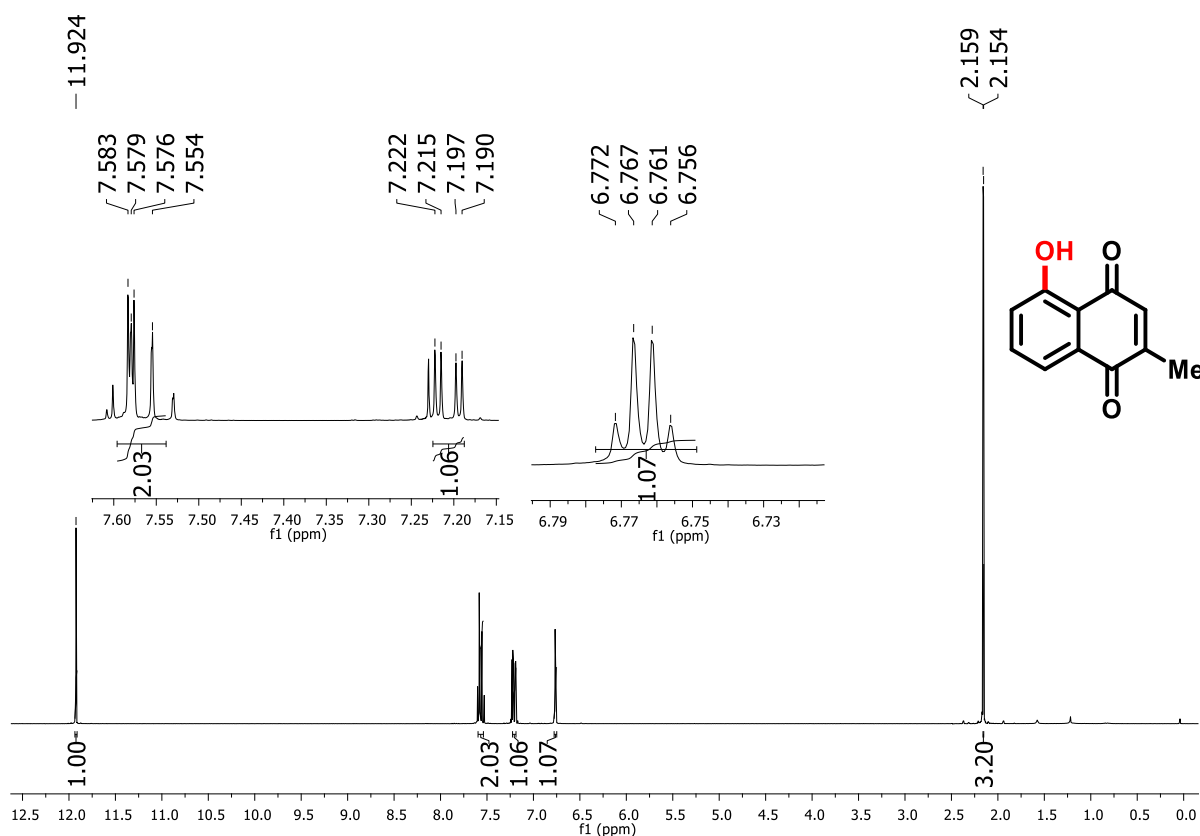


Figure 102. ^1H NMR spectrum (300 MHz, CDCl_3) of compound 186.

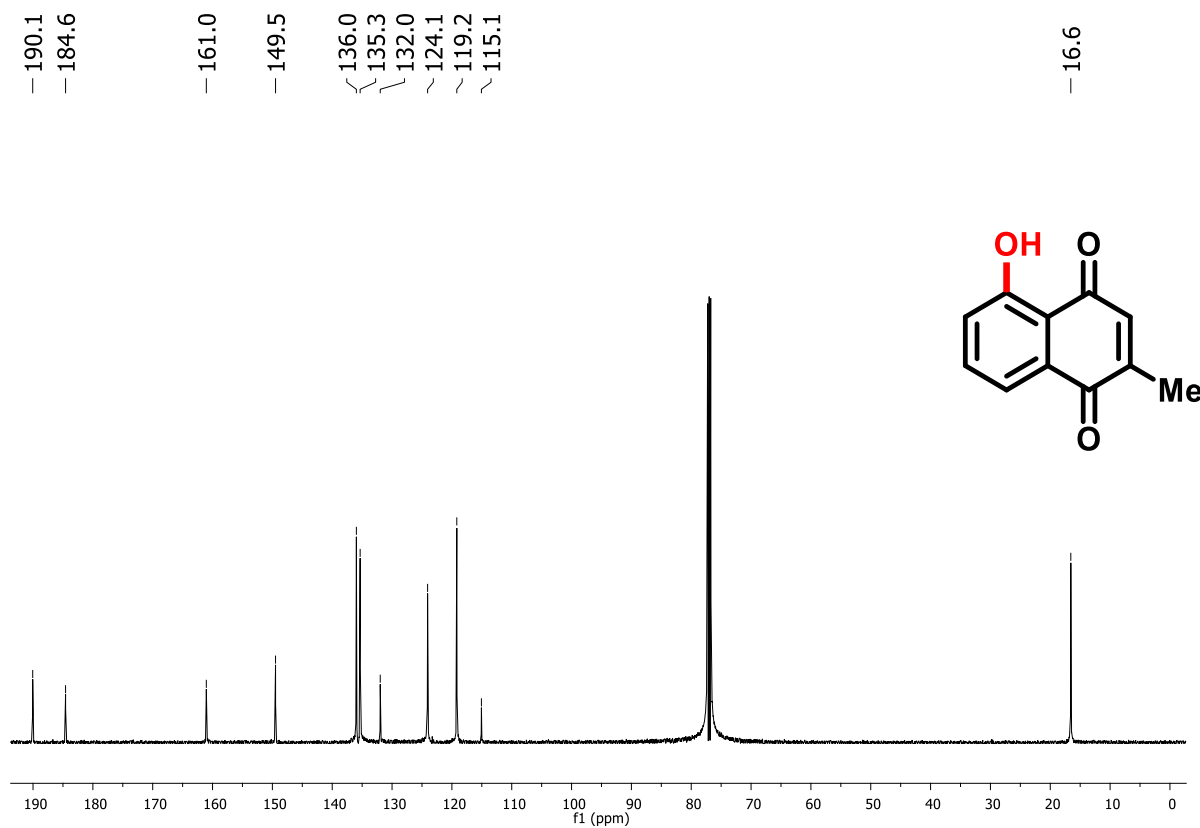


Figure 103. ^{13}C NMR spectrum (75 MHz, CDCl_3) of compound 186.

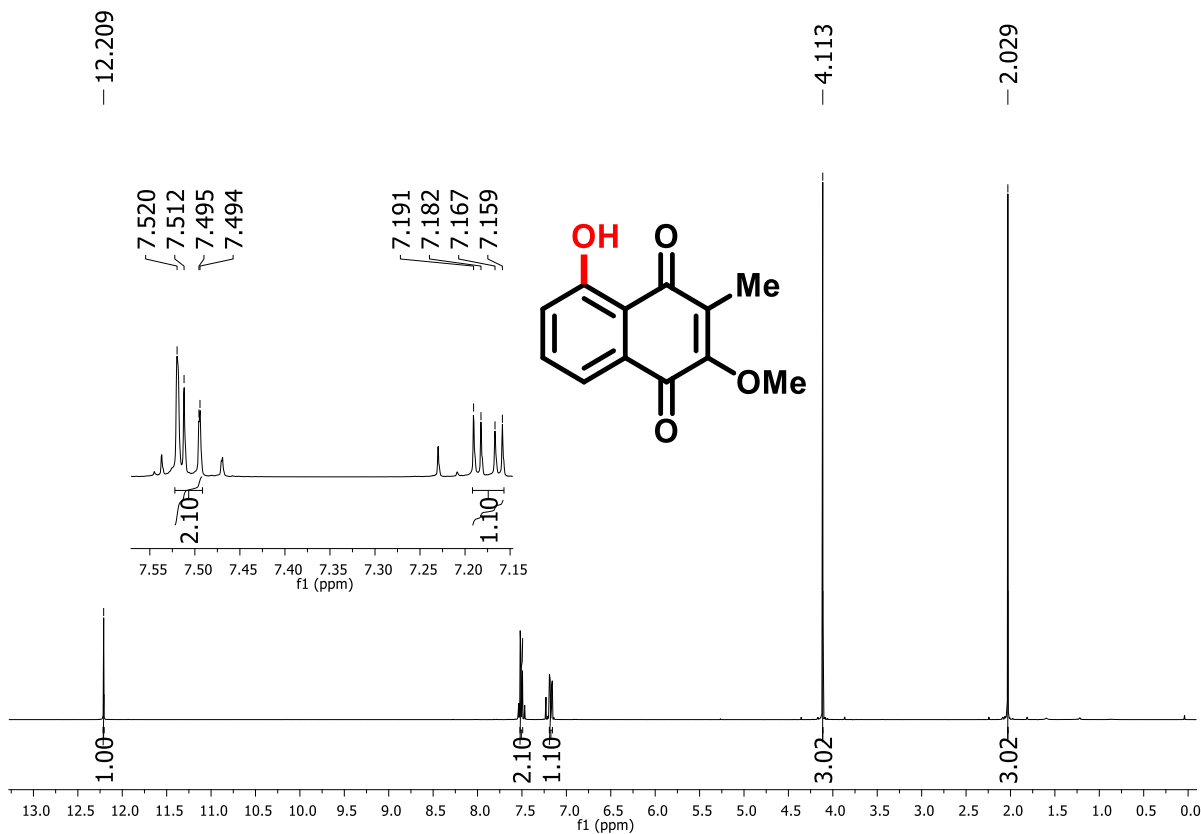


Figure 104. ¹H NMR spectrum (300 MHz, CDCl₃) of compound 191.

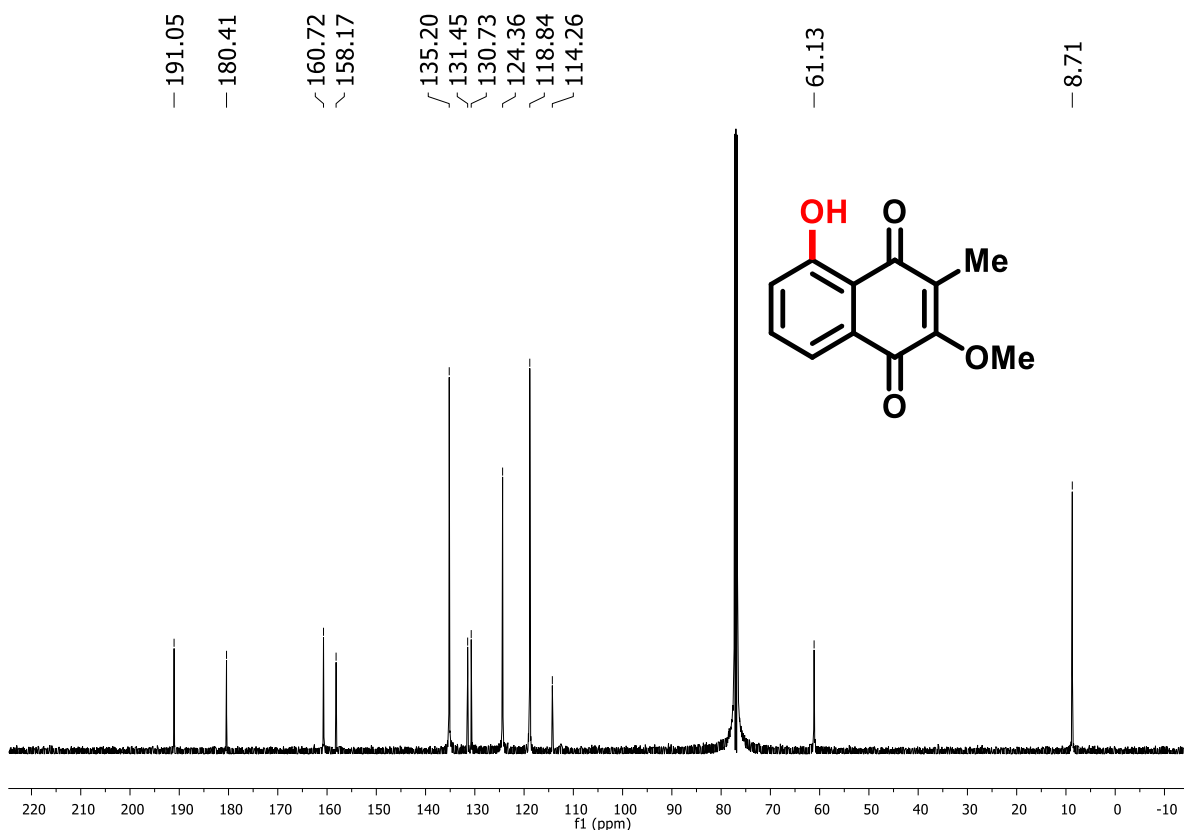


Figure 105. ¹³C NMR spectrum (75 MHz, CDCl₃) of compound 191.

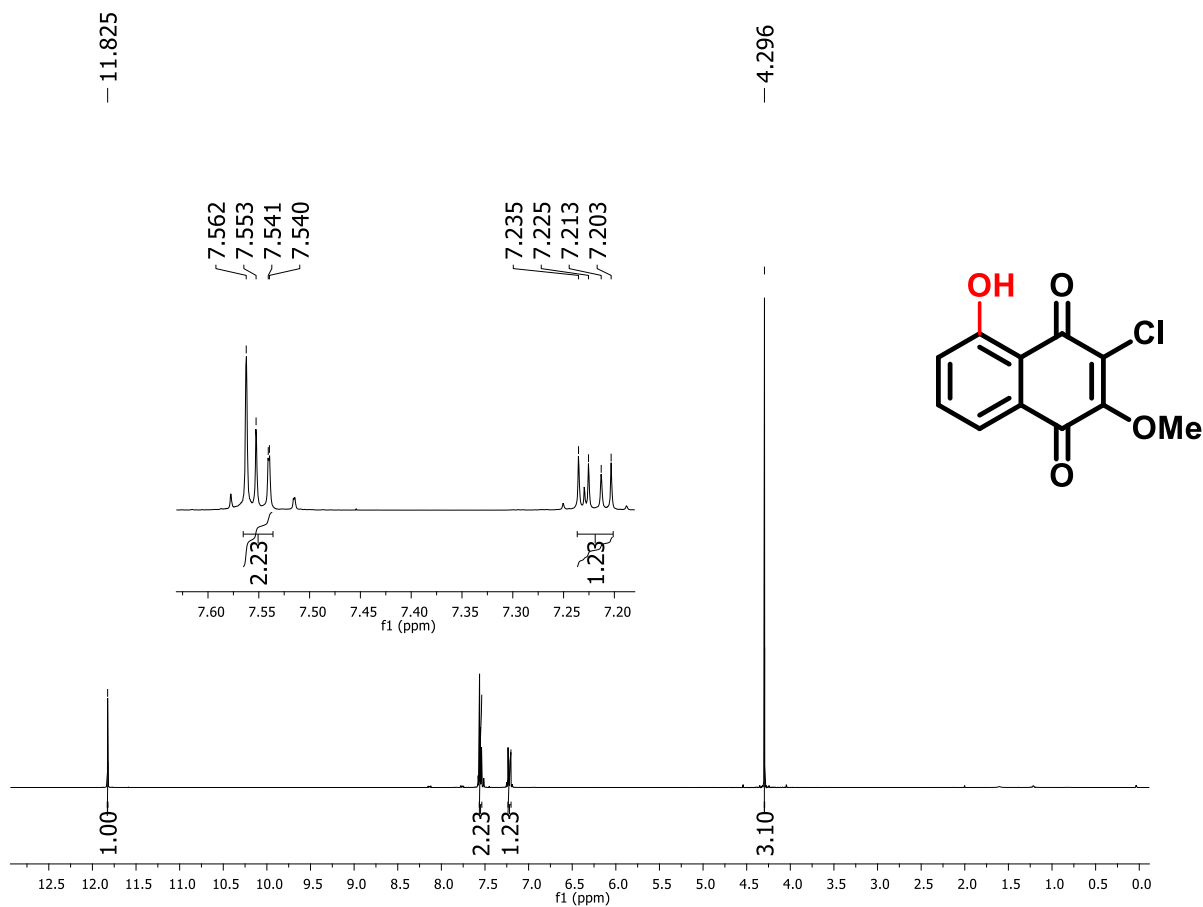


Figure 106. ^1H NMR spectrum (300 MHz, CDCl_3) of compound 192.

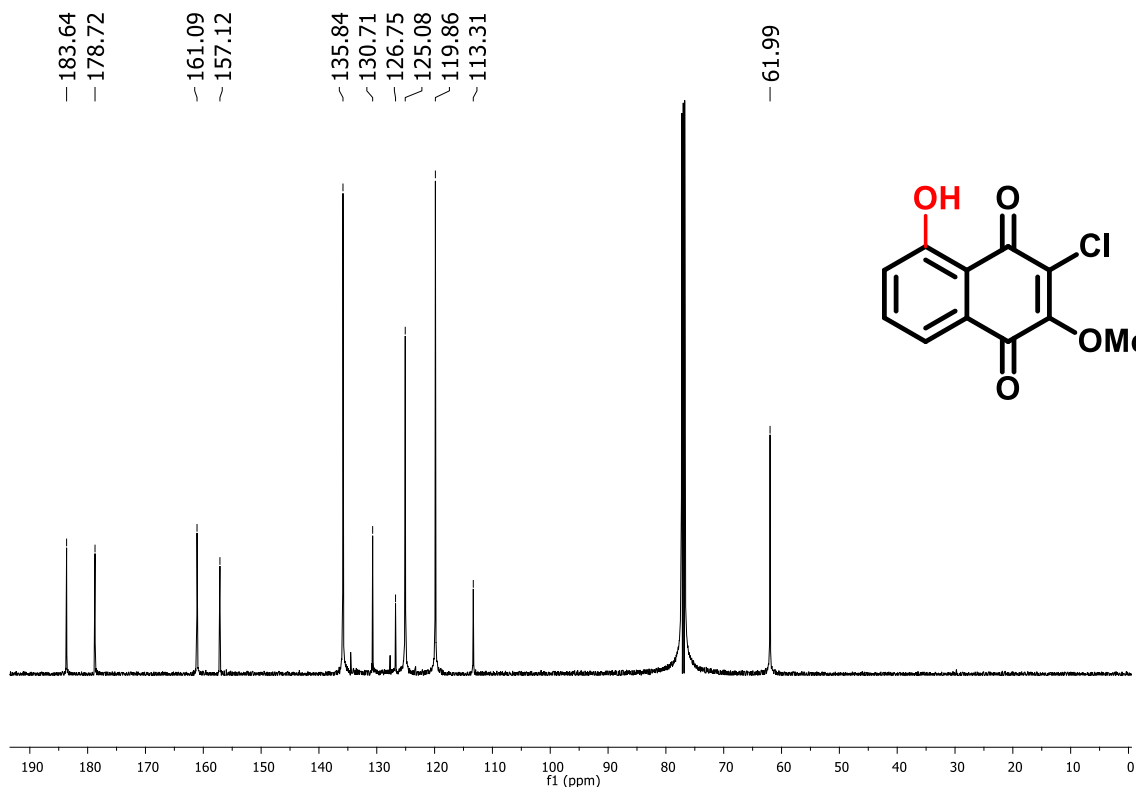


Figure 107. ^{13}C NMR spectrum (75 MHz, CDCl_3) of compound 192.

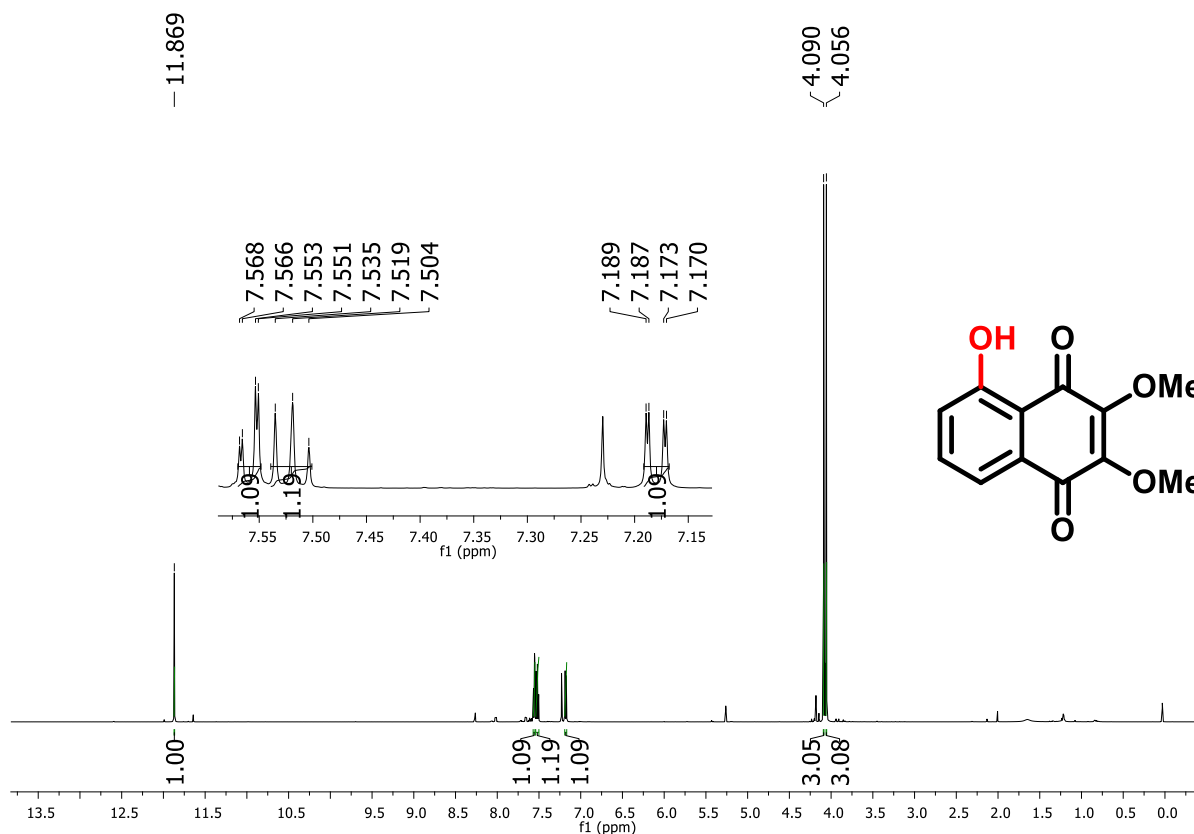


Figure 108. ^1H NMR spectrum (300 MHz, CDCl_3) of compound 193.

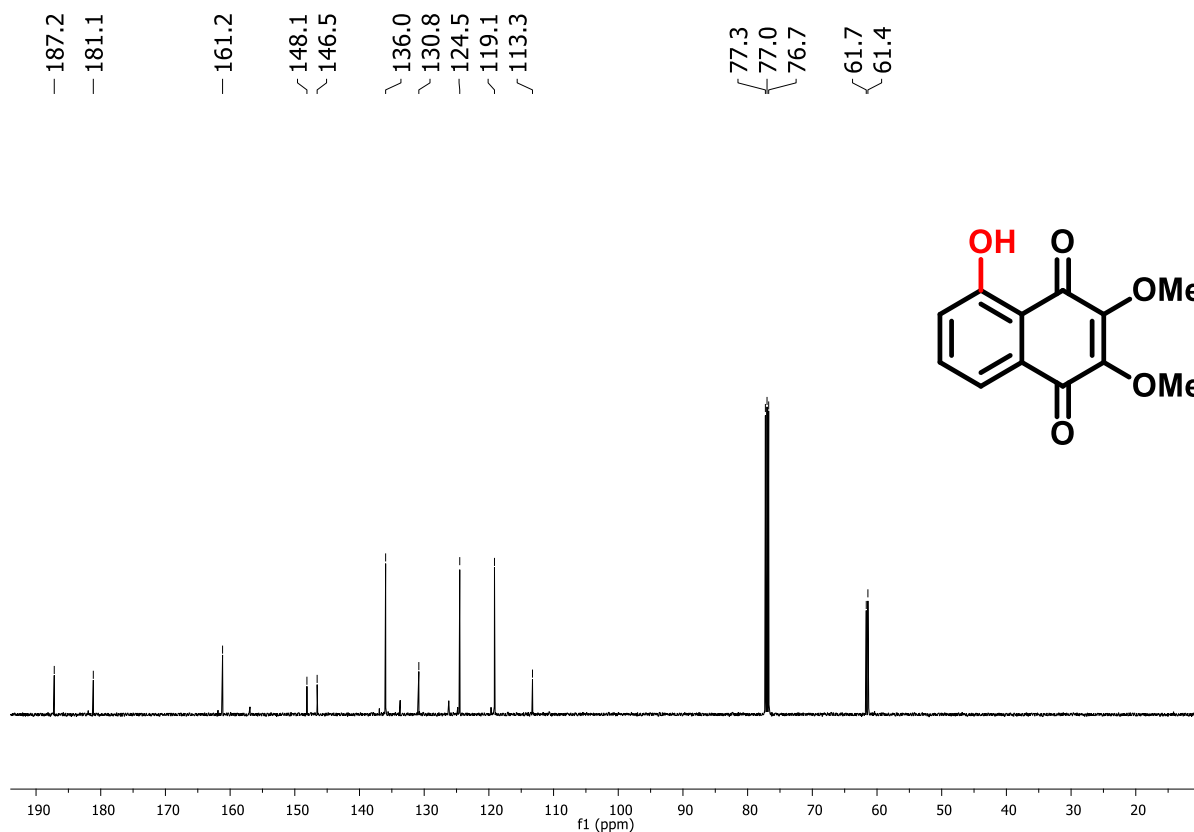


Figure 109. ^{13}C NMR spectrum (75 MHz, CDCl_3) of compound 193.

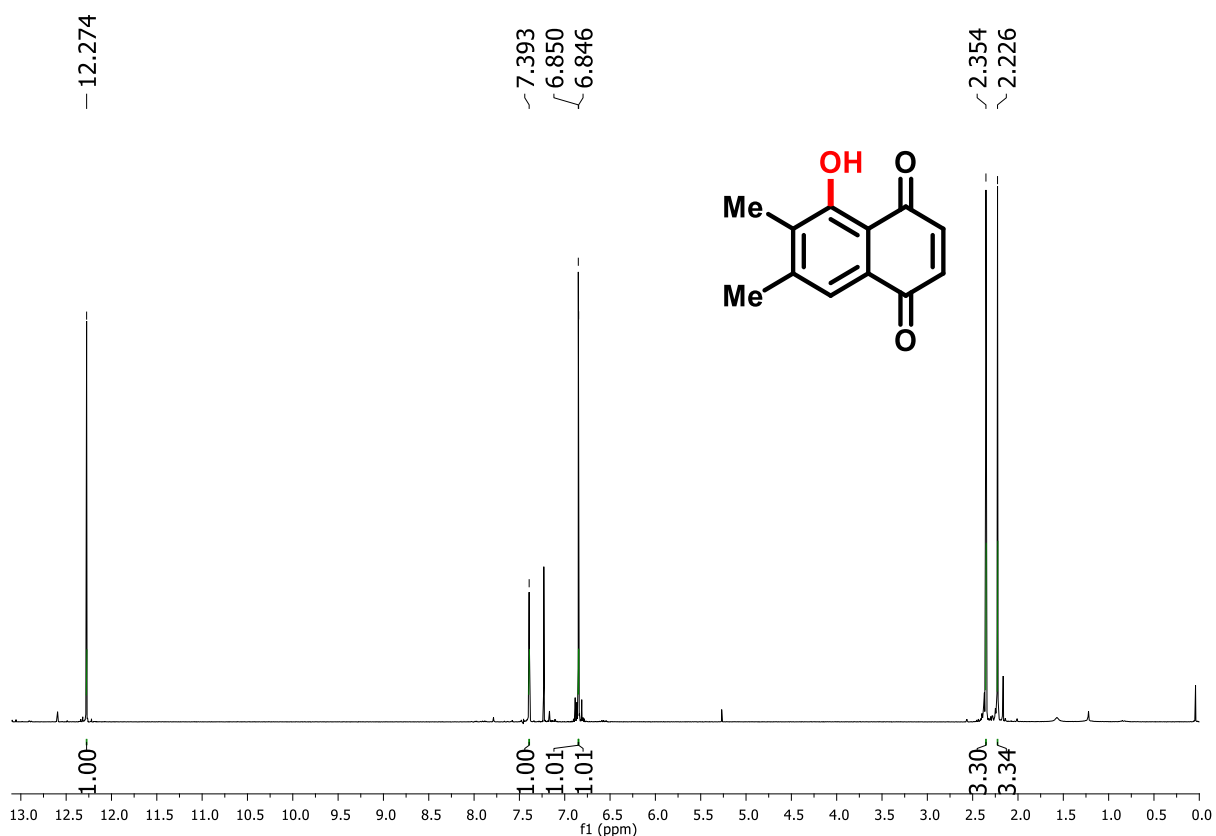


Figure 110. ^1H NMR spectrum (300 MHz, CDCl_3) of compound 194.

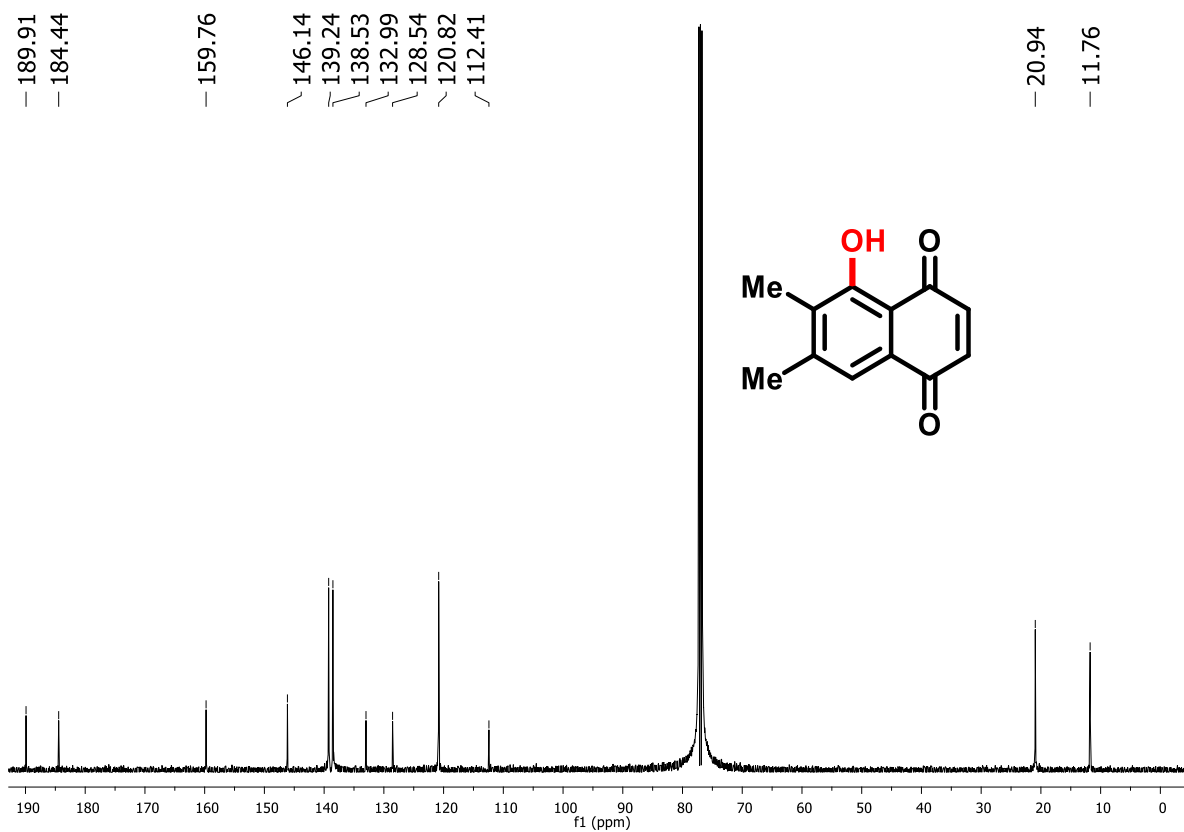


Figure 111. ^{13}C NMR spectrum (75 MHz, CDCl_3) of compound 194.

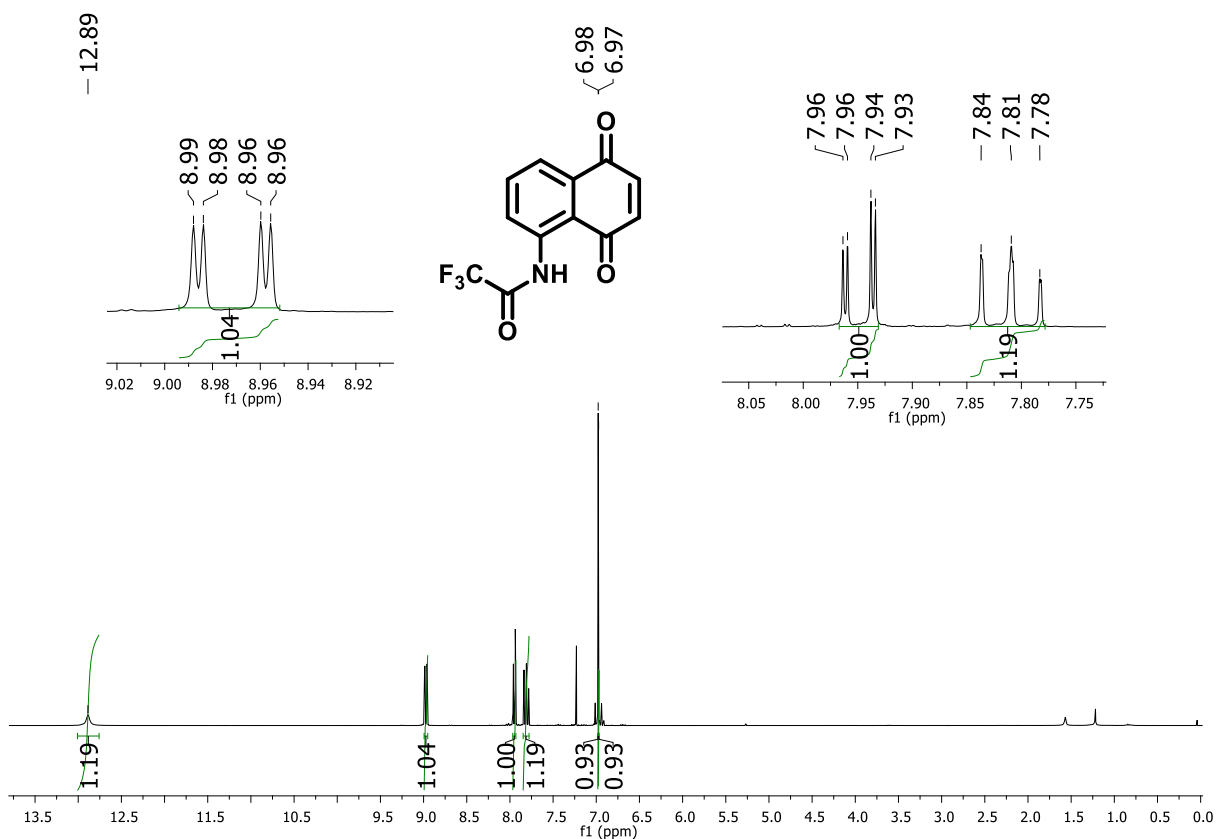


Figure 112. ¹H NMR spectrum (300 MHz, CDCl₃) of compound 196.

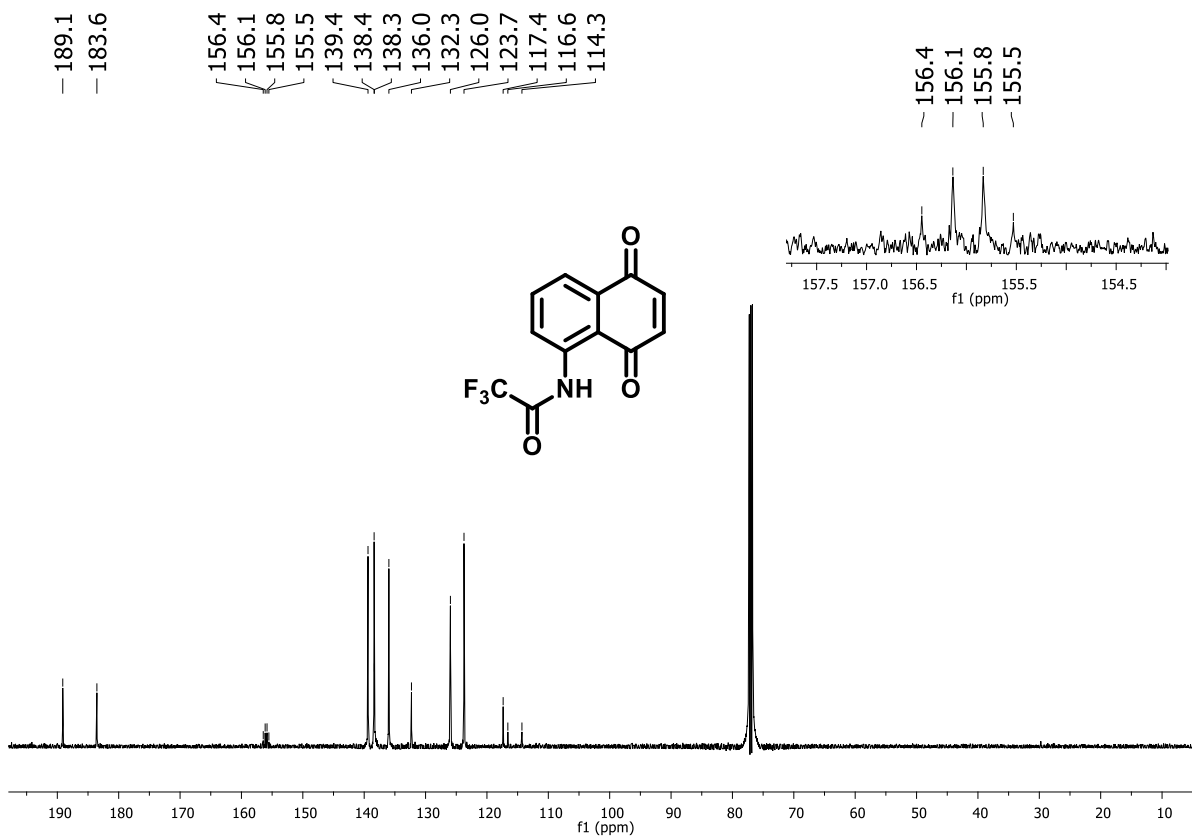


Figure 113. ¹³C NMR spectrum (75 MHz, CDCl₃) of compound 196.

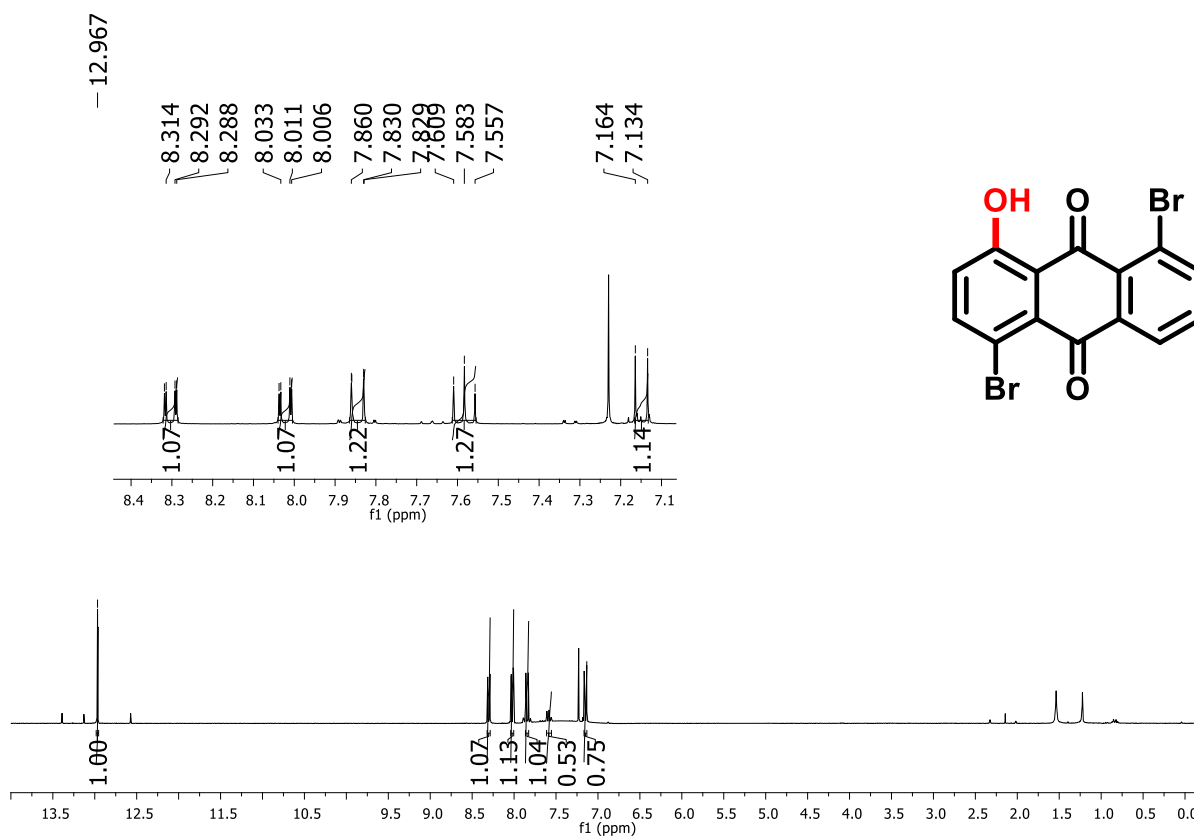


Figure 114. ¹H NMR spectrum (300 MHz, CDCl₃) of compound 198.

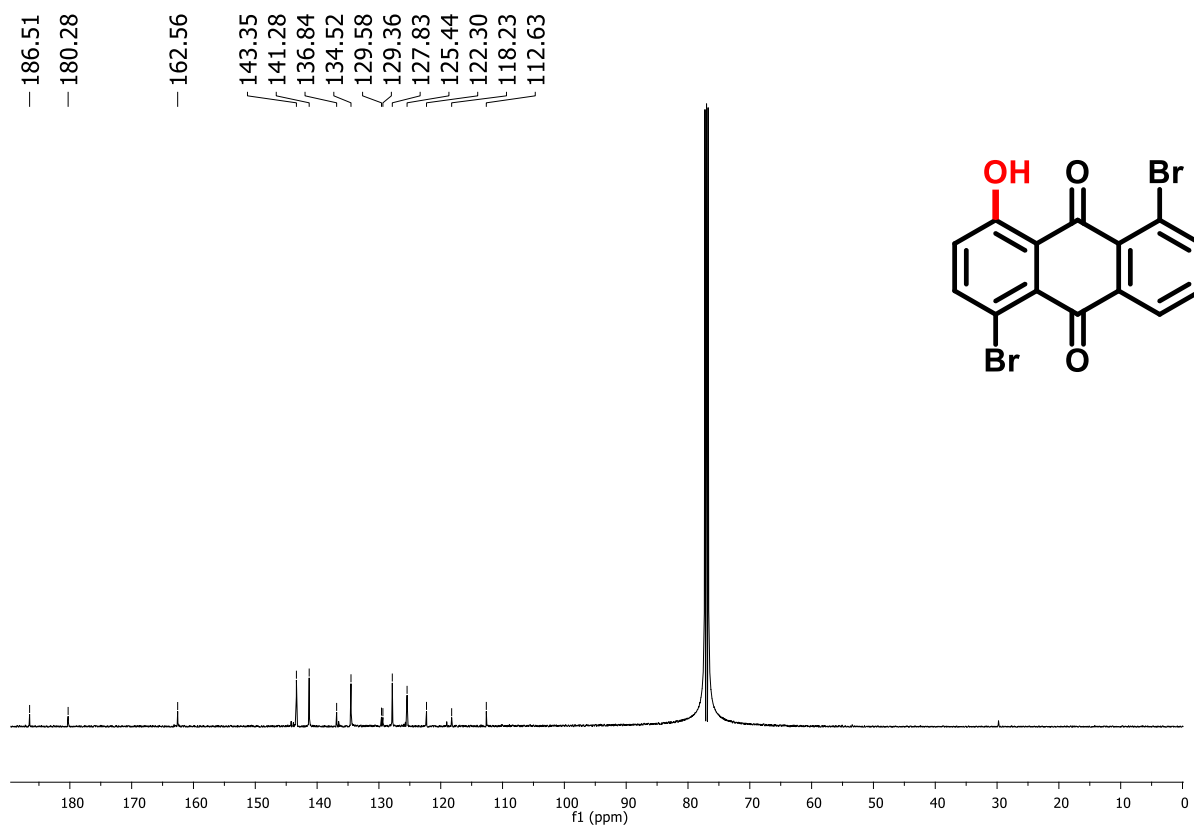


Figure 115. ¹³C NMR spectrum (75 MHz, CDCl₃) of compound 198.

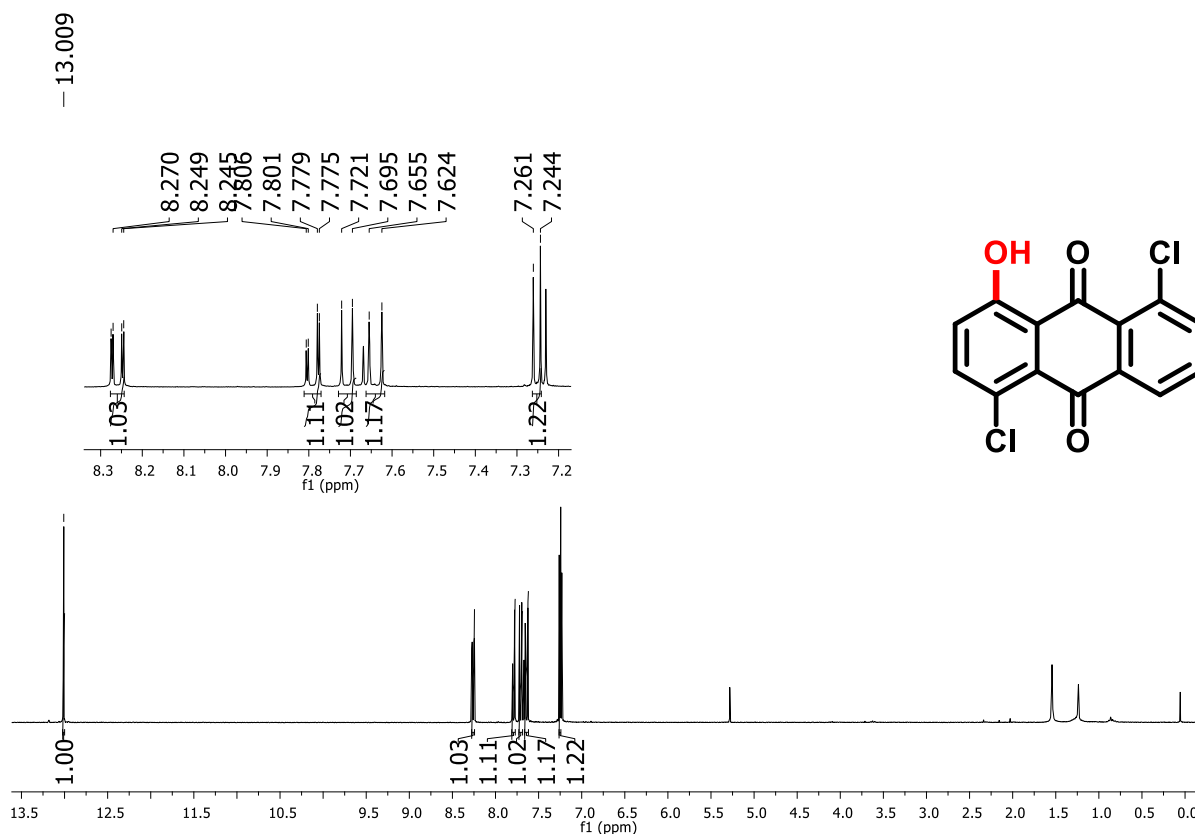


Figure 116. ^1H NMR spectrum (300 MHz, CDCl_3) of compound 199.

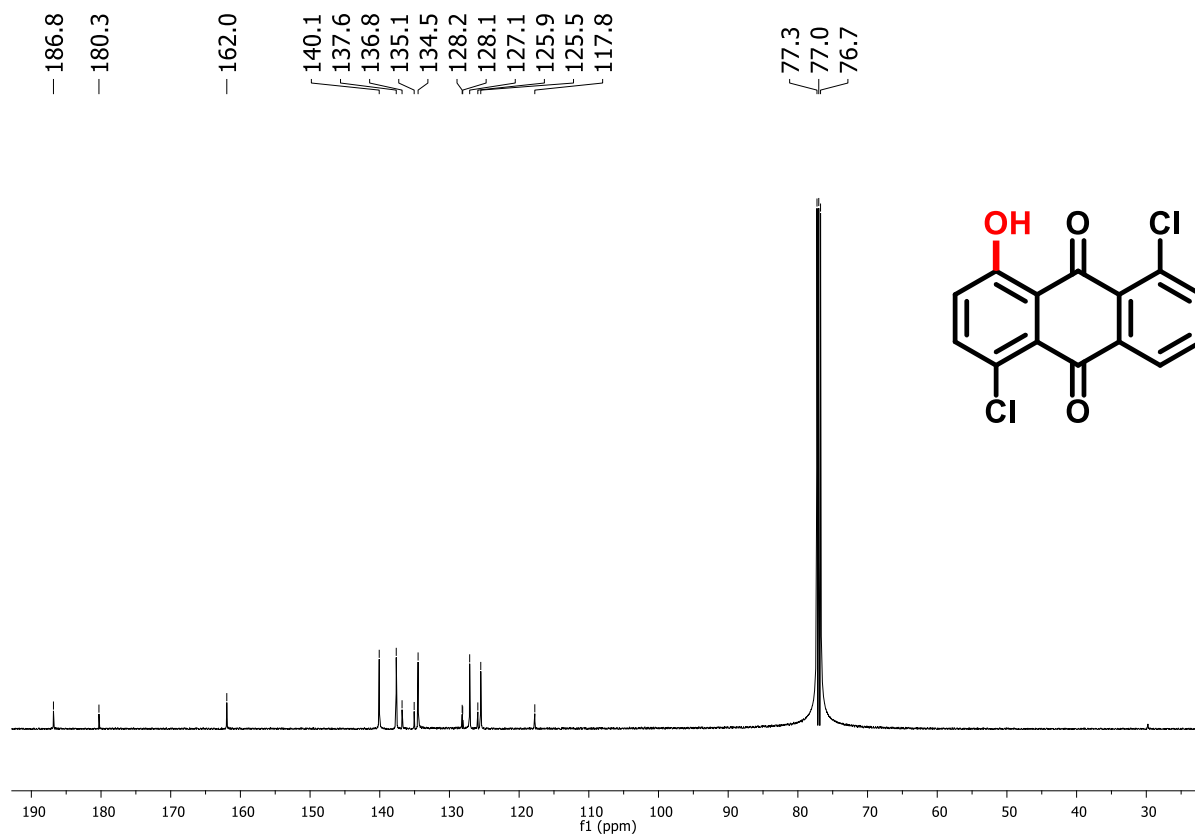


Figure 117. ^{13}C NMR spectrum (75 MHz, CDCl_3) of compound 199.

Spectra of aryl-lapimidazole

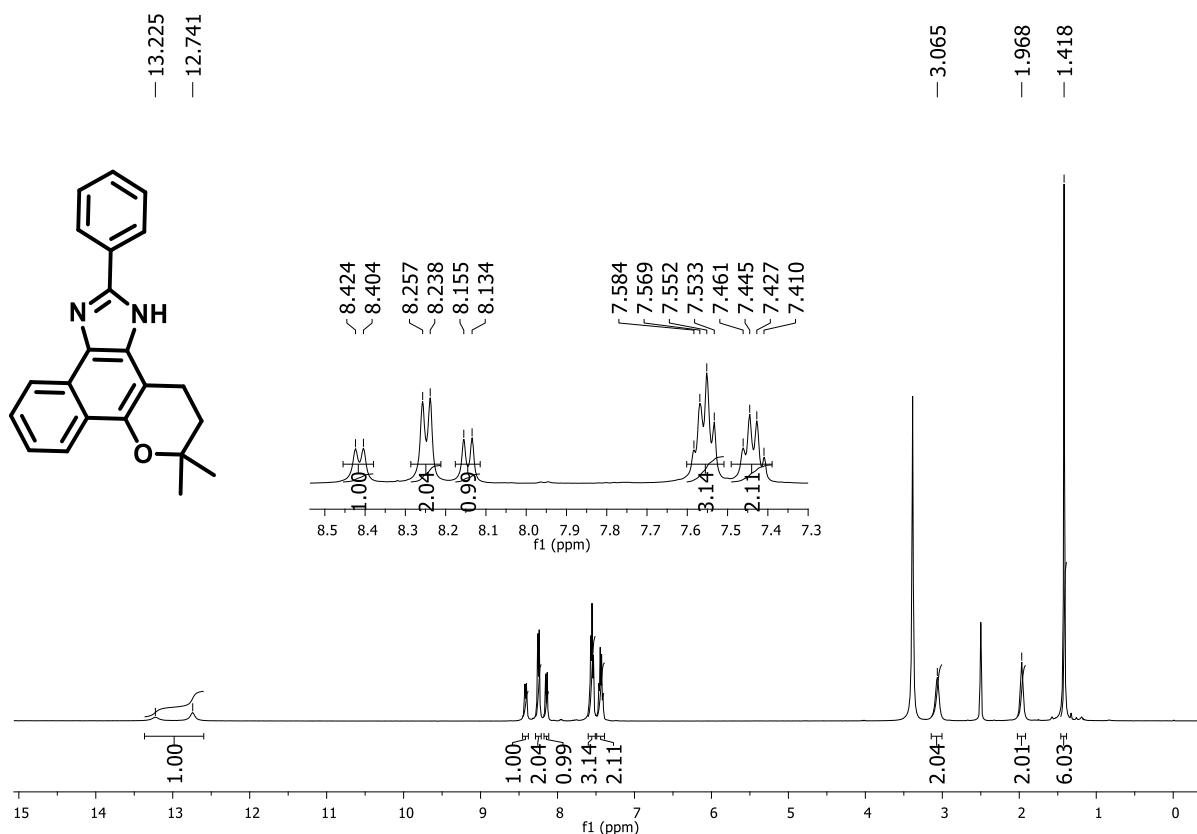


Figure 118. ¹H NMR spectrum (400 MHz, DMSO-*d*₆) of compound 234.

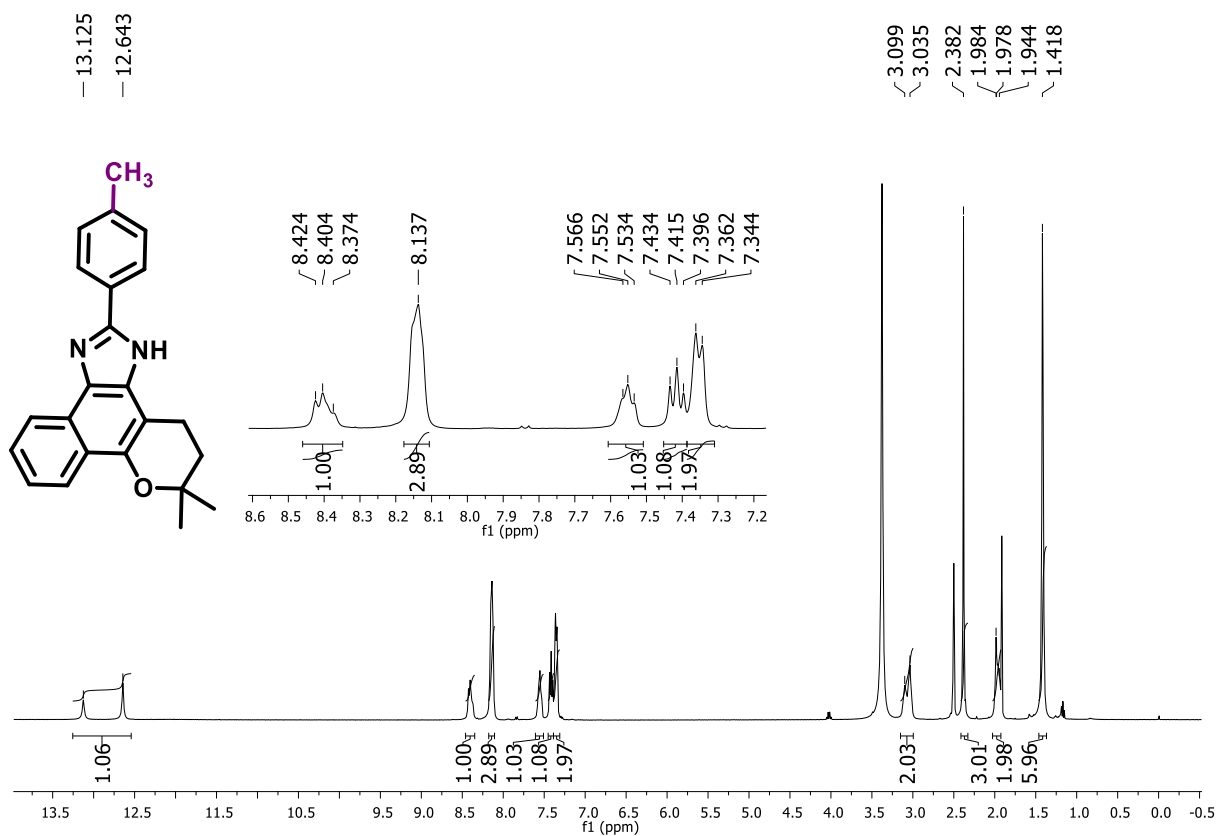


Figure 119. ¹H NMR spectrum (400 MHz, DMSO-*d*₆) of compound 237.

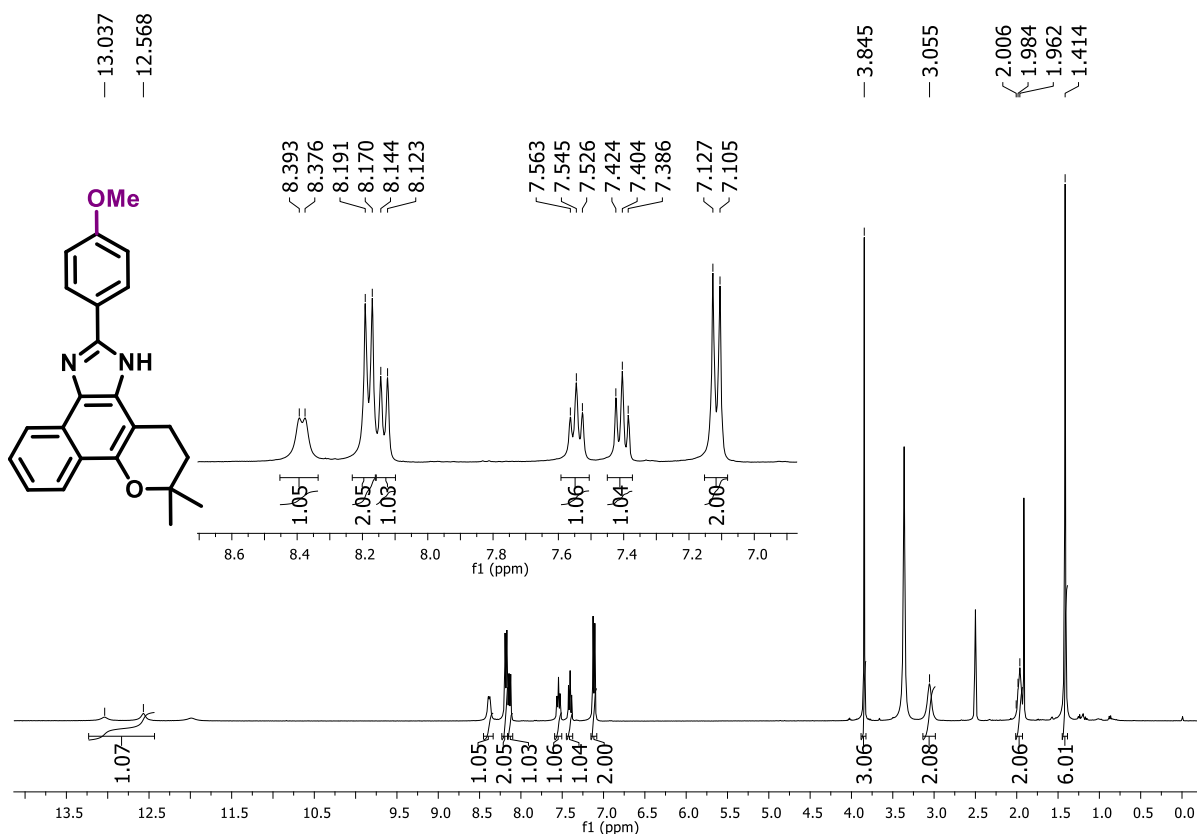


Figure 120. ¹H NMR spectrum (400 MHz, DMSO-*d*₆) of compound 238.

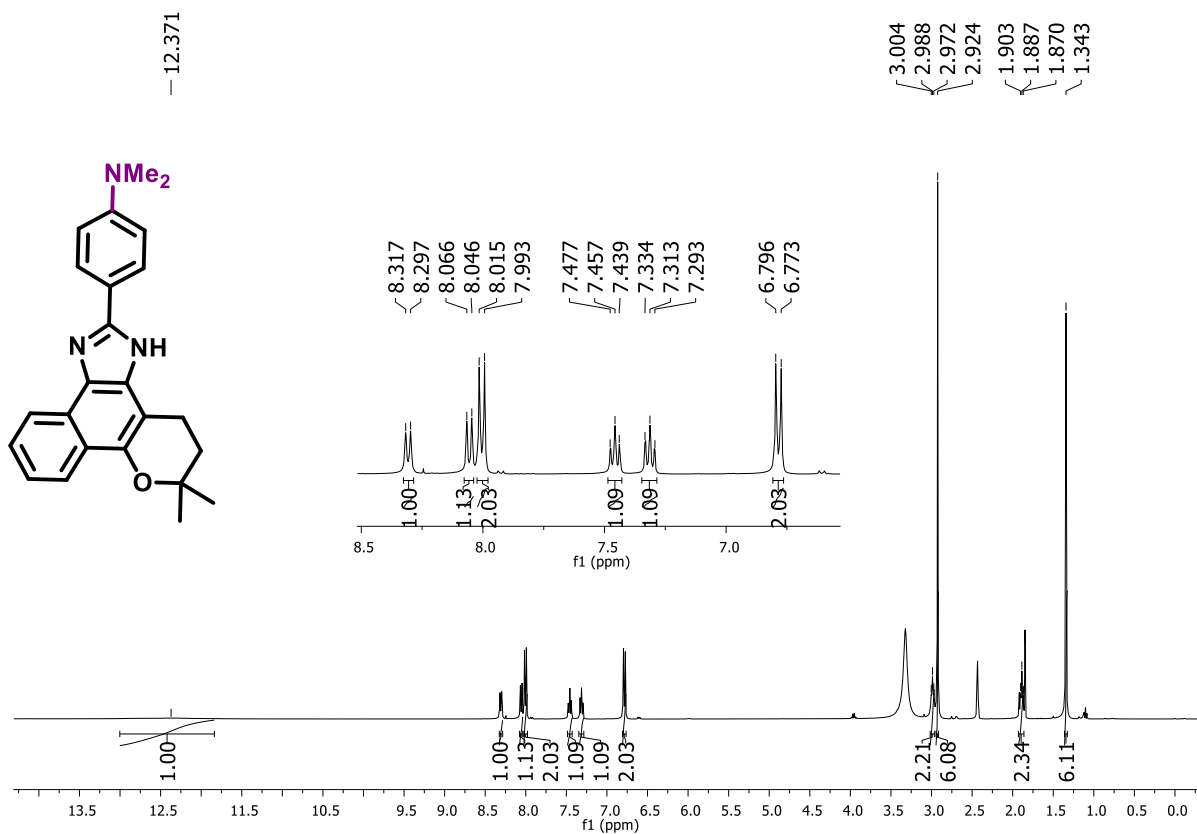


Figure 121. ¹H NMR spectrum (400 MHz, DMSO-*d*₆) of compound 239.

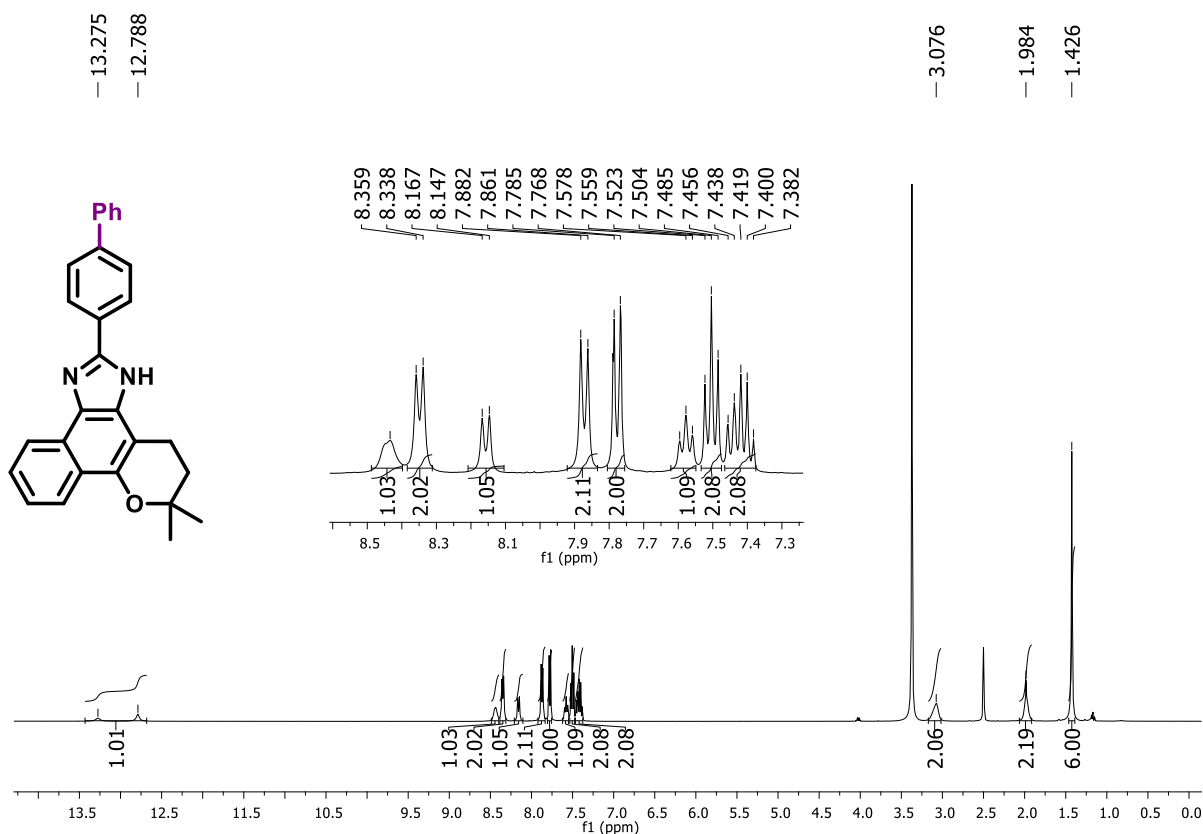


Figure 122. ¹H NMR spectrum (400 MHz, DMSO-*d*₆) of compound 240.

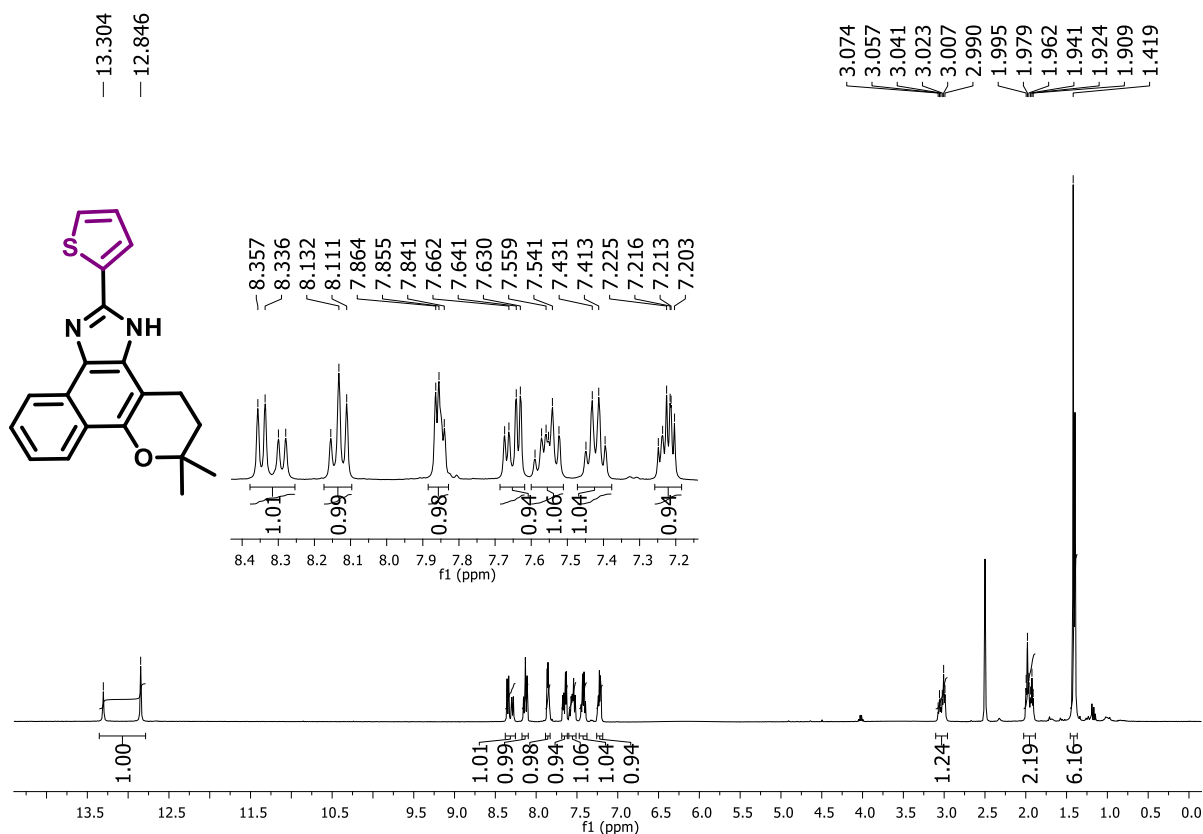


Figure 123. ¹H NMR spectrum (400 MHz, DMSO-*d*₆) of compound 241.

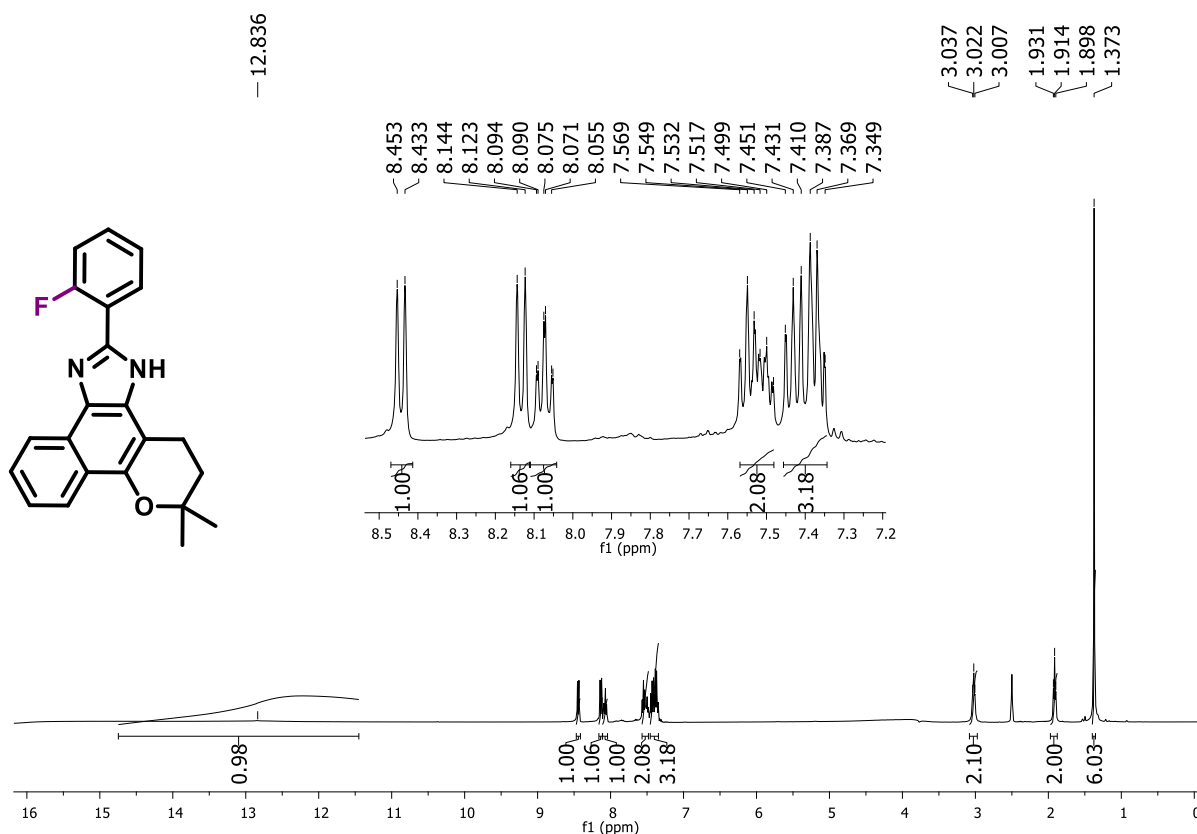


Figure 124. ¹H NMR spectrum (400 MHz, DMSO-*d*₆) of compound 242.

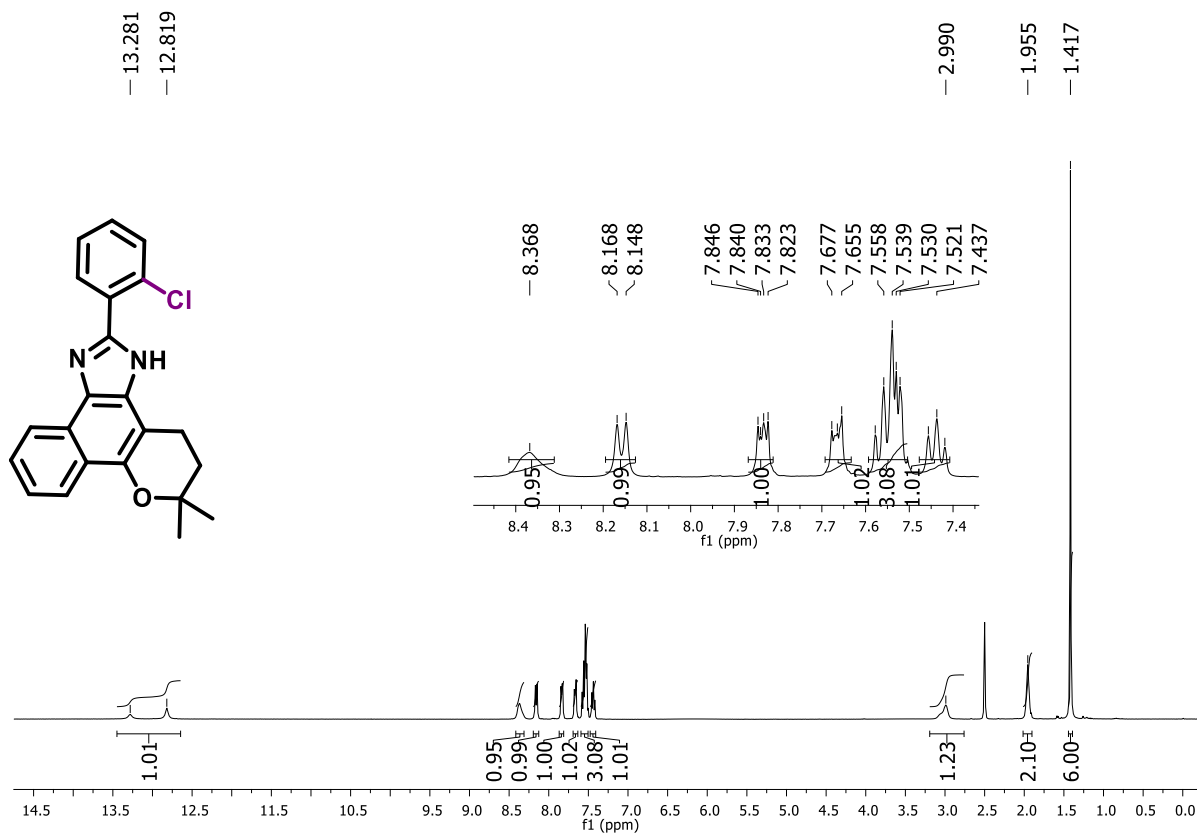


Figure 125. ¹H NMR spectrum (400 MHz, DMSO-*d*₆) of compound 243.

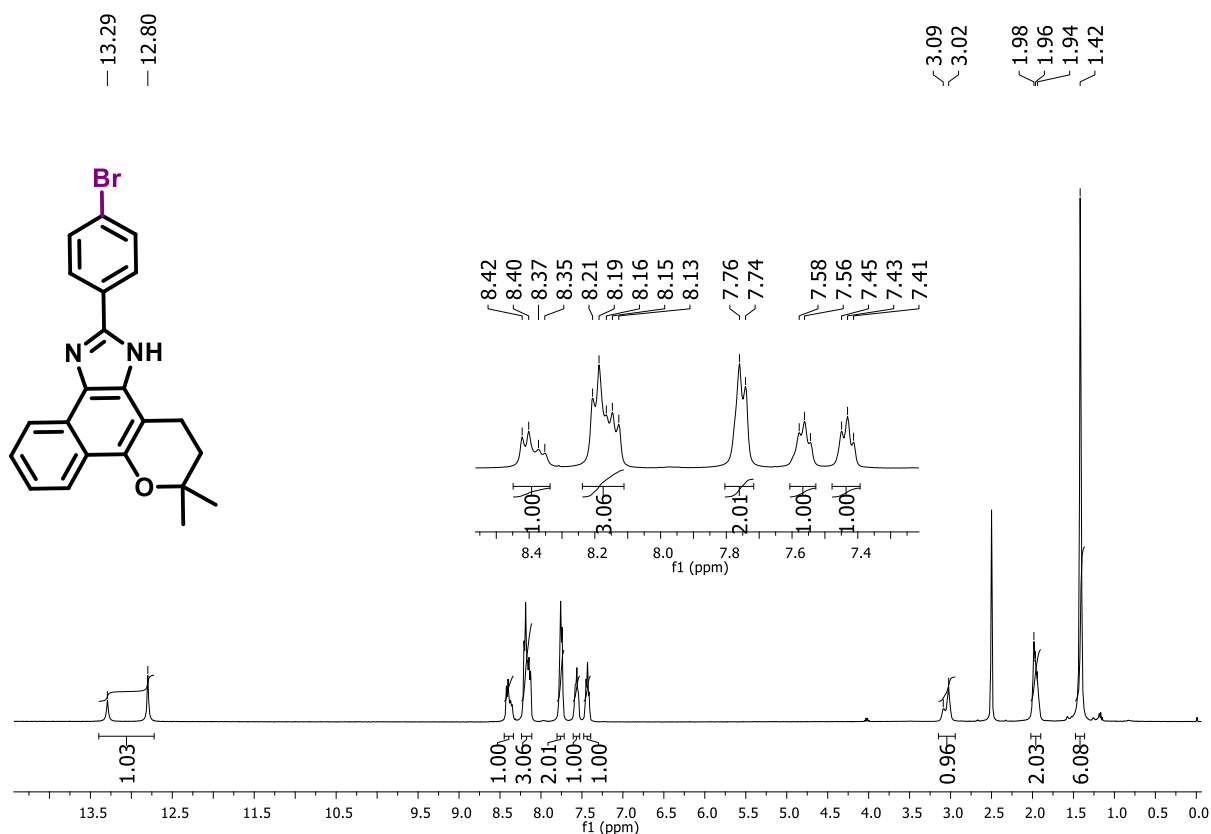


Figure 126. ¹H NMR spectrum (400 MHz, DMSO-*d*₆) of compound 244.

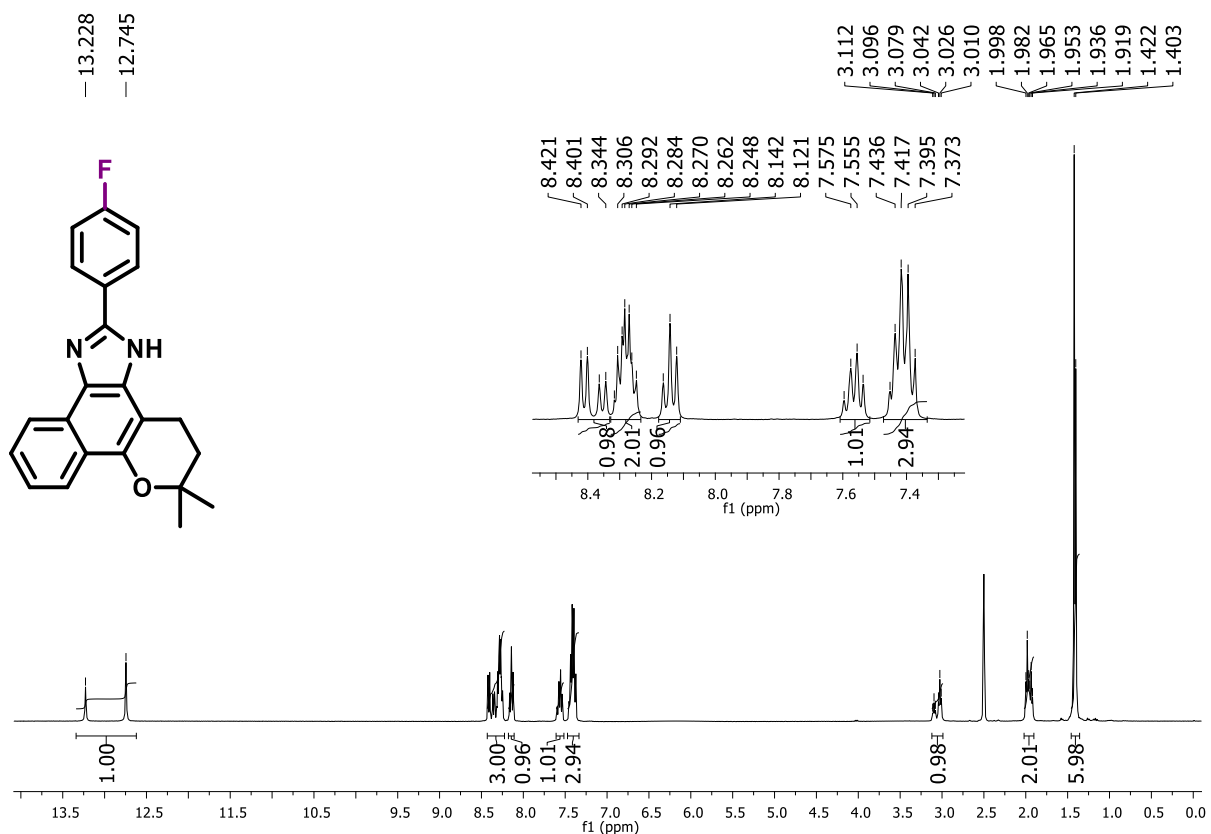


Figure 127. ¹H NMR spectrum (400 MHz, DMSO-*d*₆) of compound 245.

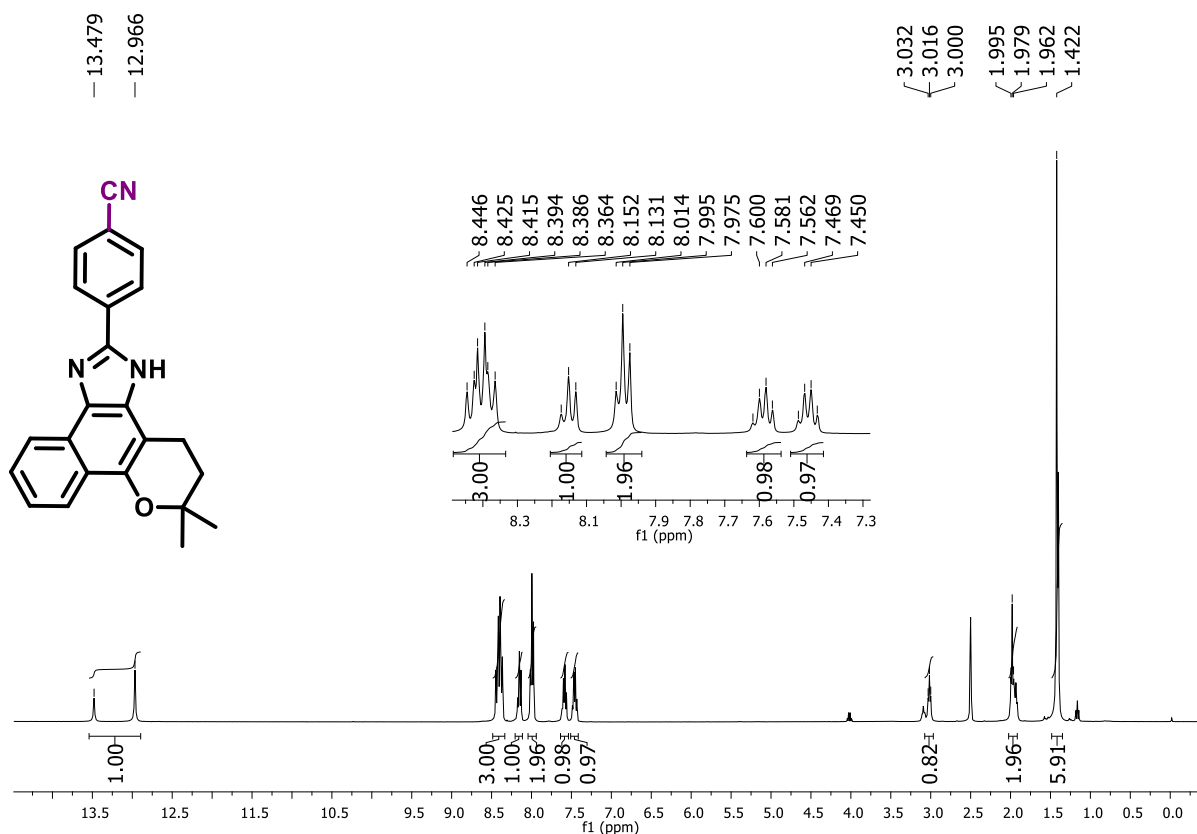


Figure 128. ¹H NMR spectrum (400 MHz, DMSO-*d*₆) of compound 246.

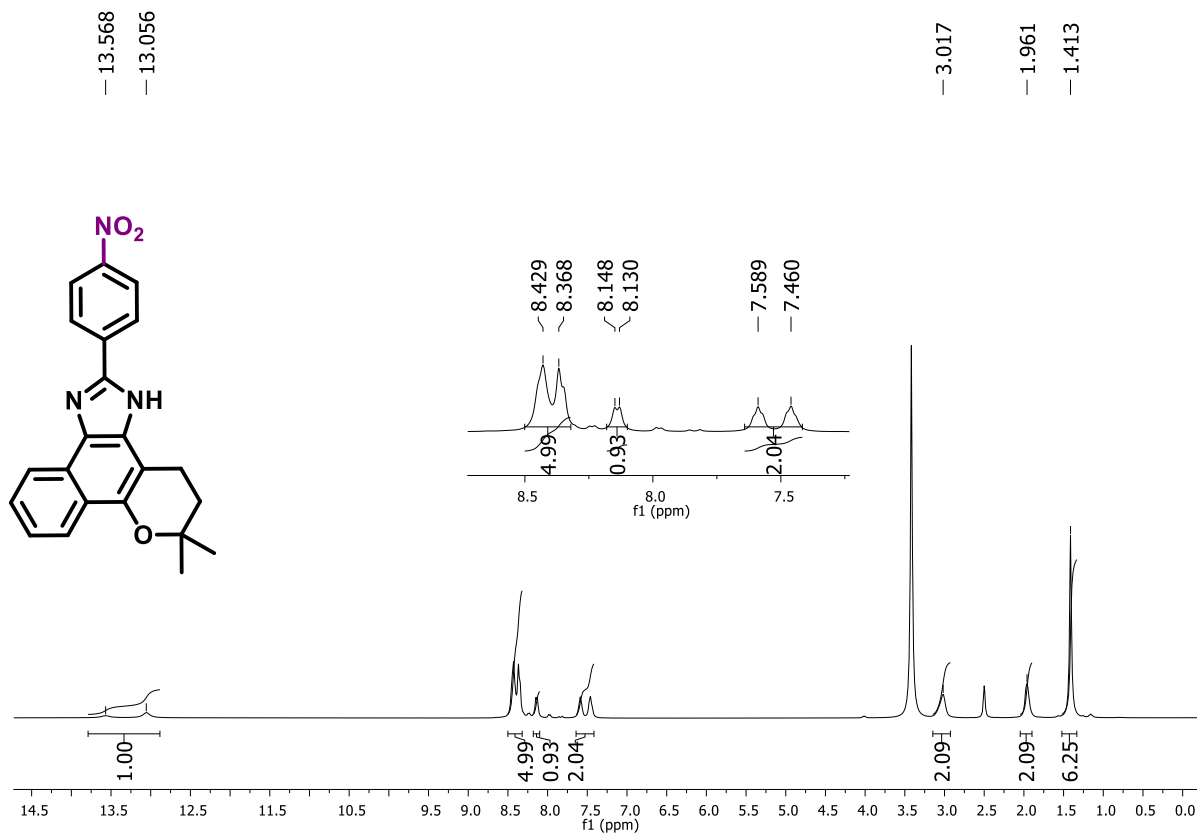


Figure 129. ¹H NMR spectrum (400 MHz, DMSO-*d*₆) of compound 247.

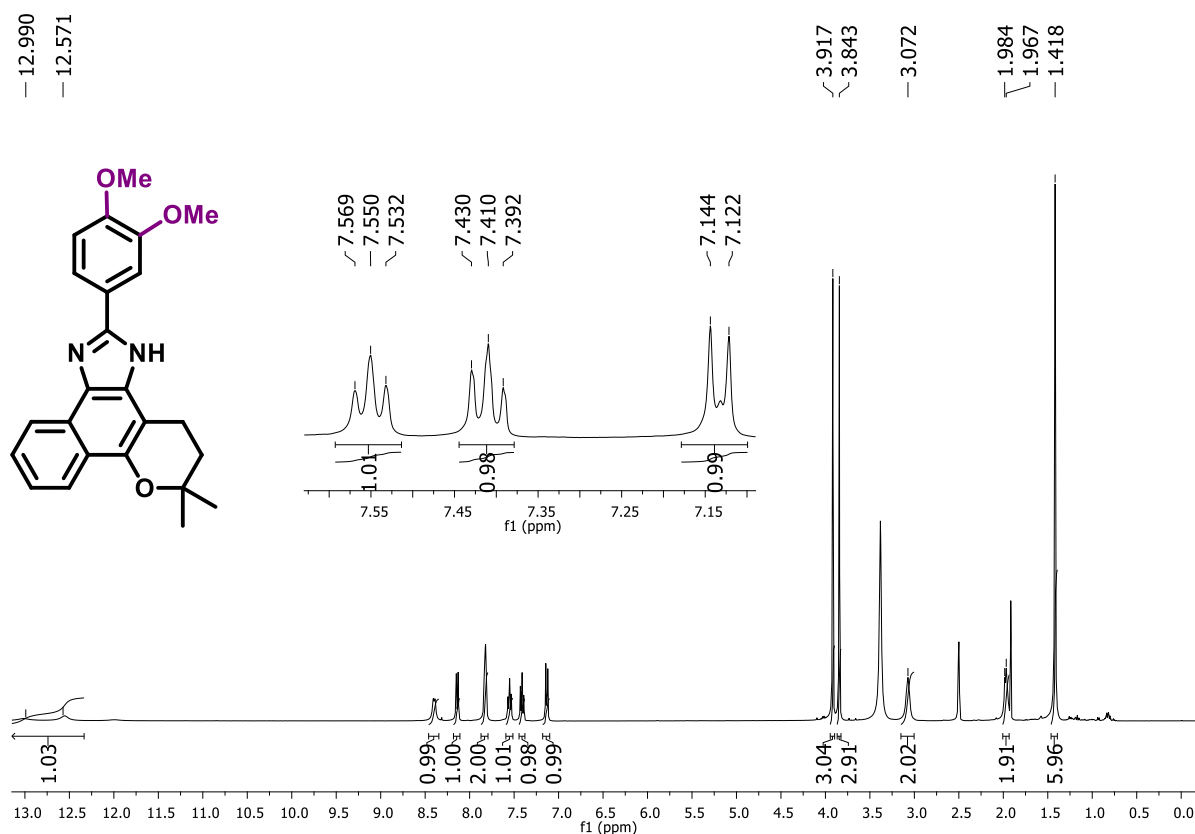


Figure 130. ¹H NMR spectrum (400 MHz, DMSO-*d*₆) of compound 248.

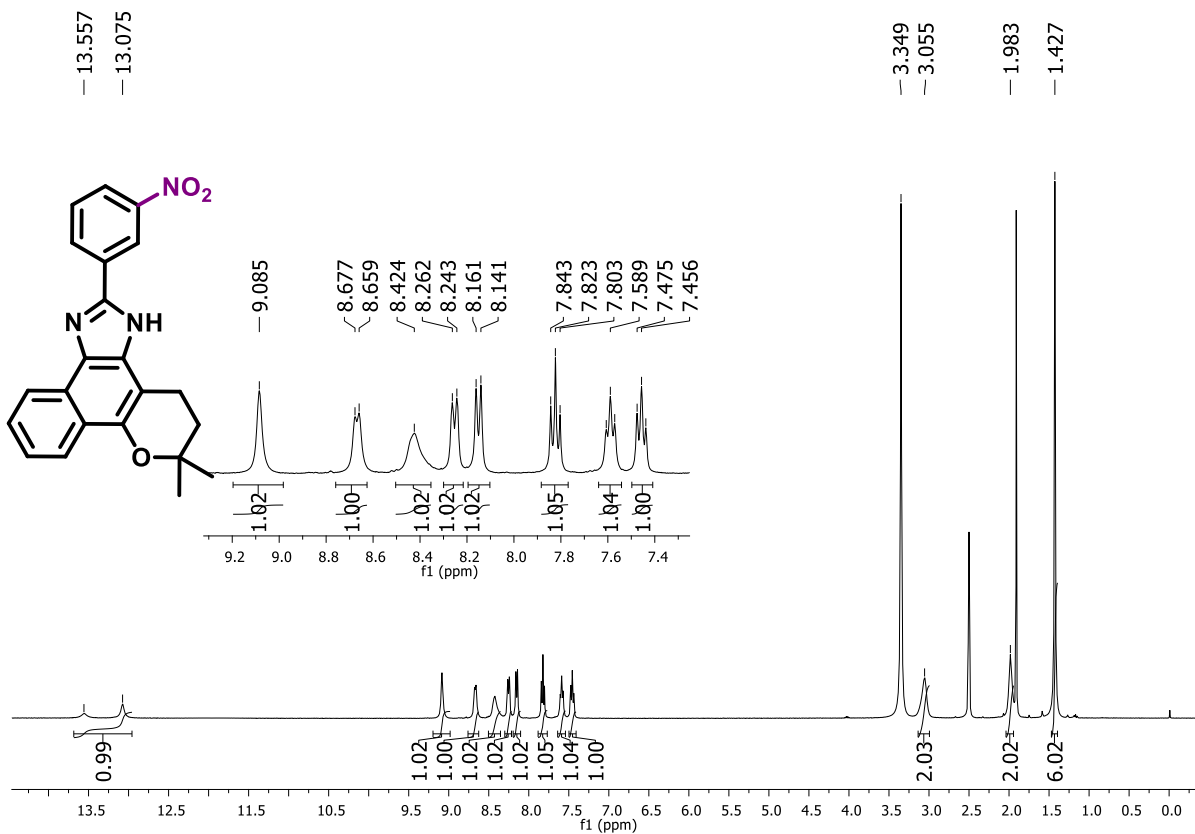


Figure 131. ¹H NMR spectrum (400 MHz, DMSO-*d*₆) of compound 249.

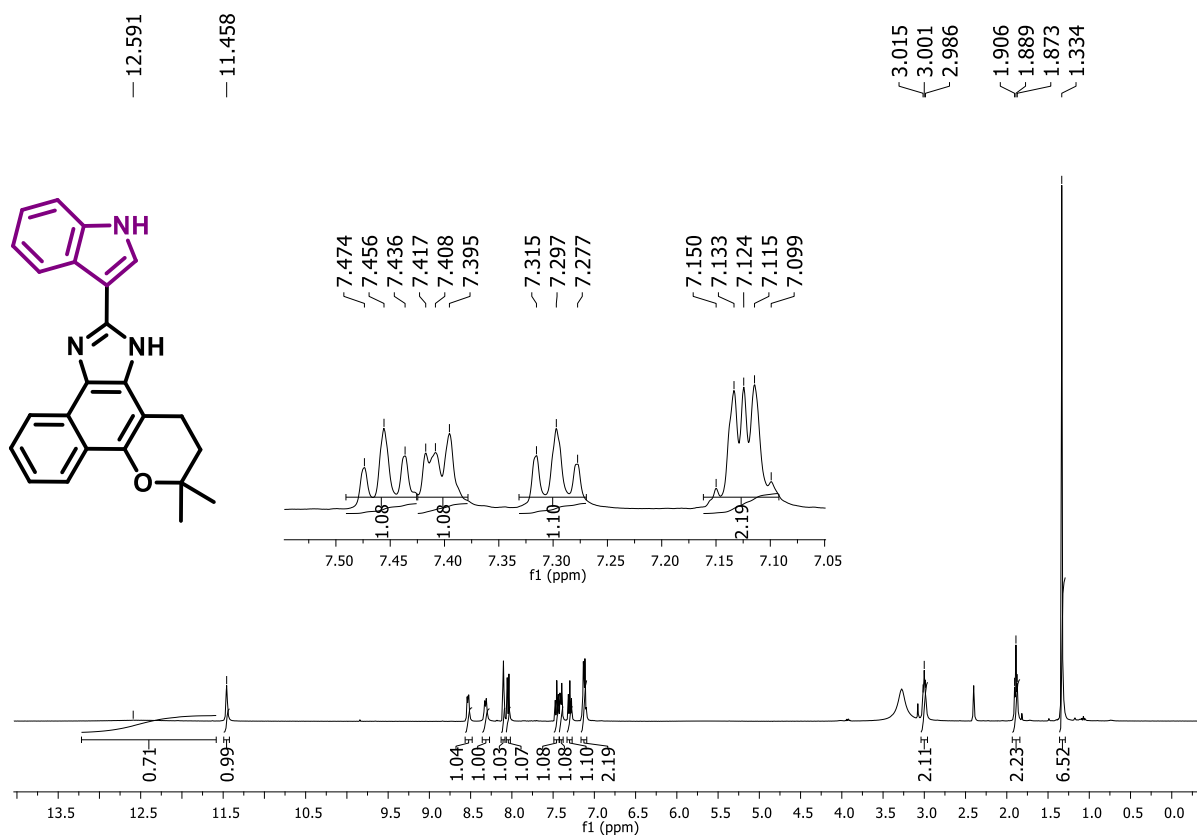


Figure 132. ^1H NMR spectrum (400 MHz, $\text{DMSO-}d_6$) of compound 250.

Spectra of annulated products

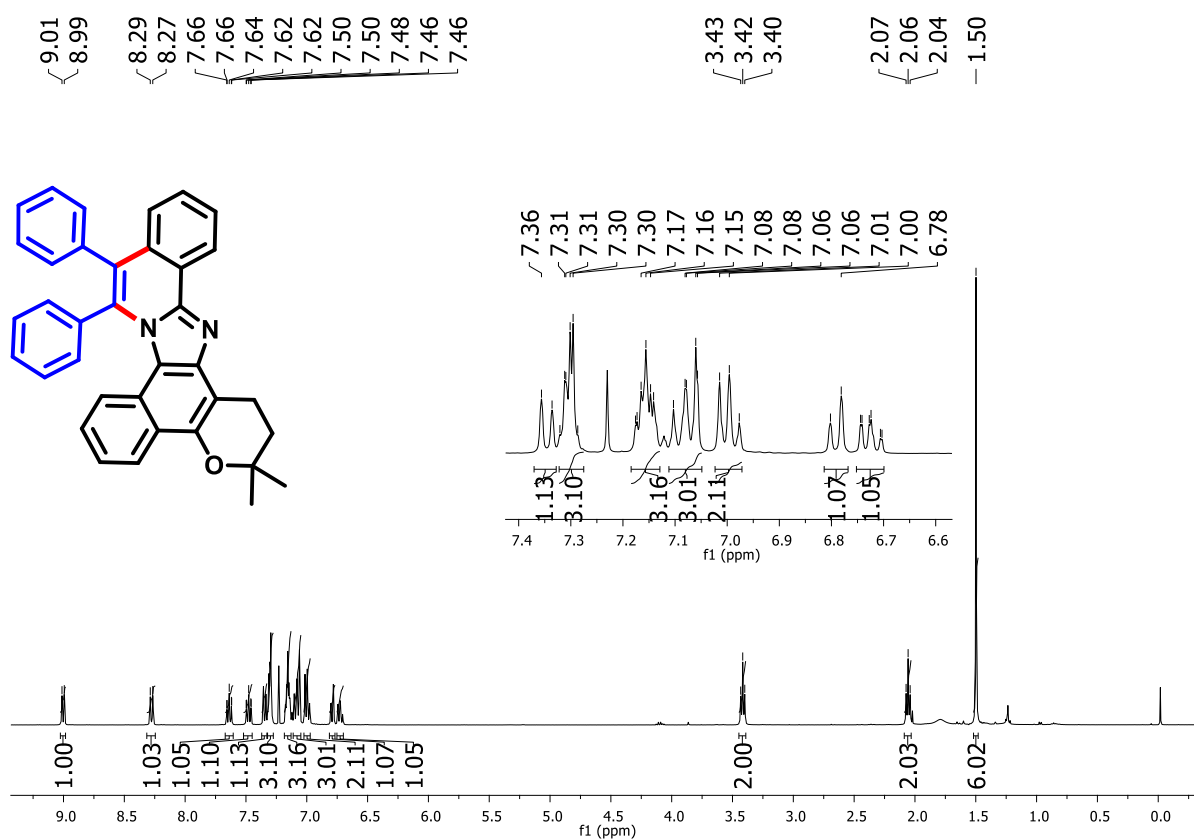


Figure 133. ^1H NMR spectrum (400 MHz, CDCl_3) of compound **235**.

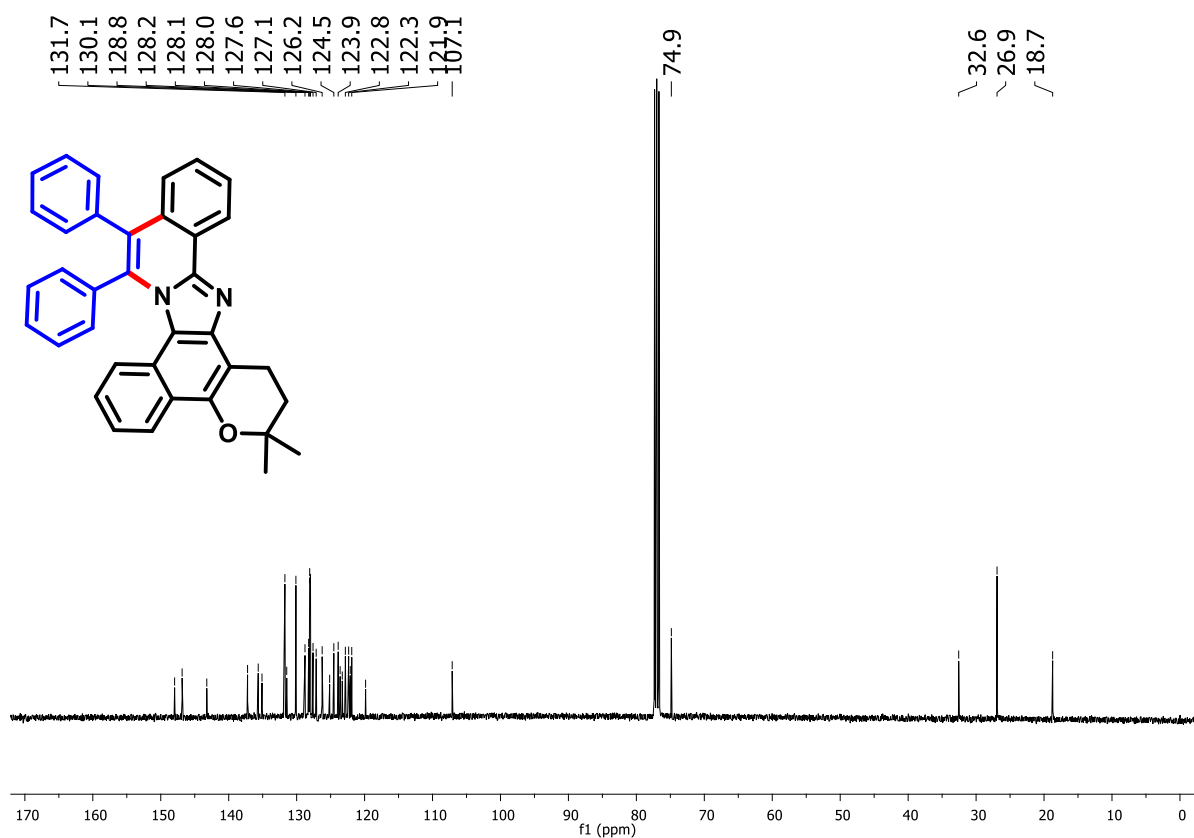


Figure 134. ^{13}C NMR spectrum (100 MHz, CDCl_3) of compound **235**.

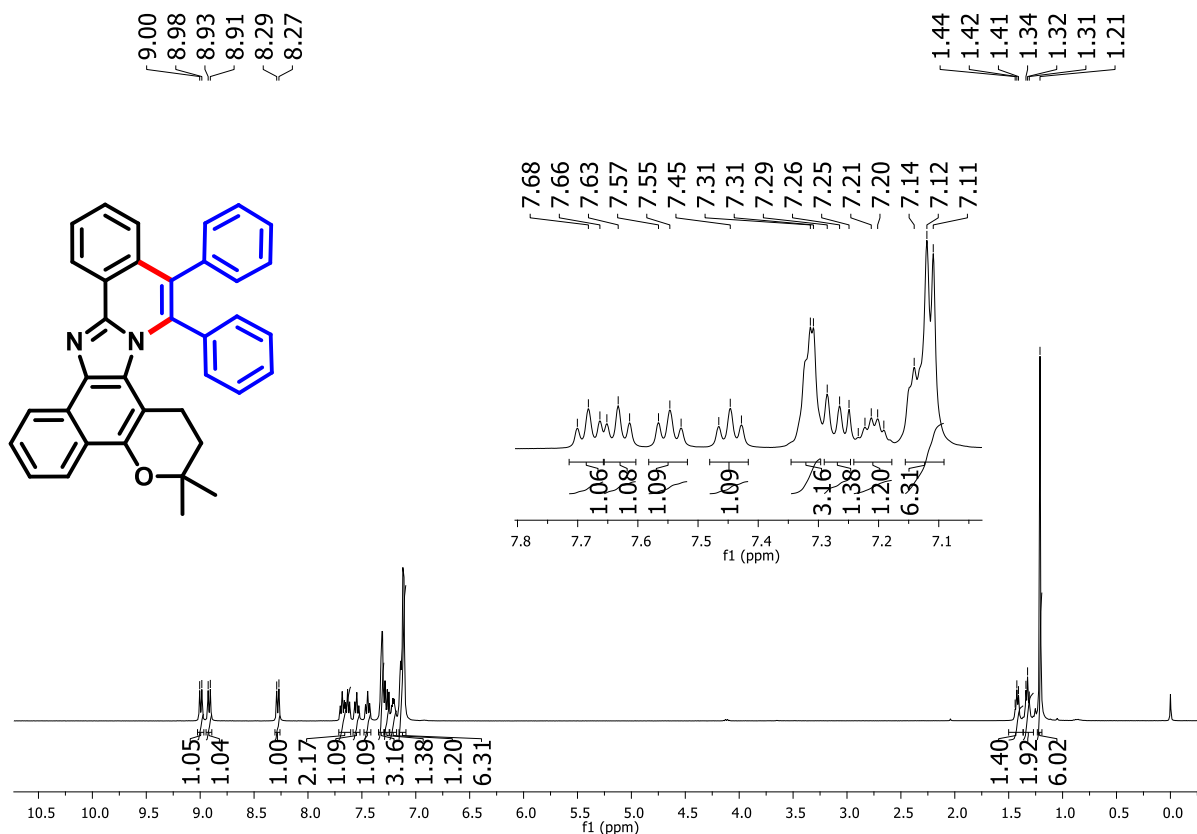


Figure 135. ^1H NMR spectrum (400 MHz, CDCl_3) of compound 236.

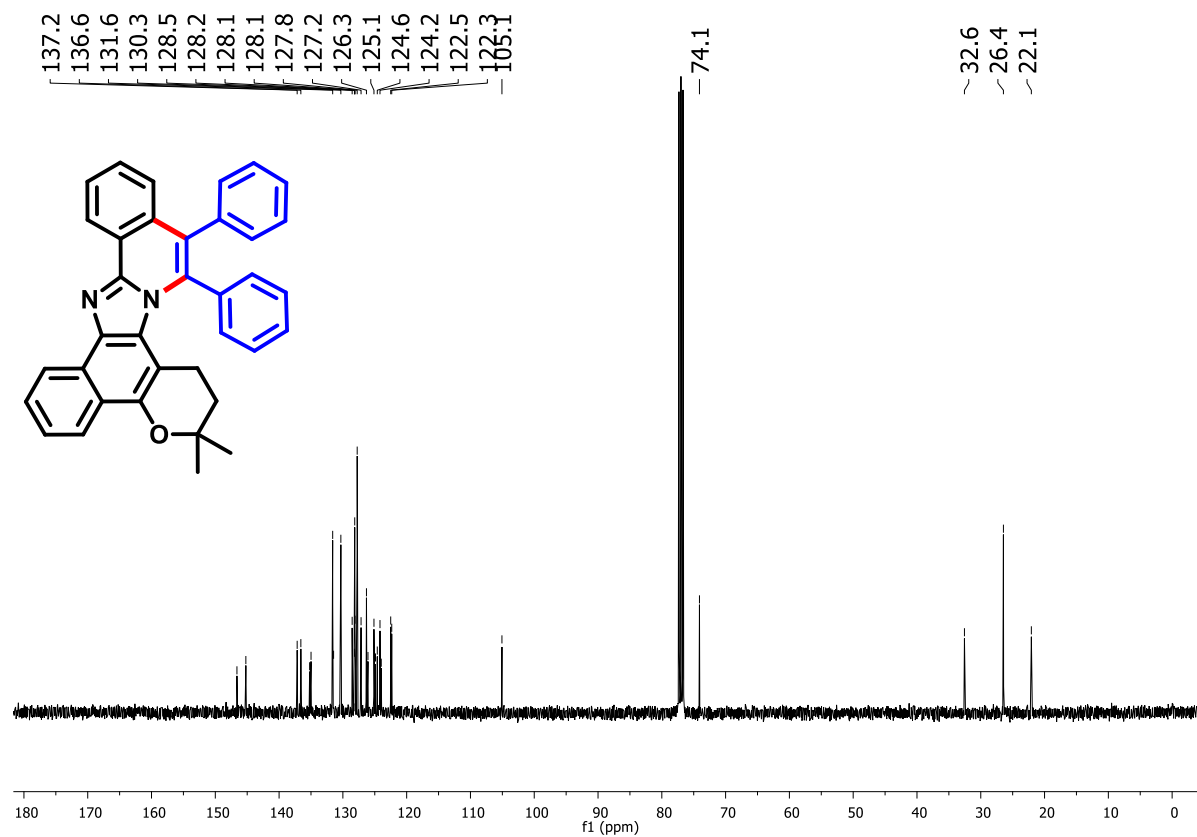


Figure 136. ^{13}C NMR spectrum (100 MHz, CDCl_3) of compound 236.

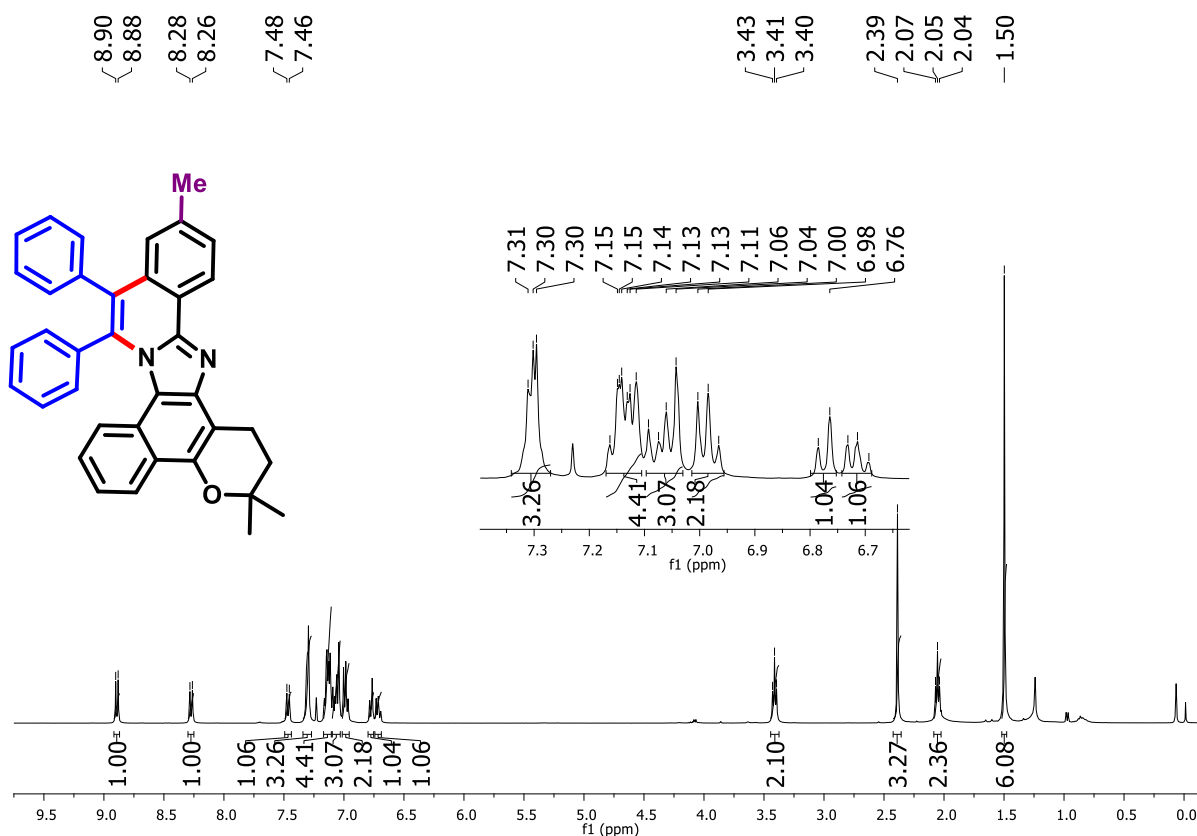


Figure 137. ¹H NMR spectrum (400 MHz, CDCl₃) of compound 257.

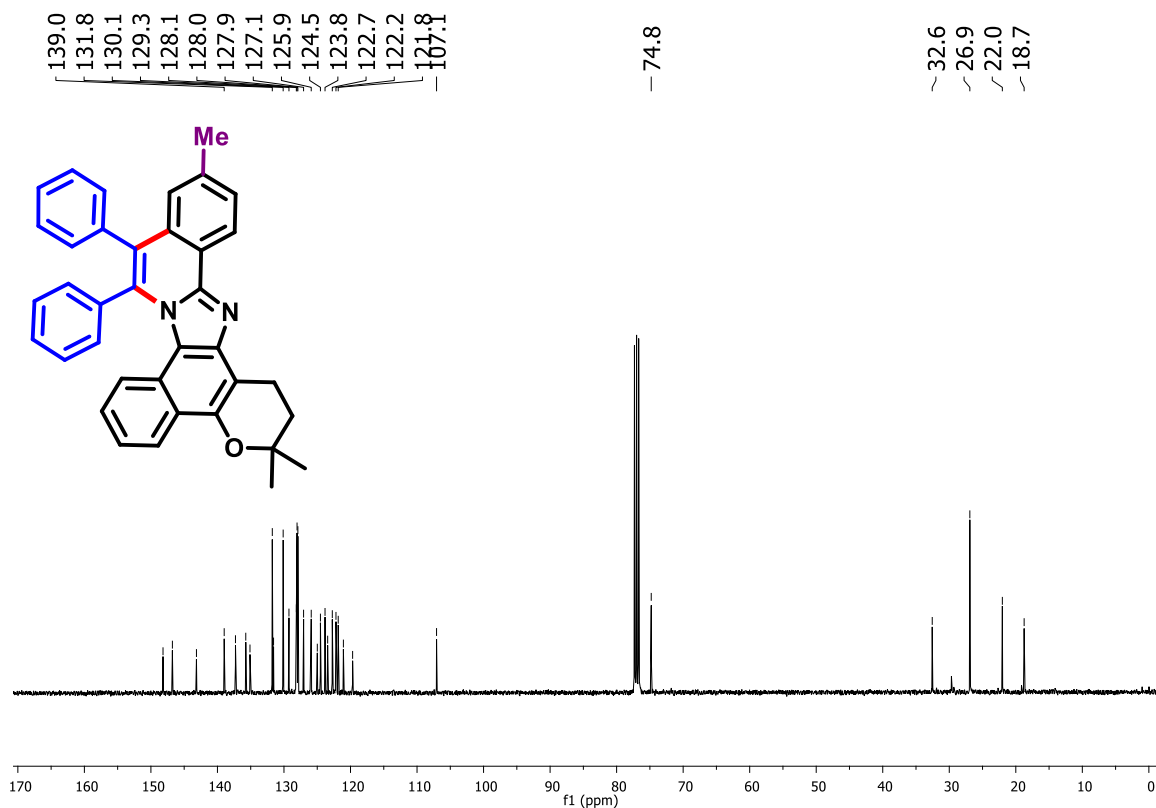


Figure 138. ¹³C NMR spectrum (100 MHz, CDCl₃) of compound 257.

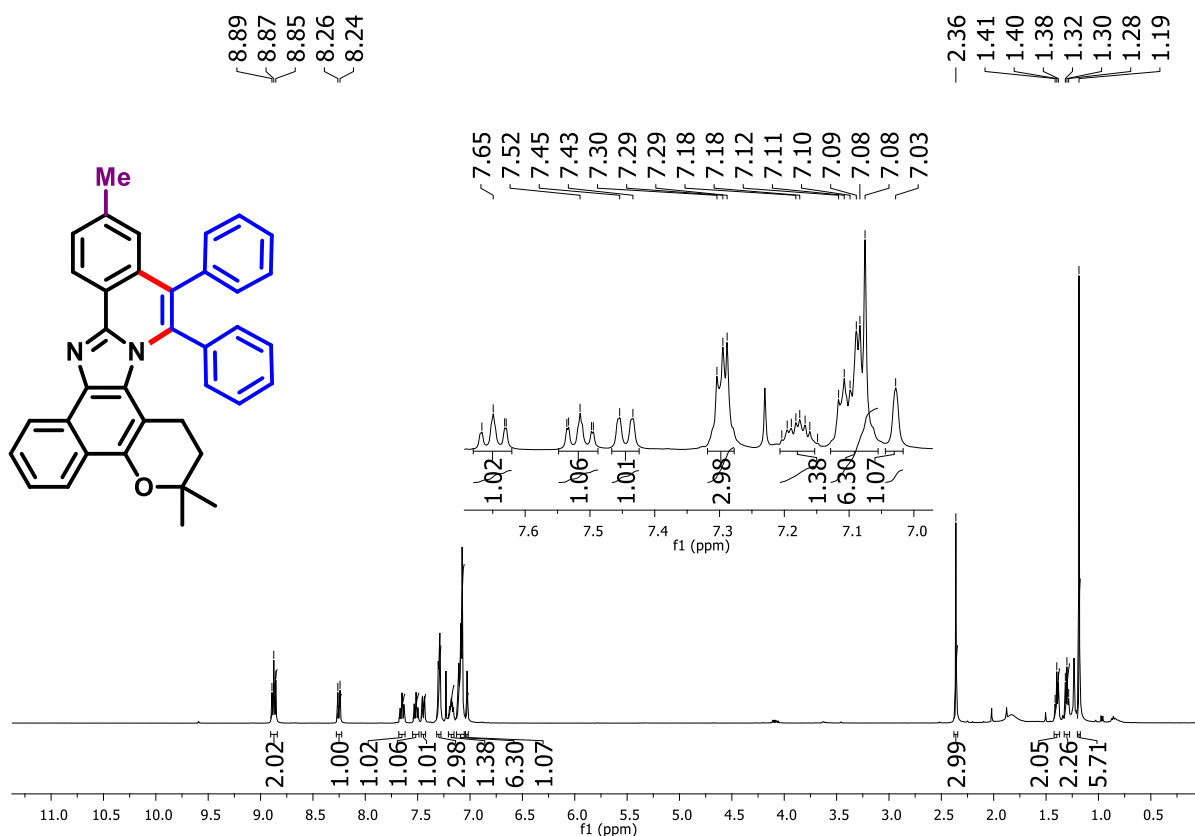


Figure 139. ¹H NMR spectrum (400 MHz, CDCl₃) of compound 258.

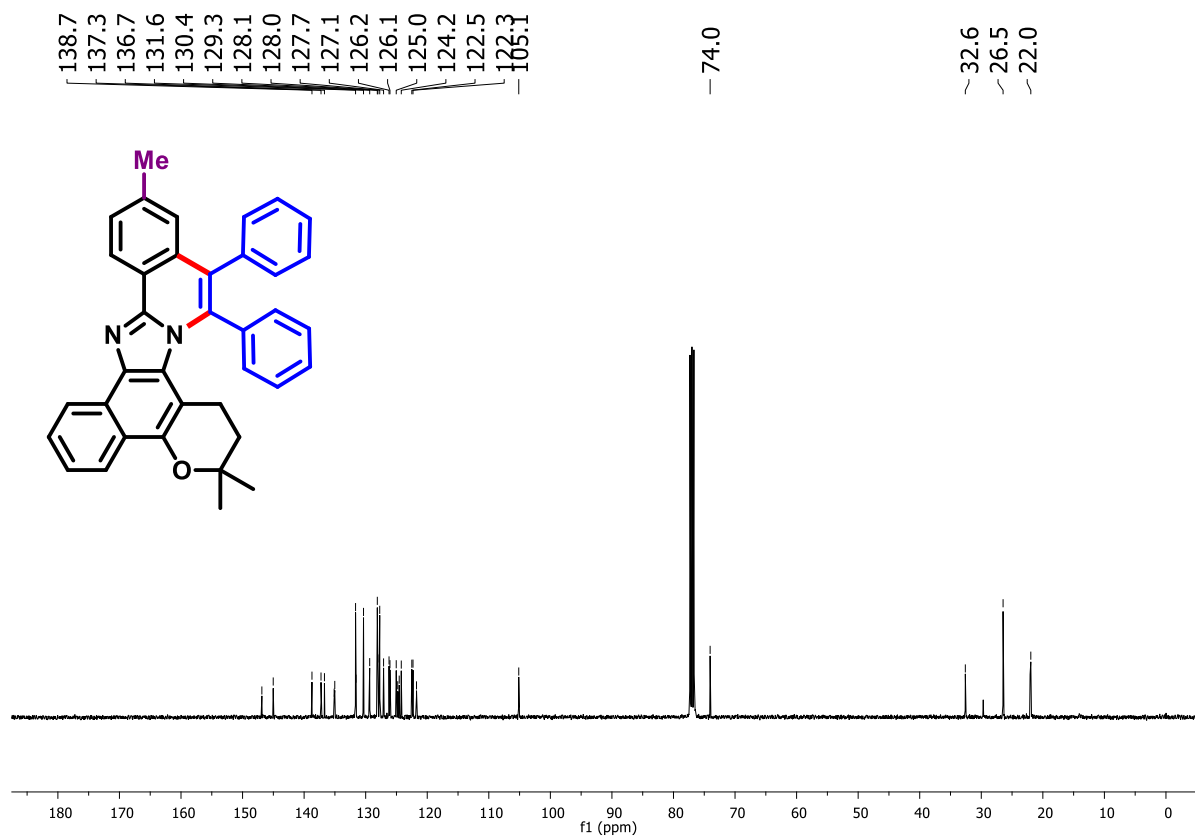


Figure 140. ¹³C NMR spectrum (100 MHz, CDCl₃) of compound 258.

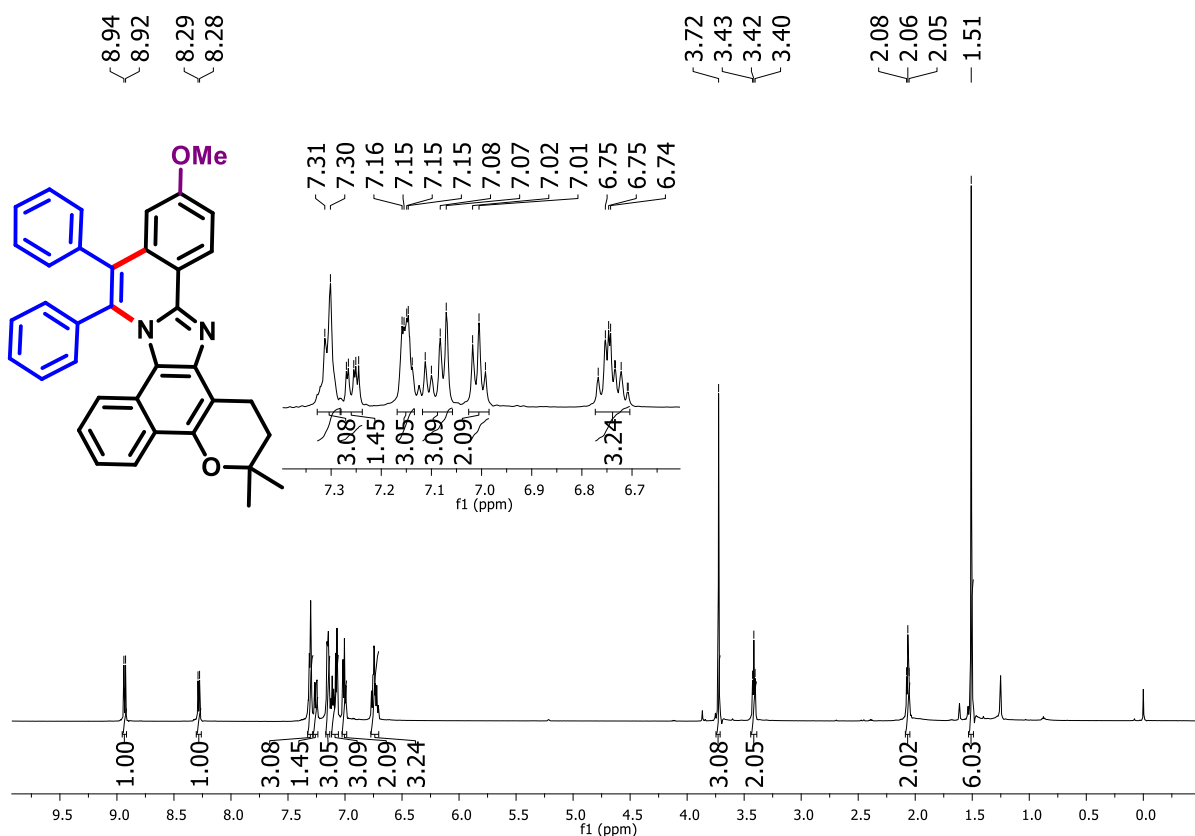


Figure 141. ¹H NMR spectrum (600 MHz, CDCl₃) of compound 259.

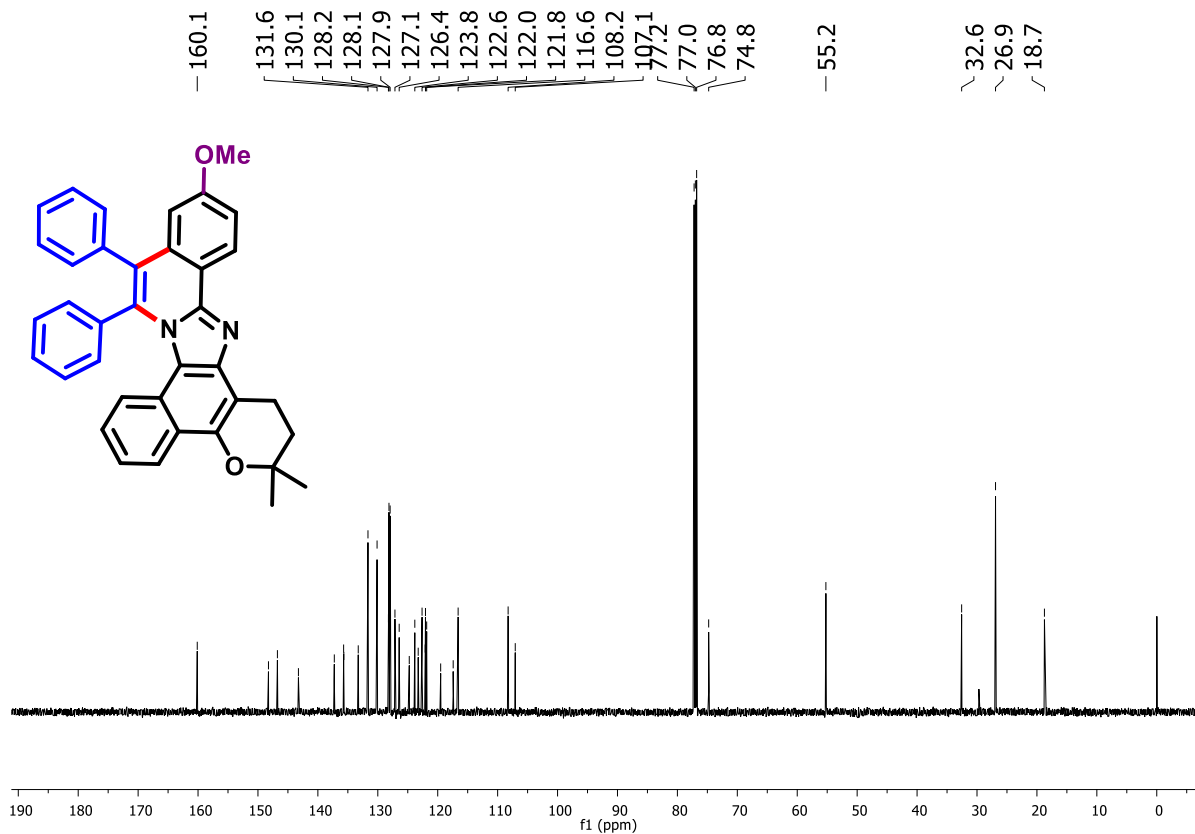


Figure 142. ¹³C NMR spectrum (150 MHz, CDCl₃) of compound 259.

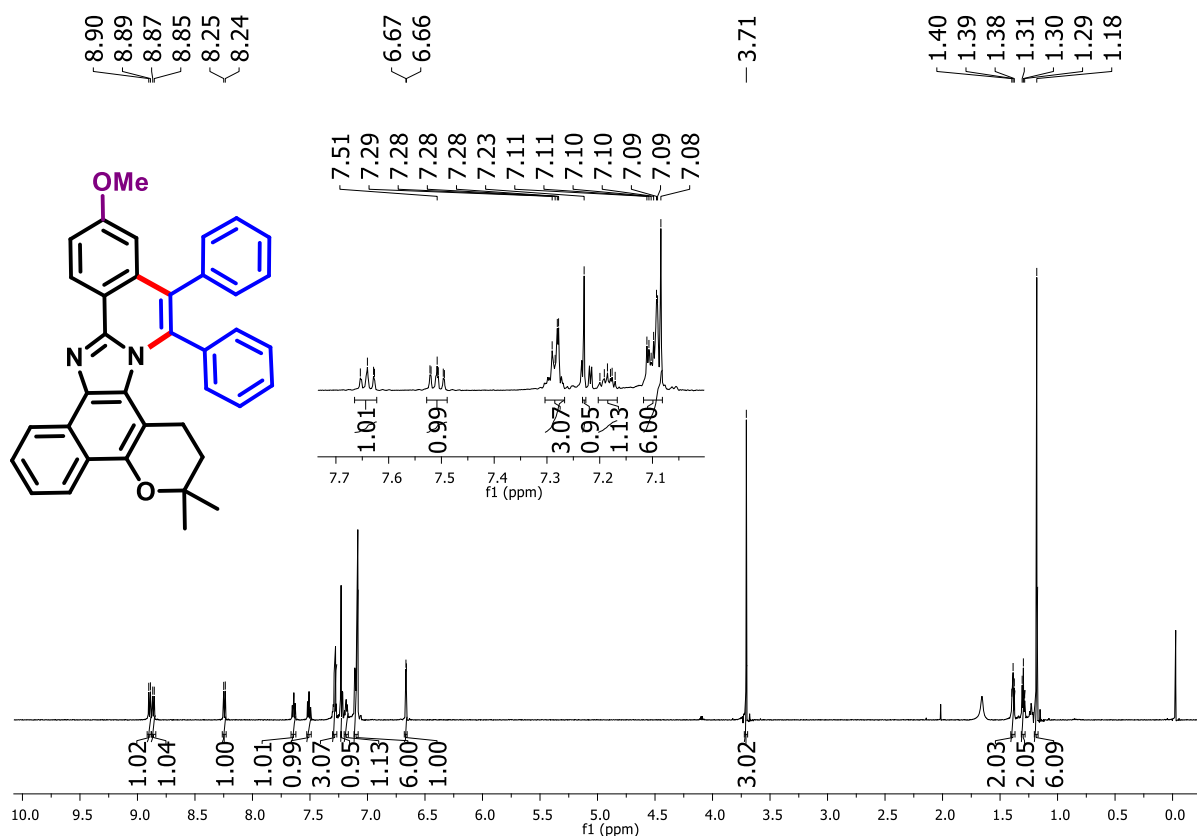


Figure 143. ¹H NMR spectrum (600 MHz, CDCl₃) of compound **260**.

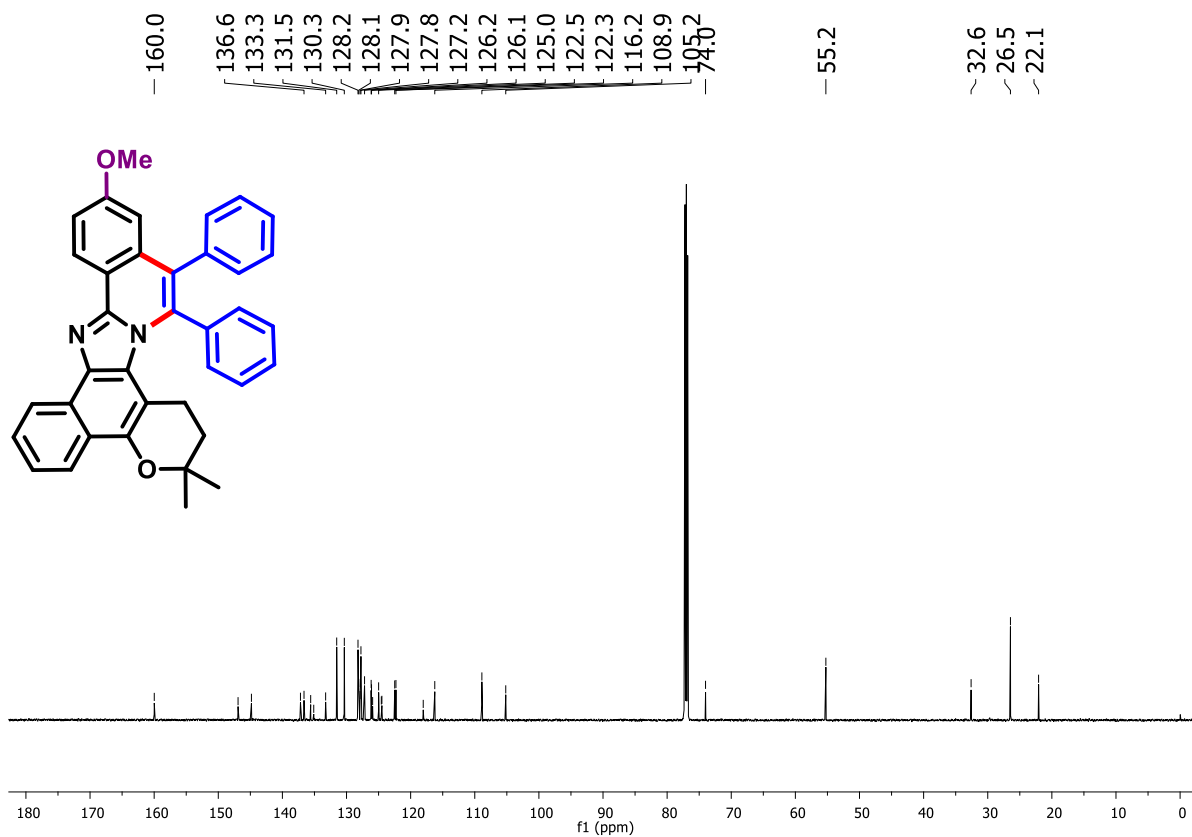


Figure 144. ¹³C NMR spectrum (150 MHz, CDCl₃) of compound **260**.

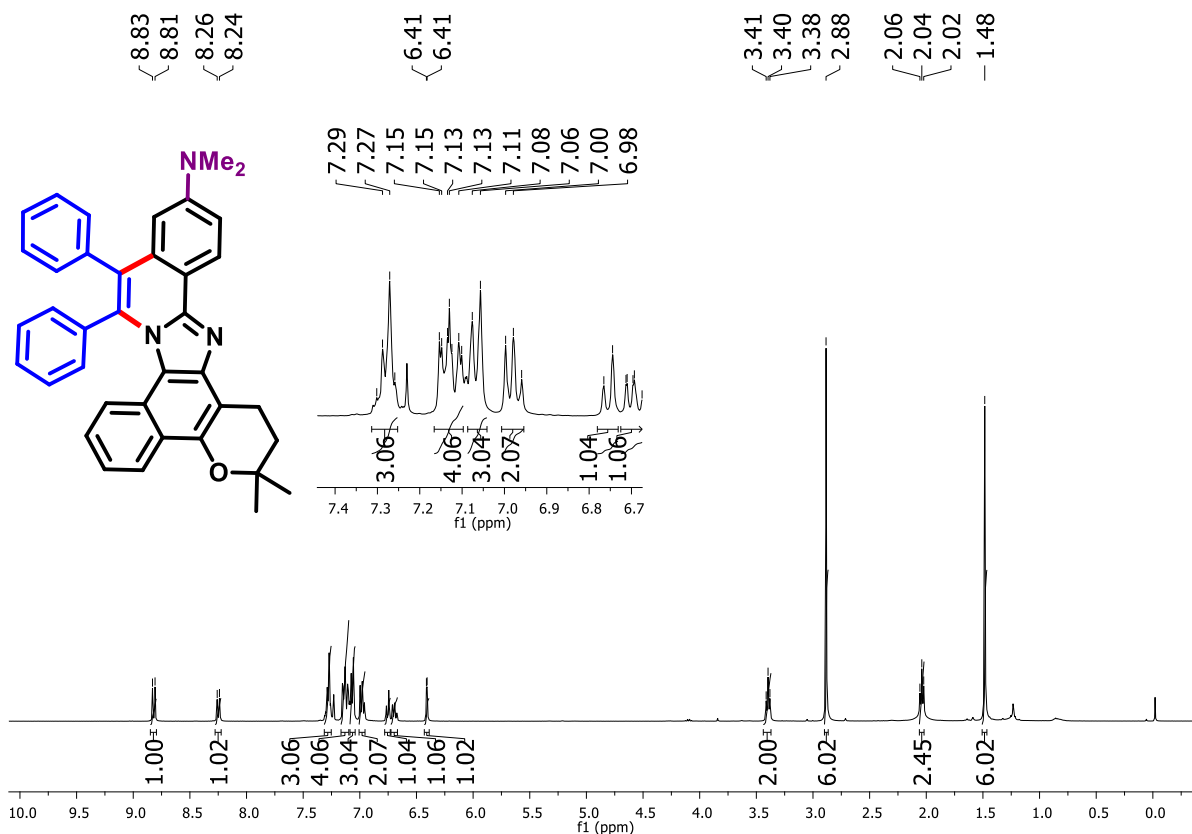


Figure 145. ¹H NMR spectrum (400 MHz, CDCl₃) of compound 261.

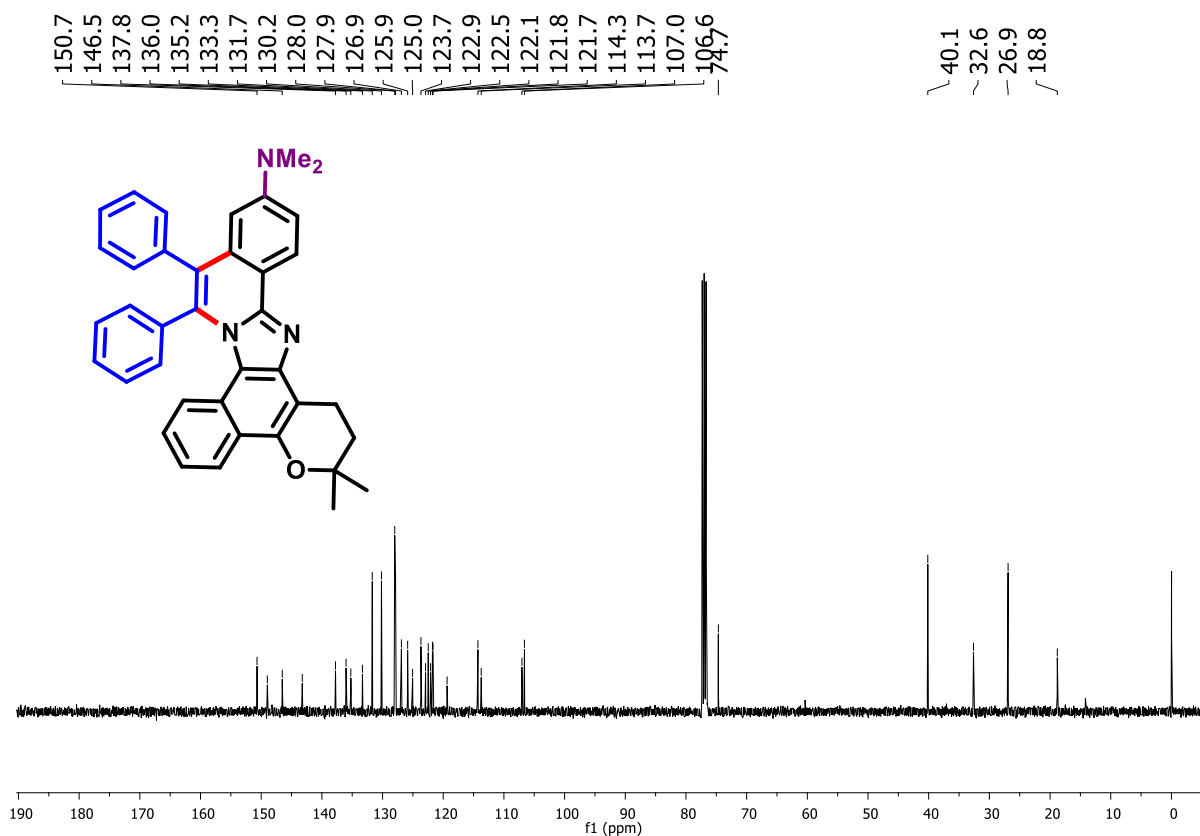


Figure 146. ¹³C NMR spectrum (100 MHz, CDCl₃) of compound 261.

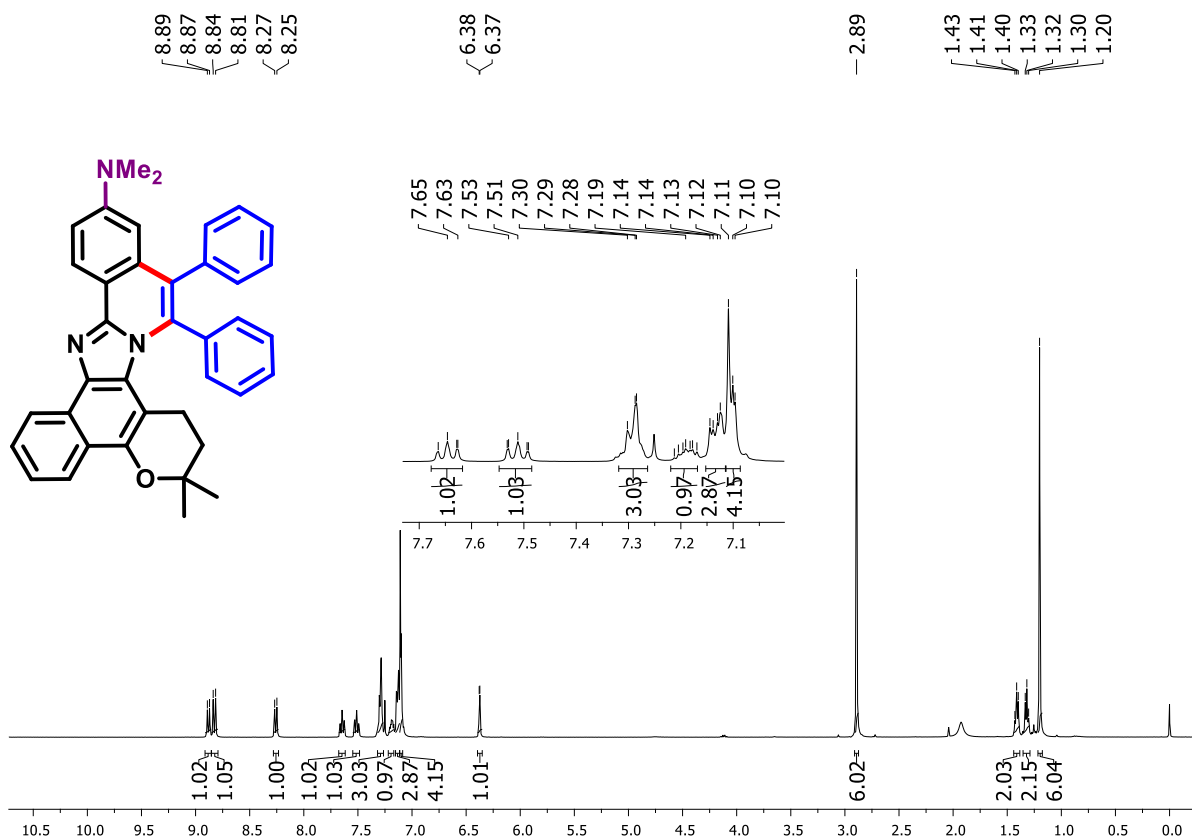


Figure 147. ¹H NMR spectrum (400 MHz, CDCl₃) of compound 262.

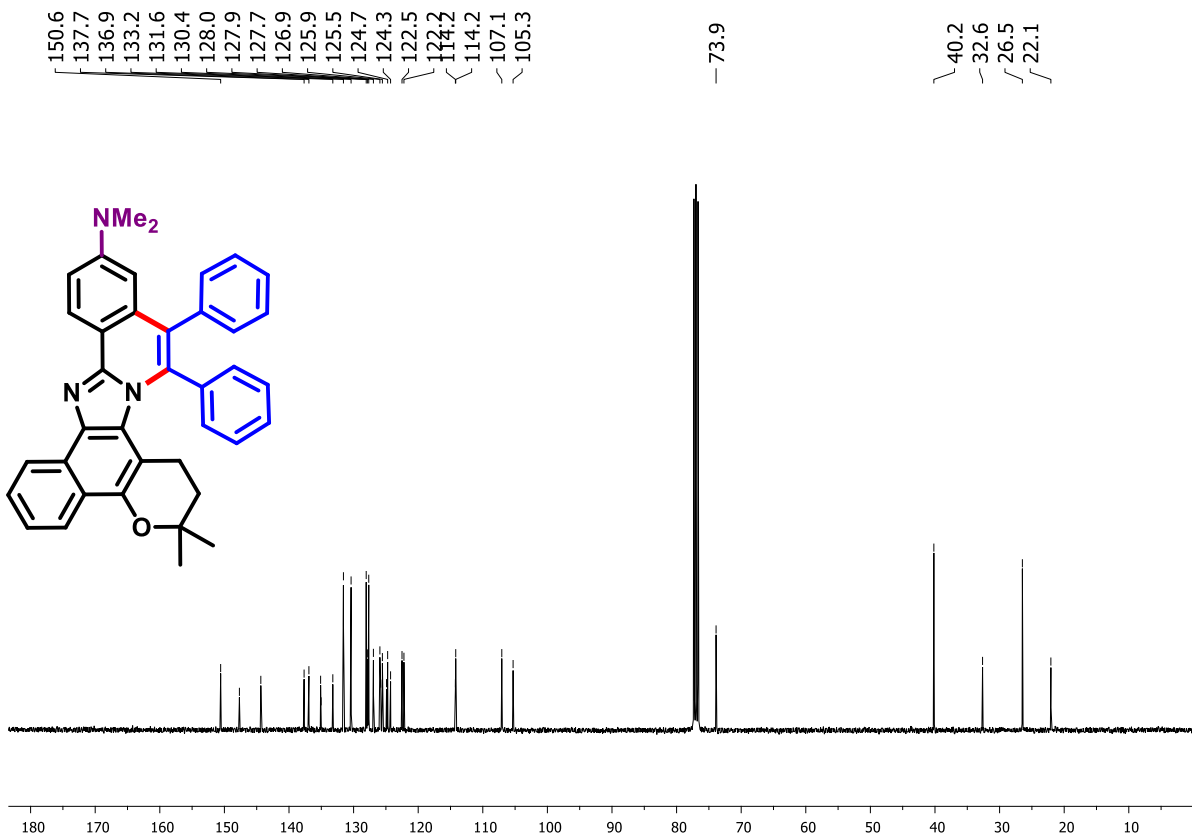


Figure 148. ¹³C NMR spectrum (100 MHz, CDCl₃) of compound 262.

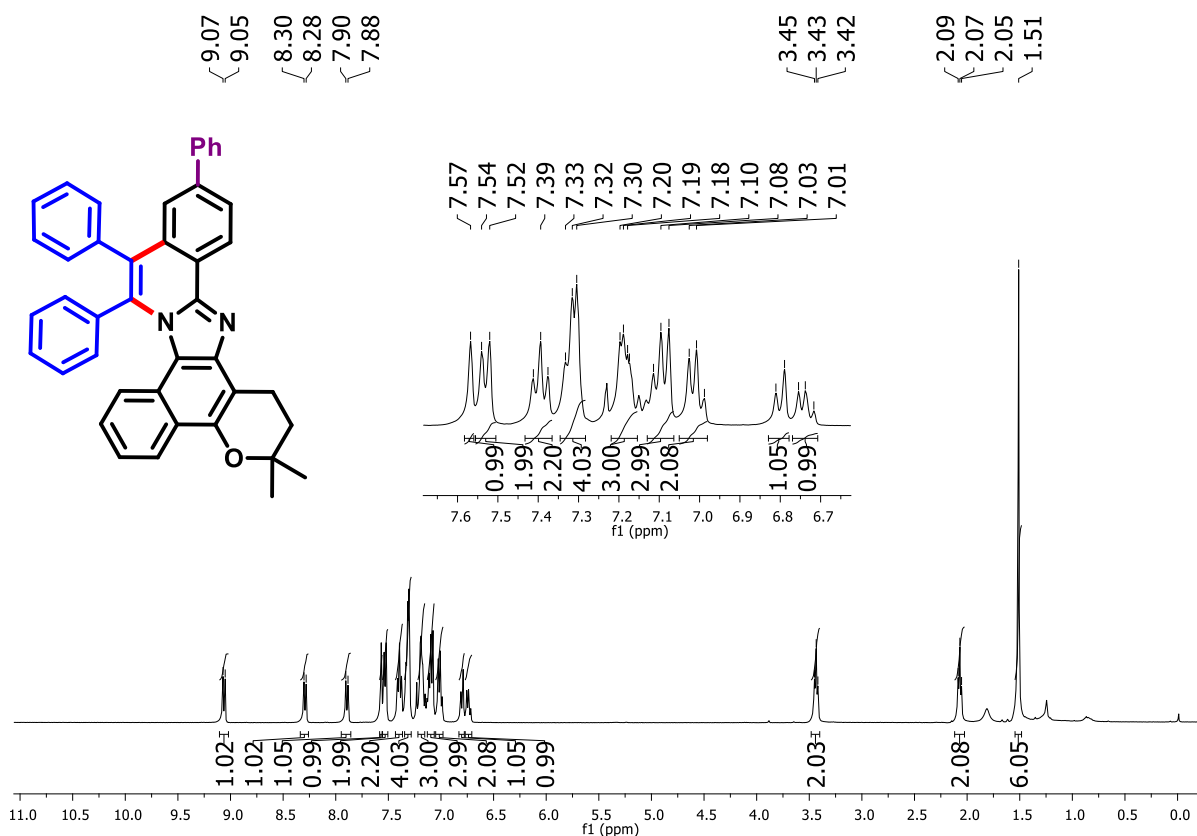


Figure 149. ¹H NMR spectrum (400 MHz, CDCl₃) of compound 263.

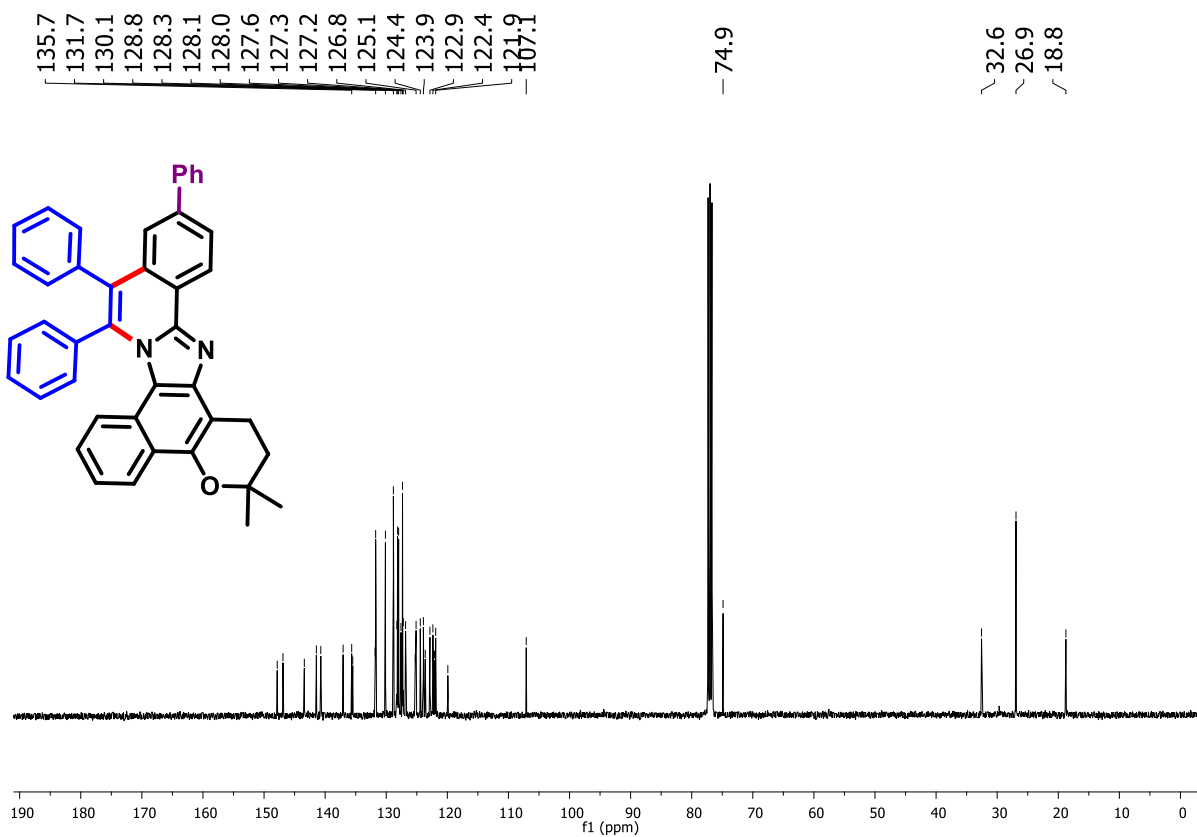


Figure 150. ¹³C NMR spectrum (100 MHz, CDCl₃) of compound 263.

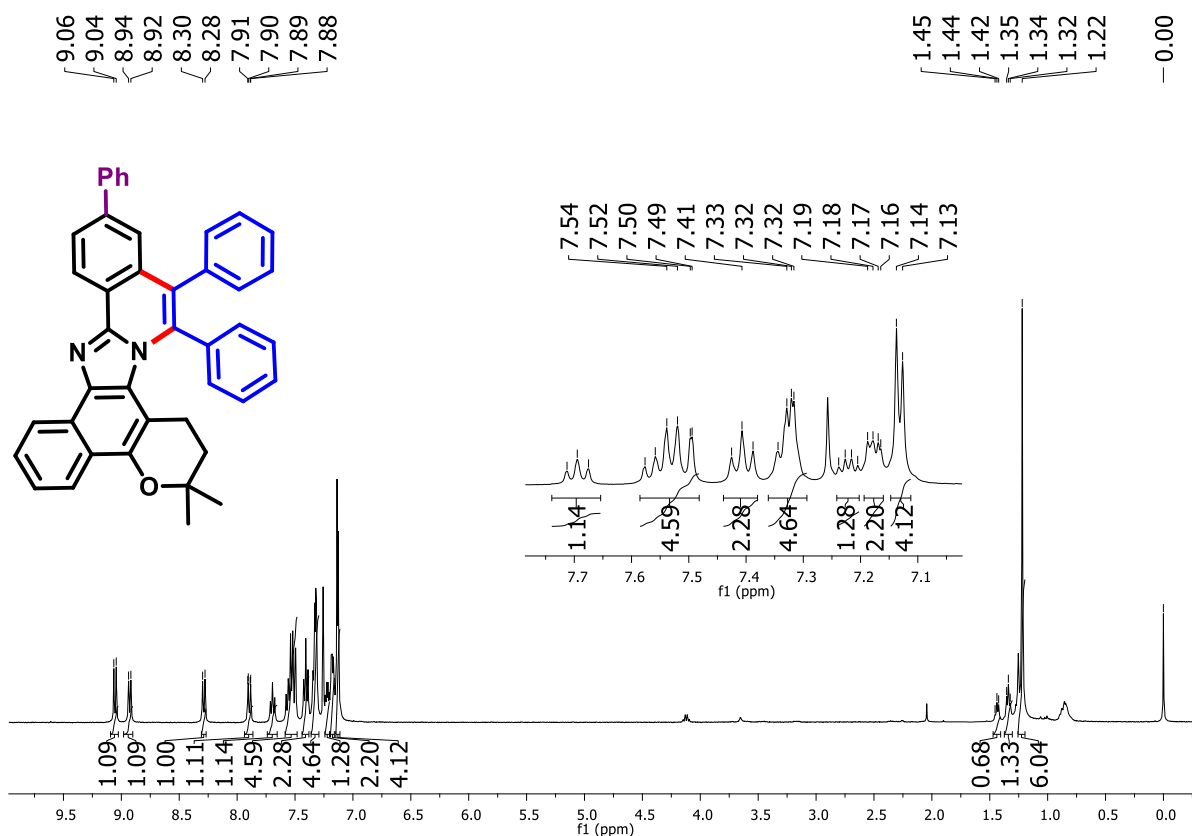


Figure 151. ¹H NMR spectrum (400 MHz, CDCl₃) of compound 264.

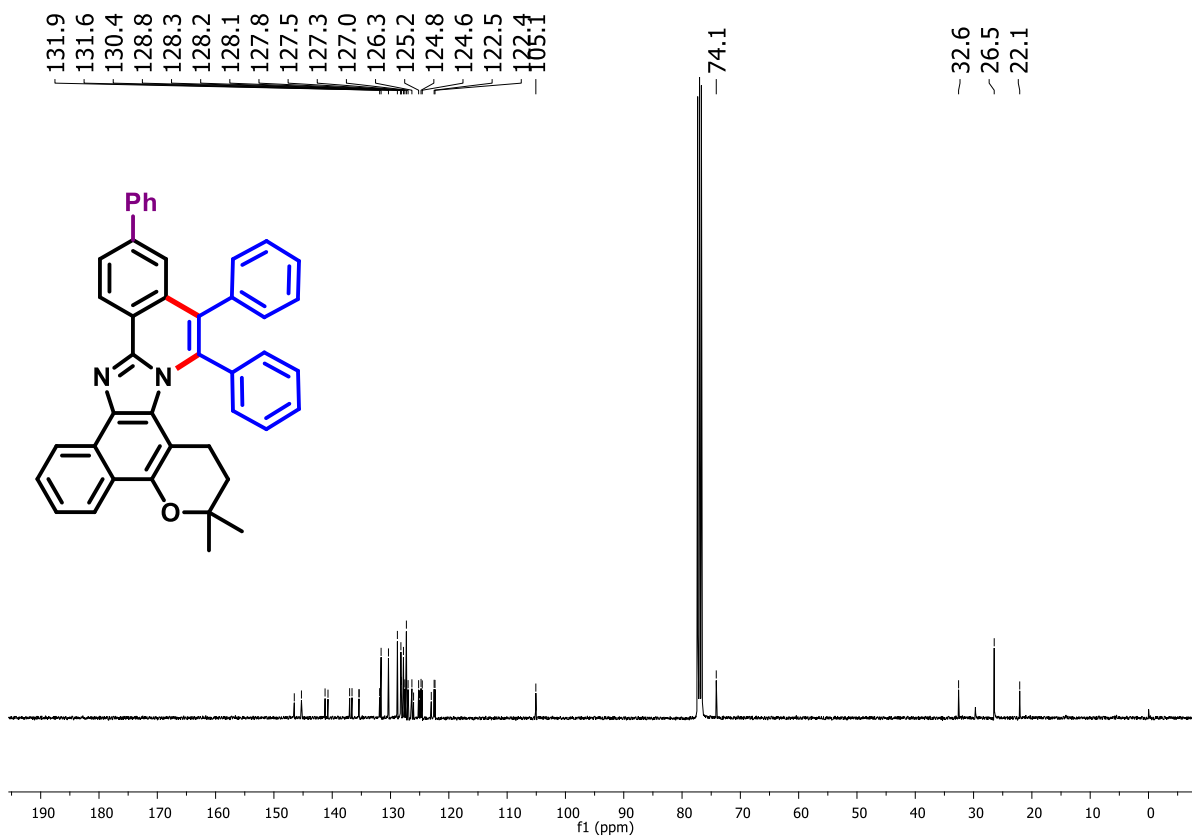


Figure 152. ¹³C NMR spectrum (100 MHz, CDCl₃) of compound 264.

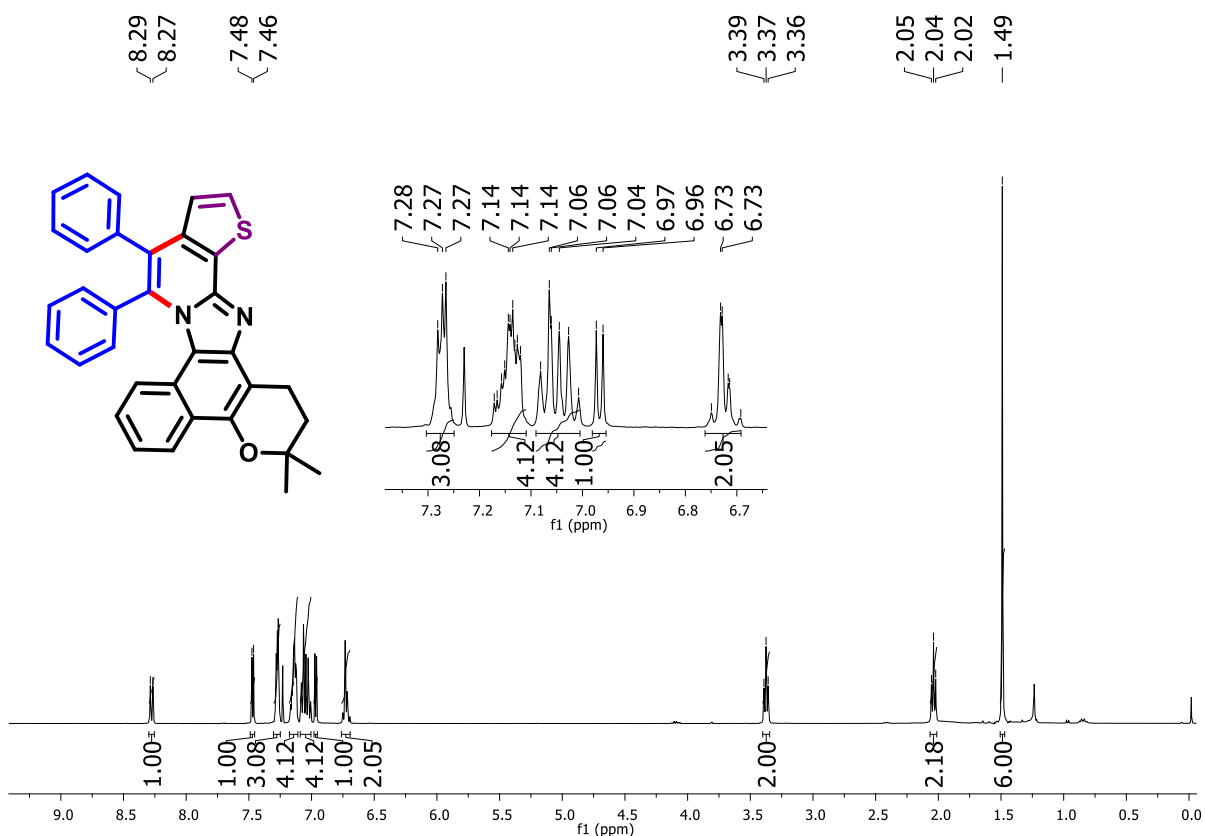


Figure 153. ¹H NMR spectrum (400 MHz, CDCl₃) of compound **265**.

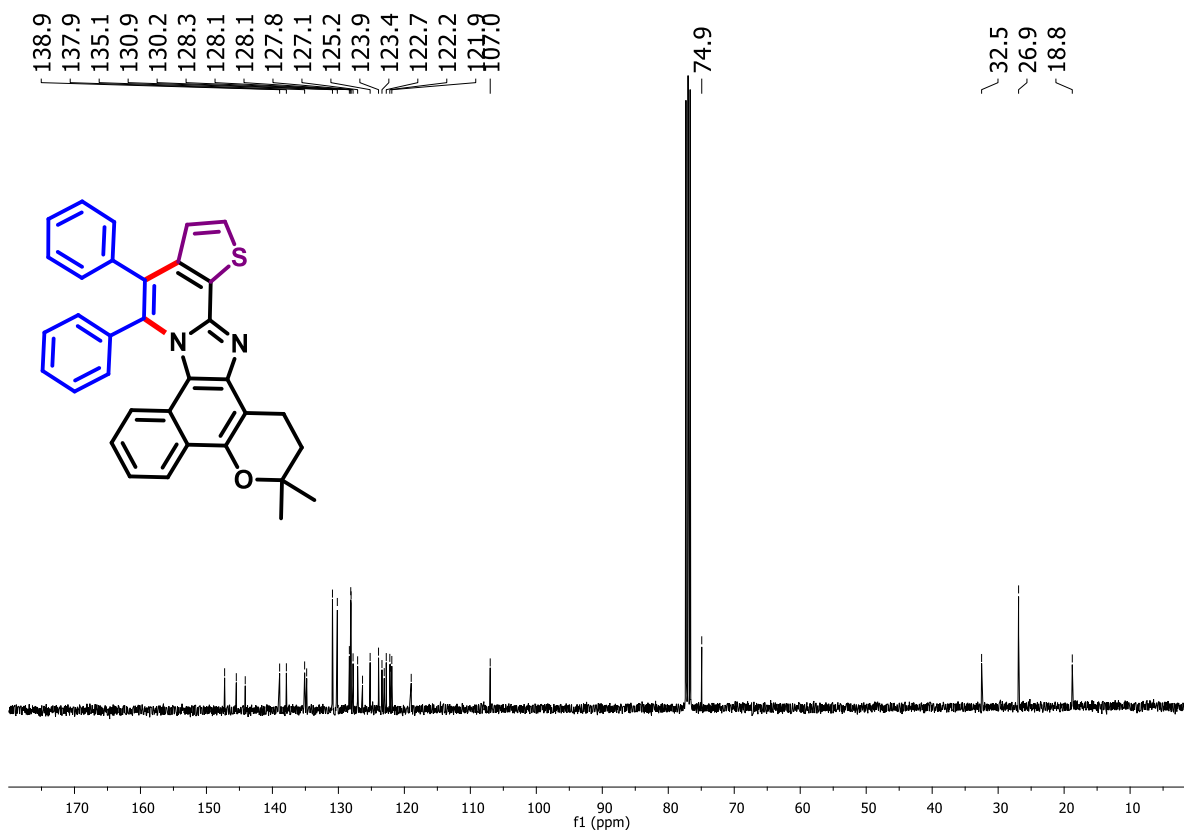


Figure 154. ¹³C NMR spectrum (100 MHz, CDCl₃) of compound **265**.

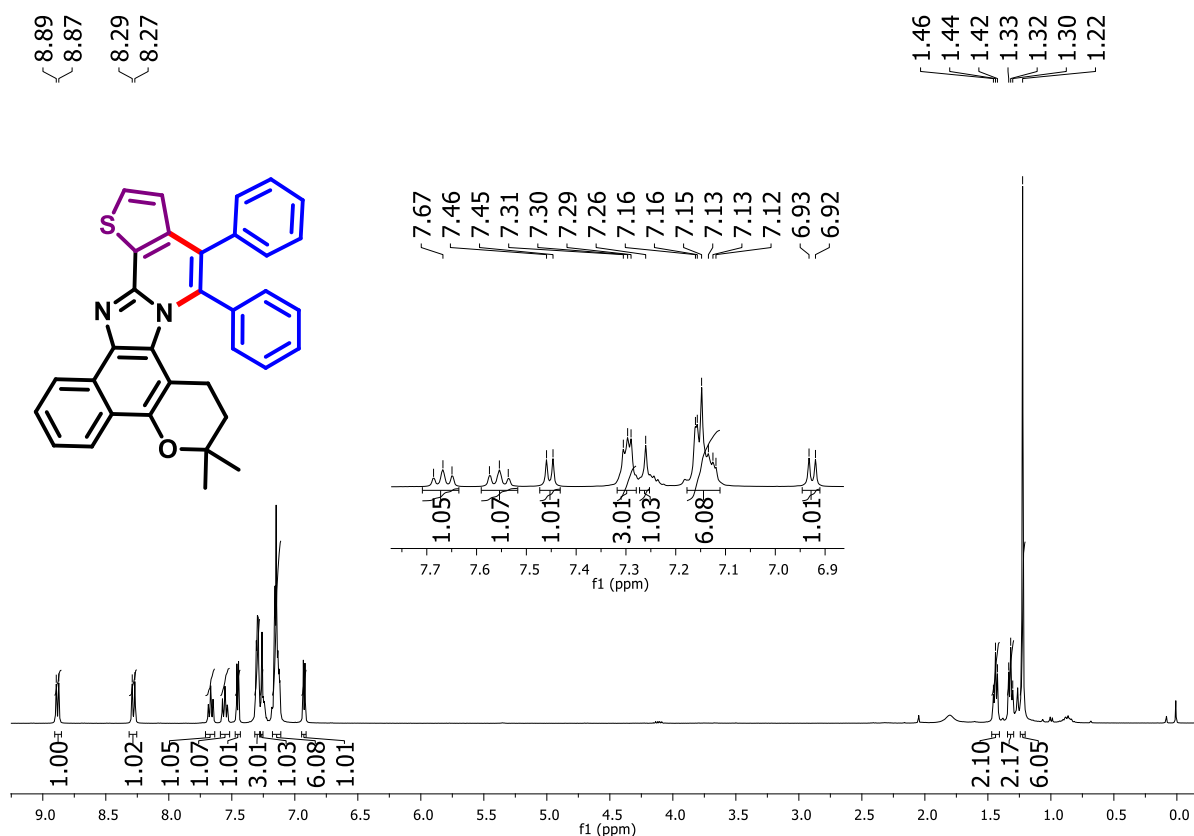


Figure 155. ¹H NMR spectrum (400 MHz, CDCl₃) of compound 266.

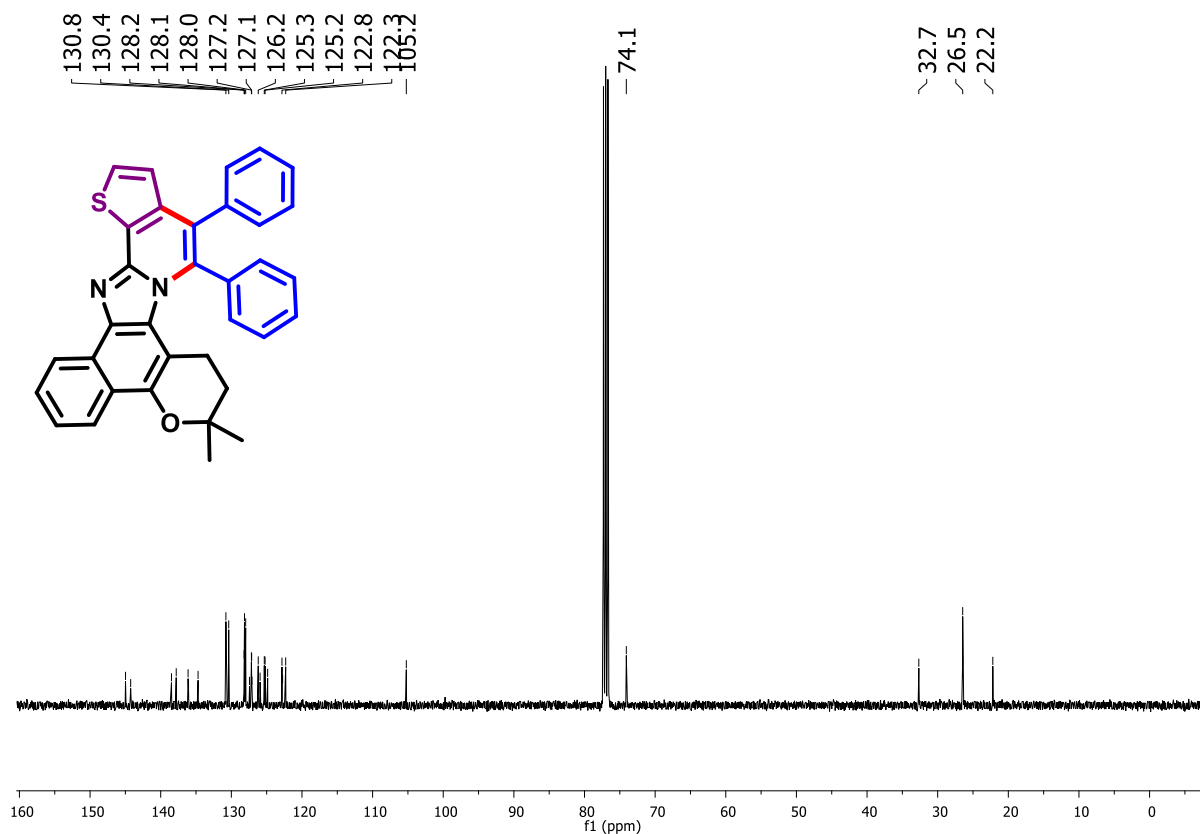


Figure 156. ¹³C NMR spectrum (100 MHz, CDCl₃) of compound 266.

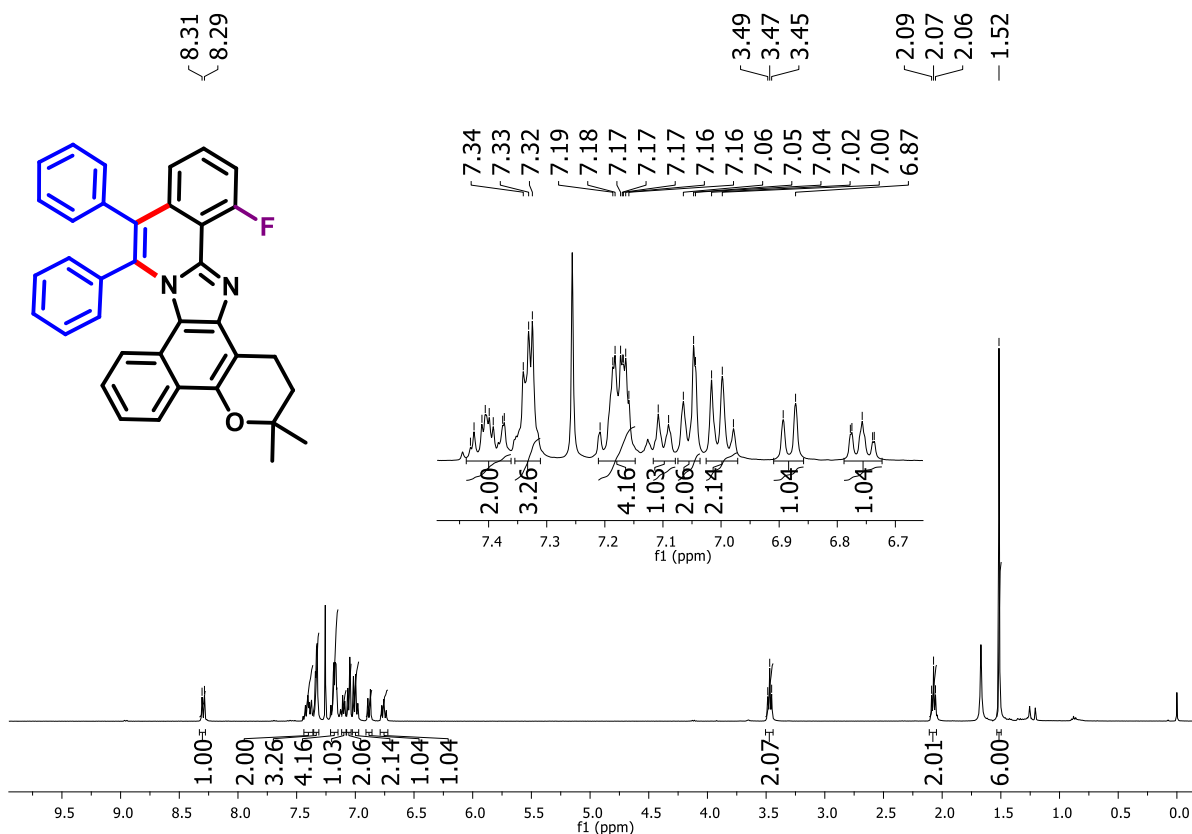


Figure 157. ¹H NMR spectrum (400 MHz, CDCl₃) of compound 267.

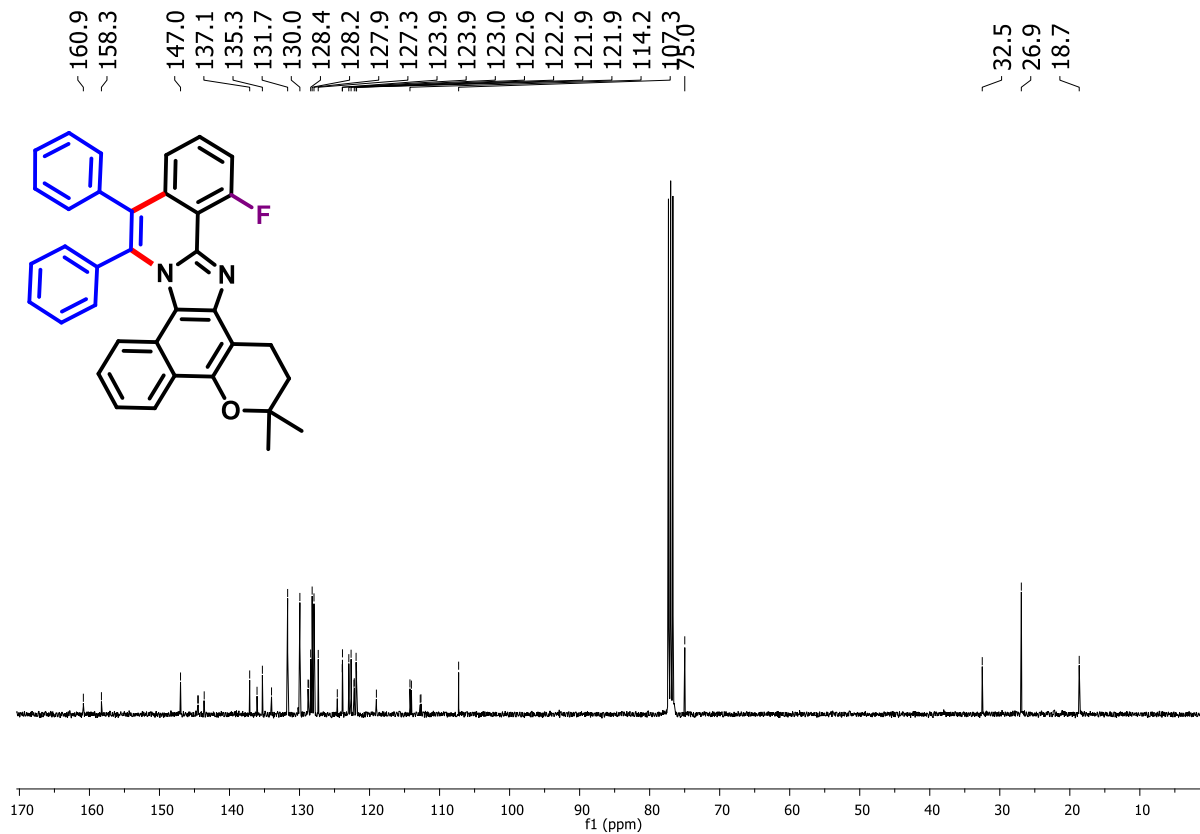


Figure 158. ¹³C NMR spectrum (100 MHz, CDCl₃) of compound 267.

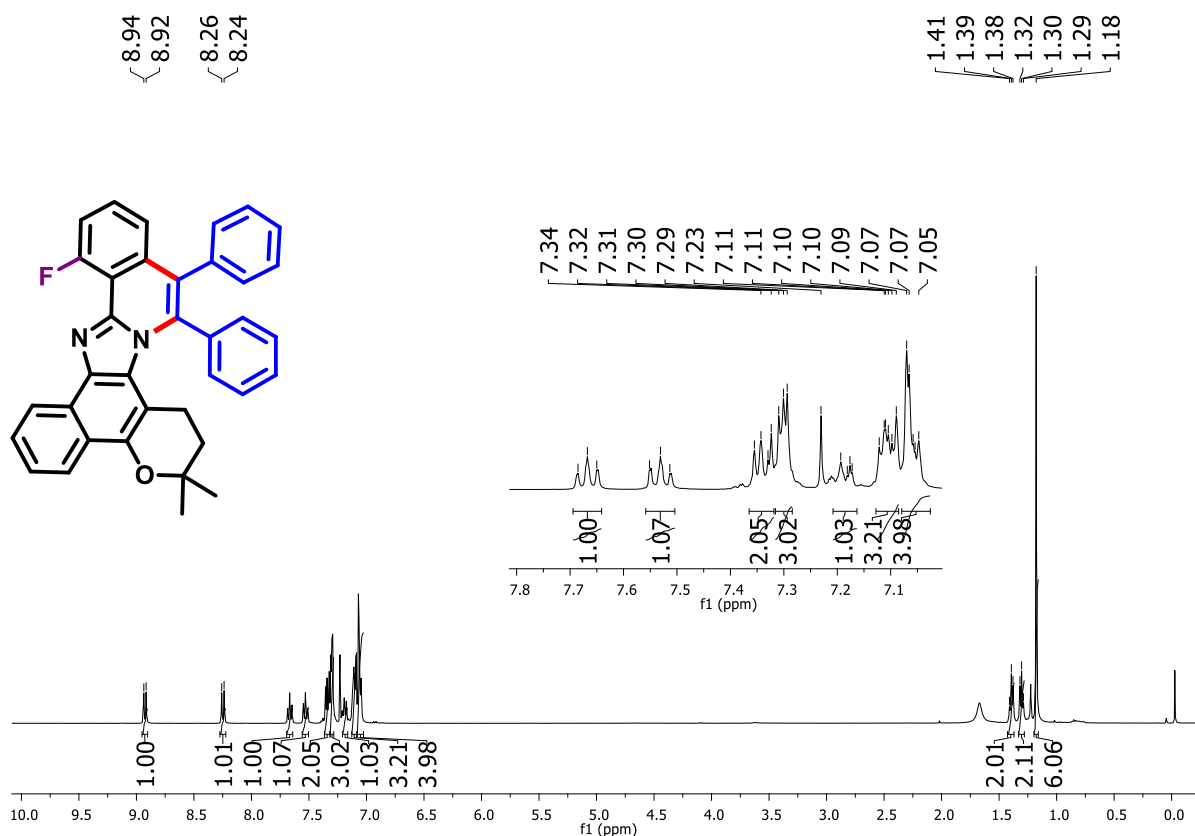


Figure 159. ¹H NMR spectrum (400 MHz, CDCl₃) of compound 268.

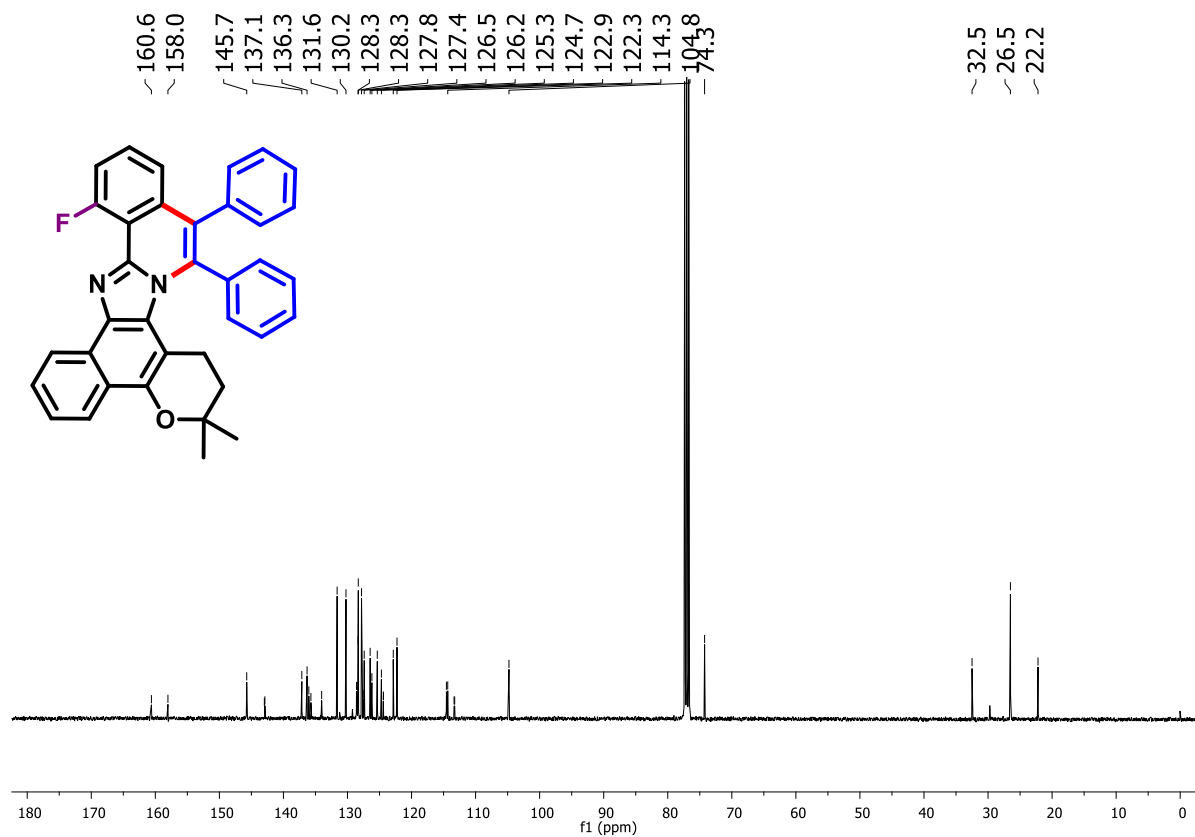


Figure 160. ¹³C NMR spectrum (100 MHz, CDCl₃) of compound 268.

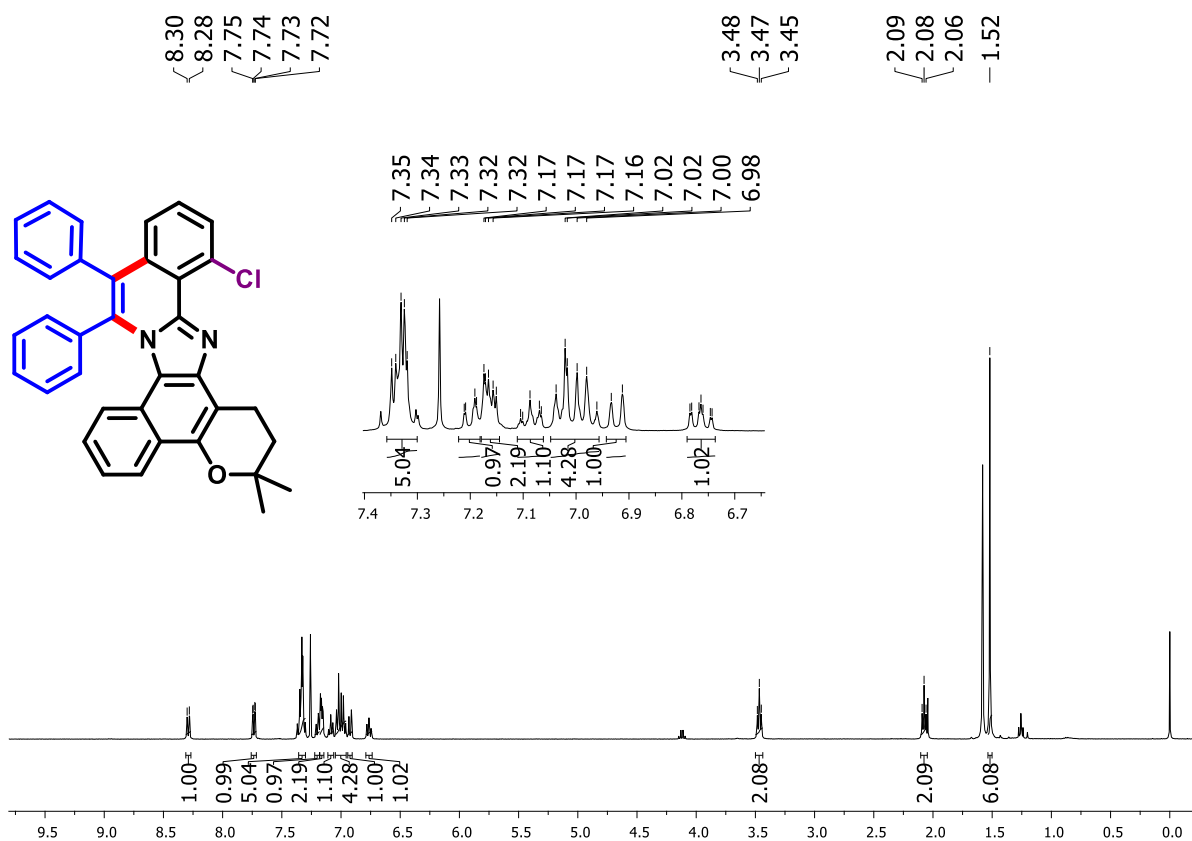


Figure 161. ¹H NMR spectrum (400 MHz, CDCl₃) of compound **269**.

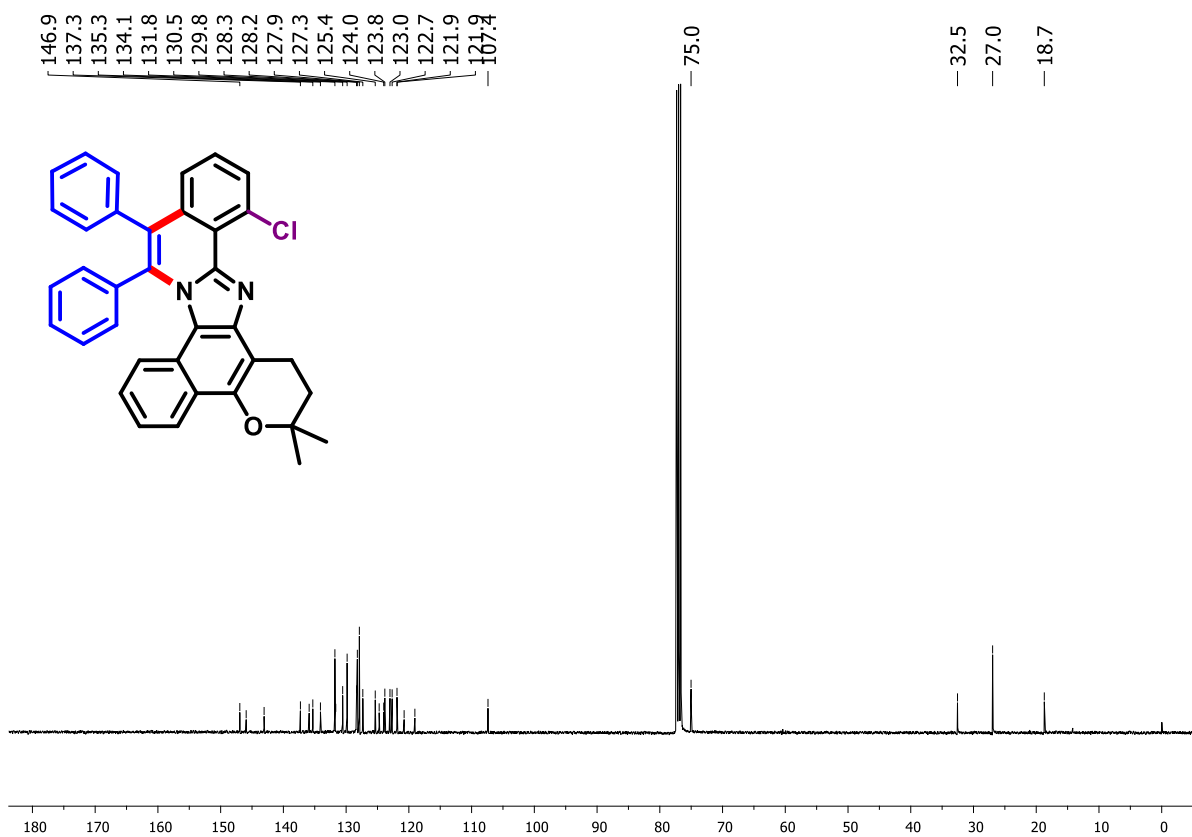


Figure 162. ¹³C NMR spectrum (100 MHz, CDCl₃) of compound **269**.

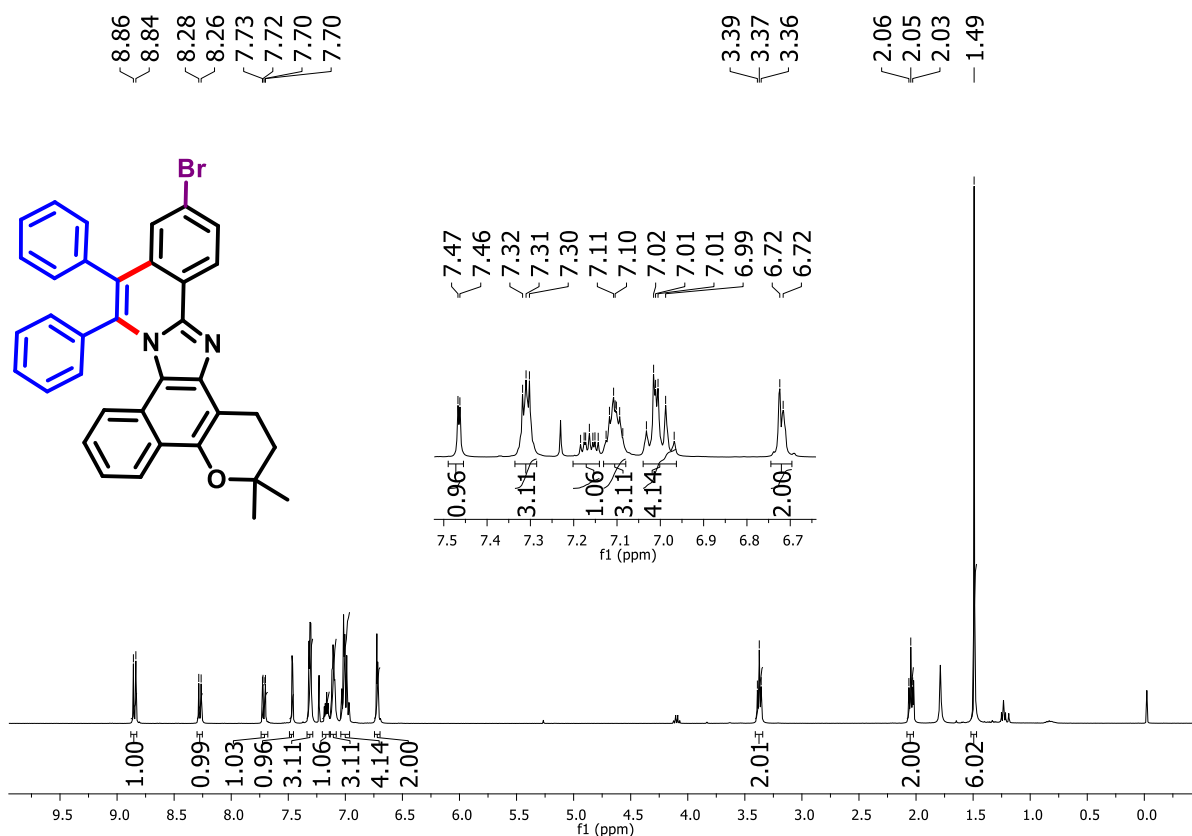


Figure 163. ¹H NMR spectrum (400 MHz, CDCl₃) of compound 271.

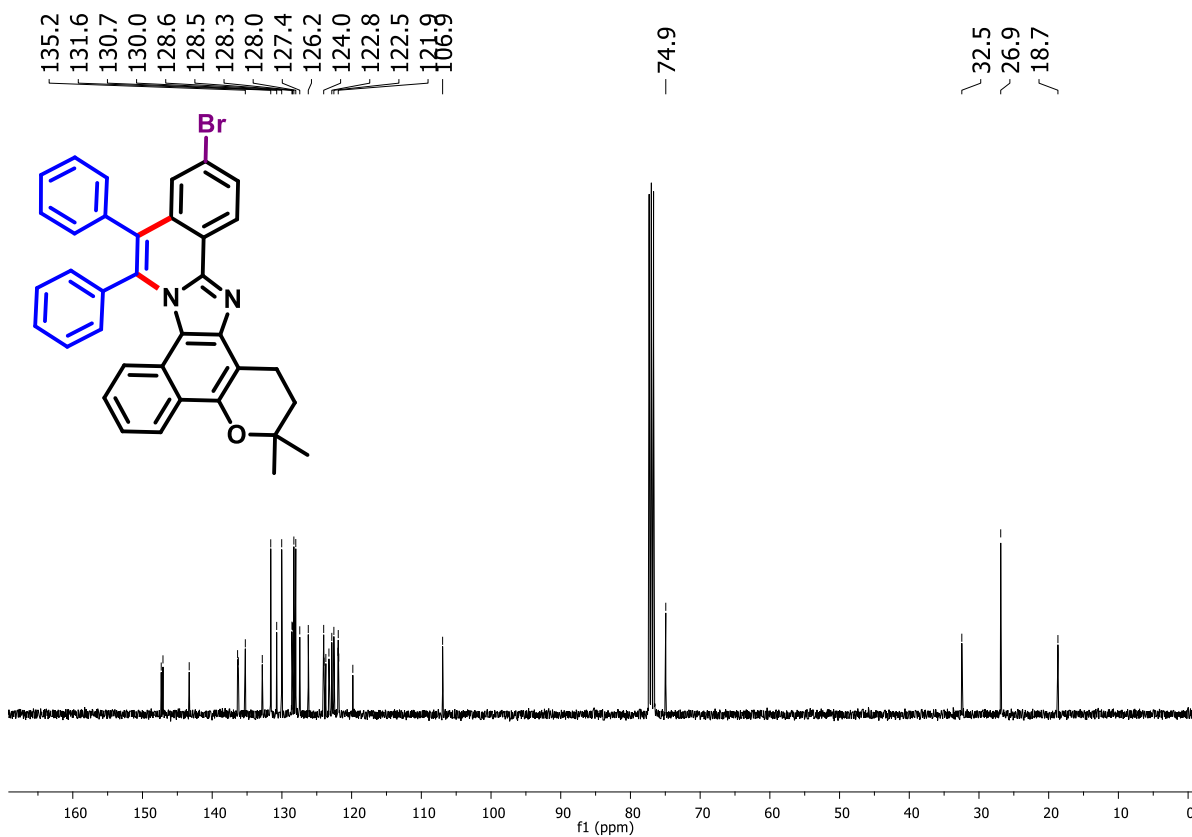


Figure 164. ¹³C NMR spectrum (100 MHz, CDCl₃) of compound 271.

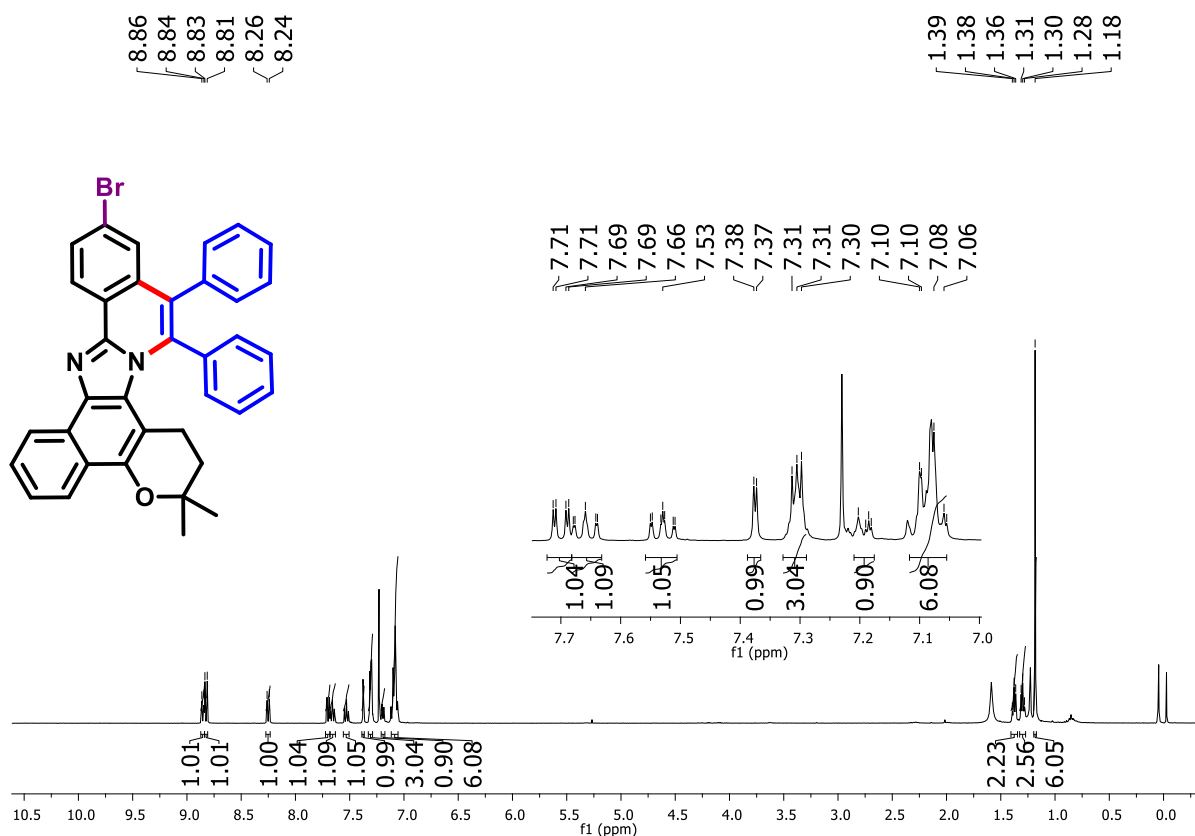


Figure 165. ¹H NMR spectrum (400 MHz, CDCl₃) of compound 272.

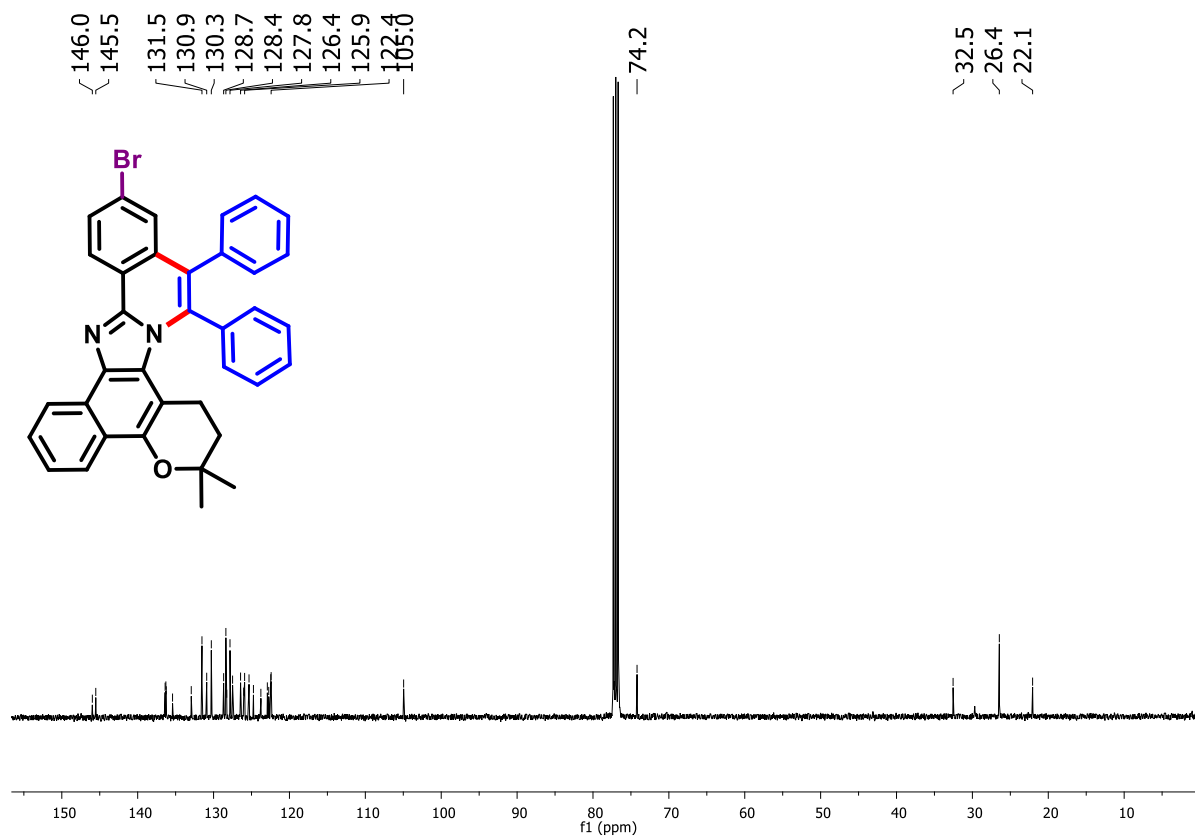


Figure 166. ¹³C NMR spectrum (100 MHz, CDCl₃) of compound 272.

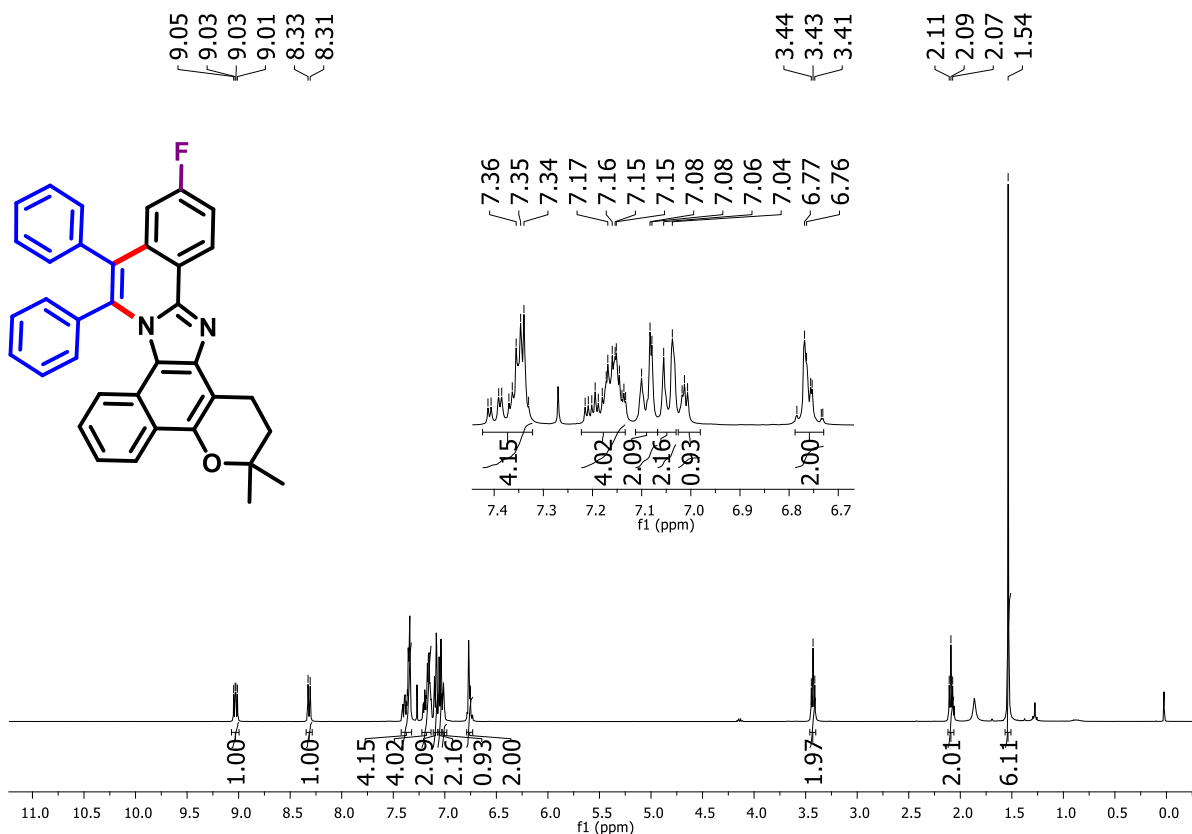


Figure 167. $^1\text{H NMR}$ spectrum (400 MHz, CDCl_3) of compound 273.

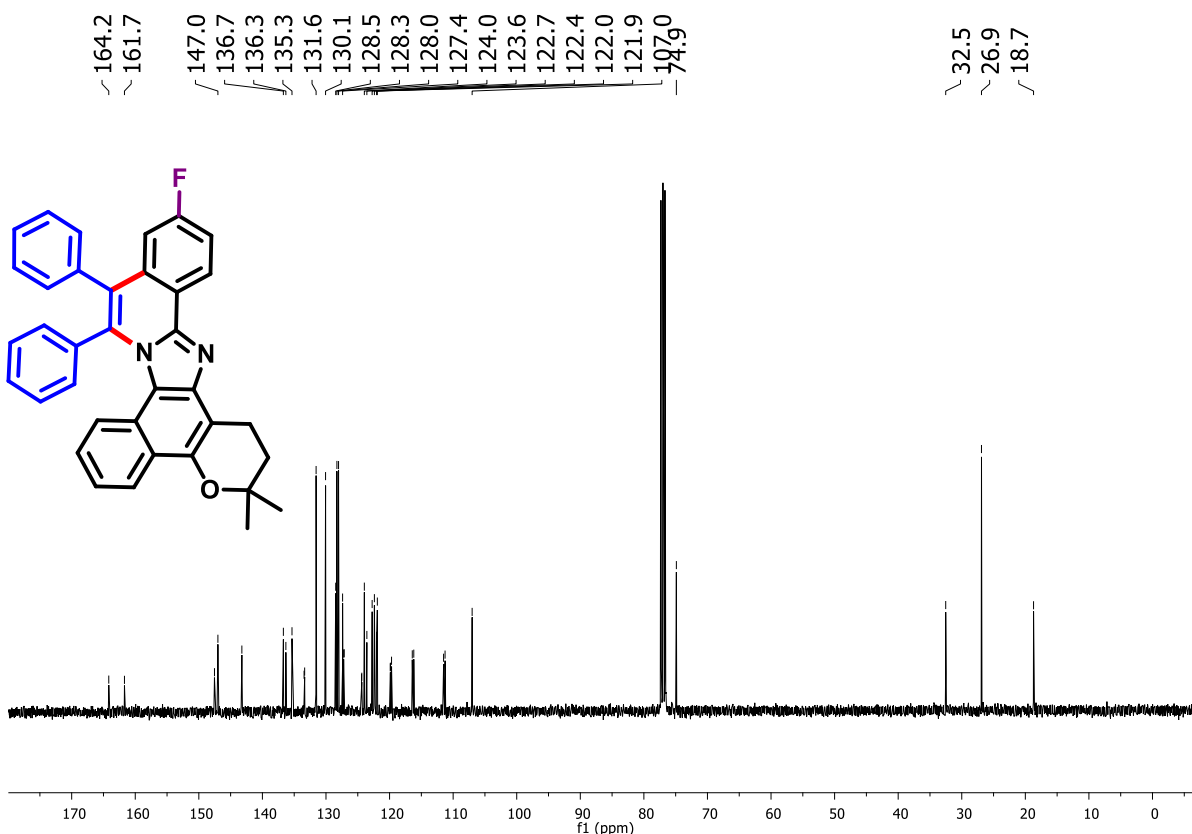


Figure 168. $^{13}\text{C NMR}$ spectrum (100 MHz, CDCl_3) of compound 273.

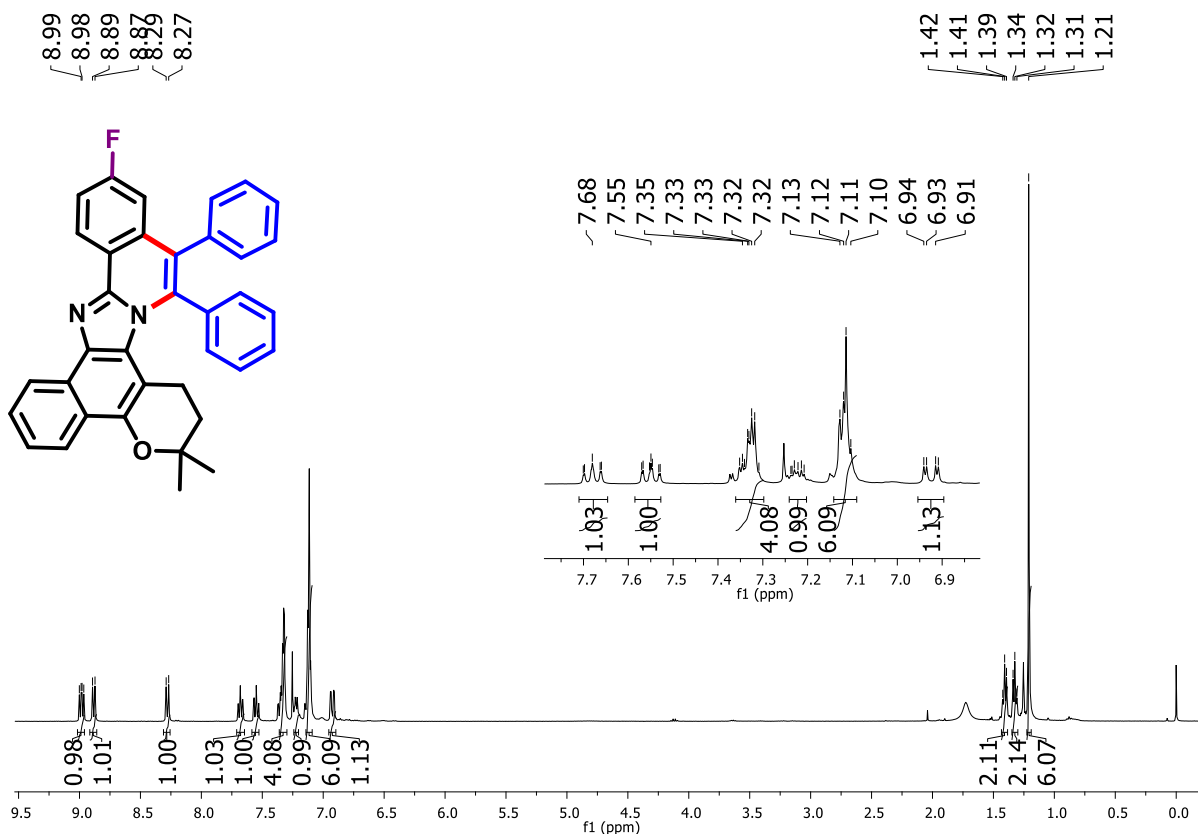


Figure 169. ¹H NMR spectrum (400 MHz, CDCl₃) of compound 274.

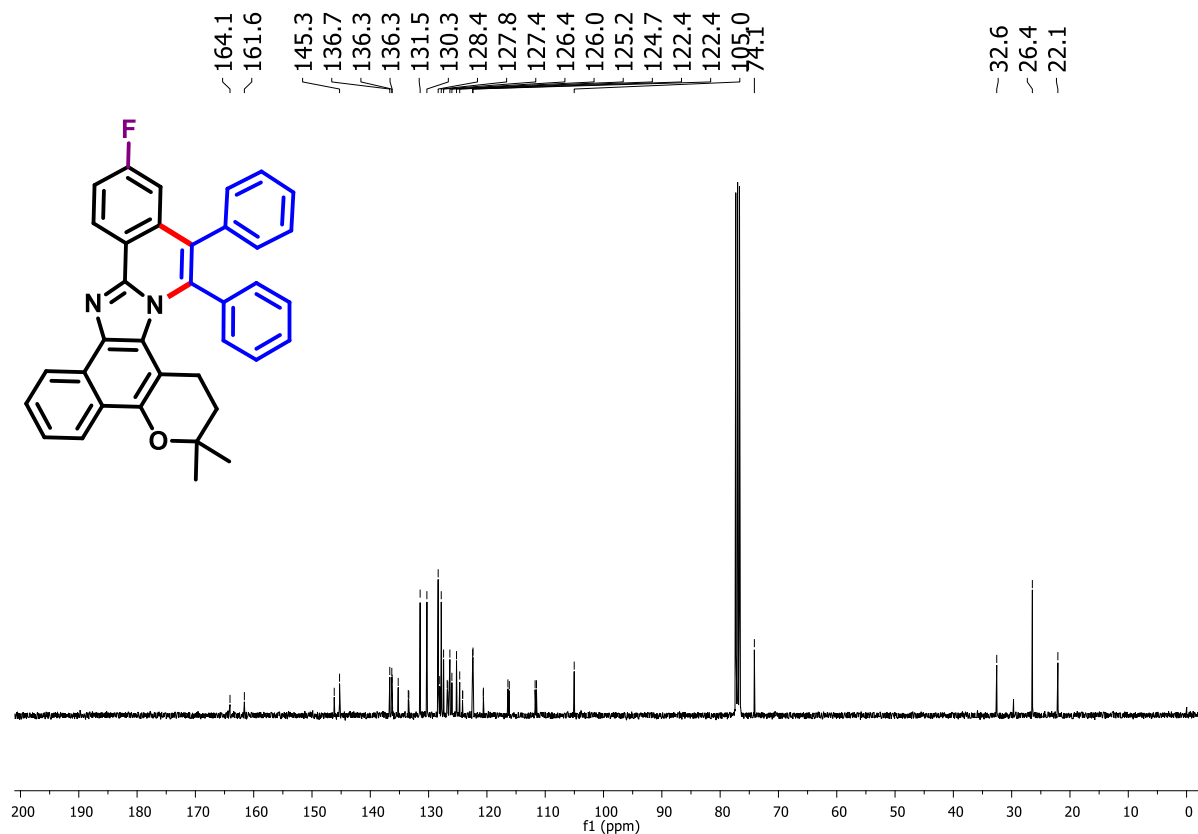


Figure 170. ¹³C NMR spectrum (100 MHz, CDCl₃) of compound 274.

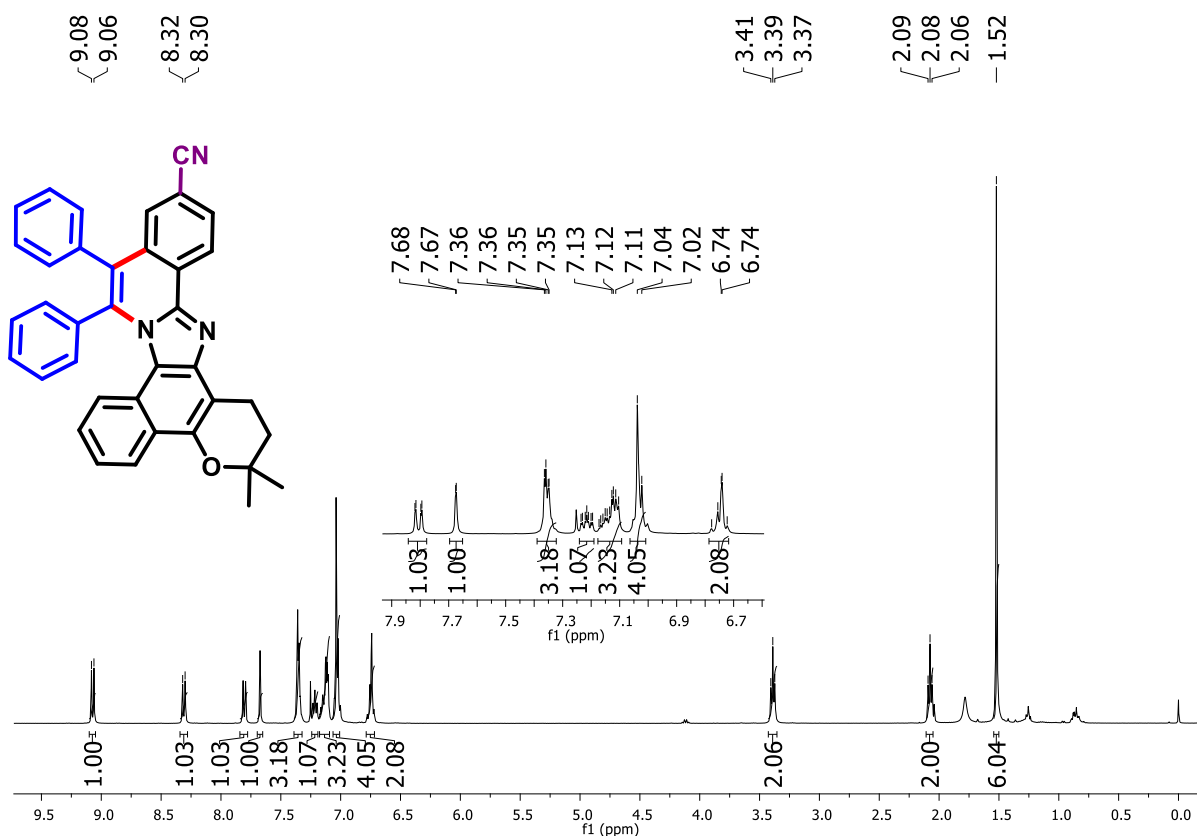


Figure 171. ¹H NMR spectrum (400 MHz, CDCl₃) of compound 275.

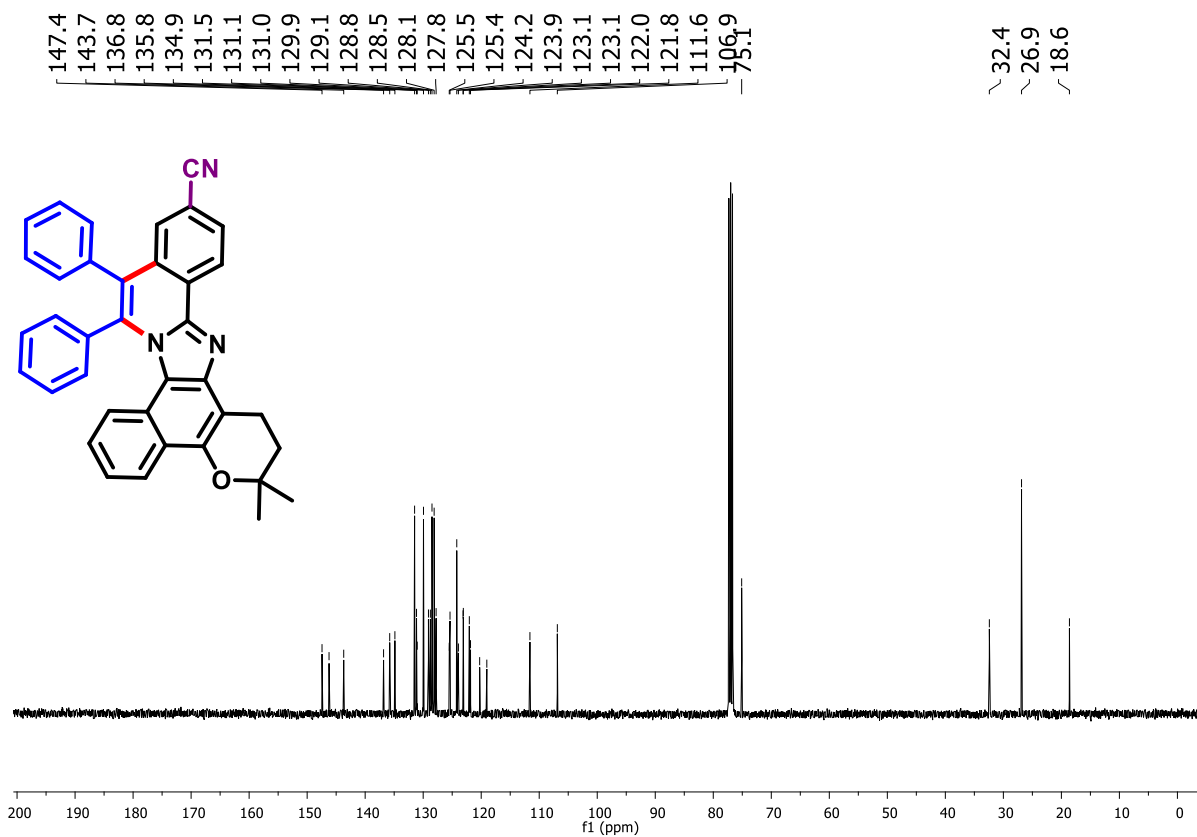
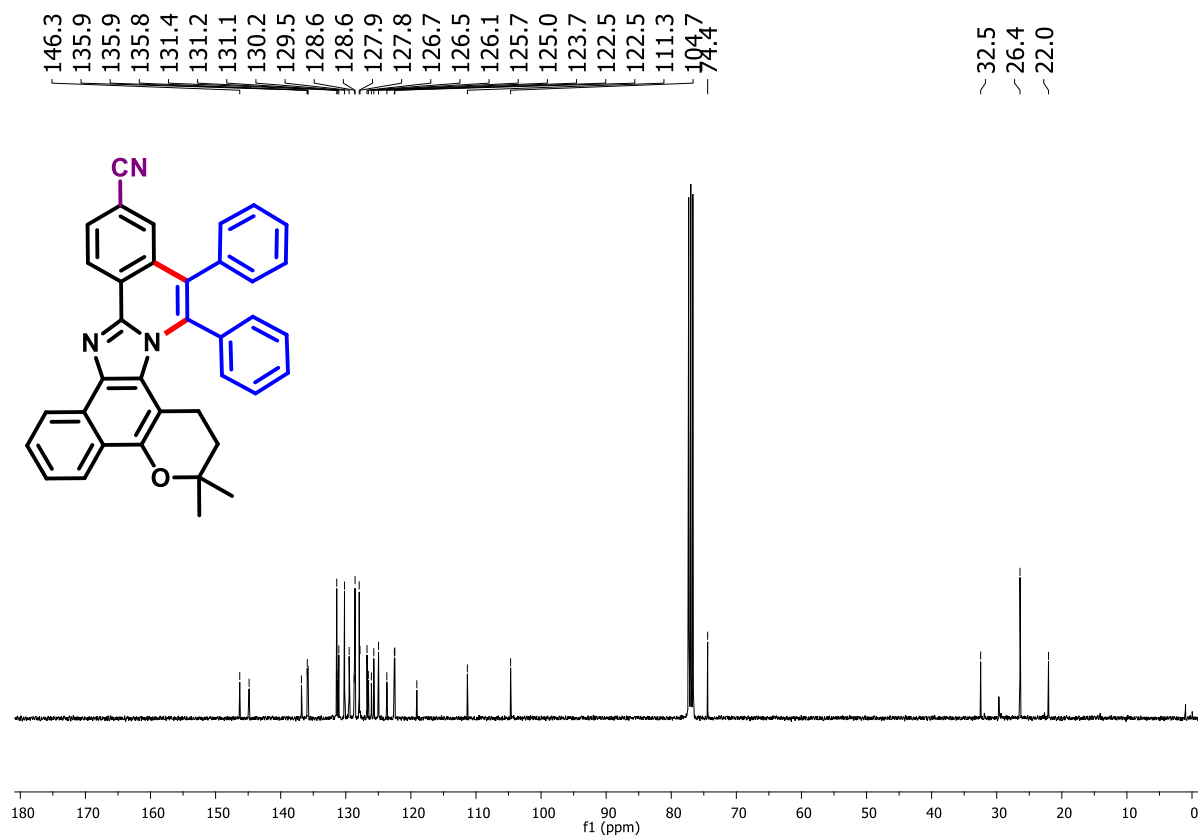
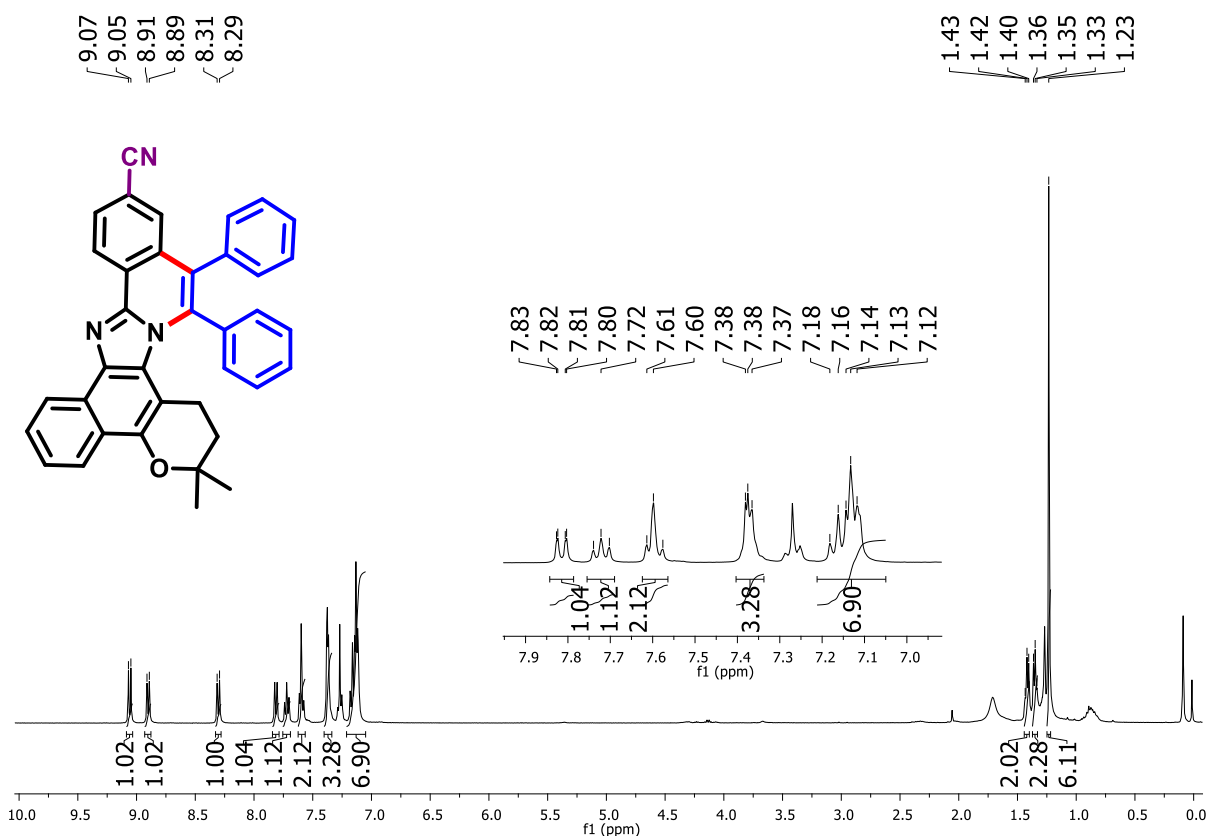


Figure 172. ¹³C NMR spectrum (100 MHz, CDCl₃) of compound 275.



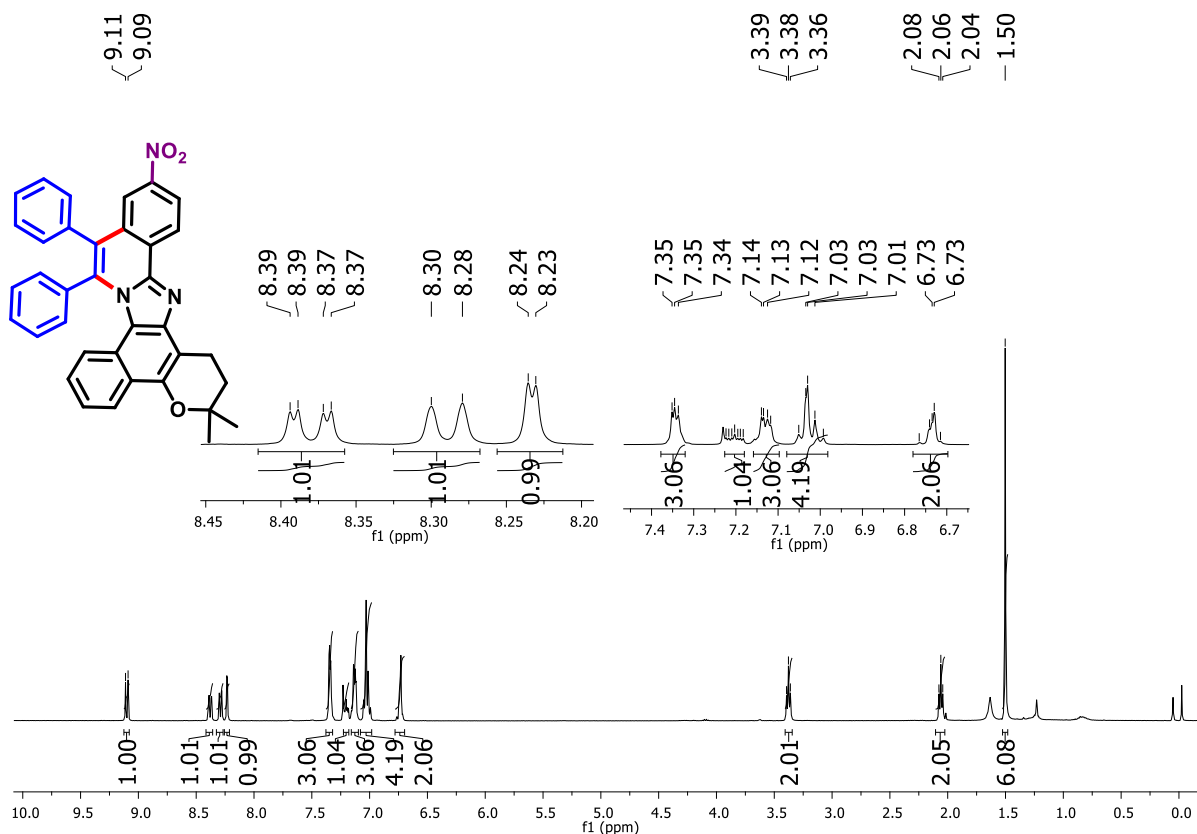


Figure 175. ¹H NMR spectrum (600 MHz, CDCl₃) of compound 277.

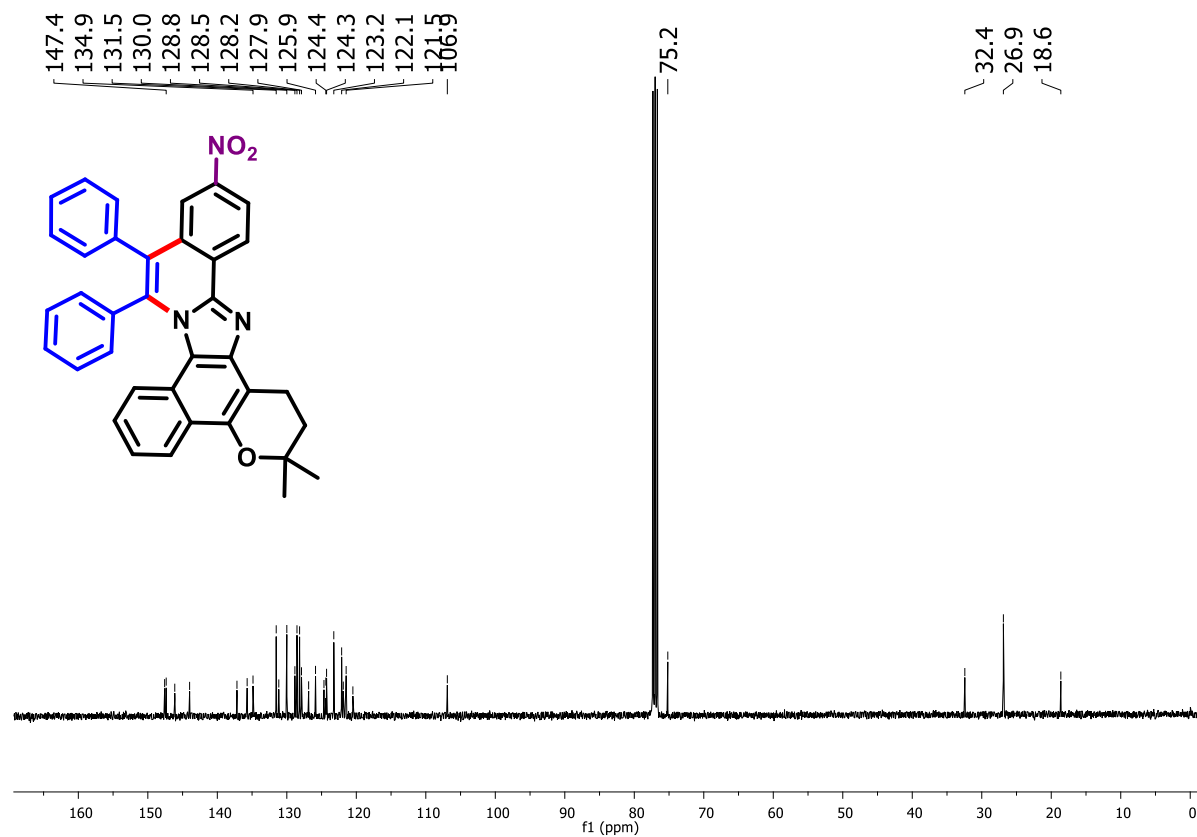


Figure 176. ¹³C NMR spectrum (150 MHz, CDCl₃) of compound 277.

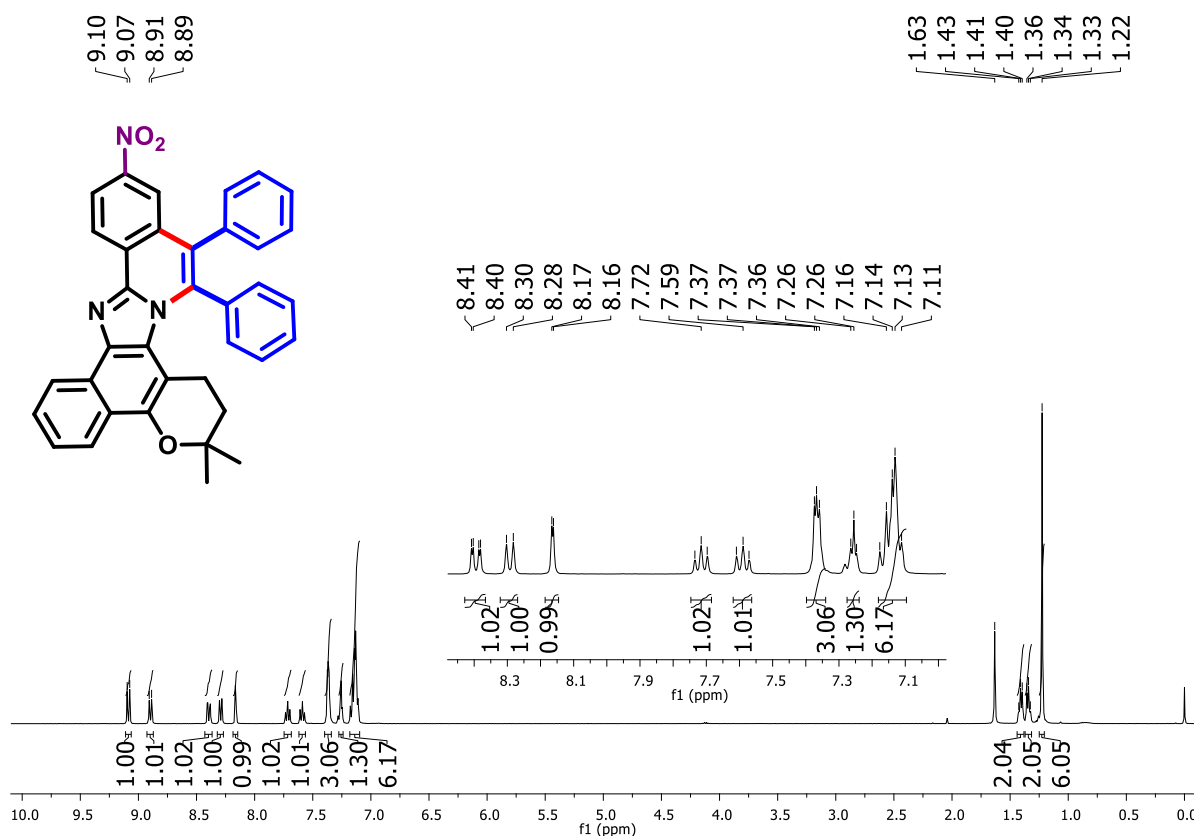


Figure 177. ¹H NMR spectrum (400 MHz, CDCl₃) of compound 278.

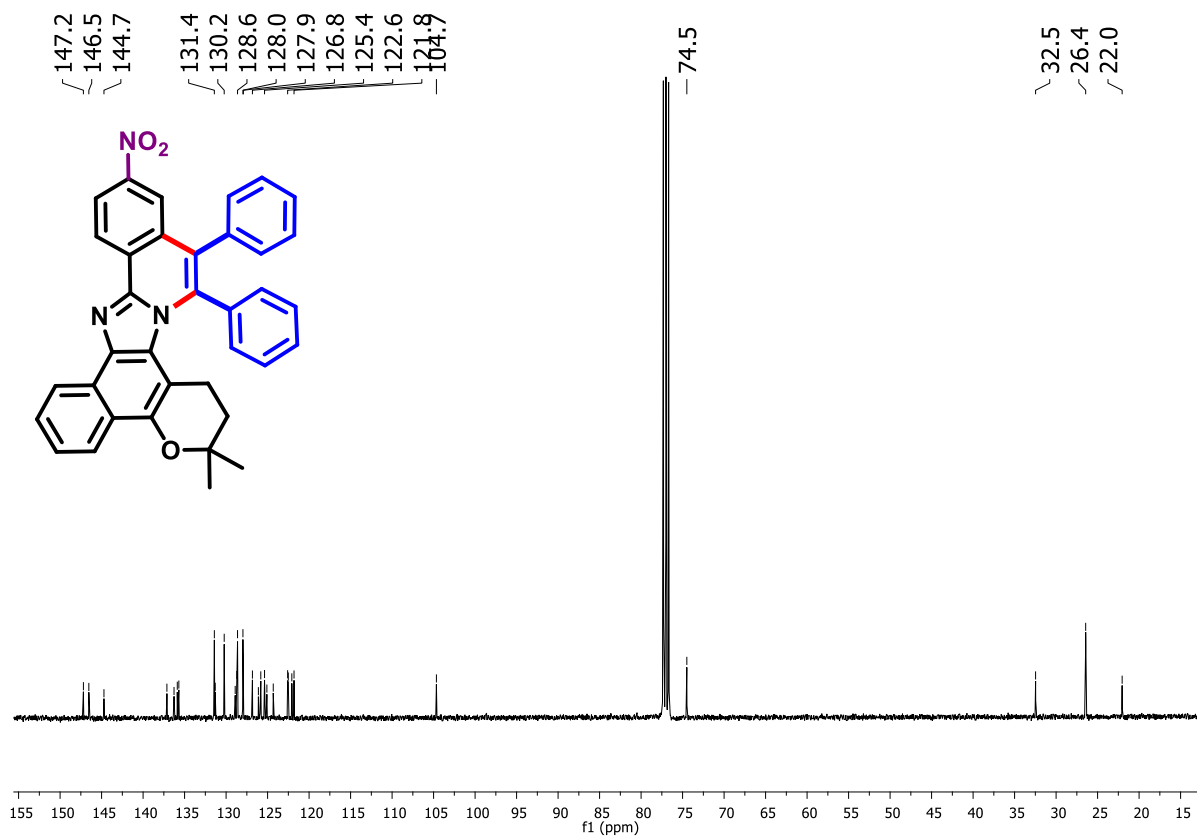


Figure 178. ¹³C NMR spectrum (100 MHz, CDCl₃) of compound 278.

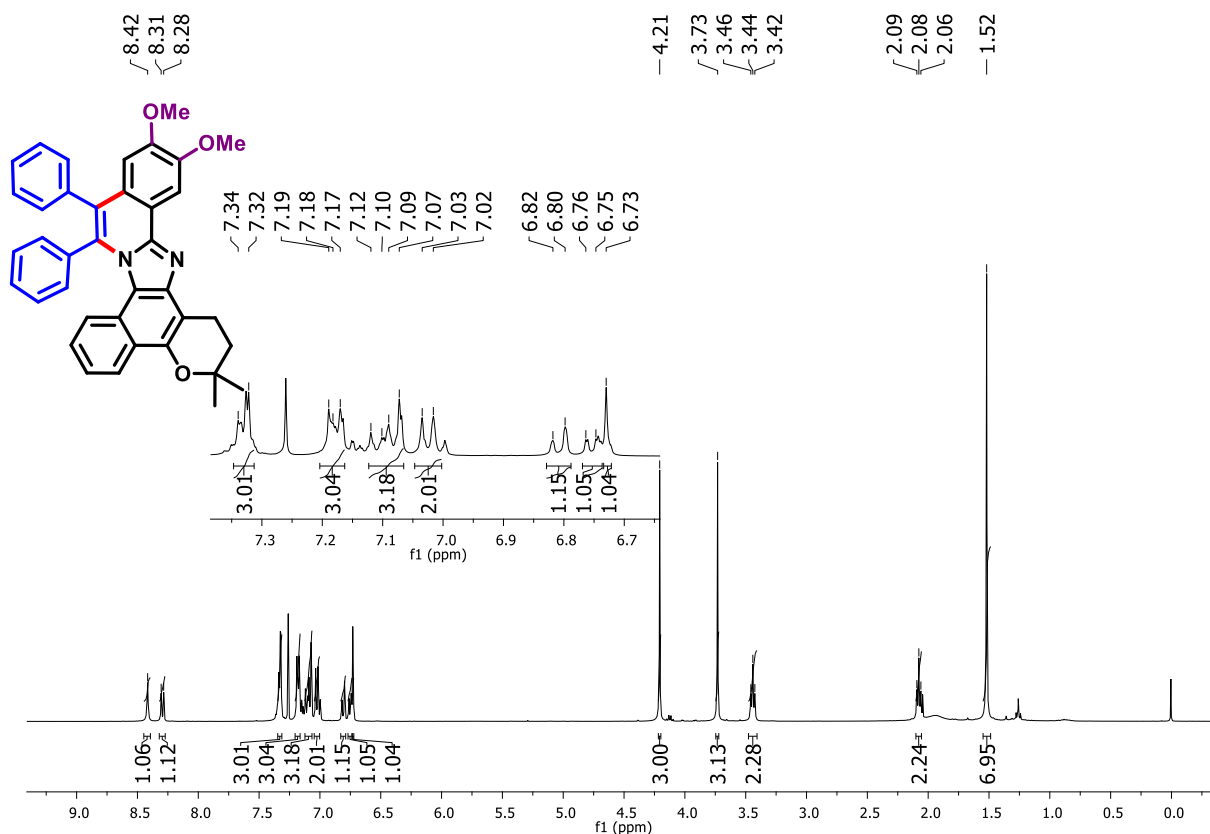


Figure 179. ^1H NMR spectrum (400 MHz, CDCl_3) of compound 279.

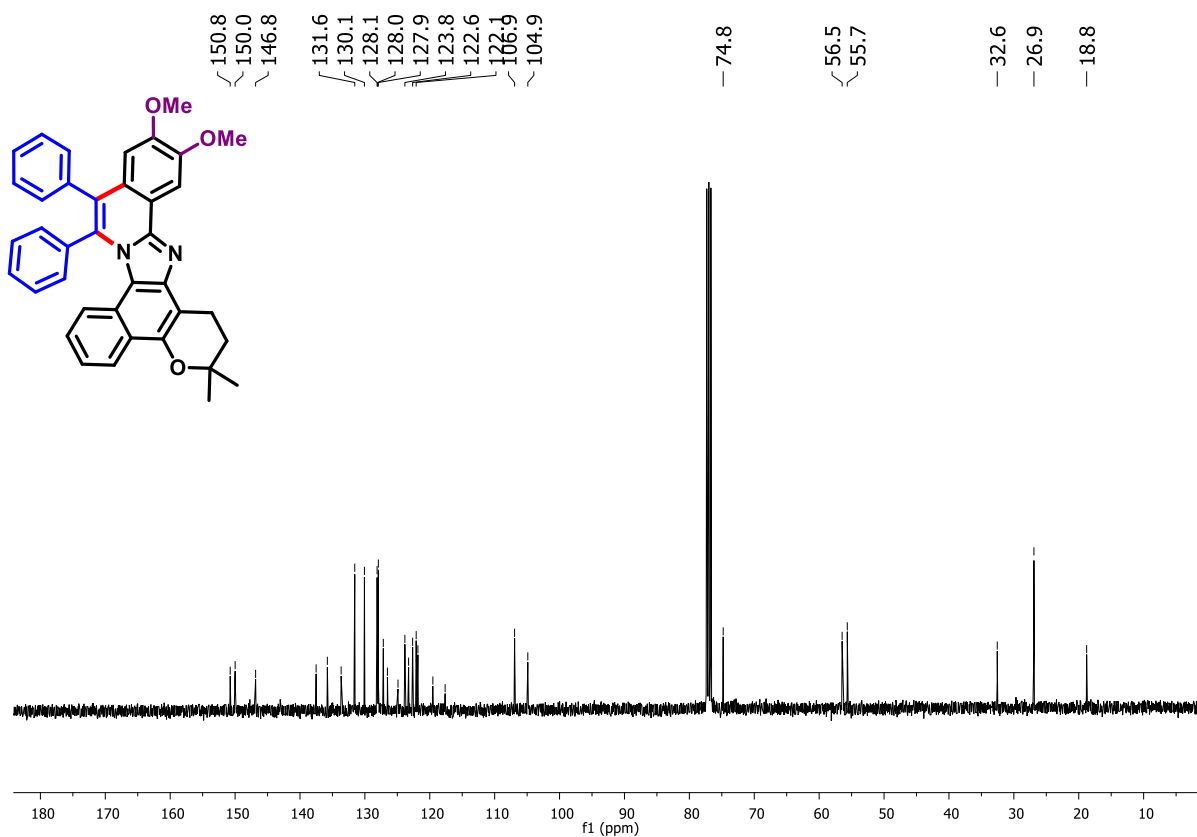


Figure 180. ^{13}C NMR spectrum (100 MHz, CDCl_3) of compound 279.

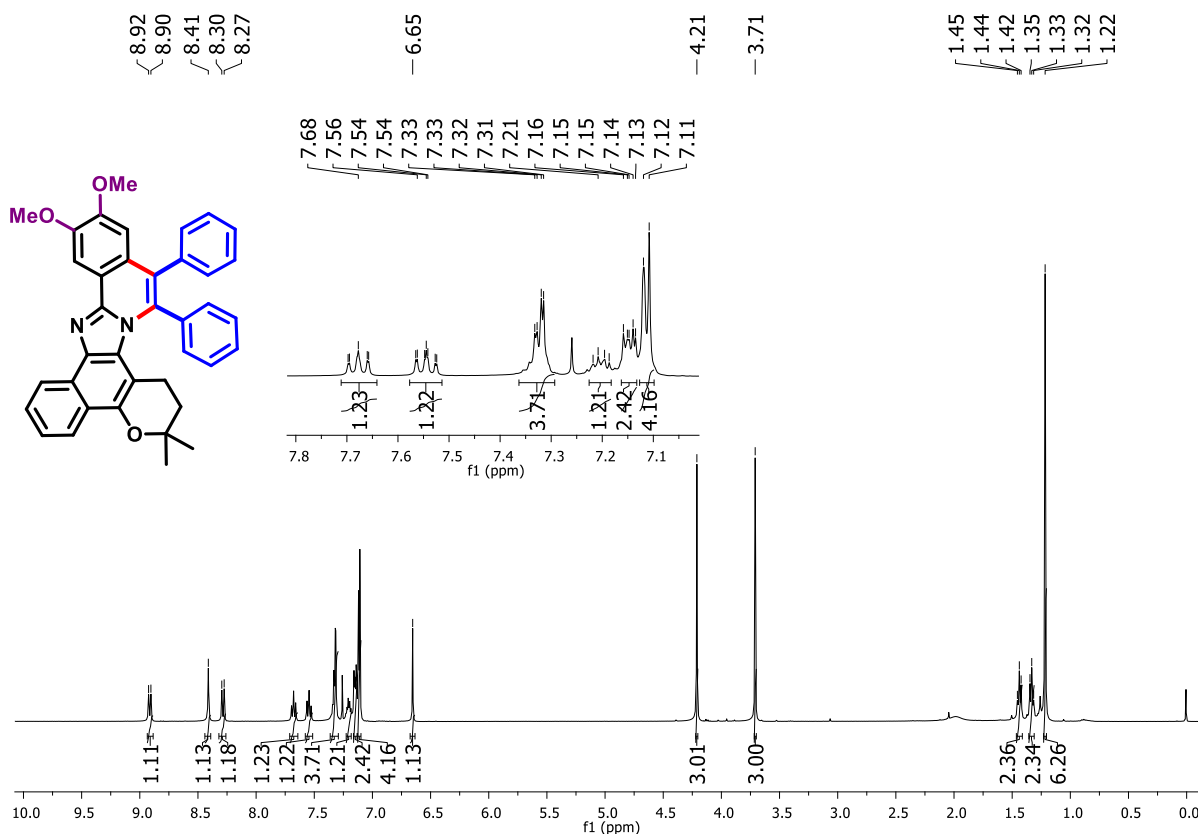


Figure 181. ¹H NMR spectrum (400 MHz, CDCl₃) of compound 280.

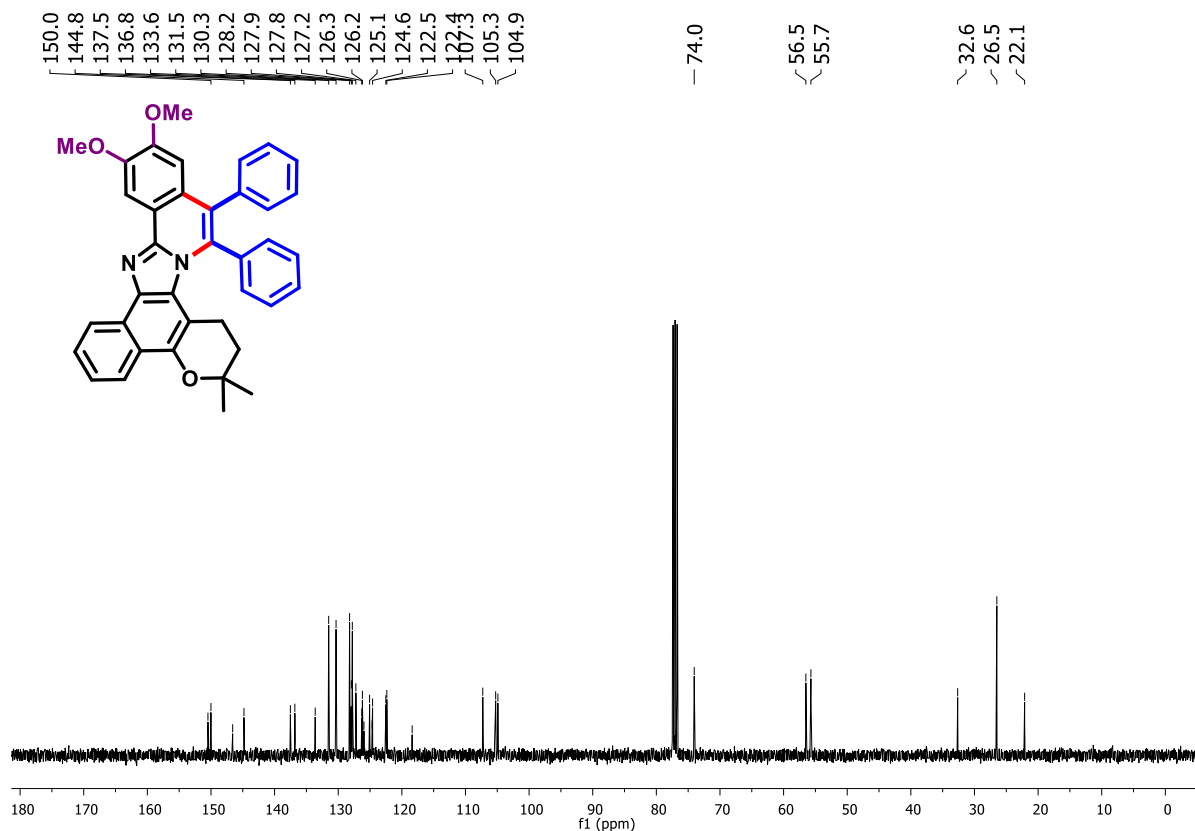


Figure 182. ¹³C NMR spectrum (100 MHz, CDCl₃) of compound 280.

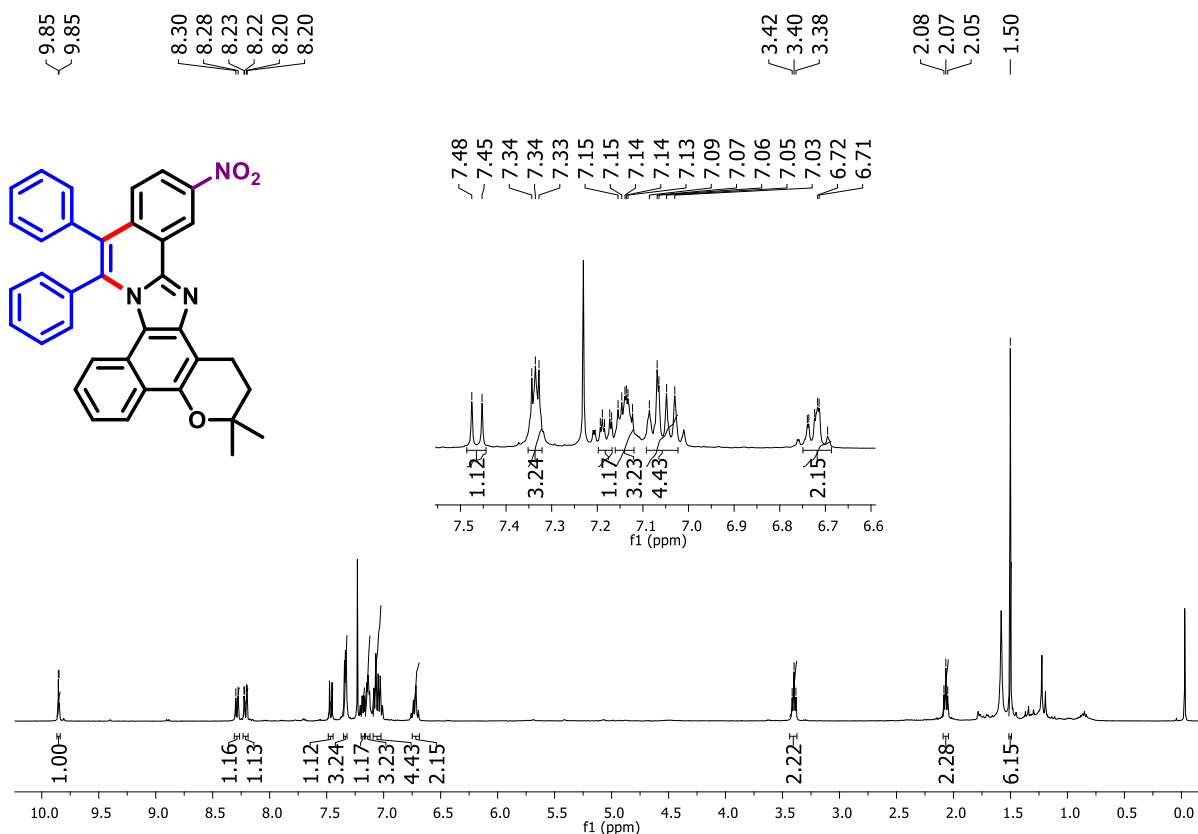


Figure 183. ¹H NMR spectrum (400 MHz, CDCl₃) of compound **281**.

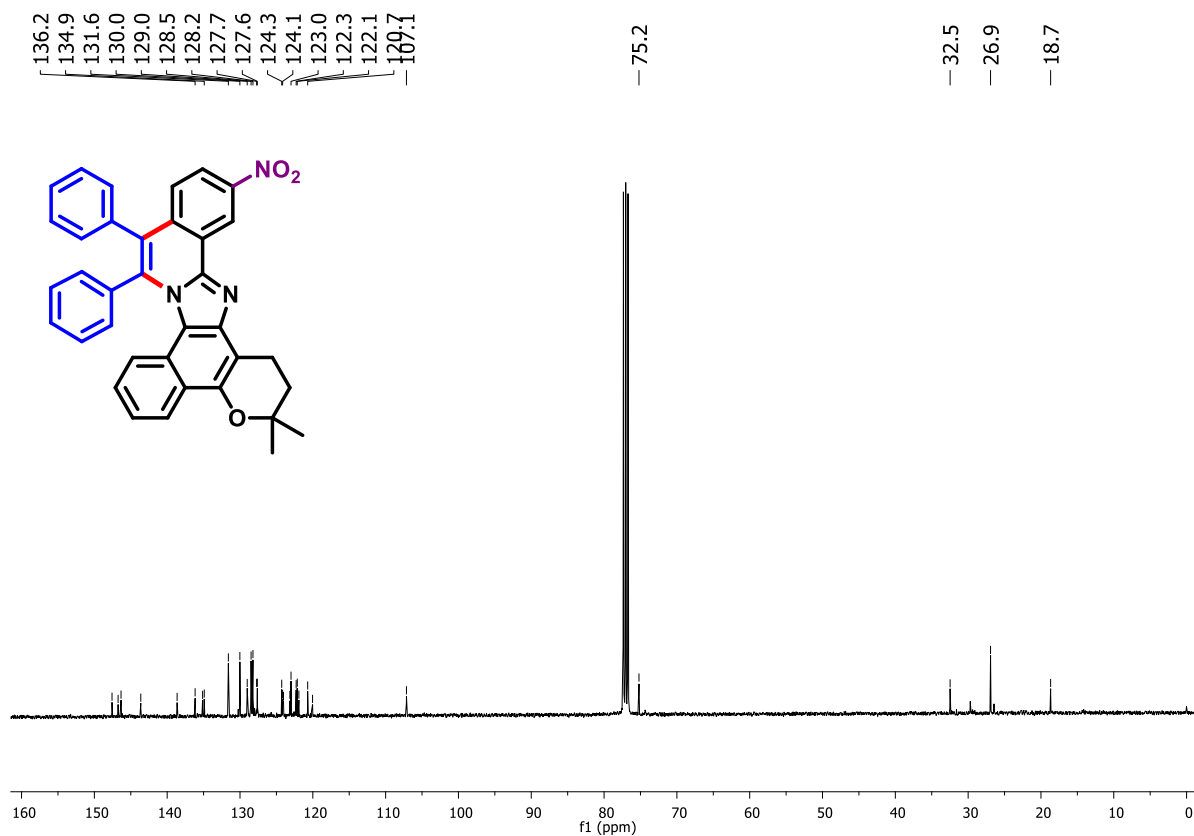


Figure 184. ¹³C NMR spectrum (100 MHz, CDCl₃) of compound **281**.